3 August 2007 | $10

Science

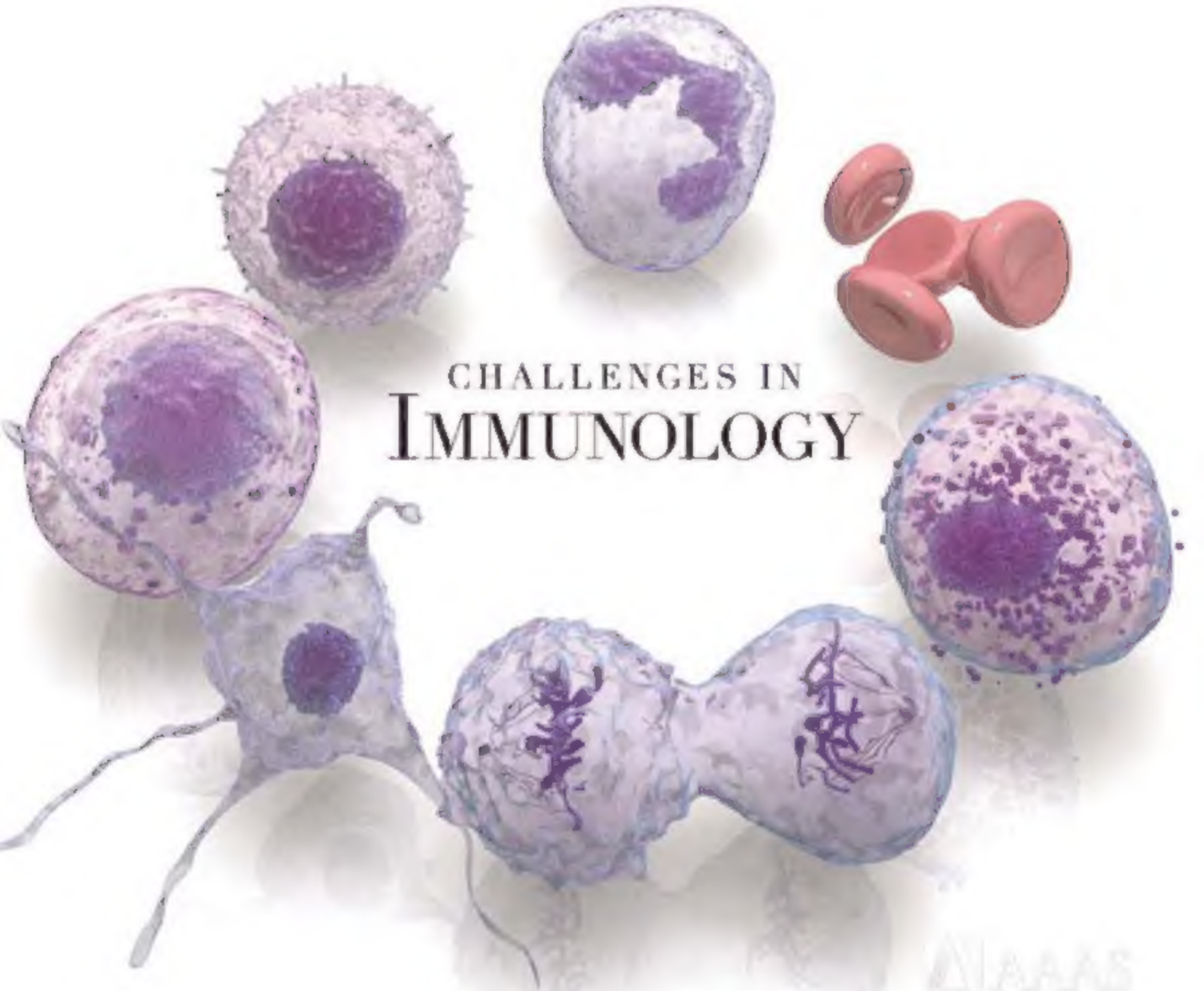

CHALLENGES IN IMMUNOLOGY

AAAS

Amazing!

INNOVATION @ WORK

Over 4,000 high quality antibodies from a single source

Sigma's AMAZING collection of high quality antibodies:

- Includes monoclonals, polyclonals, secondaries, conjugates and custom services
- Validated using a variety of methods – WB, IHC, IF, IP, ELISA
- Easily explored through Sigma's award-winning online tools
- Supported by Sigma's world-renowned technical service to assist you with your specific antibody requirements

Sigma is your source.

Go to sigma.com/antibody and be Amazed!

Our Innovation, Your Research
Shaping the Future of Life Science

Don't miss this **Amazing** opportunity: Order your copy of the all new 2007-2008 Antibodies Catalog, visit **sigma.com/antibody_cat**

SIGMA™
Life Science

The New BenchCel Automation Platform

Handles more integrations, rack styles, labware, and capacity

Liquid Handling • Labeling • Detection • Dispensing • Centrifugation • Sealing • Washing • Storage

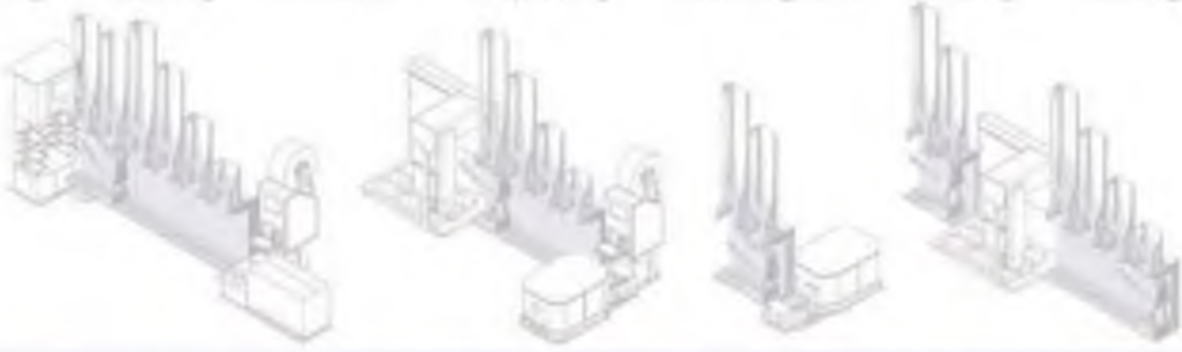

More Applications Than Ever in a Compact Workstation

The all new BenchCel® Platform is the heart of a fast and compact automation workstation that can handle applications ranging from simple microplate-processing tasks (such as barcode-labeling microplates) to sophisticated applications (such as PCR sample prep) that were only possible with full-sized automation systems. The BenchCel Platform can handle more of your applications with best-in-class features including the ability to integrate more instrumens per side; the flexibility to work with lidded microplates, deep-well microplates, and tip boxes; and the choice of two-, four-, or six-rack configurations available now with slot and front-loading rack styles. Let Velocity11 help you handle your next application with a BenchCel Platform plus your favorite combination of microplate-based instruments including liquid handlers, dispensers, readers, sealers, washers, microplate storage devices, centrifuges, and more.

Contact Velocity11 at +1.650.846.6600 for more information. For your FREE Workstation Configuration Handbook, email config@velocity11.com.

VELOCITY11®

The Speed of Discovery

www.velocity11.com

GE Healthcare

illustra™

Get attached to illustra for faster nucleic acid sample prep.

New illustra™ nucleic acid sample prep kits from GE Healthcare give you optimal yield and purity. What's more, they do this in as little as half the time it takes the best competing products. Whether you're purifying nucleic acids in plasmid, blood, tissue, cells or bacteria, you'll find that superior results and outstanding reproducibility come easily with illustra mini and midi kits.

With more than 20 years' experience in nucleic acid research, we're bringing science to life and helping transform healthcare. We call it Life Science Re-imagined.

www.gelifesciences.com/illustra

Speed is crucial to the sundew plant's success.
It reacts rapidly, bending its tentacles to bind its prey.
Some species can do this in just tenths of a second.

imagination at work

GE Healthcare Bio-Sciences AB, a General Electric Company
Björkgatan 30, 75184 Uppsala, Sweden

GE05-07. First printed 05/2007

Volume 317, Issue 5838

COVER

A showcase of cellular weapons deployed by the immune system ranges from antibody-making B cells to macrophages. A special section beginning on page 611 outlines the outstanding challenges in immunology for understanding how immune cells protect and sometimes injure us.

Illustration: Christopher Bickel

DEPARTMENTS

567 *Science* Online
568 This Week in *Science*
572 Editors' Choice
574 Contact *Science*
577 Random Samples
579 Newsmakers
682 New Products
683 *Science* Careers

EDITORIAL

571 Domestic? Forget It.
by Donald Kennedy

SPECIAL SECTION

Challenges in Immunology

INTRODUCTION

Testing Our Defenses 611

NEWS

Building an HIV-Proof Immune System 612
Mast Cells Show Their Might 614

PERSPECTIVES

Primary Immunodeficiencies: A Field in Its Infancy 617
J.-L. Casanova and L. Abel

Epigenetic Flexibility Underlying Lineage Choices in the Adaptive Immune System 620
D. Kioussis and K. Georgopoulos

Division of Labor with a Workforce of One: Challenges in Specifying Effector and Memory T Cell Fate 622
S. L. Reiner, F. Sallusto, A. Lanzavecchia

Private Lives: Reflections and Challenges in Understanding the Cell Biology of the Immune System 625
I. Mellman

Emerging Challenges in Regulatory T Cell Function and Biology 627
S. Sakaguchi and F. Powrie

See News story p. 584; Reports pp. 666, 670, 675, 678; Science's STKE material p. 567 or at www.sciencemag.org/sciext/immunology07/

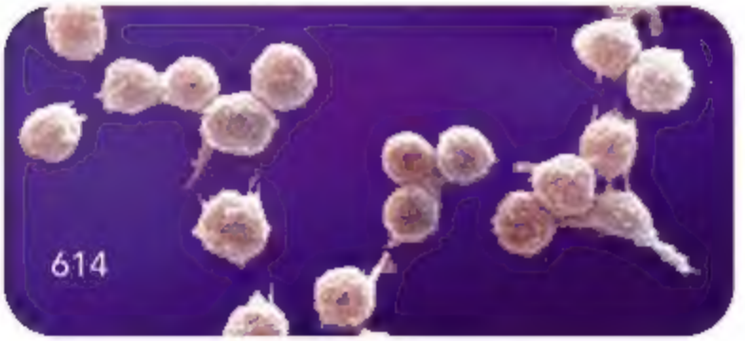

NEWS OF THE WEEK

Death Prompts a Review of Gene Therapy Vector 580
Rising Asian Threat Leaves Russia in the Lurch 581
U.S. Output Flattens, and NSF Wonders Why 582
Light-Splitting Trick Squeezes More Electricity Out of Sun's Rays 583
SCIENCESCOPE 583
A Slimy Start for Immunity? 584
>> Report p. 678
Cancer Test Dispute Pits Researcher Against a Firm She Helped Create 585

NEWS FOCUS

Middle Asia Takes Center Stage 586
Ancient Writing or Modern Fakery?
Cracking Open the Iranian Door
Ocean Observing Network Wades Into Swirling U.S. Fiscal Waters 591
Pilai Poonswad: Subduing Poachers, Ducking Insurgents to Save a Splendid Bird 592
Where Are the Invisible Galaxies? 594

CONTENTS continued >>

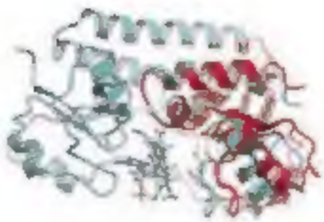

SCIENCE EXPRESS

www.sciencexpress.org

PLANETARY SCIENCE

Coupled Ferric Oxides and Sulfates on the Martian Surface
J.-P. Bibring et al.
Satellite observations show that oxidized iron minerals appear with sulfate deposits in ancient layered rocks on Mars, indicating that acidic groundwater pervaded several regions.
10.1126/science.1144174

PHYSICS

Superconducting Interfaces Between Insulating Oxides
N. Reyren et al.
The interface of two oxide insulators, $LaAlO_3$ and $SrTiO_3$, becomes superconducting at 200 millikelvin.
10.1126/science.1146006

BIOCHEMISTRY

Asymmetry in the Structure of the ABC Transporter–Binding Protein Complex BtuCD-BtuF
R. N. Hvorup et al.
The structure of a bacterial transporter for vitamin B_{12} and its binding protein partner reveals an occluded state that may represent an intermediate step in transport.
10.1126/science.1145950

MOLECULAR BIOLOGY

UHRF1 Plays a Role in Maintaining DNA Methylation in Mammalian Cells
M. Bostick et al.
Epigenetic DNA methylation patterns that persist through cell division depend on a protein that binds to hemi-methylated DNA and a methyltransferase.
10.1126/science.1147939

LETTERS

Genetics and *The Sopranos* *B. P. Possidente Jr.* 596
A Less Pessimistic View of U.S. Science Funding *J. H. Marburger III*
Evolution and Group Selection *D. P. Barash* **Response** *J. Haidt*
CORRECTIONS AND CLARIFICATIONS 597

BOOKS *ET AL.*

Five Days in August How World War II Became a Nuclear War *M. D. Gordin, reviewed by J. Krige* 598
Bomb Scare The History and Future of Nuclear Weapons *J. Cirincione, reviewed by C. F. Chyba* 599

POLICY FORUM

Identifiability in Genomic Research 600
W. W. Lowrance and F. S. Collins

PERSPECTIVES

Proteins That Promote Long Life 603
S. K. Kim
>> Report p. 660
Micelles Made to Order 604
M. A. Hillmyer
>> Reports pp. 644 and 647
Exploiting Wrinkle Formation 605
A. F. Miller
>> Report p. 650
Reproductive Dialog 606
S. McCormick
>> Report p. 656
Seeing Through Dark Matter 607
S. McGaugh
Retrospective: Anne McLaren (1927–2007) 609
J. Rossant and B. Hogan

BREVIA

NEUROSCIENCE

Defusing the Childhood Vocabulary Explosion 631
B. McMurray
Toddlers express a burst of new words as a result of their parallel acquisition of words of varying complexity, not because they acquire a new cognitive skill.

RESEARCH ARTICLE

GENETICS

Genome Transplantation in Bacteria: Changing One Species to Another 632
C. Lartigue et al.
The intact DNA genome was isolated from one *Mycoplasma* species and transferred to another, replacing the recipient's genome and conferring its own phenotype.

REPORTS

PHYSICS

Quantum Hall Effect in a Gate-Controlled *p-n* Junction of Graphene 638
J. R. Williams, L. DiCarlo, C. M. Marcus
In graphene sheets with different areas containing either electron or hole carriers, the conductance at the junctions between regions is quantized. >> Report p. 641

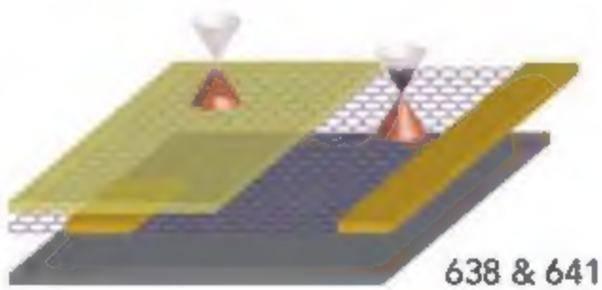

638 & 641

CONTENTS continued >>

REPORTS *CONTINUED...*

PHYSICS

Quantized Transport in Graphene *p-n* Junctions in a Magnetic Field 641
D. A. Abanin and L. S. Levitov
The mixing of quantum Hall edge states at the interface between different carrier regions in a graphene sheet accounts for the quantized transport through the gates. *>> Report p. 638*

CHEMISTRY

Cylindrical Block Copolymer Micelles and Co-Micelles of Controlled Length and Architecture 644
X. Wang et al.
A chemical system mimics living polymerization by adding block copolymers to the end of polymeric strands, forming cylindrical micelles with different lengths and functions.
>> Perspective p. 604

CHEMISTRY

Block Copolymer Assembly via Kinetic Control 647
H. Cui, Z. Chen, S. Zhong, K. L. Wooley, D. J. Pochan
Controlling the electrostatic interactions of charged polymer building blocks in water yields complex flat structures with internal patterns that can be used as templates.
>> Perspective p. 604

MATERIALS SCIENCE

Capillary Wrinkling of Floating Thin Polymer Films 650
J. Huang et al.
A drop of water placed on a free-floating thin polymer film produces a pattern of wrinkles that can be used to determine its elastic modulus and thickness. *>> Perspective p. 605*

PLANETARY SCIENCE

The Source of Saturn's G Ring 653
M. M. Hedman et al.
Saturn's tenuous G ring, which lacks a clear source, is produced by an arc of fine debris that is trapped in orbital resonance with Saturn's inner moon Mimas.

PLANT SCIENCE

The FERONIA Receptor-like Kinase Mediates Male-Female Interactions During Pollen Tube Reception 656
J.-M. Escobar-Restrepo et al.
In plants, a female-specific kinase senses the arrival of the pollen tube, setting the stage for the next stages of fertilization and potentially controlling reproductive compatibility.
>> Perspective p. 606

CELL BIOLOGY

Quantitative Mass Spectrometry Identifies Insulin Signaling Targets in *C. elegans* 660
M.-Q. Dong et al.
Identifying the genetic and protein targets of the insulin signaling pathway in *C. elegans* reveals mechanisms that potentially control the aging process. *>> Perspective p. 603*

CELL BIOLOGY

Forced Unfolding of Proteins Within Cells 663
C. P. Johnson et al.
Fluorescent labeling of cysteines in living cells reveals how mechanical stress can cause force-induced conformational changes in cellular proteins.

IMMUNOLOGY

Monitoring of Blood Vessels and Tissues by a Population of Monocytes with Patrolling Behavior 666
C. Auffray et al.
Immune cells that reside in endothelial tissues remain attached to the walls of blood vessels and survey for signs of damage and infection.

IMMUNOLOGY

Regulation of Homeostatic Chemokine Expression and Cell Trafficking During Immune Responses 670
S. N. Mueller et al.
During the immune response to a pathogen, lymph nodes temporarily block the entry of new immune cells, thereby optimizing the ongoing immune reaction.

IMMUNOLOGY

Negative Regulation of Toll-Like Receptor Signaling by NF-κB p50 Ubiquitination Blockade 675
R. J. Carmody, Q. Ruan, S. Palmer, B. Hilliard, Y. H. Chen
In mice, the innate immune response to microbes is controlled by blocking degradation of a transcriptional inhibitor, dampening an otherwise potentially dangerous response.

IMMUNOLOGY

Immune-like Phagocyte Activity in the Social Amoeba 678
G. Chen, O. Zhuchenko, A. Kuspa
The sluglike assemblies formed by social amoebae contain specialized cells that function like the phagocytes of animal immune systems, suggesting an evolutionary connection.
>> News story p. 584

606 & 656

AAAS
ADVANCING SCIENCE, SERVING SOCIETY

SCIENCE (ISSN 0036-8075) is published weekly on Friday, except the last week in December, by the American Association for the Advancement of Science, 1200 New York Avenue, NW, Washington, DC 20005. Periodicals Mail postage (publication No. 484460) paid at Washington, DC, and additional mailing offices. Copyright © 2007 by the American Association for the Advancement of Science. The title SCIENCE is a registered trademark of the AAAS. Domestic individual membership and subscription ($1 issue): $142 ($74 allocated to subscription). Domestic institutional subscription ($1 issue): $710. Foreign postage extra: Mexico, Caribbean (surface mail) 65%; other countries (air assist delivery) 185. First class, airmail, student, and canadian rates on request. Canadian rates with GST available upon request, GST #13734 8122. Publications Mail Agreement Number 1069624. Printed in the U.S.A.

Change of address: Allow 4 weeks, giving old and new addresses and 8-digit account number. Postmaster: Send change of address to AAAS, P.O. Box 96178, Washington, DC 20090-6178. Single-copy sales: $10.00 current issue, $15.00 back issue prepaid includes surface postage; bulk rates on request. Authorization to photocopy material for internal or personal use under circumstances not falling within the fair use provisions of the Copyright Act is granted by AAAS to libraries and other users registered with the Copyright Clearance Center (CCC) Transactional Reporting Service, provided that $30.00 per article is paid directly to CCC, 222 Rosewood Drive, Danvers, MA 01923. The identification code for Science is 0036-8075. Science is indexed in the Reader's Guide to Periodical Literature and in several specialized indexes.

CONTENTS continued >>

Never forget.

SCIENCENOW

www.sciencenow.org DAILY N

Bad Memories Tied to DNA
Study links enhanced ability to recall emotional events to genetic mutation

Gene Duplications Give Clues to Humanness
Different copy numbers may explain differences in diet, physical activity among primates.

A Mind for Sociability
Brain structure offers clues to evolution of human emotional intelligence

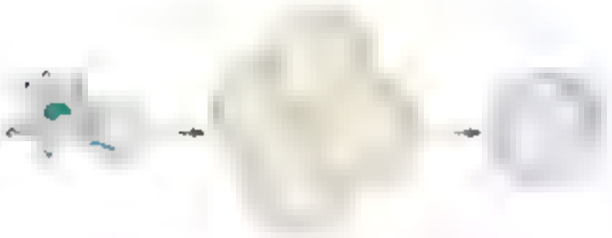

AD SECTION

Challenges in Immunology

SCIENCE'S STKE

www.stke.org SIGNAL TRANSDU

EDITORIAL GUIDE Uncovering Immunological Secrets
J. F. Foley and E. M. Adler
Three articles highlight signals controlling T cell late T cell responsiveness, and the response to cytokines secreted by T cells

PERSPECTIVE NFAT in Lymphocytes—A Factor for All Events?
E. Serfling, F. Berberich-Siebelt, A. Avots
The NFAT transcription factors may hold the key to T cell memory.

PERSPECTIVE Diacylglycerol Kinases Put the Brakes on Immune Function
B. W. Wattenberg and D. M. Raben
Diacylglycerol kinases are key negative regulators of immune responses in a broad array of cells.

REVIEW A Role for the Cytoplasmic Adaptor Protein Act1 in Mediating IL-17 Signaling
A. Linden
Act1 may play a role in local inflammatory responses mediated by interleukin-17

How a baseball player's struggle can influence postdocs.

SCIENCE CAREERS

www.sciencecareers.org CAREER RESOURCES FOR SCIENTISTS

US: The Curt Flood Effect
B. Benderly
Standing up for rights is perilous for people like postdocs who depend on subjective recommendations of supervisors.

EUROPE Beyond CSI—Environmental Forensics Picks Up in Europe
M. Anscombe
New environmental laws mean more demand for people in environmental science and law.

US: Educated Woman, Postdoc Edition, Chapter 7—Tainted Love
M. P. DeWhyse
Does Micella need to deliver gold stars and other rewards in her career, or should she just please herself?

GRANTSNET August 2007 Funding News
GrantsNet Staff
Learn about the latest research funding opportunities, scholarships, fellowships, and internships.

CREDITS: (SCIENCE NOW) FINBARR O'REILLY/REUTERS; (SCIENCE CAREERS) MAPX; CREATIVE COMMONS

Separate individual or institutional subscriptions to these products may be required for full-text access.

EDITED BY STELLA HURTLEY AND PHIL SZUROMI

Stress and Wrinkles >>

Under most circumstances, when a stiff thin film is placed under either a compressive or tensile stress, the film buckles, rather than stretches or shrinks. **Huang *et al.*** (p. 650; see the Perspective by **Miller**) placed a drop of water on a free-floating polymer film and show that the stresses caused by the surface tension between the droplet and the film cause the film to wrinkle. The periodic wrinkling pattern that formed confirms recent theoretical results, and the authors could relate the wrinkling characteristic features to the elasticity and thickness of the film. This system provides a simple, bench-top method for the study of the viscoelastic response of thin films.

Quantized Transport in Graphene Sheets

The manipulation of the carrier density and carrier sign over an entire graphene sheet (a single layer of graphite) by electrostatic gating has been demonstrated. Efforts are now being directed to local gating so that transport properties of different areas can be simultaneously manipulated in order to make device-like structures with advanced functionality. **Williams *et al.*** (p. 638, published online 28 June) show experimentally that a global bottom gate combined with a patterned top gate provides the ability to controllably form bipolar *p-n* junctions in the graphene layer (as well as unipolar *p-p* and *n-n* junctions). Subsequent magnetotransport measurements revealed quantum Hall effect behavior, the details of which depend on whether the junctions are bipolar or unipolar. **Abanin and Levitov** (p. 641, published online 28 June) theoretically explain these results in terms of quantum Hall edge-state mixing at the interface region.

An Arc Anchoring Saturn's G Ring

Saturn's G ring is a faint and narrow ring lying beyond the main set of rings. Despite being well defined, it has been unclear why it exists at this precise location; in particular, it is not flanked by moons that might shepherd it and carve it out or infuse it with vapor. **Hedman *et al.*** (p. 653), using the Imaging Science Subsystem aboard the Cassini spacecraft, show that the G ring contains a bright arc of material made up of centimeter- to meter-sized icy bodies held in a 7:6 corotation resonance with the major moon Mimas. Dust from this concentration of particles trails out to enscribe the ring.

Manipulating Micelle Formation

In solution, block copolymers can form a variety of thermodynamically controlled structures, including micelles (see the Perspective by **Hillmyer**). Polyferrocenylsilane-based block copolymers have an unusual propensity to form cylindrical micelles that are stable over a range of polymer concentrations. **Wang *et al.*** (p. 644) show that the shape and composition of the micelles can be further controlled in a process analogous to the synthesis of polymers through living polymerization. The addition of more polymer to the solution leads to its epitaxial attachment and to the growth of the micelles with narrower size distributions. With the addition of a different block copolymer, co-micelles consisting of the two different block copolymers are formed. **Cui *et al.*** (p. 647) describe a general strategy for the preparation of complex one-dimensional nanostructures from block copolymers. Unlike classical block copolymer self-assembly, in which the structure is dictated by the lengths of the two polymer blocks, assembly was controlled through electrostatic interactions and solvation. The process involves the formation in water of polymer micelle structures, which flatten upon the rapid addition of tetrahydrofuran. The resulting flattened micelles subsequently grow in an anisotropic fashion to yield unusual architectures. When the diamine additives were replaced with amine-coated gold particles, even more complex structures are obtained.

Genome Transplant

In the 1970s, it was a revolutionary advance to be able to cut and paste small sequences of DNA and to transfer an individual gene into a cell at will. **Lartigue *et al.*** (p. 632, published online 28 June) now describe the replacement of one entire bacterial genome (*Mycoplasma capricolum*) with another (*Mycoplasma mycoides*), which allows the production of a colony of cells that produced the protein products encoded by the donor genome.

Match-Making in Plants

In plants, as in animals, fertilization requires male and female gametes selectively and exclusively to meet and fuse. In plants, unlike in animals, it is not the actual gametes that participate in this dance, but rather the gametophytes, which carry immotile gametes. **Escobar-Restrepo *et al.*** (p. 656; see the Perspective by **McCormick**) have now identified one of the molecules by which the female gametophyte (the embryo sac) recognizes the male gametophyte (the pollen). A receptor kinase, FER, is situated at cell surfaces within the female gametophyte. As the pollen tube approaches, a signaling cascade is initiated in the

CREDITS (TOP TO BOTTOM): JIANGSHU HUANG/UNIVERSITY OF MASSACHUSETTS; CUI ET AL.

embryo sac that closes the door to late-arriving pollen tubes and halts the growth of the successful pollen tube, which then releases the male gamete. A good match between FER and its presumed ligand from the pollen tube appears to form the basis of reproductive compatibility.

Insulin Signaling Up-Close and Personal

Novel quantitative methods are allowing the analysis of gene and protein expression in unprecedented detail. **Dong *et al.*** (p. 660, see the Perspective by **Kim**) profiled protein abundance changes in response to perturbations of insulin and insulin-like growth factor–1 (IGF-1) signaling in *Caenorhabditis elegans* and identified 86 targets. More than half of the targets identified by this qualitative proteomics approach were not previously identified and may provide new insights into the mechanisms of diabetes and aging.

Monitoring Cellular Mechanical Stress

Cells exert and respond to mechanical forces, but investigating how these signals are transduced is a challenge. By measuring differential labeling of cysteines in stressed and relaxed cells, **Johnson *et al.*** (p. 663) identify proteins that change their structure in response to stress. Using mass spectroscopy, they determined the specific Cys residues that experience structural changes in red blood cells' spectrin unfolds as cells are stressed, and in mesenchymal stem cells, both myosin IIA and vimentin show differential labeling in tensed versus drug-relaxed cells.

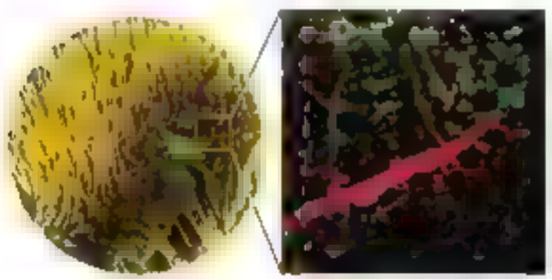

CREDIT: AUFFRAY ET AL.

Leukocytes on Border Patrol

Immune cells move between the circulation system and tissues in response to infection. Upon detection of inflammation, leukocytes initiate a highly orchestrated sequence of events, whereby they attach and roll along on the surface of the endothelium before squeezing through to the underlying tissue. **Auffray *et al.*** (p. 666) reveal a quite distinct type of behavior displayed by a population of monocytes that remain attached to the endothelium in the absence of inflammation. The resident cells appeared to survey the surface of postcapillary venules, veins, and arteries, depending on specific chemokine and integrin signals. Upon detection of inflammatory cues, the cells moved into infected sites, where they undergo differentiation into macrophages. **Mueller *et al.*** (p. 670) reveal how the down-regulation of chemokines in the lymph node prevents T lymphocytes from entering during an ongoing immune response. This delay may help to optimize the lymph node environment to produce the most effective immune response.

Keeping Tabs on a TLR Response

Toll-like receptors (TLRs) exert powerful proinflammatory responses to microbial pathogens, and TLR responses are stringently regulated during infection so that the chronic exposure of cells to microbial products can ultimately lead to a state of hyporesponsiveness. **Carmody *et al.*** (p. 675) identify an essential role for the proto-oncogene protein B cell leukemia (Bcl)–3 in negatively regulating TLR signaling. In this context, Bcl-3 blocks ubiquitination of the nuclear factor κB subunit p50, which prevents its degradation and allows it to maintain its inhibition of gene transcription in response to TLR signals. This pathway offers a means by which microbial signals can be prevented from overpowering the immune response.

Slimy Cooperative Requires Housekeeper

Phagocytes are innate immune cells found in animals that specialize in scavenging bacteria and other foreign matter. **Chen *et al.*** (p. 678, see the news story by **Leslie**) show that a similar waste disposal system helps maintain well-being in slime molds. The aggregates formed by the social amoebae *Dictyostelium discoideum*. Specialized sentinel cells engulfed bacteria and removed toxins, and were themselves ejected from the colony as it migrated. A protein related to those found in animal innate immune systems was required for this function, as well as in allowing individual amoebae to feed on their diet of bacteria when not part of a colony.

Q

Who's working to increase support for science?

Top quality research depends on comprehensive support. AAAS is present at every stage of the process – from advising on funding policy initiatives to tracking the US Federal R&D budgeting process. As the experts, we brief Congressional staffers and representatives from governments around the world. And only AAAS Funding Updates – sent out monthly – provide continual coverage of R&D appropriations. By actively working to increase support for research, AAAS advances science.
To see how, go to **www.aaas.org/support**

AAAS

ADVANCING SCIENCE SERVING SOCIETY

Mehitabel the cat

Domestic? Forget it.

READERS OLD ENOUGH TO REMEMBER DON MARQUIS' SYNDICATED New *York Sun* columns may recall that at night, a cockroach named Archy took over his typewriter to write short pieces about him and his friend, a cat named Mehitabel. Because he typed by diving on the keys, he had difficulty with upper case and punctuation, yielding a rather free-form text. In the following message forwarded to us, Mehitabel is apparently responding to recent findings on the genetic background and history of cat "domestication" (*Science*, 27 July 2007, p. 519).

– Donald Kennedy

boss, i sent archy to the keyboard to say how upset I am about the terrible treatment of cats in the papers it's because of a report in science telling all about how we cats got started pretty interesting but some of the papers are saying that's how we got domesticated domesticated hell domesticated is for dogs not us boss action needs to be taken against this slander these scientist guys did a good thing they found that the first real house cat was not that pampered egyptian pussy instead they showed our relationship with people was much older thank god for that then they looked at genes of us cats and compared them with the five small wildcats and decided we all came from the one in the middle east maybe an arab cat their idea is that the first farmers ten thousand years ago started storing grain that brought in rats and mice so then this arab cat helped out some pepers call that domestication that nonsense has gotta be stopped this was a gift not some ownership deal why do they think today we occasionally bring a bloody present into the house and lay it on the bed or the best rug it s because we want to remind everyone that we are volunteers not repressed conscripts like the damn rovers and fidos just look at how they act wagging their tails and begging for food talk about deal they got one okay but they lost their independence not me and my kind no sir heres the thing about us cats we think it's fine in the house but we're just as happy in the alley or out hunting when we do that they call us feral ever hear anyone call a dog feral by the way hell the feral dog is a coyote not some lost rover get it our gig is about independence pet us a little thats okay even pimp us up for the cat show but make one of those ownership moves and sayonara we're gone we think the scientists got it right about what went down back then in the fertile crescent after the mice got after the einkorn wheat or whatever pretty soon our ancestors were chomping em up well you might ask did they see any dog fossils in there what was old rover doing not much it appears maybe practicing pointing rats or rolling over for the farmers well when the going gets tough only the tough get going us cats are okay with the publicity but when the science story got out into the mainstream media what was said was downright disrespectful domestication indeed we don't like to be dissed boss so get off your editorial ass and do something about this nonsense

your colleague mehitabel

10.1126/science.1147839

EDITED BY GILBERT CHIN AND JAKE YESTON

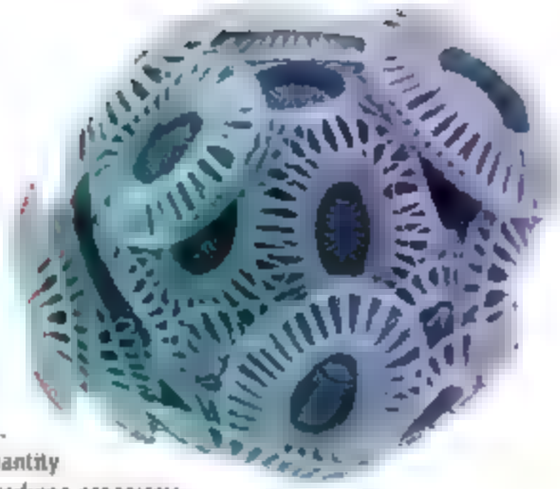

CLIMATE SCIENCE

Choose Calcifiers with Care

In contrast to near-term estimates, prediction of atmospheric CO_2 content several centuries from now is severely hampered by the multitude of poorly understood feedback mechanisms. The most important of these is probably the interaction between atmospheric CO_2 and marine calcification. In a nutshell, the amount of CO_2 absorbed by the ocean depends on the quantity depleted through calcium carbonate incorporation into the skeletons of calcifying organisms such as foraminifera and coccolithophorids. This bioactivity is a function of the alkalinity and the pH of the ocean, which in turn depend largely on the partial pressure of atmospheric CO_2, as well as the type of calcifying organism (*E. huxleyi* and *O. universa* are shown). Although the carbonate chemistry of the ocean is well known, the response of different species to changes in pH and alkalinity is incompletely understood, and large differences exist between the species that have been studied. Ridgwell *et al.* have performed model calculations for a range of calcifying behaviors. They find that the strength of CO_2-calcification feedback is dominated by the assumption of which species of calcifier contributes most to carbonate production, and that ocean CO_2 sequestration could reduce the atmospheric fossil fuel CO_2 burden by 4 to 13% in the year 3000. This long-term view is needed to help understand the full impact of current energy use. — HJS

Biogeosciences **4**, 481 (2007)

IMMUNOLOGY

Degrees of Tolerance

The affinity of a T cell receptor for its ligand [a peptide bound by a molecule of the major histocompatibility complex (pMHC)] dictates whether a T lymphocyte will become active. However, activation also depends critically on a series of parallel signals, and when these are lacking, the effect of any pMHC complex is a state of anergy (or permanent inactivation) of the T cell. This is an important means by which immune tolerance to self constituents of the body is maintained.

Using intravital imaging, Skokos *et al.* observed that as T cells engaged pMHC complexes of differing affinities for the T cell receptor in lymph nodes in the absence of coactivating signals, their behavior varied considerably. Thus, although under these conditions pMHCs of all affinities induced anergy and led to the retention of circulating T cells in the lymph nodes, only those with a high affinity triggered the flux of Ca^{2+} that signals the T cells to slow down. Medium affinity complexes, on the other hand, failed to stimulate Ca^{2+} flux, but did induce a low level of division and cytokine production. Finally, the low-affinity ligands did not evoke any biochemical event or change in cellular motility but instead rapidly induced an inactive state. Thus, a hierarchy of anergic states may exist for T cells, depending on differences in the binding strength of antigens they meet under steady state conditions. — SJS

Nat. Immunol. **8**, 835 (2007)

SURFACE SCIENCE

Getting a Leg Up

The reversible cis/trans isomerization of azobenzene and its derivatives, induced by alternating irradiation with ultraviolet and visible light, can be used for on-demand control of properties ranging from large-area hydrophobicity (by variation of surface-exposed groups) to the opening and closing of ion channels on the nanoscale. However, adsorption on metal surfaces tends to impede the isomerization process, in all likelihood through electronic effects or induced changes in the molecule's optical absorption spectrum. Comstock *et al.* show that if the phenyl rings in azobenzene are derivatized with four bulky *tert*-butyl groups, the molecule in the planar trans configuration is lifted far enough off a gold surface for irradiation with ultraviolet light to induce photoisomerization. The addition of only two *tert*-butyl "legs" proved insufficient. The reversible isomerization was monitored with scanning tunneling microscopy. PDS

Phys. Rev. Lett. **99**, 038301 (2007)

CELL BIOLOGY

Let's Get Sorted

Epithelial cells provide a barrier function in tissues by establishing and maintaining a distinctive polarity with an apical surface that faces the lumen of the tissue and a basolateral surface that faces the blood. The maintenance of the two distinct membrane domains has been studied in great detail for many years, but how the polarity originates is much less clear. Nejsum and Nelson examined this process as epithelial cells in tissue culture generated a polarized cell layer and determined whether cell-cell adhesion and the generation of distinct membrane domains were linked. By looking at fluorescently tagged versions of two similar proteins, aquaporins 3 and 5, one of which (AQP3) is basolateral, the other (AQP5) apical, while simultaneously monitoring a component of the cell adhesion machinery, E-cadherin, they observed a precise correlation

Vesicle targeting and fusion machinery localize at sites of cell-cell contact (yellow)

CREDITS (LEFT TO RIGHT): NOAA; STEVE GSCHMEISSNER/SCIENCE PHOTO LIBRARY; NEJSUM AND NELSON, *J. CELL BIOL.* **178**, 333 (2007)

between the basolateral membrane protein and newly formed cell adhesions. It seems that dur ng the establishment of polarity, newly synthesized basolateral membrane proteins leave the Golgi complex in vesicles that are specifically targeted to and fuse with the growing sites of cell adhesion, which are enriched for the docking and fusion machinery involved in basolateral membrane protein targeting. — SMH

J. Cell Biol. **178**, 323 (2007)

MATERIALS SC ENCE

Softening into Shape

Polymer particles with nanometer and micrometer dimensions have been applied to fields ranging from medical imaging to fluid rheology, but controlling particle shape during synthesis has been challenging. Champion *et al.* have devised a simple method for manipulating spherical polystyrene particles into a diverse array of shapes and sizes (including the bicones shown left). The particles were embedded in a sheet of polyvinyl alcohol and then either softened (by solvent or heat) and stretched, or else softened after first stretching the film (which created voids filled by the softened particles). Dissolution of the film then afforded the shaped free particles. Stretching was possible in either one or two directions, and it was possible to combine or repeat the two techniques. MSL

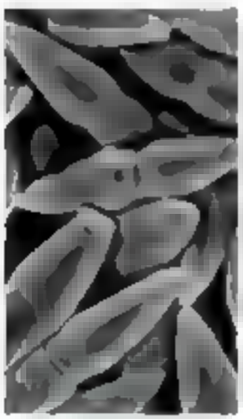

Proc. Nat. Acad. Sci. U.S.A. **104**, 11901 (2007)

GEOLOGY

Appalachian Twins

The striking change in the trend of the Appalachian mountain range—from south southwesterly to easterly through central Pennsylvania—reflects a bend in the direction of large folds in the upper crust, which elevate and expose old resistant rocks that support many of the mountains there. Similar bends are common in other mountain ranges, and their origin and timing during continent-continent collision have been enigmatic. Ong *et al.* looked at twinning in calcite crystals in limestone across Pennsylvania. The orientation of twins reflects stress acting during the initial deformation of the rocks before most of the folding began (strain hardening then locks the twins in). The data suggest that, initially, compression was to the northeast, orthogonal to the southwesterly direction of the southern Appalachians, the early formed twins in the north were then rotated clockwise. These data, and other studies of later strain, imply that the folds and thrust faults formed after this initial deformation on top of the bend and were not later rotated themselves. A rigid salient in the North American crust that became increasingly important as a barrier during collision with what is now western Africa ~300 million years ago may have caused these dynamics. — BH

Geol. Soc. Am. Bull. **119**, 796 (2007)

www.sciencemag.org

Science

1200 New York Avenue, NW
Washington, DC 20005
Editorial: 202-326-6550, FAX 202-289-7562
News: 202-326-6581, FAX 202-371-9227

Bateman House, 82-88 Hills Road
Cambridge, UK CB2 1LQ
+44 (0) 1223 326500, FAX +44 (0) 1223 326501

Subscription Services For change of address, missing issues, new orders and renewals, and payment questions: 866-434-AAAS (2227) or 202-326-6417, FAX 202-842-1065. Mailing addresses: AAAS, P.O. Box 96178, Washington, DC 20090-6178 or AAAS Member Services, 1200 New York Avenue, NW, Washington, DC 20005

Institutional Site Licenses please call 202-326-6755 for any questions or information

Reprints: Author Inquiries 800-635-7181
Commercial Inquiries 803-359-4578

Permissions 202-326-7074, FAX 202-682-0816

Member Benefits Bookstore: AAAS/BarnesandNoble.com bookstore www.aaas.org/bn; Car purchase discount: Subaru VIP Program 202-326-6417; Credit Card: MBNA 800-847-7378; Car Rentals: Hertz 800-654-2200 CDP#343457, Dollar 800-800-4000 #AA1115; AAAS Travels: Betchart Expeditions 800-252-4910; Life Insurance: Seabury & Smith 800-424-9883; Other Benefits: AAAS Member Services 202-326-6417 or www.aaasmember.org.

science_editors@aaas.org	(for general editorial queries)
science_letters@aaas.org	(for queries about letters)
science_reviews@aaas.org	(for returning manuscript reviews)
science_bookrevs@aaas.org	(for book review queries)

Published by the American Association for the Advancement of Science (AAAS), *Science* serves its readers as a forum for the presentation and discussion of important issues related to the advancement of science, including the presentation of minority or conflicting points of view, rather than by publishing only material on which a consensus has been reached. Accordingly, all articles published in *Science*—including editorials, news and comment, and book reviews—are signed and reflect the individual views of the authors and not official points of view adopted by the AAAS or the institutions with which the authors are affiliated.

AAAS was founded in 1848 and incorporated in 1874. Its mission is to advance science and innovation throughout the world for the benefit of all people. The goals of the association are to: foster communication among scientists, engineers and the public; enhance international cooperation in science and its applications; promote the responsible conduct and use of science and technology; foster education in science and technology for everyone; enhance the science and technology workforce and infrastructure; increase public understanding and appreciation of science and technology; and strengthen support for the science and technology enterprise.

Information for Authors

See pages 120 and 121 of the 5 January 2007 issue or access www.sciencemag.org/feature/contribinfo/home.shtml

EDITOR-IN-CHIEF **Donald Kennedy**
EXECUTIVE EDITOR **Monica M. Bradford**
DEPUTY EDITORS **R. Brooks Hanson, Barbara R. Jasny, Katrina L. Kelner**
NEWS EDITOR **Colin Norman**

Editorial SUPERVISORY SENIOR EDITOR Phillip D. Szuromi; SENIOR EDITOR/PERSPECTIVES Lisa D. Chong; SENIOR EDITORS Gilbert J. Chin, Pamela J. Hines, Paula A. Kiberstis (Boston), Marc S. Lavine (Toronto), Beverly A. Purnell, L. Bryan Ray, Guy Riddihough, H. Jesse Smith, Valda Vinson, David Voss; ASSOCIATE EDITORS Jake S. Yeston, Laura M. Zahn; ONLINE EDITOR Stewart Wills; ASSOCIATE ONLINE EDITOR Tara S. Marathe; BOOK REVIEW EDITOR Sherman J. Suter; ASSOCIATE LETTERS EDITOR Etta Kavanagh; INFORMATION MANAGER Gary Gale; SENIOR COPY EDITORS Jeffrey E. Cook, Cynthia Howe, Harry Jach, Barbara P. Ordway, Jennifer Sills, Trista Wagoner; COPY EDITORS Lauren Kmec, Peter Mooreside; EDITORIAL COORDINATORS Carolyn Kyle, Beverly Shields; PUBLICATIONS ASSISTANTS Ramatoulaye Diop, Chris Filiatreau, Joi S. Granger, Jeffrey Hearn, Lisa Johnson, Scott Miller, Jerry Richardson, Brian White, Anita Wynn; EDITORIAL ASSISTANTS Maris M. Bish, Emily Guise, Patricia M. Moore, Jennifer A. Seibert; EXECUTIVE ASSISTANT Sylvia S. Kihara; ADMINISTRATIVE SUPPORT Maryrose Madrid

News SENIOR CORRESPONDENT Jean Marx; DEPUTY NEWS EDITORS Robert Coontz, Eliot Marshall, Jeffrey Mervis, Leslie Roberts; CONTRIBUTING EDITORS Elizabeth Culotta, Polly Shulman; NEWS WRITERS Yudhijit Bhattacharjee, Adrian Cho, Jennifer Couzin, David Grimm, Constance Holden, Jocelyn Kaiser, Richard A. Kerr, Eli Kintisch, Andrew Lawler (New England), Greg Miller, Elizabeth Pennisi, Robert F. Service (Pacific NW), Erik Stokstad; INTERNS Benjamin Lester, Marissa Cevallos, Veronica Raymond; CONTRIBUTING CORRESPONDENTS Barry A. Cipra, Jon Cohen (San Diego, CA), Daniel Ferber, Ann Gibbons, Robert Irion, Mitch Leslie, Charles C. Mann, Evelyn Strauss, Gary Taubes; COPY EDITORS Rachel Curran, Linda B. Felaco, Melvin Gatling; ADMINISTRATIVE SUPPORT Scherraine Mack, Fannie Groom; BUREAUS New England: 207-549-7755, San Diego, CA: 760-942-3252, FAX 760-942-4979, Pacific Northwest: 503-963-1940

Production DIRECTOR James Landry; SENIOR MANAGER Wendy K. Shank; ASSISTANT MANAGER Rebecca Doshi; SENIOR SPECIALISTS Jay Covert, Chris Redwood; SPECIALIST Steve Forrester; PREFLIGHT DIRECTOR David M. Tompkins; MANAGER Marcus Spiegler; SPECIALIST Jessie Mudjitaba

Art DIRECTOR Kelly Buckheit Krause; ASSOCIATE ART DIRECTOR Aaron Morales; ILLUSTRATORS Chris Bickel, Katharine Sutliff; SENIOR ART ASSOCIATES Holly Bishop, Laura Creveling, Preston Huey, Nayomi Kevitiyagala; ASSOCIATE Jessica Newfield; PHOTO EDITOR Leslie Blizard

Science International

Europe (science@science-int.co.uk) EDITORIAL: INTERNATIONAL MANAGING EDITOR Andrew M. Sugden; SENIOR EDITOR/PERSPECTIVES Julia Fahrenkamp-Uppenbrink; SENIOR EDITORS Caroline Ash (Geneva: +41 (0) 222 346 3106), Stella M. Hurtley, Ian S. Osborne, Stephen J. Simpson, Peter Stern; ASSOCIATE EDITOR Joanne Baker; EDITORIAL SUPPORT Deborah Dennison, Rachel Roberts, Alice Whaley; ADMINISTRATIVE SUPPORT Janet Clements, Jill White; NEWS: INTERNATIONAL NEWS EDITOR John Travis; DEPUTY NEWS EDITOR Daniel Clery; CONTRIBUTING CORRESPONDENTS Michael Balter (Paris), John Bohannon (Vienna), Martin Enserink (Amsterdam and Paris), Gretchen Vogel (Berlin); INTERN Linda Zala

Asia Japan Office: Asca Corporation, Eiko Ishioka, Fusako Tamura, 1-8-13, Hirano-cho, Chuo-ku, Osaka-shi, Osaka, 541-0046 Japan; +81 (0) 6 6202 6272, FAX +81 (0) 6 6202 6271; asca@os.gulf.or.jp; ASIA NEWS EDITOR Richard Stone (+66 2 662 5818; rstone@aaas.org); CONTRIBUTING CORRESPONDENTS Dennis Normile (Japan: +81 (0) 3 3391 0630, FAX 81 (0) 3 5936 3531; dnormile@gol.com); Hao Xin (China: + 86 (0) 10 6307 4439 or 6307 3676, FAX +86 (0) 10 6307 4358; cindyhao@gmail.com); Pallava Bagla (South Asia: +91 (0) 11 2271 2896; pbagla@vsnl.com)

Africa Robert Koenig (contributing correspondent, rob.koenig@gmail.com)

EXECUTIVE PUBLISHER **Alan I. Leshner**
PUBLISHER **Beth Rosner**

Fulfillment & Membership Services (membership@aaas.org) DIRECTOR Marlene Zendell; MANAGER Waylon Butler; CUSTOMER SERVICE SUPERVISOR Pat Butler; SPECIALISTS Tamara Alfson, Laurie Baker, Latoya Casteel, Lavanda Crawford, Vicki Linton; DATA ENTRY SUPERVISOR Cynthia Johnson; SPECIALISTS Tomeka Diggs, Tarrika Hill, Erin Layne, Sheila Thomas

Business Operations and Administration DIRECTOR Deborah Rivera-Wienhold; BUSINESS MANAGER Randy Yi; SENIOR FINANCIAL ANALYSTS Michael LoBue, Jessica Tierney; FINANCIAL ANALYSTS Nicole Nicholson, Farida Yeasmin; RIGHTS AND PERMISSIONS: ADMINISTRATOR Emilie David; ASSOCIATE Elizabeth Sandler; MARKETING: DIRECTOR John Meyers; MARKETING MANAGERS Darryl Walter, Allison Pritchard; MARKETING ASSOCIATES Julianne Wielga, Mary Ellen Crowley, Alison Chandler, Marcia Leach, Wendy Wise; INTERNATIONAL MARKETING MANAGER Wendy Sturley; MARKETING EXECUTIVE Jennifer Reeves; MARKETING/MEMBER SERVICES EXECUTIVE Linda Rusk; JAPAN SALES Jason Hannaford; SITE LICENSE SALES: DIRECTOR Tom Ryan; SALES MANAGER Russ Edra; SALES AND CUSTOMER SERVICE Mehan Dossani, Iquo Edim, Kiki Forsythe, Catherine Holland; ELECTRONIC MEDIA: MANAGER Lizabeth Harman; PROJECT MANAGER Trista Snyder; ASSISTANT MANAGER Lisa Stanford; SENIOR PRODUCTION SPECIALIST Walter Jones; PRODUCTION SPECIALISTS Nichele Johnston, Kimberly Oster

Advertising DIRECTOR WORLDWIDE AD SALES Bill Moran

Product (science_advertising@aaas.org); CONSUMER & SPONSORSHIP SALES MANAGER Tina Morra: 202-326-6542; MIDWEST Rick Bongiovanni: 330-405-7080, FAX 330-405-7081 • WEST COAST/W. CANADA Teola Young: 650-964-2266 EAST COAST/E. CANADA Christopher Breslin: 443-512-0330, FAX 443-512-0331 • UK/EUROPE/ASIA Michelle Field: +44 (0) 1223-326-524, FAX +44 (0) 1223-325-532 JAPAN Mashy Yoshikawa: +81 (0) 33235 5961, FAX +81 (0) 33235 5852 SENIOR TRAFFIC ASSOCIATE Deiandra Simms

Commercial Editor Sean Sanders: 202-326-6430

Classified (advertise@sciencecareers.org); U.S.: RECRUITMENT SALES MANAGER Ian King: 202-326-6528, FAX 202-289-6742; INSIDE SALES MANAGER: MIDWEST/CANADA Daryl Anderson: 202-326-6543; NORTHEAST: Allison Millar: 202-326-6572; SOUTHEAST: Tina Burks: 202-326-6577; WEST: Nicholas Hintibidze: 202-326-6533; SALES COORDINATORS Erika Foard, Rohan Edmonson, Leonard Marshall, Shirley Young; INTERNATIONAL: SALES MANAGER Tracy Holmes: +44 (0) 1223 326525, FAX +44 (0) 1223 326532; SALES Marium Hudda, Alex Palmer; SALES ASSISTANT Louise Moore; JAPAN: Jason Hannaford: +81 (0) 52 757 5360, FAX +81 (0) 52 757 5361; ADVERTISING PRODUCTION OPERATIONS MANAGER Deborah Tompkins; SENIOR PRODUCTION SPECIALISTS Robert Buck, Amy Hardcastle; SENIOR TRAFFIC ASSOCIATE Christine Hall; PUBLICATIONS ASSISTANT Mary Lagnaoui

AAAS Board of Directors RETIRING PRESIDENT, CHAIR John P. Holdren; PRESIDENT David Baltimore; PRESIDENT-ELECT James J. McCarthy; TREASURER David E. Shaw; CHIEF EXECUTIVE OFFICER Alan I. Leshner; BOARD John E. Dowling, Lynn W. Enquist, Susan M. Fitzpatrick, Alice Gast, Linda P. B. Katehi, Cherry A. Murray, Thomas D. Pollard, Kathryn D. Sullivan

AAAS
ADVANCING SCIENCE, SERVING SOCIETY

You Stand in Front of Our Instruments All Day. We Stand Behind Them 24x7.

High Value, Cost-Effective Extensions from Applied Biosystems

With over 25 years of experience in the development, manufacture, and service of innovative instruments, and with over 1000 highly trained, dedicated service professionals, ABI Global Services is uniquely qualified to deliver a full suite of real-world lab services. From Remote Services to On-Site Application Consulting to Qualification and Professional Services and everything in between, ABI Global Services is your value-added partner to help boost your productivity and maximize the return on your technology investment.

- Instrument Repair and Maintenance
- Smart Services
- Qualification Services
- Professional Services
- On-Site Application Consulting
- Training

To learn more go to http://info.appliedbiosystems.com/service
or contact your local Applied Biosystems sales representative

Applied Biosystems


Old and new space suits.

Suited for the Moon

When humans revisit the moon in the next decade or so, aeronautical engineer Dava Newman of the Massachusetts Institute of Technology (MIT) in Cambridge hopes they will be wearing one of her creations.

Newman and her team have spent 7 years working on a suit to replace the traditional bulky, many-layered, pressurized space suit. Her idea is to apply even pressure directly to the skin by wrapping layers of cloth tightly around the body, allowing for more natural movement. Rigid supports are aligned with areas on the body that do not extend or contract with movement. The BioSuit will also be embedded with metal threads so it can be heated like a car window. If punctured by a passing meteorite, it won't deflate like the old ones but can easily be fixed by rewrapping, says Newman.

The suit's not quite ready for review by NASA, says MIT team member Christopher Carr. The wrapping part is tricky because "it's difficult to apply the same amount of pressure to certain parts of the body, like the groin and the armpits." Too much or too little pressure could cause swelling or cut off blood supply. Also, he notes, "the suit is difficult to get into, [and] you need two extra people to remove it."

Odds-On Favorite

Whether the subject is trends in housing sales or trials of a new cancer drug, news reports often have to grapple with applications of statistics and probability. ChanceWeb from Dartmouth College turns such items into lessons on statistical thinking.

Originally a newsletter penned by math professors, the site now lets readers post discussions and exercises based on media stories, papers, books, and other sources. Recent contributions have investigated possible explanations for why Europeans are now taller than Americans (a reversal of the situation 60 years ago) and slammed a 2001 report that claimed Oscar winners live nearly 4 years longer than mere nominees. The longevity boost is illusory, the entry's author concludes, the result of a statistical gaffe called selection bias.

chance.dartmouth.edu/chancewk

Monkeys Have Tin Ears

A new study finds that monkeys prefer silence to music, suggesting that some of the acoustic preferences that underlie music are unique to humans.

Cognitive scientists Joshua McDermott of the Massachusetts Institute of Technology in Cambridge and Marc Hauser of Harvard University put tamarins and marmosets in an apparatus with two chambers, each rigged to play music whenever an animal entered. In one experiment, the musical choices were a flute lullaby (65.26 beats per minute) and Alec Empire's electronic techno hit "Nobody Gets Out Alive" (369.23 beats per minute). The monkeys spent an average of about two-thirds of their time on the lullaby side, showing that they prefer slower tempos. But when given the choice of silence, lullabies, or a Mozart concerto, they spent most of their time avoiding music altogether. A similar experiment with eight humans showed a distinct preference for music, especially lullabies, over silence, the authors report in the September issue of *Cognition*.

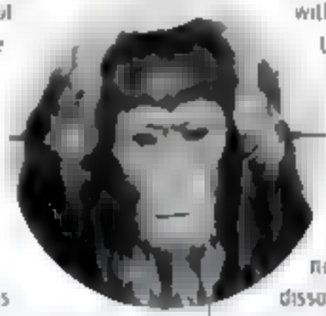

"The observations suggest that only humans have a natural, or innate, inclination to engage with music," says Isabelle Peretz of the University of Montreal in Canada, who has concluded from studies of people with amusia (tone deafness) that humans have special brain pathways for music (*Science*, 1 June 2001, p. 1636). McDermott and Hauser, who earlier found that monkeys have no preference between harmonious and dissonant music—suggest that humans' music responses may reflect a "unique evolutionary history of selection" for cognitive processes linked to emotion and motivation.

SKULL OF A POET

In Bonn this month, scientists dug up the bodies of Friedrich Schiller's wife and son in hopes of solving the "Friedrich Schiller Code", the 180-year-old mystery of Schiller's skull.

The poet's tomb in Weimar contains two skulls, and it isn't clear that either belonged to Schiller. When he died of tuberculosis at 45 in 1805, he was buried in a common grave. In 1826, officials tried to exhume the remains but found more than a dozen skulls. The local mayor declared that the largest belonged to Schiller, but doubts led to a second exhumation in 1911, which identified a different skull as Schiller's.

At least four books have been written on the controversy, but now the Weimar Classics Foundation and a German TV channel are funding what is hoped will be a definitive answer. Scientists will build face reconstructions of both skulls and compare DNA samples from them and from the bones of Schiller's wife and son. If neither skull is a match, says Ursula Wittwer-Backofen of the University of Freiburg, one of the project leaders, "Herr Schiller is lost forever."

CREDITS: (TOP TO BOTTOM) DONNA COVENEY/MASSACHUSETTS INSTITUTE OF TECHNOLOGY; KEYSTONE/GETTY IMAGES; ROGER VIOLLET COLLECTION/GETTY IMAGES

EDITED BY YUDHIJIT BHATTACHARJEE

IN THE HOT SEAT. Hawaii's spectacular volcanoes and lava flows can leave tourists with a sense of dread and wonder. The National Science Board is feeling similar emotions after its visit to the island state triggered a political eruption in the U.S. Senate.

In June, board president Steven Beering (center) led a delegation on a 7-day tour of Hawaii's many telescopes and other projects supported by the National Science Foundation (NSF), which the board oversees. In an unexpected coda, Beering also signed a "joint statement of understanding" with Republican Governor Linda Lingle (to his right) recognizing the state's efforts to promote science and technology.

State officials were thrilled by what they saw as an endorsement, but Hawaii's senior senator, Democrat Daniel Inouye, apparently didn't appreciate being blindsided by the board's foray into his backyard. So Inouye, who chairs the committee that oversees NSF's programs, decided "to send a message," in the words of one Hill aide. "It is clear that the day-to-day management structure and leadership is not serving the board or the interests of the [appropriations] committee," notes a report accompanying the Senate bill to fund NSF in 2008.

Beering says the words were a complete surprise, adding that "I am not aware of any problems." Board Executive Officer Michael Crosby (far left) says he is trying to arrange a meeting to explain the board's actions.

PIONEERS

POWERED BY FAT. Leftover cooking grease may be a waste product for most of the world. But Suzanne Hunt can't get enough of the stuff.

Hunt, who until recently directed the Worldwatch Institute's bioenergy program, has converted cooking grease from a local restaurant into biodiesel to run tractors on her family's vineyard in upstate New York. This spring, she drove a 1981 Volkswagen Rabbit pickup truck powered by the biodiesel fuel from Washington, D.C., to Central America to demonstrate the concept. Now Hunt and Shari Friedman are running a project that is training middle school students in Philadelphia to produce biodiesel by collecting leftover grease from area restaurants and performing the simple chemical processes necessary for extracting the desired methyl ester.

Hunt doesn't think biodiesel is the answer to the nation's energy needs. Tall grasses, trees, and waste hold more potential, she says, because they grow without much input and they don't compete directly as food resources. But Hunt and Friedman believe that biodiesel is a good way to show students that there are practical alternatives to petroleum for cars and trucks.

THEY SAID IT

"This computer, although assigned to me, was being used on board the International Space Station. I was informed that it was tossed overboard to be burned up in the atmosphere when it failed."

A NASA employee's explanation for the loss of a laptop, recorded in a recent report by the U.S. Government Accountability Office documenting equipment losses of more than $94 million over the past 10 years by the agency.

Honors

PRIVATE SANCTUARY. The Australian government has established a 135,000-hectare wildlife preserve on Queensland's Cape York Peninsula named after Steve Irwin, the wildlife enthusiast and television personality who died in a stingray attack last year. A scientific center on site will allow visitors and 24 researchers from the University of Queensland to study the local species, including the endangered speartooth shark and the northern quoll, a cat-sized carnivorous marsupial, and tackle management challenges such as fires and feral pigs. Prime Minister John Howard called the park, which will be closed to the public, a "fitting tribute to a passionate environmentalist."

Got a tip for this page? E-mail people@aaas.org

CREDITS: (TOP TO BOTTOM) STATE OF HAWAII; SUZANNE HUNT; AUSTRALIA ZOO

A record-breaking solar cell 583

Amoeba immunity 584

CLINICAL RESEARCH

Death Prompts a Review of Gene Therapy Vector

The death last week of a patient receiving experimental gene therapy for arthritis has triggered a federal review of all trials using the same vector. Few details have been made public, but if it turns out that the therapy is to blame, it would be another blow to the field's image. Within 8 years, one patient has died as a result of gene therapy and three have acquired leukemia. This would be the first fatality in a trial not studying a life-threatening disease.

The trial's sponsor, Targeted Genetics Corp. in Seattle, Washington, emphasizes that the company doesn't yet know what caused the patient's death. But it would be a surprise if it were the viral vector, says Chief Scientific Officer Barrie Carter, given that the vector has proved safe in hundreds of patients. He and others are watching nervously for the results of an investigation by the company and the U.S. Food and Drug Administration (FDA). Carter believes it could take weeks. "I just hope it doesn't put a mark on the entire field," says molecular orthopedist Christopher Evans of Harvard Medical School in Boston, who is also planning a test of gene therapy to treat arthritis.

The Targeted Genetics trial builds on the success of a drug called Enbrel, a protein-based treatment for rheumatoid arthritis that inhibits a pro-inflammatory cytokine called tumor necrosis factor α (TNF-α). Although Enbrel and similar drugs are effective, they don't always penetrate all joints, and they have to be injected regularly. Targeted Genetics uses a modified virus, called an adeno-associated virus (AAV), to shuttle a gene for the TNF-α inhibitory protein directly into joints. The joint cells then produce the protein, giving patients "a localized depot" of Enbrel that should work long-term, says Carter.

In rats, this strategy "was pretty impressive" at reducing inflammation and inhibiting bone destruction, says Sharon Wahl of the National Institutes of Health (NIH) in Bethesda, Maryland, who co-authored the study with Targeted Genetics. Nonhuman primate data also indicated that the approach was safe. In 2003, NIH's Recombinant DNA Advisory Committee (RAC) approved a safety study in humans. Based on those results, FDA approved a multidose study that began in fall 2005 at about 20 sites around the country.

The trial had enrolled 127 patients (32 on placebo) without any serious side effects, says Carter. Seventy-four had received a second dose. But on 20 July, one patient developed a severe adverse event that "was related in time" to a second injection, FDA says. The agency put the trial on hold. 4 days later, the patient died. FDA is reviewing the 28 other trials using AAV, including 21 active studies.

The tragedy has stirred speculation about the cause. One suspect is the gene product, because Enbrel, which suppresses one immune response, has been linked to sepsis and bacterial infections, suggests gene therapy expert Terry Flotte, dean of the University of Massachusetts Medical School in Worcester. But Carter says the protein is "not necessarily the issue" because the protein has not been detected in serum from nonhuman primates or patients.

It seems equally unlikely that the problem could be the AAV vector, says Carter. He notes that more than 500 patients have safely received AAV since 1992. However, one difference is that patients in the arthritis trial, unlike the earlier ones, received more than one dose. That raises the possibility that the patient became sensitized to the vector, leading to an adverse reaction, suggests Evans. It happened once before, in 2004, when AAV caused a mild immune reaction in two patients who received the drug in the liver (*Science*, 4 June 2004, p. 1423).

Gene therapy has restored the health of about 20 children with severe combined immunodeficiency disease. The approach is showing promise against cancer, too, experts note. "The field is extremely robust," says Arthur Nienhuis of St. Jude Children's Research Hospital in Memphis, Tennessee, and president of the American Society of Gene Therapy. Meanwhile, Carter says his company is "working furiously" to figure out what caused the death before RAC meets to consider the case in mid-September. –JOCELYN KAISER

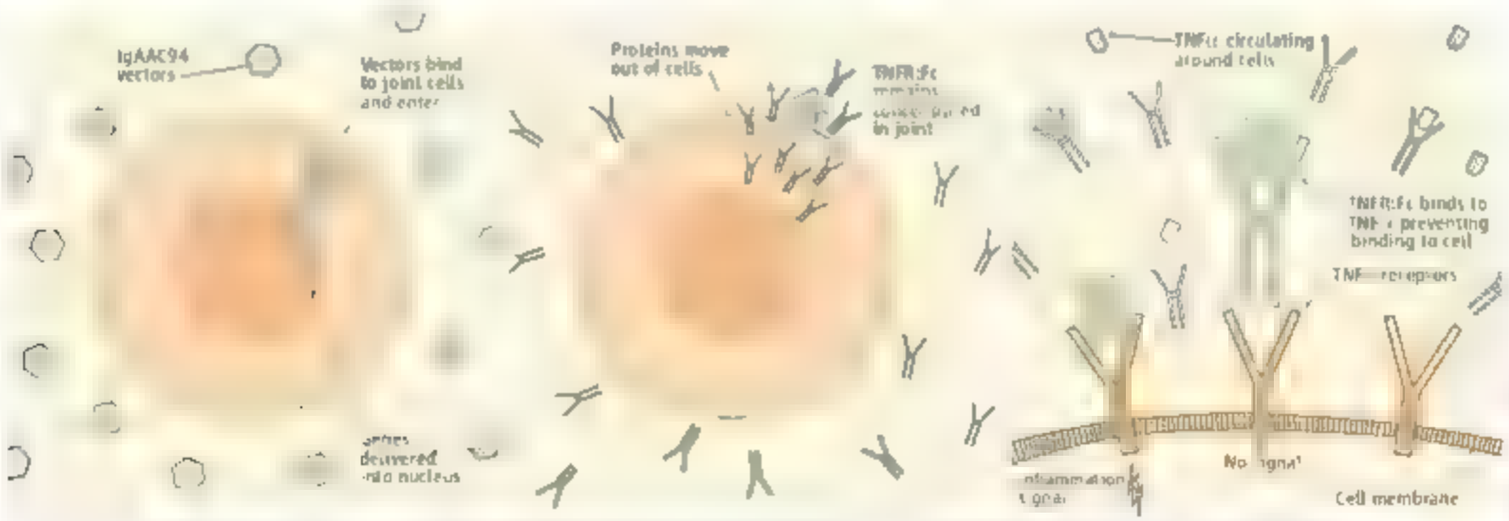

Joint effort. A Targeted Genetics vector (tgAAC94) is injected into arthritic joints; cells then make a protein (TNFR:Fc) that blocks the cytokine TNF-α.

CREDITS: TARGETED GENETICS (DESIGN: WOODARD AND CO)

BIOSECURITY

Rising Asian Threat Leaves Russia in the Lurch

The U.S. government is ending its support for former bioweapons scientists in Russia in favor of a similar but larger initiative in parts of the world that it considers potentially more dangerous to global security.

Nonproliferation experts aren't happy about the move, which State Department officials say is prompted by improving economic conditions in Russia and a rising threat in eastern and central Asia and the Middle East. There are also private grumblings at the Department of Defense, which is scaling back its own efforts because of difficulties that DOD officials have had in accessing Russian labs.

The former Soviet Union is not the same nonproliferation threat today that it was the day the ruble crashed [in 1998]," says Jason Rao, senior coordinator for Cooperative Threat Reduction at the State Department. As a result, he says, the United States can now get down to its "fighting weight" in the region and turn to places such as Pakistan, Philippines, Indonesia, and the Middle East, where a combination of transnational terrorists and emerging infectious diseases such as avian influenza pose new risks. At the same time, Rao says, an improving scientific infrastructure in Asia and the Middle East offers a better chance to combat them.

A Senate spending panel has approved $30 million in the next fiscal year for the State Department's Biosecurity Engagement Program (BEP), which was launched in 2006 with $3.9 million and currently receives $8 million. This year the department slashed by two-thirds a similar program to help biologists from Russia and neighboring countries. Meanwhile DOD is set to wind up its $4-million-a-year program to support biological research projects at Russian labs.

The shift of resources has drawn criticism from security experts who warn that Russia continues to pose a significant risk. "There are still quite a few former weapons scientists in the region whose future is uncertain," says Sonia Ben Ouagrham-Gormley of the Monterey Institute of International Studies in Washington, D.C. An aide on the Senate Foreign Relations Committee applauds the State Department's broadening scope but says committee members feel "it should not be done at the expense of efforts in the former Soviet Union."

Taming risk. U.S. officials Jason Rao (*right*) and Reynolds Salerno during a visit last year to a new BSL-3 lab in Bandung, Indonesia.

CREDIT: COURTESY OF U.S. DEPARTMENT OF STATE

State Department officials say that some of the projects to redirect Russian bioweapons scientists into other activities are now being sustained by the Russian government and that a stronger economy has made it easier for the scientists to find jobs. But administrators at the International Science and Technology Center (ISTC) in Moscow, one of two centers set up by the United States, Russia, and other countries in the early 1990s to coordinate the redirection of weapons scientists, say that's only partially correct. Many institutes have afforded raises for some scientists by laying off other researchers, according to a senior ISTC official. "The proliferation threat from the employed scientists has decreased while the threat from the recently terminated staff has likely increased," says the official, adding that the pay is still low enough to make working scientists vulnerable to offers of "uncomfortable" collaborations with rogue states.

DOD decided to pull out of Russia observers say, because of the problems it has encountered trying to implement the various projects. Last year, for example, DOD auditors visiting the State Research Center for Applied Microbiology at Obolensk were denied full access and instead were required to wait in an administrative area while lab scientists wheeled over carts of PCR machines and other equipment. Another Obolensk project was halted after the Russian government refused to allow an indigenous anthrax strain to be shipped to the United States for further study.

But such incidents, although frustrating, are not a good enough reason to disengage from Russia, says Raphael Della Ratta of the nonprofit Partnership for Global Security in Washington, D.C. "You don't just throw up your hands in despair," he says.

BEP reflects the department's view that biosecurity is more than simply monitoring former weapons labs and scientists in states that once possessed weapons of mass destruction. In Indonesia, for example, experts from the Centers for Disease Control and Prevention in Atlanta, Georgia, and other U.S. institutions will train scientists and commission a biosafety level 3 lab in Bahavet, outside Jakarta, to study agricultural diseases. A second lab in Bandung will focus on human infections. In Pakistan, the agency hopes to open a program office in Islamabad for training programs and collaborative research projects.

"Working with dangerous pathogens is inherently dual use," says Rao. "When we come in and say, 'We'll help you work with anthrax in a safe, secure, and sustainable manner,' the result is less of the stuff hanging around, a smaller risk of an accidental release, and a smaller risk of terrorists getting their hands on it. It's good for everybody."

–YUDHIJIT BHATTACHARJEE

SCIENTIFIC PUBLISHING

U.S. Output Flattens, and NSF Wonders Why

A new study by the National Science Foundation (NSF) showing that the overall number of publications by U.S. scientists has remained flat for more than a decade calls to mind the opening words of a classic 1960s folk rock anthem: "There's something happening here, what it is ain't exactly clear."

The study (nsf07320) reveals what NSF officials call an "unprecedented" and mysterious trend. Despite the continued expansion of the peer-reviewed literature, the total output of U.S. scientists stopped growing in the early 1990s and hasn't budged since then. The pattern, which cuts across all disciplines, reverses decades of steady expansion and leaves NSF officials scratching their heads for an explanation.

"We don't have a smoking gun," says Rolf Lehming, who oversees NSF's biennial compendium of leading scientific and engineering indicators and has been tracking the phenomenon since the late 1990s. The trend is especially surprising given the growth in funding, personnel, and other research inputs over the 1988–2003 period being analyzed, he notes. It also deviates from the pattern in the European Union and in emerging Asian nations, where the output has continued to grow. As a result, their scientists can claim a rising share of global publications.

The data that puzzle Lehming and other staffers from NSF's statistical shop, SRS, come from Thomson Scientific, a Philadelphia, Pennsylvania, company that tracks the global scientific publishing enterprise. Thomson monitors more than 5000 journals, tallying the demographics of the authors and the impact of their articles. That pool has actually grown over the time period. Thomson's universe of journals grew by 20%, and the average journal ran 40% more articles. And despite the proliferation of online journals and other means of communication, NSF officials believe they are using the right yardstick to measure productivity. Traditional printed journals, they say, have remained the gold standard to announce new research findings.

To interpret what they found, NSF's number crunchers took the unusual step of visiting nine prominent U.S. universities and interviewing dozens of faculty members and administrators. Although they heard many anecdotes about trends in research, a second report (nsf07204) states baldly that "data from interviews and meetings are not very useful for considering some possible explanations" for the stagnant number of publications.

Nevertheless, theories abound. Two popular ones offered by the bibliometric community include an aging scientific workforce that is growing less productive as it nears retirement and an emphasis on quality over quantity in hiring, promotion, and other rewards. Diana Hicks of the Georgia Institute of Technology in Atlanta argues strongly for a third reason: Governments around the world have been demanding greater productivity from their scientists as the price for continued support. Many Asian countries have enhanced that effort "to extract latent capacity" with additional funding, she notes. The resulting increased flow of papers has "pushed out some mediocre work" by U.S. authors, Hicks says. But the effect is so subtle, she adds, that U.S. scientists "don't think to blame anybody but themselves."

Lehming favors a fourth cause: the steep learning curve associated with collaborative research, an increasingly popular mode of operation. But he admits that there's no hard evidence for any theory. "We've beaten the data to death," he confesses. "So in the end, we decided to put the material out there and let people react."

–JEFFREY MERVIS

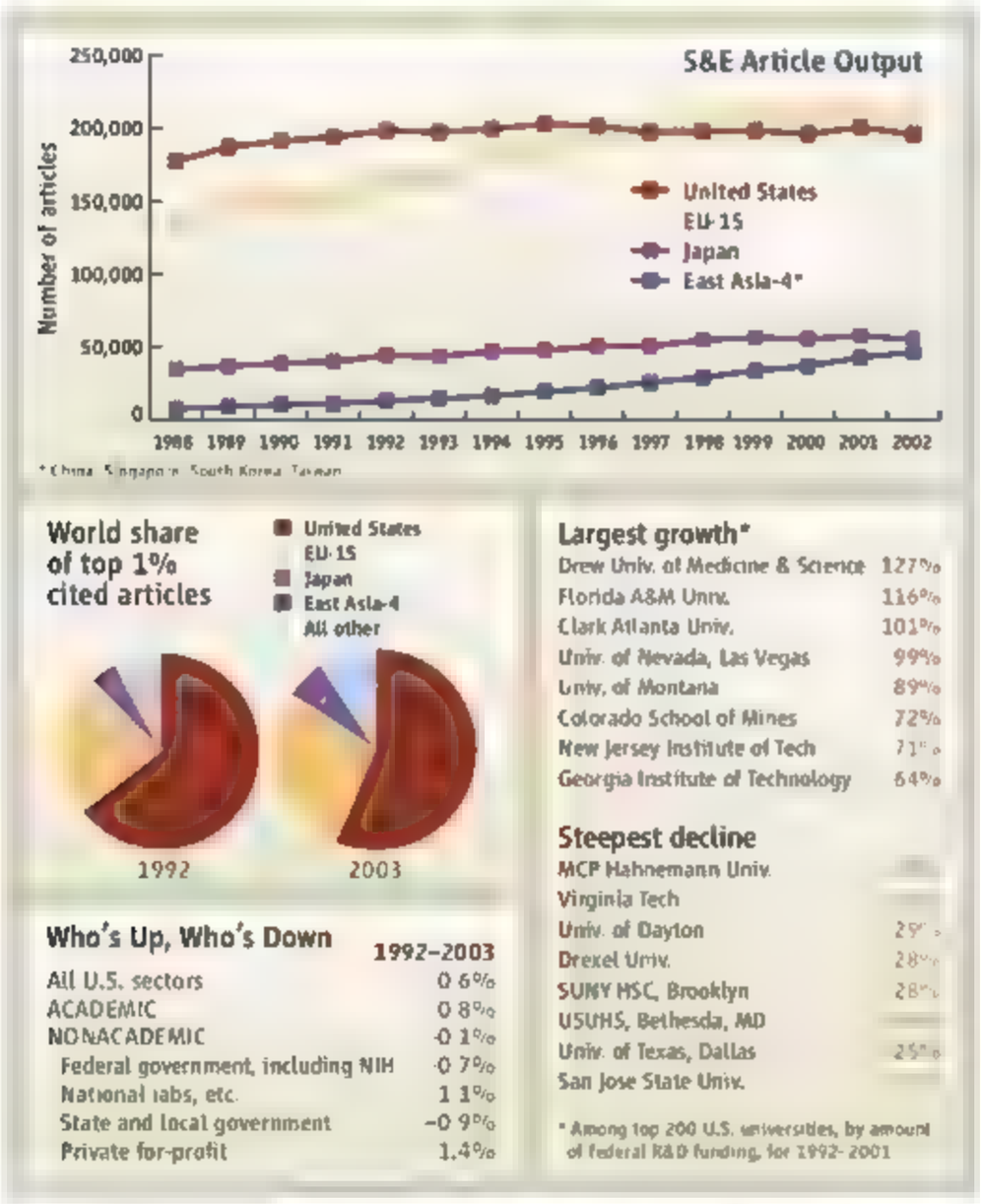

Paper trail. Although U.S. scientists have fallen behind Europe in total output, they retain a commanding lead among most-cited articles. And although the U.S. academic sector as a whole is flat, some universities have experienced a publication spike and others a steep drop.

NSF DIVISION OF SCIENCE RESOURCES STATISTICS, 2007

SOLAR POWER

Light-Splitting Trick Squeezes More Electricity Out of Sun's Rays

To create highly efficient solar cells, researchers have employed a novel engineering strategy worthy of Sun Tzu: Divide and conquer.

The scientists are part of a U.S. Department of Defense effort aimed at producing small photovoltaic modules for battlefield electronics. Commercially available solar panels convert to electricity only about a fifth of the energy across the solar spectrum that hits them; the goal of the program is to capture more than half. The team, led by researchers at the University of Delaware, Newark, has used a novel light-splitting technique to combine in a single device materials whose properties would otherwise make it difficult to work together. After only a year and a half of work, the $12 million project has yielded an unofficial record of 42.8% efficiency—beating the previous mark by about 2%.

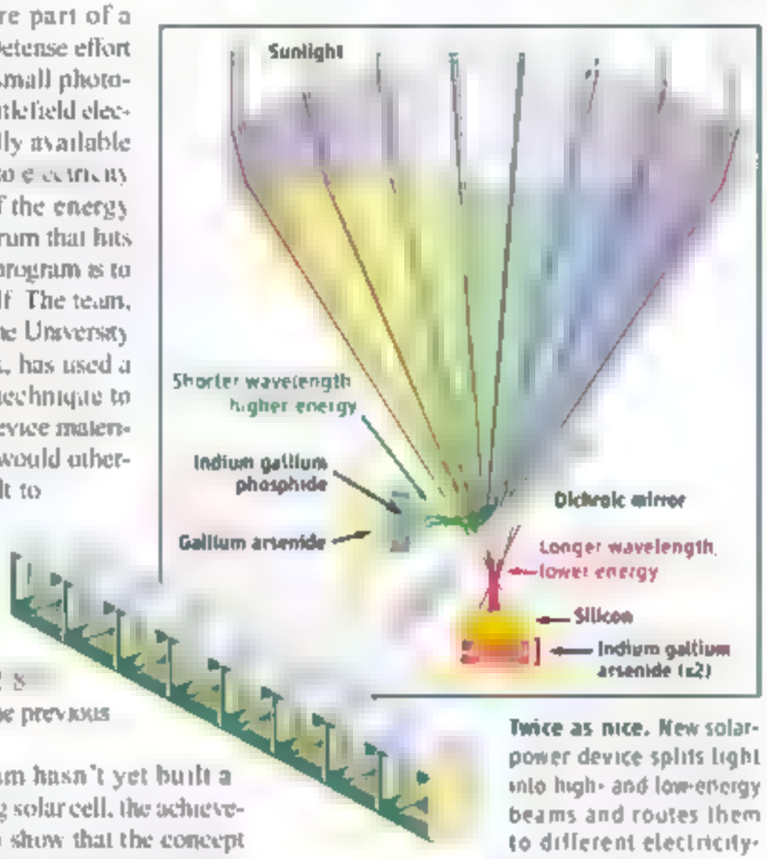

Twice as nice. New solar-power device splits light into high- and low-energy beams and routes them to different electricity-producing materials.

Although the team hasn't yet built a prototype of a working solar cell, the achievement "is important to show that the concept works," says Henry Branchorst, an engineer at Auburn University in Alabama, who focuses on high-efficiency cells and is not involved in the work. More importantly, he says, the "very interesting approach" could give solar-cell researchers a new set of options if it can be shown to be affordable. "We've completely made the choices for solar cells more flexible," says Delaware electrical engineer Christiana Honsberg.

Different varieties of semiconductors layered in solar cells respond to photons of varying energies to produce electricity. Until now, however, the requirement that the atomic structures of such layers line up to allow proper crystal growth has limited the combinations that researchers could use to gain better efficiencies. When the Defense Advanced Research Projects Agency (DARPA) tackled the problem in 2005, hoping that mobile cells could reduce the number of batteries soldiers carry for devices such as flashlights, they looked to advanced approaches such as nanotechnology or organics to solve the problem. Delaware researchers had a different idea: Use recent advances in optics to split the light and reroute it to smaller stacks of photovoltaic materials that otherwise wouldn't work together (see diagram). It's not a new concept. NASA scientists used a prism in the 1970s to create a "rainbow cell" with the same goal. "But a lot of the light gets lost using a prism," says Delaware electrical engineer and team leader Allen Barnett.

At a meeting in 2005, DARPA program manager Douglas Kirkpatrick, a physicist with experience in the lighting industry, suggested that the research team's talented optics unit use recent advances in so-called dichroic materials, which separate light into specific wavelengths. ("Where have you been all my life?" says Kirkpatrick of the eureka moment.) The research team, which included industrial as well as academic partners, took that approach and achieved with optics a 93% efficiency in processing and splitting the light in as-yet-unpublished tests. Independent officials with the National Renewable Energy Laboratory ▶

CREDITS (TOP TO BOTTOM): CREVELING/SCIENCE (ADAPTED ■ UNIVERSITY OF DELAWARE); COURTESY OF THE OFFICE OF CONGRESSMAN EDWARD J. MARKEY

SCIENCESCOPE

A War Over Indirect Costs

U.S. research universities could end up losing millions of dollars under a proposal to cut by more than half the overhead rate on $1.5 billion a year in basic research grants from the Department of Defense (DOD). Universities currently receive anywhere from 45% to 55% of the total amount of a grant for the legitimate costs associated with supporting research, including everything from electricity to cleaning animal cages. A report accompanying the 2008 defense spending bill marked up last week says a 20% cap is needed because overhead costs have "grown to unwarranted levels."

That's just not true, says Robert Berdahl, president of the Association of American Universities in Washington, D.C. The average indirect cost recovery rate has remained at about 51% for a decade, he says, despite the rising cost of supporting research. The proposed cap, if retained in the final defense spending bill now moving through Congress, could even force schools to forgo DOD grants, he adds.

–YUDHIJIT BHATTACHARJEE

Don't Be Put Off by Offsets

The head of a new congressional panel on climate change wants the U.S. government to more closely monitor the $100 million global market for voluntary carbon offsets, credits for green projects that companies and individuals purchase from specialty brokerage firms to compensate for carbon-intensive activities. Some climate scientists say offsets, which include forest projects and energy work in the developing world, are a distraction from the real need: cutting greenhouse gas emissions.

Representative Edward Markey (D–MA), chair of the House Select Committee on Energy Independence and Global Warming, feels offsets could play a positive role. But he thinks consumers need more information. He wrote the Environmental Protection Agency last week that "a lack of generally accepted standards has raised questions about the credibility of some offset products." He wants the agency to develop such standards, and he's also asked the Federal Trade Commission to devise guidelines for those who market such offsets.

–ELI KINTISCH

in Golden, Colorado, measured the overall solar-cell efficiency under simulated conditions; a separate NREL team built several of the cells used in the device. The device is based on well-known semiconductors tuned to respond to specific wavelengths using doping and other physical tweaks the researchers won't reveal. New electronics allowing parallel power generation gave them additional freedom, as cells within modules connected in series produce as much electricity as their weakest link.

Each of those advances, however, although promising in the lab, could be pricey to build. Most recent commercial solar efforts have focused on making cells cheaper to manufacture, not on increasing efficiency. Kirkpatrick says the manufactured cost goal for the program is $2 per peak watt, 45% under the current industry standard. "That's the key to success," says solar energy manager Craig Cornelius of the Department of Energy, who says it can take up to 15 years for new solar-cell architectures to make it into the marketplace.

But DARPA is hoping for faster results. With the early proof of concept in the bag, research partner DuPont has announced a 3-year commercialization effort with the Delaware team to spend up to $100 million to build prototype devices. Meanwhile, the researchers are continuing work with advanced kinds of cells, including nanotech and bio-inspired varieties, hoping later to use better performing materials in what Kirkpatrick calls a "plug and play" approach. "The building blocks are all in place," says Delaware physicist Robert Birkmire. –ELI KINTISCH

IMMUNOLOGY

A Slimy Start for Immunity?

Even slime molds get sick. Although these gooey soil dwellers, which straddle the boundary between single-celled and multicelled creatures, gobble up bacteria as food, they can also be laid low by microbial attacks. On page 678, however, researchers report that slime molds deploy cells that combat pathogens, a discovery implying that specialized immune cells preceded the advent of multicellular organisms.

Developmental biologist Adam Kuspa of Baylor College of Medicine in Houston, Texas, and colleagues also found that the germ fighters depend on a protein used by the more sophisticated defensive systems of plants and animals. The work "shows how molecules that play a role in innate immunity are already present in amoebas," says cell biologist Michel Desjardins of the University of Montreal in Canada.

Immunity's origins are murky. Because single-celled amoebas swallow their bacterial meals in much the same way that macrophages and other immune cells envelop their targets, researchers have long suspected that food consumption gave rise to this style of self-defense.

The widely studied social amoeba *Dictyostelium discoideum* has now provided strong endorsement of that idea. The amoebas, also known as cellular slime molds, lead a double life. Much of the time, they are squishy individualists. But if food runs short, as many as 100,000 cells congregate into a slinking blob known as a slug.

The Baylor team was investigating how certain transporter proteins help the amoebas slurp up fluorescent dyes, which were proxies for environmental toxins. They noticed that the dyes mainly ended up in a subset of cells, whose job appeared to be eliminating poisons.

The researchers then discovered that these cells, which they dubbed sentinel cells, also battle bacteria that menace the slug. In lab dishes, the cells snared the amoeba's main pathogen, the soil germ *Legionella pneumophila*, banishing it from the slug. Although researchers knew that some parts of the slug specialize, for example forming a spore-holding stalk, nobody had discerned these protective cells, Kuspa says.

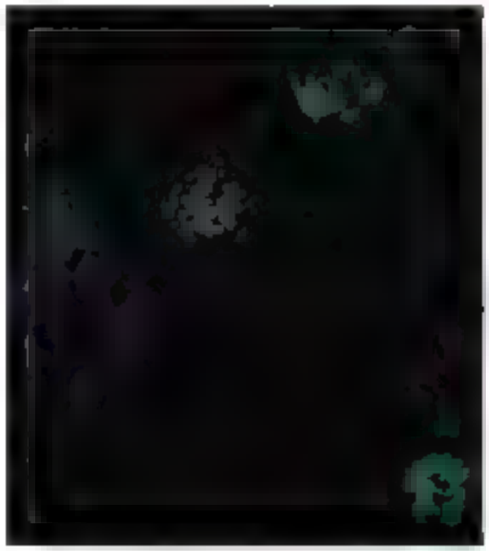

To the rescue. A crawling slime mold slug (*right*, false color) protects itself with sentinel cells. These defensive cells (*above*) capture fluorescent beads (green) much the way they do bacteria.

Once they differentiate in a slug, sentinel cells crank up production of proteins involved in immunity in other organisms, including a pathogen-detecting cell surface receptor and a so-called TIR domain protein that relays signals from such receptors. Disabling the gene for one TIR domain protein in the sentinel cell armory disrupted how cells handled bacteria. The mutant amoebas fell victim to a strain of *L. pneumophila* that they typically fight off. And although typical *D. discoideum* grow vigorously on plates coated with tasty *Klebsiella*

aerogenes, their normal food, the mutants languished. If those bacteria were dead, however, the altered amoebas thrived.

Sentinel cells circulate within the slug as if they are on patrol, and they appear to jettison globs of pathogens as the bacteria chase along. Clumps of sentinel cells also get left behind, suggesting that, like some mammalian immune cells, they sacrifice themselves for the good of the body, although the castoffs could also be the seeds of new colonies, Kuspa says. This rudimentary immune system is not a peculiarity of *D. discoideum*. Five other slime molds also sport the cells.

Sentinel cells seem to function like human neutrophils and macrophages, Kuspa and colleagues conclude. To benefit the rest of the slug, he says, "lots of the cells essentially put themselves in harm's way." Social amoebas and their kin diverged shortly after the animal-plant split, and the results suggest an early beginning for the specialized immune system now seen in multicellular organisms.

The discovery of dedicated defenses in the amoebas isn't surprising, says comparative immunologist Edwin Cooper of the University of California, Los Angeles. "If you're multicellular, you need to be sure that some of those cells are protecting against bacteria." Immunologist Ruslan Medzhitov of Yale University suggests that researchers check for rudimentary immunity in other simple eukaryotes, such as solitary amoebas and *Volvox*, a colonial organism with some cell specialization. –MITCH LESLIE

CREDITS (TOP TO BOTTOM): M. J. GRIMSON AND R. L. BLANTON, GUOKAI CHEN

FRANCE

Cancer Test Dispute Pits Researcher Against a Firm She Helped Create

PARIS—When Patrizia Paterlini first reported a cheap and rapid technology to detect tumor cells in blood 7 years ago, she hoped it might make it to the market. Today, she's fighting to prevent precisely that. Paterlini, an oncologist at the French biomedical research agency INSERM, is trying to stop Metagenex, a company in which her family owns a 44% share, from selling testing equipment based on her technology, which she says has not been sufficiently validated. Offering the test to doctors now, she says, is "unscientific." Government inspectors and two ethics panels are investigating the issue, which has also embroiled Paterlini's husband, INSERM director Christian Brechot.

At issue is an assay called isolation by size of epithelial tumor cells (ISET), in which blood samples are sucked through a membrane with pores just small enough to trap tumor cells but large enough to let through red and white blood cells. The captured cancer cells can then be fully characterized using various techniques. Standard molecular techniques to trace tumor cells in blood, such as the polymerase chain reaction, don't allow this further analysis, says Claudio Orlando of the University of Florence, who has tested ISET.

Paterlini hopes the method, first published in 2000 in the *American Journal of Pathology*, can monitor the recurrence of tumors in cancer patients or screen for cancer cells in the blood of apparently healthy people. To that end, Paterlini co-founded Metagenex in 2001 with her husband, formerly the head of her research unit. (Brechot sold his shares in the company to the couple's two children when he took the top job at INSERM.)

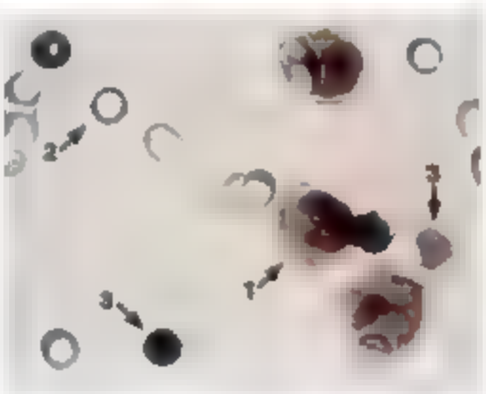

Size matters. An ISET filter has pores (2) small enough to let blood cells (3) pass, while tumor cells (1) are captured.

CREDITS (TOP TO BOTTOM): THE GLOBAL CROP DIVERSITY TRUST; G. VONA ET AL., AMERICAN JOURNAL OF PATHOLOGY 156 1 (JANUARY 2000) © AMERICAN SOCIETY FOR INVESTIGATIVE PATHOLOGY

Last year, Massachusetts Institute of Technology graduate and engineer David Znaty took over management at Metagenex. Paterlini, who has a part-time, unpaid job at the company, says she endorsed the move and even asked Znaty to take the job. Not long after, Znaty persuaded two investment companies, AXA and Banexi, to inject €2.5 million into the firm. And the Lavergne Laboratory, a diagnostic lab in Paris, bought ISET equipment from Metagenex and began offering the tests to physicians for use with their cancer patients.

Since then, accusations have been flying. According to Paterlini, Znaty has broken an agreement to conduct multicenter trials to validate the ISET technology before bringing it to the market. Without such data, it's impossible for doctors to interpret the results, she says. INSERM, which co-owns the patents to ISET, is supporting Paterlini. Orlando, too, agrees that "it is absolutely too early" to use the test clinically.

Znaty counters that Paterlini's past studies offer a sufficient scientific basis to use the test, he accuses her of trying to push him out because she wants to regain control of the company, and says her husband, and thus INSERM, has a conflict of interest. Brechot declined to be interviewed for this story, but Paterlini points out that the two other co-owners of the patents, the Universite Paris-V and the Assistance Publique–Hopitaux de Paris, are also backing her.

Jean-Claude Zerat, director of the Lavergne Lab, says he is confident that the ISET technology is mature enough for physicians to use. He says that Paterlini herself assisted the lab in implementing the technology before she fell out with Znaty, which Paterlini denies.

INSERM has asked its own independent ethics panel and France's National Consultative Ethics Committee to investigate. A government spokesperson says that inspectors from the research and health ministry have also begun a joint inquiry.

A spokesperson for the French Health Products Safety Agency says she believes Metagenex's technology is not subject to the agency's regulation, but she wasn't sure. Indeed, the INSERM panel says it wants to look at the dispute in the broader context of how new diagnostic tests should be regulated.

—[illegible]

SCIENCESCOPE

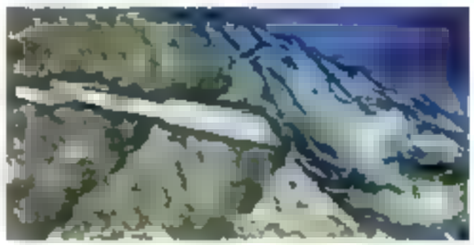

Save the Seeds

The United States would contribute up to $60 million to a so-called doomsday seed vault under a bill passed last week by the House of Representatives. The nonprofit Global Crop Diversity Trust is building the Svalbard Global Seed Vault in a mountain on Norway's Spitsbergen island to preserve 3 million seed samples from the world's crop species.

The authorization for the 5-year contribution is tucked into a controversial plan to change the formula for subsidizing U.S. farmers. The United States has already spent $6 million on the project since 2001, and supporters hope the president will seek the additional funding in his 2009 budget request next year.

—BENJAMIN LESTER

More Questions for Enviro Chief

Congress is asking more questions about the beleaguered director of the National Institute of Environmental Health Sciences (NIEHS). In a letter to the National Institutes of Health in Bethesda, Maryland, this week, Senator Chuck Grassley (R-IA) wonders whether NIEHS chief David Schwartz improperly took money from the budgets of other intramural investigators when he exceeded his approved personal lab budget of $1.8 million by $4 million (*Science*, 6 July, p. 26). The letter also asks for information about Schwartz's hiring practices and whether he recused himself from reviews of extramural grant proposals submitted by his outside collaborators. Grassley wants specific documents by 8 August.

—JOCELYN KAISER

Sarkozy Wastes No Time

PARIS—New French president Nicholas "Speedy" Sarkozy has lived up to his nickname by pushing ahead with his plan to improve the quality of research and education at 85 state-owned universities. Last week, the National Assembly endorsed his proposal to streamline university governance and give institutes more leeway in recruiting staff, handling budgets, and managing real estate. Left-wing parties, students, and some university professors' unions oppose the idea, which they say will increase competition and inequality among universities.

—MARTIN ENSERINK

Middle Asia Takes Center Stage

Long dismissed as a backwater, the vast area between Mesopotamia and the Indus Valley is now revealing a tapestry of wealthy urban centers that shaped humanity's first concerted attempt at city life

RAVENNA, ITALY—Five hundred years ago, the cities scattered across the north Italian plain exchanged goods, artists, and ideas yet clung stubbornly to their own distinctive styles and cultures. Their rivalries and trade swelled into a creative wave that transformed Europe during the Renaissance and launched the world into the modern era. Now many archaeologists believe that a similar awakening took place nearly 5000 years ago, in an even wider arc to the East spanning thousands of kilometers. New findings suggest that a string of societies, from the Russian steppes to the Arabian Peninsula, together forged the first human civilizations.

It is a radical retelling of the traditional story, which holds that civilization sprouted in Mesopotamia along the banks of the Euphrates, then on the Nile, and finally on the Indus during the 3rd millennium B.C.E., each culture largely isolated by harsh terrain and immense distances. At a meeting* here last month, archaeologists began to assemble a far more complex picture in which dozens of urban centers thrived between Mesopotamia and the Indus, trading commodities and, possibly, adopting each other's technologies, architectures, and ideas. Advocates admit they are only beginning to piece together how the urban boom unfolded across what they call Middle Asia. Nevertheless, argues Sylvia Winkelmann, an archaeologist at the University of Halle in Germany, "we have to change our view. Mesopotamia is not the only cradle of mankind—there are many."

The old take on Mesopotamia as the mother of all civilization has its roots in archaeology's obsession with major river valleys. Ancient sites in Egypt, southern Iraq, and along the Indus were relatively obvious and accessible to Western scientists. The more remote oases and inland rivers of the Iranian plateau, Central Asia, and parts of the Arabian Peninsula remained mostly terra incognita. The Cold War prolonged that isolation, as did the 1979 revolution in Iran and war in Afghanistan. Middle Asia was dismissed by many academics as a marginal region of trading paths and small settlements that supplied raw materials or goods to urban sophisticates in the three river systems.

But excavations in Iran, Turkmenistan, and Oman are prompting scholars to rethink how civilization first took a firm hold. "During the last 3 centuries of the 3rd millennium B.C.E., the Iranian plateau was an incredibly dynamic place. A transformation was taking place which finally may have led to integration," says Holly Pittman, an archaeologist at the University of Pennsylvania. But why Middle Asia's collection of sprawling civilizations suddenly collapsed remains a controversial question.

At the Ravenna meeting, a diverse band of archaeologists pledged to work together to unravel Middle Asia's cultural interactions. "This is an experiment to see if we can prove connections and similarities," says Maurizio Tosi, the University of Bologna archaeologist who hosted the gathering.

At the margins no more

Globalization is an ancient phenomenon. Anatolian obsidian used for making sharp tools is found widely in the Near East at sites dating to the 5th millennium B.C.E. By the 4th millennium B.C.E., lapis lazuli mined in Afghanistan appears in Mesopotamia and Egypt. And by the 3rd millennium B.C.E., carnelian beads crafted in the Indus River valley circulated in the Near East, and copper from Oman was worked into fine Sumerian jewelry in Mesopotamia.

Archaeologists long assumed that the impetus for much of this trade came from booming cities that sprang up in the 3rd millennium B.C.E. in southern Mesopotamia, a fertile area devoid of stone, metal, and other resources. (The Indus and Egypt, by contrast, are richer in raw materials.) That assumption was based in part on Sumerian texts and objects such as those in royal graves from circa 2500 B.C.E. in the Sumerian city of Ur. The tombs, found in the 1920s, include artifacts made of gold, silver, copper, lapis, carnelian, and dark stone originating from as far away as the Indus. The diversity and lavishness of the materials gave credence to the idea that less-developed areas to the east devoted much energy to exporting high-status goods. "Mesopotamia was the great sucking sound," says archaeologist Carl Lamberg-Karlovsky of Harvard University.

CREDIT: KENNETH GARRETT

* International Association for the Study of Early Civilizations in the Middle Asian Intercultural Space, 7–8 July.

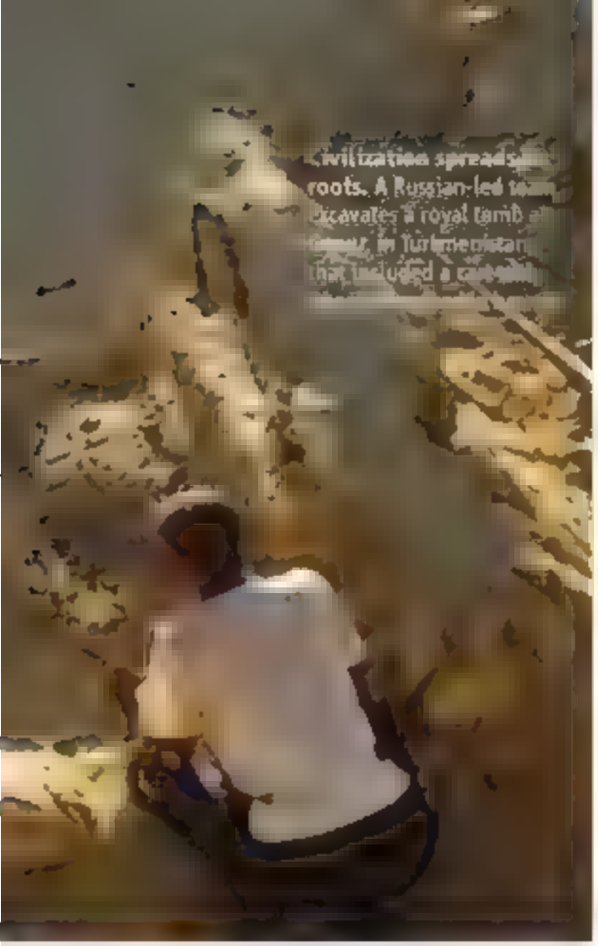

Civilization spreads its roots. A Russian-led team excavates a royal tomb at Gonur, in Turkmenistan, that included a cremation

New excavations flatly contradict that picture. The most dramatic evidence comes from the Halil River in southeastern Iran. After extensive looting of ancient cemeteries in an area south of the modern city of Jiroft in 2001, a team led by Yousef Madjidzadeh began excavating two nearby mounds (*Science* 7 November 2003, p. 973). Over five seasons, the Iranian team uncovered the remains of a city that may have rivaled contemporary Ur in its extent and wealth—a stunning discovery in an area long considered a backwater. "If not for the discovery of Jiroft, we would not have been able to bring together" the concept of multiple societies contributing to early civilization, says Tosi.

The ancient city in the mid- to late 3rd millennium B.C.E. covered more than 2 square kilometers, dominated by a large citadel flanked by a massive stepped platform to the north. A room excavated last year in the citadel includes a 2-meter-high brick human torso, ochre paint still clinging to the surface. The sculpture, says Madjidzadeh, is the largest of its kind from that era. The team also has recovered more than 400 impressions made by some 200 different seals between 2480 and 2280 B.C.E. Impressed on wet clay, the seals typically marked ownership of boxes or baskets that may have held trading goods, says Pittman, who has worked at the site. Roughly one in 10 is from Mesopotamia and two are from the Indus, but the rest are likely of local origin, she says.

Coming into view. This seal impression found near Jiroft reveals a unique iconography of a hitherto-unknown culture.

The team also found remains of carved vessels made of dark stone—steatite or chlorite—in the citadel and in the cemetery. Such vessels have long turned up in western Asia, in Ur's royal graves, around the Persian Gulf, and on the Iranian plateau. Their origin was a mystery, and they were given the vague moniker of "intercultural style," although a late-1960s excavation led by Lamberg-Karlovsky at nearby Tepe Yahya found a modest-sized factory.

In the wake of the cemetery looting, large numbers of such vessels, often incised with unique mythological designs, flooded the international art market. Many archaeologists questioned their provenance because no examples were found in situ. Madjidzadeh's finds show that the vessels were widely used locally—and may have had strong personal or religious meaning, because so many of them were apparently buried with their owners. And some were exported over vast distances. In Mesopotamia, they were considered so valuable that even plain chlorite vessels were reserved solely for kings and temples.

Although ransacked, the cemeteries provide a glimpse into the wealth of the ancient inhabitants. Madjidzadeh found one large tomb cut into limestone that appeared untouched since it was robbed in antiquity. A stairway leads down to a chamber containing eight burial areas, scattered throughout were 600 carnelian beads and other precious materials. Nearby, from the dumps left by looters, archaeologist Massimo Vidale, a visiting professor at the University of Bologna, extracted 1200 small lapis and turquoise beads, pieces of 40 or more chlorite vessels, and 40 to 50 copper vessels—at least one with ornate embossing.

The looting also provided one boon: a peek at Jiroft's heretofore-unknown origins. The robbers' holes threw up older pottery remains, and Vidale unearthed ceramics extending the settlement's past as far back as 4000 B.C.E. "This has huge significance," says Lamberg-Karlovsky, because it shows that Jiroft's existence is not just a fleeting response to Mesopotamian markets but a long-lived culture. Not all experts agree. Archaeologist Oscar Muscarella of the Metropolitan Museum of Art in New York City, for one, doubts that the site predates the 3rd millennium B.C.E. He also

CREDIT (BOTTOM): Y. MADJIDZADEH

complains that the excavation team has been too quick to make assertions and too slow to publish scholarly reports.

Moscarella does acknowledge the importance of the site. And many colleagues suspect that the culture's influence extended up the 400-kilometer-long Halil Valley, linking communities in religion and politics. But assembling the shards of evidence into a persuasive picture will take time. "In Mesopotamia, they have had 150 years to dig," says Madjidzadeh, who plans to publish on the finds this fall. "I've only had five."

To the four corners

Other sites in eastern Iran confirm that this parched region was anything but marginal. At Shahr-e Sokhta, for example, archaeologists have uncovered what was a bustling metropolis between 2550 and 2400 B.C.E., as large as 150 hectares and with at least 380 smaller sites in the surrounding region. The central site, northeast of Jiroft, is in a landlocked but fertile basin fed by the Helmand River. Artifacts from that era include lapis from Afghanistan, shells from the Pakistan coast, vessels imported from the Indus, and game boards in the style of those found in Ur. Long-distance trade appears to extend back to at least 3000 B.C.E.

The flow of goods was not just east to west. Archaeologists see a strong north-south link as well. Along the southern coast of the Persian Gulf, Serge Cleuziou of CNRS in Paris is piecing together a long, culturally complex history.

Oman in the 3rd millennium B.C.E. became an important source of copper for both Sumer and Susa, the great Elamite capital on the edge of Mesopotamia, bringing the gulf settlements substantial wealth. Ceramics found in Oman demonstrate that the region was closely connected to the coastal economy of Iran and, in turn, to Jiroft and the Iranian plateau. That connection almost certainly extended beyond the Strait of Hormuz; Indus specialists now suspect that at least some of their copper originated in Oman—a sign of a healthy overseas trading network. And Indus and Mesopotamian goods found in ancient ports along the gulf's western coast point to trade via the Arabian Sea, says Cleuziou.

That trade extended all the way to Central Asia, where archaeologists have found Omani pots. At this northern end of the trade network thrived the Bactria Margiana Archaeological Complex, or Oxus civilization, consisting of large planned urban centers set amid well-watered oases and basins. Russian archaeologist Viktor Sarianidi, working at sites such as Gonur in Turkmenistan, has evidence of a culture at the end of the 3rd millennium B.C.E. capable of long-distance trade and fine craftsmanship and having a unique artistic style and mythological system.

A Mesopotamian seal and an Indus seal found at Gonur, along with a smattering of Indus and Iranian goods, hint at the trade network's breadth—as does an Oxus-style comb in Oman. That network was enabled at least in part by the latest in transportation technology. Sarianidi recently excavated a cart with four bronze-covered wheels and a number of animal skeletons in an elaborate grave, although the tomb's dating is unclear. But at nearby Altyn-Depe, archaeologist Lubov Kircho of the Russian Academy of Sciences says her team has found models of carts dating to at least the middle 3rd millennium B.C.E.—centuries earlier than archaeologists once thought such carts were invented. The carts were pulled by bullocks and domesticated camels, she says, an innovation that would have made long-distance trade easier. The hot new transportation technology may well have spread across Middle Asia, she says.

Connecting the dots

The scatter of high-priced trade goods, seals, and pottery has revealed the existence of networks linking Middle Asia's urban centers with each other and with Mesopotamia and the Indus. Elucidating whether they embraced common ideas as well—in architecture, technology, politics, and religion—is the central challenge for the archaeologists who met in Ravenna.

CREDIT: Y. MADJIDZADEH

Ancient Writing or Modern Fakery?

RAVENNA, ITALY—They look like a child's exercise in geometry. But the images Yousef Madjidzadeh projected onto a screen last month in a sweltering lecture hall elicited gasps from archaeologists. The symbols on three baked mud tablets display a hitherto unknown writing system and likely are part of a larger archive, claimed Madjidzadeh, chief of excavations near Jiroft in southeastern Iran. He believes that these inscriptions were made between 2200 and 2100 B.C.E. and could hold the key to understanding a sophisticated urban culture in Middle Asia.

The discovery of an ancient script is a momentous find. But the circumstances surrounding the excavation have raised doubts about the tablets' authenticity. "Everyone is convinced they are fake, but no one dares say it," whispered one archaeologist after the presentation. Such criticism galls Madjidzadeh and his supporters, who say that although one tablet was found by a villager, the other two are from a carefully excavated trench. "People are skeptical because these are so different. It is hard to accept something so completely new," says Massimo Vidale, a University of Bologna archaeologist who was present during the excavation.

The first writing—cuneiform—evolved over millennia in Mesopotamia and coalesced into a coherent system by 3200 B.C.E. in the southern Iraqi city of Uruk. Not long after, another script appeared on the western edge of Mesopotamia. Dubbed proto-Elamite, after the kingdom of Elam that later flourished beside Mesopotamia, the system resembles cuneiform, although its origin and meaning are a puzzle. Centuries later, toward the end of the 3rd millennium B.C.E., another set of symbols arose on the Iranian plateau: linear Elamite. Only a handful of examples exist, mainly from the Elam capital of Susa and mainly in the form of stone carvings paired with cuneiform. Some scholars doubt it is a coherent script; they believe it is an attempt by Elamite kings to appear as modern as their Mesopotamian neighbors.

complains that the excavation team has been too quick to make assertions and too slow to publish scholarly reports.

Moscarella does acknowledge the importance of the site. And many colleagues suspect that the culture's influence extended up the 400-kilometer-long Halil Valley, linking communities in religion and politics. But assembling the shards of evidence into a persuasive picture will take time. "In Mesopotamia, they have had 150 years to dig," says Madjidzadeh, who plans to publish on the finds this fall. "I've only had five."

To the four corners

Other sites in eastern Iran confirm that this parched region was anything but marginal. At Shahr-e Sokhta, for example, archaeologists have uncovered what was a bustling metropolis between 2550 and 2400 B.C.E., as large as 150 hectares and with at least 380 smaller sites in the surrounding region. The central site, northeast of Jiroft, is in a landlocked but fertile basin fed by the Helmand River. Artifacts from that era include lapis from Afghanistan, shells from the Pakistan coast, vessels imported from the Indus, and game boards in the style of those found in Ur. Long-distance trade appears to extend back to at least 3000 B.C.E.

The flow of goods was not just east to west. Archaeologists see a strong north-south link as well. Along the southern coast of the Persian Gulf, Serge Cleuziou of CNRS in Paris is piecing together a long, culturally complex history.

Oman in the 3rd millennium B.C.E. became an important source of copper for both Sumer and Susa, the great Elamite capital on the edge of Mesopotamia, bringing the gulf settlements substantial wealth. Ceramics found in Oman demonstrate that the region was closely connected to the coastal economy of Iran and, in turn, to Jiroft and the Iranian plateau. That connection almost certainly extended beyond the Strait of Hormuz; Indus specialists now suspect that at least some of their copper originated in Oman—a sign of a healthy overseas trading network. And Indus and Mesopotamian goods found in ancient ports along the gulf's western coast point to trade via the Arabian Sea, says Cleuziou.

That trade extended all the way to Central Asia, where archaeologists have found Omani pots. At this northern end of the trade network thrived the Bactria Margiana Archaeological Complex, or Oxus civilization, consisting of large planned urban centers set amid well-watered oases and basins. Russian archaeologist Viktor Sarianidi, working at sites such as Gonur in Turkmenistan, has evidence of a culture at the end of the 3rd millennium B.C.E. capable of long-distance trade and fine craftsmanship and having a unique artistic style and mythological system.

A Mesopotamian seal and an Indus seal found at Gonur, along with a smattering of Indus and Iranian goods, hint at the trade network's breadth—as does an Oxus-style comb in Oman. That network was enabled at least in part by the latest in transportation technology. Sarianidi recently excavated a cart with four bronze-covered wheels and a number of animal skeletons in an elaborate grave, although the tomb's dating is unclear. But at nearby Altyn-Depe, archaeologist Lubov Kircho of the Russian Academy of Sciences says her team has found models of carts dating to at least the middle 3rd millennium B.C.E.—centuries earlier than archaeologists once thought such carts were invented. The carts were pulled by bullocks and domesticated camels, she says, an innovation that would have made long-distance trade easier. The hot new transportation technology may well have spread across Middle Asia, she says.

Connecting the dots

The scatter of high-priced trade goods, seals, and pottery has revealed the existence of networks linking Middle Asia's urban centers with each other and with Mesopotamia and the Indus. Elucidating whether they embraced common ideas as well—in architecture, technology, politics, and religion—is the central challenge for the archaeologists who met in Ravenna.

CREDIT: Y. MADJIDZADEH

Ancient Writing or Modern Fakery?

RAVENNA, ITALY—They look like a child's exercise in geometry. But the images Yousef Madjidzadeh projected onto a screen last month in a sweltering lecture hall elicited gasps from archaeologists. The symbols on three baked mud tablets display a hitherto unknown writing system and likely are part of a larger archive, claimed Madjidzadeh, chief of excavations near Jiroft in southeastern Iran. He believes that these inscriptions were made between 2200 and 2100 B.C.E. and could hold the key to understanding a sophisticated urban culture in Middle Asia.

The discovery of an ancient script is a momentous find. But the circumstances surrounding the excavation have raised doubts about the tablets' authenticity. "Everyone is convinced they are fake, but no one dares say it," whispered one archaeologist after the presentation. Such criticism galls Madjidzadeh and his supporters, who say that although one tablet was found by a villager, the other two are from a carefully excavated trench. "People are skeptical because these are so different. It is hard to accept something so completely new," says Massimo Vidale, a University of Bologna archaeologist who was present during the excavation.

The first writing—cuneiform—evolved over millennia in Mesopotamia and coalesced into a coherent system by 3200 B.C.E. in the southern Iraqi city of Uruk. Not long after, another script appeared on the western edge of Mesopotamia. Dubbed proto-Elamite, after the kingdom of Elam that later flourished beside Mesopotamia, the system resembles cuneiform, although its origin and meaning are a puzzle. Centuries later, toward the end of the 3rd millennium B.C.E., another set of symbols arose on the Iranian plateau: linear Elamite. Only a handful of examples exist, mainly from the Elam capital of Susa and mainly in the form of stone carvings paired with cuneiform. Some scholars doubt it is a coherent script; they believe it is an attempt by Elamite kings to appear as modern as their Mesopotamian neighbors.

Massive ceremonial platforms could be one clue to a shared culture. Such structures sprang up across the region from Mesopotamia, where they are called ziggurats, to Afghanistan—in the middle and late 3rd millennium B.C.E. Jiroft has what Madjidzadeh says is a two-stepped platform, and a smaller version recently has been found in Shahdad, a site near the modern city of Kerman, Iran. Even the central structure at the major Indus city of Mohenjo-Daro, long thought to be the remains of a later Buddhist stupa, may be a platform like those built to the west, says Giovanni Verardi of the University of Naples.

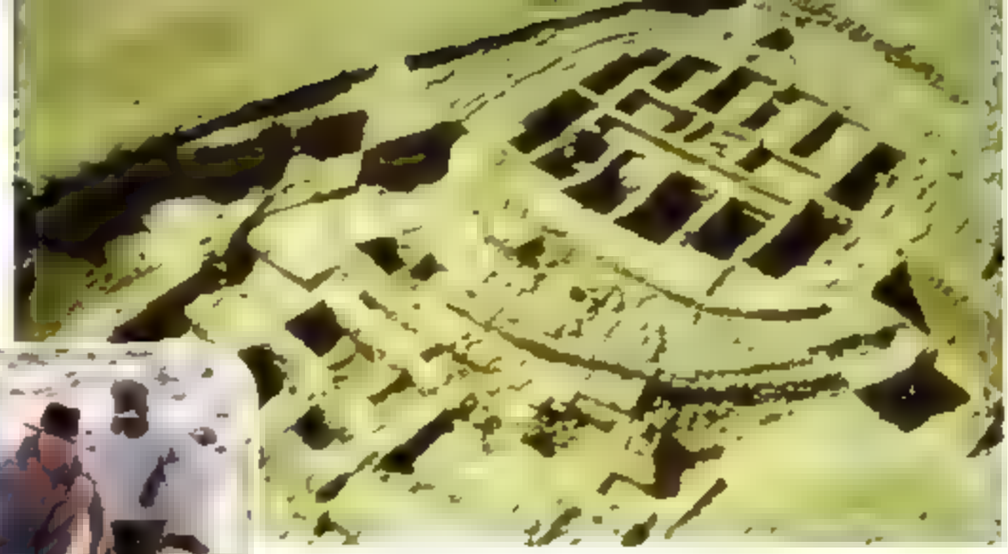

Desert pantry. On the Oman peninsula, the Hili site, excavated by Serge Cleuziou (*inset*), has a sophisticated architecture with what may be cellars for storing trade goods bound for distant lands.

One unanswered question is whether writing played an important role in Middle Asia. A script called proto-Elamite appeared circa 3000 B.C.E., and some 1500 tablets were found long ago at Susa. Scholars assumed that the script originated there, in the shadow of cuneiform. But in recent decades, proto-Elamite tablets have been unearthed across the Iranian plateau. Madjidzadeh, who found a tablet in Ozbaki, a site west of Tehran, calls the script "proto-Iranian" or "proto-plateau" to eliminate the traditional focus on the western end of the plateau. And he is betting that next season in Jiroft he will uncover an archive full of tablets related to linear Elamite, a later script (see sidebar, p. 588).

Seals and seal impressions may provide the deepest insights into the exchange of religious, mythological, and political ideas. Those found at Jiroft, for example, offer an intimate view into the belief system of the area in the mid-3rd millennium B.C.E., depicting figures such as winged goddesses with snakes sprouting from their shoulders and rulers with narrow waists wearing bird-like headgear. Pittman, a specialist in seal analysis, says the specimens offer "a whole new visual vocabulary" and demonstrate "a robust and independent culture."

Echoes of this powerful iconography appear slightly later in areas as far west as Mesopotamia, where narrow waists on seals became all the rage, and as far north as Turkmenistan, where a snake goddess shows up on Oxus seals. "There is some sort of cultural integration from the Oxus to the Iranian plateau to the Persian Gulf," says Pittman. "There are profound similarities." At the same time, she says, "each region has its own identity, its own material culture." By the end of the 3rd millennium B.C.E., cuneiform texts hint at growing wealth and power to the east. Sumerian rulers began to ally themselves with these kingdoms, cementing

Given the dearth of linear Elamite inscriptions, the Jiroft finds are attracting scrutiny. In early 2005, Madjidzadeh's team found a brick in the gateway of the main Jiroft mound. Dated to between 2480 and 2280 B.C.E., the brick is inscribed with signs that may be related to linear Elamite, Madjidzadeh says. Later that field season, a worker showed the dig director a tablet with odd symbols that he said came from a hole he dug a half kilometer from the mound.

Returning last year, Madjidzadeh had a student dig a trench at the spot. The team promptly recovered a second tablet. The next day, Madjidzadeh came to oversee the work, he uncovered the third tablet. The three tablets appear to show a progression. One has eight simple geometric signs, another has 15 slightly more complex signs, and the third has 59 signs of an even more complex nature, all inscribed in wet clay. On the back of each, apparently scratched into the mud brick after it was dry, are inscriptions that may be related to linear Elamite. Madjidzadeh believes he has stumbled on an archive and that a librarian scribe made the marks on the back of each tablet. He believes the tablets reveal linear Elamite's evolution from simple geometrical system to final complex form.

That analysis doesn't wash with some specialists. One archaeologist at the meeting suggested that the tablets could be exercises from a scribal school. Others doubt the authenticity of the geometrical markings. Earlier this year, Madjidzadeh shared photos of the tablets with Jacob Dahl, a specialist in ancient texts at Berlin's Free University. "I was shocked," Dahl recalls. "No specialist in the world would consider these to be anything but absolute fakes." The only script the geometric designs resemble, he argues, is a modern phonetic system for Eskimo.

However, Dahl is intrigued by the inscriptions on the back of the tablets, which he says could indeed be linear Elamite. He maintains that it's possible that the tablets are fake on one side, genuine on the other. Mesopotamia, he notes, is rife with objects that combine real inscriptions with those of counterfeiters.

Such assertions "are completely crazy," says University of Pennsylvania archaeologist Holly Pittman, who has worked with Madjidzadeh at Jiroft. She notes that when fine artifacts from the 3rd millennium B.C.E. began to trickle out of Afghanistan decades ago, scholars were similarly dismissive because the material did not conform to existing theories.

Madjidzadeh plans to publish soon a scholarly article laying out the details. But the controversy is likely to roil the field until he returns to Jiroft in November and expands the trench. Then the critics will eat crow, predicts Pittman. "They will be shown to be fools when he pulls out 1000 tablets," she predicts. Such extraordinary evidence may be vital to back the extraordinary claims. **–A.L.**

CREDITS (TOP TO BOTTOM): S. CLEUZIOU; M. MADJIDZADEH

Cracking Open the Iranian Door

"Let's do something!" exclaims Hassan Fazeli-Nashali, the new chief of the Archaeology Research Center in Tehran. What he has in mind is transforming Iran's sputtering archaeological enterprise into a world class effort, an ambitious goal in a country rich in unexplored ancient sites but mired in complex politics. Fazeli Nashali, 45, is undaunted. At the Ravenna meeting (see main text), he laid out a bold plan for engaging more foreign scientists and honing the skills of Iranian academics.

If Fazeli Nashali is brash, he can afford to be, thanks to his sterling credentials in an Islamic regime. "I lost my leg, so they trust me," he says, thumping the prosthetic he received after being wounded during the Iran-Iraq war 2 decades ago. "I'm a soldier of the revolution, but I've never been in politics," he adds. "And my brother is a mullah and my father was a mullah. We're a religious family, so there are no points against me." He has also won respect in his field. He received a Ph.D. from the University of Bradford, U.K., specializing in social and craft complexity in prehistoric Iran, and served most recently as head of the archaeology department at the University of Tehran, the country's top institution of higher education.

Colleagues are delighted with Fazeli Nashali's open attitude and pledge to ensure access for foreign researchers, including Americans. "This is a most dramatic and welcome initiative, and extraordinarily encouraging," says archaeologist Carl Lamberg-Karlovsky of Harvard University, who, like other Americans in recent years, has found it nearly impossible to win approval for lengthy stays. Europeans, Japanese, and Australians generally encounter less trouble, although several have had to postpone or cancel dig seasons because of visa delays.

Iran's parliament has a vocal faction that wants to halt work with foreign archaeologists, and Fazeli Nashali acknowledges that some Iranian academics oppose cooperation out of fears that foreigners will control top sites. Many colleagues doubt that Fazeli Nashali can overcome the rivalries and xenophobia. "I don't think his position is all that solid," says a Western archaeologist with long ties to Iran. "But I hope he sticks around."

Below are excerpts from a conversation with Fazeli Nashali. **–A.L.**

Visionary. Hassan Fazeli Nashali wants outsiders to help overhaul Iran's troubled archaeological community.

On his new position:
This job is hard for everybody. I plan to stay 3 years only. But I worry that international work will dry up when I leave.

On the dam crisis:
There are more than 100 [dams] under construction, and huge archaeological sites are going underwater. At just one site—in Pasagardae—we had 10 teams working for 15 seasons over 3 years until the water began to rise 3 months ago. So we face a big problem. My government will ask [foreign] archaeologists who want to come to Iran to pay for their international flight while we cover labor, subsistence, and transport costs.

On domestic excavations:
We need to open the gates for a new generation and reorient our research away from museum collecting and toward understanding social and economic transformation. The big problems in Iran are publishing scientific papers and excavating sites in a timely manner. We are paying lots of money for excavations, but we are not producing the publications to justify that money.

On international cooperation:
My main objective is to forge a link between Iranian and foreign universities. At the University of Tehran, we began a Tehran plain project in 2003 with cooperation among Leicester, Bradford, and Durham universities. We also have a project to examine the process of urbanization in the Zagros Mountains, which involves the universities of Reading, London, Tehran, and Hamadan. These kinds of projects help address the asymmetry between foreign and Iranian teams.

On politics:
Our country stands to benefit from cooperation, so I want to encourage people to come to Iran. Archaeology has been used frequently for other agendas—think of Mussolini or Hitler. And this is not the age for archaeology to be political.

agreements with diplomatic marriages.

Unlike the Italian Renaissance, the technology and ideas engendered by these Middle Asian societies ultimately did not bear fruit. From Mesopotamia to the Indus, people abandoned cities, long-distance trade ground to a halt, and civilization wilted. The Iranian plateau was particularly hard hit: Virtually no 2nd millennium B.C.E. settlements have been found there.

The crisis seems to have swept from west to east. By 1800 B.C.E., even the Indus metropolises emptied. Most archaeologists believe that a drastic climatic shift—there is evidence of prolonged drought in many areas—fueled the collapse, although experts differ over the roles of disrupted trade or social instability in the spreading calamity. Whereas cities revived in western Iran and Mesopotamia 1000 years later, sites such as Jiroft, Shahdad, Gonur, and Shahr-i Sokhta never recovered.

Although their influence waned, Middle Asia's long-lost settlements are now forcing many archaeologists to ditch the venerable Mesopotamia-centric approach, which Lamberg-Karlovsky declares "utterly demolished."

Not everyone is ready to jump aboard that bandwagon, however, until more evidence emerges about how the Middle Asian cultures interacted. "You clearly have multiple centers," says archaeologist McGuire Gibson of the University of Chicago in Illinois, who has dug in Iraq. "But Mesopotamia is still the dynamo." Philip Kohl, an archaeologist at Wellesley College in Massachusetts, says he is "skeptical of the novelty" behind the Middle Asian discussion, pointing out that most of the finds—with the exception of Jiroft—are not new. And some key players—such as Jean-François Jarrige, director of the Guimet Museum in Paris—missed the Ravenna meeting.

But backed by established scholars such as Tosi, Lamberg-Karlovsky, and Cleuziou, a new generation is staking its academic future on understanding Middle Asian cultures. The ancient mud-brick cities may never draw the crowds that today clog Florence or Venice. But scholars predict that a Middle Asian Renaissance will sweep archaeology. "Watch," Winkelmann says. "We can expect an avalanche of new research to change our view of mankind's first attempt at civilization."

–ANDREW LAWLER

CREDIT: A. LAWLER/SCIENCE

MARINE SCIENCE

Ocean Observing Network Wades Into Swirling U.S. Fiscal Waters

A fledgling integrated monitoring system holds promise for scientists, the fishing industry, and the public—if funding can be sustained

The U.S. ocean science community has long wished it had the resources to monitor the seas as thoroughly as the National Weather Service scans the skies. Last week its ship came in. The National Oceanic and Atmospheric Administration (NOAA) announced the first portion of $21.5 million in competitive grants to lay the groundwork for an Integrated Ocean Observing System (IOOS). But expanding the current network of buoys, radar stations, satellites, and gliders is only part of the challenge. For the system to succeed, scientists must also navigate treacherous budgetary waters in Washington, D.C., and learn to work with other sectors that rely upon ocean data.

Federal officials and scientists envision IOOS as a multiagency, well-connected effort to improve climate predictions, develop better navigational tools, and strengthen the monitoring of marine plants and animals. The current patchwork of instruments runs the gamut from coastal gauges that measure water temperature, currents, and salinity to midocean floats that provide hints of an emerging El Niño. But those instruments operate on varying scales, use different standards, and lack a central unifying plan, according to the U.S. Commission on Ocean Policy, which in 2004 called for an annual U.S. ocean-observing budget of $500 million by 2011. The projects also rely on the largess of individual legislators, who each year have tucked earmarks for these projects into spending measures.

In order to realize their expansive vision, ocean scientists know that they must end their addiction to special funding and become part of an ongoing national initiative. "Moving away from earmarks is something we have to do to mature," says physical oceanographer Eric Terrill of the Scripps Institution of Oceanography at the University of California, San Diego. The so-called pork was needed, say marine researchers, because the projects lacked a home within NOAA's extramural program and because the National Science Foundation has traditionally focused on marine research rather than monitoring. The 2006 NOAA budget, for example, included 10 separate ocean-observing projects funded by earmarks totaling $24 million, including nutrient and weather monitoring in Long Island Sound and buoys that help monitor bacterial levels from sewage off southern California beaches.

In the past, researchers ignored pleas not to lobby for their projects. But this year, the Washington, D.C.–based Consortium for Oceanographic Research and Education (CORE) prevailed on its members to abstain from requesting earmarks in the 2008 spending bills currently before the House and the Senate. "That was not an easy thing for people to do," says CORE's Kevin Wheeler. The change was made easier when the new Democratic majority in Congress decided to strip earmarks from NOAA's 2007 spending bill but not remove the money from the agency's budget. The funds allowed NOAA to run a competitive IOOS grants program this year that attracted 42 proposals. This year, for the first time, the agency endorsed the idea of competitive awards by asking Congress to fund an extramural IOOS program.

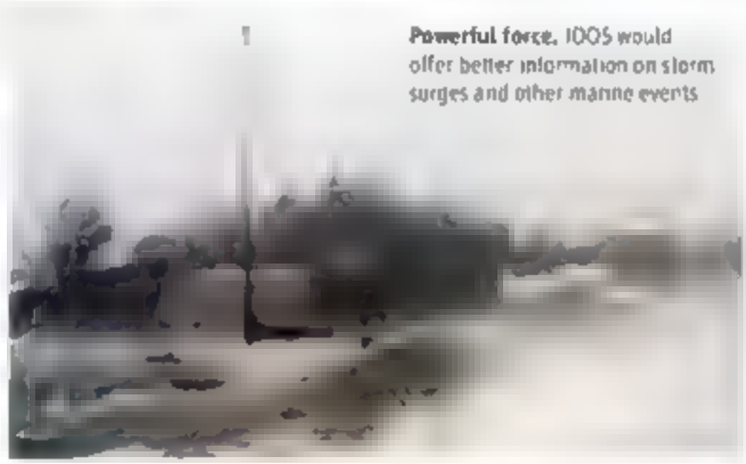

Powerful force. IOOS would offer better information on storm surges and other marine events.

CREDIT: JEAN-PIERRE MOUA/REUTERS

Some withdrawal symptoms have kicked in, however. One, say researchers, is finding the right balance between new observations and maintaining existing facilities. A joint letter by a federation of ocean-observing groups complained that NOAA's competition put too much emphasis on "demonstration projects." Among last week's winners, networks in Alaska, southern California, and Maine each got only one-third of the roughly $2 million they'd come to expect from earmarks, and Terrill says he may need to pull two buoys that have helped monitor the relation between climate and biological life off the coasts of Santa Barbara and San Diego. NOAA has already said it will tweak next year's competition to focus on "sustainment."

Getting the disparate ocean watchers to cooperate is another problem. Scientists, marine officials, and seafaring industries have organized into 11 regional associations along the U.S. coasts in an attempt to coordinate their research and observational needs. A group monitoring the Gulf of Mexico has managed to do that, says its leader, physical oceanographer Worth Nowlin of Texas A&M University in College Station, but it was a struggle. He says that some of the oil companies that fund monitoring systems agreed to share their data only after "intervention" by the U.S. Minerals Management Service, a partner in IOOS.

A third challenge is to sustain growth in the relatively modest ocean-sensing budget during a budget cycle that promises to be extremely contentious. "The [NOAA] competition was good, but the agency didn't have enough money," says Representative Thomas Allen (D-ME), who has introduced a bill, without a price tag, that would authorize a "coordinated, comprehensive" IOOS. A similar Senate bill puts the figure at $150 million annually through 2012.

The fight over NOAA's 2008 budget, for the fiscal year beginning 1 October, reflects that pressure. Citing concerns about the size of the overall budget, the White House has threatened to veto both Senate and House versions of the spending bills, which would give IOOS $50 million and $14 million, respectively. The latter amount matches NOAA's request for the program.

But supporters remain optimistic. They believe the network's ability to build lasting ties between scientists and the government is well worth the modest investment. As an example, NOAA's Jonathan Phinney lauds the "equal partnership" between federal fishery managers and academic oceanographers in an IOOS-funded study of how sardines might be affected by Pacific currents altered by climate change. "That's the only way we're going to move forward," says Phinney.

—ELI KINTISCH

PROFILE PILAI POONSWAD

Subduing Poachers, Ducking Insurgents to Save a Splendid Bird

Biologist Pilai Poonswad has earned praise for reaching out to southern Thailand's alienated Islamic communities in an effort to observe and preserve hornbills

NARATHIWAT, THAILAND—Two soldiers in dark-green fatigues and camouflage flak jackets creep through the grass in a highway median, searching for bombs. Tensions are high this morning in Narathiwat, one of three restive provinces in southern Thailand beset by an Islamic insurgency. The day before, a district official and an army colonel were killed by a roadside bomb. "I do not feel safe," confesses Pilai Poonswad, after passing the third such army patrol. The soldiers are prime targets, merely being in their vicinity entails risk, she says.

The relief is palpable as the silver pickup truck emblazoned with the Thailand Hornbill Project logo turns off on a dirt road and pulls into a village. Pilai, Southeast Asia's foremost authority on hornbills—the "canaries in the coal mine" of tropical rain forests—joins a few colleagues and a dozen men sitting cross-legged in a circle in a gazebo. The powwow begins, as the men chime in with reports on the hornbills and nests they are tracking. In Thailand, nearly half of all hornbill habitat has been logged out or converted to plantations, and this forested swath of the Kra Isthmus is one of the few areas left with adequate intact forest to support healthy populations. Data from farther south in the province, near the Malaysian border, are second-hand. Pilai urged spotters from that area not to venture out on dangerous roads.

The bird watchers have mixed news. Helmeted hornbills (*Buceros vigil*), which are choosier than other species about nesting sites, are clearly on the ropes, and white-crowned hornbills (*Berenicornis comatus*) are vanishing. But four others—the great hornbill (*Buceros bicornis*), the rhinoceros hornbill (*Buceros rhinoceros*), the wreathed hornbill (*Rhyticeros undulatus*), and the bushy-crested hornbill (*Anorrhinus galeritus*)—are rebounding. "We're seeing a steady increase in fledglings from year to year," Pilai says. In Budo-Sungai Padi National Park, some 40 breeding pairs of the six species are visited twice weekly by the villagers, most of whom once poached chicks for the illicit wildlife trade or engaged in illegal logging. These days, their subsistence incomes are increased by the hornbill project, which pays them to observe the birds.

The Thailand Hornbill Project, conceived and led by Pilai, 61, is hailed as a smashing success both for its efforts to preserve hornbills and for reaching out to Islamic communities in this predominantly Buddhist nation. And it has earned Pilai international acclaim, culminating in two major accolades in the past year: a Chevron Conservation Award and a Rolex Award for Enterprise.

"Pilai is an icon for indigenous Asian science," says Alan Kemp, a hornbill expert at the Percy FitzPatrick Institute of African Ornithology in Cape Town, South Africa. Timothy Laman, an ornithologist at Harvard University, told Rolex, "I have never met an individual who has had so much impact on conservation in their country."

Looking up. Rhinoceros hornbill numbers are on the rise.

Despite Pilai's efforts, however, the plight of hornbills in Thailand, home to 13 of Asia's 31 species, is more precarious than ever. Over the past year, the insurgency has grown in tenacity. Pilai, who spends most of her time in Bangkok, frets whenever she hears about violence in Narathiwat, 745 kilometers to the south. She fears for the safety of her local staff and the village birders, without whom the project would unravel. And the hornbills themselves are under rising pressure from illegal logging. "That's the biggest threat," says Pilai. Because felling trees is lucrative and easier than poaching, it's hard to persuade loggers to desist for hornbills' sake. "I told my team not to confront loggers," says Pilai. "Certain people I can convince, but not others."

Winning southern hearts

From the beginning of her university studies, Pilai intended to be a science teacher. She dabbled in nuclear physics before settling down in parasitology, which she still teaches at Mahidol University in Bangkok. She might never have studied hornbills if it weren't for a BBC filmmaker who hired her as an adviser and guide in Khao Yai National Park in central Thailand in 1978. Pilai knew the terrain well and volunteered to take him to where she'd seen hornbill flocks. But it was the start of breeding season, and she did not realize that the hornbills had dispersed into mating pairs. "I failed the first time out," Pilai says. But she persisted and tracked a foraging great hornbill male to its nest.

Kemp, for one, appreciates the rigors of fieldwork in Southeast Asia. In 1974, when he was setting off for 5 months of research in Borneo and India, the late Elliott McClure, a renowned ornithologist, confessed to Kemp how difficult it was to locate hornbill nests in the region—"let alone make any meaningful observations." Kemp, who by then had recorded nearly 200 nests in South Africa's Kruger National Park, managed to find a single nest in Borneo's rain forests. "Fast-forward to Thailand in 1991, my first meeting with Pilai," says Kemp, an honorary curator at Transvaal Museum in Pretoria. "She showed me some of her 70 nests in Khao Yai, and hundreds of hours of field data for both breeding and nonbreeding hornbills." In Kemp's view, Pilai proved that with "determination and forest skills, it is possible to obtain sufficient observations and nesting records of hornbills to do good science."

The more Pilai learned about hornbills, the more entranced she became. (Pilai admits she has an obsessive personality, and one obsession is food. She bemoans the shrinking Thai palate and pines for the wider variety of fruits and delicacies available in her youth.) Hornbills are known for their sometimes brightly colored casques—protrusions above the beak that may help dissipate excess body heat—and wingspans reaching nearly 2 meters. Hornbill myths abound. Borneo's Iban people, for example, believe that the birds transport the souls of dead people to God. Males are fiercely protective of females and pairs are believed to bond for life, although this remains unconfirmed due to the paucity of long-term observations. "We'd like to see if this is true," Pilai says. During mating, the

CREDIT: ROLEX/THOMAS BERTELSEN

female walls herself into a tree cavity using her feces, mud, and regurgitated food, leaving the male to forage and otherwise dote until a chick (or chicks, depending on the species) fledges a few months later.

In the early 1990s, fearing that Thai villagers would strip the forests of anything of value, especially in the impoverished south, Pilai decided that remaining a dispassionate scientist was not enough. "I could not sleep. I felt if I did nothing, the hornbills would be lost." She mulled the problem in her office in Bangkok, and in 1994, came to an epiphany: She had to join forces with southern communities. "I knew we had to express our goodwill somehow."

At the first village Pilai visited, her proposal to pay people to observe hornbills was greeted with skepticism. Exasperated, she lashed out. "I said, 'Your children will curse you for destroying the forests.'" After an awkward silence, she recalls, an assistant village chief responded: "There are times I'd like to curse my own parents for what they did to the forest." But Pilai still had to convince Muslim villagers to work with a Buddhist from Bangkok. "I asked them, 'Have you ever seen me or my team take anything but data sheets from here.' 'If you do not want this project, I can easily work somewhere else!'" Since then, Pilai has enlisted bird watchers in 11 Islamic villages. Many are sponsored by Thai families that she has persuaded to "adopt" hornbill nests.

Taking off. After attaching a wing tag, Pilai Poonswad prepares to release a great hornbill, one species that is making a comeback in Thailand.

CREDIT: BOLDT/THOMAS BERTELSEN

Not for the faint-hearted

Trekking into the backcountry of Budo-Sungai Padi National Park, dotted with bauhinia stands ablaze with copper-colored leaves, Pilai pauses to pick up what seems to be an ordinary stick. She snaps it and fragrant cinnamon wafts up. A few minutes later, she grabs what looks like a green mango. "I love picking up fruit to have a close look," she says, before dropping it suddenly. She bends down and points to patches of dark goo on the skin. The fruit is a nasty cousin of mango with toxic resin, one of the few hazards in the park, the prime one being snakes.

After an hour's hike, Pilai, accompanied by her local project manager and a village birder, reach a blind that had been fashioned from branches and palm leaves for observing a nest of a great hornbill—the largest species, with a wingspan that reaches nearly 2 meters—in a Dipterocarp tree 100 or so meters away. The blind is a charred ruin. Pilai can only speculate who might have torched it: insurgents who are rumored to maintain forest hideouts, an army patrol that mistook the blind for an insurgent shelter, or teenage arsonists. No matter who is the culprit, the destruction is a troubling sign. Fortunately, the hornbill pair is doing fine. The chick has already hatched and the parents, at first unsettled by the presence of humans, calm down amid the drone of cicadas and fly off in search of food.

Pilai heads back to camp and the two men, *Science* reporter in tow, press deeper into the forest to check on an artificial nest adopted by a great hornbill pair. The nest is a couple of kilometers away across hilly terrain; great hornbills like to spread out. By late morning, the humid air is stifling and our shirts are drenched in sweat.

As we pause to rest in a glade, we're ambushed by the nastiest, most bloodthirsty creature in the forest. It is half the length of a pinkie and has no arms or legs, but the dreaded land leech attacks with astonishing speed. Leeches cartwheel onto our shoes and bound toward our ankles, seeking flesh. One had latched on earlier and was feasting through my sock. I yank it off, and the bloodstain widens.

After vanquishing the marauders, we approach the artificial nest, strapped to a tree about 20 meters up. Pilai's team began erecting the fiberglass boxes in the park 2 years ago as an option for hornbills that fail to find a suitable home. "The forest is very fragmented at present, and suitable cavities are now the limiting factor for hornbill populations," Pilai says. Two pairs of great hornbills set up house this year in artificial nests. The species is more adaptable than other species and is even known to nest in limestone crevices.

A month ago, the mother had broken out of this nest, and the chick had resealed it; the researchers were expecting it to fledge any day. We find that it has already done so. Debris from the nest wall after the chick wriggled through the gap to the outside lies splattered on the ground around the tree.

Back at park headquarters that evening, Pilai's team welcomes several dozen schoolchildren, nearly all Muslim, for a 3-day hornbill camp. Project members give introductory slide shows about the birds, and the youngsters, most aged between 9 and 12, reciprocate with songs and skits. The next morning they will tromp into the forest to observe the nest near the burned blind. The walls of three local schools are adorned with hornbill scenes painted by the children. Pilai believes these kids will care about hornbills all their lives.

What Pilai takes the greatest pride in, she says, is that "the former poachers never go back to poaching." These days, anyone who dares to do so suffers the wrath of the community. Recently, a man from another village tried to snatch a hornbill chick but was attacked viciously by the baby's father. Little did he know that he was tangling with a helmeted hornbill—a species known for its aggressive aerial jousts. Wounds from the hornbill's beak required 10 stitches—"and the villagers cursed him," Pilai says. "If only they would curse illegal loggers, too." There's nothing she can do if someone were to skulk into the forest and cut down a nesting tree. Even Pilai's obsession for hornbills cannot save the magnificent birds—if there's no place left to nest. **–RICHARD STONE**

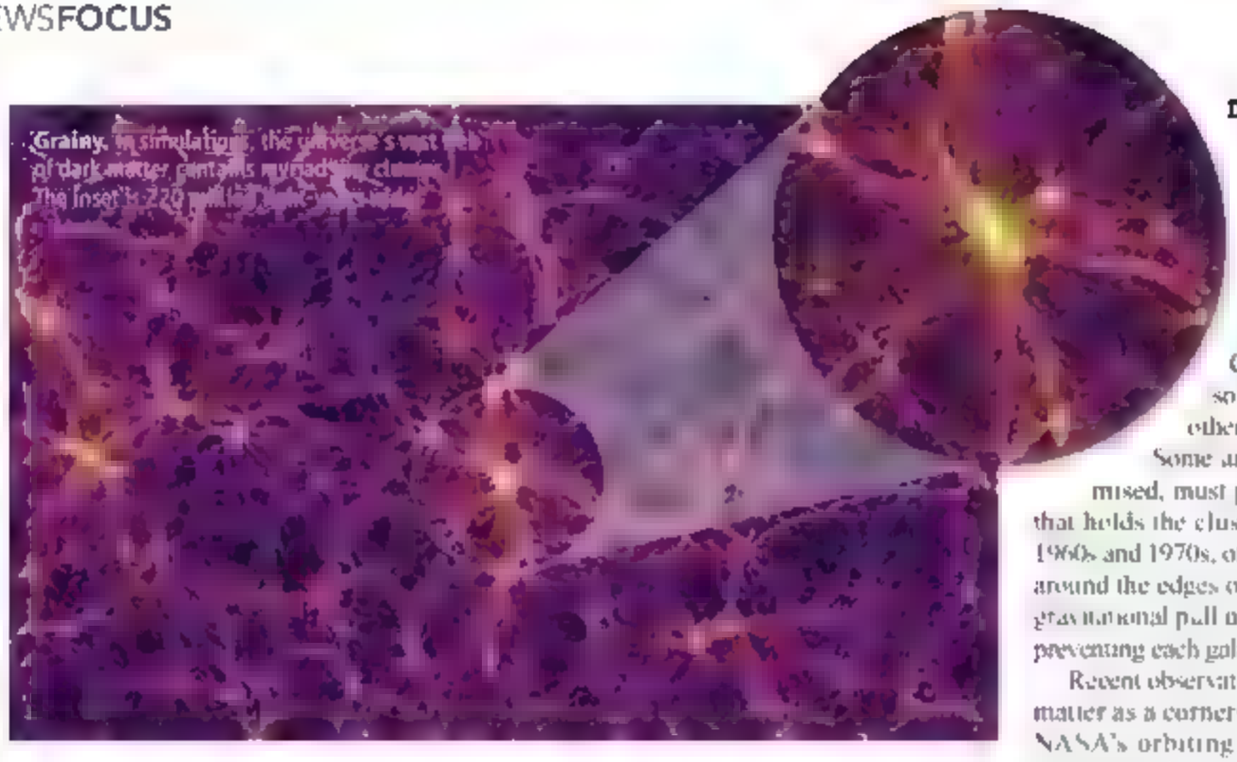

Grainy. In simulations, the universe's vast web of dark matter contains myriad tiny clumps. The inset is 220 million light-years across.

ASTRONOMY

Where Are the Invisible Galaxies?

Cosmology predicts an abundance of small galaxies made entirely of dark matter, but astronomers haven't found any yet

CARDIFF, UNITED KINGDOM—Whorls of innumerable stars, galaxies shine across the boundless darkness, their ancient light recording the nature and history of the universe. So entwined are the notions of star light and galaxy that one might expect astronomers and astrophysicists to snicker at the seemingly absurd idea of a dark galaxy—one devoid of light and stars. But many say that such things must abound, and 92 researchers gathered here recently to hash out both how to detect them and whether the fact that they haven't seen any poses a serious challenge to some fundamental theories.*

The questions have been foisted upon astronomers by cosmologists and their understanding of how the universe blossomed from the big bang. According to the increasingly refined theory, 85% of the matter in the universe is not the ordinary matter that makes up stars and galaxies, planets and people. Rather it is elusive dark matter that so far has revealed itself only through its gravity. As the infant universe grew, the dark matter condensed into enormous filaments and clumps, or "halos." These weighty objects pulled in hydrogen gas, which formed stars and galaxies.

But there's a catch. Simulations show that dark matter should have formed myriad clumps between 1/1000 and 1/1,000,000 as massive as the Milky Way galaxy. At first blush, these small halos should have accumulated gas and lit up as small "dwarf galaxies," thousands of which should whiz around the Milky Way. So far, astronomers have spotted only a few dozen nearby, although they're finding more. Various factors may have kept the small halos dark. But then space ought to teem with tiny dark galaxies, and astronomers have yet to find any. "If they don't exist, then it's an enormous problem for astrophysics," says Jonathan Davies, an astronomer at Cardiff University in the U.K.

But other astronomers say the so-called missing satellites problem is an artifact of the simulations, which do not account for how individual galaxies form. Instead, the simulations track the evolution of dark matter alone and then "paint" the galaxies onto filaments and clumps. "It could simply be that the assumptions that go into the [computer] code are wrong, and that if you do dark-matter-only simulations you get the wrong answers," says Albert Bosma of the Marseille Observatory in France.

Complicating matters, researchers do not agree on precisely what a dark galaxy is. Polite disagreement escalates to acrimony when discussion turns to the question of whether one group has actually spotted one.

* International Astronomical Union Symposium 244 Dark Galaxies and Lost Baryons, 25–29 June

Dark galaxies galore

Dark matter was dreamt up 70 years ago. In 1933, Fritz Zwicky, an astronomer at the California Institute of Technology in Pasadena, noted that some galaxies in the Coma cluster were moving so fast that the gravity of the others could not rein them in. Some unseen dark matter, he surmised, must provide the extra gravity that holds the cluster together. Then in the 1960s and 1970s, others found that stars whiz around the edges of galaxies so fast that the gravitational pull of dark matter seems to be preventing each galaxy from flying apart.

Recent observations have established dark matter as a cornerstone of cosmology, too. NASA's orbiting Wilkinson Microwave Anisotropy Probe (WMAP) has mapped in exquisite detail the afterglow of the big bang, the cosmic microwave background radiation. The temperature of the microwaves varies slightly across the sky, and the pattern reveals much about how the universe evolved. In 2003, WMAP researchers found they could account for the pattern if the universe contains precisely 4% ordinary matter, 23% dark matter, and 73% a mysterious space-stretching dark energy.

But even before then, theorists knew dark matter caused problems on smaller scales. The stuff acts like a weighty, frictionless fluid, which is easy to model. Since the 1990s, simulations have shown that it should form a multitude of small clumps. "The simulations predict that there should be thousands of dark galaxies in the halo of the Milky Way," says Carlos Frenk, a cosmologist at Durham University in the U.K. and a co-author of the state-of-the-art Millennium Simulation. "If they are not there, then the fundamentals of cold dark matter are wrong."

Discounting that possibility, theorists have tried to explain why small dark-matter halos might not evolve into visible galaxies. Ultraviolet light from the first stars should have ionized and heated the hydrogen in small clumps, preventing it from condensing into stars. Alternatively, small halos may have formed massive stars that quickly blew up in supernova explosions, blasting the remaining hydrogen into space and leaving the clumps barren. Together, the mechanisms resolve the discrepancy between the number of predicted and observed dwarf galaxies, Frenk says.

That explanation strikes some as a just-so story. Erwin de Blok of the University of Cape Town, South Africa, distrusts the simulations that predict large numbers of small halos.

CREDITS: (TOP TO BOTTOM) V. SPRINGEL/MPA GARCHING

Using the Very Large Array of radio telescopes in New Mexico, he and colleagues measured the speeds of stars in 35 galaxies and found that the simulations do not precisely reproduce the velocity distributions—the very things that dark matter was originally supposed to explain. That discrepancy suggests dark-matter-only simulations are reliable only on scales larger than galaxies, de Blok says. "Once you go to small scales, then you have to take into account the physics" of ordinary matter, he says.

Spotting the invisible

Ultimately, observations will reveal whether dark galaxies abound. Much effort has focused on radio astronomy. Dark halos might collect some atomic hydrogen, which emits radio waves of a distinct wavelength, 21 centimeters. So a dark galaxy should appear as a starless source of such hydrogen-line or HI, radiation. Astronomers have used the 64-meter dish at the Parkes Observatory in Australia to search for HI sources in the HI Parkes All-Sky Survey (HIPASS). They spotted 4315, and simulations suggested that 86 of them should be dark galaxies.

But all but a couple of the sources are associated with galaxies, the team reported 2 years ago. "That's a very big surprise," says Michael Disney of Cardiff University, who worked on HIPASS. However dark and ordinary galaxies might often line up in the sky by chance. "That leaves room for dark galaxies even though it appears that there aren't any," Disney says. More sensitive surveys called ALFALFA and AGES are under way at the Arecibo Observatory in Puerto Rico.

Others hope to track down dark galaxies by their gravity. Gravity from one galaxy can bend the light of another behind it so that the farther galaxy appears as a ring around the nearer one, an effect known as strong lensing. The details of the ring depend on the distribution of matter in the nearer galaxy and might reveal small dark galaxies orbiting it, says Leon Koopmans of the University of Groningen in the Netherlands. Since 2003, he and colleagues have spotted more than three dozen rings in data from the Sloan Digital Sky Survey, which uses a 2.5-meter telescope at Apache Point, New Mexico, and from the Hubble Space Telescope. They hope to finish the analysis within 2 years.

Some researchers aim to spot dark galaxies crashing into ordinary ones. Galaxies collide and tear one another in so-called tidal interactions, and about 8% of galaxies exhibit such damage. If dark galaxies are as common as ordinary ones, then the same fraction of seemingly isolated galaxies should have collided with invisible dark galaxies, reasons Igor Karachentsev of the Special Astrophysical Observatory of the Russian Academy of Sciences in the Republic of Karachay-Cherkessia. But analyzing about 1500 isolated galaxies from three catalogs, he found that only nine or 0.6% showed signs of a collision, suggesting that dark galaxies are rare.

Even as astronomers hunt for dark galaxies, they disagree about exactly what they're looking for. Some, such as Cardiff's Davies, say that a dark galaxy is anything dark with the mass of a galaxy. Others say that cannot be definition could include simple clouds of ordinary gas. Edward Taylor of Leiden University in the Netherlands says a dark galaxy is an ancient dark halo that collected hydrogen but never formed stars. That more specific definition appeals to many, but it may not be very helpful, either. Even Taylor says he's "fundamentally convinced that such objects do not exist." His theoretical work shows that any dark halo massive enough to collect hydrogen will eventually produce stars, too.

Object of contention. VIRGOHI 21 shines only in radio waves, shown in red contours. It could be a dark galaxy—or just debris ripped from galaxy NGC 4254.

CREDIT: R. MINCHIN/STSCI DIGITIZED SKY SURVEY/NASA/ESA

The murky case of VIRGOHI 21

The debate over the definition of a dark galaxy pales in comparison to the dispute over whether one has been spotted. In 2001, Davies, Disney, and colleagues used the Jodrell Bank radio telescope in Macclesfield, U.K., to detect an HI source that shone no visible light in the Virgo cluster about 50 million light-years away. They dubbed it VIRGOHI 21 and in 2005 they argued that its spectrum suggests it is a rotating dark galaxy that has snatched hydrogen from a nearby galaxy called NGC 4254. Images taken more recently with the Westerbork Synthesis Radio Telescope near Hoogbalen, the Netherlands, bolster their claim, they say.

But others doubt that interpretation, and only recently has a paper laying it out been accepted for publication in *The Astrophysical Journal*. Researchers working with the massive 305-meter radio dish at Arecibo have studied VIRGOHI 21 and believe it is part of a much longer stream of material ripped out of NGC 4254 by an ordinary galaxy passing at high speed. "What you're looking at is most likely the result of a tidal encounter," says Riccardo Giovanelli of Cornell University. Pierre-Alain Duc of the French Atomic Energy Commission in Saclay has used a computer to show he can model the collision.

Davies says he claims only that VIRGOHI 21 *could* be a dark galaxy. Disney goes further. "If you try to model it as tidal debris, you can't," he says. "When you look at the simulations in detail, they do not work." Such pronouncements elicit grumbles. "This is not true and it's not fair," says Brent Tully, an astronomer at the University of Hawaii, Manoa. "There are referees [for the paper] in this room. I was a referee—and I am sorry, but you didn't convince me."

Regardless of whether VIRGOHI 21 is a dark galaxy, closer to home the missing satellites problem appears slightly less alarming than it did a few years ago. Astronomers keep spotting new dwarf galaxies on the periphery of the Milky Way, narrowing the gap between the number predicted and the number observed. The Sloan survey, which covers a fifth of the sky, has identified 51, reports Eva Grebel of the University of Heidelberg in Germany. Using Sloan data and the Keck II telescope in Mauna Kea, Hawaii, Mirla Geha of the Herzberg Institute of Astrophysics in Victoria, Canada, and a colleague found eight more. "Adding these in, the problem is at least eased," Geha says.

Eased but not solved. "More and more of these objects will be found," Grebel predicts, but "probably not enough to solve the missing satellites problem." She estimates that astronomers still see only 1/5 as many spiral galaxies as the dark-matter simulations predict.

That suggests there are lots of truly dark galaxies out there. Astronomers will surely continue to look for them. After all, a dark galaxy would shine new light on the universe and glory upon its discoverer. **–ADRIAN CHO**

598 604

LETTERS | BOOKS | POLICY FORUM | EDUCATION FORUM | PERSPECTIVES

LETTERS

edited by Etta Kavanagh

Genetics and *The Sopranos*

THE SOPRANOS, THE WIDELY VIEWED HBO TELEVISION SERIES PORTRAYING contemporary Mafia life in New Jersey, recently aired its final episode. Future critics of popular culture who look back on *The Sopranos* years from now may especially appreciate its relatively sophisticated treatment of genetic themes.

By my count, the 86 episodes aired since 1999 include 20 explicit dialogs about genetics. These range from the comical ("Two beautiful kids—you must be proud… yeah, yeah … how about that huh? … I even with our genes.") to dinnertime conversation about the number of nucleotides in a chromosome, to the forensic ("cut him up in the work area" … no more of that DNA.") and the dramatic ("My God, there's nothing holding us together but DNA!").

The most in-depth discussions about heredity occur between the lead character Tony Soprano and his psychiatrist concerning the genetic basis of panic attacks in Tony's family when he discovers that his father suffered from them and that his son does, too ("He has that paternal, rotten [expletive] Soprano gene.").

Most people derive their knowledge of genetics from popular culture (*1*). *The Sopranos*, therefore, may have already shaped the genetic literacy of millions of viewers. Central questions about the relative roles of heredity and environment in human behavior can be examined through the attention paid in this series to "family" themes and discussion of (animal) traits that include depression, panic attacks, and attention deficit disorder, as well as discussions about suicide, criminality, sexual preference, substance abuse, and reproductive cloning. As *The Sopranos* takes its place in the history of American popular culture, its use of genetic dialogs may, in the long run, be recognized as one of its most revealing insights.

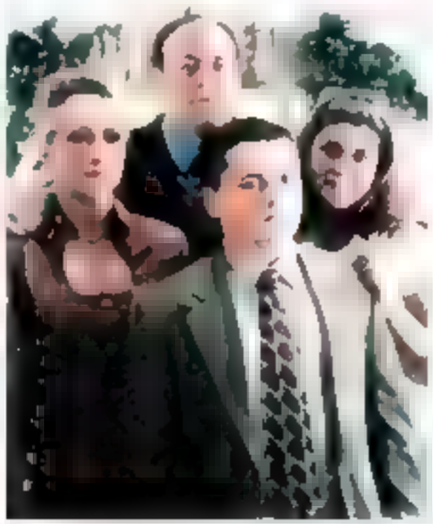

The nuclear Soprano family… celebrating an interesting genetic heritage?

BERNARD P. POSSIDENTE JR.

Biology Department, Skidmore College, Saratoga Springs, NY 12866, USA.

Reference

1. B. Bates, *Public Understand. Sci.* **14**, 47 (2005).

A Less Pessimistic View of U.S. Science Funding

REGARDING J. M. GENTILE'S LETTER "KEEPING the U.S. a world leader in science" (13 July, p. 194), readers would do well to examine my entire address to the AAAS Science Policy Forum (available at www.ostp.gov).

In my talk, I expressed alarm that the nation's research capacity in some fields is outpacing trends in federal research support that have persisted over four decades. It is simply not the case that "the United States has begun to stumble as a world leader in science and technology" or that researchers have been "left high and dry by flat federal funding." We continue to outspend and outperform all other major economies in research, and R&D funding has grown by 56% (from $91 billion to $143 billion) since 2001 (*1*). I certainly agree with Gentile that the capacity exists to do more, and that is the point. In contrast to the federal discretionary budget, whose limits are increasingly constrained by mandated programs, private-sector investments in research and development tend to grow with the economy. They currently exceed federal R&D by a factor of more than two (*2*). Research universities and other institutions are already forming innovative partnerships with state and private-sector entities to augment federal research funding, and this will certainly continue. This is a healthy trend that should be encouraged.

JOHN H. MARBURGER III

Director, Office of Science and Technology Policy, Executive Office of the President, 725 17th Street, NW, Washington, DC 20502, USA.

References

1. AAAS Report XXXIII, "Research & Development FY2008" (AAAS, Washington, DC, 2007), Table I-11, p. 59.
2. National Science Board, "Science and Engineering Indicators 2006: Highlights—National R&D Trends," vol. 1 (NSB 06-01, National Science Foundation, Arlington, VA, 2006), pp. 4–5.

Evolution and Group Selection

I WORRY THAT SOME PSYCHOLOGISTS, UNFAMILIAR with evolutionary biology, will be misled by J. Haidt's account of "The new synthesis in moral psychology" (Reviews, 18 May, p. 998). Haidt claims that whereas "[h]uman group selection was essentially declared off-limits in 1966," it is now accepted that "groups that develop norms, practices, and institutions that elicit more group-beneficial behavior can grow, attract new members, and replace less cooperative groups" (p. 1001). Although it is certainly true that such things

CREDIT: ANTHONY NESTE/THE KOBAL COLLECTION/HBO

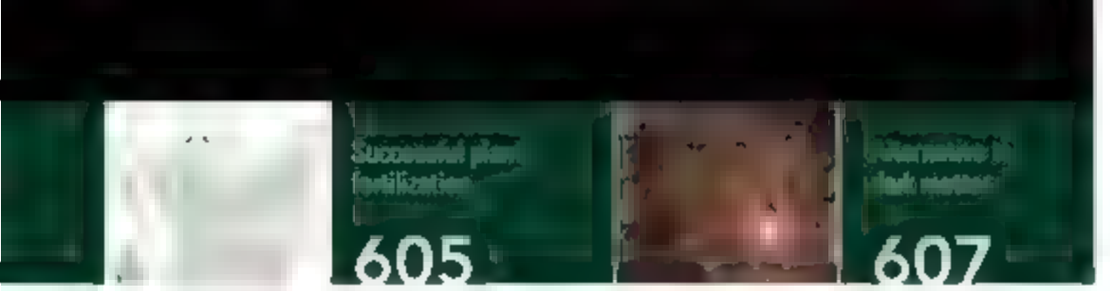

"can" happen. Haidt fails to mention that the overwhelming conviction among evolutionary theorists remains that they are most unlikely, since the selection differential between groups would have to exceed the cost differential experienced by self-sacrificial individuals within groups.

By a rhetorical sleight of hand, after describing D. S. Wilson's group-selection hypothesis for the evolution of religion, Haidt then announces—as though it were fact—that "group selection greatly increased cooperation within the group" (p. 1001). This is pure speculation, not fact, and highly controversial, contrarian speculation at that.

In another case of substituting opinion for reality, Haidt proposes his "Principle 4," arguing for the biological legitimacy of "patriotism, respect for tradition, and a sense of sacredness" (p. 1001). Perhaps, in the future, these supposed components of morality will be found to have genuine evolutionary underpinnings, but for now they seem closer to a political platform plank for the religious right, psychologists interested in achieving a new synthesis by applying evolutionary biology to human morality should bear in mind that just because these notions appeared in a *Science* Review does not make them genuine science.

DAVID P. BARASH

Department of Psychology, University of Washington, Seattle, WA 98195, USA.

Response

BARASH IS CORRECT THAT A SURVEY OF ALL evolutionary theorists would show a great deal of skepticism about group selection. That consensus, however, was forged in the 1960s and 1970s on the basis of some simplifying assumptions, most notably that phenotypes are determined solely by genotypes and that culture can be ignored. Models incorporating these assumptions showed that selection pressures operating at the individual level were almost always stronger than selection pressures operating at the group level, leading to the conclusion that genes for apparently altruistic traits can only spread if those genes are in fact "selfish" (*1*) via one of the two mechanisms of kin selection or reciprocal altruism.

But evolutionary models have become more realistic in recent years. Phenotypes (e.g., cooperator or defector) can now be modeled as joint products of genes, cultural learning, and culturally altered payoff matrices. When culture is included, the old consensus must be reexamined. The time frame shrinks from millennia to years (or less) as groups find culturally innovative ways to police themselves, to increase their phenotypic homogeneity, to lower the costs of prosocial action, and to increase the size of the pie they then share. Just look at eBay. Its genius was to make the prosocial behaviors of gossip and punishment nearly costless through its feedback systems. The eBay community is an emergent group that wiped out many other auction-related groups, without malice or genetic change. If we limit our survey of evolutionary theorists to those who study humans as cultural creatures and who allow for the bidirectional interplay of genetic and cultural evolution, we find the opposite of Barash's view. Most such theorists believe that cultural group selection has occurred and is occurring, and that such selection might well have shaped human genes whenever culturally altered selection pressures remained constant locally over many centuries. In writing my Review, I ignored the old consensus and drew instead on the new and exciting work of leading theorists such as Richerson and Boyd (*2*), Boehm (*3*), Fehr (*4*), Henrich (*5*), Maynard Smith (*6*), and Wilson (*7*), all of whom believe that natural selection works at multiple levels, including the group level.

As for Barash's final point about conservative morality, I do not believe that descriptive biology confers normative legitimacy. In my Review, I identified some areas of moral life that are highly elaborated in most cultures, but that are disliked by political liberals and dismissed by moral psychologists. I suggested that evolution may have shaped our intuitions about in-groups, authority, and purity, just as it shaped our intuitions about harm and fairness. If Barash believes that this suggestion is irresponsible because it may strengthen the religious right, then he has demonstrated the danger of moralism in science and has inadvertently illustrated all four of the principles that I proposed as comprising the new synthesis in moral psychology.

JONATHAN HAIDT

Department of Psychology, University of Virginia, Charlottesville, VA 22904, USA.

References

1. R. Dawkins, *The Selfish Gene* (Oxford Univ. Press, London, 1976).
2. P. J. Richerson, R. Boyd, *Not by Genes Alone: How Culture Transformed Human Evolution* (Univ. of Chicago Press, Chicago, 2005).
3. C. Boehm, *Hierarchy in the Forest: The Evolution of Egalitarian Behavior* (Harvard Univ. Press, Cambridge, MA, 1999).
4. E. Fehr, U. Fischbacher, *Trends Cogn. Sci.* **8**, 185 (2004).
5. J. Henrich, *J. Econ. Behav. Organ.* **53**, 3 (2004).
6. J. Maynard Smith, E. Szathmary, *The Major Transitions in Evolution* (Oxford Univ. Press, Oxford, 1997).
7. D. S. Wilson, *Darwin's Cathedral: Evolution, Religion, and the Nature of Society* (Univ. of Chicago Press, Chicago, 2002).

Letters to the Editor

Letters (~300 words) discuss material published in *Science* in the previous 3 months or issues of general interest. They can be submitted through the Web (www.submit2science.org) or by regular mail (1200 New York Ave., NW, Washington, DC 20005, USA). Letters are not acknowledged upon receipt, nor are authors generally consulted before publication. Whether published in full or in part, letters are subject to editing for clarity and space.

CORRECTIONS AND CLARIFICATIONS

Reports: "Direct evidence for a parietal-frontal pathway subserving spatial awareness in humans" by M. Thiebaut de Schotten *et al.* (30 September 2005, p. 2226). This study employed a neuroimaging method, diffusion tensor imaging tractography, to identify a fronto-parietal pathway important for spatial awareness. On the basis of the available literature [see, e.g., J. Bogy, *Les hémisphères cerebraux*. Neuroanatomie, Ed. (Springer, Berlin, 1991)] this pathway was labeled as "superior occipito-frontal fasciculus." However, further evidence from the author's laboratory (see Supporting Online Material at www.sciencemag.org/cgi/content/full/317/5838/597/DC1) led them to reconsider this labeling. The authors are now convinced that the pathway likely corresponds to the human homologous of the second branch of the superior longitudinal fasciculus (SLF II), described in the monkey brain by Schmahmann and Pandya [J. D. Schmahmann, D. N. Pandya, *Fiber Pathways of the Brain* (Oxford Univ. Press, New York, 2006)]. In the monkey, the SLF I originates in the caudal inferior parietal lobe (corresponding to the human angular gyrus) and the occipito-parietal area and projects to the dorsolateral prefrontal cortex. This modification does not change the main point of the Report, that damage to the fronto-parietal pathways is important to produce neglect. On the contrary, it renders the results even more consistent with the data reported by Doricchi and Tomaiuolo [F. Doricchi, F. Tomaiuolo, *NeuroReport* **14**, 2239 (2003)], which demonstrated that damage to the SLF in human patients with vascular lesions correlates with the presence of spatial neglect. Future studies on the implication of white matter pathways in human cognition would greatly benefit from a stereotaxic atlas of the white matter tracts in the human brain.

NUCLEAR WEAPONS

Just Another Bomb?

John Krige

"Radar won the war. The atomic bomb ended it." Many scientists are no doubt familiar with this pithy summary of the all-important role that major scientific and technological breakthroughs contributed to the defeat of fascism. It emerged as a counterweight to a hegemonic narrative that elevated nuclear weapons to the decisive instrument of victory in World War II. For years now, historians have insisted on relativizing that narrative even more by focusing on the social context in which war-fighting technologies were implemented. They have reminded us, for example, of operational analyses that helped radar succeed in the field and of the mighty financial and industrial resources that were needed to produce fissile material.

In *Five Days in August*, Michael Gordin highlights another important limitation of the catchphrase: the idea that the bomb ended the war. His fine study shows that several groups of historical actors in summer 1945 were not at all convinced of this. More to the point, he argues that the elevation of the bomb to its special status as a weapon of mass destruction was the product of a consensus that was gradually built after the bombs were used and their effects were evident. This consensus congealed into the master narrative mentioned above. Put differently, what Gordin argues is that while there is a tendency now to place the emphasis on the atomic aspect of Little Boy and Fat Man, at the time they were seen by many as just another, if more powerful, bomb.

Gordin's main point of access to this argument is the strategic plans of the military in the Pacific theater and the preparations on the island of Tinian for the air assault on Japan. Tinian is situated at the bottom tip of an archipelago close to Guam and about 1500 miles from Tokyo. After U.S. forces captured the coral island in late July 1944, the Seabees rapidly transformed it into a massive platform for an air assault on Japan using B-29s. Beginning in early 1945, hundreds of sorties were flown, which reduced one Japanese city after another to a hellish inferno using incendiary bombs. Hiroshima, Nagasaki, and other cities were spared for the atomic weapon. They were to serve as laboratories to evaluate in the field the effects of two different bomb designs and materials (only one of which had been previously tested). For the military engaged in this campaign, and for some scientists, the atomic bomb was a new weapon whose full effects were still not known. They did not assume that nuclear weapons were particularly "special" nor that the bombs that they had would win the war. A huge fleet of over 1000 planes fire-bombed Japanese targets several days after the destruction of Nagasaki. Production plans for more atomic bombs were not halted on 9 August, for fear that the bombs might still be needed to wipe out recalcitrant elements in Japan who refused to accept the terms of surrender negotiated by their authorities.

The bomb did not end the war: it was the Japanese surrender and the subsequent diplomatic negotiations around the peace terms that finally brought an end to hostilities. The atomic bomb undoubtedly played an important role in the thinking of the Japanese military and the emperor. But it cannot be uncritically elevated to the decisive factor, as so many did after the event. It was one consideration among others that included the devastating effects of incendiary bombing, the entry of the Soviet Union into the war hours after Hiroshima, the crippled state of Japanese air defenses, and the demoralized condition of the Japanese army, which could do little to halt the Soviet sweep through Manchuria.

Gordin (a historian of science at Princeton University) has done an excellent job in surveying the diverse views on what happened during those momentous five days in August 1945, in highlighting the different meanings of the atomic bomb for various groups of actors at the time, and in reconstructing the world of scientists, engineers, bomber pilots, and military planners on Tinian. In challenging again simplistic accounts of the role of atomic weapons in ending the war, he has not only made a valuable contribution to the ongoing debate on this issue. By aiming to debunk a still pervasive myth, he has emphasized one important social function of good historiography. He has also cut the ground away from those retroactive reinterpretations that have inflated the significance of atomic weapons to the gadget that ended the war—so justifying their use on a near-prostrate Japan to save American lives or playing down the significance of Japanese war crimes as compared to the horror of Hiroshima.

Gordin is right to insist that in the waning days of WWII many people had to work hard to make atomic bombs into the "special" weapons that would "shock" the Japanese to accept the humiliation of an unconditional surrender. He is right to stress that many postwar reflections on the power of the bombs uncritically assumed that they had always had the special quality that subsequently became their hallmark. However, it is one thing to argue that the unique nature of atomic weapons was not self-evident in August 1945. It is quite another to suggest, as Gordin does, that the continued

Loading the *Enola Gay*. Little Boy, a uranium gun-type bomb, "became obsolete from the moment it detonated" at Hiroshima.

CREDIT: U.S. NATIONAL ARCHIVES

The reviewer is at the School of History, Technology, and Society, Georgia Institute of Technology, 685 Cherry Street NW, Atlanta, GA 30332–0345, USA. E-mail: jon.krige@hts.gatech.edu

perception of these devices as special is as ambiguous as it was then.

We now know far more about the extensive damage caused by nuclear weapons and radiation fallout, not simply to individual victims but to the viability of society itself. We now have guided missiles that can deliver light, lethal nuclear warheads halfway around the globe in minutes rather than hours. Gordin rightly contextualizes and relativizes the boundary between atomic bombs as conventional and as special weapons at the dawn of the nuclear age. But we cannot reasonably extrapolate from that period to today. Fission and fusion bombs are very special weapons, and to allow otherwise is to open a space for an ideological and political agenda that seeks to justify their use now on the grounds that they are just another bomb.

10.1126/science.1144537

NUCLEAR WEAPONS

Moving Toward Security

Christopher F. Chyba

Since 1940, the United States has spent around six trillion dollars on its nuclear weapons program (*1*). Its arsenal still contains about ten thousand nuclear warheads—deployed and in reserve—and Russia has half again as many (*2*). Many hundreds more warheads exist in the arsenals of Great Britain, France, China, India, Pakistan, North Korea, and Israel. What is the point of these nuclear weapons?

During the Cold War the United States had, despite controversies over total warhead numbers and particular delivery systems, a rough consensus answer to this question. The purpose of strategic nuclear weapons was to deter nuclear attack, and perhaps other attacks, against the United States and its allies. In addition, battlefield nuclear weapons were available to stop a Soviet invasion of Western Europe, where NATO would find it difficult to stand up to the Warsaw Pact's larger conventional forces. Deterrence was at the core of U.S. nuclear weapons policy, but this had not been a foregone conclusion. It was rather a choice that the United States made after proposals for international management failed and successive presidents ruled out preventive attacks against nascent Soviet and Chinese nuclear weapons infrastructures (*3*).

It is less clear what role nuclear weapons should serve today, nearly 20 years after the end of the Cold War (*4*). The U.S. Congress is currently wrestling with decisions about nuclear weapons initiatives such as the so-called reliable replacement warhead and the shape of the Department of Energy's nuclear weapons complex for the year 2030. How many fission cores ("pits") will the United States need to produce annually a quarter century from now? Remarkably, Congress has been asked to reach decisions on these issues in the absence of a comprehensive U.S. policy for nuclear weapons. What risks need to be managed by these weapons, what role should the U.S. nuclear stockpile play, how should the size and shape of that stockpile serve U.S. grand strategy for national and international security; and how does this interact with nuclear proliferation? Directions for the answers to all these questions are needed if Congress is to responsibly shape the nuclear complex (*5*).

In *Bomb Scare*, Joseph Cirincione, vice president for national security at the Washington think tank Center for American Progress, describes how we got to this point and suggests solutions to three of our most pressing nuclear problems. Cirincione sketches the familiar history of how the world moved from Einstein's letter to Roosevelt warning of nuclear weapons to today's configuration of nine nuclear powers. More than a history, however this accessible account offers the reader a survey of the political science literature on why states do and do not decide to pursue nuclear weapons. Some very good work has been done on this question, and it is increasingly important to understand as the technical barriers to the manufacture of nuclear weapons slowly fall. Nuclear weapons policy must more than ever factor in these "demand-side" issues of nuclear proliferation.

Although Cirincione worries about the consequences of U.S. nuclear weapons policy under the Bush Administration—he argues that it has had ten key failures, including spurring other countries' nuclear weapons programs—he nevertheless concludes that there is still "quite a bit of good news about the prospects for reducing the threats from nuclear weapons." This is a welcome antidote to the strange confluence of nuclear nonproliferation treaty (NPT) opponents and supporters who together intone that the treaty is about to collapse. Cirincione notes that the NPT is widely considered "one of the most successful security pacts in history." He acknowledges the challenges facing it but finds that "proliferation problems cannot be solved one country at a time." Drawing on an earlier study, he argues that to do so by negotiation rewards proliferators, to do so by regime change would bring bankruptcy and isolation to the United States.

Both approaches risk encouraging nuclear proliferation (*6*). They may be needed in isolated instances, but they cannot be the pillars of a general approach to the problem.

Cirincione's analysis comes just as the U.S. political process is forcing a reconsideration of the purpose of nuclear weapons. Because Article VI of the U.S. Constitution states that ratified treaties are the "supreme Law of the Land," U.S. policy-makers have for decades been subject to the NPT's legal requirement "to pursue negotiations in good faith on effective measures relating to cessation of the nuclear arms race at an early date and to nuclear disarmament, and on a Treaty on general and complete disarmament under strict and effective international control" (*7*). Some of the most senior members of the U.S. foreign policy establishment have recently emphasized this goal as a vital policy objective (*8*). *Bomb Scare* suggests how to move toward this objective and why that movement is important to U.S. national and global security.

The reviewer is in the Department of Astrophysics and at the Woodrow Wilson School of Public and International Affairs, 216 Bendheim Hall, Princeton University, Princeton, NJ 08544, USA. E-mail: cchyba@princeton.edu

References

1. S. I. Schwartz, Ed., *Atomic Audit: The Costs and Consequences of U.S. Nuclear Weapons Since 1940* (Brookings Institution Press, Washington, DC, 1998).
2. J. Cirincione, J. B. Wolfsthal, M. Rajkumar, *Deadly Arsenals: Tracking Weapons of Mass Destruction* (Carnegie Endowment for International Peace, Washington, DC, ed. 2, 2005).
3. D. Holloway, in *U.S. Nuclear Weapons Policy: Confronting Today's Threats*, G. Burns, C. F. Chyba, Eds. (Brookings Institution Press, Washington, DC, 2006), pp. 34–74.
4. S. D. Drell, J. E. Goodby, "What Are Nuclear Weapons For?" (Arms Control Association, Washington, DC, 2005); www.armscontrol.org/pdf/USNW_2005_Drell-Goodby.pdf.
5. C. F. Chyba, in *Breaking the Nuclear Impasse: New Prospects for Security Against Weapons Threats*, J. Laurenti, C. Robichaud, Eds. (Century Foundation, New York, 2007), pp. 51–60.
6. G. Perkovich, J. Mathews, J. Cirincione, R. Gottemoeller, J. Wolfsthal, *Universal Compliance: A Strategy for Nuclear Security* (Carnegie Endowment for International Peace, Washington, DC, 2005).
7. Article VI of the Treaty on the Non-Proliferation of Nuclear Weapons (1970), the text of which can be found at www.state.gov/www/global/arms/treaties/npt1.html.
8. G. P. Shultz, W. J. Perry, H. A. Kissinger, S. Nunn, *Wall Street Journal*, 4 January 2007, p. A15.

10.1126/science.1142695

ETHICS

Identifiability in Genomic Research

Genomic data are unique to the individual and must be managed with care to maintain public trust.

William W. Lowrance and Francis S. Collins

Genomic research can now readily generate data that cover significant portions of the human genome at levels of detail unique to individuals. Data can now be categorized with respect to disease-related genes and linked to clinical, family, and social data. Identifiability, the potential for such data to be associated with specific individuals, is therefore a pivotal concern. Research, health care, police, military, and other DNA and genotype reference collections are growing. Members of the public and its leaders worry about risks of erroneous or malicious identity disclosure and consequent embarrassment, legal or financial ramifications, stigmatization; and or discrimination for insurance, employment, promotion, or loans.

If the data are considered identifiable, they may be covered by informational or genetic privacy laws, with implications for consent and other rights. They may be covered by human-subjects regulations, with implications for oversight. Controlled, conditional release may be required for the data as opposed to open public release. These can all be obstacles to the conduct of health-related research.

In the United States, personal data used in health care and or research are protected by the Common Rule on Protection of Human Subjects (*1*), and the Privacy Rule under the Health Information Portability and Accountability Act (HIPAA) (*2*–*4*). They are also protected by state and other federal laws and regulations. In the European Union (*5*), informational privacy is protected by national laws that implement the Data Protection Directive, such as the U.K. Data Protection Act (1998). Most other countries have similar laws.

How these laws apply specifically, and how adequate they are in the genomic research arena, is not entirely clear. Protection of privacy was among the issues examined by the National Institutes of Health (NIH) in a recent public consultation (*6*).

New Modes of Data Flow

Until recently, most genomic research used data and biospecimens obtained fairly directly, from the data subjects themselves or clinical repositories or specialized research collections. This will continue, as it has many advantages. But now, in efforts to increase the range and quantity of data, large-scale research platforms are being built that assemble, organize, and store data, and sometimes biospecimens, and then distribute these to researchers (see figure). The advantages of such platforms, in addition to scale, are that they can be a robust staging-point for screening data quality, fostering uniformity of data format, and facilitating analysis. Some platforms accumulate data directly (as the Framingham Heart Study does); others assemble them from a variety of sources (as The Cancer Genome Atlas, the Genetic Association Information Network, and the Wellcome Trust Case Control Consortium do and U.K. Biobank will) (*7*). Among the design and governance issues are whether and how to de-identify the data and at what stages to conduct scientific and ethics review.

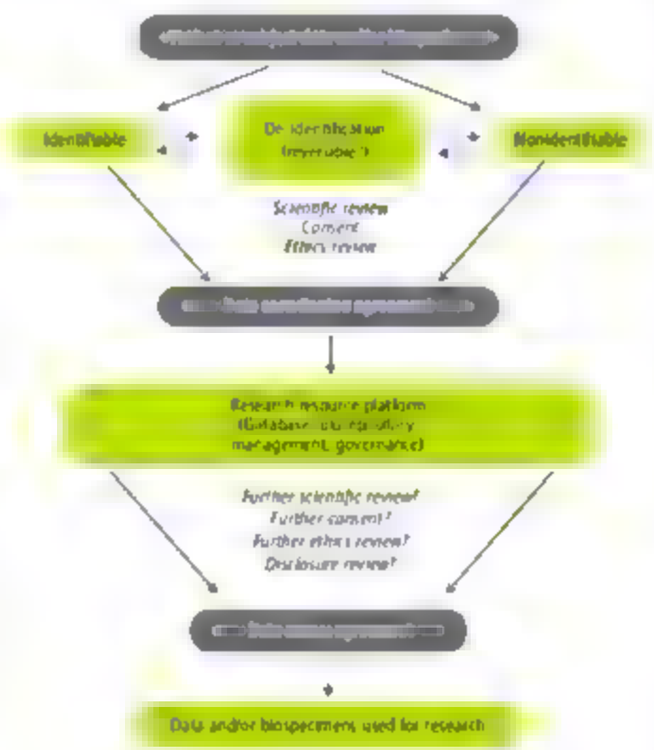

These new data flows, genomewide analyses, and novel arrangements such as the Informed Cohort scheme recently proposed by Kohane *et al.* (*8*) are relatively uncharted territory with respect to human subjects and privacy considerations. Precedent doesn't provide sufficient guidance. For example, the Human Genome and HapMap Projects have genotyped DNA from only a few hundred carefully selected people who prospectively consented to the analysis and to open publication after thorough explanation, discussion and community consultation. The projects have been scrutinized closely all along. But when the data relate to more people (by orders of magnitude) or to retrospective analysis of biospecimens, then for pragmatic reasons such painstaking selection, consent acquisition, and scrutiny can't generally be achieved.

Identifiability and Identifiers

Identifiability ranges from overtly identifiable, to potentially identifiable by deduction, to absolutely unidentifiable. The concept isn't simple, as evidenced by the European Commission's publication of an elaborate "Opinion on the concept of personal data" in June 2007, 12 years after passage of the Data Protection Directive (*9*).

In legal regimens, indirect identifiability is as important as direct. For instance, the HIPAA Privacy Rule applies to "information that identifies an individual, or with respect to which there is a reasonable basis to believe the information can be used to identify the individual" (Sec. 160.103). Similarly, the U.K. Data Protection Act applies to "data which relate to a living individual who can be identified—(a) from those data, or (b) from those data and other information which is in the possession of, or is likely to come into the possession of, the data controller" [Sec. 1.1-(1)]. If

W. W. Lowrance is a consultant in health research policy and ethics, 72 rue de St. Jean, CH-1201 Geneva, Switzerland; e-mail: lowrance@iprolink.ch. F. S. Collins is director, U.S. National Human Genome Research Institute, Bethesda, MD 20892-2152 USA; e-mail: fsc@mail.nih.gov

data aren't identifiable they shouldn't be considered "personal," and a variety of rights and obligations that apply to personal data may not be relevant.

Three sorts of identifying factors can be distinguished: demographic or administrative tags (e.g., name, social security number, e-mail address, hospital name, postal code); overt descriptors (e.g., gender, eye color, height, blood type, scars, asthma), and indirect clues (e.g., medication use, number of children, spouse's occupation, circumstances of emergency-room admission). Whether particular bits of data alone or in combination should be considered sufficient to identify a person is a matter of judgment. Much may depend on whether partial identifiers can be linked with identified or identifiable data in public or other databases.

The HIPAA Privacy Rule illustrates the practical challenges. For data to be considered adequately de-identified and therefore not subject to its provisions, a number of descriptors, which it lists, must be absent [Sec. 164.514(B)(2)] (*7*). The list contains identifiers that are linked fairly directly to name and address, such as medical record numbers or hospital discharge dates. Knowing a few elements on the list may or may not allow identification, and even knowing a person-unique fact such as social security number allows identification only if it can be traced to the person through some other source.

Identifying Through Genomic Data

Matching against reference genotype. The number of DNA markers such as single-nucleotide polymorphisms (SNPs) that are needed to uniquely identify a single person is small. Lin *et al.* estimate that only 30 to 80 SNPs could be sufficient (*10*). Thus, such data can be used, with high certitude, to confirm that two samples come from the same person; whether this can identify anybody in the usual sense depends on whether the reference data are personally identified.

Collections that can be used for matching continue to grow. Identified biospecimens from millions of people are held by criminal justice systems and armed services (*11,12*). Biospecimens and a growing number of genomic analyses are held by health-care, public health, and health research institutions. To be clear, the risk is not that a match might be found but that a de-identified data set will become linkable to a specific person because the matched data set contains personal identifiers.

Linking to nongenetic databases. A second route to identifying genotyped subjects is deduction by linking and then matching genotype-plus-associated data (such as gender, age, or disease being studied) with data in health-care, administrative, criminal, disaster response, or other databases (*10,13,14*). There is no shortage of public and commercial databases about people's lives, especially in the United States. If the nongenetic data are overtly identified, the task is straightforward. Even if such data are not fully identified, inferential narrowing-down may be possible. Statisticians have many techniques for identifying data subjects from partial data (*15,16*).

Profiling from genomic data. A number of physical attributes can now be inferred from DNA analysis, such as gender, blood type, approximate skin pigmentation, and manifestations of Mendelian disorders. Reliability of predictions will likely increase regarding height or other aspects of skeletal build, hair color and texture, eye color, and even some craniofacial features. Soon many chronic disease susceptibilities will be predictable and, before long, some behavioral tendencies will be. In 5 to 10 years, many attributes will be profilable.

Tactics for De-identifying Genomic Data

Limiting the proportion of genome released. The first option is to release only limited segments of genomes, such as sequence traces or a few variants, along with minimum necessary phenotypic or other data. But "how much" is sufficient for identifying, by any route, depends on the region and extent of genome covered, the density of mapping, the rarity of variants, the degree of linkage disequilibrium, and other factors (*17*). This makes it difficult to develop general guidance on how much to expose publicly.

Many projects do limit the portion of genome they release, especially if the release is unrestricted. Precautions can be taken, such as releasing sequence traces in such a separated manner that no individual's data can be reassembled by overlaps. But releasing too-few SNPs or too-short snippets of sequence may thwart research.

Statistically degrading data. This is possible, for example, by lumping all purines and all pyrimidines. Unfortunately, the occurrence of a T instead of a C in one data cell can mean the difference between disease and health. So for many lines of genomic research, degrading data degrades usefulness.

Sequestering identifiers via key-coding (reversibly de-identifying) (*7*). This is the method most widely used in health research. Administrative or other overt identifiers are separated from data, but a link is maintained between them via an arbitrary numerical key-code (*18*). Held securely and separately, the key allows reassociation of substantive data with identifiers if necessary. The key and responsibility for its use can be delegated to a trusted party; its use can be guided by agreed-upon criteria and subjected to oversight.

Provision of Access to Data

Open versus controlled release. A cultural habit of rapid, open release of genomic data has been pursued by the involved scientists and institutions since the beginning of the Human Genome Project (*19–20*). There is no question about the research advantages of such principles and policies. But almost certainly, the principles will have to be modified now for databases that include extensive genotypic information, to heighten the protection of identifiability (*21*).

Open data release, as with deposition in a publicly accessible Web site, is acceptable only if either (i) the data are for all practical purposes not identifiable; or (ii) consent to the release is ethically legitimate and is granted by the data subjects, or the necessity for consent is waived by a competent ethics body. Most projects now take three precautionary steps: sequestering the standard identifiers via key-coding, performing disclosure risk-reduction (such as by rounding birth date to year of birth); and providing access to the de-identified data under conditional terms.

Terms of agreements. Data-access agreements (alternatively called "certifications" or "use agreements") cover many matters. Legally they amount to contracts, and they may have to be entered into by researchers' institutions as well as the researchers.

Agreements may set limitations on purposes and uses, allowed users, or other matters covered by consent, either for the whole dataset or for particular data-subjects, and may address how data will be released. They should refer to physical, organizational, and information technology security. They may specify who will be responsible for de-identifying data and may cover key-coding, safeguarding of the key, and criteria for use of the key. They should always state that researchers will make no attempt to identify nonidentified data. They should restrict unauthorized passing on of data and should extend the chain of custody and the accompanying obligations if data are passed on. They may address linking, if linking to other datasets is contemplated that might increase identifiability. Invariably they require that derived data on individuals be protected at least as carefully as the data being provided. They may make access contingent on Institutional Review Board or other ethics committee approval and may specify the stage(s) at

which ethics review should be conducted.

Oversight. Most data-release decisions, including those made by curating principal investigators, are overseen or made by stewardship committees. This not only protects the data subjects, but it tends to maximize data sharing and to protect investigators, hosting institutions, research platforms, and funders from perceptions or acts of favoritism or impropriety.

Extremely restricted access. Examples are data enclaves in which certified researchers perform studies in databases on a special server. Because this can prevent users from taking away or sharing data examined or detailed records of the analysis, and can deter scrutiny by coauthors, manuscript reviewers, or medical products regulators, the approach must be used only as a last resort.

Scaling to Risks

Risks to data subjects, to data stewards, to researchers and their institutions, and even to the genomic research enterprise must be examined. The ease of identifying people from DNA or genomic data, without breaking laws, should not be overstated; it takes competence, perhaps a laboratory equipped for the purpose, computational power, perhaps linking to other data, and determined effort. But some risks are real. Data cordoned off and curated for research can be exposed to external view by deliberate transfer, accidental or careless release, theft, release under court order or law-enforcement demand, and release in response to freedom-of-information (FOI) request.

Data must be de-identified proportionate to reasonably expectable risks. The conditions on release should not be so burdensome as to retard research, but they must be binding. Court orders must be honored, but indiscriminate trawling through databases should be discouraged, and compelled genotype releases should be limited to the data actually needed for the investigation.

Construal of genomic "human subject." If data have been de-identified but include large amounts of genetic information, are the individuals still considered "human subjects"? The answer has important implications for consent, ethics review, and safeguards. McGuire and Gibbs have urged that "genomic sequencing studies should be recognized as human-subjects research and brought unambiguously under the protection of existing federal legislation" (*22*), but this could be unnecessarily extreme. In the United States, the Office of Human Research Protections considers that data or biospecimens collected for one purpose but then key-coded and used secondarily for research are not "individually identifiable," and therefore the research is not human-subjects research (*7*). This is a strong incentive to support de-identification and to de-identify data.

Certificates of confidentiality. These are legal assurances that the NIH and some other agencies can issue that "allow the investigator and others who have access to research records to refuse to disclose identifying information on research participants in any civil, criminal, administrative, legislative, or other proceeding, whether at the federal, state, or local level" (*23*). Their use deserves rigorous evaluation, and they may deserve administrative or legislative buttressing.

Sanctions against breach of access commitments. Generally the experience with controlled access has been positive. But the robustness and enforceability of access arrangements will be tested by the increasing provision of data to recipients who have not had prior relationships with the principal investigators who collected the data, the funding agencies, or the centers that distribute the data. Funders can consider rescinding grant support or denying future support, but they have less recourse against breaches by nongrantees. New legal penalties may be needed.

FOI requests. In a number of countries, most information held by government bodies must be made available to the public upon formal request. But there are limits, including protection against invasion of personal privacy. Given that genotype data, even though key-coded and de-identified, might be identifiable under some current or future circumstances, responses to FOI requests should negotiate to release only data relevant to the particular inquiry and to redact the data on individuals to reduce the risks.

Genetic antidiscrimination laws. As a complement to the protections discussed in this article, several countries have adopted or are considering adopting genetic antidiscrimination laws. An example is the Genetic Information Nondiscrimination Act currently under consideration in the U.S. Congress, which prohibits discrimination on the basis of genetic information with respect to health insurance and employment (*24*).

Conclusion

A proper balance between encouraging genomic research and protecting privacy and confidentiality of research participants will not be easily achieved. Only rarely will a completely open access model be defensible when sufficient amounts of genomic data are present to be unique to the individual. A variety of controlled-access models can be utilized, however, that minimally impede access by qualified investigators and at the same time keep the risk of identifying individuals low. Protection of identifiability is obligatory for maintaining the trust of our most important research partners, the public.

References and Notes

1. "Federal policy for the protection of human subjects," 45 Code of Federal Regulations (CFR) 46 (2005); www.hhs.gov/ohrp/humansubjects/guidance/45cfr46.htm.
2. Department of Health and Human Services, "Medical privacy: National standards to protect the privacy of personal health information," www.hhs.gov/ocr/hipaa.
3. National Institutes of Health, "Protecting personal health information in research: Understanding the HIPAA Privacy Rule," http://privacyruleandresearch.nih.gov/pr_02.asp.
4. Congressional Research Service, "Federal protection for human research subjects: An analysis of the Common Rule and its interactions with FDA regulations and the HIPAA privacy rule" (2005); www.fas.org/sgp/crs/misc/RL32909.pdf.
5. European Commission. *Data Protection in the European Union* (EU). www.ec.europa.eu/justice_home/fsj/privacy.
6. Genome-Wide Association Studies, http://grants.nih.gov/grants/gwas/index.htm.
7. Further information can be found in supporting material on *Science* Online.
8. I. S. Kohane *et al.*, *Science* **316**, 836 (2007).
9. EU Data Protection Working Party, "Re: Article 29, Opinion 4/2007 on the concept of personal data," adopted 20 June 2007. http://ec.europa.eu/justice_home/fsj/privacy/docs/wpdocs/2007/wp136_en.pdf.
10. Z. Lin, A. B. Owen, R. B. Altman, *Science* **305**, 183 (2004).
11. J. M. Butler, *J. Forensic Sci.* **51**, 253 (2006).
12. J. M. Butler, *Forensic DNA Typing* (Elsevier, Amsterdam, ed. 2, 2005).
13. B. Malin, L. Sweeney, *Proc. J. Am. Med. Inform. Assoc.* **2000**, 537 (2000); http://privacy.cs.cmu.edu/dataprivacy/projects/genetic/dna1.html.
14. B. Malin, *J. Am. Med. Inform. Assoc.* **12**, 28 (2005).
15. Federal Committee on Statistical Methodology, "Report on statistical disclosure limitation methodology", www.fcsm.gov/working-papers/spwp22.html.
16. American Statistical Association Web site on Privacy, Confidentiality, and Data Security; www.amstat.org/comm/cmtepc.
17. Z. Lin, R. B. Altman, A. B. Owen, *Science* **313**, 441 (2006).
18. W. W. Lowrance, *Learning from Experience: Privacy and the Secondary Use of Data in Health Research* (The Nuffield Trust, London, 2002), especially pp. 32 and 33; www.nuffieldtrust.org.uk/ecomm/files/161207learning.pdf.
19. National Human Genome Research Institute "Reaffirmation and extension of NHGRI rapid data release policies," 2003; www.genome.gov/10506537.
20. Wellcome Trust, "Policy on data management and sharing" (Wellcome Trust, London, January 2007); www.wellcome.ac.uk/doc_WTX035043.html.
21. W. W. Lowrance, *Access to Collections of Data and Materials for Health Research: A Report to the Medical Research Council and The Wellcome Trust* (Wellcome Trust, London, 2006); www.wellcome.ac.uk/doc_WTX030843.html.
22. A. L. McGuire, R. S. Gibbs, *Science* **312**, 370 (2006).
23. National Institutes of Health, Certificates of Confidentiality Kiosk, 28 February 2006. http://grants.nih.gov/grants/policy/coc.
24. H.R. 493, S. 358, 110th Congress, 1st Sess. (2007).

25. This article reflects the deliberations of a 3 to 4 October 2006 workshop on identifiability, which built upon a white paper prepared by W.W.L. Both were supported by the U.S. National Human Genome Research Institute. The authors thank the workshop participants for constructive contributions.

10.1126/science.1147699

CELL BIOLOGY

Proteins That Promote Long Life

Quantitative analysis of proteins in a long-lived worm reveals changes that both increase and shorten life span

Stuart K. Kim

The mysteries of what causes aging and how to extend life span are being tackled by applying evolving technologies to model organisms. The tiny roundworm *Caenorhabditis elegans* has been a powerhouse in this arena. A key breakthrough occurred in 1993, when worms with a mutation in the *daf-2* gene were observed to lead active and healthy lives twice as long as that of normal worms (*1*). Since then the quest to determine what makes these worms live so long has spurred powerful "top-down" genomics or proteomic approaches in wide and unbiased screens of *daf-2* mutants. On page 660 in this issue, Dong *et al.* (*2*) use mass spectrometry to identify quantitative differences in protein levels in *daf-2* versus wild-type worms. The changes in protein abundance not only identify potential longevity factors, but also indicate that *daf-2* may regulate a network of signaling pathways that both increase and decrease life span.

daf-2 encodes an insulin-like growth factor receptor that regulates expression of a large number of target genes that change cellular metabolism and slow the rate of aging in *C. elegans*. Previous approaches to identify signaling proteins acting downstream of DAF-2 have used bioinformatics (*3*), DNA microarrays (*4*–*6*), or chromatin immunoprecipitation (*7*) to identify genes that are regulated by the *daf-2* insulin-like signaling pathway. These studies profiled targets at the transcription level. For the first time, the work by Dong *et al.* profiles targets at the protein level, which are direct gene products.

To identify DAF-2 signaling targets, Dong *et al.* labeled proteins in *daf-2* worms with the stable isotope ^{15}N, and then compared the abundance of the ^{15}N-labeled proteins to that of proteins from wild-type worms containing the normal ^{14}N isotope (see the figure). Peptides labeled with ^{15}N show a slight molecular shift relative to peptides labeled with ^{14}N. Extracts from *daf-2* and wild-type young adult worms were mixed, digested with a protease, and then analyzed by mass spectrometry. In the mixed sample, each peptide generates two peaks representing labeling with either ^{14}N or ^{15}N. If the two peaks are the same size, then the corresponding peptides have the same abundance in *daf-2* and wild-type worms. If the ^{15}N peak is larger, then the protein is more abundant in *daf-2*. Conversely, if the ^{15}N peak is smaller, there is less of the protein in *daf-2*.

In the mass spectrometry analysis, Dong *et al.* identified peaks corresponding to a total of 1685 worm proteins. Of these, 47 proteins had increased abundance and 39 proteins had decreased abundance in the *daf-2* mutant relative to the wild-type worm. One challenge is to develop more powerful mass spectrometry approaches to identify more proteins, because fewer than 10% of worm proteins encoded in the *C. elegans* genome were analyzed in this study.

Dong *et al.* functionally tested seven proteins for their roles in aging by using RNA interference (RNAi) to decrease the activity of the genes that encode them. All seven genes affected life span, indicating their importance as DAF-2 targets for specifying longevity. However, the genetic results were not simple. One might expect that most of the protein changes in the *daf-2* worm are beneficial for life span, in which case the 47 proteins that have increased abundance may slow the rate of aging and the 39 proteins that have decreased expression may accelerate the rate of aging. If so, then reducing the expression of the 47 up-regulated proteins in wild-type worms by RNAi should have an effect opposite to that caused by *daf-2* mutations, resulting in rapid aging. Conversely, reducing the expression of the 39 down-regulated proteins in wild-type worms by RNAi should phenocopy the effect from *daf-2* mutations, resulting in slow aging. Instead of these results, the authors found that RNAi treatment of genes that increase protein expression in *daf-2* worms extends life span slightly, and RNAi treatment of genes that decrease protein expression shortens life span. Thus, the genetic results in wild-type worms are opposite to what might be expected on the basis of protein changes found in *daf-2* mutants.

A possible explanation for these findings is that in addition to beneficial pathways that extend life span, *daf-2* mutations also induce detrimental pathways that shorten life span. There may be a mix of pathways in *daf-2* mutants that either increase or decrease life span, with the net effect being positive. In this case, the seven genes tested with RNAi may be part of compensatory pathways, because the effects on life span were opposite to those seen in *daf-2* mutants. Another possibility is that *daf-2* mutations cause an overall change in the cellular metabolic network that is resistant to age-related degeneration. The change in the network by *daf-2* mutations may consist of small effects on many different genes that act together to make the entire metabolic network more robust. If so, then it may be difficult to recreate the beneficial effect of *daf-2* muta-

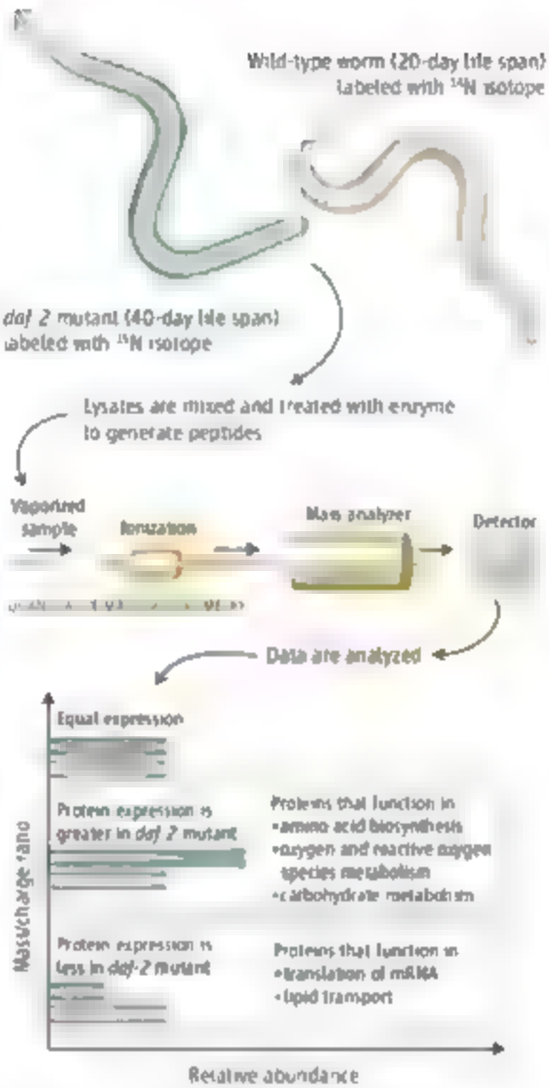

Revealing relevant factors. A mass spectrometry approach quantitates the abundance of proteins in a long-lived worm mutant (*daf-2*), providing clues to the organism's increased life span.

CREDIT: P. HUEY/SCIENCE

The author is in the Departments of Developmental Biology and Genetics, Stanford University Medical Center, Stanford, CA 94305–5329, USA. E-mail: kim@cmgm.stanford.edu

tions by using RNAi, because this strategy inactivates a single gene rather than fine-tuning many genes in the network as in *daf-2* mutants.

Now that proteomics approaches are beginning to define molecular changes associated with extreme longevity, a future challenge will be to understand how the myriad changes interact to double life span in *C. elegans*. Genetic and biochemical studies can be used to analyze the role of each of the protein targets of DAF-2 found in this study. It should also be possible to combine data from gene expression and proteomics studies about changes in *daf-2* mutants. Analysis of the integrated gene and protein network may reveal new trends in *daf-2* mutants that can slow aging.

References

1. C. Kenyon, J. Chang, E. Gensch, A. Rudner, R. Tabtiang, *Nature* **366**, 461 (1993).
2. M.-Q. Dong *et al.*, *Science* **317**, 660 (2007).
3. S. S. Lee, S. Kennedy, A. C. Tolonen, G. Ruvkun, *Science* **300**, 644 (2003).
4. J. McElwee, K. Bubb, J. H. Thomas, *Aging Cell* **2**, 111 (2003).
5. J. J. McElwee, E. Schuster, E. Blanc, J. Thornton, D. Gems, *Mech. Ageing Dev.* **127**, 458 (2006).
6. C. T. Murphy *et al.*, *Nature* **424**, 277 (2003).
7. S. W. Oh *et al.*, *Nat. Genet.* **38**, 251 (2006).

10.1126/science.1146805

MATERIALS SCIENCE

Micelles Made to Order

Precise control over the molecular structure of cylindrical micelles yields novel supramolecular architectures.

Marc A. Hillmyer

Covalently connecting two distinct polymer segments at their ends results in the formation of a class of hybrid macromolecules called block copolymers (*1*, *2*). Placed in a solvent in which one segment is soluble and the other is not, these "amphiphilic" block copolymers will self-organize into supramolecular micelles, with insoluble cores shielded from the solvent by a corona formed by the soluble segments. The most common micellar structure consists of a spherical core shielded by radiating corona chains. Elongated cylindrical micelles (*3*) or bilayer vesicles (similar to liposomes) can also be realized. The structural and chemical diversity of block copolymer micelles makes them attractive for use in applications as varied as drug delivery, personal care products, and nanolithography (*3*, *4*).

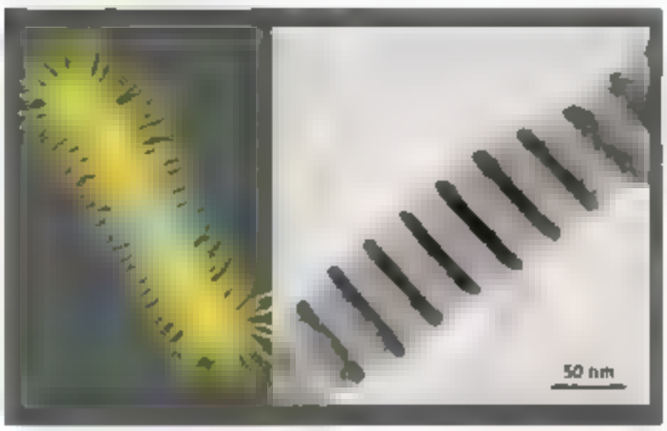

Novel types of micelles. Artist's representation of the cylindrical triblock co-micelle made by Wang *et al.* (**left**) and electron micrograph of the gold nanoparticle/block copolymer hybrid cylindrical micelle reported by Cui *et al.* (**right**). The formation of these intricate hybrid micelles demonstrates the power of block copolymer self-assembly in the preparation of novel nanostructured materials.

For these self-assembled soft materials to be most effective in applications, their size, shape, and chemical structure must be controlled precisely. Two reports in this issue describe important advances toward this overarching goal. On page 644, Wang *et al.* (*5*) show how the length and chemical composition of cylindrical block copolymer micelles can be controlled through a novel growth mechanism. And on page 647, Cui *et al.* (*6*) demonstrate that the assembly of appropriately designed triblock terpolymers (which are made from three monomers) can be directed by external agents, yielding exquisite control over the resultant cylindrical nanostructures.

The author is in the Department of Chemistry, University of Minnesota, Minneapolis, MN 55455, USA. E-mail: hillmyer@chem.umn.edu

Of the micellar structures described above, the cylindrical variants (*3*) are particularly attractive for a range of applications, for example, as artificial tissue scaffolds (*7*), in drug delivery (*8*), or to toughen cross-linked polymer resins (thermosets) (*9*). Long worm-like micelles formed by amphiphilic block copolymers are characterized by a distribution of lengths that is determined in part by the energetics of forming end caps (*10*, *11*). It has therefore been difficult to achieve precise control over their mean length (*12*).

Winnik, Manners, and co-workers have reported that block copolymers containing crystalline, organometallic core-forming blocks can form cylindrical micelles (*13*). Wang *et al.* now show how the length of these cylindrical micelles can be controlled. They first prepare a set of relatively short cylindrical micelles of a block copolymer in a selective solvent. They then add the same block copolymer, dissolved in a good solvent for both blocks, to this micellar dispersion. This method results in the controlled growth of the micelles; the more block copolymer provided in this second step, the longer the micelles become.

The linear dependence of average cylinder length on block copolymer added is reminiscent of a living polymerization, a chain polymerization where the average chain length is linearly proportional to the amount of monomer converted to polymer. These crystalline-core micelles probably grow via nucleation of the free block copolymers at the ends of the cylinders. The precise control over the micelle length is remarkable. Like the "living" chains in a typical anionic polymerization, the cylindrical micelles are stable over long periods; when a fresh block copolymer supply is added, they grow again.

Wang *et al.* also investigated the effect of adding a different block copolymer (with the same core-forming crystalline block but a distinct corona block) to preformed cylindrical micelles. The resulting "block co-micelles" contain a cylindrical midsection of one type, flanked on either end by cylindrical assemblies of the other type (see the figure, left panel). These two-component assemblies reveal the power of the growth mechanism. Just as living polymerization paved the way for a diverse array of molecular architectures, the process described by Wang *et al.* will open the door to unprecedented supramolecular assemblies.

In a distinct approach to controlling micellar structure, Cui *et al.* show that the aggregation of discrete micellar assemblies can be precisely manipulated by using appropriate

CREDIT: LEFT PANEL, P. HUEY/SCIENCE; RIGHT PANEL, ADAPTED FROM (*6*)

additives and controlling solvent quality. They show how block copolymer micelles can be coaxed to form supramicellar assemblies with distinct morphologies and chemical compositions. In the specific triblock system used by the authors, the solvent-loving block contains pendant carboxylic acids that can form ionic complexes with amine species. Upon treatment of a mixed aqueous-organic solution of these triblocks with an organic diamine, the authors observed the formation of spherical micelles. By decreasing the relative amount of water in the solution through the addition of organic solvent, these assemblies can be made to controllably aggregate and form long multicompartment cylindrical micelles, with an alternating lamellar structure in the cores of the micelles (*14*, *15*). The control over the growth process and the strikingly uniform striped wormlike micelles demonstrated by Cui *et al.* are extraordinary examples of how this tuning of the kinetic assembly of block copolymer micelles can be exploited.

Cui *et al.* illustrate the versatility of this specific triblock system by replacing the organic diamine with amine-functionalized gold nanoparticles. When the nanoparticles were added to a dispersion of spherical micelles formed from a related ABC triblock terpolymer (where A, B, and C represent chemically distinct segments), the micelles aggregated into segmented cylindrical nanostructures. Alternating organic polymer and gold nanoparticle domains formed along the long axis of the cylindrical domains (see the figure, right panel). In addition, Cui *et al.* report that by combining ABC and A′BC triblocks (where the A and A′ blocks are incompatible with both the solvent and each other) and using similar preparation procedures, undulating cylindrical micelles were produced whose cores contained nanoscopic regions with alternating A-rich and A′-rich domains.

The two reports in this issue demonstrate how the self-assembly of block copolymer amphiphiles can be controlled with unprecedented precision and how the marriage of organic, inorganic, and polymer chemistries (*16*) can yield fascinating new and exotic nanometer-scale assemblies. Control of block copolymer structure at the molecular level is crucial to the discovery of such self-assembled nanostructures, and future technological applications that use block copolymers as key components will undoubtedly benefit from these remarkable advances.

References

1. N. Hadjichristidis, S. Pispas, G. Floudas, *Block Copolymers: Synthetic Strategies, Physical Properties, and Applications* (Wiley-Interscience, New York, 2002).
2. T. P. Lodge, *Macromol. Chem. Phys.* **204**, 265 (2003).
3. R. Zana, E. W. Kaler, Eds., *Giant Micelles: Properties and Applications* (CRC Press, Boca Raton, FL, 2007).
4. J.-F. Gohy, *Adv. Polym. Sci.* **190**, 65 (2005).
5. X. Wang *et al.*, *Science* **317**, 644 (2007).
6. H. Cui, Z. Chen, S. Zhong, K. L. Wooley, D. J. Pochan, *Science* **317**, 647 (2007).
7. J. D. Hartgerink, E. Beniash, S. I. Stupp, *Science* **294**, 1684 (2001).
8. Y. Geng *et al.*, *Nat. Nanotech.* **2**, 249 (2007).
9. J. M. Dean, N. E. Verghese, H. Q. Pham, F. S. Bates, *Macromolecules* **36**, 9267 (2003).
10. Y.-Y. Won, H. T. Davis, F. S. Bates, *Science* **283**, 960 (1999).
11. S. Jain, F. S. Bates, *Science* **300**, 460 (2003).
12. V. Castelletto *et al.*, *Langmuir* **23**, 6896 (2007).
13. J. Massey, K. N. Power, I. Manners, M. A. Winnik, *J. Am. Chem. Soc.* **120**, 9533 (1998).
14. Z. Li, E. Kesselman, Y. Talmon, M. A. Hillmyer, T. P. Lodge, *Science* **306**, 98 (2004).
15. Z. Li, M. A. Hillmyer, T. P. Lodge, *Langmuir* **22**, 9409 (2006).
16. C. J. Hawker, K. L. Wooley, *Science* **309**, 1200 (2005).

10.1126/science.1144899

MATERIALS SCIENCE

Exploiting Wrinkle Formation

A simple method allows the elasticity and thickness of thin polymer films to be determined

Alina F. Miller

Wrinkle formation due to age or stretched skin is seen by many as a nuisance to be avoided, often at great financial expense, rather than as a natural phenomenon to be exploited. Skin wrinkling is just one of many natural processes that involve the formation of wrinkles. For example, plums or apples wrinkle as they become old and dehydrated, fingerprint patterns are a form of wrinkles that appear as early as 10 weeks into a pregnancy, and Earth's crust wrinkles in response to plate tectonics (*1*).

Wrinkles also form on much smaller length scales, for example, on the nanometer to micrometer scale in polymer films. These exquisite patterns have been exploited in the self-assembly of new structures and materials (*2*), have helped to explain fundamental physical phenomena (*3*), and have led to the characterization of physical properties (*4*). On page 650 of this issue, Huang *et al.* (*5*) exploit wrinkle formation of an ultrathin film on a fluid surface to determine film thickness and elasticity.

Wrinkles form when an applied compressive force acts on a rigid skin that rests on a softer foundation. For example, many fruits have a thin outer skin that surrounds a soft hydrated interior. When the fruit ages, water is lost from the interior, and the volume of the fruit decreases. Consequently, there is too much skin, which shrinks and forms wrinkles. Prunes (dried plums) provide an excellent demonstration of this phenomenon (see the photo). Wrinkling also occurs in a thin film on a thick elastic substrate when it is subjected to a uniaxial compressive strain parallel to the interface (see the figure, next page).

Huang *et al.* explored the wrinkling patterns formed under the capillary force exerted by a drop of water placed on a freely floating polymer film. They then used the wrinkle characteristics to develop a simple method to determine film thickness and elasticity. The work represents an exciting leap forward, because the wrinkling of films under capillary forces is relatively unexplored. Moreover, the authors show that the film's properties can be elucidated directly on a fluid surface, using no more than a dish of fluid and a low-magnification microscope.

Huang *et al.* induced wrinkle formation by placing a drop of water on a freely floating polymer film. The resulting wrinkles, observed with a low-magnification microscope, had two characteristic features: the number of wrinkles that emanated from the central load point and their length. These two parameters depend both on the surface tension and radius of the water drop and on the elastic properties of the film.

To investigate the effect of each of these systematically, Huang *et al.* placed water drops of incrementally increasing mass on films of varying thickness and recorded the number and length of the wrinkles formed. As the mass of the drop—and hence its radius—increased, both the number and the length of the wrinkles increased. In addition, as the film became

CREDIT: P. HUEY

The author is in the School of Chemical Engineering and Analytical Science, University of Manchester, Manchester M60 1QD, UK. E-mail: a.miller@manchester.ac.uk

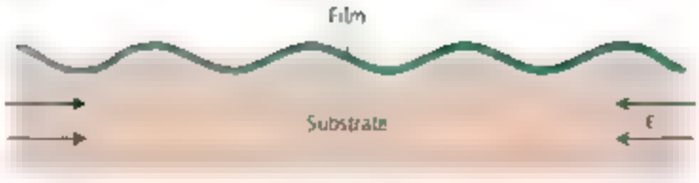

How thin films wrinkle. Wrinkle formation of a thin film in response to a uniaxial compressive strain, ε, parallel to the interface. Similar wrinkles form in the experiments of Huang *et al.*, but in their case, wrinkle patterns radiate from the center of the load.

thicker the number of wrinkles decreased, whereas their length increased. The authors used these results to develop two scaling relationships (one for the length and one for the number of wrinkles), adapting arguments made by Cerda and Mahadevan (*6*, *7*). Combination of these two scaling relationships shows that if the length and number of wrinkles are known from experimental measurement, the elasticity and thickness of the film under study can be determined by a simple calculation.

To validate their method, Huang *et al.* monitored wrinkle formation in polystyrene films that contained different amounts of plasticizer and thus had different elastic properties. Their elasticity data are equivalent to, and in some cases have higher precision than, previously reported data obtained with sophisticated, time-consuming, and expensive techniques, such as stress-induced buckling and nano-indentation (*8*). The authors also show that their calculated film thicknesses are comparable with those obtained from their x-ray reflectivity measurements.

Wrinkle formation, therefore, need not always be regarded as a nuisance. Invaluable information concerning the elasticity and thickness of ultrathin films can be determined simply by measuring the number and length of the wrinkles formed in response to a capillary force. The method developed by Huang *et al.* is not only simple, in contrast to existing techniques, it also allows both elasticity and film thickness to be determined in one easy, quick experiment. Moreover, measurements can be made directly at a fluid surface. The latter not only eliminates the introduction of artifacts but also opens up the possibility of studying dynamical relaxation processes in thin films, a matter of crucial importance for advancing material design and understanding the viscoelastic behavior of numerous biological and soft materials.

References

1. J. Genzer, J. Groenewold, *Soft Matter* **2**, 310 (2006).
2. S. P. Lacour, S. Wagner, Z. Y. Huang, A. Suo, *Appl. Phys. Lett.* **82**, 2404 (2003).
3. X. Efimenko *et al.*, *Nat. Mater.* **4**, 293 (2005).
4. C. M. Stafford *et al.*, *Nat. Mater.* **3**, 545 (2004).
5. J. Huang *et al.*, *Science* **317**, 650 (2007).
6. E. Cerda, K. Ravi-Chander, L. Mahadevan, *Nature* **419**, 579 (2002).
7. E. Cerda, L. Mahadevan, *Phys. Rev. Lett.* **90**, 074302 (2003).
8. C. M. Stafford *et al.*, *Nat. Mater.* **3**, 545 (2004).

10.1126/science.1146680

PLANT SCIENCE

Reproductive Dialog

A protein in ovule cells of a flowering plant recognizes the male pollen tube of the same species, ensuring successful fertilization

Sheila McCormick

Fertilization in higher plants requires intricate signaling between the male and female. The molecular details underlying this communication are of great interest, not only to understand plant reproduction but also to guide efforts in crossing plant species to generate new hybrids. On page 656 of this issue, Escobar-Restrepo *et al.* (*1*) show that cells in the female ovule express a protein—a type of receptor that is widely known to mediate cell-cell communication—that is required for fertilization. The unknown ligand(s) for the receptor may be present on or secreted by the pollen tube. Such a receptor-ligand interaction could control species-specific reproduction.

In flowering plants, the pollen grain (male gametophyte) contains three cells: a vegetative cell that will form the pollen tube, and two sperm cells. After release from the anther and landing on the stigma, the pollen grain extends a tube through the style, toward the ovule (see the figure). Within each ovule, there is an embryo sac (female gametophyte), typically composed of seven cells: an egg cell, a central cell, two synergid cells, and three antipodal cells. The pollen tube enters the ovule through an opening (the micropyle), penetrates one of the synergids, and bursts, thereby releasing the sperm cells. One sperm cell fuses with the egg cell to form a zygote, while the other sperm cell fuses with the central cell to form the primary endosperm cell.

A few years ago, two female gametophytic mutants, *feronia* (*2*) and *sirene* (*3*), were described in the flowering plant *Arabidopsis thaliana*. In these mutant plants, pollen tubes

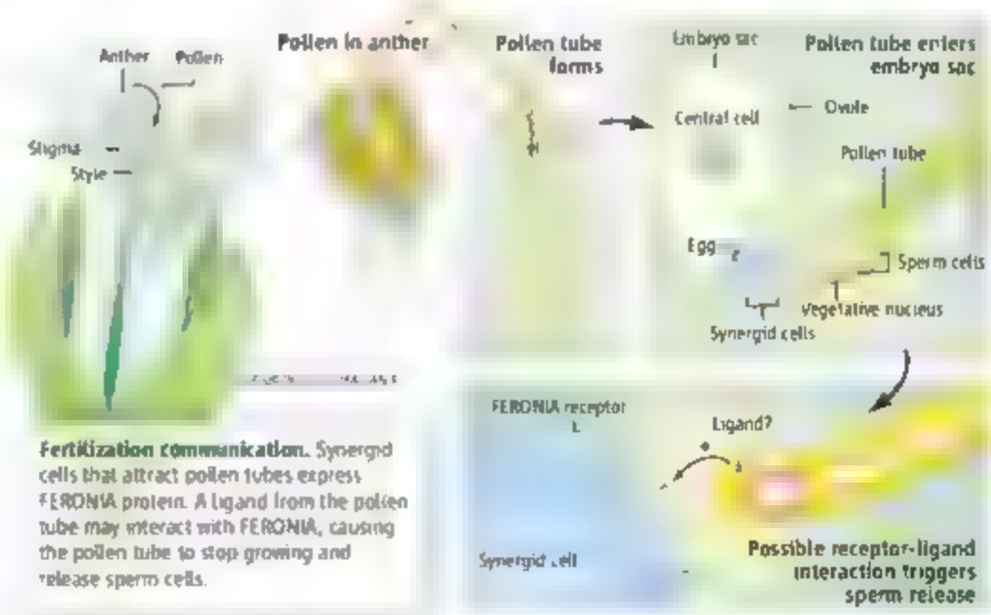

Fertilization communication. Synergid cells that attract pollen tubes express FERONIA protein. A ligand from the pollen tube may interact with FERONIA, causing the pollen tube to stop growing and release sperm cells.

The author is at the Plant Gene Expression Center, USDA Agricultural Research Service–UC Berkeley, 800 Buchanan Street, Albany, CA 94710, USA. E-mail: sheilamc@nature.berkeley.edu

were attracted to ovules and entered the micropyle, but failed to burst and release sperm, continuing to grow instead. This phenotype suggested failed communication between the pollen tube and the embryo sac, but it was not known whether *feronia* and *sirene* affected the same or different components in this dialog. Escobar-Restrepo *et al.* now show that both mutants have lesions in the same gene and that the gene encodes an enzyme that phosphorylates proteins on serine and threonine residues. The enzyme, FERONIA, belongs to the previously uncharacterized CrRLK1L-1 group of receptor-like kinases (*4*), of which there are 15 members in *A. thaliana*. The authors determined that FERONIA is located in the plasma membrane of the synergid cells.

Because the pollen tube overgrowth phenotype resembled that seen after interspecies crosses in *Rhododendron*, Escobar-Restrepo *et al.* tested whether crosses with *A. thaliana* relatives would yield similar phenotypes and thereby implicate FERONIA in interspecies barriers. Indeed, crosses of *A. thaliana* females with *Cardamine flexuosa* pollen or with pollen of a more closely related species, *Arabidopsis lyrata*, yielded a pollen tube overgrowth phenotype. Recent studies suggest that synergid cells secrete a pollen tube attractant (*5*–*7*). In addition, an ovule already targeted by a pollen tube may produce a repellent to ward off additional pollen tubes (*7*). Moreover, these attractants and repellents exhibit some degree of species specificity (*7*, *8*). In both *sirene* and *feronia* mutant plants, some ovules attracted more than one pollen tube (*2*, *3*), perhaps because the attractant persists when the first pollen tube does not burst.

Proteins involved in sexual recognition can show amino acid diversification in regions that interact with a protein from the other sex (*9*) as the proteins evolve to match each other; that is, genes with increased rates of evolution increase the frequency with which incompatibilities evolve between closely related species. Among plants related to *A. thaliana*, the extracellular domain of FERONIA has more nonsynonymous nucleotide changes than the highly conserved kinase domain. This suggests that the presumed ligand-binding region was subject to positive selection and that coevolution between FERONIA and an equivalently diverging ligand could contribute to reproductive isolation.

Escobar-Restrepo *et al.* propose a signaling pathway wherein ligand from the pollen tube interacts with FERONIA, causing the synergid cell to send another signal back to the pollen tube to stop growing and burst (see the figure). Much more information is needed to test this intriguing model. The immediate challenge is to identify the FERONIA ligand. There is no way to guess a priori what it might be; even within the LRR (leucine-rich repeat) receptor kinase group—the best-studied such group in plants—the known ligands are diverse (*10*). Potential ligand-receptor pairs might be identified through screens of mutant plants for similar phenotypes (*11*) such as pollen tube overgrowth. Yeast two-hybrid screens (*12*) are another option, in which the extracellular domain of FERONIA can be used as bait for complementary DNA libraries prepared from germinated pollen tubes.

It will also be important to determine whether disruptions of *FERONIA* homologs in other species give similar phenotypes; if so, the pollen overgrowth phenotype may occur with interspecies crosses in other plant families. It is intriguing that in the cross with *A. lyrata*, 50% of the pollinated *A. thaliana* ovules showed the pollen overgrowth phenotype, whereas the other 50% showed normal fertilization (*1*). Indeed, interspecies crosses with *A. lyrata* are possible (*13*). Escobar-Restrepo *et al.* suggest that there might be different isoforms of the ligand in *A. lyrata* with one allelic variant that recognizes the *A. thaliana* version of FERONIA.

FERONIA and its upstream and downstream signaling partners may be the key to successful sperm discharge. If so, then manipulating the components of this pathway might facilitate more promiscuous hybridizations than occur in nature.

References

1. J.-M. Escobar-Restrepo *et al.*, *Science* **317**, 656 (2007).
2. M. Huck *et al.*, *Development* **130**, 2149 (2003).
3. M. Rotman *et al.*, *Curr. Biol.* **13**, 432 (2003).
4. S. H. Shiu, A. B. Bleecker, *Plant Physiol.* **132**, 530 (2003).
5. T. Higashiyama *et al.*, *Science* **293**, 1480 (2001).
6. M. I. Márton, S. Cordts, J. Broadhvest, T. Dresselhaus, *Science* **307**, 573 (2005).
7. N. Palanivelu, D. Preuss, *BMC Plant Biol.* **6**, 10.1186/1471-2229-6-7 (2006).
8. T. Higashiyama *et al.*, *Plant Physiol.* **142**, 481 (2006).
9. B. E. Galindo, V. D. Vacquier, W. J. Swanson, *Proc. Natl. Acad. Sci. U.S.A.* **100**, 4639 (2003).
10. K. U. Torii, *Int. Rev. Cytol.* **234**, 1 (2004).
11. J. C. Fletcher, *Annu. Rev. Plant Biol.* **53**, 45 (2002).
12. W. Tang *et al.*, *Plant Cell* **14**, 2277 (2002).
13. M. E. Mavrodiev *et al.*, *Plant Physiol.* **124**, 1605 (2000).

10.1126/science.1146655

ASTRONOMY

Seeing Through Dark Matter

Stacy McGaugh

Dark matter was proposed to explain galaxy dynamics. A modification of Newton's law of gravitational force may offer a better explanation.

The universe appears to be dominated by invisible components that astronomers call dark matter and dark energy. The astronomical evidence implicating dark matter has been apparent for a generation (*1*). The rotational speeds of objects in extragalactic systems exceed what can be explained by the visible mass of stars and gas. This discrepancy has led to the inference that there is more mass than meets the eye. However, this inference requires that Newton's law of gravitational force be extrapolated well beyond where it was established. In addition, laboratory searches for dark matter have yet to bear fruit. This lack of corroboration, combined with the increasing complexity and "preposterous" nature of a once simple and elegant cosmology, leads one to wonder if perhaps instead gravity is to blame.

Simply changing the force law on some large length scale does not work (*2*). One idea that has proven surprisingly resilient is the modified Newtonian dynamics (MOND) hypothesized by Milgrom (*3*) in 1983. Rather than change the force law at some large length scale, MOND subtly alters it at a low acceleration scale around 10^{-10} m s^{-2}. In systems with gravitational accelerations above this scale (e.g., Earth, the solar system), everything behaves in a Newtonian sense. It is only when accelerations become tiny, as in the outskirts of galaxies, that the modification becomes apparent.

MOND has successfully described the rotation curves of spiral galaxies (see the figure) (*4*). In case after case, MOND correctly maps the observed mass to the observed dynamics. Why would such a direct mapping exist between visible and total mass if in fact dark matter dominates? Moreover, MOND's explicit predictions for low surface brightness galaxies have been realized (*5*). In contrast, the dark matter paradigm makes less precise predictions (*6*) for rotation curves that persistently disagree with the data (*7*).

The author is at the Department of Astronomy, University of Maryland, College Park, MD 20742-2421, USA. E-mail: ssm@astro.umd.edu

One problem is that researchers have found it difficult to create a version of MOND that satisfies the well-established tests of Einstein's general theory of relativity. This hurdle has now been overcome by Bekenstein (*8*). Testing Bekenstein's approach is in the early stages, but initial results look promising (*9*).

Despite the observational and theoretical successes, the picture for MOND is not all rosy. Many observations purport to falsify MOND, although often the evidence is less compelling than might be hoped. Perhaps the most serious observational challenge is from rich clusters of galaxies. These systems exhibit clear mass discrepancies that MOND fails to completely rectify (*10*). Even after application of the MOND formula, one still infers that there is as much unseen mass in these clusters as can be seen in stars and gas. Consequently, MOND appears to require dark matter itself—a considerable embarrassment for a theory that seeks to supplant the need for invisible mass.

It is tempting to conclude that this is the real dark matter, some fundamentally new type of particle outside the highly successful standard model of particle physics. However, it might just be the result of another missing mass problem in extragalactic astronomy: the missing baryon problem. Our inventory of ordinary matter (baryons)—the stars and gas that we can see directly—falls well short of the amount we expect from big bang nucleosynthesis (*11*). Perhaps the unseen mass required in clusters by MOND is merely these dark baryons. Indeed, this has happened before. For a long time, astronomers thought that most of the ordinary mass in clusters was visible stars. Only relatively recently have we come to appreciate that all the stars in all the cluster galaxies are outweighed by a hot, diffuse gas between them. Still more baryonic mass may await discovery there.

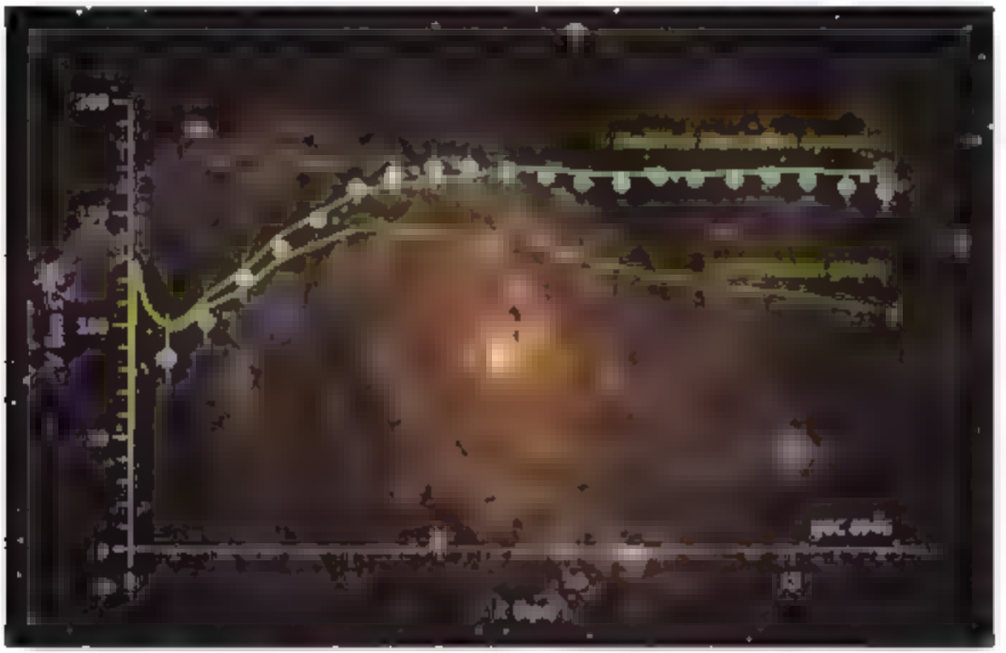

Modified gravity. The spiral galaxy NGC 6946 with its rotation curve of velocity *V* versus distance *R* from the center (blue circles) (*14*). The green line is the rotation curve computed with Newtonian gravity. The gold line is the prediction of MOND. In both cases, the one unknown parameter of the computation, the stellar mass-to-light ratio, has been set to the value expected by stellar population synthesis models (*15*). MOND provides a good description of the data with no free parameters.

The need for dark matter in clusters, even with MOND, was dramatically confirmed by the colliding "bullet" cluster (*12*). In this case the mass, as indicated by gravitational lensing, follows the galaxies rather than the gas. This implies that the unseen mass is in dense objects like brown dwarfs, but not diffuse gas. Although this provides some clue as to what the unseen mass is not, it does not tell us whether it is nonbaryonic dark matter or merely dark baryons. Moreover, although certainly puzzling for MOND, this case is also puzzling in the context of standard cosmology. The collision velocities of the components of the bullet cluster are extraordinarily high, a result much more natural to MOND than to conventional dark matter.

Another result more consistent with MOND than dark matter is the recent observation of mass discrepancies in tidal debris dwarfs (*13*). These dwarf galaxies form from the gas extruded from disks into long tidal tails as the result of collisions between massive galaxies. Because the orbits of dark matter and gas in disks are so different, these dwarfs are expected to be free of dark matter. Contrary to this expectation, they appear to show the familiar flat rotation curves.

This is precisely the behavior expected in MOND. In the conventional picture, however, we are obliged to invoke dark baryons in the disk in addition to the nonbaryonic dark matter in the halo. It is far from obvious that this can work, so the observations of Bournaud *et al.* (*13*) may pose an existential crisis for nonbaryonic dark matter.

Modern cosmology, with both dark matter and dark energy, has many genuine successes. So why should MOND work so well in describing rotation curves if, in fact, dark matter is their cause? We must understand this empirical phenomenology. If it is not the result of modified gravity, perhaps it is suggestive of something about the nature of dark matter.

If dark matter does exist in the form most commonly assumed, we should see it in the laboratory soon. Major experiments like the Large Hadron Collider and others have a good chance of detecting dark-matter particles in the near future. Moreover, measurement of a neutrino mass in excess of a few tenths of an electron volt would falsify the structure formation paradigm of standard cosmology, while perhaps going some way toward providing the missing mass in clusters with MOND. Regardless of how these experiments play out, there is clearly a great deal of fundamental physics left for us to learn. The universe may not be as cold and dark as we imagine.

References

1. S. M. Faber, J. S. Gallagher, *Annu. Rev. Astron. Astrophys.* **17**, 135 (1979).
2. S. S. McGaugh, W. J. G. de Blok, *Astrophys. J.* **499**, 41 (1998).
3. M. Milgrom, *Astrophys. J.* **270**, 365 (1983).
4. R. H. Sanders, S. S. McGaugh, *Ann. Rev. Astron. Astrophys.* **40**, 263 (2002).
5. S. S. McGaugh, W. J. G. de Blok, *Astrophys. J.* **499**, 66 (1998).
6. J. F. Navarro, C. S. Frenk, S. D. M. White, *Astrophys. J.* **490**, 493 (1997).
7. R. Kuzio de Naray, S. S. McGaugh, W. J. G. de Blok, A. Bosma, *Astrophys. J. Suppl. Ser.* **165**, 461 (2006).
8. J. D. Bekenstein, *Phys. Rev. D* **70**, 083509 (2004).
9. J. D. Bekenstein, *Contemporary Phys.* **47**, 387 (2006).
10. R. H. Sanders, *Mon. Not. R. Astron. Soc.* **342**, 901 (2003).
11. M. Fukugita, C. J. Hogan, P. J. E. Peebles, *Astrophys. J.* **503**, 518 (1998).
12. D. Clowe, A. Gonzalez, M. Markevitch, *Astrophys. J.* **604**, 596 (2004).
13. F. Bournaud *et al.*, *Science* **316**, 1166 (2007).
14. C. Carignan, P. Charbonneau, F. Boulanger, F. Viallefond, *Astron. Astrophys.* **234**, 43 (1990).
15. L. Portinari, J. Sommer-Larsen, R. Tantalo, *Mon. Not. R. Astron. Soc.* **347**, 691 (2004).

10.1126/science.1144534

PHOTO CREDIT: STACY MCGAUGH

RETROSPECTIVE

Anne McLaren (1927–2007)

A leader in mammalian development and an active voice in the ethics of human embryology research is remembered

Janet Rossant and Brigid Hogan

The death of Anne McLaren in England on 7 July 2007 has robbed us of a major leader in mammalian developmental biology and genetics. Not only was Anne a pioneer, she remained an active scientist whose influence extended across many other fields. Notably, she was a preeminent international figure in public policy debates around issues of reproductive technologies and stem cell research.

Anne's scientific career spanned more than 50 years, from early studies on embryo transfer to her most recent work on germ cell development. After receiving a D.Phil. in 1952 from Oxford University, she began her career at University College London, where she perfected techniques of embryo transfer in mice and demonstrated maternal uterine effects on embryonic patterning. This work was performed with her then-husband, Donald Michie, with whom she remained friends after they divorced in 1959. Sadly, he was with her in the car accident that took both their lives. With John Biggers, she showed for the first time that preimplantation mouse embryos cultured in a dish for 2 days could be returned to the mother's uterus to complete normal pregnancy. This combination of embryo culture and transfer enabled the development of human in vitro fertilization technologies. The media hype over the birth of these "brave new mice" in 1958 also gave Anne her first taste of public controversy around new reproductive technologies.

In 1959, Anne moved to Edinburgh to set up her own lab at the Institute of Animal Genetics, established by C. H. Waddington. There she initiated research on a broad range of topics, including embryo implantation and chimera development. She describes this period of her long career as her favorite, when genetics, epigenetics (as defined by Waddington), reproductive biology, and developmental biology were coming together to define new ways of understanding mammalian embryonic development. Her classic monograph "Mammalian Chimaeras," published in 1976, gives an amazingly current view of the power of mouse chimeras to explore a variety of biological questions.

Anne moved back to London in 1974 to direct the Medical Research Council Mammalian Development Unit. Under her guidance this became one of the world's preeminent centers for mammalian embryology and genetics. Many leading scientists developed their careers there, and many more, including us, were fortunate to receive Anne's mentorship. She was always ready to welcome visitors, give advice, and discuss scientific matters. You were subjected to tough questioning, but in a way that led to more rigorous experiments and deeper insight. As many will testify, Anne was also extremely supportive of scientists struggling to work outside the mainstream or with few resources. Her own research during this time turned to germ cell development and sex determination. With Elizabeth Simpson in the 1980s, she showed that the mouse gene encoding the male antigen H-Y was not related to the sex-determination gene on the Y chromosome. This began a chase that led to the cloning, by the Goodfellow and Lovell-Badge labs, of the true sex-determination gene, *Sry*, in 1990. She also showed the first location of germ cells in the embryo, and her work inspired the derivation of embryonic germ cell lines.

Anne was involved in the public debate about the ethics of new reproductive technologies. As a founding member of the Warnock Commission between 1982 and 1984, she provided the clear scientific background and advice that led to the first guidelines around in vitro fertilization and embryo donation for research. The U.K. Human Fertilization and Embryology Authority, founded in 1990, remains a model for other countries grappling with the increasingly complex issues surrounding reproductive technologies and human embryo research. Anne played a major role worldwide in developing guidelines in many different jurisdictions. She regarded herself as "biologist, not an ethicist," yet could communicate with ethicists, philosophers, policy-makers, politicians, and the public with clarity and precision. She believed that scientists have an ethical duty to explain their research and its possible implications for society.

Anne's influence did not decline after her statutory retirement in 1992; if anything it increased. She divided her time between ongoing research at the Gurdon Institute in Cambridge and traveling the world, advising governments and learned bodies, teaching and lecturing. She was appointed foreign secretary of the Royal Society, making her the first woman to hold a leadership position in the society since its founding in 1660. She received many awards and honors, including Dame of the British Empire in 1993, the Japan Prize with Andrzej Tarkowski, in 2002, and most recently, the March of Dimes Prize in Developmental Biology, with Janet Rossant, in 2007.

How did she manage all this—to be an outstanding scientist, public educator and policy advisor, role model and mentor, as well as a highly involved mother and grandmother? We can only offer some clues from our experiences. She had no personal ego invested in her activities, but a strong sense of social responsibility and desire to see others succeed. Anne relished all kinds of social interactions and could party long after her younger colleagues had faded. She loved young people, and they responded in kind. And she truly did not suffer from jet lag. Anne traveled the world with one small rucksack and never seemed fatigued. She also knew how to balance family and work and to be successful at both.

At her death, Anne was in her prime. An excellent celebration of her life in science was held in Cambridge on the occasion of her 80th birthday earlier this year, and it seemed she would live and work forever. Now, she would not want us to grieve for long. Rather, she would encourage us all to live life to the full, while striving for the scientific and societal ideals that she worked so hard to achieve.

10.1126/science.1147801

J. Rossant is at the Hospital for Sick Children, University of Toronto, Toronto, Ontario, Canada M5G 1X8. B. Hogan is in the Department of Cell Biology, Duke University, Durham, NC 27710, USA. E-mail: janet.rossant@sickkids.ca; b.hogan@cellbio.duke.edu

CREDIT: FIONA HANSON/PA

AAAS & NPA

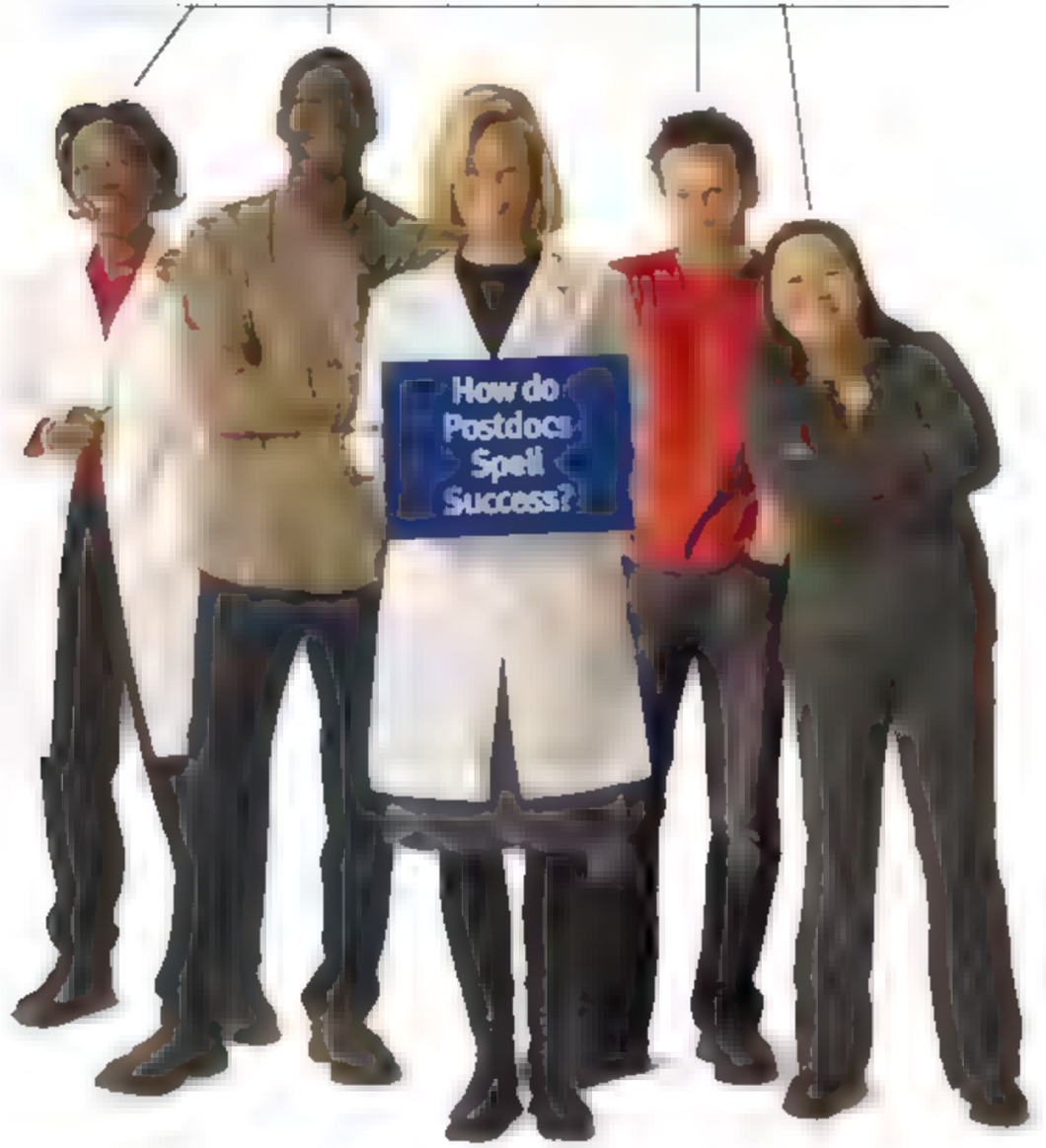

Here's your link to career advancement

AAAS is at the forefront of advancing early-career researchers offering job search, grants and fellowships, skill-building workshops, and strategic advice through ScienceCareers.org and our Center for Careers in Science & Technology.

NPA, the National Postdoctoral Association, is providing a national voice and seeking positive change for postdocs partnering with AAAS in career fairs, seminars, and other events. In fact, AAAS was instrumental in helping the NPA get started and develop into a growing organization and a vital link to postdoc success.

If you're a postdoc or grad student, go to the AAAS-NPA link to find out how to spell career success.

AAAS.org/NPA

NATIONAL POSTDOCTORAL ASSOCIATION

Science AAAS

INTRODUCT

Testing Our Defenses

CHALLENGE THE IMMUNE SYSTEM, AND YOU MIGHT WELL INDUCE A vigorous response. Challenge an immunologist, and you can be confident of eliciting something rather similar. Indeed, our rate of progress in understanding the immune system has been anything but sluggish over the past few decades. This has encouraged a mood of optimism that new vaccines for infectious diseases and immune-based therapies for cancer and autoimmune diseases are just around the corner. Yet despite this brisk pace of discovery and some enticing glimpses of how the immune system might be manipulated, there is much that is clearly left to explore about its inner workings. In this special issue, we consider a selection of fundamental immunological questions that still test investigators.

As Casanova and Abel explain (p. 617), the genetic study of human primary immunodeficiencies is an emerging field that is revealing surprises about our evolving relationship with the world of pathogens. Kioussis and Georgopoulos (p. 620) discuss the epigenetic rules that govern lymphocyte function and development, and Reiner *et al.* (p. 622) frame some of the most pertinent issues in T cell fate determination. Cell biology and immunology have long been intimate partners, and Mellman (p. 625) uses the study of antigen presentation to explain how discoveries in basic cell biology continue to underpin our understanding of the immune system. Finally, Sakaguchi and Powrie (p. 627) reveal just how much there is still to learn about the regulatory T cell and its power in preventing overzealous immune responses and autoimmunity. In News, Leslie (p. 614) describes how immunologists have struggled to understand the purpose of mast cells, and Cohen (p. 612) updates the daring efforts of gene therapists to reboot the human immune system with cells impervious to HIV. *Science*'s STKE focuses on some molecular challenges for immunologists (www.sciencemag.org/sciext/immunology07). Linden describes how the adaptor protein Act1 mediates interleukin-17 receptor signaling. Serfling *et al.* discuss the importance of NFAT transcription factors to memory lymphocytes. Finally, Wattenberg and Raben describe the negative regulation of various immune responses by diacylglycerol kinase.

We are still learning about how immune cells move around the body, and in the research section a Report by Auffray *et al.* (p. 666) describes a subset of monocytes that patrol the surfaces of blood vessels for damage and inflammation, contrasting their behavior with that of typical leukocytes. Mueller *et al.* (p. 670) offer up some intriguing evidence that lymphoid organs "close up shop" for new business during an immune response, by using chemokine regulation to prevent the admission of circulating naive lymphocytes. In research that may shed some evolutionary light on an ancient system, Chen *et al.* (p. 678 and see related News item) describe how the social amoeba *Dictyostelium* uses specialized cells akin to phagocytes in animals. Finally, Carmody *et al.* (p. 675) reveal the means by which normally potent signals mediated by the innate immune Toll-like receptors are placated by blocking ubiquitination. With so much left to discover about our immune system, there seems little doubt that immunologists will find plenty to challenge them in the years to come.

STEPHEN J. SIMPSON AND JOHN TRAVIS

Challenges in Immunology

CONTENTS

News

612 Building an HIV-Proof Immune System

614 Mast Cells Show Their Might

Perspectives

617 Primary Immunodeficiencies: A Field in Its Infancy
J.-L. Casanova and L. Abel

620 Epigenetic Flexibility Underlying Lineage Choices in the Adaptive Immune System
D. Kioussis and K. Georgopoulos

622 Division of Labor with a Workforce of One: Challenges in Specifying Effector and Memory T Cell Fate
S. L. Reiner, F. Sallusto, A. Lanzavecchia

625 Private Lives: Reflections and Challenges in Understanding the Cell Biology of the Immune System
I. Mellman

627 Emerging Challenges in Regulatory T Cell Function and Biology
S. Sakaguchi and F. Powrie

See also related Reports pages 666, 670, 675, and 678 and related News story; Online material page 567 or at www.sciencemag.org/sciext/immunology07

Science

CREDIT: C. BICKEL/SCIENCE

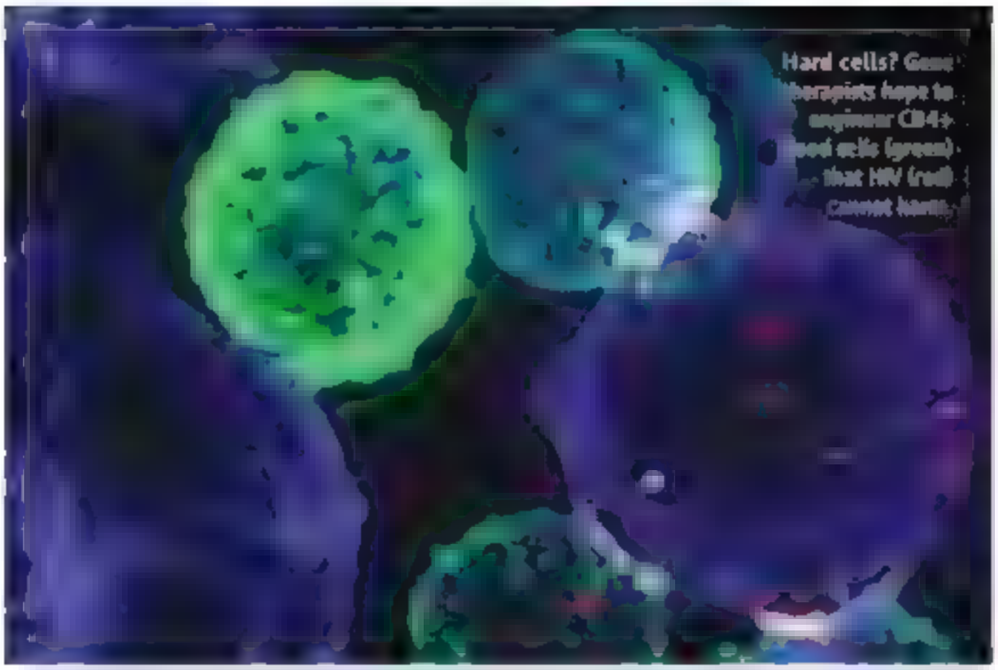

CREDIT: THOMAS HOPE/NORTHWESTERN UNIVERSITY

NEWS

Building an HIV-Proof Immune System

Despite past setbacks in the field of gene therapy, several research teams are testing whether that strategy can provide people with immune cells that are more resistant to HIV or that can cripple the virus

Except for a lucky few, everyone infected by the AIDS virus suffers a prolonged and inexorable attack that obliterates the immune system. Yes, anti-HIV drugs can stave off this destruction. But drugs can have serious toxicities, they're costly and difficult to take every day, and the virus can develop resistance to all of them. So a small group of researchers has long explored an ambitious alternative to drug therapy: introducing new genes into the bodies of HIV-infected people to help fortify their immune systems. Some are even pursuing the option of destroying the remaining immune cells in an infected person so that new, better ones can take their place. Fanciful as it sounds, scientists are hoping to reboot people's immune systems with HIV-proof cells.

Researchers haven't made much headway with this approach, which some call "intracellular immunization." But more effective gene-therapy techniques recently have begun to advance a parade of novel strategies. They include disabling a critical receptor that HIV uses to infect immune cells, silencing the regulators that turn on HIV genes, and incapacitating HIV with lab-designed antibodies. In an ironic twist, some scientists are even using forms of HIV to deliver the genes for these strategies. "These are exciting times now because the technologies are there," says immunologist Carl June, who develops HIV gene therapies at the University of Pennsylvania.

The National Institutes of Health invested more than $10 million last year in three dozen labs pursuing this pioneering HIV gene-therapy research. And as part of its Grand Challenges in Global Health initiative, the Bill and Melinda Gates Foundation has committed nearly $14 million to a project headed by Nobel laureate David Baltimore who wants to engineer the immune system to produce an ultrapotent antibody against HIV.

For the most part, industry has left the exploration of these radical ideas to academics. "One has to be somewhat optimistic to go after this type of therapy because it is labor-intensive, and we don't know all the rules yet," says Jerome Zack, an immunologist at the University of California, Los Angeles (UCLA). "The field is still waiting to be cultivated."

On trial

HIV gene therapies all adhere to the same basic principles. Researchers remove blood or bone marrow from an HIV-infected patient, isolate the immune cells that HIV targets or the blood-forming stem cells that spawn them, introduce new genes, and reinfuse the cells (see table, p. 613). Key distinctions between different labs include the viral "vectors" they design to shuttle in genes (a process called transduction) and how they culture cells to expand their number. Success depends critically on how many cells the vectors actually transduce and how long the modified cells survive once back in the body.

Gary Nabel, a leading HIV gene-therapy investigator in the 1990s who subsequently moved into AIDS vaccine research, says the field's rejuvenation owes much to improvements in the gene-carrying vectors and discoveries about the molecular weak points of HIV. "We just know so much more now than we did then," says Nabel, who heads the Vaccine Research Center at the National Institute of Allergy and Infectious Diseases in Bethesda, Maryland.

One of the earliest gene-therapy attempts to build an HIV-resistant immune system employs a ribozyme, a catalytic bit of RNA. Developed by Zack and other UCLA researchers in association with a Johnson & Johnson (J&J) division in Sydney, Australia, the ribozyme clips an HIV gene, *tat*, that the virus needs for replication, rendering it incapable of producing new copies. Nearly a decade ago, a clinician at UCLA who collaborates with Zack began a study of this ribozyme approach in 10 patients, all also receiving anti-HIV drugs. To deliver the ribozyme into each patient's cells, the researchers used a mouse retrovirus.

At the time, the most unusual aspect of the experiment was the target cell. HIV preferentially infects white blood cells that have CD4+ surface receptors, and researchers had typically focused on transducing these cells. The UCLA group decided that because the CD4+ cells are mature and have a finite life span, it made better sense to add the ribozyme gene to stem cells, marked by a cell surface protein called CD34+, that theoretically can produce CD4+ cells indefinitely. As Zack and co-workers reported in the March 2004 issue of *Human Gene Therapy*, they found that the ribozyme-containing vector was still inside CD4+ cells as long as 3 years after an infusion

of the modified stem cells, presumably because they produced progeny that survived. The strategy looked promising enough that J&J moved ahead with a larger study, which began in August 2002 and has 74 patients enrolled at UCLA and other sites.

The only other HIV gene-therapy strategy now in clinical trials pioneered the use of HIV itself as the vector. Whereas the mouse retrovirus employed by Zack and his colleagues only transduces dividing cells, HIV has no such limitation. Many in the field also contend that because lentiviruses such as HIV are not known to directly cause cancer, they are inherently safer than mouse retroviruses, one of which triggered leukemia in some children in a gene-therapy trial (*Science*, 17 June 2005, p. 1735).

The taming of HIV begins by stripping the virus down to its bare bones so that it can insert the genetic material it carries into human chromosomes but not make dangerous new copies of itself. VIRxSYS Corp. in Gaithersburg, Maryland, spliced into such a vector an "antisense" gene that stops HIV from making its crucial envelope protein. (The RNA strand made by this gene complements the messenger RNA for the protein and prevents its translation.) Once integrated into an immune cell's DNA, the antisense gene should prevent any normal HIV that gets into the cell from making new copies.

In 2003, June and co-workers used this vector to transduce CD4+ T cells taken from five people who were failing on their anti-HIV drugs. Subsequently, they gave the patients a single infusion of the modified cells. In the 14 November 2006 *Proceedings of the National Academy of Sciences*, the researchers report that the HIV vector, as expected, far more efficiently transduced cells than did mouse retroviruses. Although the study was meant to address only safety and not whether the therapy worked, one patient had a dramatic drop in HIV levels. And whereas the transduced CD4+ cells had a half-life of less than 1 month, the researchers unexpectedly found signs of the antisense-toting vector in two patients' CD4+ cells more than a year after the infusions. Two separate clinical trials in HIV-infected people, including one in which participants will stop taking their antiviral drugs, are now evaluating multiple infusions of the VIRxSYS vector.

June says it may turn out that multiple infusions aren't necessary. In the first trial, they found evidence that an infected person's own "wild-type" HIV could "package" the vector and carry it to uninfected CD4+ cells, possibly expanding the number of protected cells and extending the durability of the therapy. "Potentially, you could infuse a limited number of transduced cells that could infect their neighboring cells in vivo," says June. In most gene-therapy studies, mobilizing a retroviral vector like this would raise staggering safety concerns, but for whatever reason, and unlike other retroviral vectors, HIV integrates its genes at spots on human chromosomes unlikely to trigger cancers. (The lymphomas often seen in AIDS patients stem from general immune suppression.)

HIV GENE THERAPY TRIALS

Investigators	Sponsors	Vector	Transduced Genes Encode	Protocol	Development Stage
Jerome Zack and Ronald Mitsuyasu, UCLA	Johnson & Johnson Research Pty Sydney, Australia; NIH	Moloney murine leukemia virus	Ribozyme that targets HIV *tat*	CD34+ cells; no conditioning	74 patients in an [illegible] controlled phase II trial; Results expected early 2008
Carl June, University of Pennsylvania	VIRxSYS, Gaithersburg, Maryland; NIH	Modified HIV	Antisense that targets HIV *env*	CD4+ cells; no conditioning	Two studies with 6 patients each; results expected in 08
Carl June	Sangamo BioSciences, Richmond, California; NIH	Adenovirus	Zinc finger nuclease that targets CCR5	CD4+ cells; no conditioning	12 patients; expected to start later this year
Donald Kohn, Children's Hospital Los Angeles	NIH	Modified HIV	RevM10 that overwhelms HIV *rev*	CD34+ cells; partial ablation with busulfan	24 patients failing therapy; expected to start in early 2008
John Rossi and John Zaia, City of Hope, Duarte, California	NIH	Modified HIV	Short RNA aptamer to Rev and an RNA ribozyme against CCR5; and TAR decoy against HIV *tat*	CD34+ cells; myeloablation	5 patients with AIDS lymphoma; enrolling
Dorothee von Laer and Georg Speyer Haus, Frankfurt, Germany	Paramita Biotech Vision 7 GmbH, EU	Moloney murine leukemia virus	Peptide that disrupts HIV's gp41	CD34+ cells; partial ablation with chemotherapy	5 patients with AIDS lymphoma; start later this year
David Baltimore and Pamela Bjorkman, Caltech, Pasadena	Bill and Melinda Gates Foundation	Modified HIV	Lab-designed anti-HIV antibody	CD34+ cells	Mouse studies
Irvin Chen, UCLA	NIH	Modified HIV	Short interfering RNA that targets CCR5	CD34+ cells	Monkey studies

Tomorrow's front burners

A new generation of sophisticated therapies designed to HIV-proof the immune system promises to enter the clinic soon. For example, June, working with Sangamo BioSciences in Richmond, California, later this year plans to start trials in 12 HIV-infected people of a gene therapy designed to endow immune cells with a genetic mutation that protects them from HIV.

To infect immune cells, HIV must first bind to chemokine receptors. Researchers discovered in 1996 that people who had a naturally occurring mutation in their genes for one of these, CCR5, were strongly protected from developing AIDS—or even becoming infected in the first place—and suffered no ill effects from lacking the receptor.

Sangamo specializes in developing enzymes called zinc finger nucleases that can bind to genes, clip their DNA, and repair mutations (*Science*, 23 December 2005, p. 1894). But for the HIV gene therapy, they've created a nuclease to specifically disrupt the CCR5 gene in the same manner as the natural mutation. In the new trial, researchers will put the gene for this zinc finger nuclease into an adenovirus vector, transduce harvested CD4+ T cells of HIV-infected people, and infuse those cells back. June says this is the first gene-therapy experiment that aims to create a phenotype that's known to confer disease resistance.

A single infusion of these transduced cells will, at best, only protect a small fraction of the body's CD4+ cells. But a gene-therapy approach could have a much greater impact if scientists instead transduce the stem cells that make CD4+ cells and "condition" the existing immune system to make "space" for those stem cells.

Toward that end, Donald Kohn at Children's Hospital Los Angeles will use a chemotherapeutic agent to partially ablate the immune systems of children who are failing on anti-HIV drugs. Building on earlier work he did with mouse-based retroviral vectors, Kohn will infuse the children with their own CD34+ cells that he has transduced with an HIV-based vector to carry a gene known as *RevM10*, which produces a mutant form of the critical HIV protein Rev. When the virus infects such a transduced cell, it uses the wrong *Rev*, disrupting its replication.

Kohn says a "home run" from this conditioning would lead the vast majority of cells to express the protective gene. Still, even a much smaller percentage of protected stem cells could powerfully bolster the immune system. "Those cells over time could amplify in number because they're resistant to HIV," says Kohn. He notes, too, that the transduced

cells could at a minimum leave people with enough of an immune system to ward off serious disease.

At the nearby City of Hope in Duarte, California, John Rossi heads a study that's recently started enrolling patients in the most aggressive HIV gene therapy yet. In five people with AIDS lymphoma—a cancer of the lymph nodes, Rossi, John Zaia, and colleagues will use various chemotherapies or radiation to completely destroy each person's immune system—a dangerous procedure that is the standard of care for that highly lethal condition. The researchers will then infuse the patients with their own previously harvested immune stem cells that an HIV-based vector has transduced with three genes. The therapeutic genes encode a ribozyme that knocks down CCR5, a short RNA that interferes with the virus's ability to copy itself, and a decoy that codes for an essential HIV protein and throws a wrench in the viral replication machinery. "The nice thing is, the targets are multiple," says Rossi, who hopes this will overcome a risk in all these strategies—namely, that HIV will develop resistance to the gene therapy.

Instructive immunotherapy

At the California Institute of Technology in Pasadena, David Baltimore has teamed up with immunologist Pamela Bjorkman on an HIV gene-therapy project that he calls "instructive immunotherapy." Rather than bolstering the natural immune response, Baltimore says, "we're instructing the immune system [about] what to make."

This 5-year experiment lives up to its Grand Challenges billing with its focus on inventing virus-fighting antibodies. Gene therapists have paid antibodies little heed because HIV notoriously remains impervious to their attack. "I didn't think we should be giving up on the historically most powerful part of the immune system," says Baltimore. So he and Bjorkman are attempting to construct an antibody against HIV that's far more powerful than anything naturally produced by the immune system. Baltimore and co-workers then want to use an HIV-based vector to transduce the gene for this antibody into immune stem cells.

Baltimore originally explored intracellular immunization strategies—he even coined the term—but his work now on instructive immunotherapy reflects a belief that multiple forms of gene therapies may be needed to defeat HIV. "I'm hedging my bets," says Baltimore.

Two years into the project, Baltimore says his team is making steady progress, but they have an added hurdle to overcome. They need to craft antibody genes that will continue to function as the CD34+ stem cells mature into the B cells that ultimately secrete the antibody. Within 3 years, the scientists hope to show that this can work in chimeric mice that have humanlike immune systems. "We're very aware that this is complicated and expensive and difficult to imagine using in the less developed world," says Baltimore, noting that the Gates initiative demands that researchers work on projects applicable to the world's poor. With that in mind, Baltimore says they've been testing another strategy in mice: injecting the vector directly into the body to see if it will home in on CD34+ cells.

In the end, Baltimore and other researchers in the field imagine that different gene therapies and anti-HIV drugs will complement each other. And many anticipate that in wealthy countries, demand for a gene-therapy approach will grow as ever more people become resistant to the best anti-HIV drugs available. "With the right techniques and vectors, I think this can be just like what the Red Cross does with blood transfusions," predicts the University of Pennsylvania's June. "Unfortunately, it's going to take time."

–JON COHEN

NEWS

Mast Cells Show Their Might

Once dismissed as "allergy cells," mast cells have proven crucial for immunity. But they've also shown a dark side

They are the most reviled cells in the body. Their meddling makes our skin itch, our eyes swell, and our noses stream; the cells even provoke suffocating asthma attacks that kill thousands of people every year. In fact, these villains, known as mast cells, are responsible for so much suffering that some researchers have proposed eradicating them.

That could be a big mistake. Over the past decade or so, the reputation of these immune cells has been turned around. Researchers have learned that mast cells are vital sentinels that orchestrate counterattacks on invading bacteria and viruses. The cells link the innate immune system, which deploys a standard set of defenses, with the adaptive immune system, which customizes the body's weapons to a specific attacker. Mast cells even neutralize toxins from snakebites and bee stings (*Science*, 28 July 2006, p. 427).

However, mast cells turn out to be fickle allies. Extending the cells' disease connections far beyond allergic reactions, recent studies put them at the center of multiple sclerosis, rheumatoid arthritis, cancer, and atherosclerosis. "What this research tells you is that mast cells are key to a lot of biological processes," says immunologist Dean Metcalfe of the National Institute of Allergy and Infectious Diseases (NIAID) in Bethesda, Maryland.

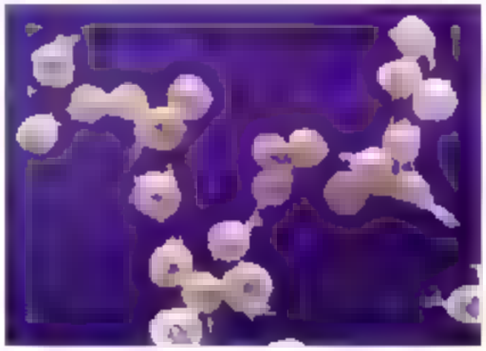

Standing guard. Mast cells from the umbilical cord.

CREDIT: FRED HOSSLER/VISUALS UNLIMITED

The catalyst for many of these discoveries was the identification of mutant mice that lack mast cells. A white-spotted coat on one of these rodents first attracted geneticists' attention in 1937. But it wasn't until the late 1970s that Yukihiko Kitamura of Osaka University Medical School in Japan and colleagues determined that the genetic defect responsible for the color change also short-circuits mast-cell development. Led by Kitamura and pathologist Stephen Galli of Stanford University in Palo Alto, California,

researchers began using the animals in the late 1980s to probe mast-cell activity. By implanting these mice with lab-grown mast cells, scientists could finally begin to elucidate the functions of the cells or parts of their molecular repertoire. The animals are "the only way to see if the effect [of mast cells] is positive, negative, or neutral," says Galli.

The good

Mast cells are microscopic chemical factories. Their product line of 10,000 compounds includes histamines that make blood vessels leaky, protein-slicing enzymes such as chymase and tryptase, and cytokines that incite inflammation and activate immune cells.

These potent potions, which the cells often stash in sacs called granules, cause misery for people who are sensitive to cat dander, ragweed pollen, and other allergens. The trouble begins when antibodies jutting from mast cells latch onto one of these substances. Once triggered this way, the cells dump their contents, or degranulate. This outpouring can elicit responses that range from local irritation, such as stuffed noses and hives, to bodywide and potentially fatal anaphylaxis. Scientists once thought these woes were a side effect of mast cells protecting us from parasitic worms, and that allergic reactions ensued when the cells instead overreacted to innocuous substances.

That rationale for the cells' existence satisfied few researchers because the costs seemed to dwarf the benefits. "Everyone knows that they make people itch, sneeze and wheeze, but why are they there?" asks immunologist George Caughey of the University of California, San Francisco.

A pair of papers published in *Nature* in 1996 marked the turning point in the thinking about mast cells. One came from microbiologist Soman Abraham of Duke University in Durham, North Carolina, and co-workers and the other from Bernd Echtenacher of the University of Regensburg in Germany and colleagues. The teams were the first to test the bacteria-fighting prowess of mice lacking mast cells. Both groups unleashed internal infections in the animals by introducing bacteria into the peritoneal cavity. And both groups found that mice with mast cells could beat back the invasion, whereas rodents devoid of the cells died.

The findings shook up the field because they were the first to show that the cells were "life-or-death critical" for fighting infection, says Caughey.

Further research has demonstrated that innate immunity depends on the mast cell taking on a range of bacteria and viruses. "It's the quintessential immunological first responder," says Joshua Boyce of Harvard Medical School in Boston. Mast cells reside just about everywhere a pathogen might try to break in: the skin, nasal passages, lungs, lining of the gut. Their membranes are studded with bacteria-sensing proteins called Toll-like receptors. Although it can gobble interlopers, a mast cell typically fights back by spilling compounds such as tumor necrosis factor (TNF) that promote inflammation and lure pathogen-killing neutrophils to the infection site.

Researchers have also been discovering surprising subtlety in mast-cell responses. "The misconception was that they are a bag of activators that goes pop," says immunologist Jean Marshall of Dalhousie University in Halifax, Canada. But research by her lab and others revealed that activated mast cells don't always degranulate. They can dole out cytokines and other effectors, giving them precise control over the behavior of other cells.

Mast cells use that power to enlist the adaptive immune system, whose soldiers are B and T lymphocytes. Before these cells join the battle, however, so-called helper T cells must rendezvous with a cell sporting a fragment, or antigen, of the invader. As Abraham and colleagues showed 4 years ago, mast cells promote encounters between antigen-presenting cells and helper T cells by inducing one of the most familiar symptoms of infection: swollen lymph nodes. Mast cells that have detected a pathogen emit TNF, which spurs nearby lymph nodes to bulk up and release molecules that draw in lymphocytes. And last year, Galli and colleagues reported that TNF from mast cells prods one antigen-presenting cell, known as a dendritic cell, to make a beeline for the nodes, where it can mingle with T cells. "In the absence of mast cells, these events don't occur, and you get a poor response from the immune system," says Abraham.

Randolph Noelle of Dartmouth Medical School in Lebanon, New Hampshire, and colleagues have also implicated the cells in immunological tolerance, in which the immune system learns not to assault the body's own tissues. Researchers knew that so-called regulatory T cells play a key role in the development of tolerance by quashing immune attacks, but they didn't know how. Last August, in an article that appeared in *Nature*, Noelle's team showed that mast cells serve as enforcers for regulatory T cells, turning down the immune system's reaction to skin grafts. That an "innate" cell is so deeply involved in this adaptive response is surprising, Noelle says.

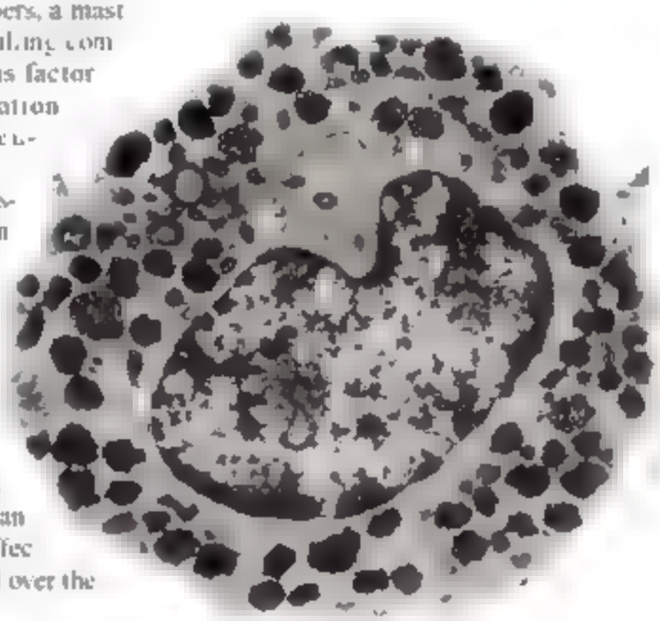

Loaded. Granules full of histamine and other effector molecules fill a mast cell.

The bad

The upside of mast cells is bigger than anyone imagined a decade ago. But so is their downside. Work by rheumatologist David Lee of Harvard Medical School, for example, indicates that mast cells help initiate rheumatoid arthritis. Five years ago, Lee and colleagues reported that mice lacking mast cells don't develop the rodent equivalent of this debilitating condition (*Science*, 6 September 2002, p. 1689). In further studies, the researchers have found that activated mast cells pump out the cytokine interleukin-1, which attracts inflammation-inducing cells to the joint. Mast cells also promote leakage of fluid into the joint, which allows in more self-targeted antibodies that might lead to damage by a cadre of defensive proteins known as complement.

In multiple sclerosis, mast cells may worsen the disease's destruction of the myelin insulation that sheathes nerves—at least if experiments on the rodent model of the condition, known as EAE, hold true for humans. Seven years ago, immunologist

CREDIT: ANN CHOBANIAN/BIOMIC

Melissa Brown of Northwestern University's Feinberg School of Medicine in Chicago, Illinois, and colleagues determined that although EAE mice still develop disease if they have no mast cells, the symptoms start later and are less severe. Brown says she assumed that mast cells in the central nervous system (CNS) exacerbated the illness. But in 2003 her group found that symptoms aren't delayed in mice lacking mast cells only in the CNS. The culprits, Brown now suspects, are mast cells hiding in the spleen and lymph nodes, where they could help activate self-destructive T cells that then travel to the CNS and target myelin.

Rogue mast cells might also contribute to the developed world's leading killer, heart disease. The cells infiltrate arterial gunk, although they are outnumbered there by macrophages and smooth muscle cells. More than 20 years of in vitro experiments by cell biologist Petri Kovanen of the Wihuri Research Institute in Helsinki, Finland, and colleagues link mast cells to plaque formation and breakage, the event that triggers most heart attacks. For example, mast cells might prompt flimsy capillaries to grow into the fatty buildup and then bleed, helping to weaken the plaque.

Biochemist Guo-Ping Shi of Harvard Medical School and colleagues have now taken this investigation into animals. In a *Nature Medicine* article published in June, they report the first data on artery clogging in mast cell–deficient mice. The animals had been crossbred with rodents that are atherosclerosis-prone. Plaques in mice without mast cells were not only smaller than ones in animals with the cells but also less likely to fracture, Shi's group found. The scientists pin the blame on proteins called cathepsins, which cause trouble in several ways. For instance, mast cells spur neighboring cells to release these enzymes, which dissolve proteins in the blood vessel walls, allowing additional smooth muscle cells to escape into the plaque.

Mast cells can break the heart in another way. Last year, physiologist Randi Silver of Weill Medical College of Cornell University in New York City and colleagues temporarily cut off blood flow to rodent hearts, simulating a heart attack. If the mice had mast cells, their hearts were more likely to display abnormal rhythms—including the often-lethal ventricular tachycardia—after blood flow resumed.

The ugly

Researchers have been trying to pin down mast cells' role in cancer since the German microbiologist Paul Ehrlich, who named the cells in the late 1800s, noticed that they swarmed around tumors. Sometimes mast cells appear to oppose the growths and sometimes to abet them.

There are more examples of the latter. Cancer biologist Lisa Coussens of the University of California, San Francisco, and colleagues have found, for example, that skin tumors exploit mast cells' proclivity for cleaning up. After an injury, mast cells release compounds that help dissolve damaged tissue. They also promote repair by, among other things, spurring angiogenesis. These actions benefit cancer cells, piping in nutrients and speeding growth. Indeed, 8 years ago, Coussens and colleagues showed in mice that the absence of mast cells hinders the progression of precancerous skin growths into tumors.

Recent results from immunologist Gunnar Nilsson of the Karolinska Institute in Stockholm, Sweden, and colleagues suggest an even more insidious partnership in Hodgkin's lymphoma, a cancer in which abnormal immune cells multiply out of control. The tumor cells get a jolt when the CD30 receptor on their surface couples with a molecule on the surface of a mast cell. The interaction also stimulates the mast cell, which releases compounds that spur inflammation needed for tumor growth.

In general, mast cells have turned out to be more subtle than scientists expected. They can perform opposing functions—for example, igniting and quenching inflammation. And as Galli notes, mast cells sometimes have contrasting effects at different times in the same process.

Their upbringing seems to determine their behavior. Unlike blood cells, which circulate and tend to be uniform, mast cells specialize for their home tissue, says immunologist Juan Rivera of the National Institute of Arthritis and Musculoskeletal and Skin Diseases in Bethesda, Maryland. The result is a multitude of varieties, each of which "responds to and is tailored to the tissue it develops in," says Lee. Researchers are just beginning to probe how a mast cell's milieu shapes its function.

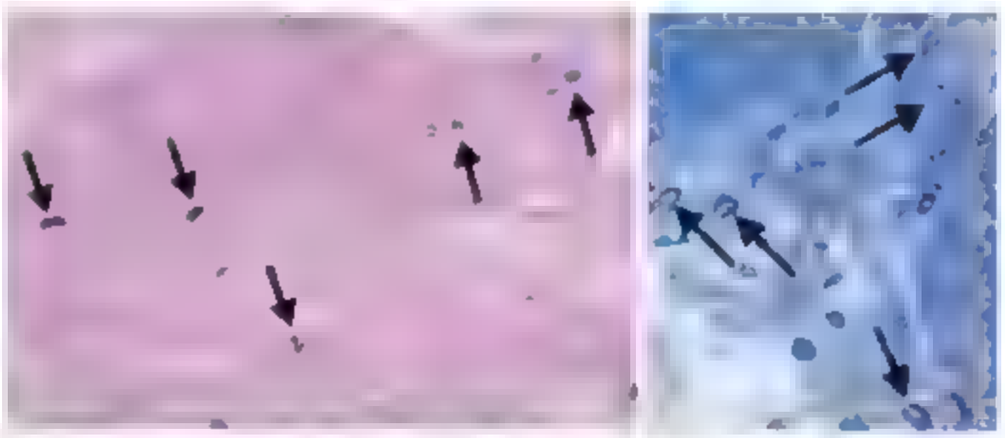

Ally or adversary? Mast cells (arrows) take up residence in colon tumors.

CREDIT: A. WEDEMEYER AND S. J. GALLI

Most work on mast-cell function carries a key caveat. The subjects were rodents. Understanding of the human cells has lagged. One reason, says Boyce, is that "there's no such thing, that we know of, as a mast cell–deficient human." Still, researchers are considering therapies that target mast cells. And that could be tricky.

Turning down mast cells could leave patients vulnerable to infection. Turning them up could prompt fatal anaphylaxis. Nonetheless, researchers are exploring the possibility that allergy and asthma drugs directed at mast cells or their contents—even good old antihistamines—will work against other conditions. One example is cromolyn, a mast-cell stabilizer found in some asthma inhalers. Shi and colleagues are testing its power against atherosclerosis in mice. And last year, in the *Journal of the National Cancer Institute*, Craig Logsdon of the University of Texas M. D. Anderson Cancer Center in Houston and colleagues reported that the inhibitor curtails growth of mouse pancreatic tumors. The researchers are now planning a clinical trial.

Plenty of mysteries remain about the Jekyll-and-Hyde nature of mast cells. But on the question of whether we can live without them, Galli says he knows where he stands. "If somebody told me I could have all my mast cells eliminated tomorrow, I wouldn't agree to that."

—MITCH LESLIE

PERSPECTIVE

Primary Immunodeficiencies: A Field in Its Infancy

Jean-Laurent Casanova[1,2,3]* and Laurent Abel[1,2]

A paradigm shift is occurring in the field of primary immunodeficiencies, with revision of the definition of these conditions and a considerable expansion of their limits. Inborn errors of immunity were initially thought to be confined to a few rare, familial, monogenic, recessive traits impairing the development or function of one or several leukocyte subsets and resulting in multiple, recurrent, opportunistic, and fatal infections in infancy. A growing number of exceptions to each of these conventional qualifications have gradually accumulated. It now appears that most individuals suffer from at least one of a multitude of primary immunodeficiencies, the dissection of which is helping to improve human medicine while describing immunity *in natura*.

The field of human primary immunodeficiencies (PIDs) has witnessed considerable success (*1*, *2*) since its emergence in the 1950s, highlighted by the discovery of X-linked agammaglobulinemia (*3*), congenital neutropenia (*4*), and severe combined immunodeficiency (SCID) (*5*). Its development has saved the lives of tens of thousands of patients with PIDs and other conditions worldwide and has given rise to ground-breaking concepts in immunology and beyond. The clinical description of over 200 diseases, for which more than 80 genetic etiologies have been described, has provided opportunities for diagnosis and genetic counseling. Moreover, an understanding of the pathogenesis of PIDs has paved the way for immunological interventions, with proof-of-principle demonstrated for new treatments, such as immunoglobulin G replacement, bone marrow transplantation, and gene therapy, in patients with PIDs (*1*). Key discoveries in fundamental biology have also emerged from the forward genetic identification of many hitherto unknown PID-causing genes, such as the ubiquitous DNA-repair regulator *ATM* in patients with ataxia telangiectasia (*6*) and a gene expressed in the thymus—the tolerance regulator gene *AIRE*—in patients with severe autoimmunity. PIDs have probably had an even greater biological impact on the definition of host gene function *in natura*—i.e., in the setting of a natural ecosystem—a unique added value of studying the human model (*8*). It is commonly thought that most, if not all PIDs, have been described. On the contrary, we would argue that there has been a subtle but profound paradigm shift, revisiting the definition of PIDs and heralding a formidable expansion of this field (Table 1).

The Expanding Universe of PID-Defining Clinical Phenotypes

What is a PID? There is, quite rightly, a consensus that "primary" refers to a disease-causing genotype. However, there is a common misconception that immunodeficiency should be defined by an "immunological phenotype" in the hematopoietic sense of the term, i.e., a detectable molecular or cellular anomaly in the blood. Such phenotypes are often quantitative, changing with the technological means available to measure them, and any threshold put forward to define a deficiency at the population level is necessarily arbitrary. Moreover, host defense is not restricted to the blood. Despite these inherent limitations, PIDs have historically been defined and classified according to immunological phenotypes (*9*). Paradoxically, epidermodysplasia verruciformis (EV)—a life-threatening inherited predisposition to warts caused by oncogenic papillomaviruses discovered in 1946 and, as such, probably the first PID to be described—was not considered to be a PID until two EV-causing genes were identified in 2002 (*10*), due to its lack of an overt immunological phenotype. A clinical definition of PIDs is therefore more rigorous, and the most conservative definition is death due to inborn errors of immunity, or a threat to life, if the illness can be rescued by drug treatment. A more controversial issue is the definition of impaired immunity. It is surprisingly still not universally accepted that any given life-threatening infection results, by definition, from an immunodeficiency, whether inherited or acquired (*11*). Life expectancy at birth did not exceed about 20 to 25 years, mostly due to infectious diseases, until the end of the 19th century and the advent of Pasteur's microbial theory of disease. This implies that most humans remain immunodeficient, although their immunodeficiency is masked by medical progress (*11*). Immunodeficiency is probably also common in other animal and plant species. In any case, given the strong epidemiological evidence documenting the importance of genetic background in predisposition to infections, any severe infectious illness may be considered a potential PID-defining phenotype (*11*). Many other relevant clinical phenotypes have been identified, including autoimmunity (*7*, *12*), angioedema (*13*), granulomas (*14*), autoinflammation (*15*), hemophagocytosis (*16*), and thrombotic microangiopathy (*17*). A few PIDs also confer predisposition to allergy (*18*) or oncogenic virus-induced cancers (*10*, *19*), and other tumors may also be associated with certain PIDs (*6*, *20*, *21*). It seems highly likely that other phenotypes defining PIDs will be discovered in the near future.

Toward a Single Phenotype per Patient

It is also commonly thought that PIDs confer predisposition to multiple phenotypes—multiple infections in particular—in individual patients, as seen in children with agammaglobulinemia (*3*), neutropenia (*4*), or SCID (*5*). However, following on from the example of EV (*10*), an increasing number of PIDs are being shown to confer predisposition to a single type of infection, or a narrower range of infections than might be expected, in otherwise healthy patients (*22*). Disorders of properdin and the terminal components of complement confer predisposition to *Neisseria* (*23*), and X-linked lymphoproliferative syndrome confers predisposition to Epstein-Barr virus disease (*19*). More recently, disorders of the interleukin-12–interferon-γ (IL-12–IFN-γ) circuit have been shown to confer predisposition to infections caused by mycobacteria and, to a lesser extent, *Salmonella* (*24*). Similarly, disorders of the Toll–IL-1 receptor–nuclear factor kappa B (TIR–NF-κB) pathway have been shown to predispose individuals to pneumococcal and, to a lesser extent, staphylococcal infections (*25*). Perhaps the most striking example is that seen with disorders of the Toll-like receptor 3 (TLR3) pathway suggested by ongoing work in our lab and UNC-93B–IFN-α/β pathway (*26*), which confer a selective predisposition to herpes simplex virus encephalitis (HSE). The infectious phenotypes that the disorders of the IL-12–IFN-γ, TIR–NF-κB, and TLR3–IFN-α/β pathways confer in humans are much narrower than those of the corresponding mutant mice at odds with the T helper cell 1–T helper cell 2

[1]Laboratory of Human Genetics of Infectious Diseases, Institut National de la Santé et de la Recherche Médicale, U550, Paris, France. [2]University Paris René Descartes, Necker Medical School, Paris, France. [3]Pediatric Hematology and Immunology Unit, Necker Children's Hospital, Paris, France.

*To whom correspondence should be addressed. E-mail: casanova@necker.fr

(T_H1/T_H2) and TLR paradigms (*8*). There is therefore much redundancy in host defense *in natura*, with nonredundant human genes ranging from the "public" genes required for protective immunity to multiple microbes to the "private" genes conferring specific immunity to one pathogen. These findings are consistent with the earlier description of mutant mice with a narrow range of vulnerability (e.g., mice deficient in Mx1, Nramp1, Ly49H, and Tlr4), although these mice were neither challenged with many pathogens nor tested in a natural ecosystem (*27*). In any case, other PIDs have also been found to confer predisposition to a very specific autoimmune phenotype (*7*, *12*). Moreover, whereas patients with mutations in the *FOXP3* (*28*) or *AIRE* (*7*) immune genes governing peripheral and central tolerance display relatively broad autoimmunity, those with disorders of cell-autonomous Fas-dependent apoptosis mostly present with autoimmune cytopenia (*29*). Finally, several PIDs confer a selective predisposition to one of several other phenotypes (*6*, *7*, *10*, *12*, *20*). Thus, it is now clear that PIDs may underlie the occurrence of a single phenotype, including a single infectious disease, in otherwise healthy patients. Furthermore, it is likely that a number of "idiopathic" syndromes may reflect hitherto unknown PIDs.

Toward Single Illnesses at Any Age

Infections in children with PIDs are commonly thought to persist constantly, to recur, or both. However, some PIDs occurring in infancy have been found to have a spontaneously favorable outcome, with no relapse in most cases. Examples include IL-12p40 and IL-12Rβ1 deficiency, associated with mycobacterial disease (*24*); IL-1 receptor–associated kinase 4 (IRAK-4) deficiency, associated with pneumococcal disease (*25*); and UNC 93B (*26*) and TLR3 deficiency again as suggested by ongoing work in our lab, associated with HSE. Patients with these disorders typically suffer from one episode of infection in childhood, rarely two, with no relapses occurring from the patient's teenage years onward. Immunity to the corresponding pathogen is therefore selectively compromised in childhood, but not in adulthood. In these PIDs, adaptive immunity to secondary infections may progressively compensate for poor innate immunity to primary infection. Alternatively, innate immune responses may improve with age. These observations strongly suggest that children with one or a few common life-threatening infections who respond to anti-infectious agents and later fare well may suffer from hitherto unknown PIDs. The possibility that inherited vulnerability in childhood and subsequent protection in adulthood in these patients results from the maturation of innate or adaptive immunity or both, may have considerable implications for the development of vaccination strategies. Conversely, some PIDs remain clinically silent for a long period and first manifest in adulthood, forming a mirror image of early-onset PIDs silenced in adulthood. Adult-onset PIDs include common variable immunodeficiency (*30*) and dominant IFN-γR1 deficiency (*24*). The late onset may reflect impaired adaptive immunity to reactivation or secondary infection, or exposure to microbes not encountered in childhood, although this is less likely. In any event, PIDs can no longer be restricted to chronic diseases of early onset, and the elucidation of PIDs underlying infectious and autoimmune diseases tightly associated with a specific age may shed light on the important and largely unknown mechanisms governing age-dependent immunity.

Toward Nonhematopoietic PIDs

Although the clinical presentation of PIDs may be much narrower than initially thought in terms of age window and range of phenotypes, the range of cells affected is broader. An absence of one or several leukocyte subsets is a hallmark of some of the most familiar PIDs, including agammaglobulinemia (*3*), congenital neutropenia (*4*), and SCID (*5*). A first hint at the involvement of nonhematopoietic cells came from the Di George and nude syndromes, which are immunological phenocopies of SCID caused by extrahematopoietic defects that preclude thymic development (*31*). Moreover, it is clear, but often overlooked, that host defense requires the action of both hematopoietic and nonhematopoietic cells, and some PIDs actually affect both types of cells. For example, dyskeratosis congenita (*27*) and ankyloblepharon ectodermal dysplasia with immunodeficiency (*32*) are associated with multiple infections, making the pathogenesis of some infections unclear. Conversely, some molecules endowed with a basic metabolic function in multiple cells appear to be particularly critical for leukocytes. These molecules include mediators of granule secretion, which are of particular importance in natural killer and T cells (*16*). Other PIDs are associated with tissue-specific infections with a single pathogen; this is the case for EV, in which keratinocytes fail to control the development of certain papillomaviruses (*10*), and HSE, in which herpes simplex virus replicates in the central nervous system (*26*).

Table 1. Multiple paradigm shifts in primary immunodeficiencies.

Primary immunodeficiencies	Conventional	Novel
Patient and population levels		
Frequency	Rare	Common
Occurrence	Familial	Sporadic
Age at onset	Childhood	Adulthood
Prognosis	Spontaneously worsening	Spontaneously improving
Phenotype level		
Disease-defining clinical phenotypes	Opportunistic infections*	Other infections and phenotypes†
Number of phenotypes per patient‡	High	Low (even single)
Number of episodes per patient§	High	Low (even single)
Disease-causing cellular phenotypes	Hematopoietic	Nonhematopoietic
Genotype level		
Disease-causing genes per patient	One (monogenic, Mendelian)	A few (oligogenic, major genes)
Mode of Mendelian inheritance	Autosomal and X-linked recessive	Autosomal dominant
Clinical penetrance	Complete	Incomplete
Mutations	Inherited from the parental genome	Germline de novo or somatic

*Infections occurring in patients with overt immunological abnormalities. †Autoimmunity, allergy, virus-induced cancer, angioedema, granulomas, hemophagocytosis, autoinflammation, thrombotic microangiopathy. ‡For example, infectious agents. §For example, infectious phenotypes.

suggesting a critical, if not exclusive role for nonhematopoietic cells in pathogenesis. Finally, other PIDs affect nonhematopoietic cells, with no detectable impact on leukocytes; for example, congenital malformations of the skull base confer a predisposition to pneumococcal meningitis (*33*), and both cystic fibrosis and primary ciliary dyskinesia impair mucociliary clearance, resulting in severe pulmonary infections (*34*). Other PIDs that affect nonhematopoietic cells will probably be discovered, particularly in patients with tissue-specific lesions.

Toward Common, Sporadic, and Complex PIDs

Rarity is generally considered a hallmark of PIDs, despite genetic epidemiological data strongly suggesting that most humans carry inborn errors of immunity. However, cases of Mendelian predisposition to common infections, such as tuberculosis, have been reported (*35*). Moreover, some individuals display autosomal recessive resistance to common pathogens, such as *Plasmodium vivax*, HIV-1, and norovirus, due to mutations in the *DARC*, *CCR5*, and *FUT2* genes, respectively. This indicates that mutant alleles conferring Mendelian resistance may be positively selected by pathogens. It also demonstrates that most (vulnerable) individuals have bona fide autosomal dominant PIDs with respect to these pathogens (*22*, *36*). Moreover, PIDs are not necessarily familial, and a number of sporadic infectious and autoimmune illnesses may result from autosomal dominant PIDs. The underlying mechanisms may involve the inheritance of mutations with incomplete penetrance from an affected parent, as in dominant STAT-1 deficiency (*24*), de novo dominant lesions in the germ line, such as dominant IFN-γR1 deficiency (*24*), or even somatic mutations, such as dominant Fas mutations in the hematopoietic lineage (*29*). Furthermore, a more complex inheritance pattern may also be involved in infectious diseases, as shown by the HbS allele conferring protection against severe *Plasmodium falciparum* malaria (*37*) and the two major susceptibility genes for leprosy, *PARK2/PACRG* and *LTA* (*38*). Similar patterns are observed for allergies, as reported for asthma and severe atopic dermatitis, for which several major susceptibility genes, including *ADAM33* (*39*) and *FLG*, encoding filaggrin (*40*), respectively, have been reported. A similar pattern has also been found for autoimmunity, with the human leukocyte antigen class II region having a major effect and other genes a more modest effect on type 1 diabetes (*41*), and for granulomatous diseases, with inflammatory bowel disease, in which the *CARD15/NOD2* (*42*) and *IL23R* (*43*) genes have been implicated. A common hypomorphic variant of *RNASEL* has also been shown to confer a predisposition to prostate cancer associated with the xenotropic murine leukemia-related retrovirus (*44*). Thus, PIDs should not be considered to be restricted to the conservative notion of rare, familial, recessive, Mendelian traits, if only because there is no such thing as a strict Mendelian trait in multigenic organisms.

Concluding Remarks

It is now clear that most, if not all individuals, suffer from at least one PID, the clinical expression of which depends on exposure to ad hoc environmental factors, infectious or otherwise. Future research will focus on the clinical description, genetic characterization, and immunological investigation of these novel PIDs. This field was ostensibly born in the 1950s, after two decades of gestation (*2*), but remains in its infancy, with considerable potential for growth. What clinical implications might we predict in this rapidly expanding field, beyond the improvement of established means of diagnosis and treatment? Novel PIDs will probably guide the development of immunostimulatory drugs, such as granulocyte colony-stimulating factor, in patients with neutropenia (*4*), IFN-γ in patients with mycobacterial diseases (*24*), and IFN-α in patients with HSE (*26*). The development of potent and safe immunosuppressive drugs, such as antibodies and chemical inhibitors, may also benefit from the description of novel PIDs. One can even predict that most specialties in human medicine will benefit considerably from the expansion of PIDs, as immunity at large is central to physiology and pathology, because most tissues are subject to environmental assaults and contain myeloid and lymphoid cells. The field of PIDs is also important for immunologists, because it provides an opportunity for the genetic dissection of protective immunity and tolerance to self in the setting of a natural ecosystem. This unique feature of the human model is important in light of the natural selection of species, because it makes it possible to define the ecologically relevant function of host defense genes most likely to be subject to evolutionary selection (*11*, *22*). The emerging connection between clinical genetics, epidemiological genetics, and evolutionary genetics, with the definition of PIDs in this context, constitutes a new frontier in immunology. Together, these disciplines make possible the genetic dissection of past and present human immunity *in natura*, thereby shedding new light on the function and evolution of the immune system.

References and Notes

1. H. Ochs, C. I. E. Smith, J. Puck, *Primary Immunodeficiencies: A Molecular and Genetic Approach* (Oxford Univ. Press, New York, ed. 2, 2007).
2. E. R. Stiehm, R. B. Johnston Jr., *Pediatr. Res.* **57**, 458 (2005).
3. M. E. Conley *et al.*, *Immunol. Rev.* **203**, 216 (2005).
4. M. S. Horwitz *et al.*, *Blood* **109**, 1817 (2007).
5. R. H. Buckley, *Annu. Rev. Immunol.* **22**, 625 (2004).
6. Y. Shiloh, *Nat. Rev. Cancer* **3**, 155 (2003).
7. I. Ulmanen, M. Halonen, T. Ilmarinen, L. Peltonen, *Curr. Opin. Immunol.* **17**, 609 (2005).
8. J. L. Casanova, L. Abel, *Nat. Rev. Immunol.* **4**, 55 (2004).
9. L. Notarangelo *et al.*, *J. Allergy Clin. Immunol.* **117**, 883 (2006).
10. G. Orth, *Semin. Immunol.* **18**, 362 (2006).
11. J. L. Casanova, L. Abel, *J. Exp. Med.* **202**, 197 (2005).
12. L. D. Notarangelo, E. Gambineri, R. Badolato, *Adv. Immunol.* **89**, 321 (2006).
13. M. M. Frank, *Curr. Opin. Pediatr.* **17**, 686 (2005).
14. H. L. Malech, D. D. Hickstein, *Curr. Opin. Hematol.* **14**, 29 (2007).
15. S. Brydges, D. L. Kastner, *Curr. Top. Microbiol. Immunol.* **305**, 127 (2006).
16. G. Menasche, J. Feldmann, A. Fischer, G. de Saint Basile, *Immunol. Rev.* **203**, 165 (2005).
17. H. M. Tsai, *Kidney Int.* **70**, 16 (2006).
18. B. Grimbacher, S. M. Holland, , M. Puck, *Immunol. Rev.* **203**, 244 (2005).
19. K. E. Nichols, C. S. Ma, J. L. Cannons, P. L. Schwartzberg, S. G. Tangye, *Immunol. Rev.* **203**, 180 (2005).
20. R. A. Gatti, *Acta Oncol.* **40**, 702 (2001).
21. F. Vulliamy, I. Dokal, *Semin. Hematol.* **43**, 157 (2006).
22. J. L. Casanova, L. Abel, *EMBO J.* **26**, 915 (2007).
23. S. Mathew, G. D. Overturf, *Pediatr. Infect. Dis. J.* **25**, 255 (2006).
24. J. L. Casanova, L. Abel, *Annu. Rev. Immunol.* **20**, 581 (2002).
25. C. Picard *et al.*, *Science* **299**, 2076 (2003).
26. A. Casrouge *et al.*, *Science* **314**, 308 (2006).
27. J. L. Casanova, E. Schurr, L. Abel, E. Skamene, *Trends Immunol.* **23**, 469 (2002).
28. H. D. Ochs, S. F. Ziegler, T. R. Torgerson, *Immunol. Rev.* **203**, 156 (2005).
29. N. Bidere, H. C. Su, M. J. Lenardo, *Annu. Rev. Immunol.* **24**, 321 (2006).
30. U. Salzer, B. Grimbacher, *Semin. Immunol.* **18**, 337 (2006).
31. G. Hollander *et al.*, *Immunol. Rev.* **209**, 28 (2006).
32. A. Puel, C. Picard, C. L. Ku, A. Smahi, J. L. Casanova, *Curr. Opin. Immunol.* **16**, 34 (2004).
33. B. Schick, A. Prescher, E. Hofmann, C. Steigerwald, W. Draf, *Eur. Arch. Otorhinolaryngol.* **260**, 518 (2003).
34. M. B. Antunes, N. A. Cohen, *Curr. Opin. Allergy Clin. Immunol.* **7**, 5 (2007).
35. A. Alcais, C. Fieschi, L. Abel, J. L. Casanova, *J. Exp. Med.* **202**, 1617 (2005).
36. C. Picard, J. L. Casanova, L. Abel, *Curr. Opin. Immunol.* **18**, 383 (2006).
37. A. C. Allison, *Genetics* **166**, 1591 (2004).
38. A. Alcais *et al.*, *Nat. Genet.* **39**, 517 (2007).
39. J. W. Holloway, G. H. Koppelman, *Curr. Opin. Allergy Clin. Immunol.* **7**, 69 (2007).
40. A. Sandilands, F. J. Smith, A. D. Irvine, W. H. McLean, *J. Invest. Dermatol.* **127**, 1282 (2007).
41. S. Onengut-Gumuscu, P. Concannon, *Curr. Opin. Immunol.* **18**, 634 (2006).
42. S. E. Girardin, J. P. Hugot, P. J. Sansonetti, *Trends Immunol.* **24**, 652 (2003).
43. R. H. Duerr *et al.*, *Science* **314**, 1461 (2006).
44. C. Bisbal, R. H. Silverman, *Biochimie* **89**, 789 (2007).

45. We thank the members of our laboratory, our collaborators and patients worldwide, and the funding grant agencies, in particular INSERM, Agence Nationale de la Recherche (ANR), and European Union. J.L.C. is an International Scholar of the Howard Hughes Medical Institute.

10.1126/science.1142963

PERSPECTIVE

Epigenetic Flexibility Underlying Lineage Choices in the Adaptive Immune System

Dimitris Kioussis[1]* and Katia Georgopoulos[2]

Although fundamental models have emerged in recent years describing how chromatin and transcription regulation interface with one another in the developing immune system, the order of events and their biological impact are still being resolved. Recent advances have provided a flexible rather than static view of chromatin regulation to reveal how both positive and negative forces work concomitantly to establish specific chromatin structures and regulate gene expression. The challenge will now be to explore new epigenetic models and validate them during lymphocyte development, with the ultimate goal of unraveling the long-sought mechanisms that support the emerging complexity of the adaptive immune response.

Lymphocyte development is ultimately determined by a succession of gene expression programs and by stage-specific networks of classical transcriptional factors, which act as drivers in the progression to specific terminal cell types (*1*, *2*). The activity of such cell fate–determining transcription factors is intimately linked to dedicated chromatin modifiers that alter accessibility of lineage-specific gene loci and provide ultimate control over this process (*3*). A consideration of the regulated development of the adaptive immune system from a nuclear perspective must take into account the extended potential to choose between alternative fates that characterizes lymphoid cells, from their earliest stages of development to their later specialization as immune cell types (Fig. 1). Such cell fate choices, acting as they do at numerous branching points, result in a diverse yet balanced immune system and depend on the coordinated acquisition of a gene expression program that favors one cell fate over another. These programs are the result of a combination of gene-activating and gene-silencing events and provide the molecular "signature" for a particular cell fate. At cell stages preceding fate choices, a subset of genes within a program may be transcriptionally primed (expressed) or poised (not expressed but readily activatable) for transcription, providing cells with the potential for differentiation into alternative lineages (Fig. 1). This state of affairs has been increasingly recognized as lineage priming that is regulated at both the transcriptional (*4*–*6*) and epigenetic (*7*, *8*) level. At these pre-decision stages, apparently opposing chromatin structures may coexist on a gene locus but resolve in subsequent stages into exclusively activating or silencing structures (Fig. 1). This type of resolution may be decided at the point of cell division, when asymmetric distribution of regulatory proteins in daughter cells can lead to differential gene expression patterns (*9*). The retention of opposing chromatin structures on lineage-specific gene loci may provide a potential at a later point for further differentiation by allowing epigenetic flexibility on key differentiation factors. Activation or repression of genes may be stably maintained through the rest of the differentiation process, or they may be "flexible," reverting to earlier states at later steps in the pathway.

During lymphocyte development, a certain set of "fixed" transcriptional decisions appears to coexist with flexible changes in gene expression. For example, T cell receptor expression is activated at the double negative (DN) stage and is maintained at subsequent stages of T cell differentiation, whereas expression of the CD8 and CD4 co-receptors fluctuates during the development of cytotoxic and helper T cell lineages.

Epigenetic flexibility may endow developing immune cells with their extended potential for alternative effector fate choices during terminal differentiation and may allow early progenitors and their late progeny to share key molecular properties. For example, both primitive hematopoietic stem cells (HSCs) and memory immune cells survive for extended periods, possibly by using similar genetic programs that contribute to their capacity to self-renew (*10*, *11*).

Modes of Epigenetic Regulation

The outcome of genetic programs set up during lymphocyte development is influenced in part by the developmentally regulated gain or loss of expression of nuclear factors that modulate basal transcription. It is also controlled by specific changes in chromatin structure in the vicinity of lineage-specific genes. Chromatin structures have been classified as closed or open-permissive, depending on whether the genes included are silenced or expressed (*12*). And a number of histone modifications (known as histone code) have been associated with such states (*13*).

Silenced chromatin, largely heterochromatic, contains a number of restrictive histone modifications, such as me[3]K9, me[3]K27, me[4]K20, and histone deacetylation, which allow for a higher-order packing and inaccessibility to transcription factors. In addition, silenced chromatin frequently contains hypermethylated DNA. Conversely, open-permissive chromatin with histone modifications, such as me[3]K4, me[3]K36, ac[3], and ac[4], contains genes that are actively transcribed and is perceived to be accessible to regulators of transcription. Recent studies in embryonic stem (ES) cells have provided evidence for a third type of chromatin, referred to as "bivalent," as a way of generating developmental plasticity through epigenetic flexibility (Fig. 1). This type combines the characteristics of both closed (me[3]K27) as well as permissive (me[3]K4) chromatin structures and marks lineage-specific genes poised for later lineage-specific activation (*7*, *8*). In a model deduced from these studies, the repressive chromatin modifications keep lineage-specific genes in a transcriptionally inactive state, while the permissive chromatin modifications keep them poised for activation once the former influence is removed. Conversely, removal of the permissive chromatin modifications may also allow the repressive chromatin modifications to prevail, thus establishing gene silencing. Increased expression of relevant transcription regulators during development may also aid the resolution of bivalent epigenetic structures into their respective activating or repressing states in a permanent fashion.

Epigenetic Flexibility in Differentiating Immune Cells?

The existence of bivalent chromatin structures and their role in providing cell fate flexibility during somatic cell differentiation and during development of the immune system need further exploration. Lineage-specific genes with flexible expression are observed throughout the lymphoid pathway, from the earliest pre-commitment steps to the later pre-effector cell stages, and these genes represent excellent candidates for testing the presence and role of bivalent epigenetic states during lymphocyte development as well as maturation to effector states (Fig. 1). For example, components of the antibody-producing machinery (e.g., immunoglobulin J and sterile transcripts from the immunoglobulin heavy chain constant regions implicated in immunoglobulin class switching) required in terminally differentiated plasma cells are expressed in early hematopoietic multipotent progenitors and are temporarily repressed during early B cell differentiation (to be reactivated in the periphery at later stages of B cell development) (*14*). Similarly, in early thymocyte precursors that lack both CD4 and CD8 co-receptors (DN), the genes for each co-receptor may acquire a bivalent chromatin state poised for

[1]Molecular Immunology, Medical Research Council (MRC) National Institute for Medical Research, The Ridgeway, London NW7 1AA, UK. [2]Cutaneous Biology Research Center, Massachusetts General Hospital, Harvard Medical School, 149 13th Street, Charlestown, MA 02129, USA.

*To whom correspondence should be addressed. E-mail: dkiouss@nimr.mrc.ac.uk

expression. This state would then resolve into activating structures at the double positive (DP) stage of T cell differentiation. After thymocytes have reached the DP ($CD4^+$ $CD8^+$) stage of development, these genes may again become temporarily poised, before their fate is determined by permanently resolving the bivalent state in a complementary fashion in mature cytotoxic (CD8) and helper (CD4) T cells (*15*). It is possible that

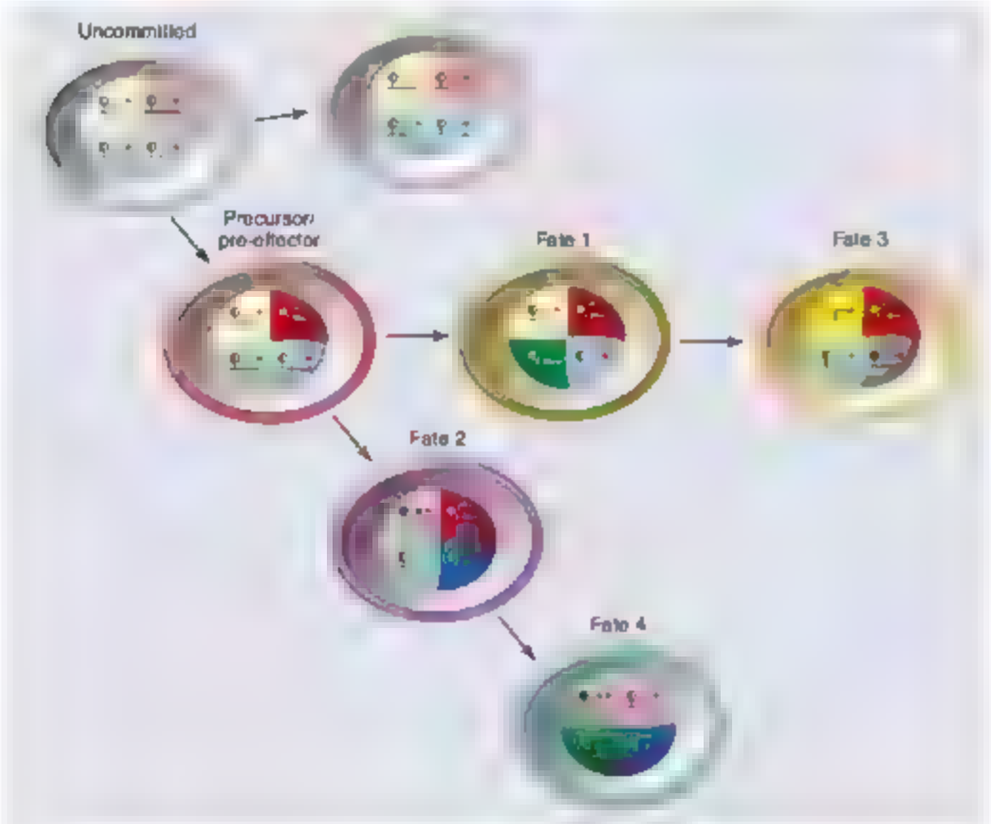

Fig. 1. Developmental progression from an uncommitted state and a precursor–pre-effector state to distinct cell fates from a gene expression–chromatin perspective. Four programs in gene expression (shown in compartments within the nucleus), whose combinatorial acquisition allows for distinct cell fate choices (depicted by the differently colored cell perimeters) to be made, are shown from the early to the later steps of the pathway. The poised (not expressed but activatable) or primed (low expression) state of the genes in these programs is indicated by a half-black, half-white circle representing bivalent chromatin and a dashed bent arrow for low or no transcription. Activated genes are indicated by a solid white circle and a solid bent arrow for transcription. Genes repressed in a permanent fashion are indicated by a solid black circle and a block (indicated by "×") on the transcriptional arrow. Different scenarios in the resolution of poised lineage-specific genetic program are entertained, leading to distinct cell fate choices. Fate choices with poised genetic programs may be reversible, whereas others without such programs may be permanent.

expression of regulatory genes such as *c-kIT-3*, *Bcl-6*, *Fox-P3*, and *RORgamma*, which influence decisions both in early T cell development and at later steps of T helper lineage maturation (*1*), may also be modulated through such flexible epigenetic mechanisms.

This handful of known examples lends evidence for a broader flexibility in the genetic programs that bestow lymphocytes with an extended differentiation potential. Genome-wide investigations on developmentally relevant cells, for example, with the use of chromatin immunoprecipitation on-chip technology (*16*, *17*) in the concurrence of restrictive and permissive chromatin modifications at various branch points of the lymphoid pathways may offer yet further examples of genetic programs poised for activation and help us define their mode of establishment and resolution. For example, it will be important to determine whether the resolution to a permissive or silenced state is permanent, or whether these can revert back to a bivalent state, which may indicate restoration of previous potential. This type of epigenetic regulation may also explain the relative ease with which lymphocytes can be reprogrammed through much of their ontogeny to their closer relatives within the hematopoietic system: the myeloid lineage. For example, the inappropriate introduction or removal of antagonistic lineage-specific transcriptional regulators (e.g., loss of PAX-5 in precursor B cells and ectopic expression of C/EBPα in mature B cells) may allow activation of a myeloid genetic program that may exist in a bivalent state in these cells (*18*–*20*).

Regulators of Epigenetic Flexibility

To date, the molecular players and their interactions that generate and regulate bivalent flexible chromatin structures and their resolution are not well defined. It is possible that epigenetic flexibility may be brought about by the concomitant action of functionally opposed chromatin regulators occupying the same chromosomal site. Precedence for such a mode of regulation is again provided in ES cells, where positive chromatin regulators and members of the trithorax complex coexist with negative regulators of the Polycomb group on lineage differentiation genes, several of which have been shown to exist in a bivalent chromatin configuration (*21*). The *CD4* and *CD8* genes lend themselves as potential paradigms for identifying such dueling epigenetic regulators during T cell development. The coexistence of opposing chromatin regulators on the *CD4* locus and its regulatory elements provides a ground for identifying such a "bimodal" regulatory network composed of competing activities and responsible for setting bivalent chromatin states and flexible transcriptional outcomes during development (*22*–*24*).

Another example for generating poised chromatin is suggested by the structure of the nucleosome remodeling and deacetylase (NuRD) complex, in which the adenosine triphosphate dependent chromatin remodeler Mi-2β that provides chromatin fluidity coexists with histone deacetylases that are usually associated with repressive chromatin structures (*25*, *26*). The coexistence of antagonistic enzymatic activities within a protein complex may ensure both proper chromatin regulation and epigenetic flexibility. The chromatin remodeler Mi-2β in the NuRD complex is one such potential direct bimodal regulator of CD4 gene expression during T cell development (*24*, *27*). A direct partner of Mi-2β in this NuRD-based chromatin-remodeling complex is Ikaros: a sequence-specific DNA binding factor implicated in early lymphocyte development (*26*, *28*, *29*). Ikaros, through its association and gene-specific targeting of such a bivalent complex in the HSC and its immediate progeny, may confer lineage plasticity and the potential for differentiation to these cells. It would be important to determine whether such an Ikaros bimodal complex effects the priming or poising of lineage-specific gene expression programs in the HSC and its early progeny.

One further challenge will be to determine whether and how opposing activities within a protein complex on a given genetic locus are regulated. For example, DNA bound chromatin-modifying complexes and their components may be amenable to modifications, such as those to histones, that could influence their overall activity and, therefore, chromatin dynamics. Another challenge is to obtain a more global view on the recruitment of such chromatin regulators to gene loci associated with lineage-specific expression signatures and determine the DNA binding activities or chromatin (histone code) platform that determines such targeting.

Nuclear Compartmentalization of Genetic Programs

In addition to the mechanisms described above, classical competition between opposing regulators

for the same DNA binding sequence at a chromosomal site or for an established chromatin (histone code) domain may also determine the transcriptional activity of a regulated gene. In these cases, fluctuating concentrations of nuclear factors with disparate activities during development can allow for a transcriptional flexibility that would obey mass action rules by establishing working equilibria between activating and silencing components (12). Such equilibria may be modified not only by varying the production of any particular factor but also by regulating the rate of their synthesis, stability, and degradation, as well as by sequestering them in different nuclear compartments. In the latter case, gene activity could be determined by moving genes into nuclear compartments where different types of regulators predominate. Indeed, the positioning of gene loci within nucleus subdomains has emerged as a potentially important determinant of gene activity (27, 30, 31). Genes associated with heterochromatic regions of the nucleus (perinuclear, centromeric clusters) seem to be silent. So far, the association is correlative, and it is unclear whether the silencing precedes or is the result of this localization. Better characterization (composition and dynamics) of such active or silencing regions will require the identification of molecules responsible (i) for setting up the environment in these domains and (ii) for the movement of genes from one region of the nucleus to another. Improvements in resolution and specificity of the tools needed for the identification and visualization of these components will be one of the most formidable technological challenges in the forthcoming years.

Concluding Remarks

The hematopoietic system, in which cell lineage choices are well characterized and a substantial number of transcription regulators of cell fate and their targets have been identified, provides an excellent paradigm to study the mechanisms that underlie lineage progression and plasticity. Initial steps in such studies are already identifying epigenetic states by which lineage priming and plasticity are achieved and are suggesting that the three discrete states of chromatin may be achieved by different mechanisms at different stages in the hematopoietic lineage. The ability to use alternative mechanisms at multiple steps during differentiation makes the hematopoietic system an important contributor to future research on epigenetic models of gene regulation in normal development and disease.

References and Notes

1. E. V. Rothenberg, *Nat. Immunol.* **8**, 441 (2007).
2. K. L. Medina, H. Singh, *Curr. Opin. Hematol.* **12**, 203 [redacted].
3. K. Georgopoulos, *Nat. Rev. Immunol.* **2**, 162 (2002).
4. K. Akashi, *Ann. N.Y. Acad. Sci.* **1044**, 125 (2005).
5. R. Mansson *et al.*, *Immunity* **26**, 407 (2007).
6. P. Laslo *et al.*, *Cell* **126**, 755 (2006).
7. B. E. Bernstein *et al.*, *Cell* **125**, 315 (2006).
8. V. Azuara *et al.*, *Nat. Cell Biol.* **8**, 532 (2006).
9. S. L. Reiner, F. Sallusto, A. Lanzavecchia, *Science* **317**, 622 (2007).
10. D. T. Fearon, P. Manders, S. D. Wagner, *Science* **293**, 248 (2001).
11. J. T. Chang *et al.*, *Science* **315**, 1687 (2007).
12. R. Festenstein, D. Kioussis, *Curr. Opin. Genet. Dev.* **10**, 199 (2000).
13. T. Kouzarides, *Cell* **128**, 693 (2007).
14. A. Delogu *et al.*, *Immunity* **24**, 269 (2006).
15. D. Kioussis, W. Ellmeier, *Nat. Rev. Immunol.* **2**, 909 (2002).
16. Y. Zheng *et al.*, *Nature* **445**, 936 (2007).
17. A. Marson *et al.*, *Nature* **445**, 931 (2007).
18. C. Cobaleda *et al.*, *Nat. Immunol.* **8**, 463 (2007).
19. H. Xie *et al.*, *Cell* **117**, 663 (2004).
20. C. V. Laiosa, M. Stadtfeld, T. Graf, *Annu. Rev. Immunol.* **24**, 705 (2006).
21. L. A. Boyer *et al.*, *Nature* **441**, 349 (2006).
22. T. H. Chi *et al.*, *Nature* **418**, 195 (2002).
23. T. Sato *et al.*, *Immunity* **22**, 317 (2005).
24. C. J. Williams *et al.*, *Immunity* **20**, 719 (2004).
25. Y. Zhang *et al.*, *Cell* **95**, 279 (1998).
26. J. Kim *et al.*, *Immunity* **10**, 345 (1999).
27. K. E. Brown *et al.*, *Mol. Cell* **3**, 207 (1999).
28. T. Yoshida *et al.*, *Nat. Immunol.* **7**, 382 (2006).
29. S. Y. Ng, T. Yoshida, K. Georgopoulos, *Curr. Opin. Immunol.* **19**, 116 (2007).
30. T. Misteli, *Cell* **128**, 787 (2007).
31. S. T. Kosak *et al.*, *Science* **296**, 158 (2002).

32. K.G. is supported by the National Institute of Allergy and Infectious Diseases, and D.K. is supported by the MRC.

10.1126/science.1143777

PERSPECTIVE

Division of Labor with a Workforce of One: Challenges in Specifying Effector and Memory T Cell Fate

Steven L. Reiner,[1*] Federica Sallusto,[2*] Antonio Lanzavecchia[2*]

In the course of the immune response against microbes, naive T cells proliferate and generate varied classes of effector cells, as well as memory cells with distinct properties and functions. Owing to recent technological advances, some of the most imposing questions regarding effector and memory T cell differentiation are now becoming experimentally soluble: How many classes of antigen-specific T cells exist, and how malleable are they in their fate and in their functional state? How might a spectrum of cell fates be imparted to the clonal descendants of a single lymphocyte? Where, when, and how does pathogen-associated information refine the instruction, selection, and direction of newly activated T cells as they perform their tasks in different locations and times? Some surprising new glimpses ahead on these subjects and other yet-unanswered questions are discussed.

Specific immunity adapts to the threat of pathogen attack with vigorous clonal expansion of a selected lymphocyte whose antigen receptor binds microbial peptide in the context of self major histocompatibility molecules. The culmination of specific immunity is the generation of effector cells that are responsible for acute elimination of the pathogen and memory cells that patrol their various tissue domains in search of evidence of re-attack.

[1]Abramson Family Cancer Research Institute of the University of Pennsylvania, Philadelphia, PA 19104, USA. [2]Institute for Research in Biomedicine, Via Vincenzo Vela 6, CH-6500 Bellinzona, Switzerland.

*To whom correspondence should be addressed. E-mail: sreiner@mail.med.upenn.edu (S.L.R.), federica.sallusto@irb.unisi.ch (F.S.), lanzavecchia@irb.unisi.ch (A.L.)

Heterogeneity is a hallmark of antigen-specific T cells. $CD4^+$ T cells make effector choices to become T helper cell 1 (T_H1), T_H2, or T_H17 cells and might likewise choose to become antigen-specific regulatory cells (1–3). In addition to choice of cytokine repertoire, effector $CD4^+$ T cells exhibit diversity in homing, such as migration to peripheral nonlymphoid tissue versus transit to lymph node follicles to promote B cell help (4). Heterogeneity of $CD8^+$ T cell effector gene expression has been described (5), although it is not clear whether this represents physiologically distinct cell fates or simply fluctuation in activation state. Memory T cells are heterogeneous, with central memory cells that patrol secondary lymphoid tissues, recapitulating the surveillance of their naïve progenitor, and effector memory cells that act as sentinels standing guard at frontline barriers (6).

Although the role and function of effector and memory subsets in protection or pathology and the nature of polarizing signals required for their differentiation are becoming increasingly clear, there are still outstanding questions that need to be addressed that relate to the mechanism of T cell fate specification. Many of these questions deal with fundamental uncertainties that are common to many areas of blood differentiation, such as the extent of fate diversity, the ontogeny and lineage relationship between opposing and kindred fates, and the degree of natural and therapeutic plasticity at different stages of differentiation.

"One Cell, One Fate" Versus "One Cell, Multiple Fates"

Signaling and transcription during T cell activation have traditionally been viewed as a uniform process. Any given naïve precursor cell could be

signaled in a unique manner, giving rise to homogeneous progeny. In this "one cell, one fate" model, heterogeneity in cell fate can be accommodated by recruitment of several clones, leading to diversity at the population level (Fig. 1). This might occur, for instance, in different anatomic zones or at differing time points during the immune response if stimulatory conditions change due to decreased availability of antigen, decline in antigen-presenting cell function, and increased competition among antigen-specific T cells (*7*).

Clonal selection during an immune response is, of necessity, intimately associated with cell division. The possibility exists, therefore, that one cell could be signaled in such a way that it gives rise to daughter cells with identical antigen receptors that adopt different fates. In a "one cell, multiple fates" model (Fig. 1), the challenge is to determine the mechanism that generates heterogeneous progeny and whether the process is deterministic or stochastic. In any model of heterogeneity, moreover, it is important to determine whether an observed change in a cell or its progeny relates to a transition in fate (inheritable differences) or simply an alteration in its functional state (stable or unstable variation within a single fate). For example, T_H1 cells that secrete interleukin-10 (IL-10) in a provisional manner in order to establish some control over inflammation may represent an altered state of T_H1 activation rather than a distinct cell fate (*8*).

Asymmetric Cell Division and Strength of Stimulation

A deterministic mechanism to generate heterogeneity, called asymmetric cell division, has recently been proposed as an explanation for achieving fate diversity in the daughter cells (*9*). On the basis of imaging studies, it appears that a naïve T cell has a prolonged interaction with the dendritic cell (DC) before its first division (*10*). This sustained contact at the level of the immunological synapse appears to coordinate the plane of cell division and the unequal partitioning of fate-determining proteins to daughter cells (*9*) (Fig. 1). Accordingly, the first daughter T cells could represent effector- and memory-fated daughters. The daughter proximal to the synapse may become signaled more strongly such that it adopts a terminally differentiated effector fate characteristic of effector and effector memory T cells, whereas the daughter distal to the synapse may remain in an intermediate stage of differentiation, which is characteristic of the central memory T cell lineage.

The extent and nature of naïve T cell differentiation are determined by the quantity and quality of stimulation, including concentration of antigen, costimulatory molecules, and cytokines, as well as the frequency of responding T cells and density of antigen-presenting DCs (*11*). As a function of the strength of stimulation, naïve T cells progress through hierarchical thresholds for proliferation, acquisition of responsiveness to homeostatic cytokines, and differentiation to effector cells. In the clonal burst of an immune response, the four-dimensional itinerary of daughter and granddaughter T cells has not yet been adequately chronicled. The subsequent interactions of these critical progeny with their antigen, cytokine, and chemokine environment could indeed be random. If daughters inherit differing migratory or signaling capacities, however, differences in their subsequent itinerary might be considered deterministic. Random and nonrandom differences in subsequent signaling might, therefore, be critical for the descendants of a workhorse of one to reach different states of differentiation, including terminally differentiated cells as well as uncommitted and less differentiated intermediates, further embellishing a spectrum of differences among clonally related T cells (Fig. 2).

The future challenge in this regard will be to determine the subsequent contact, migratory, and signaling history of daughter and granddaughter T cells, across both the $CD4^+$ and $CD8^+$ lineages and across an array of varied immune responses. How many rounds of asymmetric or symmetric division occur? To what degree do subsequent interactions appear stereotyped or random? Where do daughter cells go after division? Will the outcome of division be different for antigens presented by DCs, B cells, and macrophages?

Effector Heterogeneity—Many New Choices

Recent years have seen remarkable progress in understanding how innate immunity and other signaling processes shape the function and migration of activated T cells, but how these stimuli act on an expanding T cell clone and how much diversity is generated in immune responses remain to be determined. Indeed, with improved methods to analyze phenotype and function of effector T cells, it has become clear that the effector cells are heterogeneous in terms of their surface phenotype, cytokine production, and homing potential. Thus, in addition to the classical T_H1, T_H2, and T_H17 cells (*3*, *12*), other effector cells have been identified. These include follicular T_H cells that produce IL-10 and IL-21 (*4*), T_H0 cells producing interferon-γ (IFN-γ) and IL-4, as well as T_H cells producing both IFN-γ and IL-10 (*8*) or IFN-γ and IL-17 (*13*). Further heterogeneity is detected at the level of homing receptors with distinct subsets of central memory and effector memory cells (*6*). Although some of these properties may be related to the state of activation, most appear to define distinct T cell fates that are stable upon clonal expansion in vitro (*14*).

Many of the challenges facing our understanding of effector differentiation relate to questions of plasticity and lineage relationships. Traditionally, $CD4^+$ T cell effector fate was thought of as a binary choice between opposite fates. With increasing recognition that there are more than two $CD4^+$ effector fates (*3*, *12*), a challenge will be to understand how cells can make decisions when confronted by multiple choices. In view of the findings that mature $CD4^+$ effector fates are not adopted until after cell division (*15*), that $CD4^+$ T cells also exhibit asymmetric division (*9*), and that $CD4^+$ T cells may reengage with DCs after they have divided (*16*), it is tempting to speculate that a $CD4^+$ T cell might not make exclusive choices initially. Instead, it might generate an array of lineage-committed progenitors through limited rounds of asymmetric division. For example, the receptor for IFN-γ is polarized at the immunological synapse of $CD4^+$ T cells activated in vitro and in vivo (*9*, *17*). Because this asymmetry persists until

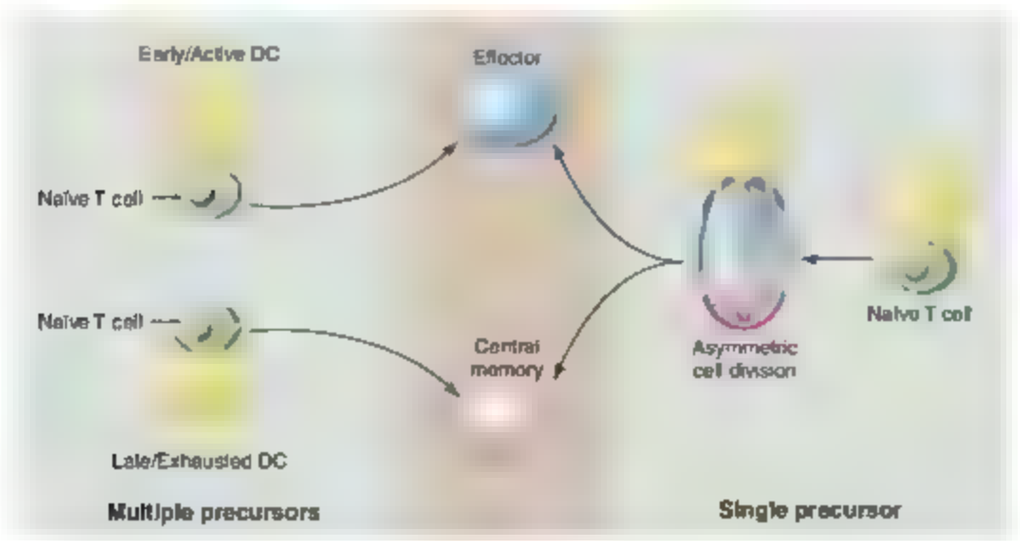

Fig. 1. Alternative models for generating heterogeneity of T cell fate during the immune response. In a "a one cell, one fate" model (left), two naïve T cells receive distinct signals from independent encounters with DCs having different states of maturation. The alternative signaling will independently elicit effector and central memory differentiation (center). Alternatively, in a "one cell, two fates" model (right), a single naïve T cell might undergo an asymmetric cell division, resulting in daughter cells that will give rise to different fates (center).

mitosis, it could result in the first CD4+ daughter T cells becoming more and less T_H1-prone. With subsequent division, daughters could further diversify as T_H2-, T_H17-, or adaptive regulatory T cell (T_{reg}) prone, as well as precursors of the central memory lineage. Selective pressures mediated by the pathogen-related signals, such as presence or absence of IL-12 or IL-23, could then determine the relative outgrowth and suppression of the various lineages, resulting in a polarized outcome. Whether the initial progeny are indeed partially committed down different paths or are all equally malleable intermediates has not yet been adequately evaluated.

How many generations of daughters recontact antigen-presenting cells and whether both initial daughters have an equal likelihood of reencountering antigen at the site of primary immunization or in peripheral tissues are not yet known. It is likely that such reencounters might influence the capacity of daughter cells to further differentiate by acquiring additional functions. At which cell division number, or after how much signaling, and in what anatomic location differentiating progeny lose their plasticity and become more epigenetically fixed in their fate are unresolved issues with important therapeutic implications for diverting burgeoning and established immune responses. Another critical challenge in effector differentiation is to better understand the role and regulation of antigen-specific regulatory cells in policing their effector kindred (*2*). Whether variant effector T cells that coexpress regulatory cytokines (*8*) and antigen-specific adaptive T_{reg}'s expressing FoxP3 (*12*, *18*) will play roles in a physiological or therapeutic setting across a wide spectrum of immune responses has not been adequately evaluated.

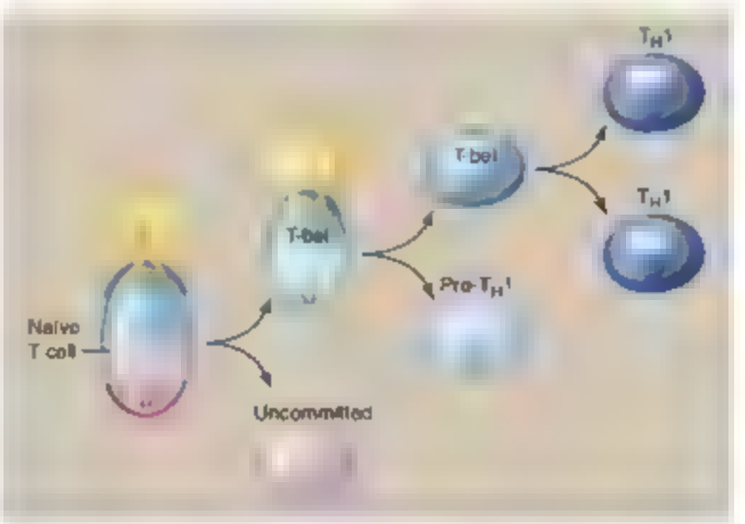

Fig. 2. Hypothetical model for generating a spectrum of differentiation among the descendants of a single clonally selected T cell. Daughter cells could encounter stochastic variation in exposure to antigen or cytokine signals, as well as deterministic differences such as unequal inheritance of fate-imposing or migratory signals. Together with further asymmetric cell division, these random and nonrandom differences in strength of stimulation could yield a diverse clonal burst, including but not limited to terminally differentiated effector progeny (T-bet–expressing T_H1 cells, in this case) as well as progeny with uncommitted and intermediate states of differentiation.

Memory Heterogeneity and "Stemness"

The ontogeny of memory T cells is controversial, with some studies suggesting a progressive development of memory cells from effectors and others suggesting an early bifurcation between commitment to the memory and effector lineages (*6*, *7*, *9*, *19*, *20*). An asymmetric first T cell division provides a potential mechanism for simultaneous generation of effector and memory daughter cells, with the proximal daughter poised to receive more antigen and cytokine signals compared to the distal cell, which can retain stem cell–like plasticity for renewal and further differentiation at a later time (*9*) (Fig. 1).

If the first distal daughter is the precursor of a central memory–like cell, then it remains to be determined what are the precursors of effector memory T cells. Are effector memory T cells simply long-lived effector cells that escaped clonal deletion, or are they continually repopulated from a stem cell–like central memory cell? Whereas the first mechanism would ensure that the spectrum of functions generated in the primary response are maintained in memory cells, the second mechanism is consistent with the finding that effector memory cells have poor reconstitution potential and that a central memory T cell can differentiate to effector cells in response to homeostatic cytokines. Because a central memory stem cell periodically engages in intercellular communication to receive membrane-bound IL-15 signaling during homeostasis, it is possible that a nonantigen-driven asymmetric division might result in a self-renewing central memory stem cell daughter and a terminally differentiated effector memory daughter.

Technical Challenges—Imaging and Modeling a Workforce of One

Modeling the immune response in vivo has relied heavily on the transfer of relatively high numbers of transgenic T cells expressing an antigen receptor of known specificity. It is increasingly apparent, however, that the behavior of 1 million transferred cells might be quite distinct from the behavior of a single cell in isolation (*19*, *21*, *22*). A high frequency of responding cells might result in strong competition, decreasing the duration and strength of the stimulus received and perhaps the likelihood of asymmetric division, which might ultimately lead to incomplete differentiation. The in vivo monitoring of a physiological immune response would require methods that allow tracking of endogenous antigen-specific T cells and, eventually, a single naïve T cell. Such minute numbers of cells, however, would make it difficult to image cell-cell interactions and clonal dynamics in situ. Given that the ability of a responding T cell to maintain contact is inversely proportional to the number of responding cells (*21*), it might be extrapolated that asymmetric division would be an invariant feature of clonal bursts with only small numbers of responding cells.

As mentioned above, a major challenge facing the field is the ability to chronicle a clonal burst adequately in vivo. Reagents and model systems to trace early events developing in situ will be critical for this task. Imaging approaches that can reveal cell fates using reporters of key transcription factor or effector molecule expression will undoubtedly be useful to this end (*13*). Being able to distinguish parent from daughter and granddaughter, as well as which are descendants of proximal and distal cells, will be important to refine a fate map of different immune responses. Reagents that can report the maturation status of DC's and local cytokine gradients may also be necessary to understand the role of the T cell's environment in promoting variance in the fate of the activated cells (*23*). The field is now faced with the exciting, yet daunting, challenge of unveiling the instructions, identity, and agenda of the cellular descendants of a single T cell called to battle.

References and Notes

1. K. M. Murphy, S. L. Reiner, *Nat. Rev. Immunol.* **2**, 933 (2002).
2. S. Sakaguchi, F. Powrie, *Science* **317**, 627 (2007).
3. B. Stockinger, M. Veldhoen, *Curr. Opin. Immunol.* **19**, 281 (2007).
4. C. G. Vinuesa, S. G. Tangye, B. Moser, C. R. Mackay, *Nat. Rev. Immunol.* **5**, 853 (2005).
5. A. Peixoto *et al.*, *J. Exp. Med.* **204**, 1193 (2007).
6. F. Sallusto, D. Lenig, R. Forster, M. Lipp, A. Lanzavecchia, *Nature* **401**, 708 (1999).
7. D. M. Catron, L. K. Rusch, J. Hataye, A. A. Itano, M. K. Jenkins, *J. Exp. Med.* **203**, 1045 (2006).
8. A. O'Garra, P. Vieira, *Nat. Rev. Immunol.* **7**, 425 (2007).
9. J. T. Chang *et al.*, *Science* **315**, 1687 (2007).
10. S. E. Henrickson, U. H. von Andrian, *Curr. Opin. Immunol.* **19**, 249 (2007).
11. A. V. Gett, F. Sallusto, A. Lanzavecchia, J. Geginat, *Nat. Immunol.* **4**, 355 (2003).
12. D. Nicoda *et al.*, *Science* **317**, 256 (2007); published online 18 June 2007 (10.1126/science.1145697).
13. I. Ivanov *et al.*, *Cell* **126**, 1121 (2006).
14. M. Messi *et al.*, *Nat. Immunol.* **4**, 78 (2003).
15. J. J. Bird *et al.*, *Immunity* **9**, 229 (1998).
16. S. Celli, Z. Garcia, P. Bousso, *J. Exp. Med.* **202**, 1271 (2005).
17. R. A. Maldonado, D. J. Irvine, R. Schreiber, L. H. Glimcher, *Nature* **431**, 527 (2004).
18. K. Kretschmer *et al.*, *Nat. Immunol.* **6**, 1219 (2005).
19. V. P. Badovinac, J. S. Haring, J. T. Harty, *Immunity* **26**, 827 (2007).
20. D. T. Fearon, P. Manders, S. D. Wagner, *Science* **293**, 248 (2001).

21. Z. Garcia *et al.*, *Proc. Natl. Acad. Sci. U.S.A.* **104**, 4553 (2007).
22. J. Nataye, J. J. Moon, A. Khoruts, C. Reilly, M. K. Jenkins, *Science* **312**, 114 (2006).
23. R. L. Reinhardt, S. Hong, S. J. Kang, Z. E. Wang, R. M. Locksley, *J. Immunol.* **177**, 1618 (2006).
24. S.L.R. is grateful for support from the NIH and the Abramson Family. A.L. and F.S. are grateful for support from the Swiss National Science Foundation and the Helmut Horten Foundation.

10.1126/science.1143775

PERSPECTIVES

Private Lives: Reflections and Challenges in Understanding the Cell Biology of the Immune System

Ira Mellman

The immune system comprises a variety of cell types whose activities must be carefully regulated to act as a coherent unit for the purpose of host defense. To perform their autonomous functions, immune cells must rely on the same basic organizational features that apply to all cells, although immune cells often exhibit remarkable degrees of specialization and adaptation. The study of these specializations has lagged behind advances in understanding the immune response and cell biology individually. As a result, there are great opportunities, but also great challenges, for new conceptual discoveries by taking a more cell-biological approach to probing the function of the immune system.

Immunology and cell biology share at least one profound common origin. Around the turn of the 19th century, Elie Metchnikoff discovered "innate immunity" by demonstrating the ability of phagocytes to detect, engulf, and kill invading microbes. His definition of this fundamental principle of immunology was wholly enabled by paying close attention to the cell biology of how phagocytes worked. Metchnikoff's attentiveness also provided some of the first fundamental principles in cell biology, including the discovery of endocytosis, the function of lysosomes, and the ability of cells to produce cytotoxic compounds. Despite this auspicious beginning, immunology and cell biology gradually drifted apart. Perhaps because of the emerging complexity of each field, immunologists became less interested in how the cells they study actually work, whereas cell biologists (at least molecular cell biologists) avoided problems involving more than one or two cells. Yet today, like Amanda and Elyot, the divorced couple in Noel Coward's play *Private Lives*, immunology and cell biology now find themselves with new spouses in adjacent hotel rooms, realizing that there had been something wonderful in their previous relationship.

In all complex problems, understanding the mechanism provides the key to understanding the problem itself, even if this relationship is hidden by a preoccupation with the problem. In immunology, this key was long ago demonstrated by the application of molecular biology to unravel how immune cells generate the diversity required for antigen recognition by antibodies and T cells. Attention to cell-biological mechanisms has similarly produced basic insights, particularly in the areas of leukocyte diapedesis, apoptosis, and transcription. What we have learned from studying cytotoxic T lymphocyte (CTL) function has been particularly noteworthy in this regard. We have learned that cytotoxic granules are in fact modified lysosomes whose distribution and secretion are polarized to the site of target-cell recognition, increasing the directionality and thereby the selectivity of the cytotoxic payload. CTL granules polarize by interacting with microtubule-dependent motor proteins after an induced reorientation of microtubule organizing centers and thus the cell's entire microtubule network after antigen recognition (*1*). Both granule biogenesis and polarity were first described with classical cell-biological approaches and then confirmed by the analysis of mutant cells isolated from individuals with various inherited immunodeficiency syndromes (*2*). These studies demonstrated that the features of granule dynamics defined for CTLs apply to other secretory cell types (such as melanocytes). Other surprises await in these systems, such as the posttranscriptional regulation of cytokine production in secretory cells (such as natural killer cells (*3*)).

A variety of other critical problems in the immune response could also be understood at a similar level of cell-biological resolution, revealing basic new information about both immunology and cell biology. We know remarkably little about the mechanisms of cytokine secretion (especially cytosolic cytokines such as interleukin-1β), how cytoplasmic scaffolds control T cell receptor signaling, how Toll-like receptor signaling is controlled at different intracellular compartments, what the immunological synapse actually does and how it works, and the mechanisms by which alterations in cell adhesion cause cellular activation or deactivation. Another central problem in immunology that has created a natural interface with cell biology, the one that we have engaged, is antigen processing and presentation. None of these are new problems. However, they have failed to capture the imagination of more than a handful of cell biologists, leaving them to immunologists, many of whom must learn the methods and criteria of cell biology on the job. The relative lack of interaction between the two communities has created a number of disconnects over the years that perhaps have made progress more difficult to achieve than it already is.

Pathways of Antigen Processing: MHCII

With the realization more than 20 years ago that major histocompatibility complex class II (MHCII) molecules bound peptides derived largely from extracellular antigens, there has been much interest in understanding the pathways and organelles involved. It was appreciated early on that an invariant chain directed newly synthesized MHCII αβ dimers to be diverted from the secretory pathway into endocytic organelles where they encountered internalized antigens (*4*, *5*). Proteases clearly degraded invariant-chain and protein antigens, with peptide loading facilitated by chaperones such as HLA-DM, and the resulting peptide-MHCII complex then proceeded from the loading site to the plasma membrane. However, the identity of the intracellular compartment(s) in which these events transpired (as well as the order of events) remained uncertain.

Initially, the issue was, in effect, ignored by collectively referring to any endocytic organelle containing MHCII as the MHCII compartment (MIIC) (*6*). This raised a problem because the endocytic pathway comprises several distinct organelles that have decidedly different functions. Worse, the term MIIC came to imply the existence of a unique compartment specific to antigen-presenting cells (APCs). This situation obscured an underlying complexity of functional importance and substituted it with a complexity (i.e., a novel organelle) that probably did not exist (*7*, *8*). MIICs were generally assumed to have the properties of late-endocytic compartments, namely because the cells most commonly used in these studies localized most of their MHCII to late endosomes and lysosomes. Yet, not all APCs accumulate MHCII in late compartments, not all antigens are processed in late compartments, and not all APCs maintain a characteristic distribution of MHCII under all conditions. This serves to illustrate the importance of understanding organelles of immune cells with

Department of Research Oncology, Genentech, 1 DNA Way, Mail Stop 212, South San Francisco, CA 94080–4990, USA, and Departments of Cell Biology and Immunobiology, Ludwig Institute for Cancer Research, Yale University School of Medicine, New Haven, CT 06520–8002, USA. E-mail: mellman.ira@gene.com

the use of the terms and criteria established to describe organelles in general, only in this way will any unusual, immune cell specific specializations be revealed and effectively communicated to those outside the field of immunology.

The problem is best illustrated by myeloid dendritic cells (DCs), which concentrate MHC II in late endosomes and lysosomes while immature, but after maturation translocate the MHC II to the plasma membrane (*9*). Yet, it is not clear that the depletion of MHC II from late compartments eliminates the ability of a given antigen to be processed and presented. Many primary B cells and B cell lines can act as efficient APCs without localizing much MHC II to late endocytic compartments (*10*). Although DCs can form peptide-MHC II complexes in lysosomes for delivery to the surface upon maturation, this may reflect the particular biology of DCs and not represent a general phenomenon. To solve these issues, we need better and more sensitive imaging and biochemical tools to identify when and where peptide-MHC II complexes form, combined with the use of genetics or conditional switches to disrupt predicted individual steps. Such tools must be applied not only to solve the problem in culture but also to investigate APCs in vivo.

Understanding the order of events remains a problem as well. Textbooks often imply that internalized antigens are converted by proteolysis to peptides, which bind at equilibrium to MHC II molecules. Yet, a variety of considerations suggest that intact antigens can bind to MHC II before degradation, with peptides being generated after exoproteolysis from both the N- and C-terminal ends (for review, see (*11*)). Such a mechanism would be consistent with the observations that protein degradation in lysosomes does not produce even a transient accumulation of peptide intermediates and that professional APCs, such as DCs and B cells, exhibit greatly attenuated levels of lysosomal and endosomal proteases, conditions that would facilitate the scalping of unfolded antigens bound to MHC II. How peptides are loaded onto MHC II molecules may be the most fundamental issue in the field, but it still awaits direct proof by kinetic analysis and biochemical reconstitution.

Presentation of Endogenous Versus Cross-Presentation of Exogenous Antigens on MHCI

When work on the MHC II system was beginning, it was appreciated that the concentration of antigen required to elicit a CD4 T cell response was small, relative to the amount required to track its behavior by biochemical or immunocytochemical techniques. It was thus formally possible that the observed pathway was not the physiologically important one. Yet, the "obvious" mechanism turned out to be correct: antigen endocytosis and intracellular formation of peptide-MHC II complexes, followed by their delivery to the plasma membrane. On the other hand, understanding antigen processing and presentation via MHC class I (MHC I) molecules presented—and continues to present—a daunting conceptual challenge. It was clear early on that the peptides recognized by $CD8^+$ T cells were often derived from cytosolic viral proteins, proteins that never reached the endoplasmic reticulum (ER) lumen and therefore should never come in contact with the peptide-binding groove of MHC I (*12*). Although the violation of compartment barriers is anathema to cell biologists, the problem was solved in a convincing fashion by the genetic identification of the ER-localized transporter associated with antigen processing (TAP) peptide translocator and the in vitro reconstitution of its activity (*13*). Elucidating how exogenous antigens are "cross-presented"

Fig. 1. Mature DCs express large quantities of self- and foreign peptides bound to MHCI and MHCII (red) molecules and can present peptide-MHC complexes to multiple T cells simultaneously (CD3, green). It is assumed, but not entirely clear, that different peptide-MHC complexes can be presented at the same time. (Photograph courtesy of Ona Bloom, Yale University School of Medicine)

on MHC I after endocytosis has eluded a similarly elegant solution.

Bevan and colleagues were the first to show that an antigen internalized by endocytosis could be loaded onto MHC I molecules, although (using fibroblasts) they had to resort to a "trick" thought to chemically disrupt endosomes after antigen uptake (*14*). More recent work has established that DCs are by far most efficient at cross-presenting peptides derived from internalized antigens (*9*). Although some peptides can be loaded within the confines of endocytic organelles (*15*), there is excellent evidence that most incoming antigens must gain access to the cytosol in order to be cleaved by the proteasome before MHC I loading (*16*). This creates two compartment barrier violations: (i) the escape of antigens or peptides across the endocytic organelle membrane to the cytosol and (ii) retransportation across (presumably) the ER membrane to bind to MHC I. Although it is clear that TAP plays a role in translocating antigen-derived peptides in the ER (*11*, *17*), how antigens egress from endocytic organelles remains a mystery. Among the suggested mechanisms are the stochastic or induced rupture of endosomes, regulated endosomal pores, and the presence of ER-derived channels responsible for retrotranslocation of misfolded proteins. The latter has received much attention after initial excitement over the possibility that forming phagosomes physically fused with the ER, a suggestion based on qualitative static electron microscopy images but not confirmed by subsequent work (*18*).

It nevertheless remains possible that ER components are present in endocytic compartments, although it has been difficult to demonstrate this point by conventional or well-accepted approaches to immunolocalization. In other words, if they are present they represent trace components, a situation quite unlike the ER, where TAP, subunits of the translocon (such as Sec61 and derlins), and the various chaperones and glycosyltransferases associated with translocation are easy to detect (*18*). There is certainly earlier evidence that some ER components can reside at least transiently in the Golgi, endosomes, or even the plasma membrane (*11*), but using elegant and sensitive assays to demonstrate their accessibility to endocytic probes (*19*) cannot be taken as definitive evidence that they perform a physiologically relevant function outside the ER. For example, small amounts of antigen may reach the ER itself by retrograde transport, as occurs for a number of viruses and bacterial toxins (*20*). A small escaped fraction of an antigen may create the signal, rather than a small endosome-localized fraction of ER components. As described above, one must use biochemical reconstitution and genetics to clinch an idea created by localization and functional studies. A problem as vexing and important as the mechanism of cross-presentation provides fertile common ground that will continue to challenge immunologists and cell biologists alike.

Antigen Targeting to DCs

With the appreciation that antigen presentation by DCs is responsible for initiating adaptive immune responses has come considerable interest in therapeutic uses of DCs in augmenting or attenuating immune responses. Antigen delivery to DCs is a minimum prerequisite for any therapeutic setting, and it is now clear that the induction of antigen-specific immunity (or tolerance) can be dramatically enhanced by targeting a desired antigen with antibodies against DCs in the presence (or absence) of a DC-maturation signal (*21*). DCs express a plethora of surface receptors, many being C-type lectins that have proved to provide effective portals of entry

Several cell-biological questions are of interest concerning these receptors: (i) Are they internalized, and where do they deliver bound antigens? (ii) Are some receptors better at programming cross-presentation? (iii) Can individual receptors target functionally distinct DC subpopulations? (iv) Does antibody binding to a given receptor trigger DC maturation, and if so, does receptor activation help to control the balance between immunity and tolerance? In general, we must ask what the relationship is between the mode of antigen endocytosis and the function of antigen presentation to T cells (Fig. 1).

In recent work published in *Science*, Dudziak *et al.* have shown that two lectin receptors on mouse DCs, DEC-205 and DCIR (33D1), are differentially expressed by two different populations of DCs in the spleen: $CD8\alpha^+$ and $CD8\alpha^-$ DCs, respectively (22). Targeting antigens via DEC-205 to the $CD8\alpha^+$ subset was found to selectively prime MHCI-restricted responses by cross-presentation, whereas MHCII-restricted responses were more efficiently triggered by DCIR targeting to the $CD8\alpha^-$ subset. This finding is consistent with the idea that cross-presentation is, in general, more the purview of $CD8\alpha^+$ DCs (23). Reversing cell-type restriction of receptor expression did not appear to change this conclusion substantially, suggesting that specializations associated with $CD8\alpha^+$ DCs may favor their ability for cross-presentation.

At the same time, in vitro work suggested that another lectin (the mannose receptor) was also quite effective at inducing the formation of peptide-MHCI complexes from exogenous antigen in bone marrow cultures and macrophages, where subpopulation identities are less clear (24). The mannose receptor appeared to deliver bound antibody to early endocytic compartments, suggesting that cross-presentation may occur from here as opposed to in late endosomes and lysosomes, which was the case for loading onto MHCII. Although these results suggest that the receptor used and route of antigen entry may also help determine the resulting form of antigen presentation, the data relied only on low-resolution qualitative immunofluorescence to outline the intracellular localization of delivered antigens—criteria too limited to support a firm conclusion. Moreover, the data did not account for the fact that DEC-205, which also efficiently mediates MHCI-restricted cross-presentation, has been extensively characterized as delivering its bound antigens to late endosomes and lysosomes as opposed to early compartments (25). In any event, these findings highlight a whole new problem set involving the relative contributions of endocytosis and DC subpopulations in determining the nature of the immune response.

Looking Forward by Looking Backward

There are many other problems that would benefit immediately from a more effective and bidirectional relationship between immunologists and cell biologists. For example, the dynamics and function of the immunological synapse remain incompletely understood, in part because these critically important structures have yet to be subjected to the type of rigorous analysis applied to "simpler" problems of cell adhesion. The relationship between autophagy and antigen presentation in viral immunity is also emerging as critical (26, 27). Signaling in immune cells will provide a rich area to mine, and some direct interchange over what lipid rafts can and cannot do would be of great value in itself. Finally, there is the issue that immunologists have always appreciated far better than most molecular cell biologists, the in vivo or systems-level context. Immunology exists to study the way the immune system works as a whole to confer protection against disease. Broad and conceptually profound, it is understandably difficult for the field to devote equivalent attention to the cellular mechanisms involved. However, further progress will require such effort, and the best path forward will be to take steps to make the language, concepts, and culture of immunology more accessible to colleagues in cell biology to attract them in and to outsource what may be too diversionary to learn. One area that is particularly ripe for spectacular advance is in the area of in vivo or "intravital" imaging. Although still in a largely descriptive phase of development, immunologists are nicely demonstrating to cell biologists the conceptual value of this platform. When this area is combined with emerging technologies to permit intervential experiments using actuation switches and quantitative molecular reporters, we will have entered a new age of "systems cell biology" combining the best of both worlds.

Like Efyot and Amanda, immunology and cell biology were once intimate partners; we find ourselves again in close proximity, but this time with the chance to rekindle a beautiful relationship.

References

1. J. C. Stinchcombe, E. Majorovits, G. Bossi, S. Fuller, G. M. Griffiths, *Nature* **443**, 462 (2006).
2. J. Stinchcombe, G. Bossi, G. M. Griffiths, *Science* **305**, 55 (2004).
3. D. B. Stetson *et al.*, *J. Exp. Med.* **198**, 1069 (2003).
4. P. R. Wolf, H. L. Ploegh, *Annu. Rev. Cell Dev. Biol.* **11**, 267 (1995).
5. P. Cresswell, *Annu. Rev. Immunol.* **12**, 259 (1994).
6. P. J. Peters, J. J. Neefjes, V. Oorschot, H. L. Ploegh, H. J. Geuze, *Nature* **349**, 669 (1991).
7. P. Pierre *et al.*, *Immunity* **4**, 229 (1996).
8. M. J. Kleijmeer, S. Morkowski, J. M. Griffith, A. Y. Rudensky, H. J. Geuze, *J. Cell Biol.* **139**, 639 (1997).
9. I. Mellman, R. M. Steinman, *Cell* **106**, 255 (2001).
10. S. Amigorena, J. R. Drake, P. Webster, I. Mellman, *Nature* **369**, 113 (1994).
11. E. S. Trombetta, I. Mellman, *Annu. Rev. Immunol.* **23**, 975 (2005).
12. A. R. Townsend, J. J. Skehel, *J. Exp. Med.* **160**, 552 (1984).
13. M. T. Heemels, H. Ploegh, *Annu. Rev. Biochem.* **64**, 463 (1995).
14. M. W. Moore, F. R. Carbone, M. J. Bevan, *Cell* **54**, 777 (1988).
15. L. Shen, L. J. Sigal, M. Boes, K. L. Rock, *Immunity* **21**, 155 (2004).
16. A. Rodriguez, A. Regnault, M. Kleijmeer, P. Ricciardi-Castagnoli, S. Amigorena, *Nat. Cell Biol.* **1**, 362 (1999).
17. A. Y. C. Huang, A. T. Bruce, D. M. Pardoll, H. I. Levitsky, *Immunity* **4**, 349 (1996).
18. M. Savina *et al.*, *Cell* **126**, 157 (2006).
19. A. L. Ackerman, A. Giodini, P. Cresswell, *Immunity* **25**, 607 (2006).
20. J. M. Lord, L. M. Roberts, *J. Cell Biol.* **140**, 733 (1998).
21. L. Bonifaz *et al.*, *J. Exp. Med.* **196**, 1627 (2002).
22. D. Dudziak *et al.*, *Science* **315**, 107 (2007).
23. P. Schnorrer *et al.*, *Proc. Natl. Acad. Sci. U.S.A.* **103**, 10729 (2006).
24. S. Burgdorf, A. Kautz, V. Böhnert, P. A. Knolle, C. Kurts, *Science* **316**, 612 (2007).
25. K. Mahnke *et al.*, *J. Cell Biol.* **151**, 673 (2000).
26. H. K. Lee, J. M. Lund, B. Ramanathan, N. Mizushima, A. Iwasaki, *Science* **315**, 1398 (2007).
27. D. Schmid, M. Pypaert, C. Münz, *Immunity* **26**, 79 (2007).

10.1126/science.1142955

PERSPECTIVE

Emerging Challenges in Regulatory T Cell Function and Biology

Shimon Sakaguchi[1] and Fiona Powrie[2]

Much progress has been made in understanding how the immune system is regulated, with a great deal of recent interest in naturally occurring $CD4^+$ regulatory T cells that actively engage in the maintenance of immunological self-tolerance and immune homeostasis. The challenge ahead for immunologists is the further elucidation of the molecular and cellular processes that govern the development and function of these cells. From this, exciting possibilities are emerging for the manipulation of regulatory T cell pathways in treating immunological diseases and suppressing or augmenting physiological immune responses.

Walter B. Cannon, the originator of the concept of homeostasis, emphasized in his book *The Wisdom of the Body* that "When a factor is known which can shift a homeostatic state in one direction it is reasonable to look for a factor or factors having an opposing

effect." The immune system is not an exception to this. It harbors not only effector lymphocytes capable of attacking invading microbes but also an inhibitory population of T cells, called regulatory T (T_{reg}) cells. These lymphocytes are specialized in suppressing excessive or misguided immune responses that can be harmful to the host, for example, against normal self-constituents in autoimmune disease, innocuous environmental substances in allergy, or commensal microbes in certain inflammatory diseases (*1*, *2*). On the other hand, overzealous T_{reg} responses can impede host protective immunity to infectious disease and cancer. Recent advances in our understanding of the molecular mechanisms that control T_{reg} cell development have opened new avenues of investigation, but key questions concerning the antigen specificity of T_{reg} cells, their homeostasis, and mechanism of action remain. Here we discuss our current understanding of the biology and function of T_{reg} cells and how they might be clinically exploited to control physiological and pathological immune responses to self- and nonself-antigens.

Naturally occurring $CD4^+$ T_{reg} cells, which constitute approximately 10% of peripheral $CD4^+$ T cells in normal individuals, characteristically express CD25, the interleukin-2 (IL-2) receptor α chain, which is a component of the high-affinity IL-2 receptor (*1*, *2*). $CD4^+CD25^+$ T_{reg} cells play a nonredundant role in maintaining immunological self-tolerance and immune homeostasis. Their importance is made evident by the fact that the depletion of this population from normal rodents produces a variety of autoimmune inflammatory diseases, whereas reconstitution with $CD4^+$ $CD25^+$ T cells can inhibit disease development (*1*, *2*). They are produced by the normal thymus as a functionally distinct and mature population, although there is evidence that T cells with similar immune suppressive activity can be generated from naive T cells in the periphery.

The identification of the transcription factor forkhead box p3 (Foxp3) as being specifically expressed by T_{reg} cells and crucial for their function has provided a molecular framework for dissecting T_{reg} function (*3*–*5*) (Fig. 1). Mutations in the gene encoding Foxp3 in humans and mice result in impaired development and function of $CD4^+CD25^+$ natural T_{reg} cells and lead to autoimmune inflammatory pathology. This is best exemplified by a human genetic disease called IPEX (immune dysregulation, polyendocrinopathy, enteropathy, X-linked) syndrome, which is characterized by autoimmune disease (including type 1 diabetes and thyroiditis), allergy, and inflammatory bowel disease (IBD) (*6*). Further evidence for Foxp3 as a key controller of the development and suppressive function of natural T_{reg} cells comes from experiments in which transduction of the gene is sufficient to convert naive T cells into T_{reg}–like cells (*3*–*5*). Notably, Foxp3 inhibits transcription of the gene encoding IL-2 and up-regulates the expression of CD25 and other T_{reg} cell–associated molecules (*3*, *4*). The resulting inability of $Foxp3^+$ T_{reg} cells to produce IL-2 appears to make them highly dependent on exogenous IL-2 for survival (*7*–*9*). Accordingly, mice genetically deficient in IL-2, CD25, or CD122 (the IL-2 receptor β chain) and humans with genetic deficiency of CD25 have both reduced numbers and impaired function of $Foxp3^+$ T_{reg} cells and succumb to severe autoimmune inflammatory disease (*8*, *10*).

A key question that has emerged from these findings is how Foxp3 orchestrates the cellular and molecular programs involved in T_{reg} function. Recent studies have shown that Foxp3 binds to other transcription factors such as NFAT (nuclear factor of activated T cells) and AML1 (acute leukemia-1) Runx1 (runt-related transcription factor 1) and potentially interacts with activator protein 1 and nuclear factor κB (*11*–*13*). It is this Foxp3-NFAT-Runx1 complex, together with other coactivator or corepressor proteins, that is responsible for the observed repression of the IL-2 and other cytokine genes, as well as the activation of the genes for CD25, cytotoxic lymphocyte–associated antigen–4 (CTLA-4), and glucocorticoid-induced TNF receptor family–related protein (GITR) by binding to their respective promoters (*11*, *12*). MicroRNA genes also appear to be important in T_{reg} cell development; for example, T cell–specific depletion of Dicer, a ribonuclease enzyme required for processing double-stranded RNA, hampers thymic development of $Foxp3^+$ T cells and elicits IBD (*14*). In addition, it has been shown by genome-wide analysis combining chromatin immunoprecipitation with mouse genome tiling array profiling that Foxp3 directly or indirectly controls hundreds of genes, which include those that encode nuclear factors controlling gene expression and chromatin remodeling, membrane proteins, and signal transduction molecules (*15*, *16*). Assuming that the proteins encoded by Foxp3-controlled genes contribute to the suppressive activity of T_{reg} cells, it seems likely that further analysis of these pathways will provide insight into T_{reg} mechanisms of action.

In addition to the thymic production of natural $Foxp3^+$ T_{reg} cells, naive T cells in the periphery acquire Foxp3 expression and T_{reg} function in several experimental settings, including in vitro antigenic stimulation in the presence of transforming growth factor β (TGF-β) or after chronic antigen stimulation in vivo (*17*, *18*) (Fig. 1). Recent studies indicate that the intestine is a site of $Foxp3^+$ T_{reg} cell development and that specialized intestinal dendritic cells (DCs) promote Foxp3 expression via a mechanism that is dependent on local TGF-β and retinoic acid, a vitamin A metabolite (*19*–*21*). Peripheral development of $Foxp3^+$ T_{reg} cells may therefore represent a mechanism that helps broaden the T_{reg} repertoire in specialized anatomical sites. Recent studies have also revealed a reciprocal relationship between the development of $Foxp3^+$ T_{reg} and effector T cells, so that naive $CD4^+$ T cells differentiate into $Foxp3^+$ T_{reg} cells in the presence of TGF-β or into T helper 17 (T_H17) cells (which secrete IL-17, a potent proinflammatory cytokine) in the presence of TGF-β and IL-6 (*22*, *23*). Therefore, TGF-β, which can be ubiquitously expressed in tissues, has the paradoxical effect of inducing distinct T cell subsets that appear to have opposing effects on immune responses. Moreover, IL-2 facilitates the differentiation of naive $CD4^+$ T cells into T_{reg} cells but inhibits their differentiation into T_H17 cells, whereas IL-6 suppresses Foxp3 expression in T_{reg} cells in addition to enhancing T_H17 cell development (*23*, *24*). These results serve to illustrate the complexity of cytokine-mediated control of the differentiation of $Foxp3^+$ T_{reg} cells in the periphery, and further work is required to identify tissue-specific factors that influence the balance between T_{reg} and effector T cells in distinct tissue sites.

Although peripherally induced T_{reg} cells resemble thymically derived T_{reg} cells in phenotype and aspects of their function, future comparative studies of their functional and genetic stability, including the status of chromatin remodeling of the Foxp3 locus, need to be performed with the two populations (*25*). It should also be noted that, in contrast to mouse naive T cells, in which it is difficult to induce Foxp3 by in vitro T cell receptor (TCR) stimulation, human naive peripheral blood T cells readily express Foxp3 upon TCR stimulation although the expression level is generally much lower and more transient than in natural T_{reg} cells (*26*). Indeed, it is not yet established whether induced T_{reg} cells have identical functions to those of natural T_{reg} cells, to what extent they contribute to the pool of $Foxp3^+$ T_{reg} cells in the periphery, and whether this activation-induced Foxp3 expression in non-T_{reg} cells serves as a T cell intrinsic brake on immune responses.

$Foxp3^+$ T_{reg} cells can both directly and indirectly suppress the activation and proliferation of many cell types, including T cells, B cells, DCs, natural killer (NK) cells, and NKT cells in vivo and/or in vitro (*27*, *28*). In vitro suppression of TCR-stimulated proliferation of other T cells is a commonly used assay for assessing T_{reg} cell suppressive activity, however, the mechanisms involved are incompletely understood. A number of different mechanisms have been linked to T_{reg} activity, including cell contact–dependent inhibition of the activation and proliferation of antigen-presenting cells (APCs) and T cells, the killing of either APCs or T cells or both, and suppression via cytokines such as IL-10 and TGF-β (*2*, *27*, *28*). These results suggest that $Foxp3^+$ T_{reg} cells do not suppress

[1]Department of Experimental Pathology, Institute for Frontier Medical Sciences, Kyoto University, Kyoto 606-8507, Japan. [2]Sir William Dunn School of Pathology, University of Oxford, Oxford OX1 3RE, UK.

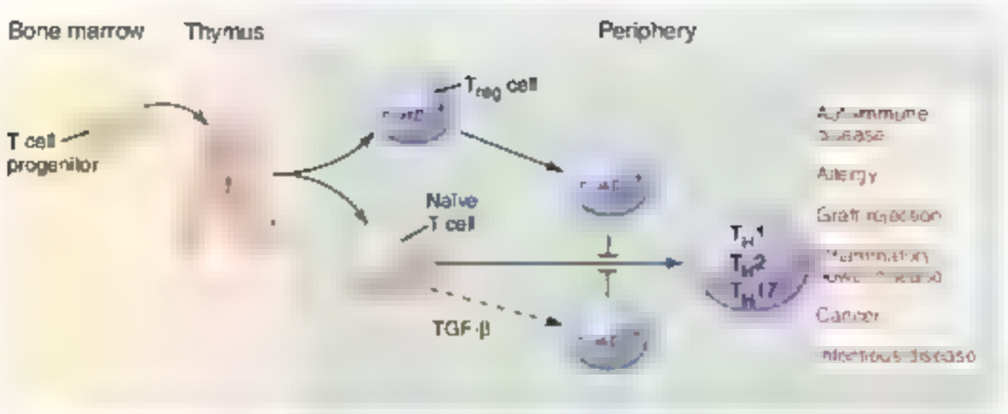

Fig. 1. Foxp3$^+$ natural T_{reg} cells produced by the normal thymus suppress the activation and expansion of naive T cells and their differentiation to effector T cells, including T_H1, T_H2, and T_H17 cells, which mediate a variety of pathological and physiological immune responses. Foxp3$^+$ T_{reg} cells can also be generated from naive T cells in the periphery, although the physiological significance of this T_{reg}-generative pathway remains to be determined.

immune responses by a single mechanism but use a variety of pathways in a context-dependent manner; for example, depending on cytokine milieu, the activation status of APCs, and the strength of antigen stimulation. A key challenge therefore is to validate putative mechanisms of T_{reg} activity in vivo and define the circumstances in which these operate. An important factor may be the site of action of T_{reg} cells. Elegant studies by intra-vital imaging with two-photon microscopy to examine the in vivo behavior of activated T_{reg} cells in lymph nodes suggest that they may hamper the access of effector T cells to DCs (*29*, *30*). There is also evidence that T_{reg} cells act in tissues to control established inflammation and that T_{reg} cell production of IL-10 plays a functional role (*2*). IL-10–secreting Foxp3$^+$ T cells are rare in the spleen but abundant in the inflamed intestine and also become detectable at the site of inflammation in autoimmune disease or chronic infection (*31*). This indicates that there is compartmentalization of the T_{reg} response and that mechanisms of suppression may be influenced by the anatomical location and dictated by the nature of the inflammatory response being regulated. It is also imperative to the host that appropriate effector responses can be activated after infection with pathogens. The production of IL-6 by activated DCs has been shown to overcome T_{reg}-mediated suppression in vitro (*32*). However, further information on the cellular and molecular pathways that control the delicate balance between effector and regulatory T cells in vivo is required.

The specialized immunological properties of Foxp3$^+$CD4$^+$ T_{reg} cells suggest that they might be clinically exploited to control a variety of physiological and pathological immune responses (*2*, *10*). These cells can recognize a broad repertoire of self- and nonself-antigens including pathogens (*33*), although their total repertoire is apparently more skewed to recognizing self-antigens (*34*, *35*). Phenotypically they appear in an "antigen-activated" state in the thymus, as illustrated by their high expression levels of various accessory molecules, including adhesion molecules (*10*). Thus, they are poised to exert suppressive function whenever exposed to relevant antigens and thus are suited for controlling autoimmunity. In addition, in contrast to their in vitro hyporesponsiveness to TCR stimulation, many natural T_{reg} cells are in a proliferative state in vivo, presumably as a consequence of the recognition of self-antigens and possibly commensal microbes, and can be stimulated to proliferate by antigenic stimulation (*10*). They are also functionally stable, retaining their suppressive activity after clonal expansion (*10*). By exploiting this stable and robust suppressive activity as well as proliferative capacity, strategies that clonally expand antigen-specific natural T_{reg} cells while inhibiting the activation and expansion of effector T cells may be useful to strengthen or reestablish self-tolerance in autoimmune disease or induce tolerance to nonself-antigens in organ transplantation, allergy, and IBD, or augment feto-maternal tolerance in pregnancy (Fig. 1). As a reciprocal approach, selective reductions in the number or function of natural T_{reg} cells while retaining or enhancing effector T cells may be a strategy for provoking and augmenting tumor immunity in cancer patients or microbial immunity in chronic infection. Biologicals and small molecules with such differential effects on T_{reg} cells and effector T cells may represent a next generation of therapeutic reagents for suppressing or enhancing immune responses with a high level of selectivity (*36*).

Besides Foxp3$^+$ T_{reg} cells, there are a number of Foxp3-nonexpressing T cells with immune suppressive activity that are in the scope of clinical use. These include CD4$^+$ cells producing IL-10 or TGF-β as well as CD8$^+$ T_{reg} cells with different modes of suppression (*28*, *37*). Although the physiological role of these populations in immune homeostasis is not known, they do offer the advantage for clinical use that antigen-specific T_{reg} cells can be prepared relatively easily.

It is now firmly established that Foxp3$^+$ T_{reg} cells, naturally arising or induced, constitute an indispensable component of the immune system. Further elucidation of the molecular and cellular basis of their development and function will facilitate our understanding of immune tolerance and homeostasis and provide ways to better control immune responses for the benefit of the host.

References and Notes

1. S. Sakaguchi, *Cell* **101**, 455 (2000).
2. K. J. Maloy, F. Powrie, *Nat. Immunol.* **2**, 816 (2001).
3. S. Hori, T. Nomura, S. Sakaguchi, *Science* **299**, 1057 (2003).
4. J. D. Fontenot, M. A. Gavin, A. Y. Rudensky, *Nat. Immunol.* **4**, 330 (2003).
5. R. Khattri, T. Cox, S. A. Yasayko, F. Ramsdell, *Nat. Immunol.* **4**, 337 (2003).
6. R. S. Wildin, S. Smyk-Pearson, A. H. Filipovich, *J. Med. Genet.* **39**, 537 (2002).
7. R. Setoguchi, S. Hori, T. Takahashi, S. Sakaguchi, *J. Exp. Med.* **201**, 723 (2005).
8. J. D. Fontenot, J. P. Rasmussen, M. A. Gavin, A. Y. Rudensky, *Nat. Immunol.* **6**, 1142 (2005).
9. L. M. D'Cruz, L. Klein, *Nat. Immunol.* **6**, 1152 (2005).
10. S. Sakaguchi, *Nat. Immunol.* **6**, 345 (2005).
11. Y. Wu *et al.*, *Cell* **126**, 375 (2006).
12. M. Ono *et al.*, *Nature* **446**, 685 (2007).
13. S. F. Ziegler, *Annu. Rev. Immunol.* **24**, 209 (2006).
14. B. S. Cobb *et al.*, *J. Exp. Med.* **203**, 2519 (2006).
15. A. Marson *et al.*, *Nature* **445**, 931 (2007).
16. Y. Zheng *et al.*, *Nature* **445**, 936 (2007).
17. W. Chen *et al.*, *J. Exp. Med.* **198**, 1875 (2003).
18. I. Apostolou, H. von Boehmer, *J. Exp. Med.* **199**, 1401 (2004).
19. D. Mucida *et al.*, *Science* **317**, 256 (2007).
20. C.-M. Sun *et al.*, *J. Exp. Med.*, in press.
21. J. L. Coombes *et al.*, *J. Exp. Med.*, in press.
22. M. Veldhoen *et al.*, *Immunity* **24**, 179 (2006).
23. E. Bettelli *et al.*, *Nature* **441**, 235 (2006).
24. A. Laurence *et al.*, *Immunity* **26**, 371 (2007).
25. S. Floess *et al.*, *PLoS Biol.* **5**, e38 (2007).
26. M. A. Gavin *et al.*, *Proc. Natl. Acad. Sci. U.S.A.* **103**, 6659 (2006).
27. H. Von Boehmer, *Nat. Immunol.* **6**, 338 (2005).
28. E. M. Shevach, *Immunity* **25**, 195 (2006).
29. Q. Tang *et al.*, *Nat. Immunol.* **7**, 83 (2006).
30. C. E. Tadokoro *et al.*, *J. Exp. Med.* **203**, 505 (2006).
31. H. H. Uhlig *et al.*, *J. Immunol.* **177**, 5852 (2006).
32. C. Pasare, R. Medzhitov, *Science* **299**, 1033 (2003).
33. I. J. Suffia *et al.*, *J. Exp. Med.* **203**, 777 (2006).
34. M. S. Jordan *et al.*, *Nat. Immunol.* **2**, 301 (2001).
35. C. S. Hsieh *et al.*, *Nat. Immunol.* **7**, 401 (2006).
36. T. Yamaguchi *et al.*, *Immunity*, in press.
37. M. G. Roncarolo *et al.*, *Immunol. Rev.* **212**, 28 (2006).
38. S.S. is supported by the Japan Science and Technology Agency. F.P. is a Wellcome Trust Senior Fellow in basic biomedical science.

10.1126/science.1142331

Q AAAs

Who inspires brainwaves while I study water waves?

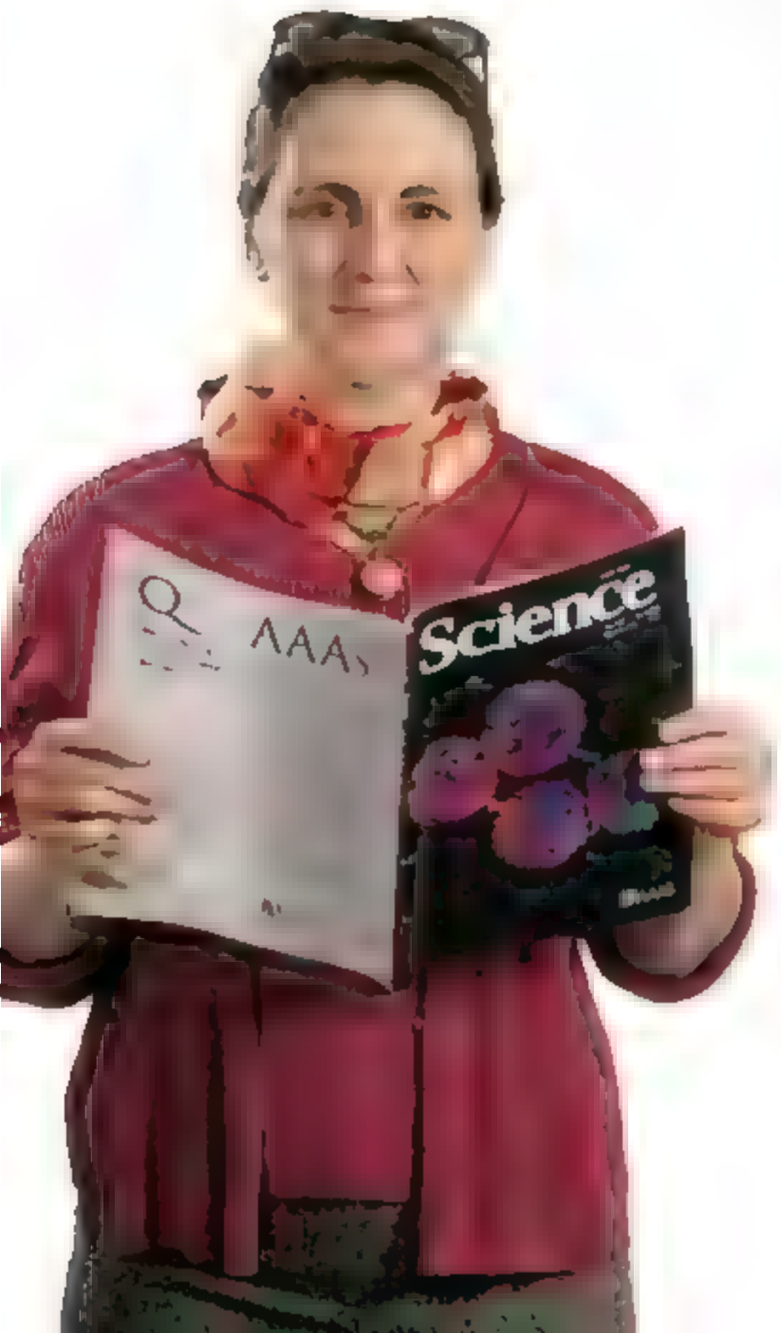

"I study the mathematical equations that describe the motion of water waves. Different equations represent different waves – waves coming onto a beach, waves in a puddle, or waves in your bathtub. Then when I've surfed the math, I like nothing better than to spend the rest of the day surfing the waves.

This field is very important. The better we can model water waves, the better we can predict the patterns of beach erosion and natural disasters such as the tsunami in South East Asia. And this research can be applied to all sorts of regions around the world.

Being a member of AAAS means I get to learn about areas of interest I might not otherwise encounter. It gives me valuable opportunities to exchange ideas with colleagues in other fields. And this helps me find new approaches to my own work."

Dr. Katherine Socha is an assistant professor of mathematics at St. Mary's College, Maryland. She's also a member of AAAS.

See video clips of this story and others at www.aaas.org/stories

Katherine Socha, Ph.D
Assistant Professor of Mathematics
and AAAS member

AAAS
ADVANCING SCIENCE SERVING SOCIETY

Defusing the Childhood Vocabulary Explosion

Bob McMurray

Between birth and adulthood, children learn about 60,000 words, or an average of 8 to 10 words per day. Studies consistently reveal that, during the second postnatal year, word learning accelerates dramatically (*1*). Although the acceleration is continuous and not stagelike (*2*, *3*), this so-called vocabulary explosion is a foundational phenomenon that theories of language acquisition must address.

Common explanations posit specialized mechanisms that build on the first words to better acquire new words. Early words may force changes, like the naming insight, or reorganize conceptual structures. Processes like syntactic bootstrapping and mutual exclusivity may also leverage known words to acquire new ones (*4*, *5*).

This paper demonstrates computationally that specialized processes are unnecessary to explain the vocabulary explosion. Acceleration is guaranteed in any system in which (i) words are acquired in parallel, that is, the system builds representations for multiple words simultaneously, and (ii) the difficulty of learning words is distributed such that there are few words that can be acquired quickly and a greater number that take longer. This distribution of difficulty derives from many factors, including frequency, phonology, syntax, the child's capabilities, and the contexts where words appear.

Such a system was simulated by generating a Gaussian distribution of time to acquisition for 10,000 words. Figure 1A shows the number of words at each difficulty level. Most are acquired at 4000 time steps, whereas a few are easier. To simulate learning, at each time step each word accrues a point. When a word crosses its time-to-acquisition threshold, it is learned. This model exhibits the characteristic pattern of slow learning followed by acceleration (Fig. 1B, black line). Deceleration is seen at the end of acquisition, something that has been hypothesized (*3*) but not examined empirically [Supporting Online Material (SOM) text S2].

Further simulations examined mechanisms that leverage initial words to facilitate learning. As each word was acquired, a benefit was added to unlearned words (SOM text S3), accelerating learning (Fig. 1B, blue line). However, acquisition also accelerated when each learned word incurred a cost (red line).

Analytically, the number of words acquired by the model within a given time window is the integral of the ease-of-acquisition distribution over that window. In a Gaussian distribution, the first quarter (e.g., 0 to 2000 time steps) has a smaller integral than the second (2000 to 4000). Hence, the rate of acquisition will appear to accelerate at the later time points (Fig. 1A). Acceleration should thus be observed in any distribution in which the number of words at a given difficulty level correlates positively with difficulty, that is, if there are fewer easy words than moderate or difficult ones (SOM text S4). Additionally, the central limit theorem suggests that, because many factors contribute to time to acquisition, their individual distributions sum to a Gaussian (assuming reasonable independence).

Given this generality, a time-to-acquisition distribution was developed from real language. Word frequency was used as a proxy for difficulty by linearly scaling the log frequency of the 2000 most frequent words of English in adult- and child-directed speech (SOM text S5). This model showed acceleration (Fig. 1C). Interestingly, child-directed speech yielded faster early learning, whereas adult-directed speech was faster later—the optimal distribution may change with age. Acceleration was also seen in a fixed-threshold model, where each word had the same threshold but at each time step only one (randomly chosen from a distribution based on the same log-frequencies) received a point. Thus, acceleration in vocabulary growth could arise from occurrence statistics alone.

The vocabulary explosion is a by-product of parallel learning and variation in the time to learn words. Although words accumulate evidence at a constant rate, the outcome accelerates. The ease-of-acquisition distribution provides a framework for integrating linguistic, psychological, and statistical factors in word learning. These mundane structural features of the organism-environment complex, not specialized learning processes, determine the form of growth. Specialized processes are not causally necessary to explain acceleration; such processes may in fact arise in response to acceleration, or they may offset other processes that slow learning (*6*). Moreover, the model's generality suggests that any parallel learning system (e.g., motor patterns and concepts) should behave similarly. Acceleration is an unavoidable by-product of variation in difficulty. It should not be misconstrued as evidence for specialized learning.

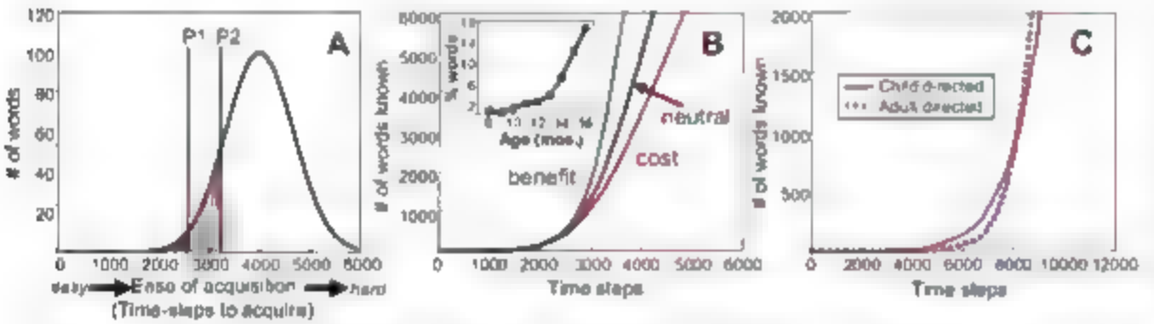

Fig. 1. (**A**) A Gaussian distribution of time to acquisition. Between 0 and 2600 time steps (P1), 1481 words are acquired. An additional 3966 are acquired in the next 600 (P2). (**B**) Vocabulary size as a function of time in initial simulations, and when learning a word offers a cost or benefit to future learning. (Inset) Percentage of words on MacArthur Communicative Development Inventory produced by children as a function of age (SOM text S1). (**C**) Acquisition in simulations based on word frequency.

References and Notes

1. L. Bloom, *One Word at a Time: The Use of Single Word Utterances Before Syntax* (Mouton, The Hague, 1973).
2. J. Ganger, M. Brent, *Dev. Psychol.* 40, 621 (2004).
3. P. Bloom, *How Children Learn the Meanings of Words* (MIT Press, Cambridge, MA, 2000).
4. I. Nazzi, J. Bertoncini, *Dev. Sci.* 6, 136 (2003).
5. E. Markman, in *Perspectives on Language and Thought: Interrelations in Development*, J. P. Byrnes, S. A. Gelman, Eds. (MIT Press, Cambridge, MA, 1991), pp. 72–106.
6. D. Swingley, R. N. Aslin, *Cognit. Psychol.* 54, 99 (2007).

7. The author thanks R. Aslin, P. Bloom, J. Freeman, P. Gupta, J. Horst, K. McGregor, and especially L. Samuelson and M. Blumberg for helpful comments on earlier drafts of this manuscript; C. Manson for assistance with the figure; and G. Oden for suggesting the central limit theorem. This research was supported by NIH grant DC008089-01.

Supporting Online Material

www.sciencemag.org/cgi/content/full/317/5838/631/DC1
SOM Text
References

20 April 2007; accepted 14 June 2007
10.1126/science.1144073

Department of Psychology, E11 SSH, University of Iowa, Iowa City, IA 52242, USA. E-mail: bob-mcmurray@uiowa.edu

Genome Transplantation in Bacteria: Changing One Species to Another

Carole Lartigue, John I. Glass,* Nina Alperovich, Rembert Pieper, Prashanth P. Parmar, Clyde A. Hutchison III, Hamilton O. Smith, J. Craig Venter

As a step toward propagation of synthetic genomes, we completely replaced the genome of a bacterial cell with one from another species by transplanting a whole genome as naked DNA. Intact genomic DNA from *Mycoplasma mycoides* large colony (LC) virtually free of protein, was transplanted into *Mycoplasma capricolum* cells by polyethylene glycol–mediated transformation. Cells selected for tetracycline resistance, carried by the *M. mycoides* LC chromosome, contain the complete donor genome and are free of detectable recipient genomic sequences. These cells that result from genome transplantation are phenotypically identical to the *M. mycoides* LC donor strain as judged by several criteria.

It has been known ever since Oswald Avery's pioneering experiments with pneumococcal transformation more than six decades ago, that some bacterial can take up naked DNA (*1*). This DNA is generally degraded or recombined into the recipient chromosome to form genetic recombinants. DNA molecules several hundred kilobase pairs (kb) in size can sometimes be taken up. In recent studies with competent *Bacillus subtilis* cells, Akamatsu and colleagues (*2*, *3*) demonstrated cotransformation of genetic markers spread over more than 30% of the 4.2-megabase pair (Mb) genome using nucleoid DNA isolated from gently lysed *B. subtilis* protoplasts. Artificial transformation methods that employ electroporation or chemically competent cells are now widely used to clone recombinant plasmids. Generally, the recombinant plasmids are only a few kilobase pairs in size, but bacterial artificial chromosomes (BACs) greater than 300 kb have been reported (*4*). Recombinant plasmids coexist with host-cell chromosomes and replicate independently. Two other natural genetic transfer mechanisms are known in bacteria. These are transduction and conjugation. Transduction occurs when viral particles pick up chromosomal DNA from donor bacteria and transfer it to recipient cells by infection. Conjugation involves an intricate mechanism in which donor and recipient cells come in contact and DNA is actively passed from the donor into the recipient. Neither of these mechanisms involves a naked DNA intermediate.

In this paper, we report a process with a different outcome, which we call "genome transplantation." In this process, a whole bacterial genome from one species is transformed into another bacterial species, which results in new cells that have the genotype and phenotype of the input genome. The important distinguishing feature of transplantation is that the recipient genome is entirely replaced by the donor genome. There is no recombination between the incoming and outgoing chromosomes. The result is a clean change of one bacterial species into another.

Work that is related to the process we describe in this paper has been carried out or proposed for various species. Itaya *et al.* transferred almost an entire *Synechocystis* PCC6803 genome into the chromosome of a recipient *B. subtilis* cell using the natural transformation mechanism. The result was a chimeric chromosome had the phenotype of the *B. subtilis* recipient cell. Most of the *Synechocystis* genes were silent (*5*). A schema for inserting an entire *Haemophilus influenzae* genome as overlapping BAC's into an *Escherichia coli* recipient has also been proposed; however, those authors have pointed out difficulties arising from incompatibility between the two genomes (*6*). Transplantation of nuclei as intact organelles into enucleated eggs is a well-established procedure in vertebrates (*7*–*9*). Our choice of the term "genome transplantation" comes from the similarity to eukaryotic nuclear transplantation in which one genome is cleanly replaced by another.

Genome transplantation is a requirement for the establishment of the new field of synthetic genomics. It may facilitate construction of useful microorganisms with the potential to solve pressing societal problems in energy production, environmental stewardship, and medicine. Chemically synthesized chromosomes must eventually be transplanted into a cellular milieu where the encoded instructions can be expressed. We have long been interested in defining a minimal genome that is just sufficient for cellular life (*10*, *11*) and have advocated the approach of chemically synthesizing a genome as a means for testing hypotheses concerning the minimal set of genes. The societal and ethical implications of this work have been explored (*12*, *13*).

Fabricating a synthetic cell by this approach requires the introduction of the synthetic genome into a receptive cytoplasm. We chose mycoplasmas (members of the class *Mollicutes*) for building a synthetic cell. This choice was based on a number of characteristics specific to this bacterial taxon. The essential features of mycoplasmas are small genomes, use of UGA to encode tryptophan (rather than a stop codon), and the total lack of a cell wall. A small genome is easier to synthesize and less likely to break during handling. The altered genetic code facilitates cloning in *E. coli* because it curtails the expression of mycoplasma proteins. The absence of a cell wall makes the exterior surfaces of these

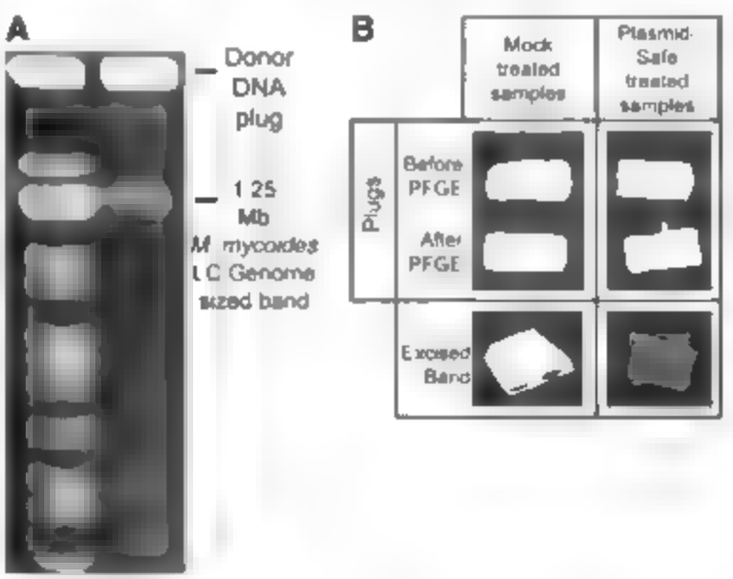

Fig. 1. Demonstration that the DNA in the blocks was intact and circular, whereas the DNA in the band that migrated into the gel was linear. (**A**) A pulsed-field gel loaded with a plug containing *M. mycoides* LC DNA. The 1× TAE buffer gel was separated by electrophoresis for 20 hours and then stained with SYBR gold. The marker lane contains Bio-Rad *Saccharomyces cerevisiae* genomic DNA size markers. Note the large amount of DNA remaining in the plug. (**B**) The plugs are shown either before PFGE or after PFGE, and the genome sized band produced after PFGE, and either with or without treatment with the Plasmid-Safe DNase. The nuclease enzyme digests linear DNA, but has no effect on circular duplex DNA. These data indicate the band of DNA that migrated into the gel was exonuclease-sensitive and, therefore, linear.

The J. Craig Venter Institute, Rockville, MD 20850, USA.

*To whom correspondence should be addressed. E-mail: jglass@jcvi.org

bacteria similar to the plasma membranes of eukaryotic cells and may simplify our task of installing a genome into a recipient cell by allowing us to use established methods for insertion of large DNA molecules into eukaryotic cells.

We elected to develop our genome transplantation methods using two fast-growing mycoplasma species, *Mycoplasma mycoides* subspecies *mycoides*, Large Colony strain GM12, and *Mycoplasma capricolum* subspecies *capricolum*, strain California kid, as donor and recipient cells, respectively. They divide every 80 and 100 min, respectively. These organisms are both opportunistic pathogens of goats, but can be grown in the laboratory under Biosafety Level 2 conditions. In preparation for our experiments, it was necessary to sequence both genomes and compare them to determine the degree of relatedness. We found that 76.4% of the 1,083,241-bp draft sequence of the *M. mycoides* LC genome (*14*) could be mapped to the 1,010,023-bp *M. capricolum* genome (*15*), and thus content matched on average at 91.5% nucleotide identity. The remaining ~24% of the *M. mycoides* LC genome contains a large number of insertion sequences not found in *M. capricolum*.

At the outset, we explored a number of methods for genome transplantation. The process had three key phases: isolation of intact donor genomes from *M. mycoides* LC, preparation of recipient *M. capricolum* cells, and installation of the isolated genome into the recipient cells. We chose our donor and recipient cells for genome transplantation on the basis of our observation that plasmids containing a *M. mycoides* LC origin of replication complex (ORC) can be established in *M. capricolum*, whereas plasmids with an *M. capricolum* ORC cannot be established in *M. mycoides* LC (*16*).

Donor Genomic DNA Preparation

Manipulation of whole chromosomes in solution exposes the DNA to shear forces that can cause breakage. Thus, it was important to minimize genome manipulation during the detergent and proteolytic enzyme treatments by suspending the cells in agarose blocks. Intact chromosomes were immobilized in the resulting cavern in the agarose that originally held the cell. Digested protein components, lipids, RNAs, and sheared genomic DNAs could then be removed by dialysis or electrophoresis from the immobilized intact genomic DNA.

Whole, intact genomic DNA isolation was performed using a CHEF Mammalian Genomic DNA Plug Kit from Bio-Rad. Briefly, we grew *M. mycoides* LC cells containing tetracycline resistance (*tetM*) and β-galactosidase genes (*lacZ*) (*17*) at 37°C to moderate density in SP4 medium (*18*), supplemented with 10 μg/ml of tetracycline and, in some experiments, 10 μg/ml of streptomycin. Cells (10 to 100 ml of culture) were reduced to a pellet by centrifugation at 4575*g* for 15 min at 10°C. We resuspended cells in 20 ml of 10 mM Tris (pH 6.5) plus 0.5 M sucrose, spun as before, and resuspended again in 1 ml (~1 to 5 × 10^9 cells/ml). We incubated the cell suspension for 15 min at 50°C, then mixed it with an equal volume of 2% low-melting-point (LMP) agarose in 1× TAE buffer [40 mM Tris-acetate and 1 mM EDTA]. After 5 min at 50°C, the mixture of cells and LMP agarose (2 ml) was distributed in 100-μl aliquots into plug molds. The 20 plugs solidified at 4°C. Embedded mycoplasma cells were lysed and proteins were digested at 50°C for 24 hours by addition of 6 ml of proteinase K reaction buffer [100 mM EDTA (pH 8.0), 0.2% sodium deoxycholate, and 1% sodium lauryl sarcosine, with 240 μl of proteinase K (>600 U/ml). The 20 plugs were then washed four times at room temperature for 1 hour in 20 ml of 1× Tris-EDTA buffer [Tris-HCl (20 mM) and EDTA (50 mM), (pH 8.0)] with agitation and stored in 10 ml of Tris-EDTA buffer at 4°C.

We wanted to confirm that our gentle preparation of the genomic DNA yielded intact circular molecules. We subjected some agarose plugs to pulsed-field gel electrophoresis (PFGE) in a 1% LMP gel in TAE, with contour-clamped homogeneous electric field (*19*) (CHEF DR III, Bio-

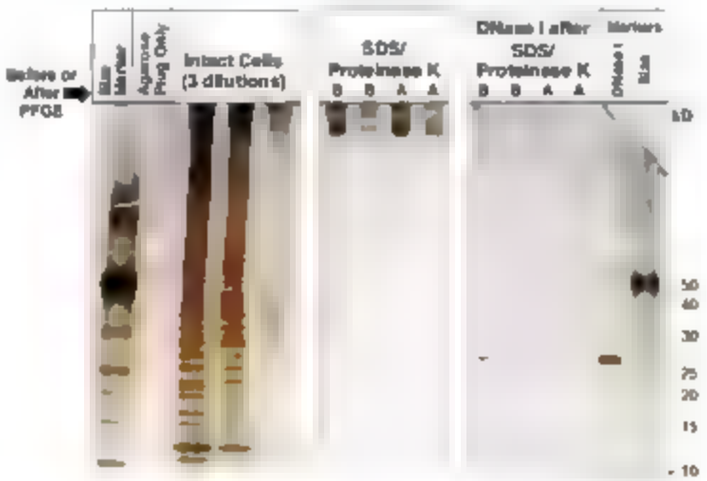

Fig. 2. SDS–polyacrylamide gel electrophoresis (SDS-PAGE) analysis of isolated *M. mycoides* LC DNA in agarose blocks shows that there were no detectable proteins associated with the DNA. The gels were silver-stained. (**Left**) The three lanes labeled "Intact cells" were three dilutions of *M. mycoides* LC cells that were boiled in SDS and loaded onto the gel. (**Middle**) Agarose blocks with the *M. mycoides* LC DNA that were boiled in SDS and loaded on the protein gel either before (B) or after (A) PFGE. (**Right**) To determine whether the material at the top of the gel was protein or DNA, we treated the blocks, before and after PFGE, with DNase I. One of the markers was DNase I.

Table 1. Results of a series of transplantation experiments.

Experiment date	Number of colonies			
	Negative controls		*M. mycoides* LC transplants	Total *M. capricolum* recipient cells
	No donor DNA	No recipient cells		
3/28/06	0	0	1	4×10^9
4/13/06	2*	0	~65	8×10^8
4/19/06†	0	0	1	1×10^9
5/25/06	0	0	1	6×10^8
6/07/06	0	0	16	5×10^8
6/08/06	0	0	17	2×10^8
6/28/06	0	0	8	7×10^8
7/06/06	0	0	3	6×10^9
9/07/06	0	0	2	3×10^{10}
11/17/06‡	0	0	~100	2×10^8
11/24/06‡	0	0	~100	5×10^8
12/13/06	0	0	20	4×10^8
1/04/07	0	0	17	5×10^7
1/18/07	0	0	20	2×10^7
3/01/07	0	0	24	6×10^7
3/20/07§	0	0	134	5×10^7
3/21/07§	0	0	81	3×10^7
3/29/07§	0	0	132	2×10^7

*We attribute these two colonies to laboratory error, and we never saw any colonies on the no-donor-DNA control plates in any later experiments. †After this experiment, we did six experiments not listed here that produced no transplant clones. ‡We attribute the higher genome transplantation efficiency in these experiments to the inclusion of streptomycin in the SP4 medium used to grow the *M. mycoides* LC donor genomes.

Rad). Pulse times were ramped from 60 to 120 s over 24 hours at 3.5 V cm⁻¹. After migration, plugs were removed from the wells and stored in 10 ml of Tris-EDTA buffer (as described above) at 4°C and used as source of intact genomic DNA for chromosome transplantation experiments. During PFGE, intact circular bacterial chromosomes become caught in the agarose and do not migrate, whereas full-length linearized DNA, as well as smaller DNA fragments, RNAs, proteins, and any other charged cellular molecules remaining after the detergent and enzyme digestion were removed from the plug by electrophoresis (*20*). A SYBR gold (Molecular Probes) stained pulsed-field gel (Fig. 1A) showed a band of DNA that had the same electrophoretic mobility as a 1125-Mb linear DNA size marker (about the same size as the *M. mycoides* LC genome), plus an intense band at the position of the wells, which suggested that a large amount of DNA was still in the plugs. Extensive digestion of the plug and the excised ~1125-Mb band with Plasmid-Safe adenosine triphosphate (ATP) dependent deoxyribonuclease (DNase) (Epicentre Biotechnologies) clearly degraded the excised 1125-Mb band (Fig. 1B). Plasmid-Safe ATP-dependent DNase digests linear double-stranded DNA to deoxyribonucleotides and, with lower efficiency, closed-circular and linear single-stranded DNA. The enzyme has no activity on nicked or closed-circular double-stranded DNA or supercoiled DNA. This is compatible with the presence of a large amount of circular genomic DNA in the plug. As we became more experienced with genome isolation, the amount of apparently linearized DNA in our preparations diminished.

We analyzed the plugs to confirm that the DNA encased in them was naked. Plugs loaded on SDS polyacrylamide gels after boiling in SDS showed no detectable protein by silver staining, which indicated that the majority of the DNA was naked (Fig. 2). In order to make sure that the DNA was completely deproteinated during the genome transplantation, agarose plugs treated with detergent and proteinase K were subjected to liquid chromatography followed by tandem mass spectrometry (LC-MS/MS) on an ion-trap mass spectrometer (*21*). Five *M. mycoides* peptides, each for a different protein and from a separate plug, were identified (table S1). Because LC-MS/MS analysis is very sensitive and provides excellent sequence coverage, the peptide quantities are extremely small. Only one peptide per protein was detected, which makes it highly unlikely that any undigested proteins were present in these agarose plug samples. In addition, we detected no *M. mycoides* LC peptides in plugs not exposed to PFGE. There was also a background in the samples run on PFGE of many peptides not encoded by *M. mycoides* LC, such as keratin peptides. All of these peptides, including the five encoded by *M. mycoides* LC, could be contaminants introduced during the PFGE.

The final step in donor genome preparation entailed liberation of the DNA from agarose encasement. Before transplantation experiments, the agarose plugs containing *M. mycoides* LC genomic DNA (before or after PFGE) were washed 2 times 30 min in 1 ml of 0.1× Tris-EDTA buffer [Tris-HCl (2 mM) and EDTA (5 mM) (pH 8.0)] with gentle agitation. The buffer was completely removed, and the agarose plugs were melted at 65°C with 1/10th volume of 10× β-agarase buffer [10 mM bis Tris-HCl (pH 6.5) and 1 mM EDTA] for 10 min. The molten agarose was cooled for 10 min to 42°C and incubated overnight at the same temperature with 2.5 units of β-agarase I (New England Biolabs) per 100 μl of plug. We calculated each plug contained ~10 μg of DNA (~8 × 10^9 genomes).

Recipient Cell Preparation and Genome Transplantation Reaction Conditions

We prepared the *M. capricolum* recipient cells in a 6-ml culture of SOB medium (*22*) containing 1% fetal bovine serum and 0.5% glucose. Incubation was at 37°C until the medium pH was 6.2. Cells (5 to 50 × 10^7 cells ml⁻¹) were then spun in a centrifuge at 4575*g* for 15 min at 10°C. As pH decreased from 7.4 to 6.2, regularly rod *M. capricolum* cells changed shapes dramatical-

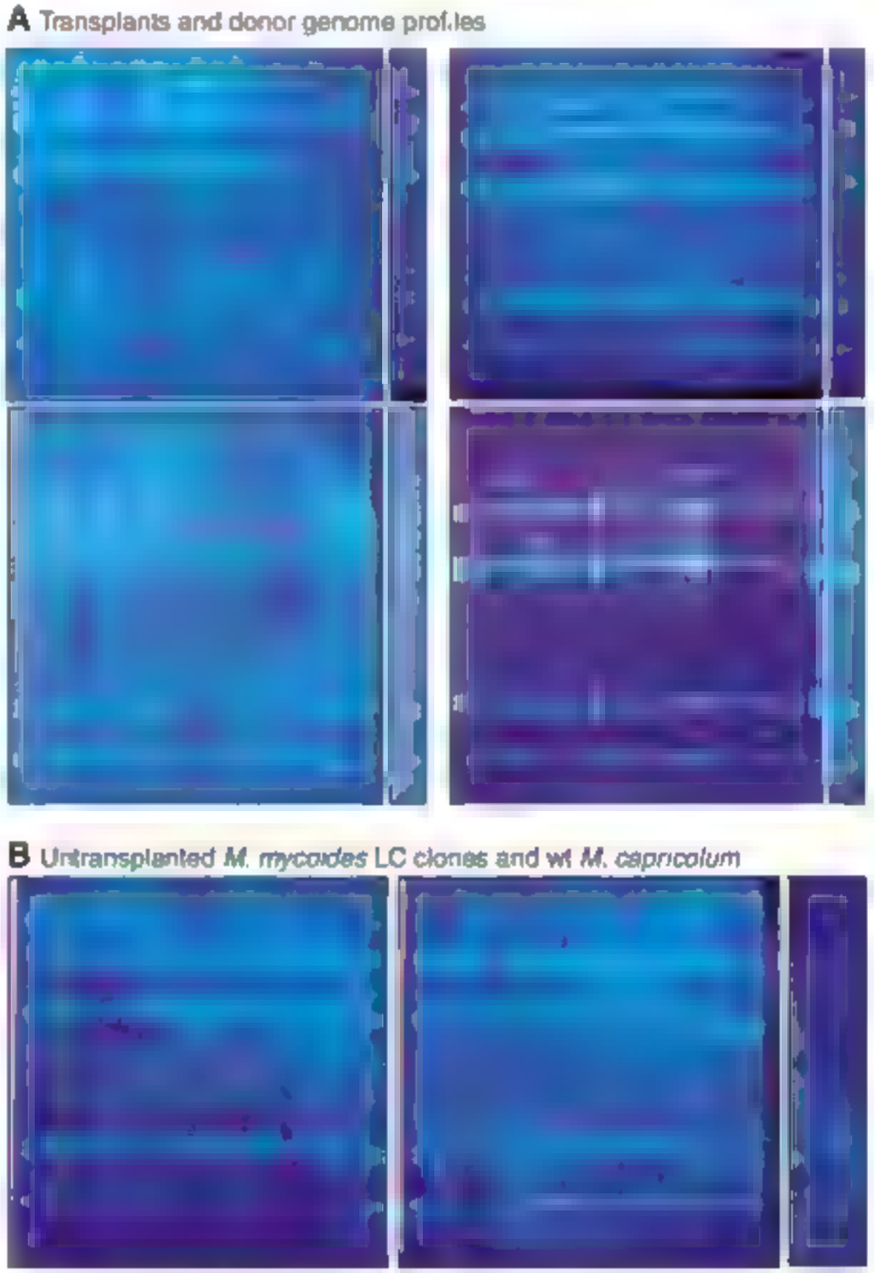

Fig. 3. Southern blots of (**A**) 75 transplants and (**B**) 37 different *M. mycoides* LC filter clones. The blots were probed with a PCR amplicon that hybridized to the IS1296 insertion sequences. Although different samples all had multiple copies of the IS1296, they had slightly different patterns on the blots, which indicated movement of the element. For the transplants (A), the donor cell genomes are shown in the single lanes. As a control (B), Southern blots of recipient cells (wild-type *M. capricolum*) are shown in the single lane. The IS196 probe from *M. mycoides* LC genomic DNA was amplified by PCR using primers IS1296P1F (AAGCGTTTAGAATAGAAGGGCTA) and IS1296P1R (CTGAATTGTACAGGAGACAATCC).

ly. Cells became longer, thinner, and branched. In poor medium, inhibition of DNA replication due to nucleotide starvation is known to induce branching in *M. capricolum* cells (*23*, *24*). Cells were washed once [Tris 10 mM and NaCl 250 mM (pH 6.5)], resuspended with 200 μl of $CaCl_2$ (0.1 M), and held on ice for 30 min. During that period, 20 μl of β-agarase–treated plugs (~50 ng/μl) were delicately transferred into 400 μl of SP4 medium without serum [SP4 (−)], with wide-bore genomic pipette tips, and incubated 30 min at room temperature. For the genome transplantation, *M. capricolum* cells mixed with 10 μg of yeast transfer RNA (Invitrogen) were gently transferred into the 400 μl of SP4 (−) containing 70 μl of *M. mycoides* LC whole-genomic DNA. An equal volume of 2× fusion buffer [Tris 20 mM, NaCl 500 mM, $MgCl_2$ 20 mM, polyethylene glycol 8000 (PEG; USB Corporation no. 19959) 10%] was added, and the contents were mixed by rocking the tube gently for 1 min. After 30 min at 37°C, 10 ml of SP4 was added, and the cells were incubated for 3 hours at 37°C to allow recovery. Finally, cells were spun at 4575*g* for 15 min at 10°C, resuspended in 0.7 ml of SP4, and plated on SP4 agar plates containing 3 μg/ml tetracycline and 150 μg/ml X-gal (5-bromo-4-chloro-3-indolyl β-D-galactopyranoside, Sc).

The plates were incubated at 37°C until large blue colonies, putatively *M. mycoides* LC, formed after ~3 days. Sometimes, after ~10 days smaller *M. capricolum* colonies, both blue and white, were visible. Thus, all of these colonies were tetracycline-resistant, as evidenced by their surviving the antibiotic selection, and only some expressed β-galactosidase. These colonies might be the result of recombination. We observed that these colonies appeared after almost twice as many days as it took for the transplants to become visible (*25*). Individual colonies were picked and grown in broth medium containing 5 μg/ml of tetracycline. During propagation, the tetracycline concentration was progressively increased to 10 μg/ml. When we first developed this technique, we subjected all plugs to PFGE. Later, we found this step was unnecessary. We observed no significant difference in transplantation yield as a result of PFGE of the plugs.

Every experiment included two negative controls. To ensure that the *M. mycoides* genomic DNA contained no viable cells, one control was processed exactly as described above except no *M. capricolum* recipient cells were used. Similarly, in another control, *M. capricolum* recipient cells were mock-transplanted without any donor DNA. The results of a series of experiments are shown in Table 1. No colonies were ever observed in controls lacking recipient cells; thus, the donor DNA was free of any viable contaminating *M. mycoides* LC cells. When donor DNA and recipient cells were both present, from 1 to >100 putative transplants were obtained in individual experiments. As we became more experienced with this technique, the yield of transplant colonies increased.

Fig. 4. Colony hybridization of the *M. mycoides* LC (genome donor), *M. capricolum* (recipient cell), and transplants from four different experiments that were probed with a polyclonal antibody specific for the *M. capricolum* VmcE and VmcF surface antigens or with monoclonal antibodies specific for the *M. mycoides* LC VchL surface antigen (*29*).

Analysis of Putative Transplants

The blue, tetracycline-resistant colonies resulting from *M. mycoides* LC genome transplantation were to be expected if the genome was successfully transplanted. However, colonies with that phenotype could also result from recombination of a fragment of *M. mycoides* LC genomic DNA containing the *tetM* and *lacZ* genes into the *M. capricolum* genome. To rule out recombination, we examined the phenotype and genotype of the transplanted clones.

Genotype analysis. We analyzed several transplant clones after synthesis with the polymerase chain reaction (PCR) using primers specific for each species to determine whether the putative transplants had *M. mycoides* LC sequences other than the selected *tetM* and *lacZ* marker genes. We used PCR primers specific for IS*1296* insertion sequences, which are present in 11 copies in the sequenced *M. mycoides* LC genome, but are absent in the *M. capricolum* genome. Similarly, we used PCR primers specific for the *M. capricolum* arginine deiminase gene,

which is not present in *M. mycoides* LC. The IS1296 PCR produced an amplicon only when the template was the *M. mycoides* wild-type strain or was one of the transplanted clones. Similarly the *M. capricolum* arginine deiminase PCR generated an amplicon with the *M. capricolum* template DNA, but not with the *M. mycoides* LC wild-type DNA or DNAs from transplant clones. The PCR experiments left open the possibility that fragments of the *M. mycoides* LC genome containing an IS1296, the *tetM* gene, and the *lacZ* gene had recombined into the *M. capricolum* genome in such a way that they destroyed the arginine deiminase gene (fig. S1). A more convincing genotypic analysis that looked at the overall genome used Southern blot analysis of the donor and recipient mycoplasmas and a series of putative transplants. Genomic DNA from each of these species was digested with the restriction enzyme HindIII and run on a 1% agarose gel. Southern blots were prepared and probed with IS1296 sequences. As expected, no probe hybridized to the wild-type *M. capricolum* lane (Fig. 3A). We did this analysis on every transplant we obtained, as well as a series of *M. mycoides* LC clones (Fig. 3B). Analysis of Southern blots of 37 wild-type *M. mycoides* LC clones and 75 putative transplants showed that 34 (92%) and 44 (59%), respectively, were essentially identical to the *M. mycoides* LC donor DNA blot; the rest showed variations in the banding patterns. We assume that variation was the result of IS element transposition. We hypothesize that mobility of the IS1296 element may be somewhat suppressed in *M. mycoides* LC cells. However, there may be no suppression of transposon mobility immediately following introduction of the donor genome into the *M. capricolum* cytoplasm. This is evidence of a transitional period when the *M. mycoides* LC donor genomes reside in a cellular milieu whose *M. capricolum* content is initially high, but diminishes with each cell division. Next, we did sample sequencing of whole-genome libraries generated from two transplant clones. Our analysis of more than 1300 random sequence reads from the genome of each clone (totaling ~1.09 million bases for each clone) showed that all reads matched *M. mycoides* LC sequence (*26*). We cannot rule out the possibility that small regions of the donor genomes recombined with identical regions of *M. capricolum* recipient cell genome; however, those regions would be very small. There are 20 identical regions of between 395 and 972 base pairs. The above results were all consistent with the hypothesis that we have successfully introduced *M. mycoides* LC genomes into *M. capricolum* followed by subsequent loss of the capricolum genome during antibiotic selection.

Phenotype analysis. We examined the phenotype of the transplanted clones in two ways. In one, we looked at single-gene products characteristic of each of these two mycoplasmas. Using colony-Western blots, we probed donor and recipient cell colonies and colonies from four different transplants with murine antibodies specific for the *M. capricolum* VmcE and VmcF surface antigens and with murine antibodies specific for the *M. mycoides* LC VchL surface antigen. In both assays, *M. mycoides* LC VchL specific antibodies bound the transplant blots with the same intensity as it bound the *M. mycoides* LC blots (Fig. 4). Similarly, the antibodies specific for the *M. capricolum* VmcE and

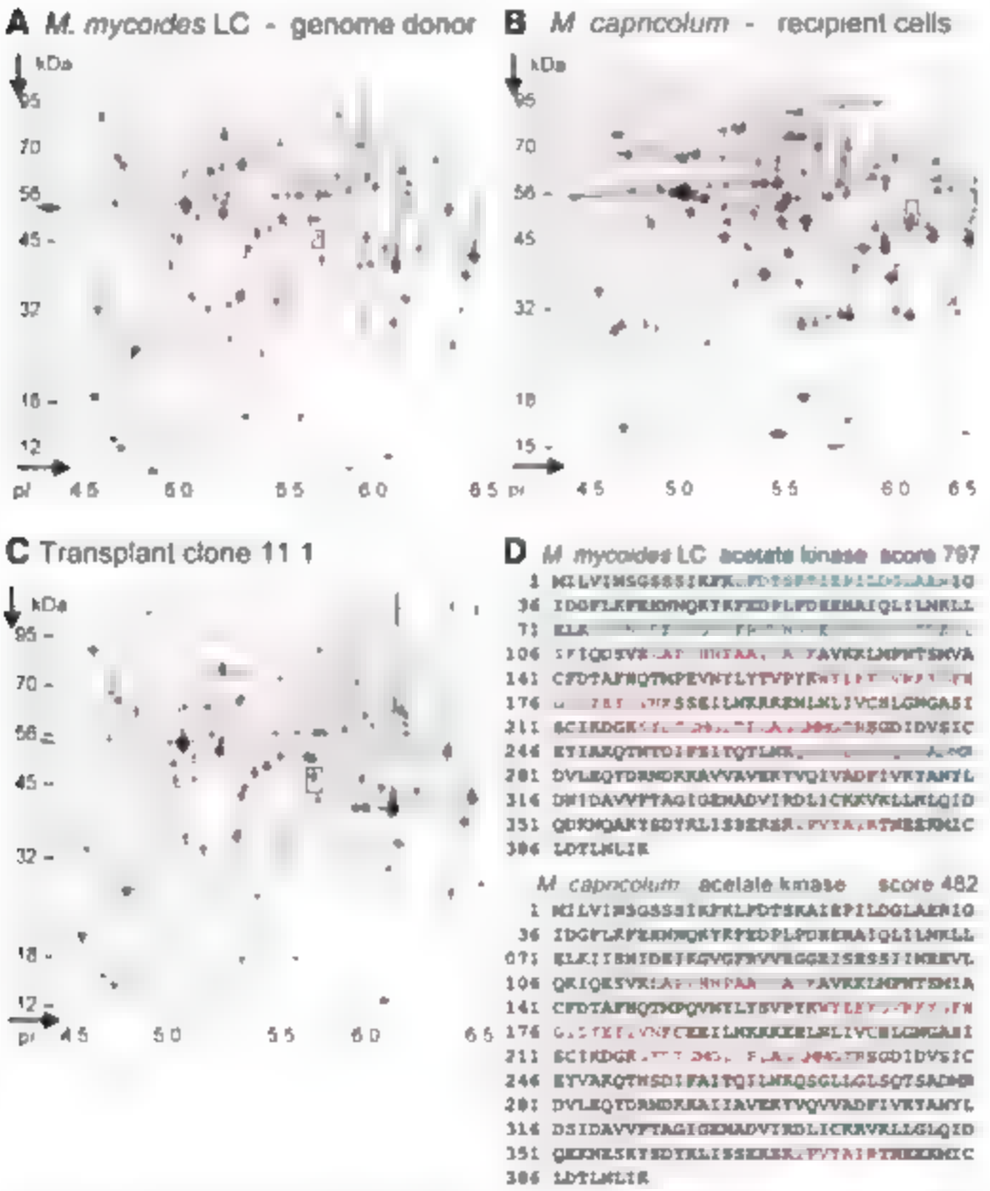

Fig. 5. Proteomic analysis. Two-dimensional gels were run using cell lysates from (**A**) *M. mycoides* LC, (**B**) *M. capricolum*, and (**C**) a transplant clone (11 1). Standard conditions were used for the separation of protein spots in the first dimension on immobilized pH gradient (IPG) strips (pH range 4 to 7) and in the second, SDS-PAGE, dimension (molecular mass 8 to 200 kD) (*30*). The gels were stained with Coomassie brilliant blue G-250, and 96 spots were excised from each of the gels. Spots 71 (A), 23 (B), and 8 (C) were identified as acetate kinase. (**D**) *M. capricolum* acetate kinase showed a clear alkaline pH shift. The sequence coverage map for trypsin-digested peptides obtained from MALDI-MS peptide mass fingerprint (PMF) data localizes peptide sequences of acetate kinase [spot 8 (C)] matching mass/charge ratio (*m/z*) values in the PMF. Peptide sequences in red were identical to the two *Mycoplasma* species; peptide sequences in blue were unique to *M. mycoides* LC.

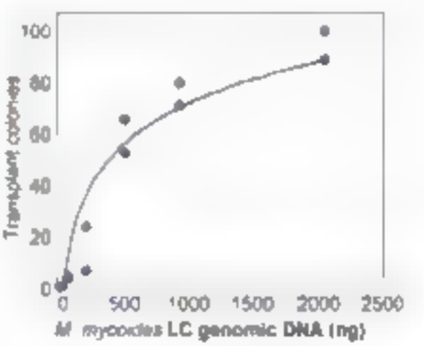

Fig. 6. Genome transplantation as a function of the amount of *M. mycoides* LC genomic DNA transplanted. Transplant colonies were observed on two different plates. We observed no colonies on either the no-recipient-cell control or the mock-transplanted control plates.

VmcF did not bind the to the transplant blots. In the second proteomic analysis, cell lysates of all three strains were examined by using differential display in two-dimensional electrophoresis (2-DE) gels, followed by identification of proteins spots with matrix-assisted laser desorption ionization (MALDI) mass spectrometry. The 2-DE spot patterns of the *M. mycoides* LC and the transplanted clone were identical within the limits of 2-DE, however, the *M. capricolum* 2-DE spot patterns were very different. More than 50% of the respective spots could not be matched among the gels (Fig. 5, A to C). More evidence was gained from MALDI-MS data that the transplant proteome was identical to the *M. mycoides* LC proteome and did not have any *M. capricolum* features. For nearly 90 identified spots of the transplant, confidence scores obtained with the Mascot algorithm were invariably equal or higher for *M. mycoides* LC than for *M. capricolum* proteins, despite high sequence homologies. although there were nine protein spots with confidence scores that indicated they were derived from *M. capricolum* genes, each case proved to be an artifact of either sequencing errors or gene bioinformatics annotation errors (table S2). As an example, Fig. 5D visualizes peptides in acetate kinase matching only the sequence of the respective *M. mycoides* LC protein. Thus, the phenotypic assays affirmed that the transplants were likely *M. mycoides* LC and were not the result of a *M. capricolum*–*M. mycoides* LC mosaic produced by recombination between the donor and recipient cell genomes after the transplantation of the *M. mycoides* LC genome and before the two genomes segregate during cell division.

Optimization of Genome Transplantation Efficiency

To determine what factors govern genome transplantation efficiency, we varied the number of *M. capricolum* recipient cells and the amount of *M. mycoides* LC genomic DNA used in transplantation experiments. Transplant yield was optimal when 10^7 to 5×10^7 cells were used. At lower donor DNA concentrations, there was a linear relation between the amounts of genomic DNA transplanted and transplant yield. Yields began to plateau at higher donor DNA concentrations (Fig. 6).

Concluding Remarks

These data demonstrate the transplantation of whole genomes from one species to another such that the resulting progeny are the same species as the donor genome. However, they do not explain the mechanism of the transplant. This is not natural DNA transformation, where linear DNA enters the cytoplasm and recombines into the resident chromosome. Our genome transplantation does not entail recombination, and our donor molecule is circular. In addition, our recipient mycoplasma cells have not been shown to be competent for natural transformation, nor are any DNA uptake genes identified in the *M. capricolum* genome. We presume that organisms carrying both donor and recipient cell genomes occurred at least transiently at early times after transplantation. Only 1 recipient cell in ~150,000 was transplanted in our most efficient experiments. This low efficiency has so far prevented a demonstration of transient mosaicism. Although our donor and recipient are distinct species, they are phylogenetically close relatives. Genome transplantation works for the species we have chosen, but we do not know for what other species it will work.

Because mycoplasmas are similar to mammalian cells with respect to their lack of a cell wall, we experimented with a series of approaches that are effective for transferring large DNA molecules into eukaryotic cells. These included cation- and detergent-mediated transfection, electroporation, and compaction of the donor genomes using various cationic agents. None of those approaches proved effective for whole-genome transplantation (see SOM). Our PEG-based method may be akin to PEG-driven cell fusion methods developed for eukaryotic cells. To test this hypothesis, two parental strains of *M. capricolum*, one carrying a *tetM* marker in the chromosome and the other one with the chloramphenicol-resistance marker (CAT) in a stable ORC plasmid, were both prepared as "recipient" cells, mixed, and incubated in the presence of the fusion buffer as described above for transplantation experiments. We plated cells on SP4 agar containing both tetracycline (3 μg/ml) and chloramphenicol (50 μg/ml). In the presence of 5% PEG, we obtained progeny resistant to both antibiotics. No colonies grew in the absence of 5% PEG. The number of colonies increased ~30 times when we pretreated cells with $CaCl_2$. Sequencing analysis of 30 clones showed that all had both the *tetM* and CAT markers in the cells at the expected chromosomal and plasmid locations. Thus, we concluded that with our PEG-based method, *M. capricolum* cells fuse. Those results agree with membrane studies by Rottem and colleagues demonstrating that fusion of *M. capricolum* cells is maximal in 5% PEG (27). Gene transfer into *Mycoplasma pulmonis* was also mediated by PEG at concentrations likely to fuse cells, albeit only small DNA segments are transferred (28). We can imagine that, in some instances, the cells may fuse around the naked *M. mycoides* LC genomes. Those genomes, now encapsulated in *M. capricolum* cytoplasm, express the *tetM* protein, which allows the large fused cells to grow and divide once plated on the SP4 agar containing tetracycline. Cells lacking the *M. mycoides* genome do not grow. Eventually, now, in the absence of PEG and through a process of cell division and chromosome segregation, normal, albeit tetracycline-resistant β-galactosidase producing *M. mycoides* cells produce large blue colonies on the plate. This basic approach of PEG-mediated genome transplantation may allow other species to be transplanted with naked genomes containing antibiotic-resistance genes.

Some bacterial cells have multiple large chromosomes. This suggests the existence of natural mechanisms for chromosome transfer between species. However, we have no evidence that genome transplantation as described here occurs in nature. We observed that in the absence of treatment with detergent and proteinase K, nucleoids from *M. mycoides* LC cells would not produce transplants. Given the improbability of the natural occurrence of free-floating bacteria, genomes that are both deproteinized and intact, genome transplantation could be a phenomenon unique to the laboratory. Still, we have discovered a form of bacterial DNA transfer that permits recipient cells to be platforms for the production of new species with the use of modified natural genomes or manmade genomes generated by the methods being developed by synthetic biologists.

References and Notes

1. O. T. Avery, C. M. MacLeod, M. McCarty, *J. Exp. Med.* **79**, 137 (1944).
2. T. Akamatsu, H. Taguchi, *Biosci. Biotechnol. Biochem.* **65**, 823 (2001).
3. Y. Saito, H. Taguchi, T. Akamatsu, *J. Biosci. Bioeng.* **101**, 334 (2006).
4. H. Shizuya *et al.*, *Proc. Natl. Acad. Sci. U.S.A.* **89**, 8794 (1992).
5. M. Itaya, K. Tsuge, M. Koizumi, K. Fujita, *Proc. Natl. Acad. Sci. U.S.A.* **102**, 15971 (2005).
6. R. A. Holt, R. Warren, S. Flibotte, P. I. Missirlis, D. E. Smailus, *Bioessays* **29**, 580 (2007).
7. I. Wilmut, A. E. Schnieke, J. McWhir, A. J. Kind, K. H. Campbell, *Nature* **385**, 810 (1997).
8. J. B. Gurdon, J. A. Byrne, *Proc. Natl. Acad. Sci. U.S.A.* **100**, 8048 (2003).
9. R. Briggs, T. J. King, *Proc. Natl. Acad. Sci. U.S.A.* **38**, 455 (1952).
10. J. I. Glass *et al.*, *Proc. Natl. Acad. Sci. U.S.A.* **103**, 425 (2006).
11. C. A. Hutchison III *et al.*, *Science* **286**, 2165 (1999).
12. M. K. Cho, D. Magnus, A. L. Caplan, D. McGee, *Science* **286**, 2087 (1999).
13. M. S. Garfinkel, D. Endy, G. E. Epstein, R. M. Friedman, *Synthetic Genomics, Options for Governance* (report of the project "Synthetic Genomics: Risks and Benefits for Science and Society," funded by Alfred P. Sloan Foundation of New York), in preparation.
14. This whole-genome shotgun project has been deposited at DNA Database of Japan (DDBJ), European Molecular Biology Laboratory (EMBL), and GenBank under the project accession AAZK00000000. The version described in this paper is the first version, AAZK01000000.
15. GenBank accession number NC_007633.
16. C. Lartigue, A. Blanchard, J. Renaudin, F. Thiaucourt, P. Sirand-Pugnet, *Nucleic Acids Res.* **31**, 6610 (2003).
17. The donor cells containing the *tetM* and *lacZ* genes were made through integration of an *M. mycoides* LC ORC plasmid [see (16)] containing those genes near the *M. mycoides* LC ORC. The location of the plasmid insertion can be seen in the genome sequence.
18. J. G. Tully, D. L. Rose, R. F. Whitcomb, R. P. Wenzel, *J. Infect. Dis.* **139**, 478 (1979).
19. G. Chu, D. Vollrath, R. W. Davis, *Science* **234**, 1582 (1986).
20. S. M. Beverley, *Nucleic Acids Res.* **16**, 925 (1988).
21. Materials and methods are available as supporting material on Science Online.
22. D. Hanahan, *J. Mol. Biol.* **166**, 557 (1983).
23. S. Seto, M. Miyata, *J. Bacteriol.* **180**, 256 (1998).
24. S. Seto, M. Miyata, *J. Bacteriol.* **181**, 6073 (1999).
25. To minimize the risk of contaminating our transplant cultures with *M. mycoides* LC cells from our donor genome preparation process, we used three different

hoods for our cell culture work: one for *M. mycoides* LC donor cell preparation, one for *M. capricolum*, and one for working with transplant clones
26. There was no sequence that was unique to *M. capricolum*. Of the 24 reads that did not match the *M. mycoides* LC or *M. capricolum* genome sequences, most were either very short reads (<200 bases) or the result of chimeric clones, which is to be expected owing to the active transposons in *M. mycoides* LC and also as part of library construction. The data for the two transplant clones that were sequenced are posted at the National Center for Biotechnology Information, NIH, NCBI Trace File Archives (accession numbers 1807995910 through 1807998555)
27. M. Tarshis, M. Salman, S. Rottem, *Biophys. J.* 64, 709 (1993)
28. A. M. Teachman, C. T. French, H. Yu, W. L. Simmons, K. Dybvig, *J. Bacteriol.* 184, 947 (2002)
29. The murine antibodies were gifts from M. Foecking, T. Marten, K. Wise, and M. Calcutt at the University of Missouri.
30. C. L. Gatlin *et al.*, *Proteomics* 6, 1530 (2006).
31. We thank C. Merryman, L. Young, and M. Assad-Garcia for many discussions about genome transplantation; and D. Rusch, G. Sutton, S. Yooseph, and J. Johnson for bioinformatics analyses. The bulk of the work was supported by Synthetic Genomics. The proteome analysis was funded in part through the Pathogen Functional Genomics Resource Center, managed and funded by the Division of Microbiology and Infectious Diseases, National Institute of Allergy and Infectious Diseases, NIH, Department of Health and Human Services, and operated by the J. Craig Venter Institute. J.C.V. is Chief Executive Officer and Co-Chief Scientific Officer of Synthetic Genomics, Inc., a privately held entity that develops genomic-driven strategies to address global energy and environmental challenges. H.O.S. is Co-Chief Scientific Officer and on the Board of Directors of Synthetic Genomics, Inc. C.A.H. is Chairman of the Synthetic Genomics, Inc., Scientific Advisory Board. All three of these authors hold Synthetic Genomics, Inc., stock, and the J. Craig Venter Institute owns a significant fraction of Synthetic Genomics, Inc. Following the disclosure policy of this journal, the authors disclose that the Venter Institute has filed for a patent application on some of the techniques described in this paper

Supporting Online Material
www.sciencemag.org/cgi/content/full/1144622/DC1
Materials and Methods
SOM Text
Fig. S1
Tables S1 and S2
References

3 May 2007; accepted 21 June 2007
Published online 28 June 2007
10.1126/science.1144622
Include this information when citing this paper

REPORTS

Quantum Hall Effect in a Gate-Controlled *p-n* Junction of Graphene

J. R. Williams,[1] L. DiCarlo,[2] C. M. Marcus[2]*

The unique band structure of graphene allows reconfigurable electric-field control of carrier type and density, making graphene an ideal candidate for bipolar nanoelectronics. We report the realization of a single-layer graphene *p-n* junction in which carrier type and density in two adjacent regions are locally controlled by electrostatic gating. Transport measurements in the quantum Hall regime reveal new plateaus of two-terminal conductance across the junction at 1 and ½ times the quantum of conductance, e^2/h, consistent with recent theory. Beyond enabling investigations in condensed-matter physics, the demonstrated local-gating technique sets the foundation for a future graphene-based bipolar technology.

Graphene, a single-layer hexagonal lattice of carbon atoms, has recently emerged as a fascinating system for fundamental studies in condensed-matter physics (*1*), as well as a candidate for novel sensors (*2*, *3*) and postsilicon electronics (*4*–*10*). The unusual band structure of single-layer graphene makes it a zero-gap semiconductor with a linear (photon-like) energy-momentum relation near the points where valence and conduction bands meet. Carrier type (electron-like or hole-like) and density can be controlled by using the electric-field effect (*10*), obviating conventional semiconductor doping, for instance via ion implantation. This field-effect doping via local gates would allow graphene-based bipolar technology devices comprising junctions between hole-like and electron-like regions, or *p-n* junctions, to be reconfigurable using only gate voltages to distinguish *p* (hole-like) and *n* (electron-like) regions within a single sheet. Although global control of carrier type and density in graphene using a single back gate has been investigated by several groups (*11*–*13*), local control (*8*, *9*) of single-layer graphene has remained an important technological milestone. In addition, *p-n* junctions are of great interest for low-dimensional condensed-matter physics. For instance, recent theory predicts that a local step in potential would allow solid-state realizations of relativistic (Klein) tunneling (*14*, *15*) and a surprising scattering effect known as Veselago lensing (*16*), comparable to scattering of electromagnetic waves in negative-index materials (*17*).

We report the realization of local top gating in a single-layer graphene device that, combined with global back gating, allows individual control of carrier type and density in adjacent regions of a single atomic layer. Transport measurements at zero perpendicular magnetic field B and in the quantum Hall (QH) regime demonstrate that the functionalized aluminum oxide (Al_2O_3) separating the graphene from the top gate does not significantly dope the layer nor affect its low-frequency transport properties. We studied the QH signature of the graphene *p-n* junction and found new conductance plateaus at 1 and $\frac{1}{2}e^2/h$, consistent with recent theory addressing equilibration of edge states at the *p-n* interface (*18*).

Graphene sheets were prepared via mechanical exfoliation using a method (*19*) similar to that used in (*10*). Graphite flakes were deposited on 300 nm of SiO_2 on a degenerately doped Si substrate. Inspection with an optical microscope allowed potential single-layer regions of graphene to be identified by a characteristic coloration that arises from Fabry-Perot interference (Fig. 1A). These micrometer-scale regions were contacted with thermally evaporated Ti-Au (5-40 nm) that was patterned using electron-beam lithography. Next, a ~30-nm layer of oxide was deposited atop the entire substrate. As illustrated (Fig. 1B), the oxide consisted of two parts, a nonconvalent functionalization layer (NCFL) and Al_2O_3. This deposition technique (*19*) was based on a recipe successfully applied to carbon nanotubes (*20*). The NCFL serves two purposes. One is to create a noninteracting layer between the graphene and the Al_2O_3, and the other is to obtain a layer that is catalytically suitable for the formation of Al_2O_3 by atomic layer deposition (ALD). The NCFL was synthesized by 40 pulsed cycles of NO_2 and trimethylaluminum (TMA) at room temperature inside an ALD reactor. Next, five cycles of H_2O-TMA were applied at room temperature to prevent desorption of the NCFL. Lastly, Al_2O_3 was grown at 225°C with 300 H_2O-TMA ALD cycles. To complete the device, a second step of electron-beam lithography defined a local top gate (5-40 nm Ti-Au) covering a region of the device that includes one of the metallic contacts.

A completed device, similar in design to that shown in the optical image in Fig. 1A, was cooled in a ^{3}He3 refrigerator and characterized at temperatures T of 250 mK and 4.2 K. Differential resistance, $R = dV/dI$, where I is the current and V the source-drain voltage, was measured by standard lock-in techniques with a current bias

[1]School of Engineering and Applied Science, Harvard University, Cambridge, MA 02138, USA. [2]Department of Physics, Harvard University, Cambridge, MA 02138, USA.
*To whom correspondence should be addressed. E-mail: marcus@harvard.edu

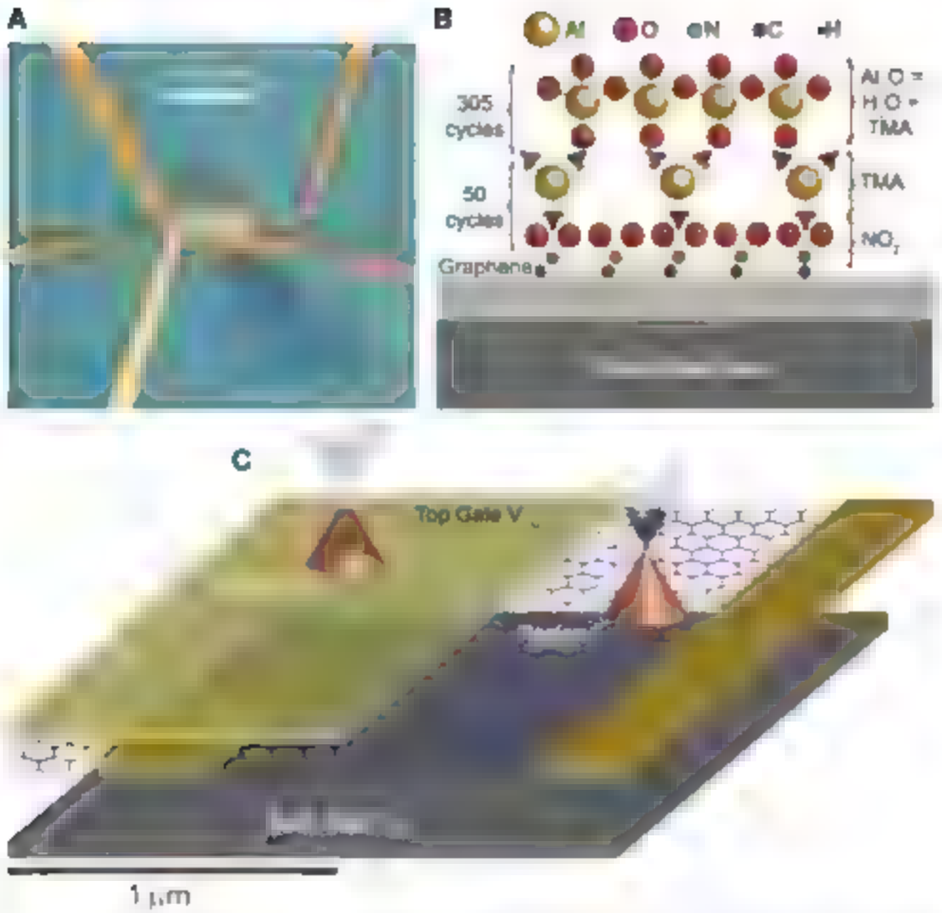

Fig. 1. (**A**) Optical micrograph of a device similar to the one measured. Metallic contacts and top gate appear in orange and yellow, respectively. Darker regions below the contacts are thicker graphite from which the contacted single layer of graphene extends. (**B**) Illustration of the oxide deposition process. A noncovalent functionalization layer is first deposited with NO_2 and TMA (50 cycles), and Al_2O_3 is then grown by ALD using H_2O TMA (305 cycles yielding ~30-nm thickness). (**C**) Schematic of the device measured in this experiment.

of 1 nA_{rms} at 95 Hz for T = 250 mK and 10 nA_{rms} for T = 4.2 K. The voltage across two contacts on the device, one outside the top-gate region and one underneath the top gate, was measured in a four-wire configuration, eliminating series resistance of the cryostat lines but not contact resistance. Contact resistance was evidently low (~1 kohm), and no background was subtracted from the data. A schematic of the device is shown in Fig. 1C.

The differential resistance, R, as a function of back-gate voltage, V_{BG}, and top-gate voltage, V_{TG}, at B = 0 (Fig. 2A) demonstrates independent control of carrier type and density in the two regions. This two-dimensional (2D) plot reveals a skewed, crosslike pattern that separates the space of top-gate and back-gate voltages into four quadrants of well-defined carrier type in the two regions of the sample. The horizontal and diagonal edges correspond to charge neutrality, i.e., the Dirac point, in regions 1 and 2, respectively. The slope of the charge-neutral line in region 2, along with the known distances to the top gate and back gate, gives a dielectric constant $\kappa \sim 6$ for the functionalized Al_2O_3. The center of the cross at (V_{TG}, V_{BG}) ~ (−0.2 V, −2.5 V) corresponds to charge neutrality across the entire graphene sample. Its proximity to the origin of gate voltages demonstrates that the functionalized oxide does not chemically dope the graphene substantially.

Slices through the 2D conductance plot at fixed V_{TG} are shown in Fig. 2C. The slice at V_{TG} = 0 shows a single peak commonly observed in devices with only a global back gate (*19*, *20*). By using a Drude model away from the charge-neutrality region, we estimated mobilities of ~7000 cm^2/Vs (*19*). The peak width, height, and back-gate position are consistent with single-layer graphene (*19*, *20*) and

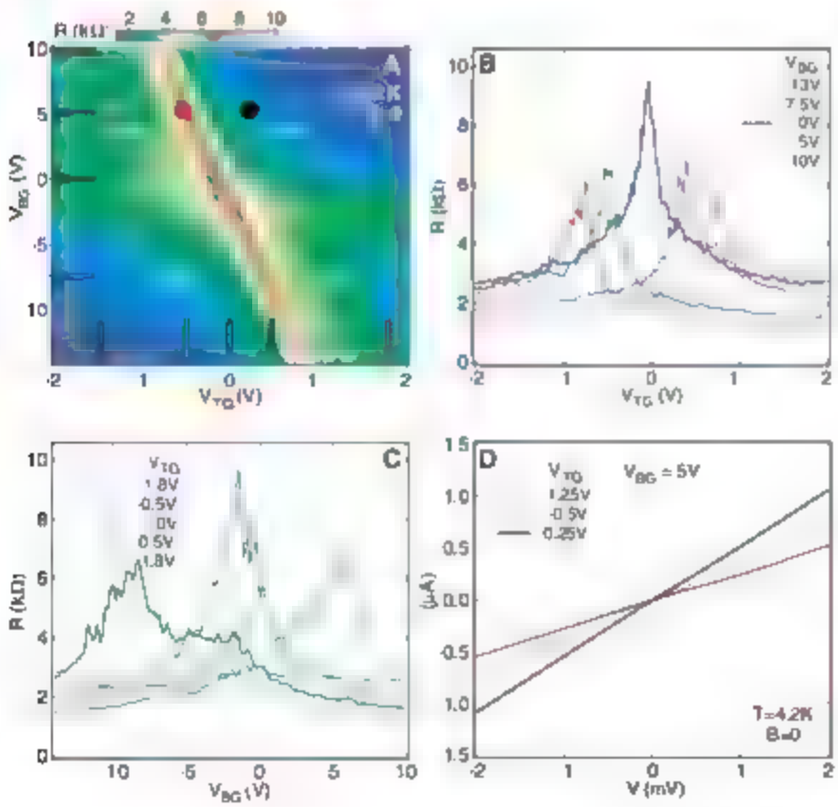

Fig. 2. (**A**) Two-terminal differential resistance R as a function of V_{TG} and V_{BG} at B = 0 and T = 4.2 K, demonstrating independent control of carrier type and density in regions 1 and 2. Labels in each of the four quadrants indicate the carrier type (first letter indicates carrier type in region 1). (**B** and **C**) Horizontal slices at V_{BG} and vertical slices at V_{TG} settings corresponding to the colored lines superimposed on Fig. 2A. (**D**) *I-V* curves at the gate voltage settings corresponding to the solid circles in Fig. 2A are representative of the linear characteristics observed everywhere in the plane of gate voltages.

provide evidence that the electronic structure and degree of disorder of the graphene are not strongly affected by the oxide. Slices at finite V_{TG} reveal a doubly peaked structure. The weaker peak, which remains near $V_{BG} = -2.5$ V at all V_{TG}, corresponds to the Dirac point of region 1. The stronger peak, which moves linearly with V_{TG}, is the Dirac point for region 2. The difference in peak heights is a consequence of the different aspect ratios of regions 1 and 2. Horizontal slices at fixed V_{BG} corresponding to the horizontal lines in Fig. 2A are shown in Fig. 2B. These slices show a single peak, corresponding to the Dirac point of region 2. This peak becomes asymmetric away from the charge-neutrality point in region 1. We note that the V_{BG} dependence of the asymmetry is opposite to that observed in (9), where the asymmetry is studied in greater detail. The changing background resistance results from the different density in region 1 at each V_{BG} setting. Current-voltage (I-V) characteristics, measured throughout the (V_{TG}, V_{BG}) plane, show no sign of rectification in any of the four quadrants or at either of the charge-neutral boundaries between quadrants (Fig. 2D), as expected for reflectionless (Klein) tunneling at the p-n interface (*14*, *15*).

In the QH regime at large B, the Dirac-like energy spectrum of graphene gives rise to a characteristic series of QH plateaus in conductance, reflecting the presence of a zero-energy Landau level that includes only odd multiples of $2e^2/h$ (that is, 2, 6, 10, ... $\times e^2/h$) for uniform carrier density in the sheet (*21*–*23*). These plateaus can be understood in terms of an odd number of QH edge states (including a zero-energy edge state) at the edge of the sheet, circulating in a direction determined by the direction of B and the carrier type. The situation is somewhat more complicated when varying local density and carrier type across the sample.

A 2D color plot of differential conductance $g = I/R$ as a function of V_{BG} and V_{TG} at $B = 4$ T is shown in Fig. 3A. A vertical slice at $V_{TG} = 0$ through the p-p and n-n quadrants (Fig. 3B) reveals conductance plateaus at 2, 6, and $10e^2/h$ in both quadrants, demonstrating that the sample is single layer and that the oxide does not significantly distort the Dirac spectrum.

QH features are investigated for differing filling factors ν_1 and ν_2 in regions 1 and 2 of the graphene sheet. A horizontal slice through Fig. 3A at filling factor $\nu_1 = 6$ is shown in Fig. 3C. Starting from the n-n quadrant, plateaus are observed at $6e^2/h$ and $2e^2/h$ at top-gate voltages corresponding to filling factors $\nu_2 = 6$ and $\nu_2 = 2$, respectively. Crossing over to the n-p quadrant by further decreasing V_{TG}, a new plateau at $3/2\,e^2/h$ appears for $\nu_2 = -2$. In the $\nu_2 = -6$ region, no clear QH plateau is observed. Another horizontal slice at $\nu_1 = 2$ shows $2e^2/h$ plateaus at both $\nu_2 = -6$ and $\nu_2 = 2$ (Fig. 3D). Crossing into the n-p quadrant, the conductance exhibits QH plateaus at $1e^2/h$ for $\nu_2 = -2$ and near $3/2\,e^2/h$ for $\nu_2 = -6$.

For ν_1 and ν_2 of the same sign (n-n or p-p), the observed conductance plateaus follow

$$g = \min(|\nu_1|, |\nu_2|) \times 2e^2/h \qquad (1)$$

This relation suggests that the edge states common to both regions propagate from source to drain, whereas the remaining $|\nu_1| - |\nu_2|$ edge states in the region of highest absolute filling factor circulate internally within that region and do not contribute to the conductance. This picture is consistent with known results on conventional 2D electron gas systems with inhomogeneous electron density (*24*–*26*).

Recent theory (*18*) addresses QH transport for filling factors with opposite sign in regions 1 and 2 (n-p and p-n). In this case, countercirculating edge states in the two regions travel in the same direction along the p-n interface (Fig. 3F), which presumably facilitates mode mixing between parallel-traveling edge states. For the case of complete mode mixing, that is, when current entering the junction region becomes fully and randomly distributed among the $|\nu_1| + |\nu_2|$ parallel-traveling modes, quantized plateaus are expected (*18*) at values

$$g = \frac{|\nu_1| \cdot |\nu_2|}{|\nu_1| + |\nu_2|} \cdot 2e^2/h \qquad (2)$$

A table of the conductance plateau values given by Eqs. 1 and 2 is shown in Fig. 3E. Plateau values at $1e^2/h$ for $\nu_1 = -\nu_2 = 2$ and at $3/2\,e^2/h$ for $\nu_1 = 6$ and $\nu_2 = -2$ are observed in the experiment. Notably, the $3/2\,e^2/h$ plateau suggests uniform mixing among four edge states (three from region 1 and one from region 2). All observed conductance plateaus are also seen at $T = 4$ K and for B in the range from 4 to 8 T (Supporting Online Material (SOM) text).

We do find some departures between the experimental data and Eqs. 1 and 2, as represented in the grid of Fig. 3E. For instance, the plateau near $3/2\,e^2/h$ in Fig. 3D is seen at a value of $1.4e^2/h$, and no clear plateau at $3e^2/h$ is observed for $\nu_1 = -\nu_2 = 6$. We speculate that the conductance in these regions being lower than their expected values is an indication of incomplete mode mixing. We also observe an unexpected peak in conductance at a region in gate voltage between the two $1e^2/h$ plateaus at $\nu_1 = -\nu_2 = 2$. This rise in conductance is clearly seen for V_{TG} values between −1 and 2 V and V_{BG} values between −5 and 2 V. This may result from the possible existence of puddles of electrons and holes near the charge-neutrality points of regions 1 and 2, as previously suggested (*27*).

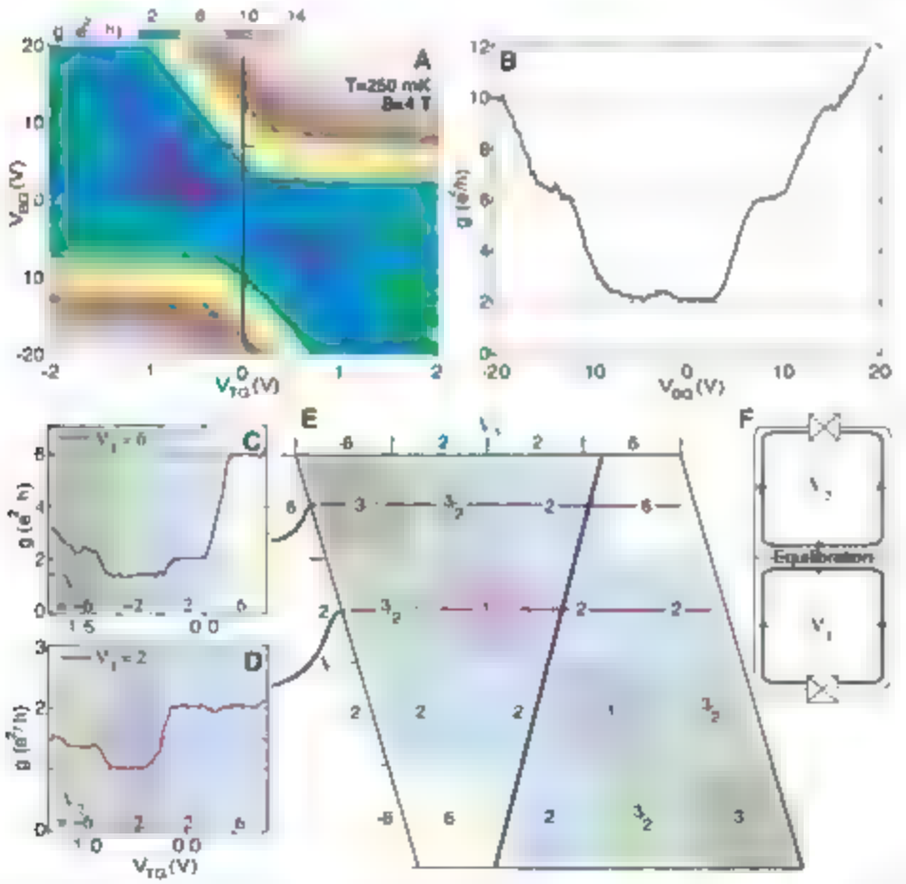

Fig. 3. (**A**) Differential conductance g as a function of V_{TG} and V_{BG} at $B = 4$ T and $T = 250$ mK. (**B**) Vertical slice at $V_{TG} = 0$, traversing p-p and n-n quadrants. Plateaus are observed at $2e^2/h$ and $6e^2/h$, the QH signature of single-layer graphene. (**C**) Horizontal slice at $\nu_1 = 6$ showing conductance plateaus at 6, 2, and $3/2\,e^2/h$. (**D**) Horizontal slice at ν_2 showing QH plateaus at 2, 1, and $3/2\,e^2/h$. (**E**) Table of conductance plateau values as a function of filling factors calculated with Eqs. 1 and 2. Black, purple, and red lines correspond to slices in (B), (C), and (D), respectively. (**F**) Schematic of countercirculating edge states at filling factors $\nu_2 = -\nu_1 = 2$.

References and Notes

1. A. K. Geim, K. S. Novoselov, *Nat. Mater.* **6**, 183 (2007).
2. F. Schedin *et al.*, http://arXiv.org/abs/cond-mat/0610809

3. E. H. Hwang, S. Adam, S. Das Sarma, A. K. Geim, http://arXiv.org/abs/cond-mat/0610834.
4. C. Berger *et al.*, *Science* **312**, 1191 (2006); published online 12 April 2006 (10.1126/science.1125925).
5. Z. Chen, Y.-M. Lin, M. J. Rooks, P. Avouris, http://arXiv.org/abs/cond-mat/0701599.
6. M. Y. Han, B. Özyilmaz, Y. Zhang, P. Kim, http://arXiv.org/abs/cond-mat/0702511.
7. A. Rycerz, J. Tworzydło, C. W. J. Beenakker, *Nature Phys.* **3**, 172 (2007).
8. M. C. Lemme, T. J. Echtermeyer, M. Baus, H. Kurz, *IEEE Electron Device Lett.* **28**, 282 (2007).
9. B. Huard *et al.*, *Phys. Rev. Lett.* **98**, 236803 (2007).
10. K. S. Novoselov *et al.*, *Science* **306**, 666 (2004).
11. K. S. Novoselov *et al.*, *Nature* **438**, 197 (2005).
12. Y. Zhang, Y.-W. Tan, H. Stormer, P. Kim, *Nature* **438**, 201 (2005).
13. H. B. Heersche, P. Jarillo-Herrero, J. B. Oostinga, L. M. K. Vandersypen, A. F. Morpurgo, *Nature* **446**, 56 (2007).
14. M. Katsnelson, K. S. Novoselov, A. K. Geim, *Nature Phys.* **2**, 620 (2006).
15. V. V. Cheianov, V. I. Fal'ko, *Phys. Rev. B* **74**, 041403(R) (2006).
16. V. V. Cheianov, V. Fal'ko, B. L. Altshuler, *Science* **315**, 1252 (2007).
17. D. R. Smith, J. B. Pendry, M. C. K. Wiltshire, *Science* **305**, 788 (2004).
18. D. A. Abanin, L. S. Levitov, *Science* **317**, 641 (2007).
19. Information on materials and methods is available on *Science* Online.
20. D. B. Farmer, R. G. Gordon, *Nano Lett.* **6**, 699 (2006).
21. P. Gusynin, S. G. Sharapov, *Phys. Rev. Lett.* **95**, 146801 (2005).
22. A. Abanin, P. A. Lee, L. S. Levitov, *Phys. Rev. Lett.* **96**, 176803 (2006).
23. N. M. R. Peres, F. Guinea, A. H. Castro Neto, *Phys. Rev. B* **73**, 125411 (2006).
24. D. A. Syphers, P. J. Stiles, *Phys. Rev. B* **32**, 6620 (1985).
25. R. J. Haug, A. H. MacDonald, P. Streda, K. von Klitzing, *Phys. Rev. Lett.* **61**, 2797 (1988).
26. S. Washburn, A. B. Fowler, H. Schmid, D. Kern, *Phys. Rev. Lett.* **61**, 2801 (1988).
27. E. H. Hwang, S. Adam, S. Das Sarma, *Phys. Rev. Lett.* **98**, 186806 (2007); also available at http://arXiv.org/abs/cond-mat/0610157.

28. We thank L. S. Levitov, D. A. Abanin, C. H. Lewenkopf, and P. Jarillo-Herrero for useful discussions; Z. Chen at IBM T. J. Watson Research Center for suggesting the NO_2 functionalization process, and D. Monsma for assistance in implementing it. Research supported in part by INDEX and by the NSF through the Harvard Nanoscale Science and Engineering Center.

Supporting Online Material

www.sciencemag.org/cgi/content/full/1144657/DC1
Materials and Methods
SOM Text
Fig. S1

4 May 2007; accepted 15 June 2007
Published online 28 June 2007
10.1126/science.1144657
Include this information when citing this paper

Quantized Transport in Graphene *p-n* Junctions in a Magnetic Field

D. A. Abanin and L. S. Levitov*

Recent experimental work on locally gated graphene layers resulting in *p-n* junctions has revealed the quantum Hall effect in their transport behavior. We explain the observed conductance quantization, which is fractional in the bipolar regime and an integer in the unipolar regime, in terms of quantum Hall edge modes propagating along and across the *p-n* interface. In the bipolar regime, the electron and hole modes can mix at the *p-n* boundary, leading to current partition and quantized shot-noise plateaus similar to those of conductance, whereas in the unipolar regime transport is noiseless. These quantum Hall phenomena reflect the massless Dirac character of charge carriers in graphene, with particle/hole interplay manifest in mode mixing and noise in the bipolar regime.

The transport properties of graphene, [two-dimensional sheets of graphite (*1*)], in particular the high carrier mobility and tunability of transport characteristics, make this material attractive for applications in nanoelectronics (*2*, *3*). Various methods have been developed for patterning graphene sheets into prototype devices such as quantum-dot transistors (*1*) and nanoribbons (*4*, *5*), followed by the demonstration of local control of carrier density in a graphene sheet (*6*). Besides possible device applications, graphene junctions are predicted to host new and exciting phenomena reflecting the massless Dirac character of carriers in this material, such as Klein tunneling (*7*), particle collimation (*8*), quasibound states (*9*), and Veselago lensing (*10*). In addition, interesting phenomena are expected in gated graphene bilayers, where field-effect transport can be induced by tuning the gap at the Dirac point (*11*). These applications make the gating of graphene a topic of great interest.

Recently, a graphene *p-n* junction with individual control of carrier density in two adjacent regions with a pair of gates above and below it was reported (*12*). The density in each region could be varied across the neutrality point, allowing *p-n*, *p-p*, and *n-n* junctions to be formed at the interface. The interface width was quite small, owing to the 30-nm distance to the top gate and its sharp edge. Transport measurements, carried out in the quantized Hall effect (QHE) regime at magnetic fields $3\ \mathrm{T} < B < 8\ \mathrm{T}$, revealed ohmic two-terminal conductance taking quantized values $g = 6, 2, 1$, and 1 in the units of conductance quantum e^2/h, where h is Planck's constant. The QHE plateaus with $g = 2$ and 6 were observed in the unipolar regime, whereas the quantized plateaus with $g = 1$ and ½ of similar quality were observed in the bipolar regime. Whereas conductance of $6e^2/h$ and $2e^2/h$ is a hallmark of the integer QHE in graphene (*13*, *14*), quantized conductance values of ½ and 1 are unusual and call for explanation.

We interpret these observations by linking them to the properties of the Dirac-like carriers, which give rise to bipolar electron and hole QHE edge modes at the *p-n* interface (Fig. 1). The behavior at the interface is explained by employing ideas from the theory of quantum-chaotic transport (*15*, *16*). Although in our case the edge modes carry charge along the *p-n* interface all in the same direction (in a chiral rather than chaotic fashion), we argue that intermode scattering within the *p-n* interface region gives rise to dynamics with features analogous to those known for quantum-chaotic systems.

In this analogy, the QHE states at the sample boundary play the role of perfect lead channels of chaotic quantum dots (*15*, *16*), bringing charge to the *p-n* interface and carrying it away into reservoirs. However, several physical effects causing conductance fluctuations in chaotic dots are absent in our case, leading to quantization of two-terminal conductance not known for the dots. In particular, the effective lead channels are quantized more perfectly than in the dots, owing to backscattering suppression in QHE transport. In addition, the quantum-mechanical interference effects, which lead to sample-specific conductance fluctuations, can be suppressed in our case because of self-averaging, as well as dephasing and electron-electron scattering. Other effects that can affect the edge-state transport at the *p-n* interface are

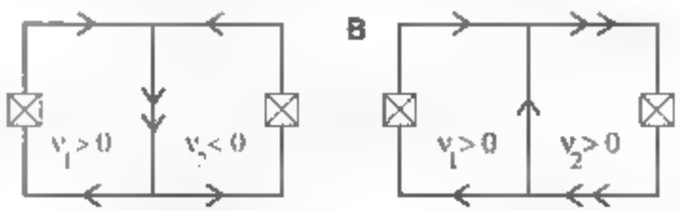

Fig. 1. Schematic of QHE edge states for the (**A**) bipolar regime and (**B**) unipolar regime of a graphene junction. In (A), the edge states counter-circulate in the *n* and *p* regions, bringing electrons and holes from different reservoirs to the *p-n* interface. Mode mixing at the interface leads to the two-terminal conductance (Eq. 1). In (B), because the edge states circulate in the same direction without backscattering or mixing, conductance is determined by the modes permeating the whole system, $g = \min(|\nu_1|, |\nu_2|)$.

Department of Physics, Center for Materials Sciences and Engineering, Massachusetts Institute of Technology, 77 Massachusetts Avenue, Cambridge, MA 02139, USA.

*To whom correspondence should be addressed. E-mail: levitov@mit.edu

intermode relaxation and coupling to electronic states in QHE bulk, causing dephasing in a manner similar to that of the voltage-probe model (*21*). Whereas these regimes yield similar results for conductance, they will manifest themselves differently in other characteristics, in particular in electron shot noise (*22*), which can be used for detailed characterization of transport mechanisms.

Because of particle-hole symmetry of carriers in graphene, the QHE in this material occurs symmetrically about the neutrality point at the densities $\nu = \pm 2, \pm 6, \pm 10, \ldots$ (*13*, *14*). In each of these quantized states, there are $n = |\nu|$ edge modes propagating in different directions at $\nu > 0$ and $\nu < 0$ (*23*, *24*). For the bipolar case, assuming QHE at densities $\nu_1 > 0$ and $\nu_2 < 0$ on either side of the boundary, this gives ν_1 and ν_2 edge modes circulating in opposite directions that merge to form a multimode edge state at the *p*-*n* interface (Fig. 1A). These modes supply to the *p*-*n* interface particles from both the *n* and *p* reservoirs. After propagating together along the interface, these particles arrive at the sample boundary where they are ejected into the edge modes, which split up and return to reservoirs.

The observed conductance quantization can be readily explained by assuming full mixing of these modes at the *p*-*n* interface, so that for each particle the probability to be ejected into any of the $N = \nu_1 + \nu_2$ modes equals $p_N = 1/N$, irrespective of its origin. The two-terminal conductance is then obtained by multiplying p_N by the numbers of the modes, giving

$$g_{pn} = \frac{\nu_1 \nu_2}{\nu_1 + \nu_2} = 1, \frac{3}{5}, 3, \frac{5}{7}, \ldots \qquad (1)$$

where $\nu_{1,2} = \pm 2, \pm 6, \pm 10, \ldots$ This agrees with the observed quantized values (*12*) (Fig. 2).

The character of QHE edge transport in the unipolar regime is quite different. In this case, *n*-*n* or *p*-*p*, the edge modes in both regions circulate in the same direction. As a result, some modes are coupled to both reservoirs, whereas the others are connected to only one of the reservoirs (Fig. 1B). With backscattering suppressed by QHE, the conductance across the boundary is solely due to those edge modes that permeate the entire system, making contact with both reservoirs. This gives the observed nonclassical conductance values

$$g_{nn} \quad g_{pp} \quad \min(\nu_1, \nu_2) \quad 2, 6, 10, \ldots \qquad (2)$$

where $\nu_{1,2} = \pm 2, \pm 6, \pm 10, \ldots$, in agreement with the known results for the quantized conductance of constrictions between different QHE states (*25*, *26*). The nondissipative character of transport in the unipolar regime (Eq. 2), resulting from suppressed backscattering, can be revealed by measuring noise. In the absence of current partitioning inside the sample, we expect only thermal Johnson-Nyquist noise $S \quad 2g k_B T$ (where k_B is the Boltzmann constant and T is temperature) in this regime, but no shot-noise contribution (Fig. 3).

The conductance values given by Eqs. 2 and 1 occur in a particular pattern (*12*) that can be described as follows (Fig. 2): Electron density in graphene induced by the back gate is $n_1 = (\kappa/4\pi e)$ $V_b d$, where d is the distance to the gate, V_b is the voltage on it, and κ is the dielectric constant. Similarly, in the locally gated region we have n_2 $(\kappa/4\pi e)(V_b d + V_t h)$, where h and V_t are the distance to the top gate and the voltage on it. For the Landau-level filling factors $\nu_{1,2} = (hc/eB)n_{1,2}$ we find

$$\nu_1 \quad l_B^2(\kappa/2e)V_b d$$

$$\nu_2 \quad l_B^2(\kappa/2e)(V_b d + V_t h) \qquad (3)$$

where l_B is the magnetic length. The values V_b and V_t, corresponding to integer QHE states, are inside parallelograms with the boundaries approximately given by $\nu_{1,2} = 0, \pm 4, \pm 8, \ldots$, as appropriate for the fourfold degenerate graphene Landau levels (*13*, *14*). The resulting conductance pattern, shown in Fig. 2 for realistic parameter values, strikingly resembles the experimental results (*12*).

How is the conductance in Eq. 1 affected by quantum-mechanical interference effects? Random-matrix theory (RMT) of chaotic transport predicts (*15*, *16*) ensemble-averaged conductance $\bar{g} = n_1 n_2 (n_1 + n_2 + 1 \quad 2/\beta)$, where $n_{1,2}$ is the open channel number and $\beta = 1$, 2, or 4 for the three random-matrix universality classes. In our QHE case, with the channel numbers $n_{1,2}$ $\nu_{1,2}$ and $\beta = 2$, RMT predicts that $\bar{g}$ is identical to Eq. 1. Similarly, a semiclassical description of transport in chaotic cavities (*17*), where mixing is due to the dynamics in the cavity, yields conductance values close to the classical result for two conductors connected in series.

To clarify the origin of the mode mixing at the *p*-*n* interface, we studied electron-density distribution for the gate geometry used in (*12*). A numerical solution of the Laplace problem for the electrostatic potential in between the gates revealed that the *p*-*n* density step is about 40 nm wide, a few times larger than the magnetic length at $B = 8$ T. Comparison to the known results (*27*) for a compressible region sandwiched between incompressible regions then suggests the presence at the *p*-*n* interface of additional QHE

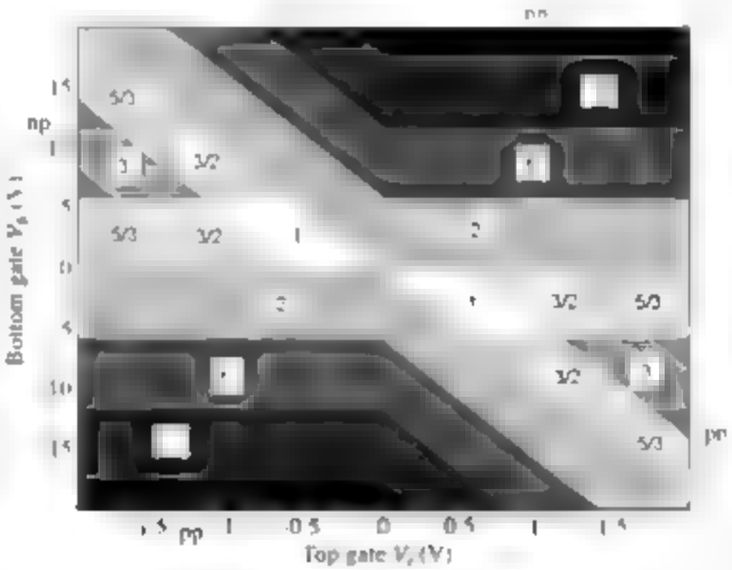

Fig. 2. Two-terminal conductance versus gate voltage, given by Eq. 1 in the bipolar case ($\nu_1 > 0$, $\nu_2 < 0$) and by Eq. 2 in the unipolar case ($\nu_{1,2}$ of equal sign). The boundaries of QHE regions are specified by $\nu_{1,2} = 0, \pm 4, \pm 8, \ldots$, with the gate voltage dependence of $\nu_{1,2}$ given by Eq. 3. The parameters used are as follows: distance to the top gate $h = 30$ nm, distance to the back gate $d = 300$ nm, magnetic length $l_B = 10$ nm, and dielectric constant $\kappa = 3$.

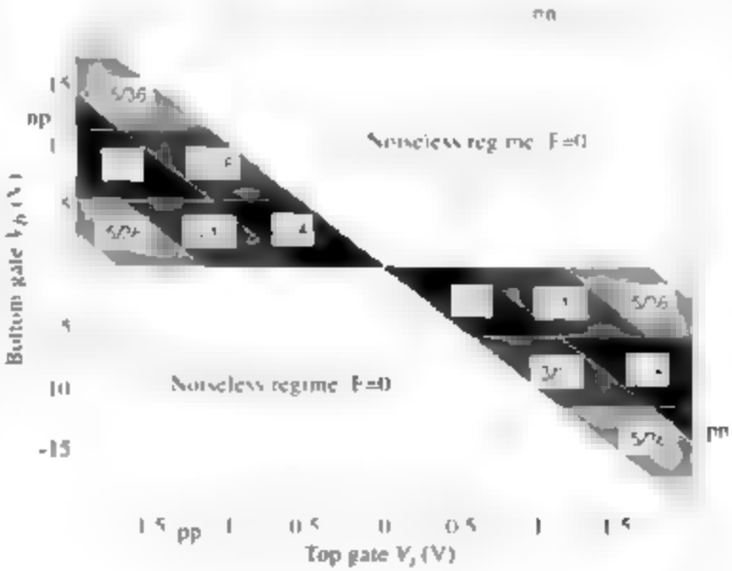

Fig. 3. Shot-noise Fano factor (Eq. 8) plotted versus gate voltages for the same parameter values as those in Fig. 2. The noise is zero in the unipolar regime (*p*-*p* or *n*-*n*), reflecting the absence of QHE edge-state backscattering and current partition at the junction interface. In the bipolar regime, because of edge mode mixing at the *p*-*n* interface, noise is finite, exhibiting a quantized plateau structure similar to that of conductance.

modes which, in the presence of disorder, can facilitate interchannel scattering and mixing.

In the fully coherent regime, conductance would exhibit universal fluctuations (UCF). The magnitude of UCF predicted for chaotic transport (20) in our case depends on the channel numbers as follows

$$\mathrm{var}(g) = \frac{\nu_1^2\nu_2^2}{(|\nu_1| + |\nu_2|)^2\,((|\nu_1| + |\nu_2|)^2 - 1)} \quad (4)$$

Applied to the observed plateaus with (ν_1,ν_2) = (2, 2), (2, 6), and (6, 2), Eq. 4 indicates that these plateaus would not have been discernible in a system with fully developed UCF. We therefore conclude that the observed quantization of g depends on some mechanism that suppresses UCF. For example, the suppression could easily be understood if Thouless energy for the states at the *p-n* interface was small as compared with k_BT. The reduced UCF would then result from averaging over the k_BT energy interval. However, the plateaus in (12) remain unchanged when the temperature is reduced from 4 K to 250 mK, making such a scenario unlikely.

The UCF suppression may signal a fundamental departure of chiral QHE dynamics from that of the earlier-studied systems. However, at this point we cannot exclude other, more mundane explanations. In particular, time-dependent fluctuations of system parameters can supercede mesoscopic fluctuations, turning the observed time-averaged quantities into ensemble-averaged quantities. This self-averaging could arise naturally because of a fluctuating electric field at the *p-n* interface induced by voltage noise on the gates. Another, more interesting explanation could be that UCF suppression indicates the presence of dephasing due to the coupling of the chiral modes to the localized states in the bulk, or some other intrinsic mechanism.

Current partition because of mode mixing at the *p-n* interface will manifest itself in the finite shot-noise intensity. To find noise, we take into account that the mixing of the reservoir distributions, no matter of what origin, results in particle energy distribution of a double-step form

$$n(\varepsilon) = \frac{|\nu_1|}{N}n_1(\varepsilon) + \frac{|\nu_2|}{N}n_2(\varepsilon) \quad (5)$$

where $n_{1,2}(\varepsilon) = n_F(\varepsilon \pm \frac{1}{2}eV_{sd})$. [Here, $n_F(\varepsilon)$ is the Fermi distribution, and V_{sd} is the source-drain voltage.] In an analogy with diffusive systems (28) and chaotic cavities (17, 19), this distribution serves as a Kogan-Shulman–like extraneous source of current fluctuations

$$J = \int n(\varepsilon)[1 - n(\varepsilon)]d\varepsilon = \frac{|\nu_1\nu_2|}{N^2}|eV_{sd}| \quad (6)$$

We relate the noise source J to the fluctuations of the two-terminal current by noting that, because fluctuating current of intensity J is injected into each open channel, the current fluctuations flowing into the *n* and *p* regions will be $J_1 = |\nu_1|J$ and $J_2 = |\nu_2|J$. Converting these fluctuations into voltage fluctuations and adding the contributions of the *n* and *p* regions, we find the voltage fluctuations δV induced between the reservoirs

$$\langle\delta V^2\rangle = \frac{J_1}{\nu_1^2} + \frac{J_2}{\nu_2^2} = \left(\frac{1}{|\nu_1|} + \frac{1}{|\nu_2|}\right)J \quad (7)$$

Current noise can now be obtained as $S = g^2\langle\delta V^2\rangle$, where g is the conductance (Eq. 1). It is convenient to characterize noise by the Fano factor $F = S/I$ (where I is current), describing noise suppression relative to Poisson noise. We find

$$F = \frac{|\nu_1||\nu_2|}{(|\nu_1| + |\nu_2|)^2} = \frac{1}{4}, \frac{3}{16}, \frac{5}{36}, \ldots \quad (8)$$

where $\nu_{1,2}$ = 2, 6, 10.... The result (Eq. 8) is identical in form to the shot-noise Fano factors of chaotic cavities (17, 19). The Fano factor values (Eq. 8) should be contrasted with $F \approx 0.29$ that is predicted for a *p-n* junction in the absence of magnetic field (8).

Another regime for noise is possible if electrons, while traveling along the *p-n* interface, have enough time to transfer energy to each other via inelastic processes. This will occur if $\tau_{el} \ll L/v$, where τ_{el} is the characteristic electron energy relaxation time, v is the drift velocity, and L is the *p-n* interface length. [A similar regime was analyzed for diffusive (28) and chaotic (19) transport.] In this case, the electron energy distribution is characterized by an effective temperature T_{eff} that is determined by the balance of the energy supplied from reservoirs and electron thermal energy flowing out

$$\frac{1}{2}\frac{|\nu_1\nu_2|}{|\nu_1| + |\nu_2|}V_{sd}^2 = \frac{\pi^2}{6}(|\nu_1| + |\nu_2|)k_B^2T_{eff}^2 \quad (9)$$

The extraneous fluctuations (Eq. 6), evaluated for the Fermi distribution with $T = T_{eff}$, give $J = k_BT_{eff}$. Repeating the reasoning that has led to Eq. 8, we find the noise intensity $S = gk_BT_{eff}$. This expression resembles the Nyquist formula, except for the factor of 2 missing because the fluctuations (Eq. 6) occur only in the *p-n* region but not in the leads. Because $T_{eff} \propto V_{sd}$, this noise is linear in V_{sd}. Similar to the $T = 0$ shot noise, it can be characterized by the Fano factor $\tilde{F} = (3F)^{1/2}/\pi$, with F given by Eq. 8.

Finally, noise can be used to test which of the UCF suppression mechanisms discussed above, self-averaging or dephasing, occurs in an experiment (12). For coherent transport, noise exhibits mesoscopic fluctuations, similar to UCF, that can be analyzed within an RMT framework. In the absence of time-reversal symmetry, RMT yields an ensemble-averaged Fano factor

$$\bar{F} = \frac{|\nu_1\nu_2|}{(|\nu_1| + |\nu_2| + 1)(|\nu_1| + |\nu_2| - 1)} \quad (10)$$

(see Eq. 11 in (20)). For $\nu_{1,2}$ = 2, 4, 6..., this gives $\bar{F}$ = 4/15, 12/63, 36/143.... These values, expected when transport is coherent but self-averaged, are different from those in Eq. 8 that are obtained from an incoherent-mixing model.

The quantized transport observed in graphene *p-n* junctions (12) is of different character in the unipolar and bipolar regimes. In the first case, transport is dissipationless, with conductance quantized to an integer. In the second case, mode mixing at the *p-n* interface creates a situation similar to that studied in quantum-chaotic transport. Conductance quantized to fractional values observed in (12) then results from intrinsic or extrinsic suppression of UCF. These transport regimes can be unraveled by using electron shot noise (predicted to be finite in the bipolar regime and zero in the unipolar regime), with quantized plateau structure similar to that of conductance.

References and Notes

1. A. K. Geim, K. S. Novoselov, *Nat. Mater.* **6**, 183 (2007).
2. Y.-W. Son, M. L. Cohen, S. G. Louie, *Nature* **444**, 347 (2006).
3. A. Rycerz, K. J. Tworzydło, C. W. J. Beenakker, *Nat. Phys.* **3**, 172 (2007).
4. Z. Chen, Y.-M. Lin, M. J. Rooks, P. Avouris, preprint available at http://arXiv.org/abs/cond-mat/0701599.
5. M. Y. Han, B. Oezyilmaz, Y. Zhang, P. Kim, preprint available at http://arXiv.org/abs/cond-mat/0702511.
6. B. Huard *et al.*, preprint available at http://arXiv.org/abs/0704.7626.
7. M. I. Katsnelson, K. S. Novoselov, A. K. Geim, *Nat. Phys.* **2**, 620 (2006).
8. V. V. Cheianov, V. I. Fal'ko, *Phys. Rev. B* **74**, 041403 (2006).
9. P. G. Silvestrov, K. B. Efetov, *Phys. Rev. Lett.* **98**, 016802 (2007).
10. V. V. Cheianov, V. Fal'ko, B. L. Altshuler, *Science* **315**, 1252 (2007).
11. T. Ohta, A. Bostwick, T. Seyller, K. Horn, E. Rotenberg, *Science* **313**, 951 (2006).
12. J. R. Williams, L. DiCarlo, C. M. Marcus, *Science* **317**, 638 (2007).
13. K. S. Novoselov *et al.*, *Nature* **438**, 197 (2005).
14. Y. Zhang, Y.-W. Tan, H. L. Stormer, P. Kim, *Nature* **438**, 201 (2005).
15. C. W. J. Beenakker, *Rev. Mod. Phys.* **69**, 731 (1997).
16. H. U. Baranger, P. A. Mello, *Phys. Rev. Lett.* **73**, 142 (1994).
17. Ya. M. Blanter, E. V. Sukhorukov, *Phys. Rev. Lett.* **84**, 1280 (2000).
18. D. Agam, I. Aleiner, A. I. Larkin, *Phys. Rev. Lett.* **85**, 3153 (2000).
19. S. Oberholzer *et al.*, *Phys. Rev. Lett.* **86**, 2114 (2001).
20. D. V. Savin, H.-J. Sommers, *Phys. Rev. B* **73**, 081307(R) (2006).
21. M. Büttiker, *Phys. Rev. B* **38**, 9375 (1988).
22. Ya. M. Blanter, M. Büttiker, *Phys. Rep.* **336**, 1 (2000).
23. N. M. R. Peres, F. Guinea, A. H. Castro Neto, *Phys. Rev. B* **73**, 125411 (2006).
24. D. A. Abanin, P. A. Lee, L. S. Levitov, *Phys. Rev. Lett.* **96**, 176803 (2006).
25. R. J. Haug, A. H. MacDonald, P. Streda, K. von Klitzing, *Phys. Rev. Lett.* **61**, 2797 (1988).
26. S. Washburn, A. B. Fowler, H. Schmid, D. Kern, *Phys. Rev. Lett.* **61**, 2801 (1988).
27. A. V. Khaetskii, V. I. Fal'ko, G. E. W. Bauer, *Phys. Rev. B* **50**, 4571 (1994).
28. K. E. Nagaev, *Phys. Lett. A* **169**, 103 (1992).

29. We thank C. M. Marcus, L. DiCarlo, J. R. Williams, P. Kim, and P. Jarillo-Herrero for discussions and Ya. M. Blanter and E. V. Sukhorukov for comments. This work is supported by the NSF Materials Research Science and Engineering Center (grant DMR 02132802) and NSF (grant DMR-0304019).

4 May 2007; accepted 21 June 2007
Published online 28 June 2007;
10.1126/science.1144672
Include this information when citing this paper.

Cylindrical Block Copolymer Micelles and Co-Micelles of Controlled Length and Architecture

Xiaosong Wang,[1]* Gerald Guerin,[1] Hai Wang,[1] Yishan Wang,[1] Ian Manners,[1,2]† Mitchell A. Winnik[1]†

Block copolymers consist of two or more chemically different polymers connected by covalent linkages. In solution, repulsion between the blocks leads to a variety of morphologies, which are thermodynamically driven. Polyferrocenyldimethylsilane block copolymers show an unusual propensity to forming cylindrical micelles in solution. We found that the micelle structure grows epitaxially through the addition of more polymer, producing micelles with a narrow size dispersity, in a process analogous to the growth of living polymer. By adding a different block copolymer we could form co-micelles. We were also able to selectively functionalize different parts of the micelle. Potential applications for these materials include their use in lithographic etch resists, in redox-active templates, and as catalytically active metal nanoparticle precursors.

Block copolymers, which consist of two or more different polymers covalently linked together, form a range of structures when placed in a selective solvent. These assemblies include micelles with a solvent-insoluble core and a solvent-swollen corona (*1*). The shapes and sizes of the structures that form are typically determined by the lengths of the polymer blocks, their affinity for each other and for the solvent, and temperature (*2*). Long micelles with a narrow diameter are particularly useful (*3*). For example, cylindrical aggregates of a peptide-amphiphile have been used as a fibrous scaffold for the mineralization of hydroxyapatite (*4*). Polyethylene oxide poly(ethylene-*alt*-propylene) (PEO-PEP) cylinders incorporated into epoxy resins greatly enhance the toughness of the resins (*5*). Cylindrical micelles with a polyferrocenylsilane (PFS) core and a cross-linked corona have been used as a template for creating linear arrays of silver nanoparticles (*6*). Whereas spherical block copolymer micelles are able to carry dyes and other drug analogs into cells (*7*), cylindrical micelles can orient and stretch in a flowing stream in a manner that is ideal for flow-intensive drug delivery applications (*8*, *9*). Thus, cylindrical micelles are interesting in part because of their potential applications in nanotechnology and medicine.

Block copolymer micelles are normally formed under conditions close to thermodynamic control and are studied in a kinetically frozen state (*2*, *10*). Most diblock copolymers form spherical micelles, whereas only a narrow range of compositions are able to form cylindrical micelles (*2*). In contrast, PFS block copolymers such as PFS-polyisoprene (PFS-PI), PFS-polydimethylsiloxane (PFS-PDMS), and PFS-polymethylvinylsiloxane (PFS-PMVS) form rod-like micelles for a broad range of block ratios. This process occurs in a variety of solvents that are selective for the complementary block and yields structures with a cylindrical organometallic core (*11*–*14*). We previously provided evidence that the crystalline nature of PFS is a key feature that promotes the formation of cylinders for such a broad range of compositions (*14*). Here, we show that these micelles can undergo chain extension in ways that recall key features of living polymerization to form structures of controlled segment length and composition.

Living polymerization refers to a diverse class of systems in which molecules or other microscopic units form long chains by continuous addition to the reactive chain ends, without termination or transfer steps (*15*). Examples include the synthesis of linear macromolecules (*16*) and the growth of actin and microtubule filaments through self-assembly of the appropriate proteins (*17*, *18*). The defining feature of this type of reaction is that after all the monomer units in solution have been consumed, the chain ends remain active and will continue to react once additional monomer is added. The chain length increases linearly with the amount of added monomer and frequently the resulting product has a narrow contour length distribution (CLD). If the added monomer is different from the one initially polymerized, one obtains a block copolymer consisting of chemically different segments sharing a common junction. This is the method used to synthesize the PFS block copolymers examined here.

We begin by considering cylindrical micelles formed by a PFS_{53}-PI_{320} diblock copolymer in hexane (the subscripts refer to the number-averaged degree of polymerization). [All of the polymers considered here have a narrow molar mass distribution (*19*) (table S1).] Undisturbed, the micelle structures were stable over a period of months. However, when aliquots of additional polymer dissolved in a common good solvent such as tetrahydrofuran (THF) or toluene were added, the micelles, by transmission electron microscopy (TEM), appeared to become longer (fig. S1). To enable us to follow changes in length distribution, we sonicated the solution to form shorter micelles with a mean length of ~250 nm (Fig. 1A). Addition of more polymer dissolved in THF led to an increase in the apparent hydrodynamic radius R_h^{app} as monitored by dynamic light scattering (DLS) and by an increase in micelle length, as seen in Fig. 1. Two noteworthy features of these structures are their rigidity and their relatively narrow length distribution. The mean micelle length increased from 250 nm to 500, 750, and 2000 nm (Fig. 1, B to D, respectively), roughly proportional to the amount of PFS_{53}-PI_{320} added. Simply adding 1 mg of PFS_{53}-PI_{320} in 0.1 ml of THF to 1 ml of hexane, comparable to the amount of polymer present in the solution in Fig. 1B, gave a different result. Large aggregates of ill-defined shape could be seen by TEM. We infer that preexisting micelles are necessary initiators for controlled micelle growth.

To test this idea, we examined micelles of a different polymer sample of similar composition (PFS_{48}-PI_{264}) in decane, using static and dynamic light scattering (SLS and DLS) experiments as well as TEM measurements. Direct formation of

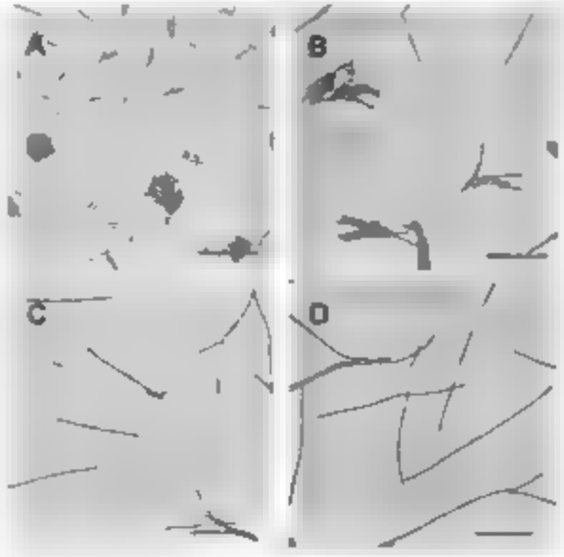

Fig. 1. TEM images for (A) sonicated PFS_{53}-PI_{320} micelles in hexane (0.5 mg/ml); (B to D) elongated micelles after adding 0.5 mg (B), 1 mg (C), and 2 mg (D) of PFS_{53}-PI_{320} in THF (0.1 ml) to 1.0-ml solutions of (A). Scale bars, 500 nm.

[1]Department of Chemistry, University of Toronto, Toronto, Ontario M5S 3H6, Canada. [2]School of Chemistry, University of Bristol, Bristol BS8 1TS, UK.

*Present address: Department of Colour and Polymer Chemistry, University of Leeds, Leeds LS2 9JT, UK.

†To whom correspondence should be addressed. E-mail: mwinnik@chem.utoronto.ca; ian.manners@bristol.ac.uk

the micelles by heating and then cooling the solution led to long cylinders (>2 μm), which would make the study of their growth by TEM and light scattering difficult. After sonicating the solution, the micelles fragmented to give shorter structures. Sonication and dilution yielded rod-like micelles with a mean length (L_w) of 98 nm, an aggregation number of 310 molecules per micelle, an apparent radius of gyration R_g^{app} = 38.3 nm (fig. S2), and a hydrodynamic radius R_h = 32.8 nm. For micelle growth experiments, approximately equal aliquots of the sonicated micelles (~1.0 ml, 0.050 mg/ml; table S2) were transferred into six tared vials, and then five increasing amounts (samples B to F) of a solution of PFS_{48}-PI_{264} in THF (2.316 mg/ml) were added. As a control (sample A), a similar amount of THF alone was added to one of the vials.

The cells were covered to prevent dust from entering the solutions, and the THF was allowed to evaporate as the solutions were aged at 21°C for 7 days. After the initial SLS and DLS experiments, the samples were carefully sealed and stored in the dark for an additional 20 weeks to test their long-term stability. The TEM and SLS data in Fig. 2 are taken from these samples aged for 5 months.

The CLD of sample A is shown in Fig. 2A. The number-average length (L_n^{TEM} = 105 nm) is consistent with that of the initial sonicated sample. The CLD of sample E is shown in Fig. 2B. Here, the value of L_n^{TEM} has shifted to 510 nm with a L_w/L_n ratio of 1.6, similar to its value of 1.4 for sample A. In Fig. 2C we present Guinier-Holtzer plots of $qR_\theta/\pi\mathcal{K}_0Kc$ (where q is the scattering vector, R_θ is the Rayleigh ratio, M_0 is the copolymer weight-average molecular weight, K is the optical constant, and c is polymer concentration), plotted as a function of q, for the six samples. The solid lines correspond to the best fit of the data to the form factor for thin rigid rods [(19), equations S3 and S4]. These plots highlight the presence of elongated structures in the solution, because such objects exhibit a plateau at high q. The magnitudes of the plateau values, from which the number of polymer molecules per unit length ($N_{mol/L}$) can be calculated, were obtained as a fitting parameter for all of the samples, but the presence of the plateau is clearly evident in the two uppermost curves. Note that the samples approach their plateau values at lower q values as the amount of polymer added is increased. This behavior is expected for solutions containing rods of increasing length, and is mirrored in the upward curvature at low q for the longer micelles seen in the plots of R_g^{app} as a function of q (fig. S3B). All samples are characterized by similar values of $N_{mol/L}$ ≈ 3 molecules/nm, and this property remained constant as the samples were subjected to long-term aging.

Values of L_n are plotted against c in Fig. 2D. These data exhibit three remarkable features. The first is the overall finding of these experiments that addition of polymer in THF solution leads to the growth of existing micelles while preserving the internal structure, as reflected in the essentially

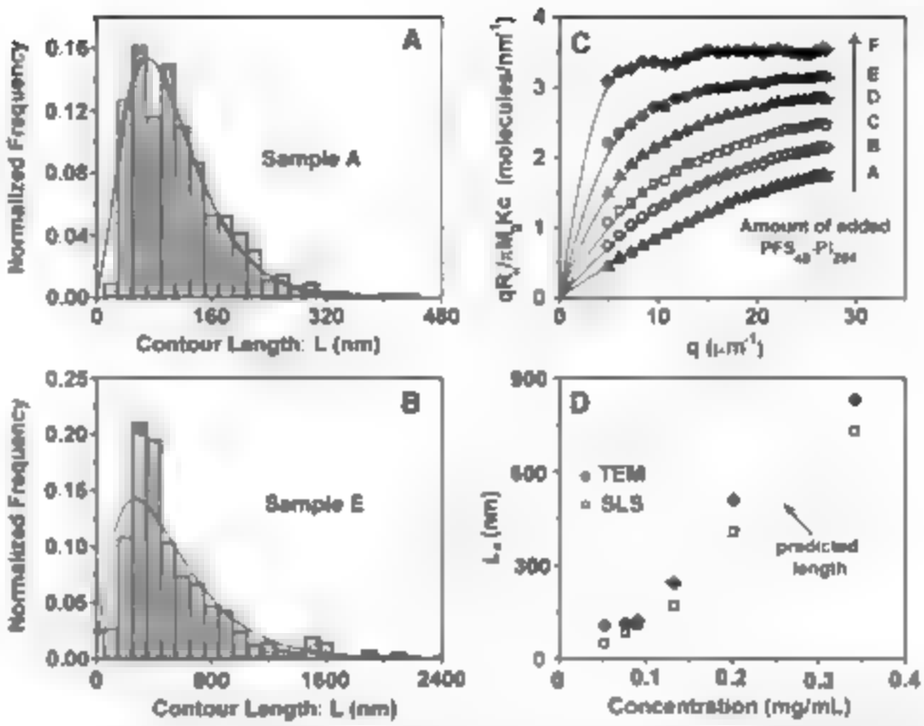

Fig. 2. Properties of sonicated PFS_{48}-PI_{264} micelles in *n*-decane (0.05 mg/ml). (**A**) Contour length distribution (CLD) obtained from TEM images after treatment with 0.03 ml of THF (sample A). (**B**) CLD for sample E. The lines correspond to the expression $F(L) = L\exp(-2L/L_n)$. (**C**) Plots of $qR_\theta/\pi M_0Kc$ versus q for sample A, and after addition of 0.01, 0.02, 0.04, 0.07, and 0.12 ml of PFS_{48}-PI_{264} in THF (2.316 mg/ml) (samples B to F, respectively). The lines represent the best fit to equations S3 and S4 (19) for thin rigid rods with a Zimm-Schulz distribution of lengths. (**D**) Number-average length L_n versus total polymer concentration for the solutions in (C) deduced from TEM-CLD (•) and SLS (□) experiments. The dashed line is the predicted value for monodisperse rods assuming uniform growth of existing micelles as a function of polymer concentration. The samples were aged for 5 months before the SLS and TEM measurements.

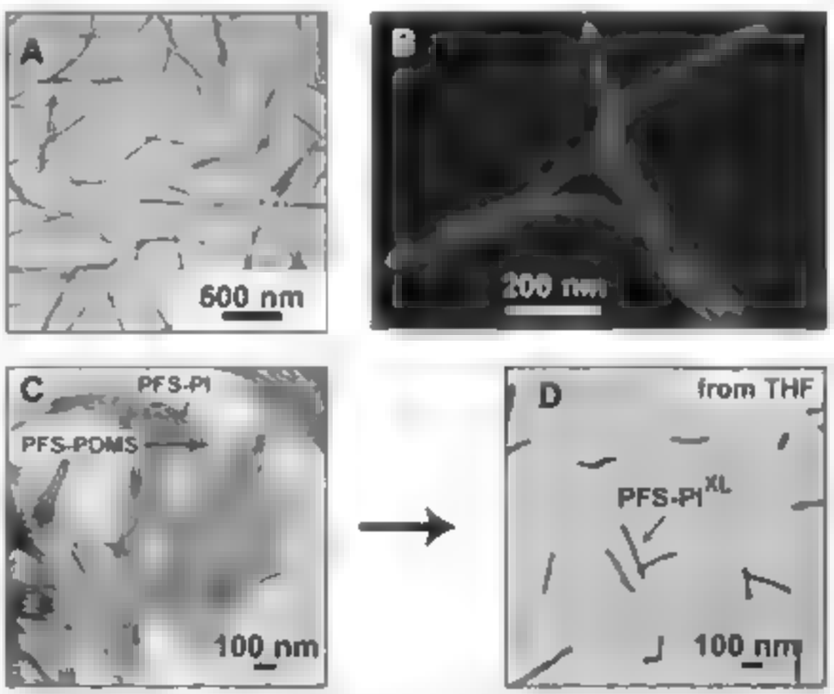

Fig. 3. (**A** and **B**) Bright-field (A) and dark-field (B) TEM images of triblock co-micelles $M_{(PFS_{48}\text{-}PMVS_{300})}$-*b*-$M_{PFS_{53}\text{-}PI_{320}}$-*b*-$M_{(PFS_{48}\text{-}PMVS_{300})}$ formed by adding PFS_{48}-$PMVS_{300}$ (1.0 mg in 0.1 ml of THF) to a solution (0.5 mg/ml) of sonicated PFS_{53}-PI_{320} micelles in decane. (**C**) A TEM image of sample prepared in hexane/THF (10:1 v/v) of $M_{PFS_{40}\text{-}PDMS_{210}}$-*b*-$M_{PFS_{53}\text{-}PI_{320}}$-*b*-$M_{PFS_{40}\text{-}PDMS_{210}}$ triblock co-micelles. (**D**) The PI corona chains were then cross-linked (XL) by reaction with tetramethyldisiloxane and the sample was transferred to THF solution, which dissolved the PFS-PDMS chains but left the cross-linked PFS_{53}-PI^{XL}_{320} structures intact.

constant value of N_{agg}. Values of L_n increase linearly with c as one would expect for a living polymerization. The second feature is the concordance between L_n values determined by light scattering and by contour length analysis of the TEM images, with slightly larger values obtained by TEM (table S4). Finally, we note the long-term stability of the micelles (fig. S3). Even on a time scale of months, there is little evidence for unimer dissociation and new micelle formation, nor is there any indication of micelle fusion in dilute solution. The absence of micelle fusion suggests that the micelle growth happens via the addition of free chains on the preexisting micelle, rather than by "self-nucellization" of the free chains followed by addition to the ends of preexisting micelles. It is interesting that most of the distributions (Fig. 2, A and B, and fig. S4) can be well fitted with the Zimm-Schulz expression $F(L) = L^z \exp(-zL/L_n)$. This is also the expression developed by Israelachvili (*20*) for the CLD of one-dimensional micelles formed under equilibrium conditions, but we note an important difference: Our finding that L_n increases linearly with concentration is different from the square-root dependence predicted by that model.

Another important characteristic of a living polymerization is that the chain ends will react with the addition of a different monomer. Starting with PFS_{53}-PI_{320} cylinders in decane-THF mixtures, we prepared short rod-like seeds of PFS_{53}-PI_{320} micelles in decane (L_n = 200 nm, 0.5 mg/ml) by sonication. To a 1.0-ml aliquot of this solution, we added 0.1 ml of THF containing 1.0 mg of PFS_{40}-$PMVS_{330}$ and monitored the solution by DLS. The apparent R_h of the aggregates increased gradually until reaching a constant value. A TEM image of these micelles (Fig. 3A) shows that the addition of the second block copolymer did not disrupt the original shape of the cylinders, but their length increased to ~1000 nm, which suggests that block co-micelles were formed.

A clearer indication of the micelle structure is provided by the dark-field TEM image in Fig. 3B. In a dark-field image, components containing heavy elements scatter more electrons and appear bright against the dark carbon film. The structures in Fig. 3B are characterized by a thin central line flanked by two thicker segments. The thin lines can be attributed to the PFS cores of a central PFS_{53}-PI_{320} block, whereas the thicker segments arise from the additional electron scattering of the silicon-rich PMVS corona that surrounds a PFS core. By TEM, we could not observe any micelles containing only PFS-PMVS copolymer, which indicates that micelle growth starts from both ends of the PFS_{53}-PI_{320} micelle and leads to a triblock architecture which we denote $M_{PFS_{40}\text{-}PMVS_{330}}$-*b*-$M_{PFS_{53}\text{-}PI_{320}}$-*b*-$M_{PFS_{40}\text{-}PMVS_{330}}$ (where M denotes micelle, b denotes block structure, and the subscripts are the components of each block).

The susceptibility of the PI chains of PFS-PI micelles to cross-linking provides another proof of the ability of the system to form triblock co-micelles. By adding a THF solution of PFS_{40}-$PDMS_{330}$ to a solution of PFS_{53}-PI_{320} micelles in hexane, we produced co-micelles of $M_{PFS_{40}\text{-}PDMS_{330}}$-*b*-$M_{PFS_{53}\text{-}PI_{320}}$-*b*-$M_{PFS_{40}\text{-}PDMS_{330}}$ (Fig. 3C). The middle block of the co-micelles contains vinyl groups in the PI corona, whereas the PDMS corona chains of the two side blocks have no reactive functionality. We have shown that the vinyl groups of PI or PMVS in the corona of PFS micelles can be cross-linked using Pt(0)-catalyzed hydrosilylation (*13*). Using the same chemistry, with tetramethyldisiloxane as the cross-linking agent, we were able to cross-link the vinyl-containing PI blocks of the triblock co-micelles and fix the structure of the center block of the aggregates. When this sample was dried and then exposed to THF, the soluble PDMS chains dissolved, and only the cross-linked (PFS_{53}-PI^{XL}_{320}) central block remained (Fig. 3D).

These findings show that the micelles in this hexane-THF mixture are sufficiently robust to support the hydrosilylation reaction to cross-link the PI corona chains. We also discovered that the semicrystalline PFS core of the micelle itself is accommodating to PFS chains of somewhat different length. The number-average degree of polymerization of the PFS portion of the polymers (PFS_{40}-$PDMS_{330}$) that grow off the ends of the PFS_{53}-PI_{320} micelles is about 80% of that of the chains in the preformed micelles.

Micelle growth cannot occur, however, if the ferrocenylsilane block has a different chemical structure that prevents crystallization. Poly(ferrocenylmethylethylsilane) (PFMES) is an amorphous polymer, and PFMES-PMVS forms spherical micelles in hexane. When a THF solution of PFMES-PMVS is added to a hexane solution of sonicated PFS_{53}-PI_{320} micelles, the product appears by TEM to be a mixture of spherical micelles and unchanged PFS_{53}-PI_{320} micelles (fig. S6).

Figure 4 summarizes the nucleation and growth steps involved in the self-assembly of PFS-PI diblock copolymers in alkane solvents. The free chains formed upon heating the initial sample undergo homogeneous nucleation upon cooling and aging to form a discrete number of nuclei that serve as initiation sites for chain growth. Free chains deposit on the ends of the rod-like structures, accompanied or driven by epitaxial crystallization of the PFS blocks. Once this process is complete, growth stops. When more polymer, dissolved in a common good solvent such as THF, is added to the solution, "chain growth" is reinitiated, leading to longer rod-like structures or triblock co-micelles.

The mechanism for block copolymer self-assembly in solution demonstrated here enables the production of rods with a narrow distribution of lengths, as well as the synthesis of segmented rod-like structures with control over segment length and composition. The blocks containing vinyl groups in their corona can be selectively cross-linked. Such cylindrical structures with controlled lengths and compositions are of interest as etch resists, reactive redox-active templates, conductive wires, and patternable precursors to magnetic and catalytic Fe nanoparticles.

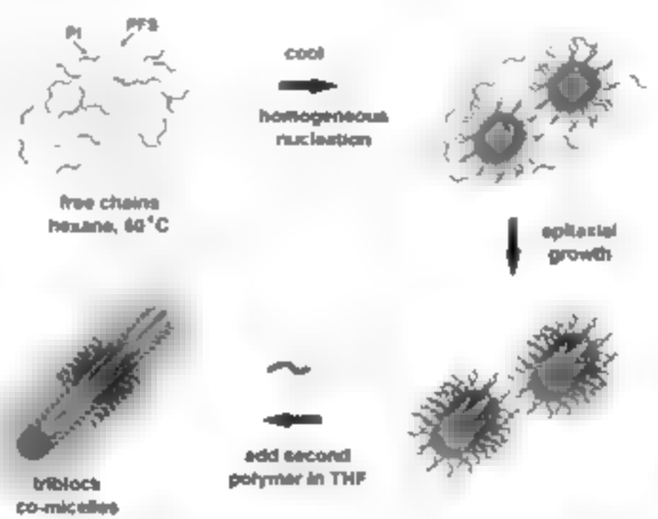

Fig. 4. A mechanism for the self-assembly of PFS-PI block copolymers in alkane solvents. Homogeneous nucleation followed by epitaxial growth yields cylindrical micelles with a semicrystalline core and a relatively narrow distribution of lengths. The rod ends remain active to further growth if additional polymer containing a PFS block is added to the system. As shown, the second polymer and PFS-PI have different soluble blocks.

References and Notes

1. J. Rodriguez-Hernandez, F. Checot, Y. Gnanou, S. Lecommandoux, *Prog. Polym. Sci.* **30**, 691 (2005).
2. E. B. Zhulina, M. Adam, I. LaRue, S. S. Sheiko, M. Rubinstein, *Macromolecules* **38**, 5330 (2005).
3. S. Jain, F. S. Bates, *Science* **300**, 460 (2003).
4. J. D. Hartgerink, E. Beniash, S. I. Stupp, *Science* **294**, 1684 (2001).
5. J. M. Dean, N. E. Verghese, H. Q. Pham, F. S. Bates, *Macromolecules* **36**, 9267 (2003).
6. K. S. Wang, H. Wang, N. Coombs, M. A. Winnik, I. Manners, *J. Am. Chem. Soc.* **127**, 8924 (2005).
7. R. Savić, L. B. Luo, A. Eisenberg, D. Maysinger, *Science* **300**, 615 (2004).
8. Y. Kim, P. Dalhaimer, D. A. Christian, D. E. Discher, *Nanotechnology* **16**, S484 (2005).
9. P. Dalhaimer, F. S. Bates, D. E. Discher, *Macromolecules* **36**, 6873 (2003).
10. Y. Y. Won, T. H. Davis, F. S. Bates, *Macromolecules* **36**, 953 (2003).
11. J. Massey, K. N. Power, I. Manners, M. A. Winnik, *J. Am. Chem. Soc.* **120**, 9533 (1998).
12. J. Raez, I. Manners, M. A. Winnik, *J. Am. Chem. Soc.* **124**, 10381 (2002).
13. X. S. Wang, A. Arsenault, G. A. Ozin, M. A. Winnik, I. Manners, *J. Am. Chem. Soc.* **125**, 12686 (2003).
14. J. A. Massey *et al.*, *J. Am. Chem. Soc.* **122**, 11577 (2000).
15. B. O'Shaughnessy, D. Vavylonis, *Phys. Rev. Lett.* **90**, 118301 (2003).
16. O. W. Webster, *Science* **251**, 887 (1991).
17. S. C. Greer, *Adv. Chem. Phys.* **94**, 261 (1996).

18. S. C. Greer, *Annu. Rev. Phys. Chem.* 53, 173 (2002).
19. See supporting material on *Science* Online
20. J. Israelachvili, *Intermolecular and Surface Forces* (Academic Press, London, ed. 2, 1992), p. 359.
21. Supported by a European Union Marie Curie Chair (I.M.), a Wolfson Research Merit Award from the Royal Society of Chemistry (I.M.), and the Natural Sciences and Engineering Research Council of Canada. We thank L. Herrera for helpful discussions.

Supporting Online Material
www.sciencemag.org/cgi/content/full/317/5838/644/DC1
Materials and Methods
Figs. S1 to S6
Tables S1 to S4

15 February 2007; accepted 22 June 2007
10.1126/science.1141382

Block Copolymer Assembly via Kinetic Control

Honggang Cui,[1] Zhiyun Chen,[2] Sheng Zhong,[1] Karen L. Wooley,[2]* Darrin J. Pochan[1]*

Block copolymers consist of two or more chemically different polymer segments, or blocks, connected by a covalent linkage. In solution, amphiphilic blocks can self-assemble as a result of energetic repulsion effects between blocks. The degree of repulsion, the lengths of the block segments, and the selectivity of the solvent primarily control the resultant assembled morphology. In an ideal situation, one would like to be able to alter the morphology that forms without having to change the chemistry of the block copolymer. Through the kinetic manipulation of charged, amphiphilic block copolymers in solution, we are able to generate different nanoscale structures with simple block copolymer chemistry. The technique relies on divalent organic counter ions and solvent mixtures to drive the organization of the block copolymers down specific pathways into complex one-dimensional structures. Block copolymers are increasingly used as templating materials; thus, the ability to control the formation of specific patterns and structures is of growing interest and applicability.

The broader development of nanoscale technologies requires methods to fabricate and manipulate material at the nanometer-length scale. This includes techniques that manipulate individual atoms or clusters, as well as materials that will self-assemble into organized patterns, often through solution-based processes. Molecules with varying chemical interactions are needed to drive the assembly, and this has been accomplished in block copolymers (*1*–*7*), surfactants (*8*), proteins (*9*), DNA (*10*, *11*), peptides (*12*, *13*), peptide amphiphiles (*14*), and polypeptides (*15*). This broad range of molecules was needed to tailor nanostructures with potential impact on disparate, emerging fields such as nanomedicine (*14*), organic photovoltaics (*16*, *17*), and self-assembled spintronics (*18*, *19*) or optoelectronic devices (*11*, *20*).

Linear triblock copolymers, produced with common polymerization techniques, provide an opportunity to develop self-assembly strategies for complex nanostructure formation that do not necessarily require the altering of the molecule chemistry to create a wide range of structures. The chemical tunability of amphiphilic block copolymers has been used previously to produce micelles and nanostructures in solution (*1*, *7*, *21*–*22*). Polymeric micelle size and shape can be designed through monomer selection, chain architecture design, and variation of solution conditions (e.g., solvent mixtures, pH manipulation, salt concentration, and temperature) (*1*, *7*, *21*, *23*). However, the slow kinetics of block copolymers in solution, due to the slow exchange of chains between micelles because of the higher molecular weight of the molecules, hinders assembled structures from reaching global equilibrium states (*21*, *24*–*26*). We specifically take advantage of this lack of global equilibrium in amphiphilic charged block copolymers to produce complex, one-dimensional nanostructures. The block copolymers are controllably forced down specific assembly pathways through a combination of solvent mixing and the complexation of a charged, hydrophilic block with divalent, organic counterions. The resultant assemblies are kinetically trapped but stable because of the inability of the system to thermodynamically equilibrate.

The system we used consists of a linear poly(acrylic acid)-*block*-poly(methyl acrylate)-*block*-polystyrene (PAA-*b*-PMA-*b*-PS) triblock copolymer, tetrahydrofuran (THF)/water mixed solvents, and organic diamines (Fig. 1A). Various micelles with different packing geometries, such as disks and toroids, have been constructed using this system (*4*, *22*, *27*, *28*). This multicomponent assembly system allows control over the thermodynamics and kinetics of block copolymer assembly in the following ways. The selectivity of water for PAA allows the manipulation of interfacial curvature between the hydrophilic corona and hydrophobic core within a micelle, thus providing a means to control local micelle geometry. Organic diamine complexation with chargable PAA corona blocks influences both intermicellar interactions and the intramicellar PAA corona block conformation. By the use of different solvent-mixing protocols, the pathway through which polymer assembly occurs can be manipulated.

The controlled assembly pathway generally begins with diamine complexation with the PAA block in pure THF solution producing PAA-diamine aggregates. Subsequent addition of water has the combined effect of aggregating the hydrophobic PMA and PS blocks while concurrently swelling and eventually solubilizing the PAA-diamine complexes into micelle coronas. The combination of the PAA-diamine complexation with subsequent solvent mixing produces a unique block copolymer assembly pathway resulting in the nanostructures displayed in Figs. 1, B and C. The cylindrical nanostructures consist of PAA_{94}-*b*-PMA_{109}-*b*-PS_{44} with 1,2-ethylenediaminediethylamine (EDDA) as the ammonium counterion.

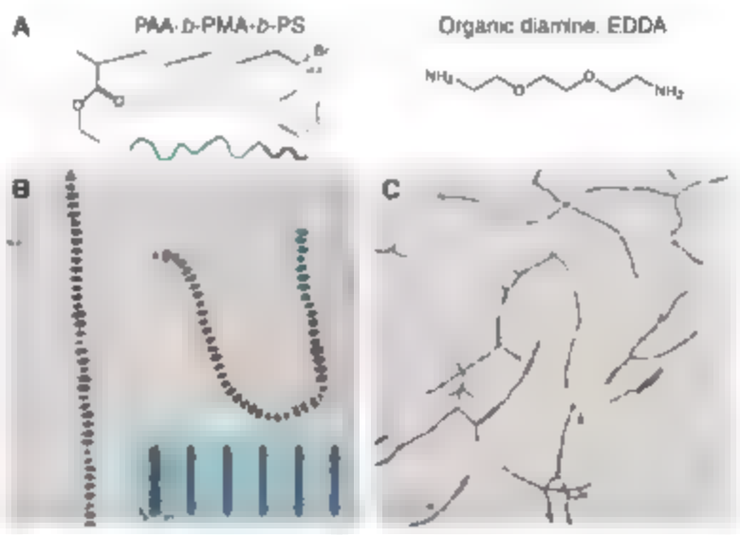

Fig. 1. (**A**) Molecular structures of triblock copolymer, PAA-*b*-PMA-*b*-PS, and organic diamine (EDDA). (**B** and **C**) TEM images of one-dimensional assembled structures of PAA_{94}-*b*-PMA_{109}-*b*-PS_{44} at 67% THF/water solution in the presence of EDDA (molar ratio of amine groups: acid groups = 1:1). The samples were stained with uranyl acetate aqueous solution. (B, inset) Schematic drawing of cross section of one-dimensional assembled structures. PMA-PS stripes are illustrated as gray and dark blue bands. Light blue bands denote PAA concentrated area. EDDA, which is complexed with the PAA block, is not drawn for clarity.

[1]Department of Materials Science and Engineering and Delaware Biotechnology Institute, University of Delaware, Newark, Delaware 19716, USA. [2]Center for Materials Innovation, Department of Chemistry and Department of Radiology, Washington University in Saint Louis, Saint Louis, Missouri 63130, USA.

*To whom correspondence should be addressed. E-mail: klwooley@artsci.wustl.edu (K.L.W.); Pochan@udel.edu (D.J.P.)

by interaction with the acrylic acid residues of the PAA [see table S1 and (29) for block copolymer molecular details]. The periodic stripes perpendicular to the cylinder axes indicate the alternating layers of hydrophilic PAA complexed with EDDA and hydrophobic PMA-PS domains. The dark stripes are PAA layers that are positively stained as a result of uranyl cations interacting with carboxylic acid side chains of the PAA. The light stripes are composed of PS and PMA hydrophobic segments with a thickness of ~20 nm (Fig. 1B, inset). It is notable that this assembly is not a typical hydrophobic core hydrophilic corona micelle but rather a cylinder with alternating layers of hydrophilic and hydrophobic components arranged perpendicular to the cylinder axis.

The specific assembly pathway to produce the striped cylinders is as follows. PAA_{94}-*b*-PMA_{103}-*b*-PS_{88} was first dissolved in THF to form a 0.1 weight percent homogeneous solution. Next, EDDA was added to give a molar ratio of amine group/acid group = 1:1. The EDDA complexed with the PAA block affording PAA-diamine aggregates. Water was then added slowly (~8 ml water per hour added to 20-ml THF block copolymer solution with a syringe pump) both to initiate aggregation of the hydrophobic blocks and to solubilize the PAA-diamine complexes. This slow addition of water first caused polymer phase separation into polymer-rich domains with a local lamellar nanostructure due to phase segregation of unlike blocks (*22*). Once sufficient water was added, the phase-separated polymer droplets were solubilized into discrete micelles through the segregation of the hydrophobic blocks into hydrophobic core domains and the hydration of PAA-diamine into the corona. At high water content (THF:water = 1:4), stable, spherical micelles formed (Fig. 2A). THF was then pipetted into the spherical micelle solution to produce a final volumetric ratio of THF:water = 2:1. During the original slow addition of water to the block copolymer diamine:THF solution, a 2:1 THF:water ratio produced block copolymer droplets with local lamellar structure (*22*). By forcing the system back to this solvent composition, the spherical block copolymer micelles were forced to aggregate into a locally ordered lamellar nanostructure. Transmission electron microscopy (TEM) images taken immediately after the THF addition demonstrated that all of the micelles polymerized along a preferred growth axis (Fig. 2B). Further aging for several hours allowed additional one-dimensional growth of these structures into long (up to microns in length) structures with uniform widths as shown in Fig. 1, B and C.

In amphiphilic block copolymer dilute solutions, two kinetic processes are possible in response to solvent compositional changes. One is a relatively fast intramicellar process of obtaining local preferred interfacial curvature in isolated micelles through fast local chain adjustment. The second is the relatively slow process of reaching a global equilibrium by means of intermicellar interactions [through infrequent intermicellar single-chain exchange (*21*, *24*, *25*) or micelle fusion or fission]. When combined, the mismatch of the two kinetic processes can produce the well-defined hierarchical structure in Fig. 1, B and C, and Fig. 2C schematically demonstrates the proposed mechanism. Upon quick introduction of THF, the local packing geometry of isolated micelles changes before intermicellar aggregation takes place. Because local chain adjustment is a much faster process than intermicellar interactions, oblate spheres or discoidal micelles form with the addition of THF (Fig. 2C, step 1). Although the local flat interfacial curvature is desired in the system, the resultant dispersed structures are not stable in the low-water-content solution and undergo aggregation. However, the aggregation is one-dimensional because the disklike micelles have PAA-diamine faces that experience long-range, attractive electrostatic interactions with other diamine-rich PAA faces in high THF content solution. [See figs. S1 to S4 and (*29*) for data and accompanying discussion about the electrostatic nature of the interactions between the PAA blocks and the multivalent amine counterions.] Direct visualization of several separate disklike micelles in the intermediate assembly stage can be seen in Fig. 2D, as marked by black arrows, supporting the concept that these segmented cylinders are formed by one-dimensional collapse of discotical micelles. In addition, the diameter and volume of each cylindrical segment is comparable to the dimensions of the separate spherical micelles before aggregation, further supporting the fusion mechanism. Branching appears as growth defects, as observed in Fig. 2, E and F. Theoretical prediction has shown that branching could occur in the one-dimensional aggregation of dipolar fluids when construction of a branch provides a lower free energy than the formation of a free chain end (*30*). In the current work, branching probably oc-

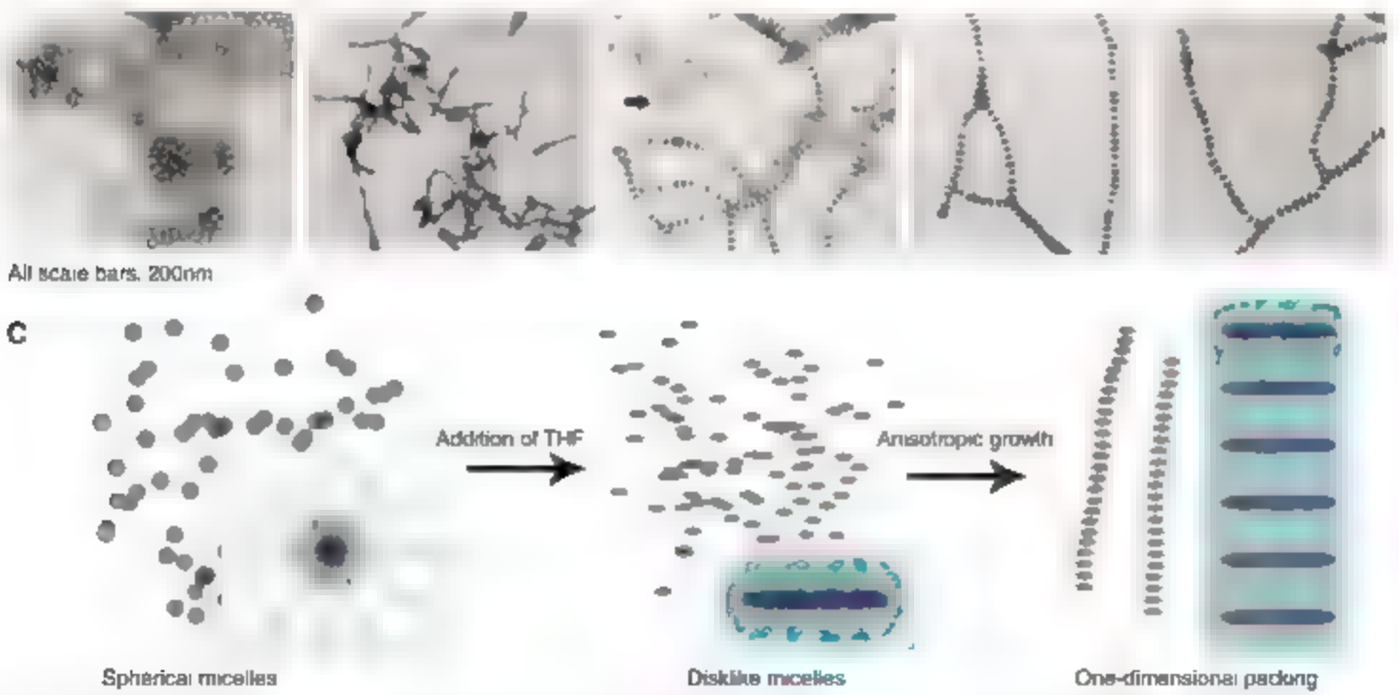

Fig. 2. (**A**) Spherical micelles of PAA_{94}-*b*-PMA_{103}-*b*-PS_{88} formed at the 1:4 ratio of THF to water in the presence of EDDA (molar ratio of amine groups:acid groups = 1:1). (**B**) TEM image of one-dimensional aggregation of spherical micelles immediately after introducing THF into original solution to reach a 2:1 final ratio of THF to water. Further growth of these short structures led to a giant one-dimensional supra-assembly, as shown in Fig. 1, B and C. (**C**) Growth mechanism of spherical micelles. Sphere-disk transition occurred first as THF was introduced. Anisotropic shape of disk-like micelles allows for one-dimensional preferred growth. Inserted schematic illustrates proposed chain packing of spherical micelles, disklike micelles and one-dimensional packing structures. (**D**) Separate disklike micelles marked as black arrow. (**E** and **F**) Branches appear as growth defect. The samples were stained with uranyl acetate aqueous solution.

curs because of polydispersity in size and shape of assembling micelle units. As intermicellar interaction proceeds, there is a chance that some spherical micelles do not have enough time to adjust their packing geometry before assembling into a growing cylinder. This curved surface could then allow two disklike micelles to attach, forming a branch. An alternative branching mechanism could be polydispersity in the sizes of disks, with slightly larger disks having more PAA-diamine surface area, so that two additional disks could assemble, thus forming a branch.

The periodic spacing of PAA was then used as a template to interact with oppositely charged inorganic nanoparticles to construct periodic hybrid materials. Hybrid superstructures were created by immersing assembled one-dimensional structures into primary amine–coated gold nanoparticle aqueous suspension for several minutes. Dark stripes in Fig. 3, A and B, are due to the high electron density of gold nanoparticle rich PAA regions. Lattice fringes of gold nanoparticle single crystals can be clearly seen in high-resolution TEM imaging (Fig. 3C). In high-angle annular dark-field (HAADF) imaging, the gold stripes are visualized as parallel bright lines (Fig. 3, D and E).

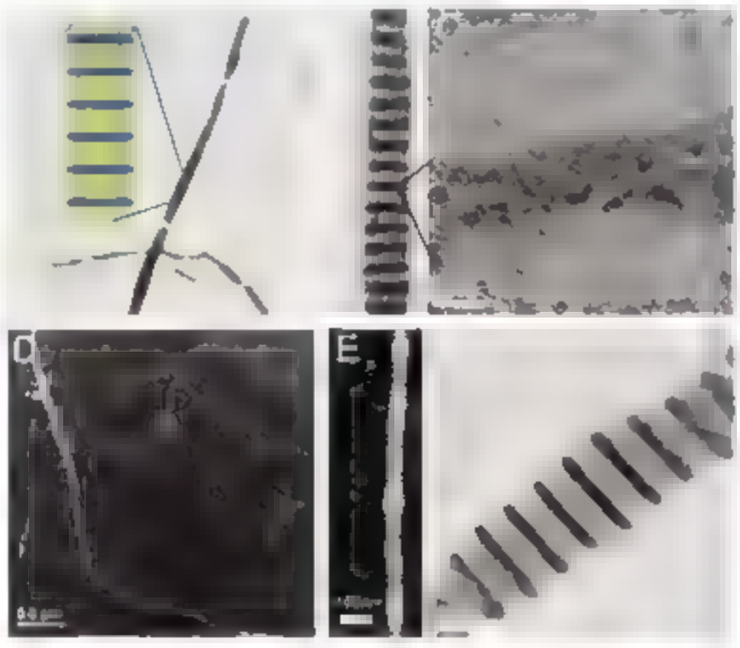

Fig. 3. TEM images of directed gold nanoparticle assembly in the charged PAA region. (**A** and **B**) Bright-field images. Dark stripes are concentrated gold nanoparticle areas. Insert shows proposed structures. Yellow dots denote gold nanoparticles. (**C**) High-resolution TEM (HRTEM) imaging of lattice structure of gold single crystals. (**D** and **E**) high-angle annular dark field (HAADF) imaging of periodic gold stripes. Gold particles appear as bright stripes. (**F**) TEM image of periodic gold stripes when polyamine functionalized gold particles are used as counterions.

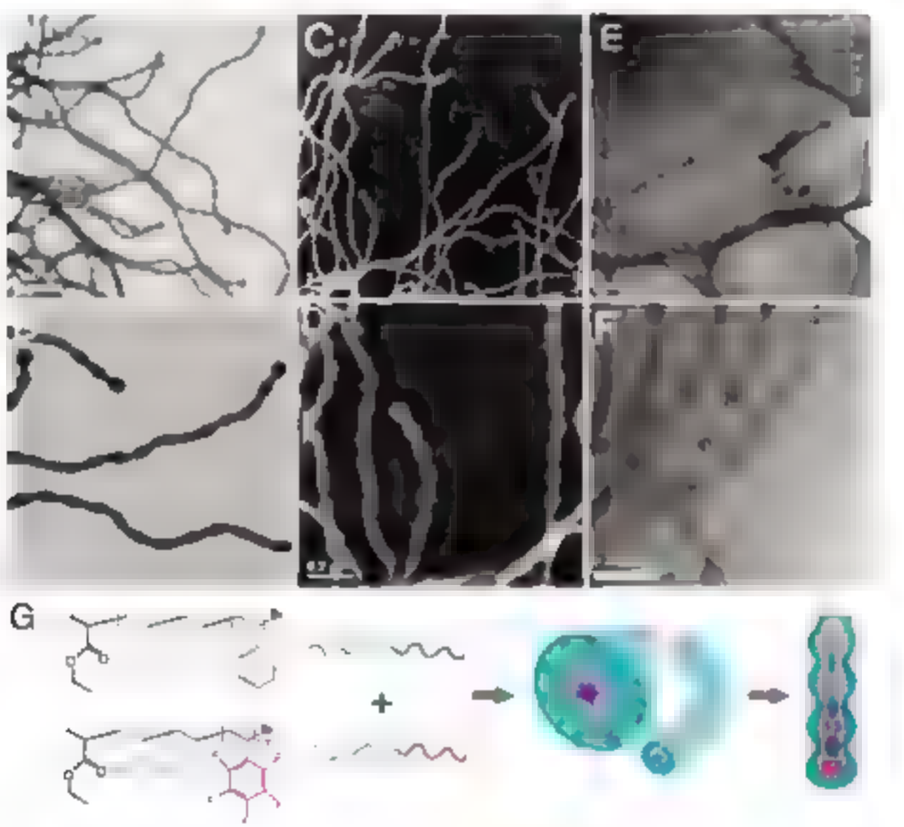

Fig. 4. Nanostructured multicompartment cylinders. (**A** and **B**) Bright-field TEM images. Dark regions present polypentafluorostyrene-chain rich area. (**C** and **D**) HAADF images of cylindrical micelles with internal phase-separated cores. (**E**) Cryogenic TEM (cryo-TEM) image of uniform cylindrical micelle at 40% water/THF solution. (**F**) Cryo-TEM image of cylindrical micelles with internal phase-separated cores at 67% water/THF solution. (**G**) Schematic illustration of formation of multicompartment cylinders.

Another advantage of using charged corona blocks is that multivalent counterions, such as functionalized inorganic nanoparticles, can be used to influence local micelle structure and act as the stimulus for the formation of one-dimensional segmented nanostructures. This approach may be used in concert with, or as an alternative to, the addition of solvent. If the block copolymer is designed correctly, when spherical micelles come into contact with multifunctional inorganic nanoparticles, they should transform into disks that attractively collapse into segmented cylinders. This concept has been implemented with the addition of positively charged gold nanoparticles into a 50% THF water suspension of PAA_{64}-*b*-PVA_{80}-*b*-PS_{130} spherical micelles, as described without added diamine. Each gold nanoparticle had on average six primary amine groups on the surface and functioned as a multivalent counterion to complex with PAA. When they were added to the block copolymer spheres, the spheres collapsed into one-dimensional structures with alternating stripes of gold nanoparticle rich layers and hydrophobic layers, both perpendicular to the primary axis of the assembly. The distance between PAA gold-laden stripes was then 40 nm, as compared to approximately 20 nm between PAA layers for the sample in Fig. 1, B and C. This increased interlayer spacing was due to the increase of the PS block length to 130 from 44 monomer repeat units. Apparently, the structures shown in Fig. 3F were not a consequence of pure one-dimensional growth of spherical micelles, because the diameter of the final cylindrical structures is about twice as large as the original spherical micelles. However, the addition of charged gold nanoparticles was able to influence the assembly of spheres in a preferred direction. The multivalent functionalized nanoparticle can be chosen independently, and the spacing between inorganic-rich layers of the final one-dimensional assembly can be tuned by choosing different relative polymer block lengths.

By taking advantage of slow kinetics of block copolymer chains in solution and the complexation of charged blocks with multivalent counterions, one can also produce complex micelles containing multiple hydrophobic blocks within the same micelle core that can undergo local, intramicellar phase separation. To obtain a single polymeric micelle geometry, such as cylinders, with each micelle core constituted by multiple hydrophobic blocks, at least two different, linear triblock copolymers are required, with similar overall molecular weight and relative block ratios but

different core block chemistry. The key point for choosing the different chemistries of the two hydrophobic blocks is that the two blocks experience a high degree of mutual immiscibility. In the current experiment, polystyrene (PS) and poly(2,3,4,5,6-pentafluorostyrene) (PPFS) were employed as the different, third hydrophobic blocks in the two triblock copolymers (PAA_{96}-*b*-PMA_{103}-*b*-PS_{117} and PAA_{93}-*b*-PMA_{99}-*b*-$PPFS_{100}$) (*29*). Equal molar amounts of the two triblock copolymers with different respective third blocks were dissolved in pure THF. EDDA was then added to reach a final 1:1 molar ratio of amine groups to acid groups. The diamines underwent complexation with the PAA blocks, thereby forming aggregates with PAA-diamine cores. Notably, these aggregates contained each of the triblock copolymers with both PS and PPFS hydrophobic blocks because of the simple trapping of unlike hydrophobic blocks in the same aggregate by PAA-diamine complexation. Next, introduction of water into the THF solution to a final ratio of THF:water = 1:2 provided for the formation of cylindrical micelles. However, the existence of the original mixed triblock copolymer aggregates, as a result of PAA and diamine complexation, forced the local co-assembly of unlike third hydrophobic blocks into the same micelle core. In addition, the lack of chain exchange in solution that disallows global chain migration and maintains nonequilibrated micelle structures, combined with the fact that the PAA chains in the corona of the newly formed micelles were still complexed with diamines and were not freely mobile within the micelle, guarantee the stability of the mixed-core micelle. The immiscibility of the two different hydrophobic blocks, PS and PPFS, eventually resulted in internal phase separation on the nanoscale, producing multicompartment micelles. The images shown in Fig. 4, A to D, were taken after 4 days of aging a solution of mixed hydrophobic core cylinders. Internal phase separation is clearly indicated by the strong undulations along the cylinder surfaces and the TEM contrast variation along the cylinders. The larger, darker, and more spherical regions within the cylinders are hypothesized to be regions that are concentrated in PAA_{96}-*b*-PMA_{103}-*b*-$PPFS_{100}$ triblock copolymer. First, there is a higher interfacial energy between PPFS and PMA, relative to PS and PMA, causing more chain stretching within PPFS-rich core domains so as to limit PPFS interactions with surrounding PMA blocks. Second, the greater electron density of the PPFS block provides a greater ability to scatter electrons and produce darker images in the TEM. The thinner region of the undulating cylinder would then be occupied primarily by PAA_{93}-*b*-PMA_{99}-*b*-PS_{117} (Fig. 4G). This internal cylinder phase separation only occurred at relatively higher amounts of water in the mixed solvent solutions. Cryo-TEM showed uniform cylinders without undulation on the surface at only 40% water:THF solution after 4 days (Fig. 4E). However, multicompartment cylinders could be observed as the water percentage increased to 67% (Fig. 4F). Reports in the literature have shown similar undulating cylinder morphologies through polymer blending, but with, at most, only three periods of undulation that always started from semispherical end caps (*21*). Clearly, the undulations shown here are not exclusively correlated with the spherical end caps and are obvious throughout the length of the cylinders. Safran *et al.* have demonstrated that the curvature energy of a cylinder with undulations could be lower than that of a nonundulating cylinder (*31*). However, the undulations observed here, although locally induced by unfavorable energetic interactions between PPFS and PS, are only possible kinetically because of the forced mixing of unlike hydrophobic core blocks as a result of PAA complexing with diamines and a specific solvent-mixing pathway.

Both the multicompartment cylinders with phase-separated cores and the cylindrical nanostructures with alternating layers of chemistry perpendicular to the cylinder axes are results of a solution assembly strategy to create structures with increased complexity with standard linear block copolymer architectures and chemistries. The key parameters are the combination of charged block interactions with multivalent counterions to influence both intra- and intermicellar interactions and solvent mixing to control the assembly pathways.

References and Notes

1. Z. B. Li, E. Kesselman, Y. Talmon, M. A. Hillmyer, T. P. Lodge, *Science* **306**, 98 (2004).
2. S. Jain, F. S. Bates, *Science* **300**, 460 (2003).
3. B. M. Discher *et al.*, *Science* **284**, 1143 (1999).
4. D. J. Pochan *et al.*, *Science* **306**, 94 (2004).
5. J. Raez, I. Manners, M. A. Winnik, *J. Am. Chem. Soc.* **124**, 10381 (2002).
6. L. F. Zhang, A. Eisenberg, *Science* **268**, 1728 (1995).
7. R. H. Zheng, G. J. Liu, X. H. Yan, *J. Am. Chem. Soc.* **127**, 15358 (2005).
8. R. Zana, Y. Talmon, *Nature* **362**, 228 (1993).
9. P. Ringler, G. E. Schulz, *Science* **302**, 106 (2003).
10. P. W. K. Rothemund, *Nature* **440**, 297 (2006).
11. C. A. Mirkin, R. L. Letsinger, R. C. Mucic, J. J. Storhoff, *Nature* **382**, 607 (1996).
12. J. Cornelissen *et al.*, *Science* **293**, 676 (2001).
13. J. P. Schneider *et al.*, *J. Am. Chem. Soc.* **124**, 15030 (2002).
14. G. A. Silva *et al.*, *Science* **303**, 1352 (2004).
15. A. P. Nowak *et al.*, *Nature* **417**, 424 (2002).
16. W. U. Huynh, J. J. Dittmer, A. P. Alivisatos, *Science* **295**, 2425 (2002).
17. L. Schmidt-Mende *et al.*, *Science* **293**, 1119 (2001).
18. O. Kahn, C. J. Martinez, *Science* **279**, 44 (1998).
19. M. Ouyang, D. D. Awschalom, *Science* **301**, 1074 (2003).
20. V. Percec *et al.*, *Nature* **419**, 384 (2002).
21. S. Jain, F. S. Bates, *Macromolecules* **37**, 1511 (2004).
22. H. G. Cui, Z. Y. Chen, K. L. Wooley, D. J. Pochan, *Macromolecules* **39**, 6599 (2006).
23. T. P. Lodge, *Macromol. Chem. Phys.* **204**, 265 (2003).
24. R. Lund, L. Willner, D. Richter, E. E. Dormidontova, *Macromolecules* **39**, 4566 (2006).
25. Y. Y. Won, H. T. Davis, F. S. Bates, *Macromolecules* **36**, 953 (2003).
26. E. E. Dormidontova, *Macromolecules* **32**, 7630 (1999).
27. Z. Y. Chen *et al.*, *J. Am. Chem. Soc.* **127**, 8592 (2005).
28. Z. B. Li *et al.*, *Langmuir* **21**, 7533 (2005).
29. Materials and methods are available as supporting material on Science Online.
30. I. Tlusty, S. A. Safran, *Science* **290**, 1328 (2000).
31. S. A. Safran, *Statistical Thermodynamics of Surfaces, Interfaces, and Membranes* (Addison-Wesley, New York, 1994).

32. We thank NSF for funding, specifically the Nanoscale Interdisciplinary Research Teams program under grant DMR-0210247. Any opinions, findings, conclusions, or recommendations expressed in this material are those of the authors and do not necessarily reflect the views of NSF. We also thank the W. M. Keck College of Engineering electron microscopy laboratory at the University of Delaware and the nuclear magnetic resonance facilities of the Department of Chemistry at Washington University in Saint Louis.

Supporting Online Material

www.sciencemag.org/cgi/content/full/317/5838/647/DC1
Materials and Methods
Figs. S1 to S4
Table S1
References

26 February 2007; accepted 20 June 2007
10.1126/science.1141768

Capillary Wrinkling of Floating Thin Polymer Films

Jiangshui Huang,[1,2] Megan Juszkiewicz,[2] Wim H. de Jeu,[2,3] Enrique Cerda,[4] Todd Emrick,[2] Narayanan Menon,[2]* Thomas P. Russell[2]*

A freely floating polymer film, tens of nanometers in thickness, wrinkles under the capillary force exerted by a drop of water placed on its surface. The wrinkling pattern is characterized by the number and length of the wrinkles. The dependence of the number of wrinkles on the elastic properties of the film and on the capillary force exerted by the drop confirms recent theoretical predictions on the selection of a pattern with a well-defined length scale in the wrinkling instability. We combined scaling relations that were developed for the length of the wrinkles with those for the number of wrinkles to construct a metrology for measuring the elasticity and thickness of ultrathin films that relies on no more than a dish of fluid and a low-magnification microscope. We validated this method on polymer films modified by plasticizer. The relaxation of the wrinkles affords a simple method to study the viscoelastic response of ultrathin films.

Thin sheets are much more easily bent than stretched by external forces. Even under purely planar tension, a sheet will often deform out of plane to form wrinkles. This is an everyday phenomenon that can be seen on our skin as it is stretched by smiling, scars, or age.

on the film of cream that floats on warm milk, or on the skin of fruit as it dries.

This familiar instability occurs because the elastic energy required to stretch a sheet is reduced by the out-of-plane bending that accompanies wrinkling. Cerda and Mahadevan (*1*, *2*) considered a situation in which a rectangular elastic sheet is clamped at its ends and stretched. Beyond a critical strain, the sheet wrinkles. Minimization of the total elastic energy leads to scaling relationships between the amplitude and wavelength of the wrinkles. Their arguments have been applied to a variety of contexts, including the mechanics of artificial skins (*3*, *4*) and surgical scars (*5*).

We report on a study of wrinkling of films under capillary forces, which has thus far remained relatively unexplored. Because thin films are often immersed in fluid environments, both in biological and in synthetic soft materials, the elastic deformation of films under surface tension is relatively commonplace. Thin polymer films form an ideal experimental setting in which to explore wrinkling phenomena: We study films with very high aspect ratios (the ratio of diameter D to thickness h is $D/h \sim 5 \times 10^4$), which can be treated accurately in the framework of two-dimensional elasticity.

We used films of polystyrene (PS; atactic, number-average molecular weight M_n = 91,000, weight-average molecular weight M_w = 95,500, radius of gyration $R_g \sim 10$ nm) spin-coated onto glass substrates. The film thickness h was varied from 31 to 233 nm, as measured by x-ray reflectivity with a precision of 0.5 nm (*6*, *7*). A circle of diameter D = 22.8 mm was scribed onto the film with a sharp edge. When the substrate was dipped into a petri dish of distilled, deionized water, a circular piece of the PS film detached from the substrate. Because PS is hydrophobic, the film floated to the surface of the water where it was stretched flat by the surface tension γ of the air-water interface at its perimeter.

Wrinkles were induced in the stretched, floating film by placing a drop of water in the center of the film (Fig. 1), by placing a solid disk in the center of the film (fig. S1A), or by poking the film with a sharp point (fig. S1B) to produce a fixed out-of-plane displacement. All these methods of loading lead to qualitatively similar wrinkling patterns, radiating from the center of the load. We emphasize a crucial difference between loading with a solid and a fluid: The wrinkling induced in Fig. 1 is primarily due not to the weight of the drop, but to the capillary force exerted on the film by the surface tension at the air-water-PS contact line. The radial stress σ_{rr} induced at the edge of the drop is dominated by the surface tension, which for the conditions of Fig. 1 is about 100 times as great as the radial stress developed due to the weight of the drop ($mg/2\pi a$), where m is the mass of the drop and a its radius. Indeed, a solid object of weight and contact area comparable to those of the drops shown in Fig. 1 would produce no discernible wrinkling. The contact angle of the drop on PS is 88° ± 2°, and thus the geometry of the drop on the film is approximately that of a hemisphere on a flat surface (with perhaps some deformation of the film close to the contact line itself). In view of this attractively simple geometry and the degree of experimental control afforded by loading with a fluid, we focus on wrinkling induced by fluid capillarity as in Fig. 1.

We observe the wrinkling pattern using a digital camera mounted on a low-magnification microscope (Fig. 1). Two obvious quantitative descriptors of the wrinkling patterns are the number of wrinkles N and the length of the wrinkle L as measured from the edge of the droplet. N is determined by counting. Because the terminus of the wrinkle is quite sharply defined and not sensitive to lighting and optical contrast, we are also able to measure L directly from the image. The radius of the circle in which the entire wrinkle pattern is inscribed (see top left of Fig. 1) is determined with a precision of 3%.

The central question in understanding this wrinkling pattern is, how are (N, L) determined by the elasticity of the sheet (thickness h, Young's modulus E, and Poisson ratio A) and the parameters of the loading (surface tension γ and radius of the drop a). To study systematically the effect of loading and elasticity, we placed water drops at the center of the film using a micropipette, increasing the mass of the drop in increments of 0.2 mg. As the radius of the drop was increased, both L and N increased.

We first focus on N, which is found to increase as $N \propto \sqrt{a}$. However, as is evident in Fig. 1, N is smaller in thicker films. The combined dependence of N on a and h is correctly captured by the scaling $N \sim a^{1/2}h^{-3/4}$, as shown in Fig. 2. To understand this scaling, the arguments of Cerda and Mahadevan (*2*) may be adapted to a radial geometry (*3*, *8*). Because the number of wrinkles remains constant at all radial distances r from the center of the pattern, the wavelength of wrinkles varies according to $\lambda = 2\pi r/N$.

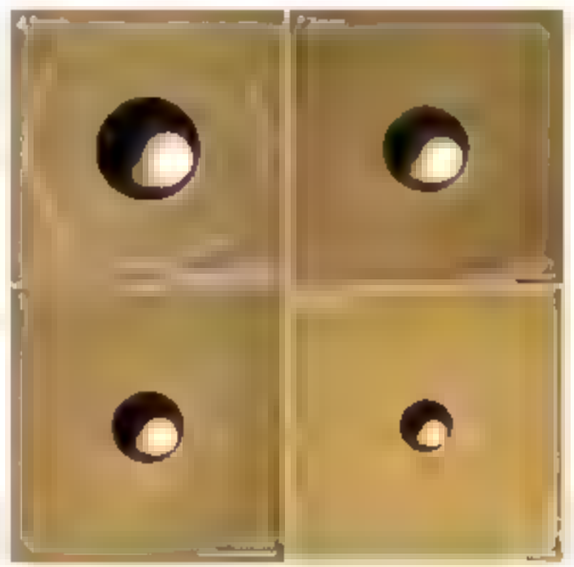

Fig. 1. Four PS films of diameter D = 22.8 mm and of varying thicknesses floating on the surface of water, each wrinkled by water drops of radius a = 0.5 mm and mass m = 0.2 mg. As the film is made thicker, the number of wrinkles N decreases (there are 111, 68, 49, and 31 wrinkles in these images), and the length of wrinkles L increases. L is defined as shown at top left, measured from the edge of the water droplet to the white circle. The scale varies between images, whereas the water droplets are approximately the same size.

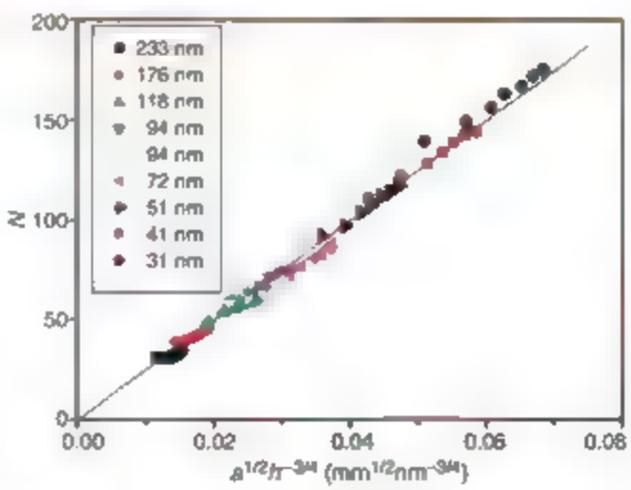

Fig. 2. The number of wrinkles N as a function of a scaling variable, $a^{1/2}h^{-3/4}$. Data for different film thicknesses h (indicated by symbols in the legend) collapse onto a single line (the solid line is a fit, $N = 2.50 \times 10^3 a^{1/2}h^{-3/4}$). The extent of reproducibility is indicated by the open and solid inverted triangles, which are taken for two films of the same nominal thickness.

[1]Department of Physics, University of Massachusetts, Amherst, MA 01003, USA. [2]Polymer Science and Engineering Department, University of Massachusetts, Amherst, MA 01003, USA. [3]FOM Institute for Atomic and Molecular Physics, Amsterdam, Netherlands. [4]Departamento de Física, Universidad de Santiago de Chile, Santiago, Chile.

*To whom correspondence should be addressed. E-mail: russell@pse.umail.umass.edu (T.P.R.); menon@physics.umass.edu (N.M.)

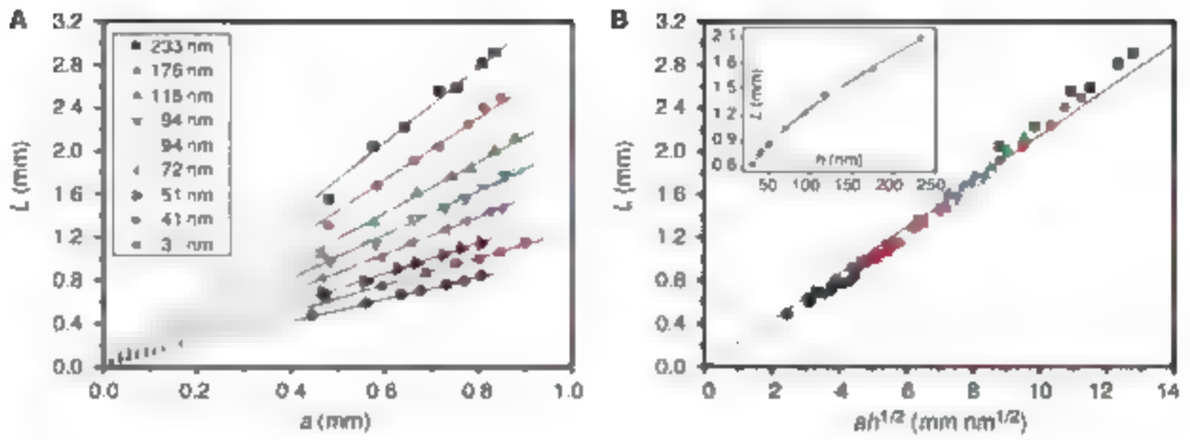

Fig. 3. (**A**) Wrinkle length L is proportional to the drop radius a. For fixed loading, L increases with thickness h, as shown by the different symbols. (**B**) An approximate data collapse is achieved by plotting L against the variable $ah^{1/2}$. The inset at the top left shows the relation between L and h for a fixed radius of the water droplet $a = 0.6$ mm. The black line is the best fit of the data to a power-law dependence: $L = 0.0872\ h^{0.58}$; the red line is the best fit to a square root: $L = 0.129\ h^{1/2}$

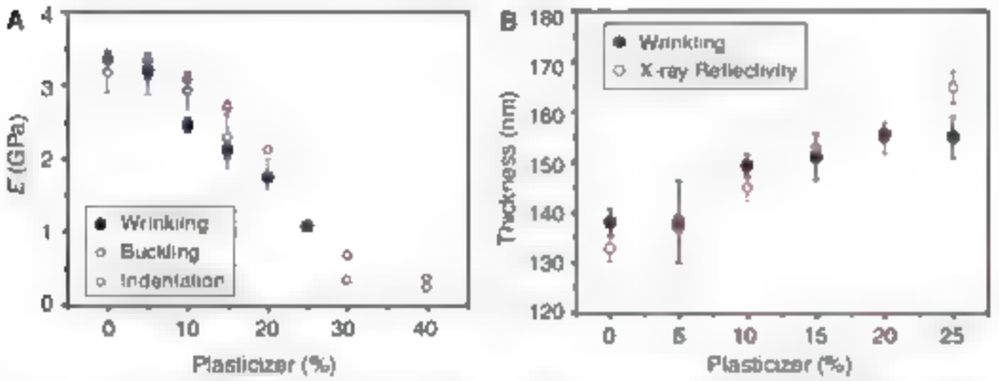

Fig. 4. (**A**) Young's modulus E versus concentration (by weight %) of plasticizer (dioctyl phthalate). E is computed from the wrinkling pattern (solid black symbols) by means of Eqs. 2 and 3. Data from other techniques (*12*) are shown for comparison. (**B**) Thickness h versus plasticizer concentration. h is computed from Eqs. 2 and 3; compare with data from x-ray reflectivity measurements (*7*). The error bars are the standard errors of the measurements.

This wavelength can be computed from a minimization of the bending transverse to the folds and the stretching along their length, which leads to

$$\lambda \sim B\,\sigma_a^{-1/4} r^{1/2} \qquad (1)$$

where the bending modulus $B = Eh^3/12(1-\nu^2)$ (*9*). For a circular film with a radial stress due to surface tension γ at the edge of the film and another surface tension γ at the boundary of the droplet, $\sigma_a \sim \gamma a^2/r^2$ (*10*). We thus obtain

$$\lambda \sim C_\lambda \left(\frac{12(1-\nu^2)\gamma}{E}\right)^{1/4} a^{1/2} h^{1/2} \qquad (2)$$

where C_λ is a numerical constant. C_λ may be obtained from an analytical solution of the elastic problem or from an experiment like ours where all relevant parameters are known. Using literature values of $E = 3.4$ GPa and $\nu = 0.33$ for PS (*11*), and $\gamma = 72 \pm 0.3$ mN m, we obtain $C_\lambda = 3.62$ from the slope of the fit line in Fig. 2.

Before discussing wrinkle length, we make some qualitative remarks regarding the evolution of the wrinkle pattern. The wrinkles shown in the images are purely elastic deformations and can be removed without the formation of irreversible, plastic creases (except possibly at the very center of the pattern). Despite this, the number of wrinkles in the pattern is hysteretic because there is an energy barrier as well as a global rearrangement involved in removing wrinkles. In Fig. 2, the drops are slowly increased in size by gentle addition of increments of water and thus represent our best experimental approximation to the equilibrium number of wrinkles. There is no measurable effect of contact line pinning. Nevertheless, the first droplet added invariably overshoots the equilibrium value of N, as may be seen in the slight curvature of individual sets of data in Fig. 2. The length of the ridge shows much less hysteresis because the length can locally increase or decrease continuously. This effect is clearly seen when the wrinkle pattern evolves as the drop is allowed to shrink by evaporation (fig. S2).

The length L of the wrinkle increased linearly with a, the radius of the drop, as shown in Fig. 3A. A simple argument for a linear increase was presented by Cerda (*5*), where the length of the wrinkle is dictated by the radial distance at which stress due to an out-of-plane force F applied at the center of a film decays to the value of the tension τ applied at the distant boundaries. Thus gives $L \sim a(F/a\tau)^{1/2}$. In our situation $F \sim 2\pi a\gamma$ and $\tau = \gamma$, thus yielding a linear dependence $L \sim a$. However, the data in Fig. 3A clearly show a dependence on thickness h, which is not captured by this argument. The dependence on a and h is reasonably well described by the purely empirical power-law scaling shown in Fig. 3B: $L \sim ah^{1/2}$ (as shown in the inset to the figure, an unconstrained fit to a power-law yields a slightly better fit of $L \sim ah^{0.58}$). This scaling is dimensionally incomplete and an additional factor of (length)$^{1/2}$ needs to be taken into account. In terms of the available physical variables, the only possibility is $(E/\gamma)^{1/2}$, leading to

$$L = C_L \left(\frac{E}{\gamma}\right)^{1/2} ah^{1/2} \qquad (3)$$

where C_L is a constant. From the fit shown in Fig. 3B, we obtain $C_L = 0.031$. E and h appear in Eq. 3 in the combination Eh, which is the stretching modulus of the sheet. This indicates that the length is defined purely by in-plane stresses. However, an attempt to write the radial stresses in a manner that is consistent with Eq. 3 yields an answer for $\sigma_a(a)$ that is independent of surface tension, which is implausible. Thus, the dependence of L on h and a is adequately constrained by the experimental data and is well described by Eq. 3 but does not yet have a definitive explanation.

A measurement of λ and L allows a determination of both E and h for a film, based on Eqs. 2 and 3. As a demonstration of this technique, we vary the elastic modulus of PS by adding to it varying amounts of di-octylphthalate, a plasticizer. As can be seen in Fig. 4A, we find good agreement with published data (*12*) obtained by other techniques. As a further test of our technique, we note that accompanying the large variation (greater than 300%) in Young's modulus, there is also a subtle change (of about 10%) in the thickness of the film as a function of the mass fraction, x, of plasticizer. The determination of thickness by means of Eqs. 2 and 3 yields a value that is in very close agreement

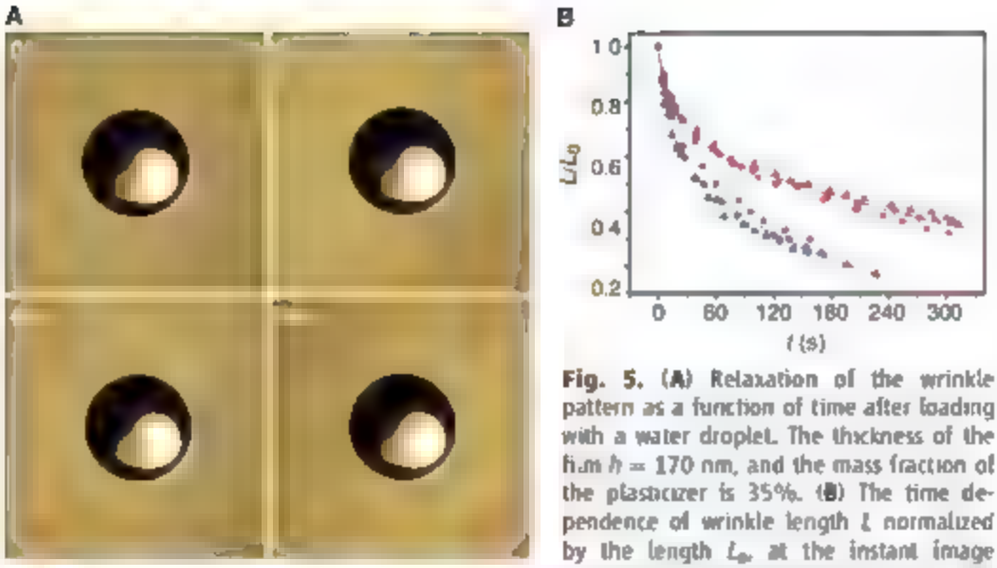

Fig. 5. (**A**) Relaxation of the wrinkle pattern as a function of time after loading with a water droplet. The thickness of the film h = 170 nm, and the mass fraction of the plasticizer is 35%. (**B**) The time dependence of wrinkle length L normalized by the length L_0 at the instant image capture commenced. Data are shown for plasticizer mass fractions of 35% (blue symbols) and 32% (red symbols). The plot symbols differentiate experimental runs, showing reproducibility of the time dependence. Solid lines show fits to a stretched exponential: $L(t)/L_0 = \exp[-(t/\tau)^{\beta}]$.

(Fig. 4B) with our x-ray reflectivity measurements of h. Thus, measurements of both modulus and thickness can be achieved by a wrinkling assay with comparable or higher precision, and with very basic instrumentation, when compared to the other techniques on display in Fig. 4, each of which involves sophisticated equipment and yields only one of E or h.

Further in contrast to the few other methods available for measuring the modulus of extremely thin films, such as nano-indentation (*13*) or stress-induced buckling (*12*), the measurement is performed with the film on a fluid surface, rather than mounted on a solid substrate. This allows the possibility for the film to relax internal mechanical stresses that can develop either in the spin-coating process or during transfer to a solid substrate. Apart from the ability to make measurements on a state that is not pre-stressed, this opens the possibility of measuring bulk relaxational properties of the film without concerns about pinning to a substrate. In Fig. 5A, we show a sequence of images visualizing the time-dependent relaxation of the wrinkle pattern formed by a capillary load. At increasing time, the wrinkles smoothly reduce in length and finally disappear. The strains that develop in response to the capillary load (*14*) can relax due to the viscoelastic response of the PS charged with a large mass fraction of plasticizer. In Fig. 5B, we show the time dependence of wrinkle length, $L(t)$, for two sets of films with different plasticizer mass fraction, x. $L(t)$ can be fit with a stretched exponential function $L_0 \exp[-(t/\tau)^{\beta}]$, where τ decreases with increasing plasticizer concentration, and $\beta \approx 0.50 \pm 0.02$, typical of polymer viscoelastic response near the glass transition (*13*, *15*).

Thus, capillary-driven wrinkle formation can be used as the basis for a metrology of both the elastic modulus and the thickness of ultrathin films by means of a very elementary apparatus—a low-magnification microscope and a dish of fluid. This simple technique can also be used to study dynamical relaxation phenomena in ultrathin films.

References and Notes

1. E. Cerda, K. Ravi-Chander, L. Mahadevan, *Nature* **419**, 579 (2002).
2. E. Cerda, L. Mahadevan, *Phys. Rev. Lett.* **90**, 074302 (2003).
3. K. Efimenko *et al.*, *Nat. Mater.* **4**, 293 (2005).
4. J. Genzer, J. Groenewold, *Soft Matter* **2**, 310 (2006).
5. E. Cerda *J. Biomech* **38**, 1568 (2005).
6. T. P. Russell, *Mat Sci Rep.* **5**, 171 (1990).
7. Supporting material is available on *Science* Online.
8. J.-C. Geminard, R. Bernal, F. Melo, *Eur. Phys. J. E* **15**, 117 (2004).
9. L. D. Landau, E. M. Lifshitz, *Theory of Elasticity, Course of Theoretical Physics* (Butterworth-Heinemann, India ed. 3, 1986), vol. 7.
10. S. Timoshenko, J. Goodier, *Theory of Elasticity* (McGraw-Hill, New York, ed. 3, 1987).
11. J. Brandrup, E. H. Immergut, *Polymer Handbook* (Wiley, New York, ed. 3, 1989).
12. C. M. Stafford *et al.*, *Nat. Mater.* **3**, 545 (2004).
13. K. Miyake, N. Satomi, S. Sasaki, *Appl. Phys. Lett.* **89**, 031925 (2006).
14. H. Bodiguel, C. Fretigny, *Eur. Phys. J. E* **19**, 185 (2006).
15. N. G. McCrum, B. E. Read, G. Williams, *Anelastic and Dielectric Effects in Polymeric Solids* (Wiley, London, 1967).

16. We acknowledge support from the Center for University of Massachusetts–Industry Cooperative Research Program (J.H.); the NSF–supported Materials Research Science and Engineering Center on Polymers at the University of Massachusetts (W.H.J.); the U.S. Department of Energy, Office of Basic Energy Science, through DE-FG-0296 ER45612 (T.P.R.); and the NSF through contracts NS -DMR 0606216 (N.M.) and NSI CBET 0609107 (T.S.E., T.P.R., and N.M.). We gratefully acknowledge useful conversations with A. D. Dinsmore.

Supporting Online Material

www.sciencemag.org/cgi/content/full/317/5838/650/DC1
Materials and Methods
Figs. S1 and S2

3 May 2007; accepted 15 June 2007
10.1126/science.1144616

The Source of Saturn's G Ring

Matthew M. Hedman,[1]* Joseph A. Burns,[1,2] Matthew S. Tiscareno,[1] Carolyn C. Porco,[3] Geraint H. Jones,[4,5] Elias Roussos,[4] Norbert Krupp,[4] Chris Paranicas,[4] Sascha Kempf[7]

The origin of Saturn's narrow G ring has been unclear. We show that it contains a bright arc located 167,495.6 ± 1.3 km from Saturn's center. This longitudinally localized material is trapped in a 7:6 corotation eccentricity resonance with the satellite Mimas. The cameras aboard the Cassini spacecraft mainly observe small (1 to 10 micrometers) dust grains in this region, but a sharp decrease in the flux of energetic electrons measured near this arc requires that it also contain larger (centimeter- to meter-sized) bodies whose total mass is equivalent to that of a ~100-meter-wide ice-rich moonlet. Collisions into these bodies may generate dust, which subsequently drifts outward to populate the rest of the G ring. Thus, the entire G ring could be derived from an arc of debris held in a resonance with Mimas.

The G ring is unique among Saturn's major rings in that, before the arrival of the Cassini spacecraft, there was no obvious explanation for its location. The dust-sized particles that dominate this ring's optical properties should erode quickly in Saturn's magnetosphere, yet there was no direct evidence for larger source bodies that could replenish the dust and no clear explanation for the concentration of such bodies in this one region (*1*–*5*). Unlike the E and F rings, which are closely associated with satellites that could either directly supply material to the ring (Enceladus) or potentially confine the ring particles into a narrow region (Prometheus and Pandora), the G ring is located 168,000 km from Saturn's center, over 15,000 km from the nearest known satellite. However, using data from the remote-sensing and in situ instruments onboard

[1]Department of Astronomy, Cornell University, Ithaca, NY 14853, USA. [2]Department of Theoretical and Applied Mechanics, Cornell University, Ithaca, NY 14853, USA. [3]Cassini Imaging Central Laboratory for Operations, Space Science Institute, Boulder, CO 94043, USA. [4]Max Planck Institut für Sonnensystemforschung, Katlenburg-Lindau 37191, Germany. [5]Mullard Space Science Laboratory, Department of Space and Climate Physics, University College London, Holmbury St. Mary, Dorking, Surrey RH5 6NT, UK. [6]Applied Physics Laboratory, Johns Hopkins University, Laurel, MD 20723, USA. [7]Max Planck Institut für Kernphysik, Saupfercheckweg 1, 69117 Heidelberg, Germany.

*To whom correspondence should be addressed. E-mail: mmhedman@astro.cornell.edu

the Cassini spacecraft, we have identified a structure that may be the source of this mysterious ring.

The Imaging Science Subsystem (ISS) onboard the Cassini spacecraft (*6*) obtained its most comprehensive view of the G ring on 19 September 2006, revealing a localized brightness enhancement near the ring's inner edge around 167,500 km from Saturn's center (Fig. 1). This feature extends over ~60° in longitude and has a radial full width at half maximum (FWHM) of 250 km, much less than the ~6000-km radial extent of the entire G ring (see Figs. 2, 3).

At least five other image sequences obtained during the first 2 years of the Cassini mission observed this arc (Fig. 3 and supporting online material (SOM)), demonstrating that it is a persistent feature of the ring. Based on these measurements, we estimate that the arc's mean orbital motion is 445.475° ± 0.007°/day (period 0.808126 ± 0.000013 day), where the uncertainty permits a 5° shift in the arc's position over 2 years. Given current measurements of Saturn's gravitational potential (*7*), this mean motion corresponds to an orbital semimajor axis a = 167,495.6 ± 1.3 km.

The arc's mean motion is extremely close to the Mimas 7:6 corotation eccentricity resonance (CER) at 445.484°/day (a = 167,493.4 km) (*8*). Corotation resonances have been invoked previously to explain arcs in Neptune's rings (*9*–*11*). In our case, perturbations from Mimas can constrain particles to librate around any of six stable longitudes λ where the resonant argument $\varphi_{CER} = 7\lambda_M - 6\lambda - \varpi_M$ equals 180° (λ_M and ϖ_M are the satellite Mimas' mean longitude and pericenter, respectively). An ensemble of such trapped particles could produce a longitudinally confined structure ~60° wide like the observed arc. Furthermore, throughout the first 3 years of the Cassini mission, the arc's peak has remained near one of the six stable points with $\Delta\varphi_{CER} < 4°$.

To verify this model, we conducted numerical simulations of 3830 massless test particles initially placed within 20 km of the Mimas 7:6 CER (see SOM). Most simulated particles (2820) were clearly trapped in the CER (with $\Delta\varphi_{CER}$ < 150°) over our 80-year integration. The dominant libration period was 1273 ± 3 days, significantly longer than the interval covered by the currently available observations. The marginally significant (0.009° ± 0.007°/day) drift in the arc's observed position relative to the stable points could therefore be part of a libration cycle. The mean epicyclic eccentricity of the simulated particles ranges from 0.0001 to 0.001 depending on $\Delta\varphi_{CER}$, consistent with the arc's ~250-km radial width (equivalent to an eccentricity ~ 0.0007).

Besides scattering light, the G ring and its arc also absorb magnetospheric particles, leaving detectable imprints on the local plasma environment. In fact, before Voyager took its first pictures of the G ring, Pioneer 11 detected subtle but persistent longitudinally averaged decreases (macrosignatures) in high-energy (>10 MeV) proton fluxes in this region (*12*). More recently, the Magnetospheric Imaging Instrument's Low Energy Magnetospheric Measurements System (LEMMS) onboard the Cassini spacecraft (which measures the flux of electrons with energies between 20 keV and 40 MeV) (*13*) has detected microsignatures (localized depletions in the electron flux) around the G ring. At ~12:13 universal time (UT) on 5 September 2005, this instrument observed an unprecedented ~50% decrease in electron flux while Cassini was moving outbound from Saturn (Fig. 2), and a candidate signature was detected inbound at ~11:58 UT. Two previous passages near the G ring did not show a strong absorption (see SOM).

Using the arc's orbital period determined above, Cassini's location relative to the arc can be plotted for all three passages near the G ring (Fig. 4). The 5 September 2005 passage was much closer to the arc than the others and, when mapped to the equatorial plane, the outbound microsignature's radial profile was 250 km wide, consistent with the arc's inferred density profile (Fig. 2). The absorption signature is most apparent in the LEMMS channels that measure mega electron volt electrons. Electrons with energies around 1 MeV near the G ring have net azimuthal speeds close to the Keplerian orbital rate, allowing for the formation of very deep absorption signatures. These data strongly suggest that material associated with the arc causes this deep absorption.

The inferred position of the outbound microsignature in Saturn's equatorial plane is displaced roughly 3000 km exterior to the arc (Fig. 2), but this is not too surprising because similar displacements are observed in the signatures of Saturn's small and mid-sized satellites (*14*, *15*). Depletions in charged particles will drift and fill in at different rates, depending on the electrons' energies and the pitch angles of the electrons' trajectories around the magnetic field lines, so the

Fig. 1. Images of the G ring arc obtained on 19 September 2006 at 12:37, 13:11, 13:44, and 14:18 UTC from top to bottom. A bright arc moves from right to left through the field of view.

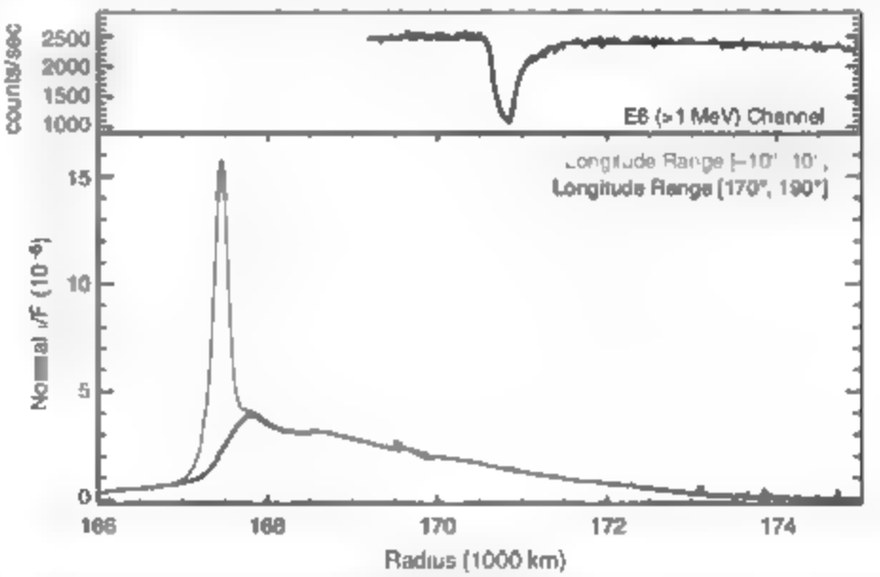

Fig. 2. (Top) The charged-particle flux detected by LEMMS channel E6 (*13*, *15*) during Cassini's passage over the arc region on 5 September 2005. The radial scale here corresponds to the equatorial distance of the unperturbed magnetic field lines that thread Cassini at the time of the observation. **(Bottom)** Average (offset-subtracted) radial brightness profiles of the G ring at different longitudes relative to the arc's peak based on data from 19 September 2006. The profiles through the arc (gray) and elsewhere (black) are essentially identical outside 168,000 km, whereas the arc is the sharp peak at 167,500 km in the gray profile. The absorption feature's radial width is comparable to the visible arc's. The 3000-km radial offset between the two signatures may be caused by magnetospheric effects (see SOM).

microsignature could be displaced by larger-scale magnetospheric processes or through a deformation of the local magnetic field by the arc itself.

For a given set of electron pitch angles (near 30° during this observation) and energies (which determine the electron's drift rate relative to the arc), and assuming absorbers composed primarily of water ice, the total arc mass can be estimated from the magnitude of the LEMMS absorption (*16*). For energies between 1 and 10 MeV the observed depletion implies a total mass between 10^3 and 10^{10} kg (see SOM). If all this material were gathered into a single body, that object would be roughly 100 m across. Because the gyroradii of 1-MeV electrons are on the order of a few kilometers here, the absorption signature's 250-km width indicates that this mass is not in a single body but is instead distributed among multiple objects.

The arc observed in imaging data has a peak normalized reflectance (or normal *I/F*, see SOM) that increases from 10^{-6} to 10^{-5} between phase angles of 90° and 165°. Such strong forward scattering implies that the cameras mostly see dust grains 1 to 10 μm across (*17*). The *I/F* values indicate that the normal optical depth in this dust is ~10^{-5}, implying that the entire arc contains between 10^5 and 10^6 kg of dust, which is much less than the absorbing mass required by the in situ data. The arc must therefore contain a population of larger particles ranging from centimeters to meters across. The size distribution of these larger objects is not strongly constrained, but if we assume for simplicity that the larger bodies in the arc are on average 1 m across, their total optical depth would only be around 10^{-7}, well below our current optical detection limit and comparable to previous estimates based on Voyager and Pioneer data (*1*). We propose that impact ejecta from these objects supply the dust that forms not only the visible arc but ultimately also the rest of the G ring.

The bulk of the visible G ring lies exterior to the arc, and the radial brightness profile of the outer part of the G ring decays exponentially with a scale length of approximately 3500 km (*18*) (fig. S2). Curiously, the Cosmic Dust Analyzer's (CDA) High Rate Detector (HRD) onboard the Cassini spacecraft (*19*) recorded an impact with an exceptionally large dust grain at 10:38:25 UT on 5 September 2005, when the spacecraft passed through the ring plane at 176,700 km, near the outermost edge of the visible G ring. Although the exact size of this grain is uncertain, it produced damage that was never observed in laboratory experiments with grains less than 100 μm across, so this grain was probably at least 100 μm in size. We can explain both of these phenomena with a simple model similar to one

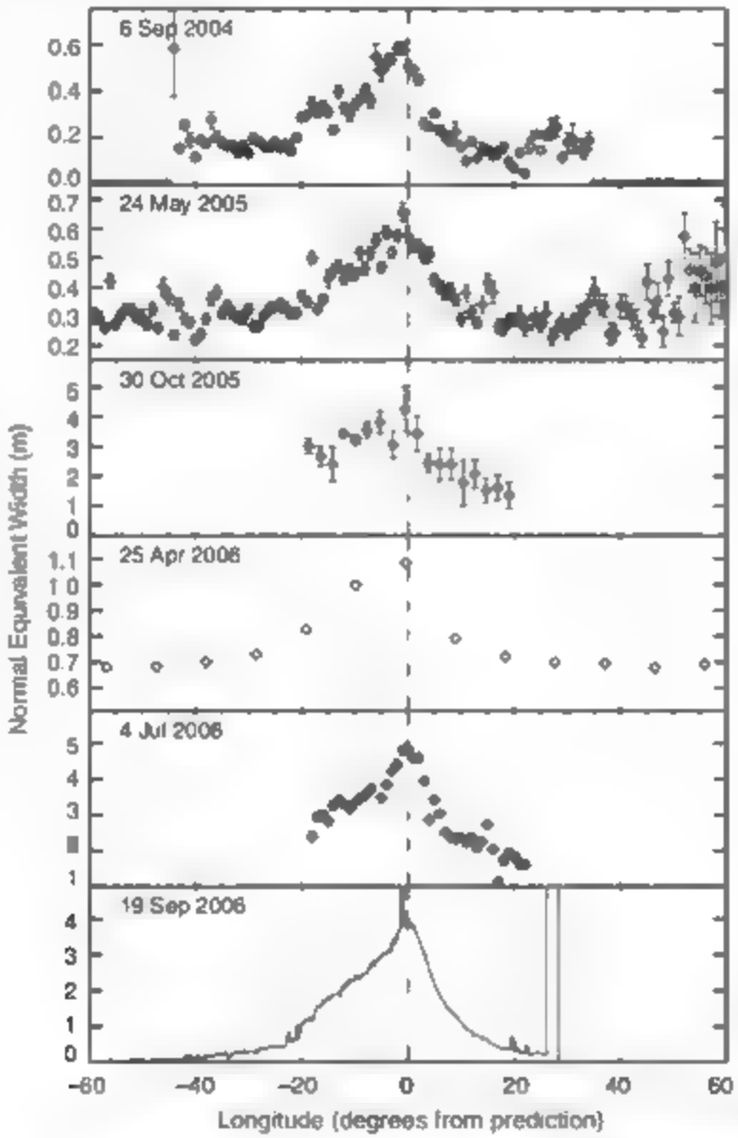

Fig. 3. Six profiles of the G-ring arc's radially integrated brightness (see SOM) versus longitude relative to a coordinate system rotating with a mean motion of 445.475°/day. Errors are based on random noise in the images. These errors are 0.02 and 0.1 m for the 25 April 2006 and 19 September 2006 data, respectively, and so are not plotted. The arc's longitudinal extent is <60°, as expected for a collection of particles trapped in a 7:6 resonance.

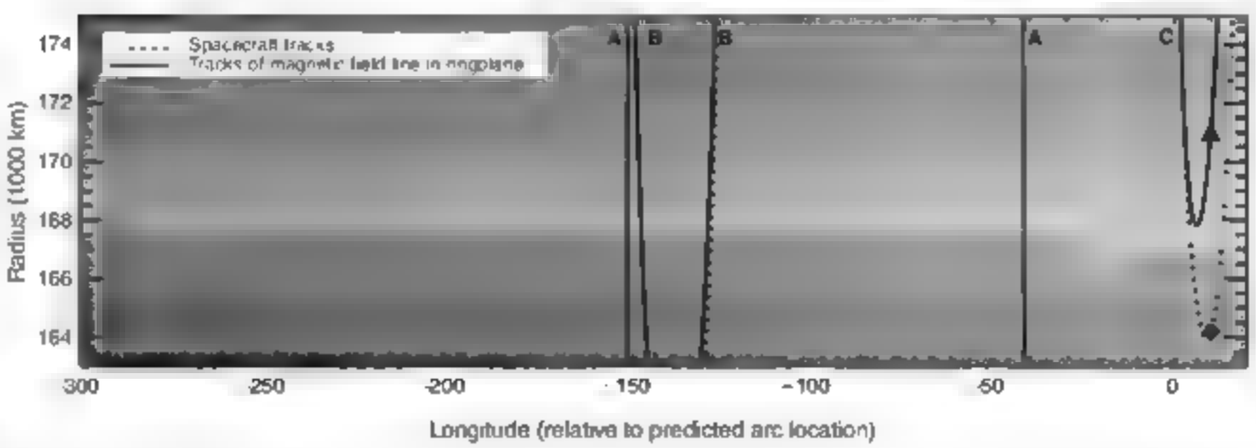

Fig. 4. Correlation between remote-sensing and in situ data. The background image shows the G ring's brightness as a function of radius and longitude measured relative to the arc's center (at 0°). The dotted lines trace Cassini's orbit during its three passages through this region (A = 1 July 2004, B = 14 April 2005, C = 5 September 2005). The solid lines show where an unperturbed magnetic field line threading through the spacecraft would intersect the ring plane during these times. The triangle and diamond mark the time of the strongest absorption detected by LEMMS on 5 September 2005 (Fig. 2).

previously proposed for other dusty rings (*17*, *20*), where small grains released from the arc drift outward under the influence of nongravitational drag forces (such as plasma drag) while they are steadily eroded by collisions with ions, atoms, and smaller grains.

Consider that the visible arc represents dust released from the surfaces of larger bodies by collisions. Although the source bodies are trapped in the Mimas resonance, interactions with Saturn's magnetosphere allow dust to escape this region (*17*). The magnetospheric plasma corotates with the planet's magnetic field (period ~ 0.45 days) (*21*), so its mean motion is much faster than the dust grains' Keplerian orbital motion. Momentum transfer from the plasma therefore causes the dust to drift outward over time. For a particle of mass m located at semimajor axis a and with an orbital velocity v, a drag force F_D will cause a motion $da/dt = a v(F_D/m)$. In general F_D is proportional to the particle's surface area whereas m is proportional to its volume, so $da/dt \propto 1/s$, where s is the dust grain's linear size.

As the dust grains drift outward, they will be steadily eroded by collisions with plasma ions, energetic particles, and other small grains. So long as the collisions do not completely shatter the drifting grain (*17*), the mass loss rate will be proportional to the impactor flux times the grain's cross-sectional area, so $ds/dt \propto s^2$ and $da/dt \propto s^0$. Thus, $ds/da \propto s$. Given that the G ring is narrow ($\delta a/a \sim 0.05$) and assuming that the drag forces and erosion rates do not vary significantly across this region, s should therefore decay exponentially with distance from the source region δa; that is, $s = s_0 e^{-\delta a/3D}$, where s_0 is the initial particle size, e is the base of natural logarithms, and $3D$ is a scale length determined by the orbital and magnetospheric environments.

The G ring's brightness and optical depth τ at a given δa are proportional to the integral of the particle cross section over the differential particle size distribution at that location [$\tau = \int \pi s^2 n(s,\delta a) ds$]. Assuming that the ring is in a steady state, continuity requires that the number flux of particles of a size s at a distance δa from the arc equal the flux of particles of size s_0 released from the arc, which requires that $n(s,\delta a) = n(s_0,0)$ (see SOM). Hence, τ scales like s^3 and the optical depth also decreases exponentially with radial distance from the arc source, but with a scale length of D instead of $3D$: $\tau = \tau_0 e^{-\delta a/D}$. This simple, generic model therefore produces a radial brightness profile with the same basic shape as that observed in the remote-sensing data. Furthermore, the shorter scale length in the optical depth means that although the brightness of the ring at 176,700 km is reduced by over an order of magnitude, individual particle sizes are reduced by only a factor of 2 or 3, so the grain detected by CDA could have been as small as about 200 μm across when it escaped the arc (if at all, still small enough to be subject to nongravitational accelerations).

References and Notes

1. M. R. Showalter, J. N. Cuzzi, *Icarus* **103**, 124 (1993).
2. R. Canup, L. W. Esposito, *Icarus* **126**, 28 (1997).
3. H. B. Throop, L. W. Esposito, *Icarus* **131**, 152 (1998).
4. J. J. Lissauer, R. G. French, *Icarus* **146**, 12 (2000).
5. I. dePater, S. C. Martin, M. R. Showalter, *Icarus* **172**, 446 (2004).
6. C. C. Porco *et al.*, *Space Sci. Rev.* **115**, 363 (2004).
7. R. A. Jacobson *et al.*, *Astron. J.* **132**, 2520 (2006).
8. Mimas' 7:6 inner Lindblad resonance also lies nearby at 445 411°/day (a = 167 513 km).
9. P. Goldreich, S. Tremaine, N. Borderies, *Astron. J.* **92**, 490 (1986).
10. C. C. Porco, *Science* **253**, 995 (1991).
11. F. Namouni, C. C. Porco, *Nature* **417**, 45 (2002).
12. J. A. van Allen, *J. Geophys. Res.* **88**, 6911 (1983).
13. S. M. Krimigis *et al.*, *Space Sci. Rev.* **114**, 233 (2004).
14. G. H. Jones *et al.*, *Science* **311**, 1412 (2006).
15. E. Roussos *et al.*, *Icarus*, in press.
16. J. N. Cuzzi, J. A. Burns, *Icarus* **74**, 284 (1988).
17. J. A. Burns, D. P. Hamilton, M. R. Showalter, in *Interplanetary Dust*, E. Grün, B. Gustafson, S. Dermott, H. Fechtig, Eds. (Springer, New York, 2001), pp. 641–725.
18. Slight deviations from an exponential profile occur around 168 200 and 169 800 km. The latter feature shows longitudinal structure and is probably associated with the Mimas 8:7 inner Lindblad resonance.
19. R. Srama *et al.*, *Space Sci. Rev.* **114**, 465 (2004).
20. J. A. Burns, M. R. Showalter, G. E. Morfill, in *Planetary Rings*, R. Greenberg, A. Brahic, Eds. (Univ. of Arizona Press, Tucson, AZ, 1984), pp. 200–272.
21. D. Gurnett *et al.*, *Science* **316**, 442 (2007).

22. We thank the staff at the Space Science Institute, Jet Propulsion Laboratory, and Cornell University for planning and delivering the imaging data, and M. Kusterer of the Johns Hopkins University Applied Physics Laboratory (JHUAPL) for UVIS data reduction. We also acknowledge the support of the Cassini Project and NASA's Planetary Geology & Geophysics program. MJM/UVIS was in part financed by the German Bundesministerium für Bildung und Forschung through the German Aerospace Center (DLR) under contract 50 OH 0103 and by the Max Planck Gesellschaft. The work at JHUAPL was supported by NASA under contract NAS5-97271 with the Johns Hopkins University. G.H.J. was partially supported by the Science and Technology Facilities Council, UK.

18 April 2007; accepted 14 June 2007
10.1126/science.1143964

The FERONIA Receptor-like Kinase Mediates Male-Female Interactions During Pollen Tube Reception

Juan-Miguel Escobar-Restrepo,[1] Norbert Huck,[1] Sharon Kessler,[1] Valeria Gagliardini,[1] Jacqueline Gheyselinck,[1] Wei-Cai Yang,[2] Ueli Grossniklaus[1]*

In flowering plants, signaling between the male pollen tube and the synergid cells of the female gametophyte is required for fertilization. In the *Arabidopsis thaliana* mutant *feronia* (*fer*), fertilization is impaired: the pollen tube fails to arrest and thus continues to grow inside the female gametophyte. *FER* encodes a synergid expressed, plasma membrane–localized receptor-like kinase. We found that the FER protein accumulates asymmetrically in the synergid membrane at the filiform apparatus. Interspecific crosses using pollen from *Arabidopsis lyrata* and *Cardamine flexuosa* on *A. thaliana* stigmas resulted in a *fer*-like phenotype that correlates with sequence divergence in the extracellular domain of FER. Our findings show that the female control of pollen tube reception is based on a *FER*-dependent signaling pathway, which may play a role in reproductive isolation barriers.

In contrast to animals, where the products of meiosis differentiate directly into gametes, the meiotic products of higher plants undergo further mitotic divisions to form multicellular haploid structures called gametophytes, which in turn produce the gametes. To accomplish fertilization, the gametophytes communicate with and recognize each other. In angiosperms, the male gametophyte (pollen) germinates on the stigma and the growing pollen tube delivers the two nonmotile sperm cells to the female gametophyte (embryo sac). Proper delivery depends on signals from the female gametophyte (*1*, *2*). These chemotactic signals guide the pollen tube into the micropylar opening of the ovule, the reproductive structure that harbors the female gametophyte. In the majority of flowering plants, including *Arabidopsis thaliana* (Brassicaceae), the female gametophyte consists of seven cells: the egg cell, the two synergids (which lie just inside the micropylar opening of the ovule), the central cell, and the three antipodals (*3*) (Fig. 1A). In *Torenia fournieri* (Scrophulariaceae), the two synergids are necessary for pollen tube guidance (*4*). In most species, one of the synergids degenerates prior to or coincident with the pollen tube approaching the micropyle (*5*). The pollen tube grows into the degenerating synergid through the filiform apparatus, a structure formed by invaginations of the cell wall of

[1]Institute of Plant Biology and Zürich-Basel Plant Science Center, University of Zurich, Zollikerstrasse 107, CH-8008 Zürich, Switzerland. [2]Key Laboratory of Molecular and Developmental Biology, Institute of Genetics and Developmental Biology, Chinese Academy of Sciences, Beijing 100101, China.

*To whom correspondence should be addressed. E-mail: grossnik@botinst.uzh.ch

both synergids (*6*). Pollen tube reception in the ovule involves the arrest of pollen tube growth (Fig. 1B), the rupture of the pollen tube, and the release of the sperm cells, which are subsequently targeted to the egg and central cells for fertilization (*7*). Once the pollen tube has ruptured, attraction of further pollen tubes ceases; thus, only a single pollen tube will normally enter each micropyle.

Recent work in *A. thaliana* has shown that pollen tube reception is controlled by female gametophytic factors (*8*, *9*). In heterozygous *feronia* (*fer*) and *sirene* (*sir*) mutants, all female gametophytes develop normally but half of the ovules remain unfertilized. In these ovules, the pollen tube continues to grow inside the female gametophyte, fails to arrest its growth, and does not rupture to release the sperm cells (Fig. 1C). Pollen from these mutants, however, can fertilize wild-type ovules, indicating that pollen tube growth and sperm delivery are unaffected (*8*, *9*). Detailed cytological and ultrastructural analyses have shown that the synergids are normally specified and differentiated (*8*), which suggests that these mutants identify components of an active signaling process in which female gametophytic factors control pollen tube behavior and hence fertilization. Only a small number of factors involved in pollen germination, pollen tube growth, and guidance are known at the molecular level (*10*–*15*). The molecular events underlying the female control of pollen tube reception are unknown. Here, we show that *FER* encodes a kinase-active receptor-like kinase, which is localized to the plasma membrane and, in particular, is asymmetrically localized to the filiform apparatus of the synergid cells. Interspecific crosses indicate that the interaction of the FER receptor-like kinase with a putative ligand on the pollen tube may be involved in reproductive isolation barriers.

To gain insight into the molecular bases of the signaling event underlying pollen tube reception, we molecularly cloned *FER* with the use of positional methods (*16*). We mapped the mutation to At3g51550, which in the *fer* mutant contains a 4 base pair (bp) insertion corresponding to the footprint left after excision of a *Ds* transposon (Fig. 1D). Because *sir* shows the same phenotype, we sequenced the coding region of At3g51550 in the mutant and found a single base pair deletion (Fig. 1E). Both mutations lead to frameshifts that result in premature stop codons; therefore, *FER* and *SIR* are identical.

A genomic fragment carrying At3g51550 plus 2.6 kb and 1.2 kb of upstream and downstream sequences, respectively, complements the *fer* phenotype (table S1), demonstrating that At3g51550 corresponds to the *FER* gene (fig. S1, A and B). The *FER* open reading frame contains a single 175-bp intron in the 5′ untranslated region and produces a transcript of 2682 bp, which encodes a putative receptor-like serine-threonine kinase (RLK) (Fig. 1F).

FER, which is a unique gene in *A. thaliana*, belongs to the CrRLK1L-1 subfamily of kinases, no members of which have a known function (Fig. 2A) (*17*). Plant RLKs belong to a monophyletic gene family with more than 600 members (*18*). RLKs are transmembrane proteins that receive signals through an extracellular domain and subsequently activate signaling cascades via their intracellular kinase domain, a molecular function consistent with the role of *FER* in a signaling process.

To determine the activity of the predicted intracellular kinase domain, we tested whether FER autophosphorylates in an in vitro kinase assay. The predicted intracellular domain (FERwt) and a kinase-inactive version (FERKR) were fused to glutathione *S*-transferase (GST). GST and GST-FERKR exhibited no kinase activity, whereas GST-FERwt was autophosphorylated (Fig. 2B). In addition, experimentally verified phosphorylation sites were present in the *FER* kinase domain (*19*) (Fig. 1F). Taken together, these findings show that *FER* encodes a kinase-active RLK involved in a novel signaling pathway that plays a critical role in the last stages of the communication between female and male gametophytes required for fertilization.

To evaluate whether the expression of *FER* is consistent with its proposed role in pollen tube

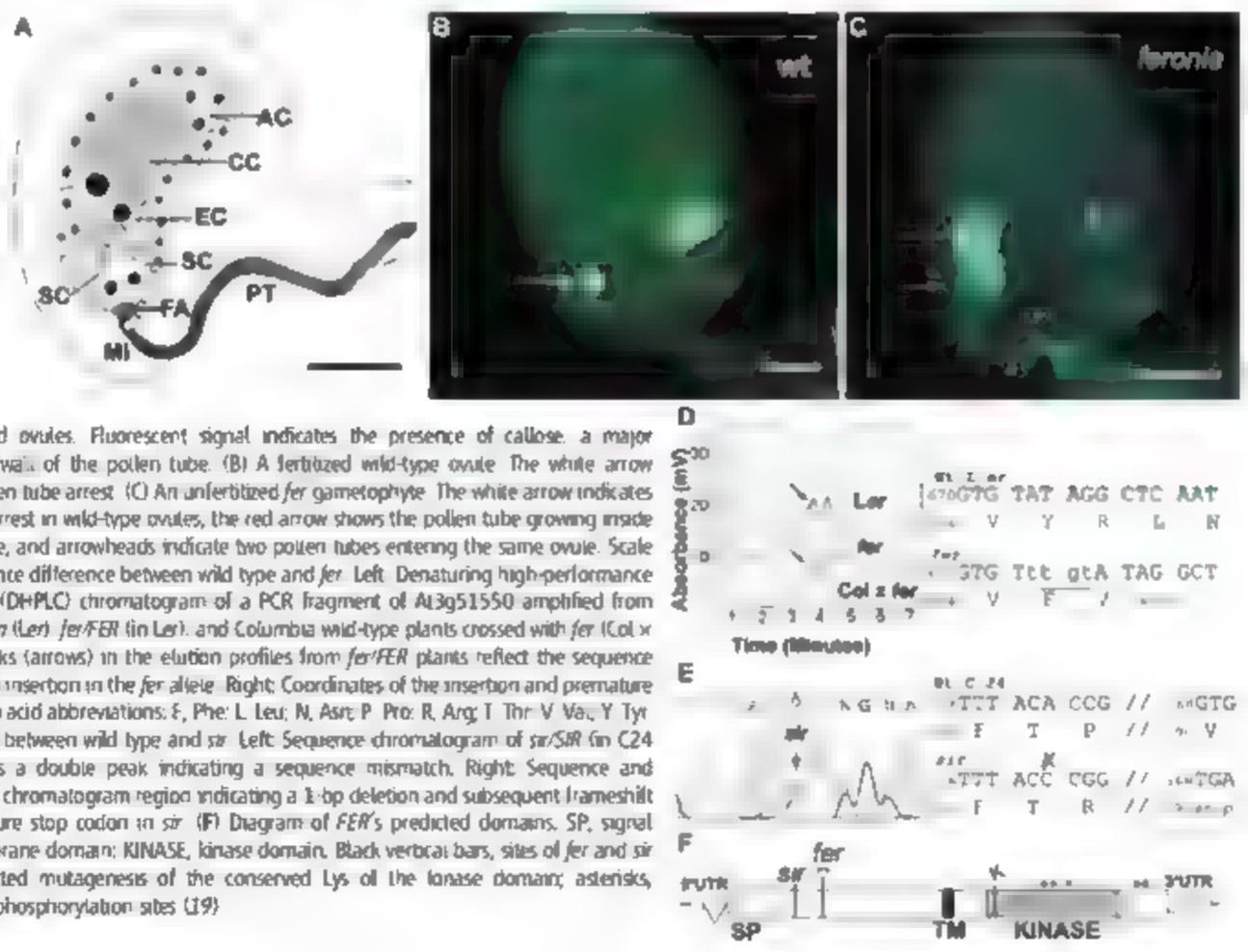

Fig. 1. Pollen tube reception is mediated by the FERONIA RLK. (**A**) Diagram of a mature female gametophyte. Abbreviations: AC, antipodal cells; CC, central cell; EC, egg cell; SC, synergid cells; FA, filiform apparatus; MI, micropyle; PT, pollen tube. Scale bar, 30 μm. (**B** and **C**) Epifluorescence micrographs of Aniline Blue–stained ovules. Fluorescent signal indicates the presence of callose, a major component of the cell wall of the pollen tube. (B) A fertilized wild-type ovule. The white arrow indicates the site of pollen tube arrest. (C) An unfertilized *fer* gametophyte. The white arrow indicates the site of pollen tube arrest in wild-type ovules, the red arrow shows the pollen tube growing inside the female gametophyte, and arrowheads indicate two pollen tubes entering the same ovule. Scale bars, 30 μm. (**D**) Sequence difference between wild type and *fer*. Left: Denaturing high-performance liquid chromatography (DHPLC) chromatogram of a PCR fragment of At3g51550 amplified from DNA of Landsberg *erecta* (Ler) *fer*/*FER* (in Ler), and Columbia wild-type plants crossed with *fer* (Col × *fer*). The additional peaks (arrows) in the elution profiles from *fer*/*FER* plants reflect the sequence difference due to a 4-bp insertion in the *fer* allele. Right: Coordinates of the insertion and premature stop codon in *fer*. Amino acid abbreviations: F, Phe; L, Leu; N, Asn; P, Pro; R, Arg; T, Thr; V, Val; Y, Tyr. (**E**) Sequence difference between wild type and *sir*. Left: Sequence chromatogram of *sir*/*SIR* (in C24 accession); arrow shows a double peak indicating a sequence mismatch. Right: Sequence and coordinates of the same chromatogram region indicating a 1-bp deletion and subsequent frameshift that leads to a premature stop codon in *sir*. (**F**) Diagram of *FER*'s predicted domains. SP, signal peptide; TM, transmembrane domain; KINASE, kinase domain. Black vertical bars, sites of *fer* and *sir* mutations; K, site-directed mutagenesis of the conserved Lys of the kinase domain; asterisks, experimentally located phosphorylation sites (*19*).

reception, we examined the temporal and spatial expression pattern of *FER*. Quantitative real-time reverse transcription polymerase chain reaction (RT-PCR) revealed *FER* mRNA throughout the mature plant—specifically in leaves, buds, flowers, and siliques—but it was not detected in mature pollen (Fig. 2C). By in situ hybridization, *FER* transcripts were detected in floral apices, young ovule primordia, and young anthers with immature pollen (Fig. 3, A to C). In older anthers harboring mature pollen, *FER* transcript was not detected (Fig. 3D), consistent with the quantitative real-time RT-PCR experiments and the female-specific role of *FER* in fertilization. In emasculated flowers, a very weak *FER* signal was detected throughout mature unfertilized ovules, and a stronger signal could be detected in the synergid cells (Fig. 3E). After fertilization, *FER* transcripts were detected in globular embryos (Fig. 3G), consistent with the finding that in rare cases where fertilization of *fer* gametophytes is achieved, the resulting homozygous embryos abort (*8*). In our complementation experiments, both the defect in pollen tube reception and embryo lethality were rescued by a wild-type *FER* transgene, demonstrating that *FER* is also required after fertilization (table S1). A genomic fragment containing the putative *FER* promoter (1.3 kb upstream of the start codon) was fused to the bacterial *uidA* gene encoding β-glucuronidase (GUS) to confirm the weak expression of *FER* observed in mature female gametophytes. Using a chromogenic substrate for GUS, we found that the *FER* promoter is highly active in the synergid cells (Fig. 3, I and J). Thus, the spatiotemporal expression pattern of *FER* is consistent with a function in pollen tube reception.

To investigate the subcellular localization of FER, we bombarded onion epidermal cells with a *FER-GFP* construct driven by the *FER* promoter (*pFER::FER-GFP*). The FER-GFP (green fluorescent protein) fusion protein was localized to the plasma membrane (Fig. 4, A and B), in contrast to GFP driven by the constitutive 35S promoter (*35S::GFP*), which is detected throughout the cell (Fig. 4, C and E). The *pFER::FER-GFP* construct was also stably transformed into *A. thaliana* and fully complemented the *fer* mutation (table S1), and the fusion protein was localized at the plasma membrane in leaf epidermal cells (Fig. 4D). Unfertilized ovules accumulated high levels of GFP signal in the lower part of the synergids (Fig. 4F) where the filiform apparatus is located. Weaker GFP fluorescence was detected in the membranes of the synergid cells and in the surrounding maternal sporophytic cells, as well as faintly in the egg cell (Fig. 4G). Because the filiform apparatus is a structure rich in plasma membrane, we tested whether the asymmetric distribution of FER might simply be due to an enrichment of plasma membrane in the area. Therefore, we compared

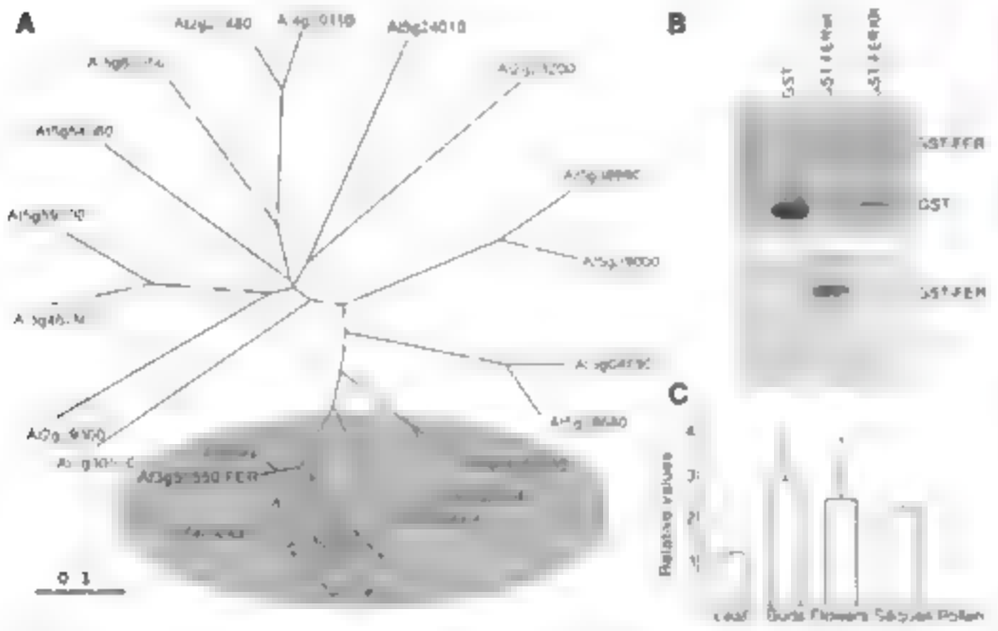

Fig. 2. FERONIA, a plant-specific widely expressed RLK, phosphorylates itself. (**A**) Unrooted tree showing *FER* and homologs from different species. The *FER* homologs, whose clade is supported by a 100% bootstrap value, are in the shaded area. The other plant species together with *A. thaliana* in this clade are *A. lyrata*, *B. oleracea*, *B. rapa*, and *C. flexuosa* homologs 1, 2, 3, and 4 (Brassicaceae); *Oryza sativa* (Os., Poaceae), and *Populus trichocarpa* (Salicaceae). The rest of the tree contains the *A. thaliana* members of the CrRLK1L-1 subfamily of kinases. The branch length scale bar represents 0.1 substitutions per site. (**B**) FER autophosphorylates during in vitro kinase assays. Top: Coomassie-stained gel of proteins used in the kinase assays. Bottom: Phosphorimager scan of gel in top panel. GST and GST-FERKR (FER Lys^{563} → Arg in Ler FER Lys^{565} → Arg in Col-0) have no kinase activity, whereas GST-FERwt is autophosphorylated. (**C**) Quantification of *FER* transcripts in leaves, closed flower buds, open flowers, and siliques (collected 1 to 4 days after hand pollination) and mature pollen grains. Transcript levels were normalized to 18S ribosomal RNA; means and SEs of three independent experiments are shown.

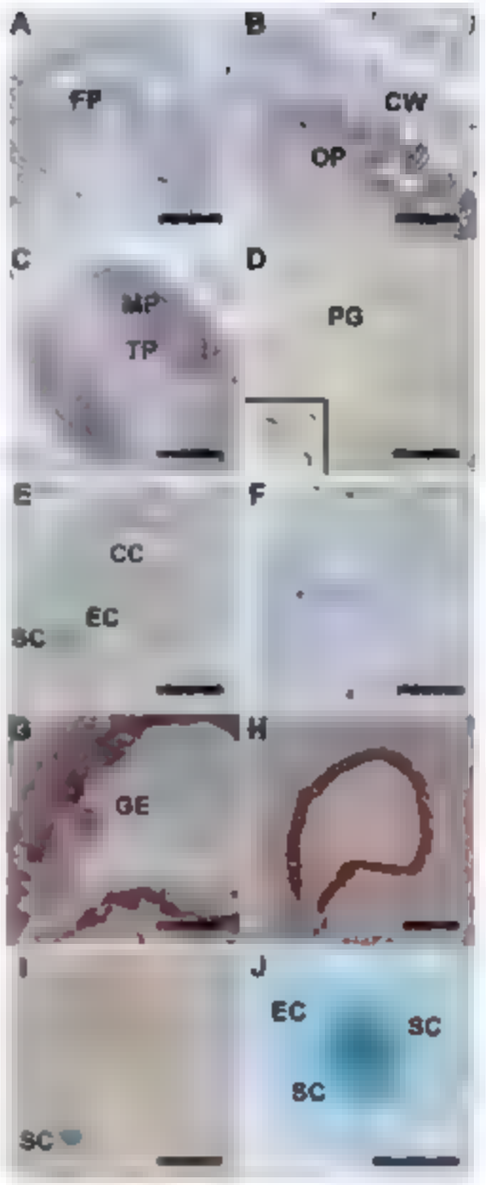

Fig. 3. *FERONIA* is expressed in developing primordia and synergid cells. (**A** to **H**) In situ hybridization with an antisense *FER* probe [(A) to (E), (G)] or with a sense probe [(F) and (H)]. *FER* mRNA is present in the floral apex (A) and in ovule primordia (B). *FER* mRNA is expressed in anthers and microspores during early pollen development (C), but the transcript levels in mature pollen (D) are below the limit of detection (inset shows the sense control). (E) *FER* transcript can be detected in the synergid cells of the female gametophyte. (F) Sense control in the female gametophyte. (G) After fertilization, *FER* mRNA was detected in globular embryos. (H) Sense control in a fertilized ovule with a globular embryo. (I and J) Analysis of the *FER* upstream transcriptional regulatory region. (I) *pFER::GUS* is active in both synergid cells. (J) Higher magnification of the synergids from another ovule. Scale bars, 100 μm (A), 30 μm [(B), (E), (F), (I), (J)], 15 μm (C), 70 μm (D), and 50 μm [(G) and (H)]. Abbreviations: FP, floral apex; OP, ovule primordia; CW, carpel wall; MP, microspore cells; TP, tapetum cells; PG, pollen grain; CC, central cell; EC, egg cell; SC, synergid cell; GE, globular-stage embryo.

the distribution of FER to that of another GFP fusion construct that has a plasma membrane localization motif and is expressed in the female gametophyte (*pAtD123::EGFP-AtROP6C*). Under the same conditions, FER-GFP levels were much higher in the filiform apparatus than in the rest of the synergids' cell membranes when compared to EGFP-AtROP6C (Fig. 4E). This finding suggests that FER is polarly transported to the filiform apparatus. Taken together, the data are consistent with a model in which FER, localized in the filiform apparatus, binds a putative ligand on the approaching male gametophyte, which then triggers the molecular events involved in pollen tube reception.

Because a signal transduction cascade initiated by the interaction of the FER RLK with a putative pollen ligand seems necessary for fertilization, it is possible that changes in the components of this interaction could act as reproductive isolation barriers. To some extent, the interaction between the pollen tube and the synergid is similar to sperm-egg interactions in animals (*20*), but it occurs at the level of gametophytes rather than gametes. For example, divergence in the protein sequence of the putative ligand-binding extracellular domain of FER or changes in the pollen ligand could prevent interspecific fertilization events. Interestingly, in interspecific crosses of *Rosidopsida* species, pollen tube growth does not arrest. This results in pollen tube overgrowth in the female gametophyte, similar to the phenotype observed in *fer* (*21*, *22*). If our model is correct, an interspecific cross where wild-type *A. thaliana* is pollinated by a related Brassicaceae species with a sufficiently divergent ligand might also produce a *fer*-like phenotype. Therefore, we performed interspecific crosses between *A. thaliana* and different Brassicaceae species. In most crosses, the pollen germinated but failed to grow toward the ovules, as reported previously (*23*, *26*). In crosses with the close relative *Arabidopsis lyrata*, pollen tubes were correctly targeted to the ovule but only 43.9% of the embryo sacs received pollen tubes and were fertilized; 5.2% of the ovules were fertilized with more than one pollen tube in the same micropyle, showing pollen tube overgrowth inside the female gametophyte (fig. S1C), and 50.9% of the ovules had pollen tubes that continued to grow inside the female gametophyte as was observed in *fer* mutants (fig. S1D) ($n = 813$ ovules). In crosses with a more distant relative *Cardamine flexuosa*, only 7.7% of *A. thaliana* ovules attracted pollen tubes, of these, 1.6% had pollen tubes that entered the micropyle and stopped as previously reported (*27*), 0.8% had pollen tubes coiling outside the micropyle, and in 5.3% of the ovules the pollen tubes entered the micropyles but reception failed, resulting in a *fer*-like phenotype ($n = 363$ ovules) (fig. 4J). In summary, around 50% and 70% of the *A. lyrata* and *C. flexuosa* pollen tubes that entered a wild-type *A. thaliana* embryo sac, respectively, displayed a *fer*-like phenotype.

Given the involvement of the *FER* signal transduction cascade in the interaction between the pollen tube and the receptive synergid, it is likely that *FER* plays a role in the failed pollen tube reception in these interspecific crosses. In the *A. thaliana* × *A. lyrata* crosses, about half of the pollen tube reception events were normal, demonstrating the capacity of the *A. lyrata* pollen tube for a normal reception response. However, in the same cross, *fer*-like phenotypes were observed. This suggests two possible reasons for failed receptions: (i) They are caused by a divergent ligand that is inefficiently recognized by the receptor domain of the *A. thaliana* FER RLK, or (ii) they result from the presence of two polymorphic forms of the putative ligand, one that is and one that is not recognized by the *A. thaliana* FER RLK. In the case of *C. flexuosa*, the ligand or ligands are predicted to have diverged to a degree that they cannot be recognized by the *A. thaliana* FER RLK, thereby causing the *fer*-like phenotype in *A. thaliana* ovules. We expect that a divergence in the sequence of the putative ligand would also be reflected in sequence divergence in FER's extracellular domain, which is proposed to interact with this ligand.

To test this hypothesis, we isolated *FER* homologs in these species and calculated the ratio between the number of nonsynonymous substitutions per nonsynonymous site (K_a) and the number of synonymous substitutions per synonymous site (K_s) (*28*) as an indication of their divergence in pairwise comparisons between *A. thaliana* and *A. lyrata* (one *FER* homolog) or *C. flexuosa* (four *FER* homologs) (fig. 4K and fig. S1D). In all comparisons, higher K_a/K_s values occurred in the putative

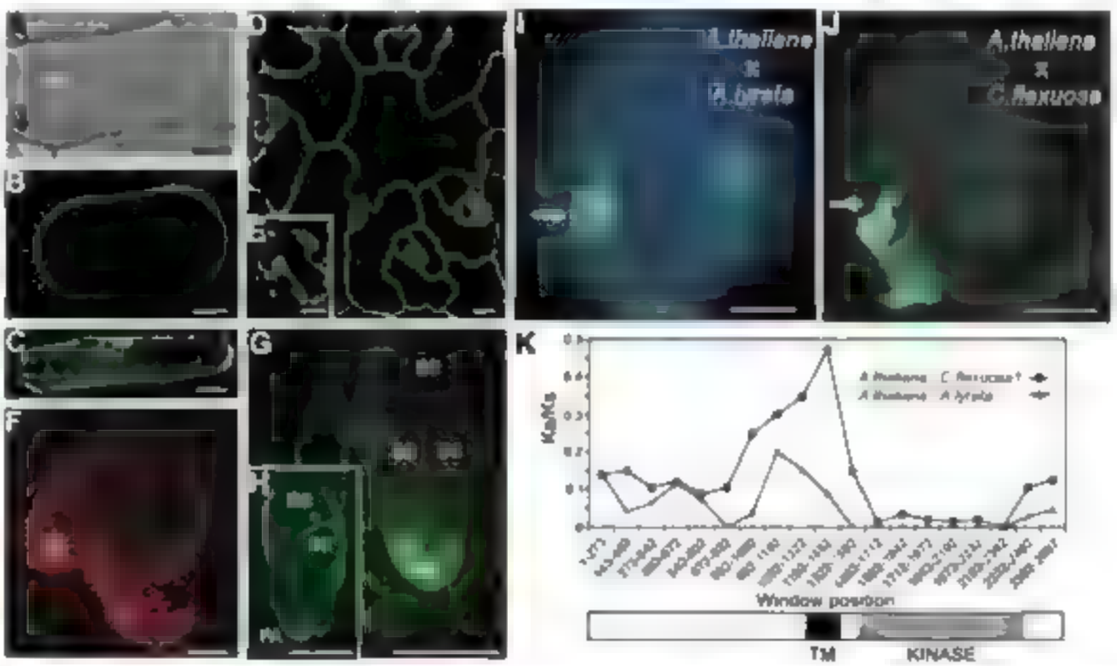

Fig. 4. FERONIA is a cell membrane–localized RLK targeted to the filiform apparatus, and sequence divergence in its extracellular domain correlates with *feronia*-like phenotypes in interspecific crosses. (**A**) Transmission image of a plasmolyzed onion epidermal cell transiently expressing FER-GFP under *FER* promoter (*pFER::FER-GFP*). Black arrow points to cell wall; white arrow points to cell membrane. (**B**) Confocal laser scanning microscopy (CLSM) single optical section of (A) with FER-GFP localized at the periphery of the cell membrane. (**C**) Epifluorescence micrograph of an onion cell transiently expressing (*35S::GFP*). (**D**) CLSM single optical section of leaf epidermis of an *A. thaliana* plant stably transformed with *pFER::FER-GFP*. (**E**) *A. thaliana* leaf epidermal cell transiently expressing (*35S::GFP*). (**F**) Ovule from the same plant as in (D) under CLSM; GFP signal in green, chlorophyll autofluorescence in red. (**G**) Maximum projection of several sections of the micropyle area of ovule in (F) showing FER-GFP accumulation in the filiform apparatus of the synergids. (**H**) Maximum projection of several sections of *pAtD123::EGFP-AtROP6C* female gametophyte. Upper arrow indicates upper part of synergids; lower arrow indicates region of filiform apparatus. (**I**) Gametophyte of a wild-type *A. thaliana* plant pollinated with pollen from *A. lyrata*, showing pollen tube overgrowth (white arrow). (**J**) Gametophyte of a wild-type *A. thaliana* plant pollinated with pollen from *C. flexuosa*, showing pollen tube overgrowth (white arrow). (**K**) K_a/K_s ratios calculated using a sliding window analysis with windows of 86 codons and a step size of 43 codons of the coding region of *FER* (excluding the signal peptide) in *A. thaliana*, *A. lyrata*, and *C. flexuosa* homolog 1. The least divergent homolog of *C. flexuosa* is shown. Scale bars, 30 μm [(A), (B), (F), (I), (J)], 60 μm (C), 10 μm [(D) and (E)], 20 μm [(G) and (H)]. SC, synergid cell; FA, filiform apparatus; EC, egg cell.

ligand-binding extracellular region, which indicates that this domain shows the greatest degree of amino acid diversification and evolves faster than the highly conserved intracellular kinase domain (*29*). The high sequence divergence in the extracellular domain of FER may contribute to reproductive isolation between two species, as has been proposed for other genes involved in recognition at fertilization (*30*).

Our data suggest that FER acts in the filiform apparatus to control the behavior of the pollen tube to achieve fertilization. We propose that the interaction between the putative male ligand and the extracellular domain of the FER RLK triggers a signal transduction cascade inside the synergid cell. A subsequent signal then feeds back from the synergid to the pollen tube, causing growth arrest and the release of the sperm cells. Conceptually, this process is similar to the signaling events occurring during the self-incompatibility reaction in *Brassica* spp. (*31*). In an incompatible pollination, a pollen ligand interacts with a stigma-expressed RLK, inducing a signaling cascade in female papillar cells, which then signal back to the pollen and inhibit its germination. Further studies of the *FER* signaling pathway will help to uncover the molecular mechanism of fertilization and reproductive isolation in plants. Furthermore, the manipulation of the *FER* pathway might allow the generation of hybrids between otherwise incompatible species.

References and Notes

1. M. Hülskamp, K. Schneitz, R. E. Pruitt, *Plant Cell* **7**, 57 (1995).
2. S. M. Ray, S. S. Park, A. Ray, *Development* **124**, 2489 (1997).
3. U. Grossniklaus, K. Schneitz, *Semin. Cell Dev. Biol.* **9**, 227 (1998).
4. T. Higashiyama *et al.*, *Science* **293**, 1480 (2001).
5. R. N. Kapil, A. K. Bhatnagar, *Phytomorphology* **25**, 334 (1975).
6. B. Q. Huang, S. D. Russell, *Int. Rev. Cytol.* **140**, 233 (1992).
7. S. D. Russell, *Int. Rev. Cytol.* **140**, 357 (1992).
8. M. Huck, J. M. Moore, M. Federer, U. Grossniklaus, *Development* **130**, 2149 (2003).
9. M. Rotman *et al.*, *Curr. Biol.* **13**, 432 (2003).
10. C. R. Schopfer, M. E. Nasrallah, J. B. Nasrallah, *Science* **286**, 1697 (1999).
11. M. Nishina *et al.*, *J. Biol. Chem.* **278**, 36389 (2003).
12. S. Kim *et al.*, *Proc. Natl. Acad. Sci. U.S.A.* **100**, 16125 (2003).
13. M. L. Márton, S. Cordts, J. Broadhvest, T. Dresselhaus, *Science* **307**, 573 (2005).
14. W. Tang, D. Kelley, I. Ezcurra, R. Cotter, S. McCormick, *Plant J.* **39**, 343 (2004).
15. K. von Besser, A. C. Frank, M. A. Johnson, D. Preuss, *Development* **133**, 4761 (2006).
16. See supporting material on *Science* Online.
17. S. H. Shiu, A. B. Bleecker, *Plant Physiol.* **132**, 530 (2003).
18. S. H. Shiu, A. B. Bleecker, *Proc. Natl. Acad. Sci. U.S.A.* **98**, 10763 (2001).
19. T. S. Nühse, A. Stensballe, O. N. Jensen, S. C. Peck, *Plant Cell* **16**, 2394 (2004).
20. P. Primakoff, D. G. Myles, *Science* **296**, 2183 (2002).
21. V. Kaul, J. L. Rouse, E. G. Williams, *Can. J. Bot.* **64**, 282 (1986).
22. E. G. Williams, V. Kaul, J. L. Rouse, B. F. Palser, *Aust. J. Bot.* **34**, 413 (1986).
23. S. J. Hiscock, H. G. Dickinson, *Theor. Appl. Genet.* **86**, 744 (1993).
24. M. K. Kandasamy, J. B. Nasrallah, M. E. Nasrallah, *Development* **120**, 3405 (1994).
25. M. Hülskamp, S. D. Kopczak, T. F. Horejsi, B. K. Kihl, R. E. Pruitt, *Plant J.* **8**, 703 (1995).
26. K. K. Shimizu, K. Okada, *Development* **127**, 4511 (2000).
27. K. K. Shimizu, *Popul. Ecol.* **44**, 221 (2002).
28. M. Nei, T. Gojobori, *Mol. Biol. Evol.* **3**, 418 (1986).
29. S. H. Shiu *et al.*, *Plant Cell* **16**, 1220 (2004).
30. W. J. Swanson, V. D. Vacquier, *Nat. Rev. Genet.* **3**, 137 (2002).
31. A. Kachroo, M. E. Nasrallah, J. B. Nasrallah, *Plant Cell* **14**, S227 (2002).

32. Supported by the University of Zürich, grants from the Swiss National Science Foundation (U.G.) and the National Science Foundation of China (W.-C.Y.), and a Human Frontier Science Program fellowship (S.K.). We thank C. Baroux and P. Barrell for help with confocal analyses, D. Weigel and J.-E. Faure for seeds, M. Curtis, R. Blanvillain, and P. Gallois for plasmids, P. Kopf for technical assistance; and M. A. Collinge and S. E. Schauer for discussions and comments on the manuscript. GenBank accession numbers for *FER* homologs are as follows: *B. oleracea*, EF681131; *A. lyrata*, EF681133; *A. thaliana* Ler, EF681137; *C. flexuosa* 1, EF681134; *C. flexuosa* 2, EF681135; *C. flexuosa* 3, EF681136; *C. flexuosa* 4, EF681132.

Supporting Online Material

www.sciencemag.org/cgi/content/full/317/5838/656/DC1
Materials and Methods
Fig. S1
Table S1
References

9 April 2007; accepted 14 June 2007
10.1126/science.1143562

Quantitative Mass Spectrometry Identifies Insulin Signaling Targets in *C. elegans*

Meng-Qiu Dong,[1] John D. Venable,[1] Nora Au,[2,3] Tao Xu,[1] Sung Kyu Park,[1] Daniel Cociorva,[1] Jeffrey R. Johnson,[1] Andrew Dillin,[2] John R. Yates III[1]*

DAF-2, an insulin receptor–like protein, regulates metabolism, development, and aging in *Caenorhabditis elegans*. In a quantitative proteomic study, we identified 86 proteins that were more or less abundant in long-lived *daf-2* mutant worms than in wild-type worms. Genetic studies on a subset of these proteins indicated that they act in one or more processes regulated by DAF-2, including entry into the dauer developmental stage and aging. In particular, we discovered a compensatory mechanism activated in response to reduced DAF-2 signaling, which involves the protein phosphatase calcineurin.

The insulin signaling pathway and insulin-like growth factor 1 (IGF-1) signaling pathway are conserved from invertebrates to mammals (*1*, *2*). DAF-2, the sole homolog of the insulin receptor or IGF-1 receptor in *C. elegans*, controls the expression of presumably a large number of downstream targets by negatively regulating DAF-16, a FoxO transcription factor (*3*–*8*). In this study, we integrated technological advancements in quantitative mass spectrometry (MS) (*9*–*11*), including labeling multicellular organisms with the ^{15}N stable isotope, to identify DAF-2 signaling targets. We made direct measurements of proteins as opposed to mRNAs, which are not final gene products. Our method allows for the identification of targets not regulated at the transcription level. The MS techniques demonstrated in this study can be readily used to determine protein abundance changes as a result of genetic or pharmacological perturbations.

We prepared lysates from wild-type (WT), *daf-16(mu86)* null, or *daf-2(e1370ts)* worms in their first day of adulthood, a period important for regulation of longevity by DAF-2 signaling (*8*). These lysate samples were mixed at a 1:1 ratio with a reference sample in which all proteins were labeled with ^{15}N (atomic enrichment of $^{15}N \geq 96\%$) [(*12*) and fig. S1]. This reference sample was a lysate of WT worms fed with bacteria that were grown in a medium enriched in ^{15}N. Soluble proteins (S100 fraction) from the lysate mixtures were then digested and analyzed by MS. A total of 1685 proteins were identified. Using its ^{15}N-labeled counterpart as a reference, we determined the relative abundance of each unlabeled (i.e., ^{14}N-labeled) protein with a modified version of the RelEx software (*10*). We also assessed the relative abundance of individual proteins by spectral counting (SC), in which we counted how many times the unlabeled version of a protein was identified by the fragmentation spectra of its peptides. Spectral counts correlate with protein abundance (*11*). We detected little difference between the *daf-16* and WT samples (fig. S2A), reflecting the fact that *daf-16* and WT adult worms were phenotypically similar under our experimental conditions (*3*, *4*, *6*–*8*). In contrast, we observed many protein abundance changes in the *daf-2* mutants as compared with those in WT worms (fig. S2B), with an obvious correlation (i) between the RelEx and SC measurements ($r = 0.59$) and (ii) between the

[1]Scripps Research Institute, La Jolla, CA 92037, USA. [2]Salk Institute for Biological Studies, La Jolla, CA 92037, USA. [3]University of California at San Diego, La Jolla, CA 92093, USA.

*To whom correspondence should be addressed. E-mail: jyates@scripps.edu

two *daf-2* samples ($r = 0.83$, fig. S3). Using stringent criteria that emphasize high-quality measurements and consistent changes (table S1), we identified 86 proteins that were differentially expressed in the S100 fraction of the *daf-2* sample (tables S2 and S3). Of these proteins, 47 were more abundant and 39 were less abundant than those in the WT sample. A subset of these proteins corresponds to known DAF-16 target genes, including superoxide dismutase *sod-3* (*7*, *13*).

To assess the quality of the quantitative MS results, we used selected reaction monitoring (SRM) to validate a subset of these results. For SRM, we measured the intensity of a specific fragment ion from a specific precursor ion (*12*). SRM is suitable for monitoring selected peptides at multiple time points. We reasoned that if a protein is truly regulated in *daf-2* mutants, then the difference in its abundance between the WT and the *daf-2* mutant animals should increase gradually during the temperature shift from 15°C (permissive for *e1370*) to 20°C (semi-permissive) and 25°C (nonpermissive). This was indeed the case with the three proteins that we monitored (Fig. 1, A to C). Western blotting results also correlated directly with MS results for nine proteins tested (Fig. 1, D to L, and fig. S4). Thus, the SRM and Western blotting results confirmed the accuracy of the quantitative proteomic results.

Other researchers have previously identified DAF-16 target genes that barely overlapped between studies (*13*, *16*). To help clarify this issue, we compared results (tables S2 and S3) and found that ours matched best with a microarray analysis by Murphy *et al.* (*13*). In total, only 35 proteins identified in this study were identified in previous studies (tables S2 and S3). The remaining 51 proteins may be previously unrecognized targets of the DAF-2 signaling pathway.

To understand the protein abundance changes in the context of protein function, we adopted GoMiner software (*17*) to classify the differentially expressed proteins on the basis of their annotation in the gene ontology database (table S2). Proteins whose abundance decreases in *daf-2* mutant animals were enriched for functions in translation elongation and lipid transport. In contrast, proteins that became more abundant in *daf-2* mutant animals were enriched for functions in amino acid biosynthesis, oxygen and reactive oxygen species metabolism, and carbohydrate metabolism [including gluconeogenesis and the glyoxylate cycle (GC), a modified version of the tricarboxylic acid cycle].

To determine whether the signaling targets identified in this study function in DAF-2–dependent processes such as dauer formation, we used RNA interference (RNAi) to analyze a subset of these targets (Fig. 2A). We found that *npa-1* RNAi suppressed dauer formation in *daf-2* mutants as strongly as did *daf-16* RNAi. *npa-1* encodes a polyprotein precursor for multiple fatty acid binding and retinol-binding proteins (www.wormbase.org). This result suggests that NPA-1, which has increased abundance in the *daf-2* mutant (tables S2 and S3), plays a critical role in dauer formation. Several genes functioning in carbohydrate metabolism also seem to be important for *daf-2* dauer formation (Fig. 2A).

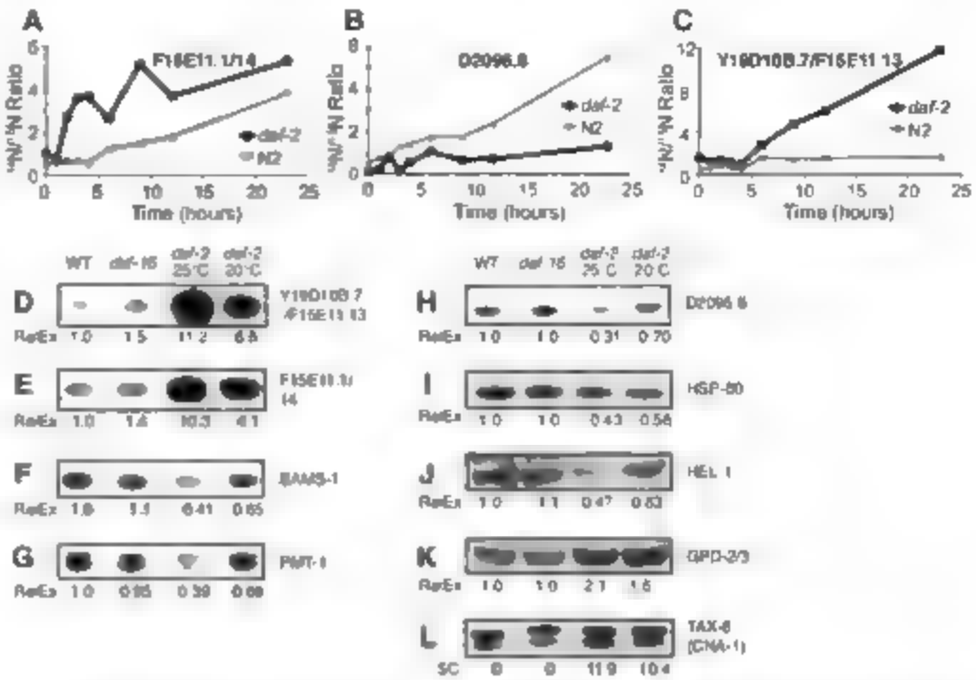

Fig. 1. Confirmation of quantitative proteomic results by SRM and Western blotting. (**A** to **C**) SRM quantitation of the abundance of F15E11.1/14, D2096.8, and Y19D10B.7/F15E11.13 in WT (N2) and *daf-2* mutant animals after a temperature shift from 15° to 20°C for 3 hours and then to 25°C for 20 hours. Samples were collected (at times indicated), lysed, and mixed at a 1:1 ratio with a ^{15}N-labeled standard derived from WT worms. The S100 fractions were analyzed. (**D** to **L**) The amounts of nine proteins in the S100 fraction of WT, *daf-16(mu86)*, or *daf-2(e1370ts)* worms were visualized by Western blotting. Shown below the blot of each protein is the relative abundance of that protein normalized to the WT amount as determined by RelEx with the use of a ^{15}N-labeled standard [(D) to (K)] or by normalized SC (L).

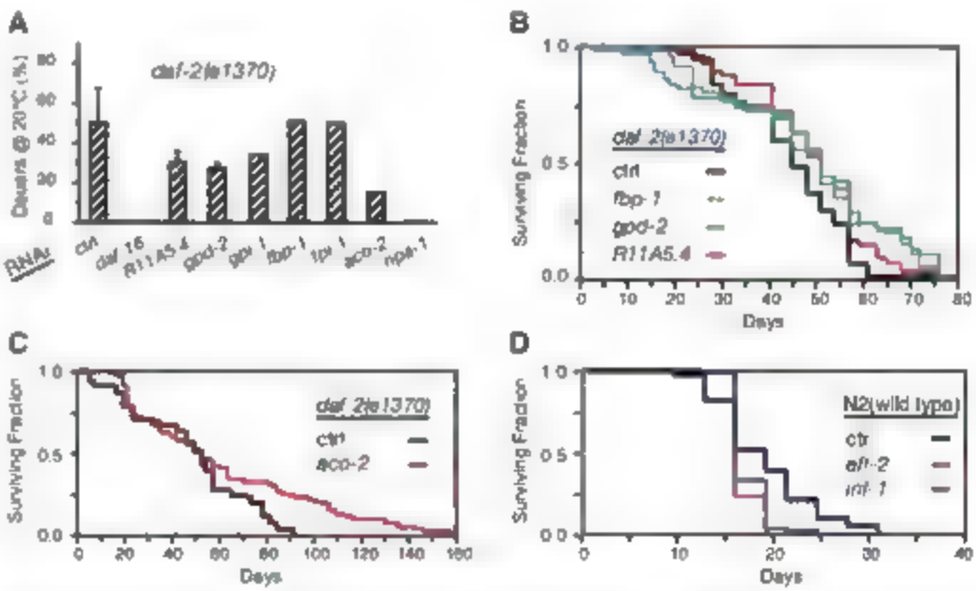

Fig. 2. Function of a subset of the identified DAF-2 signaling targets in life-span regulation, dauer formation, or both. (**A**) Suppression of dauer formation of *daf-2(e1370ts)* animals by RNAi of *npa-1* and several genes involved in carbohydrate metabolism. Percentages of dauers were averaged from four (for Ctrl, *daf-16*, *R11A5.4* and *gpd-2* RNAi) or two (for RNAi of the remaining genes) independent experiments ($n > 110$ animals in each experiment). Error bars indicate SE. Ctrl, control. (**B** and **C**) Effects of *fbp-1*, *gpd-2*, *R11A5.4*, and *aco-2* RNAi on the life span of *daf-2(e1370)* mutant animals (one experiment, $n \geq 39$ animals). (**D**) Effects of RNAi of *inf-1*, a translation initiation factor, and *eft-2*, an elongation factor, on the life span of WT worms (one experiment, $n \geq 80$ animals). All P values are less than 0.05 (log-rank tests) between sample and control.

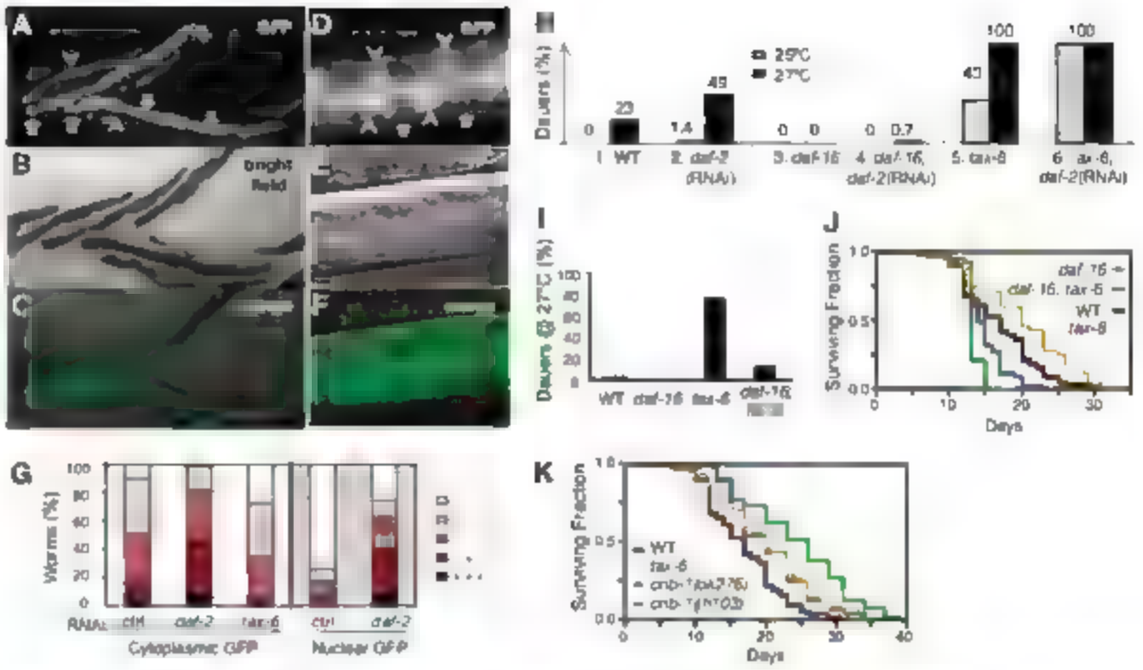

Fig. 3. Identification of TAX-6 as a target and a positive regulator of DAF-2 signaling. (**A** to **F**) TAX-6::GFP was expressed in neurons (open arrows) and in the cytoplasm (solid arrows) and nucleus (arrowheads) of intestinal cells. *tax-6(p675); Ex[pAK13]* animals were imaged at magnifications 100× [(A) to (C)] and 400× [(D) to (F)]. DIC, differential interference contrast. (**G**) Expression of TAX-6::GFP in the intestine of animals treated with control, *daf-2*, or *tax-6* RNAi. The intensity of cytoplasmic and nuclear TAX-6::GFP in the intestine was scored separately. Percentages of worms expressing strong (+++), intermediate (++), weak (+), very weak (+/−), or background (−) TAX-6::GFP in the intestine were averaged from three experiments ($n \geq 39$ animals in each experiment). (**H**) Effects of the *tax-6(p675)* mutation on dauer formation and a synthetic effect with *daf-2* RNAi. WT ("1" and "2"), *daf-16 (mu86)* ("3" and "4"), and *tax-6(p675)* ("5" and "6") animals were treated with *daf-2* ("2," "4," and "6") or control RNAi ("1," "3," and "5") at 27°C (black, one experiment) or 25°C (gray, average of two experiments) ($n > 120$ animals in each experiment). (**I**) *daf-16(mu86)* suppressed *tax-6(p675)* dauer formation (average of two experiments, $n > 300$ animals per experiment). (**J**) *daf-16(mu86)* suppressed the long life span of *tax-6(p675)* mutant animals (one experiment, $n \geq 80$ animals, $P < 0.01$, log-rank test). (**K**) *cnb-1* mutants displayed an extended life span (one experiment, $n \geq 80$ animals, $P < 0.01$, log-rank test).

Given the importance of insulin signaling and IGF-1 signaling in aging, we asked whether these targets play a role in life-span regulation and we focused on a subset of proteins involved in gluconeogenesis, GK, or translation. RNAi of some of the genes that we tested showed no significant effect on life span (table S4). However, RNAi of *R11.A5.4* (phosphoenolpyruvate carboxykinase), *fbp-1* (fructose bisphosphatase), *gpd-2* (glyceraldehyde 3-phosphate dehydrogenase), and *acn-2* (aconitase) further extended the life span of *daf-2* mutants ($P < 0.05$, log-rank test) (Fig. 2, B and C) and so did RNAi of *pgi-1* (glucose phosphate isomerase) (*18*). RNAi of *eft-2* (an elongation factor) or *inf-1* (an initiation factor) shortened the life span of WT worms ($P < 0.05$, log-rank test) (Fig. 2D). Because R11A5.4, FBP-1, GPD-2, ACO-2, and GPI-1 showed increased abundance in the *daf-2* mutant, whereas EFT-2 and INF-1 showed decreased abundance (table S2), these results suggest that abundance changes of proteins involved in carbohydrate metabolism or translation do not necessarily contribute to the longevity of *daf-2* mutants. Instead, such changes may reflect a compensatory mechanism or mechanisms activated by a reduction in DAF-2 signaling.

Another protein exemplifying a compensatory mechanism is TAX-6 or CNA-1, the *C. elegans* calcineurin A protein that is the catalytic subunit of a serine or threonine protein phosphatase. The activity of calcineurin A requires the regulatory subunit calcineurin B (CNB-1 in *C. elegans*) (*19*). TAX-6 and CNB-1 are expressed in multiple cell types (*20*, *21*) including intestinal epithelial cells (Fig. 3, A to F), a site of action for DAF-16 (*22*). Neither *tax-6* nor *cnb-1* has been implicated in the DAF-2 signaling pathway. Both genes lack the DAF-16 binding element (*13*) in a 1.5-kb region upstream of the start codon.

Our MS result indicated a higher TAX-6 abundance in *daf-2* mutant worms as compared to WT worms (table S2). This was verified by Western blotting (Fig. 1L) and by comparing the green fluorescent protein (GFP) signal in animals expressing a TAX-6::GFP fusion protein (Fig. 3G) (*20*). When these worms were treated with *daf-2* RNAi, cytoplasmic as well as nuclear TAX-6::GFP increased in intestinal cells.

Both *tax-6* and *cnb-1* loss-of-function mutants displayed phenotypes that were similar to but weaker than those of *daf-2* mutants, such as an extended life span and increased propensity to entering the dauer phase (Fig. 3, H to K, fig. S5, and table S4). *tax-6(p675)* acted synergistically with *daf-2(RNAi)* (Fig. 3H), and *daf-16(mu86)* partially suppressed *tax-6(p675)* (Fig. 3, I and J). Thus, the TAX-6 and CNB-1 complex (i) facilitates DAF-2 signaling in life-span regulation and dauer formation and (ii) acts in parallel to DAF-16 or acts both upstream of and in parallel to DAF-16. Further epistasis analysis suggested that *tax-6* acts upstream of or in parallel to *age-1*, which encodes a phosphatidylinositol 3-kinase downstream of *daf-2* (see supporting online material text).

Although TAX-6 facilitates DAF-2 signaling, TAX-6 itself is regulated by DAF-2 because reduced DAF-2 signaling results in increased abundance of TAX-6. Thus, TAX-6 is part of a feedback loop that acts to maintain DAF-2 signaling at normal levels. This again suggests a compensatory mechanism. We propose that the life span of *daf-2* mutants results from two types of changes: One change extends life span (e.g., SOD-3) and the other, represented by the compensatory mechanism(s) involving TAX-6 and several proteins functioning in carbohydrate metabolism or translation, shortens life span. Thus, ablation of the compensatory mechanism can further extend the life span of *daf-2* mutants (e.g., by *acn-2* RNAi). Further investigation of the compensatory mechanism and DAF-2 signaling targets identified here is likely to aid the research of diabetes and aging in mammals.

References and Notes

1. A. R. Saltiel, C. R. Kahn, *Nature* **414**, 799 (2001).
2. M. F. White, *Am. J. Physiol. Endocrinol. Metab.* **283**, E413 (2002).
3. C. Kenyon, J. Chang, E. Gensch, A. Rudner, R. Tabtiang, *Nature* **366**, 461 (1993).
4. K. D. Kimura, H. A. Tissenbaum, Y. Liu, G. Ruvkun, *Science* **277**, 942 (1997).
5. S. Ogg *et al.*, *Nature* **389**, 994 (1997).
6. D. Gems *et al.*, *Genetics* **150**, 129 (1998).
7. Y. Honda, S. Honda, *FASEB J.* **13**, 1385 (1999).
8. A. Dillin, D. K. Crawford, C. Kenyon, *Science* **298**, 830 (2002).
9. J. Kruglyak *et al.*, *Nat. Biotechnol.* **21**, 927 (2003).
10. J. D. Venable, M. Q. Dong, J. Wohlschlegel, A. Dillin, J. R. Yates III, *Nat. Methods* **1**, 39 (2004).
11. H. Liu, R. G. Sadygov, J. R. Yates III, *Anal. Chem.* **76**, 4193 (2004).
12. Materials and methods are available as supporting material on *Science* Online.
13. C. T. Murphy *et al.*, *Nature* **424**, 277 (2003).
14. J. J. McElwee, E. Schuster, E. Blanc, J. Thornton, D. Gems, *Mech. Ageing Dev.* **127**, 458 (2006).
15. S. S. Lee, S. Kennedy, A. C. Tolonen, G. Ruvkun, *Science* **300**, 644 (2003).
16. S. W. Oh *et al.*, *Nat. Genet.* **38**, 251 (2006).
17. B. R. Zeeberg *et al.*, *Genome Biol.* **4**, R28 (2003).

18. M. Hansen, A. L. Hsu, A. Dillin, C. Kenyon, *PLoS Genet.* **1**, 119 (2005).
19. J. Lee *et al.*, *J. Mol. Biol.* **344**, 585 (2004).
20. A. Kuhara, H. Inada, I. Katsura, I. Mori, *Neuron* **33**, 751 (2002).
21. J. Bandyopadhyay *et al.*, *Mol. Biol. Cell* **13**, 3281 (2002).
22. M. Jibiru, J. R. Berman, C. Kenyon, *Cell* **115**, 489 (2003).
23. We thank WormBase (www.wormbase.org); the *Caenorhabditis* Genetics Center; A. Kuhara, I. Mori, I. Katsura, J. Ahnn, and T. Blumenthal for databases and reagents; and M. Koelle, L.-I. Du, A. Aslanian, I. Cheeseman, and members of the Yates and Dillin laboratories for help with the manuscript, experiments, and grant applications. M. MacCoss and C. Wu helped determine the atomic enrichment of ^{15}N in labeled worms. J.V. was supported by a NIH National Research Service Award fellowship. This work was supported by NIH grants DK067598, DK074798, DK070696, and P41 RR11823-10.

Supporting Online Material
www.sciencemag.org/cgi/content/full/317/5838/660/DC1
Materials and Methods
SOM Text
Figs. S1 to S5
Tables S1 to S4
References

16 January 2007; accepted 12 June 2007
10.1126/science.1139952

Forced Unfolding of Proteins Within Cells

Colin P. Johnson,[1]*†‡ Hsin-Yao Tang,[2]* Christine Carag,[1]†‡
David W. Speicher,[2]† Dennis E. Discher[1,2]†‡¶

To identify cytoskeletal proteins that change conformation or assembly within stressed cells, in situ labeling of sterically shielded cysteines with fluorophores was analyzed by fluorescence imaging quantitative mass spectrometry and sequential two-dye labeling. Within red blood cells, shotgun labeling showed that shielded cysteines in the two isoforms of the cytoskeletal protein spectrin were increasingly labeled as a function of shear stress and time, indicative of forced unfolding of specific domains. Within mesenchymal stem cells—as a prototypical adherent cell—nonmuscle myosin IIA and vimentin are just two of the cytoskeletal proteins identified that show differential labeling in tensed versus drug-relaxed cells. Cysteine labeling of proteins within live cells can thus be used to fluorescently map out sites of molecular-scale deformation, and the results also suggest means to colocalize signaling events such as phosphorylation with forced unfolding.

Force-induced changes in protein conformation have long been postulated to contribute to the deformability of cells (*1*, *2*). Likewise, in cell adhesion, forces of pico-Newton magnitude that result from cells pulling on matrix (*3*) are believed to induce conformational changes that initiate essential anchorage signals (*4*, *5*). Single-molecule measurements indeed show that domain unfolding occurs in reversible extension of purified cytoskeletal, motor, and matrix adhesion proteins (*9*–*12*), and simulations of the molecular dynamics of protein extension have helped to clarify mechanisms (*13*–*15*). Direct cell-level evidence is lacking or even contrary to forced unfolding (*16*), although cytoskeletal association of a large and rare conformation-sensitive antibody has suggested extension of a proline-rich region in one protein within spread, fixed cells (*17*). The more broadly directed "shotgun" approach here is applied to live cells under physiological stresses and exploits small thiol-reactive probes that permanently label force-sensitive domains.

Cysteine (Cys) is a moderately hydrophobic amino acid that is frequently shielded by tertiary or quaternary protein structure. Labeling of cysteine's SH moiety has been exploited in solution denaturation studies on a few small purified proteins (*18*, *19*), as well as in an anemia-causing prolinx mutation in the red blood cell (RBC) protein spectrin (*20*). In addition, forced unfolding of single proteins with core-sequestered disulfides demonstrates reduction of the S-S within seconds by reactive thiols in the medium (*21*, *22*). We show here, in intact cells, that force-induced changes in protein structure can also expose for relatively rapid reaction specific buried Cys (Fig. 1) in a number of key cytoskeletal proteins. Sequential *n*-dye labeling with different color fluorophores ($n = 2$ here) proves to be a facile approach to amplifying signals from shielded sites relative to prelabeled surface sites (*23*). We illustrate the range of this in situ "Cys shotgun" approach, first with the relatively simple human RBC, which allows for the most direct demonstration of forced unfolding in fluid-stressed cells, then, with human mesenchymal stem cells (MSCs) under cell-generated tension.

Red blood cells deform under the incessant stresses of blood flow, and the spectrin membrane cytoskeleton has proven central to cell deformability (*24*). Spectrin's α and β chains interact to cross-link F-actin in this cell, and in single-molecule studies, spectrin's tandem array of helical bundle domains (Fig. 1) are found to unfold at low forces [~picoNewton (*25*–*27*)] that could be generated by just a few myosin motor molecules. There are 20 Cys in α-spectrin and 15 Cys in β-spectrin, and some of these appear buried in crystal structures (Fig. 1) and homology models. To assess exposure of Cys in unfolding of spectrin and all of the other RBC membrane proteins, cells were reversibly lysed to make hemoglobin-depleted pink "ghosts" that were resealed with entrapment of the Cys-reactive fluorophore IAF DANS. Dye-loaded cells were then either held static in suspension at various temperatures or else sheared over a physiological range of stresses with a standard fluid shearing device. After 5 min or more, cells were relysed, excess dye was quenched, and cells were imaged to assess membrane labeling (Fig. 2A).

Solubilized cells were denatured, and all Cys that were not dye-labeled were alkylated with iodoacetamide (IAM). Separation of membrane proteins by one-dimensional (1D) SDS polyacrylamide gel electrophoresis (SDS-PAGE), followed by densitometry, showed 50% more IAF DANS fluorescence in the bands of α- and β-spectrin from the shear samples (Fig. 2A, 15 min at 37°C); sequential two-dye labeling magnifies this difference to >500%, as described below. Labeling under shear is only enhanced for spectrin. Labeling of the other major membrane proteins (ankyrin, protein 4.1, actin, etc.)

Fig. 1. Force-induced changes in protein structure within cells are hypothesized to expose novel binding sites for ligands. This example of a molecular dynamics simulation shows that Cys^{2147} in β-spectrin exposes 0 $Å^2$ surface area (of 224 $Å^2$) until forced extension [e.g., (*15*)] exposes the –SH for reaction with a thiol-reactive fluorescent dye.

[1]Biophysical Engineering Lab, University of Pennsylvania, Philadelphia, PA 19104, USA. [2]Systems Biology Division—The Wistar Institute, Philadelphia, PA 19104, USA.

*These authors conducted experiments.
†These authors designed, refined, and analyzed experiments.
‡These authors modeled the data and wrote the paper.
¶To whom correspondence should be addressed. E-mail: discher@seas.upenn.edu

was not affected by fluid shear, which suggests, together with additional results below, that mixing is not limiting.

Liquid chromatography coupled tandem MS (LC-MS/MS) was used to identify and quantify IAEDANS-modified Cys sites in spectrin bands after excision and trypsinization. Within α- and β-spectrin, respectively, 13 and 14 IAEDANS-Cys were detected (table S1). Because surface-exposed Cys are predominantly IAEDANS labeled and buried Cys are largely inaccessible until subsequent denaturation and IAM labeling, site-specific ratios of (IAEDANS/IAM) ion chromatogram elution profiles (e.g., Fig. 2B) quantify Cys exposure. A majority of ratios are the same for shear and static samples, but at least six Cys sites are distinct with results for the ratio of dye-labeling rates over time $\phi(t) = [(\text{IAEDANS/IAM})_{\text{shear}} / (\text{IAEDANS/IAM})_{\text{static}}]$ that are typically in the range of $\phi \approx 5$ to 10 at 60 min, but as high as 36 (Fig. 2C). Cleavage patterns of β-spectrin treated with NTCB (2-nitro-5-thiocyanobenzoic acid), which cleaves peptide bonds at unlabeled Cys (fig. S1A), are distinct for shear and static samples, consistent with qualitative differences in Cys exposure.

The structure of shear-sensitive β-R8-9 (*28*) shows the shear-labeled $Cys^{\beta1167}$ is 100% buried or shielded within a tertiary fold at least until force induces localized unfolding (Fig. 1). A recombinant multidomain construct β-R5-9 was, therefore, Cys-labeled at different temperatures for a fixed time and then analyzed by both fluorescence imaging and MS. Construct labeling is significant only at temperature $T > 25$°C (Fig. 2D), with evidence from MS of $Cys^{\beta1167}$ labeling at 25°C. This apparent transition corresponds to the transition midpoint temperature (T_m) of β-R9 (*29*) and correlates with both the thermally induced loss of helicity and the loss of mechanical stability of R9 as determined by atomic force microscopy (AFM) forced extension. At higher temperatures, additional repeats are labeled as helicity is lost.

The shear-sensitive $Cys^{\alpha1203}$ was also studied in solution with a recombinant α-R12 domain for which modeling predicts partial shielding (Fig. 2E). At a given temperature, the ratio of dye-labeling rates $\Phi(T)$ for urea-denaturing conditions versus native conditions relates to the steric protection of a partially exposed cysteine (*19*) (fig. S2). The recombinant's $\Phi(37°C) = 4$ approximates the LC-MS/MS result for shear versus static cells' $\Phi(37°C) = 5$ (Fig. 2C). Normalization and rescaling to the folded state maximum $\Phi_{max} = \Phi(4°C)$ gives the fraction folded, and this decreases with T in parallel again with the helicity loss upon heating (Fig. 2E and fig. S2).

Within RBCs, the labeling kinetics for IAEDANS provides a basis for dramatically increasing the shear/static labeling ratio. Surface-exposed Cys in spectrin label to saturation within 30 to 60 min with a first-order rate constant (0.13 min^{-1}) (Fig. 3A), whereas in the shear sample, the ~50% enhanced labeling is slower (0.04 min^{-1}), consistent with a second population of shear-exposed Cys sites. In sequential two-dye labeling, static-accessible sites are labeled to near saturation with IAEDANS (blue), and then shear is applied with labeling by a second (green) Cys-reactive fluorophore (Fig. 3B). *N*-(4,4-Difluoro-1,3,5,7-tetramethyl-4-bora-3a,4a-diaza-s-indacene-2-yl) iodoacetamide (BODIPY-IA) labeling of spectrin within RBCs increases with both time and stress, yielding results for the shear/static ratio of ~5 to 6.5 after 60 min at the highest shears of $\sigma = 0.8$ to 1.7 Pa. Site-specific MS gave $\langle\phi\rangle \approx 10$ (Fig. 2C).

The effective labeling rate k for the secondary BODIPY-IA labeling reaction is 30 times as fast in maximally sheared cells as in static cells (Fig. 3B) and fits to a force (f)-dependent Linderstrøm-Lang (fLL) scheme in which shear stress, proportional to f, shifts the conformational equilibrium

$$N \underset{k_{U\to N}e^{+\Delta x f/k_BT}}{\overset{k_{N\to U}e^{-\Delta x f/k_BT}}{\rightleftharpoons}} U \xrightarrow{k_2} P$$

Similar to forced unfolding in the cited single-molecule studies, the folded state N shifts toward unfolded state U with a force bias on the forward and reverse reactions, and the activated transition state P^* along the reaction coordinate x is at the respective distances Δx (>0, $N \rightarrow P^*$) and $\Delta x'$ (<0, $U \rightarrow P^*$). Here, the U state's exposed Cys can be labeled by dye at concentration c and rate k_2 to yield measured

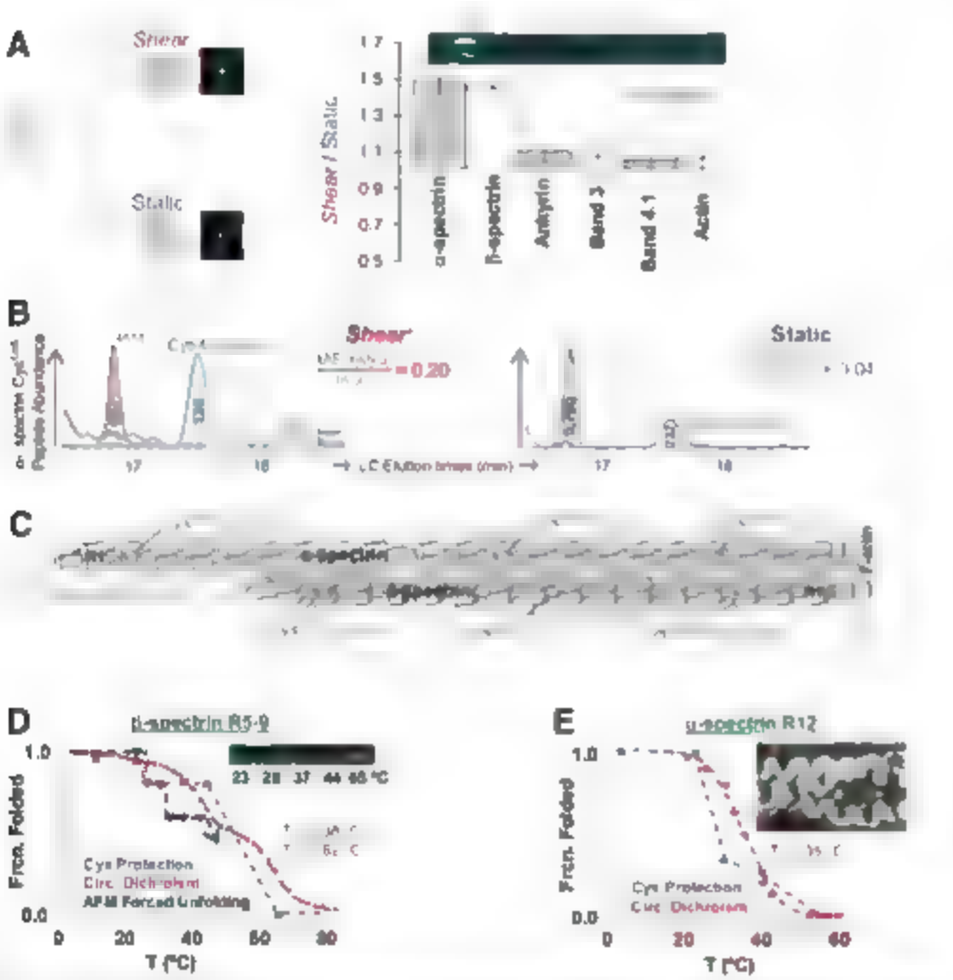

Fig. 2. In-cell labeling of RBCs under stressed versus static conditions demonstrates force-enhanced labeling of spectrin sites with Cys identification by quantitative MS. (**A**) Inset images show shear-distorted or round RBC ghosts fixed by glutaraldehyde, as well as fluorescence microscopy of membranes after IAEDANS reaction under either shear (stress $\sigma = 0.93$ Pa) or static conditions (60 min, 37°C). SDS 1D-PAGE separations of ghost lysates demonstrate shear-enhanced labeling of α- and β-spectrin, but no significant differences for other membrane proteins (±5D). (**B**) Extracted ion chromatograms for α12's Cys^{1203}-containing peptide from shear and static samples. Ratios of peak areas for IAEDANS- and IAM-labeled peptides provide measures of relative dye labeling. (**C**) Positions along α- and β-spectrin with shear/static–labeling differentials, $\phi \geq 2$ (see table S1). (**D**) Recombinant β-R5-9 construct labeled in solution by IAEDANS with increasing temperature reveals a step-wise increase in labeling extent, this is inverted and normalized to report fraction folded. The increase at $T > 23$°C coincides with unfolding of repeat β9, as determined by both circular dichroism (CD) and forced unfolding with an AFM. The numbered T_m are the two melting temperatures from CD. (**E**) Homology model of α-R12 with Cys^{1203} highlighted in yellow. Fraction of α12 folded versus temperature based on cysteine labeling results (blue) and CD measurements (red) (*28*).

product P (table S1 and fig. S1B). The analytical solution to the fLL scheme (SOM text) fits well to the spectrin in-cell experiments here when we use parameter values similar to those obtained from single-molecule studies on spectrin, such as $k_{ff} \approx 0.002$ min^{-1} (25). The fits are also consistent with expectations that (i) the refolding rate is only important in the static sample and at low stress, (ii) labeling is limiting at very high stress, and (iii) labeling in the intermediate stress regime is sufficiently rapid that the rate of exposure of sequestered Cys is exponential with respect to stress.

Consistent with past speculations that spectrin unfolding occurs to some extent within RBCs (1, 30), about 40% of spectrin's domains studied as isolated domains unfold with $T_m < 37$°C (29). Within stable cells, IAEDANS labeling of spectrin Cys occurs slowly at low temperature as expected (fig. S3A), and, although site-selective labeling rates will be needed for an accurate assessment of in-cell melting of spectrin, 60 min of labeling yields an apparent melting curve (fig. S3B) in close agreement with the summed melting profile calculated from individual recombinant spectrin domains (29). Moreover, at all temperatures up to thermal disruption of cells (~45°C), shear enhances labeling of spectrin but not actin (fig. S3).

Mechanically induced changes in protein structure within other cells are likely to be of importance not only to cell deformability but also to various mechano-signaling processes. MSCs, for example, are contractile (31) and strain the underlying matrix in differentiation (32). Traction force measurements on soft matrices show that MSCs, like many tissue cells (4), generate stresses (~kPa) that are ~1000 times fluid shear stresses imposed on RBCs. Inhibition of nonmuscle myosin II (NMM II) with the drug blebbistatin (33) relaxes and softens MSCs (31) and also blocks differentiation. For molecular insight into structural changes, as well as a proteomic characterization of MSCs, the Cys shotgun method was applied to these adherent stem cells with and without blebbistatin (fig. S4).

The membrane-permeable Cys-reactive fluorophore monobromobimane (mBBr) shows labeling of the cytoskeleton, nucleus, and other structures after fixation and washing, without perturbing cell area (fig. S4A). This suggests that labeling does not greatly disturb MSCs (23). Cell lysates for the tensed cells and blebbistatin-relaxed cells were Cys-quenched, and, once again, 1D SDS-PAGE was followed by densitometry and then LC-MS/MS analyses of all prominently labeled bands (>40 kD) (fig. 4B). The cytoskeletal proteome of MSCs (table S2) appears typical of nucleated cells in consisting of actin, myosin, the actin-binding proteins filamin and nonerythroid spectrin, as well as tubulin and the mesenchymal intermediate filament protein vimentin. Site-specific differences in Cys labeling with blebbistatin are seen in several proteins, and two prove illustrative.

Nonmuscle myosin IIA shows greater mBBr-labeling in the tensed state of MSCs for which immunofluorescence imaging shows cytoskeletal striation (Fig. 4C). In contrast, blebbistatin disorganizes NMM II, consistent with blocking it in a low-affinity state for actin (34). MS analysis identifies Cys^{90} as a differentially labeled site, and homology models of NMM II show this site is buried between the head and rod domains. Transient allosteric changes that occur in stress generation during NMM II's normal ATP hydrolysis likely expose Cys^{90}, whereas blebbistatin

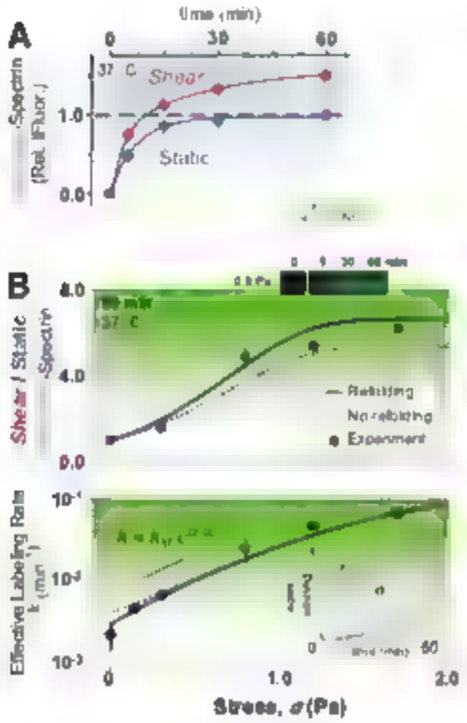

Fig. 3. Stress-dependent kinetics and sequential two-dye labeling for amplification. (**A**) Sheared (σ = 0.93 Pa) versus static RBCs show distinct labeling kinetics for spectrin. IAEDANS labeling (at 2.5 mM) of the static-labeled, surface-exposed spectrin sites fit a first-order rate of 0.13 min^{-1}; the shear-exposed sites (66% more from fit) label more slowly at 0.04 min^{-1}. (**B**) Sequential labeling entails labeling of the surface Cys (blue) for 30 min, after which BODIPY-IA (green) is added at >10-fold excess (6 mM). Half of the cells are then exposed to shear with timed aliquots again quenched by IAM and analyzed by densitometry of the green fluorescent spectrin. BODIPY-spectrin at 60 min increases with σ (top) as does the effective rate of labeling (bottom). Error bars (±SD) indicate three or more measurements (six for σ = 0). The data are fit by the exact solution of the fLL reaction for $P(t)$, either with or without refolding (SOM text). The intermediate regime of stress (dotted black line) is dominated by unfolding and increases exponentially with stress, exhibiting a characteristic stress of $\sigma_u \approx 0.5$ Pa and giving $k_{uf} \approx 0.004$ min^{-1}. (Inset) The effect of force on computed kinetics using the fit parameters.

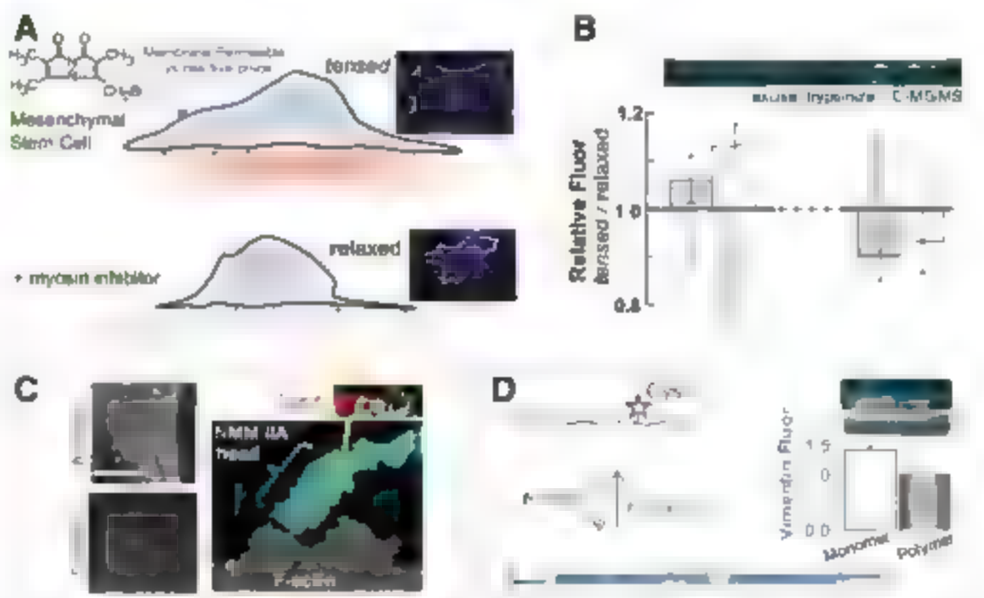

Fig. 4. In-cell labeling of human stem cells either tensed or relaxed. (**A**) The membrane-permeable Cys-reactive fluorophore mBBr was added to 1-week cultures of MSCs with active myosins and tensed cytoskeletons and also to MSCs treated with myosin-inhibiting blebbistatin for 1 day to relax the cells. Imaging shows homogeneous labeling with 0.5 mM mBBr for 40 min. (**B**) SDS-PAGE and densitometry of samples (±SD, three experiments) that were either blebbistatin treated (relaxed) or untreated (tensed) show several protein bands in which the fluorescence intensities are different (normalized to protein load). Lysates were quenched with β-mercaptoethanol (50 mM) before analysis. (**C**) Immunofluorescence imaging of NMM IIA in tensed cells (top) and relaxed cells (bottom) indicates a spatial redistribution of myosin with drug. Scale, 5 μm. MS analyses of excised myosin bands detected labeling of Cys^{90}, which appears buried within the fold of NMM IIA homology models. (**D**) Vimentin labeling in monomeric and polymeric forms display different degrees of fluorescence (error bar from two experiments), which indicates that polymerization sterically blocks Cys^{327} for labeling.

eliminates force-generation and keeps this site buried.

Differential labeling in MSCs is also found at the single Cys site of vimentin (Fig. 4D). Cys^{327} is in the central coil that mediates coiled-coil polymerization (*35*). Quaternary structure changes in solution have been exploited previously to understand hemoglobin tetramerization [e.g., (*36*)], as well as actin-binding interfaces [e.g., (*37*)], and here blebbistatin-induced depolymerization of vimentin with Cys exposure in the MSCs appears consistent with blebbistatin-induced softening of the cells (*32*). Purified vimentin confirms enhanced labeling as monomer (~50% more) versus polymer (Fig. 4D), and Western blot analysis plus immunofluorescence imaging of MSCs grown on various matrices show that chronic blebbistatin treatment consistently down-regulates vimentin (fig. S4, B and C). Short treatments with blebbistatin (~1 hour instead of 1 day) also show that mBBr vimentin measured in cell lysates increases significantly even though Western blots and immunofluorescence indicate no differences in overall expression. In-cell labeling thus identifies structural changes with tensed cell but not relaxing cells.

Nucleated cells typified by MSCs have a complex intracellular force map when inferred from cell tractions in the surrounding matrix (*1*, *32*, *38*), and even simple cells such as RBCs sustain stresses at the molecular level in unknown ways (*1*, *29*). The overall Cys-shotgun methodology here not only provides evidence of force-induced changes that propagate in both tertiary and quaternary structures within cells but also, through LC-MS/MS, provides useful proteomic information, as well as new opportunities for fluorescence imaging. In addition, whereas fluorescence resonance energy transfer imaging of labeled proteins within cells [e.g. (*39*)] might allow imaging of force-induced conformational changes in real time, the time-integrated analyses here are complementary and also readily extended to engineered sites in wild-type and mutant proteins for in-cell assessments of perturbations. This idea seems very likely to extend to coincidence detection of Cys labeling with posttranslational events such as phosphorylation so as to precisely colocalize conformational changes with signaling events.

References and Notes

1. E. A. Evans, R. Skalak, *Mechanics and Thermodynamics of Biomembranes* (CRC Press, Boca Raton, FL, 1980) p. 190.
2. H. P. Erickson, *Proc. Natl. Acad. Sci. U.S.A.* **91**, 10114 (1994).
3. M. Q. Balaban *et al.*, *Nat. Cell Biol.* **3**, 466 (2001).
4. K. A. Beningo, M. Dembo, I. Kaverina, J. V. Small, Y. L. Wang, *J. Cell Biol.* **153**, 881 (2001).
5. F. J. Alenghat, D. E. Ingber, *Sci. STKE* **2002** (119), PE6 (2002).
6. E. A. Evans, D. A. Calderwood, *Science* **316**, 1148 (2007).
7. V. Vogel, M. Sheetz, *Nat. Rev. Mol. Cell Biol.* **7**, 265 (2006).
8. A. Bershadsky, M. Kozlov, B. Geiger, *Curr. Opin. Cell Biol.* **18**, 472 (2006).
9. M. Rief, M. Gautel, F. Oesterhelt, J. M. Fernandez, H. E. Gaub, *Science* **276**, 1109 (1997).
10. A. F. Oberhauser, P. E. Marszalek, H. P. Erickson, J. M. Fernandez, *Nature* **393**, 181 (1998).
11. I. Schwaiger, C. Sattler, D. R. Hostetter, M. Rief, *Nat. Mater.* **1**, 232 (2002).
12. G. Lee *et al.*, *Nature* **440**, 246 (2006).
13. M. Sotomayor, K. Schulten, *Science* **316**, 1144 (2007).
14. P. M. Williams *et al.*, *Nature* **422**, 446 (2003).
15. V. Ortiz, S. O. Nielsen, M. L. Klein, D. E. Discher, *J. Mol. Biol.* **349**, 638 (2005).
16. M. I. Abu-Lail, T. Ohashi, R. L. Clark, H. P. Erickson, S. Zauscher, *Matrix Biol.* **25**, 175 (2006).
17. Y. Sawada *et al.*, *Cell* **127**, 1015 (2006).
18. J. H. Ha, S. N. Loh, *Nat. Struct. Biol.* **5**, 730 (1998).
19. J. A. Silverman, P. B. Harbury, *J. Biol. Chem.* **277**, 30968 (2002).
20. C. P. Johnson *et al.*, *Blood* **109**, 3538 (2007).
21. P. Carl, C. H. Kwok, G. Manderson, D. W. Speicher, D. E. Discher, *Proc. Natl. Acad. Sci. U.S.A.* **98**, 1565 (2001).
22. A. P. Wiita, S. R. Ainavarapu, H. H. Huang, J. M. Fernandez, *Proc. Natl. Acad. Sci. U.S.A.* **103**, 7222 (2006).
23. Materials and methods are available as supporting material on Science Online.
24. N. Mohandas, E. A. Evans, *Annu. Rev. Biophys. Biomol. Struct.* **23**, 787 (1994).
25. M. Rief, J. Pascual, M. Saraste, H. E. Gaub, *J. Mol. Biol.* **286**, 553 (1999).
26. R. Law *et al.*, *Biophys. J.* **85**, 3286 (2003).
27. L. G. Randles, R. W. Rounsevell, J. Clarke, *Biophys. J.* **92**, 571 (2007).
28. H. Kutanoja, R. I. MacDonald, A. Mondragon, *Structure* **12**, 645 (2004).
29. X. An *et al.*, *J. Biol. Chem.* **281**, 10527 (2006).
30. J. C. Lee, D. E. Discher, *Biophys. J.* **81**, 3178 (2001).
31. R. McBeath, D. M. Pirone, C. M. Nelson, K. Bhadriraju, C. S. Chen, *Dev. Cell* **6**, 483 (2004).
32. A. J. Engler, S. Sen, H. L. Sweeney, D. E. Discher, *Cell* **126**, 677 (2006).
33. A. F. Straight *et al.*, *Science* **299**, 1743 (2003).
34. B. Ramamurthy, C. M. Yengo, A. F. Straight, T. J. Mitchison, H. L. Sweeney, *Biochemistry* **43**, 14832 (2004).
35. H. Herrmann, U. Aebi, *Annu. Rev. Biochem.* **73**, 749 (2004).
36. E. Chiancone, D. L. Currell, P. Vecchini, E. Antonini, J. Wyman, *J. Biol. Chem.* **245**, 4105 (1970).
37. S. Sun, M. Foster, P. Matsudaira, *Mol. Biol. Cell* **8**, 421 (1997).
38. N. Wang *et al.*, *Am. J. Physiol. Cell Physiol.* **282**, C606 (2002).
39. V. S. Kraynov *et al.*, *Science* **290**, 333 (2000).

40. We thank V. Ortiz for the Molecular Dynamics image, X. An for purified protein, A. Engler for culture and help with MSCs, and A. Kashina for helpful comments on the manuscript. We gratefully acknowledge support from NIH grants (D.E.D., D.W.S.), NIH Training Grants (C.P.J., C.C.), as well as NSF and Muscular Dystrophy Association grants (D.E.D.).

Supporting Online Material

www.sciencemag.org/cgi/content/full/317/5838/663/DC1
Materials and Methods
SOM Text
Figs. S1 to S4
Tables S1 and S2
References and Notes

12 January 2007; accepted 27 June 2007
10.1126/science.1139857

Monitoring of Blood Vessels and Tissues by a Population of Monocytes with Patrolling Behavior

Cedric Auffray,[1] Darin Fogg,[1] Meriem Garfa,[1] Gaelle Elain,[1] Olivier Join-Lambert,[2,3] Samer Kayal,[1,2,3] Sabine Sarnacki,[2,3] Ana Cumano,[4] Gregoire Lauvau,[5] Frederic Geissmann[1,2,3]*

The cellular immune response to tissue damage and infection requires the recruitment of blood leukocytes. This process is mediated through a classical multistep mechanism, which involves transient rolling on the endothelium and recognition of inflammation followed by extravasation. We have shown, by direct examination of blood monocyte functions in vivo, that a subset of monocytes patrols healthy tissues through long-range crawling on the resting endothelium. This patrolling behavior depended on the integrin LFA-1 and the chemokine receptor CX_3CR1 and was required for rapid tissue invasion at the site of an infection by this "resident" monocyte population, which initiated an early immune response and differentiated into macrophages.

Mammalian monocytes consist of two major subsets of circulating cells (*1*, *2*), which arise from a common hematopoietic progenitor, the macrophage and dendritic cell (DC) precursor (MDP, or monoblast) that also gives rise to conventional resident spleen DCs (cDCs) and several tissue macrophage subsets (*3*, *4*). So-called "inflammatory" monocytes express the cell surface protein Ly6c (Gr1), the chemokine receptor CCR2, and the adhesion molecule L-selectin and are selectively recruited to inflamed tissues and lymph nodes (*1*, *5*). They are able to differentiate into inflammatory DC (*1*, *6*, *7*) and can replenish resident cell compartments in the skin, digestive tract, and lung (*3*, *8*). The second subset of monocytes has been termed "resident" in mice (*1*, *2*) because they were found in both resting and inflamed tissues, although their functions are still unknown. This subset is defined by a smaller size, high expression of the chemokine receptor CX_3CR1 and LFA-1 integrin, and by the lack of expression of Ly6c (Gr1), CCR2, and L-selectin (*1*, *2*). Two monocyte subsets can also be identified in humans (*9*), with ($CD14^+$ $CD16^-$) monocytes resembling mouse inflammatory monocytes and ($CD14^{low}$ $CD16^+$) monocytes sharing a phenotype similar to that of mouse resident monocytes (*1*). Resident and

inflammatory monocytes thus appear to be defined by distinct sets of adhesion molecules and chemokine receptors, which suggests different modes of tissue trafficking.

To explore this possibility further, we developed a strategy to study the behavior and functions of blood monocytes in real time under steady state or inflammatory conditions. Intravital confocal microscopy imaging was undertaken in vivo in a way that allowed us to observe cells within capillaries and postcapillary vessels in the dermis (Fig. 1A) and in larger veins and arteries, that is, mesenteric vessels (Fig. 1B) (*10*). $Cx_3cr1^{gfp/+}$ mice, which express green fluorescent protein (GFP) in monocytes [but also in natural killer (NK) cells and some T cells] and $Rag_2^{-/-}$, $\gamma_c^{-/-}$, $Cx_3cr1^{gfp/+}$ mice, in which monocytes are the only blood cells expressing GFP, were used as reporters (Fig. 1, C and D) (*10*).

Intravital microscopy observation of tissues in the steady state revealed that monocytes within most blood vessels in the dermis (Fig. 2, A and B, and movies S1 and S2) and in the branches of the mesenteric vein and the mesenteric artery (Fig. 2C, fig. S1, and movies S3 and S4) exhibited a constitutive "crawling" type motility. In contrast, rolling gfp^+ monocytes were observed only transiently after surgery in the mesenteric veins (fig. S1 and movies S3 and S4) but not in arteries (movie S4). Analysis of gfp signal intensity per pixel indicated that crawling monocytes belonged predominantly to the gfp^{high} subset ($(CX_3CR1)^{high}$ Gr1$^-$) as compared with monocytes that perform rolling in the same vessels (Fig. 2D and fig. S2). These finding suggested either that gfp^{high} monocytes were crawling inside blood vessels onto endothelial cells, despite the blood flow, or that they were located outside the lumen of the blood vessel. When the green gfp signal was omitted, crawling gfp^{high} monocytes appeared as dark spots on confocal sections of the vessel labeled in red with the fluorescent dextran, indicating that monocytes are located inside the blood vessels (Fig. 2E and movie S5). Crawling polymorphonuclear neutrophils (PMN) or lymphocytes would appear as dark crawling cells in the blood of mice; however, gfp$^+$ crawling cells were not observed in the steady state (movie S1), suggesting that these cells did not behave in the same way and that gfp$^+$ monocytes were the majority of cells that crawl on the endothelium in the steady state.

Although monocytes were located inside the vessels, overlay of individual cell tracks plotted after aligning their starting positions indicated that the direction of their crawling movement was not dependent on the blood flow (Fig. 2F). Extravasation was rarely observed in the steady state. The path of individual cells indicated that monocytes in blood vessels appeared to describe loops (25%), hairpin (17%), waves (38%), mixed pattern (9%), and short path (<40 μm, 11%) (Fig. 2, G to J, and fig. S3). The average instantaneous velocity of crawling monocytes was 4 to 20 μm/min (average 12 μm/min) (Fig. 2K and fig. S4). The distance traveled by individual cells was, on average, only half their path length, indicating that the cells have a high confinement ratio (Fig. 2L). The result of these crawling movements was that in small postcapillary venules, after an hour, monocytes appeared to have extensively monitored the endothelium of a given vessel (Fig. 2B and movie S2), leading us to describe their behavior as patrolling.

The velocity profile of flow in blood vessels is generally parabolic across the cross section of the vessel, and calculated values decrease to zero at the blood vessel wall (*11*). However, crawling against the mainstream blood flow is counterintuitive, and this suggested that monocytes were closely adherent to the luminal side of the endothelium. We therefore explored the molecular basis of monocyte patrolling. Lymphocytes and PMNs have been shown to roll at speeds of 40 μm/sec under conditions of flow at sites of inflammation along the endothelium of postcapillary venules (*12*, *13*). This initial contact allows endothelial membrane-bound chemokines to activate leukocyte integrins through $G\alpha_i$-linked chemokine receptor (*14*). Changes in integrin affinity then allow the rolling leukocytes to stick firmly, occasionally crawl onto the endothelial cell toward the closest intracellular cell junction (*15*, *16*), and diapedese across the endothelium. Patrolling was slower than rolling by a factor of 100 to 1000 and was observed in the steady state. Long-range and independent of the direction of bloodstream blood flow and of extravasation. However, it appears to involve a "firm binding" to endothelium, and therefore we reasoned that integrin may be involved. Gfp^{high} (Gr1$^-$) monocytes express the β_2 integrins LFA-1

[1]Institut Nationale de la Santé et de la Recherche Medicale (INSERM) U838, Laboratory of Biology of the Mononuclear Phagocyte System, and Cellular and Molecular Imaging core facility, Institut Federatif de Recherche Necker-Enfants Malades, Paris, France. [2]University Paris-Descartes, Paris, France. [3]Hôpital Necker-Enfants Malades, AP-HP, Paris, France. [4]INSERM U668, Unité de Développement des Lymphocytes, Institut Pasteur, Paris, France. [5]INSERM E03-44, Institut de Pharmacologie Moleculaire et Cellulaire, Nice, France.

*To whom correspondence should be addressed. E-mail: geissmann@necker.fr

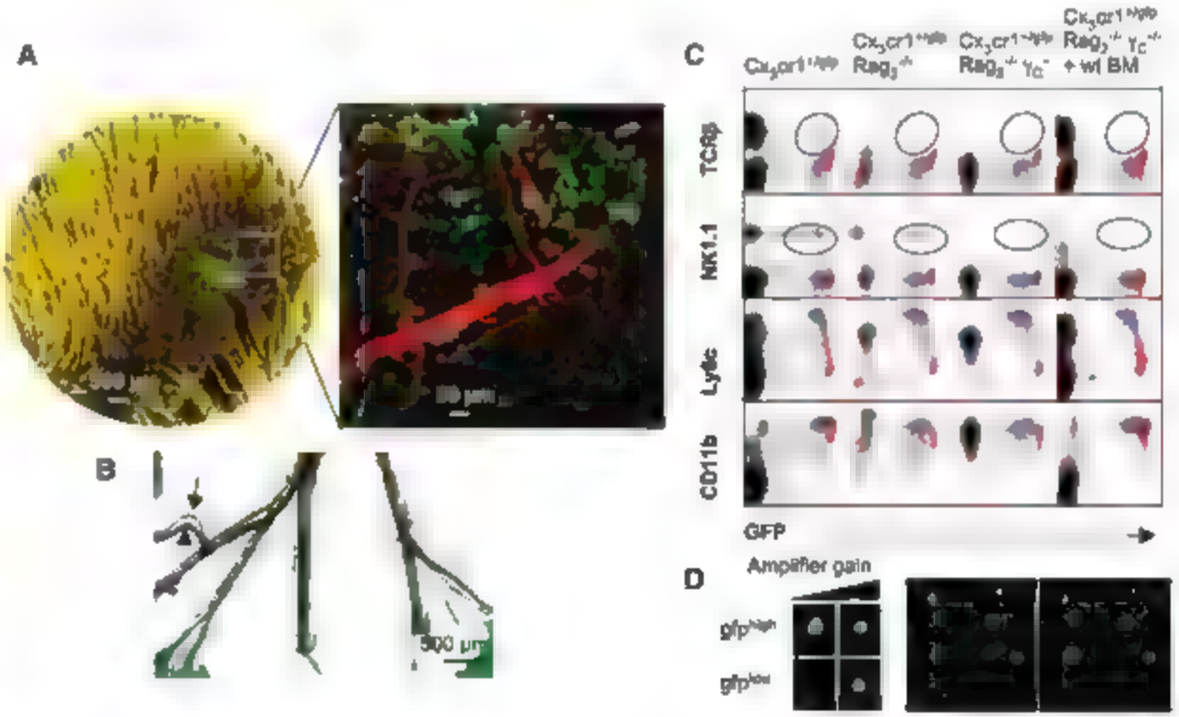

Fig. 1. Intravital imaging of mouse monocytes. **(A)** CX_3CR1-expressing cells express gfp in reporter mice, and dermal blood vessels are labeled in red rhodamine-conjugated dextran. **(B)** The branches of the mesenteric vein (arrowhead) and mesenteric artery (arrow) are surgically exposed. **(C)** Flow cytometry analysis of blood leukocytes from $Cx_3cr1^{gfp/+}$ mice, $Rag_2^{-/-}$ $Cx_3cr1^{gfp/+}$ mice, $Rag_2^{-/-}$, $\gamma c^{-/-}$ $Cx_3cr1^{gfp/+}$ mice, and $Rag_2^{-/-}$ $\gamma c^{-/-}$, $Cx_3cr1^{gfp/+}$ mice reconstituted with wild-type lymphoid cells. **(D)** Gr1$^+$ (gfp^{low}) and Gr1$^-$ (gfp^{high}) monocytes were sorted by flow cytometry and examined by confocal microscopy. Based on gfp intensity, Gr1$^-$ (gfp^{high}) monocytes sorted by fluorescence-activated cell sorting (FACS) are easily distinguishable by confocal microscopy from FACS-sorted Gr1$^+$ (gfp^{low}) monocytes labeled with a far-red cell tracker (shown in blue in the middle panel).

(CD11a/CD18, $\alpha_L\beta_2$) and Mac-1 (CD11b/CD18, $\alpha_M\beta_2$) (*1*). Intravenous injection of blocking antibodies to either CD11a or CD18, but not of antibodies to CD11b or control immunoglobulin (Ig), resulted in the rapid, complete, and prolonged release of monocytes from the endothelial wall (Fig. 3, A and B, and movie S6), indicating that LFA-1 is required for crawling. Gfp^{high} monocytes also express high levels of the chemokine receptor CX_3CR1 (*1*), whereas its ligand, fractalkine, is a transmembrane molecule expressed on endothelial cells (*17*, *19*). CX_3CR1-fractalkine interaction in vitro has been described to mediate adhesion between monocytes and endothelial cells through activation of integrins (*20*) and through an intrinsic adhesion function (*18*, *20*, *21*). The number of crawling monocytes was reduced by two-thirds in CX_3CR1-deficient

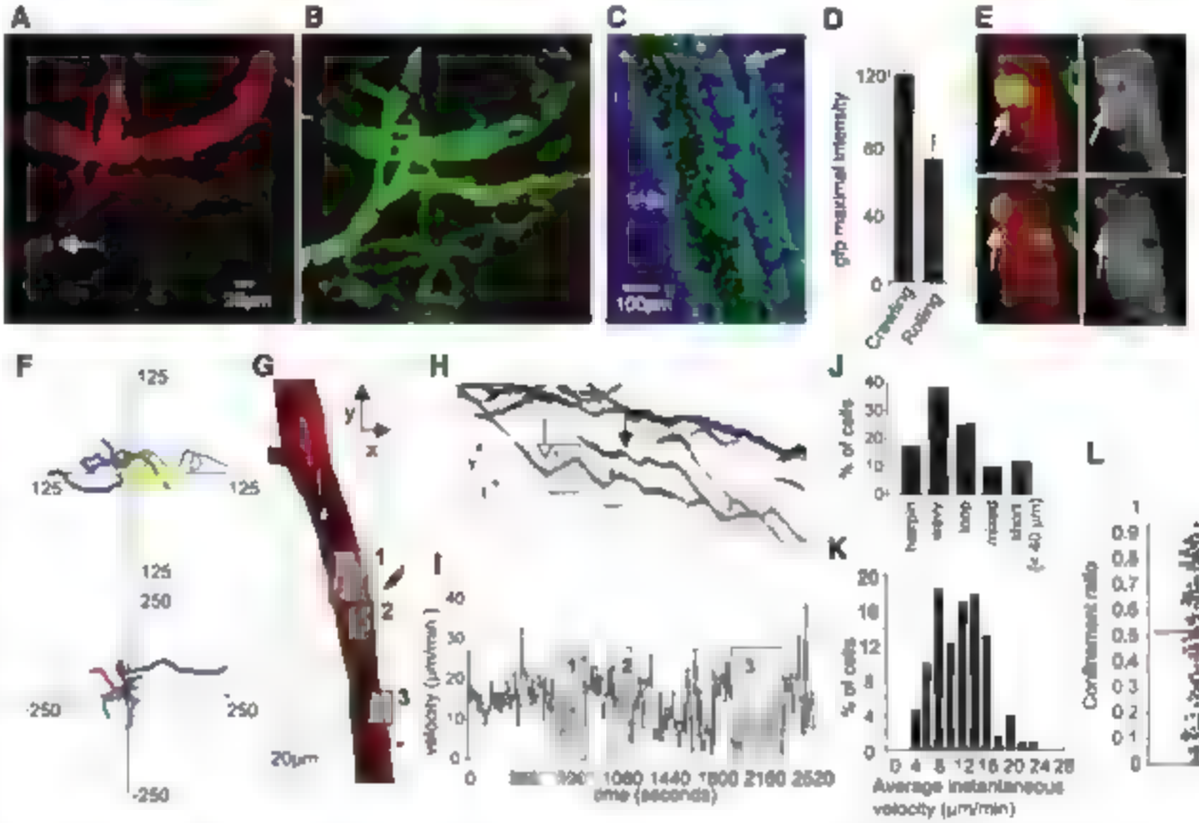

Fig. 2. Gfp^{high} $Gr1^-$ monocytes crawl inside blood vessels. (**A**) Dermal blood vessels in $Rag_2^{-/-}$, $\gamma_c^{-/-}$ $Cx_3cr1^{gfp/+}$ reporter mice. Monocytes appear as green dots (arrows). (**B** and **C**) Green signal from images of time-lapse series are summed to display the path of labeled cells in the dermis (B) and mesenteric vessels (C). In (C), the open arrow indicates a branch of the mesenteric vein, and the closed arrow indicates a branch of the mesenteric artery. (**D**) gfp maximal pixel intensity was calculated as indicated in fig. S2. (**E**) Confocal section (6 μm) examined with red (intravenous dextran) and green (gfp^+ monocytes) signals, or for the red signal only (shown in gray, right panel). Cells that are located within the vessels appear as a dark signal (arrow). (**F**) Overlay of monocyte tracks from two representative vessels, plotted after aligning their starting positions. (**G** to **I**) Path (G), kymograph (H), and instantaneous velocity (I) of a cell from movie S1. (**J**) Monocyte paths were classified as loops, hairpin, waves, mixed pattern, and short path (<40 μm) (fig. S3). (**K**) Average velocity was calculated as indicated in (*10*). (**L**) Confinement ratio of gfp^{high} monocytes. Scatter plot represents the ratio of the distance to origin of tracked cells versus their path length.

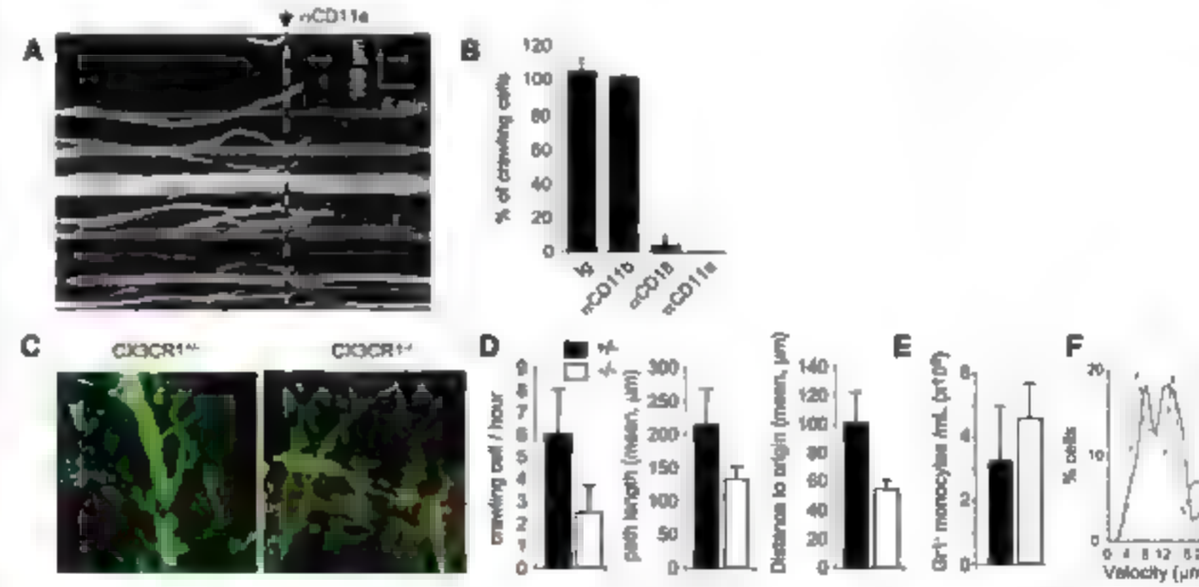

Fig. 3. Monocyte crawling is mediated in vivo through the integrin LFA-1 and the chemokine receptor CX_3CR1. (**A**) Kymograph of a time-lapse series before and after intravenous injection of CD11a-blocking antibody (4 mg per kg of weight). (**B**) Percentage of crawling cells was determined as a ratio between the numbers of cells crawling before and 10 min after injection of control Ig or blocking antibody directed against CD11b, CD18, and CD11a. Experiments were repeated at least three times for each antibody. (**C**) Maximum projection of time-lapse series obtained from intravital microscopy experiments in postcapillary venules of the ear in steady-state conditions. (**D**) Histograms represent number of crawling cells per hour, mean path length of these crawling cells, and distance to origin, either in $Rag_2^{-/-}$, $\gamma_c^{-/-}$ $Cx_3cr1^{gfp/+}$ or $Rag_2^{-/-}$, $\gamma_c^{-/-}$ $Cx_3cr1^{gfp/gfp}$ mice in the steady state. (**E**) Histograms represent number of Gr1$^+$ monocytes in the blood of 10-week-old $Rag_2^{-/-}$, $\gamma_c^{-/-}$ $Cx_3cr1^{gfp/+}$ and $Rag_2^{-/-}$, $\gamma_c^{-/-}$ $Cx_3cr1^{gfp/gfp}$ mice. (**F**) Representation of the crawling velocity of Gr1$^-$ monocytes from $Rag_2^{-/-}$, $\gamma_c^{-/-}$ $Cx_3cr1^{gfp/+}$ (solid line) and $Rag_2^{-/-}$, $\gamma_c^{-/-}$ $Cx_3cr1^{gfp/gfp}$ (dashed line) mice.

mice, and the average path length of crawling cells was reduced by one-half, resulting in a six-fold decrease in patrolling (Fig. 3, C and D, and movie S7), whereas the velocity of the remaining crawling monocytes and the numbers of circulating blood gfp^{high} monocytes were similar in *Cx3cr1*$^{+/-}$ and *Cx3cr1*$^{-/-}$ mice (Fig. 3, E and F, and fig. S5). It is notable that blocking antibodies to LFA-1 can detach crawling monocytes in *Cx3cr1*$^{-/-}$ mice, which suggests that CX$_3$CR1-dependent crawling is largely mediated through LFA-1 in vivo.

The patrolling monocytes are ideally located to provide immune surveillance of endothelial cells and surrounding tissues. In response to tissue damage, gfp^{high} monocytes extravasated rapidly within 1 hour and invaded the surrounding tissues after exposure to irritants (Fig. 4, A and B), aseptic wounding (Fig. 4C), and peritoneal infection with *Listeria monocytogenes* (Fig. 4D). To study in depth the kinetics, phenotype, and functions of extravasated monocytes, we used the *L. monocytogenes* peritoneal infection model, because extravasated cells can easily be recovered by peritoneal lavage. In this model, extravasation of Gr1^{+} gfp^{high} monocytes peaked at 2 hours after infection, at a time when PMN is only beginning to enter the peritoneum and several hours before the extravasation of conventional Gr1^{+} gfp^{low} monocytes is observed and was significantly delayed in patrolling-deficient *Cx3cr1*$^{-/-}$ mice (Fig. 4D and table S1). Therefore, patrolling was associated with and required for, early extravasation and tissue invasion by Gr1^{-} gfp^{high} monocytes. Extravasated Gr1^{-} gfp^{high} monocytes were responsible for an early inflammatory response (Fig. 4, E and F, and fig. S6). At 1 and 2 hours after infection, Gr1^{-} gfp^{high} monocytes were the only producers of tumor necrosis factor- α (TNFα), a cytokine central to inflammation, as detected by intracellular flow cytometry and polymerase chain reaction (PCR) (Fig. 4F). Genes coding for interleukin-1 (IL-1), lysozyme, defensins, complement, pattern recognition receptors such as TLRs, scavenger receptors, and IgFc receptors, and chemokines involved in the recruitment and activation of other effector cells were also up-regulated (Fig. 4E and fig. S6).

Notably, the production of TNF and IL-1 was transient and turned off at 8 hours (Fig. 4F).

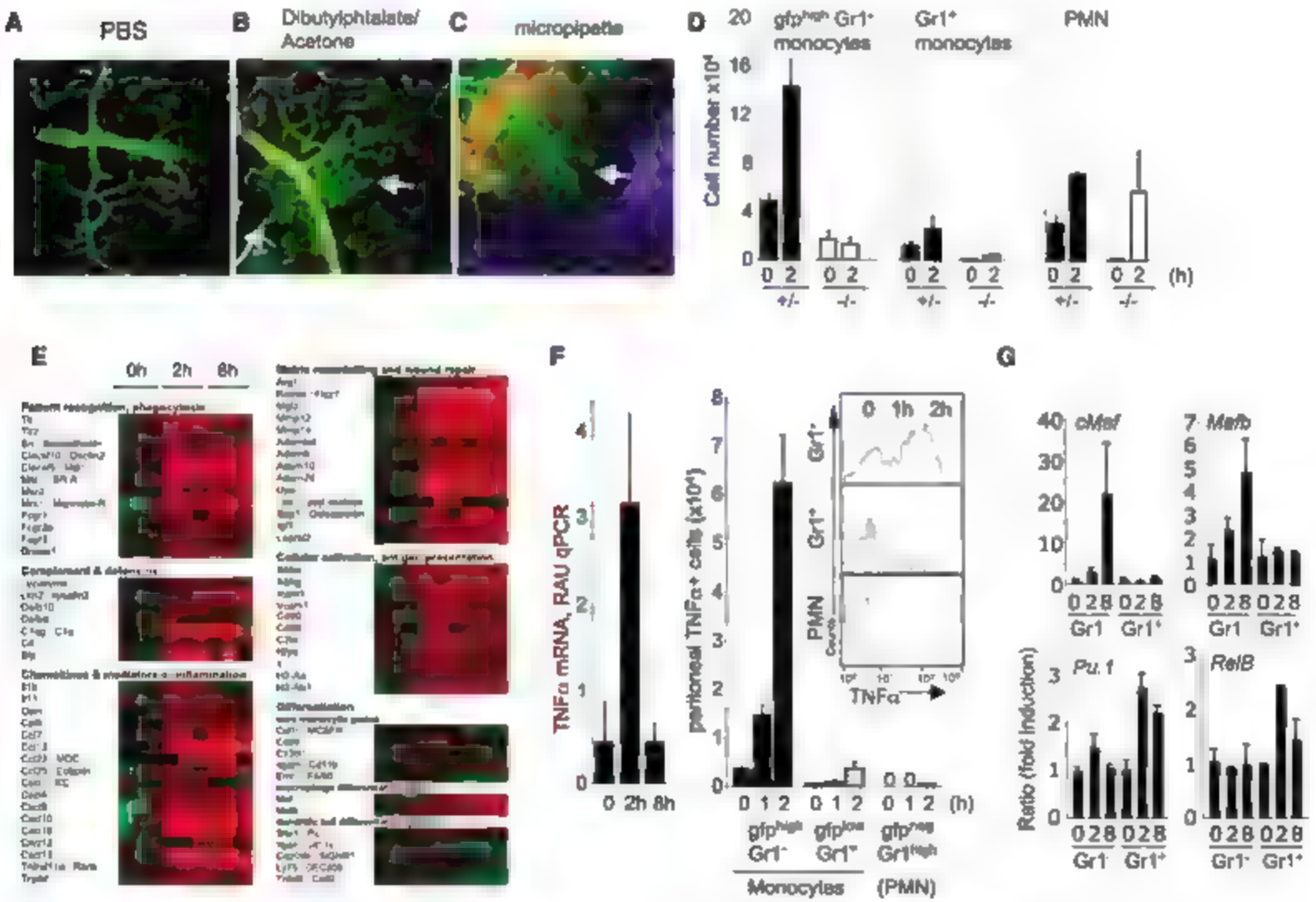

Fig. 4. Rapid tissue invasion by patrolling Gfp^{high} Gr1^{-} monocytes after tissue damage or infection. (**A** to **C**) Crawling gfp^{high} monocytes in the mouse dermis are tracked for 1 hour after application of phosphate-buffered saline (PBS) (A) or 1:1 dibutylphtalate acetone (B), or after aseptic damage with a microinjection pipette loaded with a far-red dye (shown in blue) (C). (**D**) Number of extravasated cells recovered from the peritoneal cavity of mice infected with *L. monocytogenes*. (**E**) Analysis of gene expression on purified GFP^{high} monocytes (fig. S6) (*10*). (**F**) GFP^{high} monocytes recovered from the peritoneum of infected mice are the main producers of TNFα in vivo at 2 hours after *L. monocytogenes* infection (Data are mean ± SD, $n = 3$ in each group; representative experiment out of four). (**G**) Extravasated Gr1^{-} gfp^{high} monocytes initiated a macrophage differentiation program, at the expense of DC differentiation, whereas Gr1^{+} gfp^{low} monocytes initiated a DC differentiation program. Regulation of Mafb, cMaf, Pu.1, and RelB genes was analyzed as described in figs. S6 and S7.

whereas extravasated Gr1⁻ gfp[high] monocytes turned on—at 2 and 8 hours—genes involved in tissue remodeling (22), including arginase I, Fizz1, Mgl2, and mannose receptor (MR) (Fig. 4E and fig. S9).

Indeed, the study of the balance of transcription factors that specifies the alternative macrophage or dendritic cell fate of monocytes (23) indicated that extravasated Gr1⁻ gfp[high] monocytes initiated a typical macrophage differentiation program, characterized by up-regulation of cMaf and MafB but not RelB and Pu.1 (sfpi1) (Fig. 4G and figs. S6 and S7). In contrast, the conventional Gr1⁺ gfp[low] monocytes initiated a DC differentiation program, as described previously (1, 6), by up-regulating RelB and Pu.1 but not cMaf and MafB (Fig. 4G and fig. S6). Analysis of the expression of a larger panel of genes differentially regulated in monocyte-derived macrophages and DC supported this conclusion (fig. S8).

These findings demonstrate a new mechanism of leukocyte crawling on endothelial cells and a new role for LFA-1. The present data also assign a function to gfp[high] Gr1⁻ monocytes. Patrolling of blood vessels by these resident monocytes allow rapid tissue invasion by monocytes in case of damage and infection, followed by the initiation of an innate immune response and their differentiation into macrophages. This is in contrast to the role of Gr1⁺ monocytes, which reach the inflammatory site later and give rise to inflammatory DCs (1, 6). This reveals an unsuspected dichotomy of the differentiation potential and functions of blood monocyte subsets during infection. The extravasation of patrolling Gr1⁻ gfp[high] monocytes is likely to be dependent on a yet-unidentified signal(s) from damaged tissue and/or endothelium. Interestingly, the existence of a pool of "marginated" monocytes expressing CD16⁺ has been proposed in humans (24) and may correspond, at least in part, to the patrolling behavior that we describe here, suggesting a similar in vivo function of mouse resident CX_3CR1^{high} (gfp[high]) Gr1[low] monocytes and human CX_3CR1^{high} CD16⁺ CD14[low] monocytes. Monocytes are abundant in arthritis and atherosclerotic lesions (25, 26), and CX_3CR1, TNF-α, and LFA-1 have been implicated in the pathogenesis of these inflammatory diseases (27, 28); thus, patrolling monocytes may contribute to their pathogenesis and may represent a target for treatment.

References and Notes

1. F. Geissmann, S. Jung, D. R. Littman, *Immunity* **19**, 71 (2003).
2. C. Sunderkotter et al., *J. Immunol.* **172**, 4410 (2004).
3. C. Varol et al., *J. Exp. Med.* **204**, 171 (2007).
4. D. K. Fogg et al., *Science* **311**, 83 (2006).
5. R. T. Palframan et al., *J. Exp. Med.* **194**, 1361 (2001).
6. N. V. Serbina, T. P. Salazar-Mather, C. A. Biron, W. A. Kuziel, E. G. Pamer, *Immunity* **19**, 59 (2003).
7. S. H. Naik et al., *Nat. Immunol.* **7**, 663 (2006).
8. F. Ginhoux et al., *Nat. Immunol.* **7**, 265 (2006).
9. B. Passlick, D. Flieger, H. W. Ziegler-Heitbrock, *Blood* **74**, 2527 (1989).
10. Materials and methods are available as supporting material on Science Online.
11. M. L. Smith, D. S. Long, E. R. Damiano, K. Ley, *Biophys. J.* **85**, 637 (2003).
12. T. A. Springer, *Cell* **76**, 301 (1994).
13. A. Fischer, B. Lisowska-Grospierre, D. C. Anderson, T. A. Springer, *Immunodefic. Rev.* **1**, 39 (1988).
14. G. Constantin et al., *Immunity* **13**, 759 (2000).
15. M. Phillipson et al., *J. Exp. Med.* **203**, 2569 (2006).
16. A. R. Schenkel, Z. Mamdouh, W. A. Muller, *Nat. Immunol.* **5**, 393 (2004).
17. J. F. Bazan et al., *Nature* **385**, 640 (1997).
18. A. M. Fong et al., *J. Exp. Med.* **188**, 1413 (1998).
19. T. Imai et al., *Cell* **91**, 521 (1997).
20. S. Goda et al., *J. Immunol.* **164**, 4313 (2000).
21. C. A. Haskell, M. D. Cleary, I. F. Charo, *J. Biol. Chem.* **275**, 34183 (2000).
22. G. H. Ghassabeh et al., *Blood* **108**, 575 (2006).
23. Y. Bakri et al., *Blood* **105**, 2707 (2005).
24. B. Steppich et al., *Am. J. Physiol. Cell Physiol.* **279**, C578 (2000).
25. M. Iwahashi et al., *Arthritis Rheum.* **50**, 1457 (2004).
26. A. Schlitt et al., *Thromb. Haemost.* **92**, 419 (2004).
27. H. Umehara et al., *Arterioscler. Thromb. Vasc. Biol.* **24**, 34 (2004).
28. P. Lesnik, C. A. Haskell, I. F. Charo, *J. Clin. Invest.* **111**, 333 (2003).

29. We thank M. Sieweke (CIML, Marseille, France) and N. Hogg (Cancer Research UK, London, UK) for expert advice and the gift of reagents. We are also grateful to J. L. Casanova, P. Revy, B. Lucas, and S. Amigorena for expert advice and critical reading of the manuscript; C. Grolleau (Roper Scientific, Paris, France) for expert advice in the use of the Metamorph Software; Jennifer Wong for help in setting up the imaging of mesenteric vessels; and all the members of INSERM U838 for discussion and support. C.A. was a fellow of the Fondation de France. This work was supported by grants (to F.G.) from the Fondation Schlumberger, the Agence Nationale de la Recherche (grant JRAP2005), the City of Paris, the Fondation de France, the Fondation pour la Recherche Médicale, and a European Young Investigator award.

Supporting Online Material
www.sciencemag.org/cgi/content/full/317/5838/666/DC1
Materials and Methods
Figs. S1 to S8
Table S1
References
Movies S1 to S7

22 March 2007; accepted 29 June 2007
10.1126/science.1142883

Regulation of Homeostatic Chemokine Expression and Cell Trafficking During Immune Responses

Scott N. Mueller,[1*] Karoline A. Hosiawa-Meagher,[2] Bogumila T. Konieczny,[1] Brandon M. Sullivan,[3] Martin F. Bachmann,[4] Richard M. Locksley,[3] Rafi Ahmed,[1] Mehrdad Matloubian[2]

The chemokines CCL21 and CXCL13 are immune factors that dictate homing and motility of lymphocytes and dendritic cells in lymphoid tissues. However, the means by which these chemokines are regulated and how they influence cell trafficking during immune responses remain unclear. We show that CCL21 and CXCL13 are transiently down-regulated within lymphoid tissues during immune responses by a mechanism controlled by the cytokine interferon-γ. This modulation was found to alter the localization of lymphocytes and dendritic cells within responding lymphoid tissues. As a consequence, priming of T cell responses to a second distinct pathogen after chemokine modulation became impaired. We propose that this transient chemokine modulation may help orchestrate local cellularity, thus minimizing competition for space and resources in activated lymphoid tissues.

A cardinal property of cells of the immune system is mobility, allowing them to navigate the body and combat invading pathogens. This is modulated by a complex array of chemokines and their receptors, which provide the molecular signals to direct cells to where they are required (1). Many chemokines are up-regulated in cells and tissues in response to inflammatory stimuli such as infection (2). In contrast, the lymphoid chemokines CCL21, CCL19, and CXCL13 are constitutively expressed in restricted areas for steady-state attraction of cells (3). CCL21 expression by fibroblastic reticular cells (FRCs) of the T cell zones in the spleen and lymph nodes (LN) facilitates effective interaction between dendritic cells (DCs) and T cells, whereas CXCL13 expression on follicular dendritic cells guides B cells and follicular T helper (T_H) cells into B cell zones (4, 5). The critical role of these homeostatic chemokines in attracting cells into lymphoid organs and in initiating antigen-specific responses is well established (3, 6). However, less is known about the impact that acute immune responses have on the expression of homeostatic chemokines and how this affects lymphocyte trafficking within lymphoid tissues.

[1]Emory Vaccine Center and Department of Microbiology and Immunology, Emory University School of Medicine, Atlanta, GA 30322, USA. [2]Department of Medicine, Division of Rheumatology, University of California, San Francisco, CA 94143, USA. [3]Howard Hughes Medical Institute and Department of Medicine and Department of Microbiology and Immunology, University of California, San Francisco, CA 94143, USA. [4]Cytos Biotechnology AG, Wagistrasse 25, 8952 Schlieren, Switzerland.

*To whom correspondence should be addressed. E-mail: mueller@microbio.emory.edu

To address these questions, we examined expression of CCL21 and CXCL13 in the spleen by immunofluorescence after infection of mice with lymphocytic choriomeningitis virus (LCMV) (7). In contrast to the up-regulation of chemokines observed in peripheral tissues during inflammation (8, 9), we found reduced expression of these chemokines in the spleen after LCMV infection (Fig. 1A). To examine this down-regulation in more detail, we assayed spleen homogenates for CCL21 and CXCL13 protein by enzyme-linked immunosorbent assay (ELISA). Down-regulation of the lymphoid chemokines was observed in the spleen (Fig. 1B) and also in peripheral LN (Fig. 1C and fig. S1). CCL21 down-regulation began within 3 days of infection, reaching levels 70- to 80-fold less than that detected before infection within 8 days (Fig. 1B). Importantly, modulation was transient, and we observed relatively normal CCL21 expression within 2 weeks after LCMV infection (Fig. 1B). The down-modulation of CXCL13 was also transient but with slightly delayed kinetics; levels remained low at 2 weeks after infection and returned to normal within 5 weeks (Fig. 1B). This transient modulation of the homeostatic chemokines correlated with the generation of virus-specific T and B cell responses after infection.

To determine whether regulation of lymphoid chemokine expression after infection occurred at the transcriptional level, we quantified CCL21 and CXCL13 mRNA by real-time reverse transcription polymerase chain reaction (RT-PCR). About 100-fold less CCL21 mRNA and 10-fold less CXCL13 mRNA was detectable in whole spleens, as well as in isolated cells of the

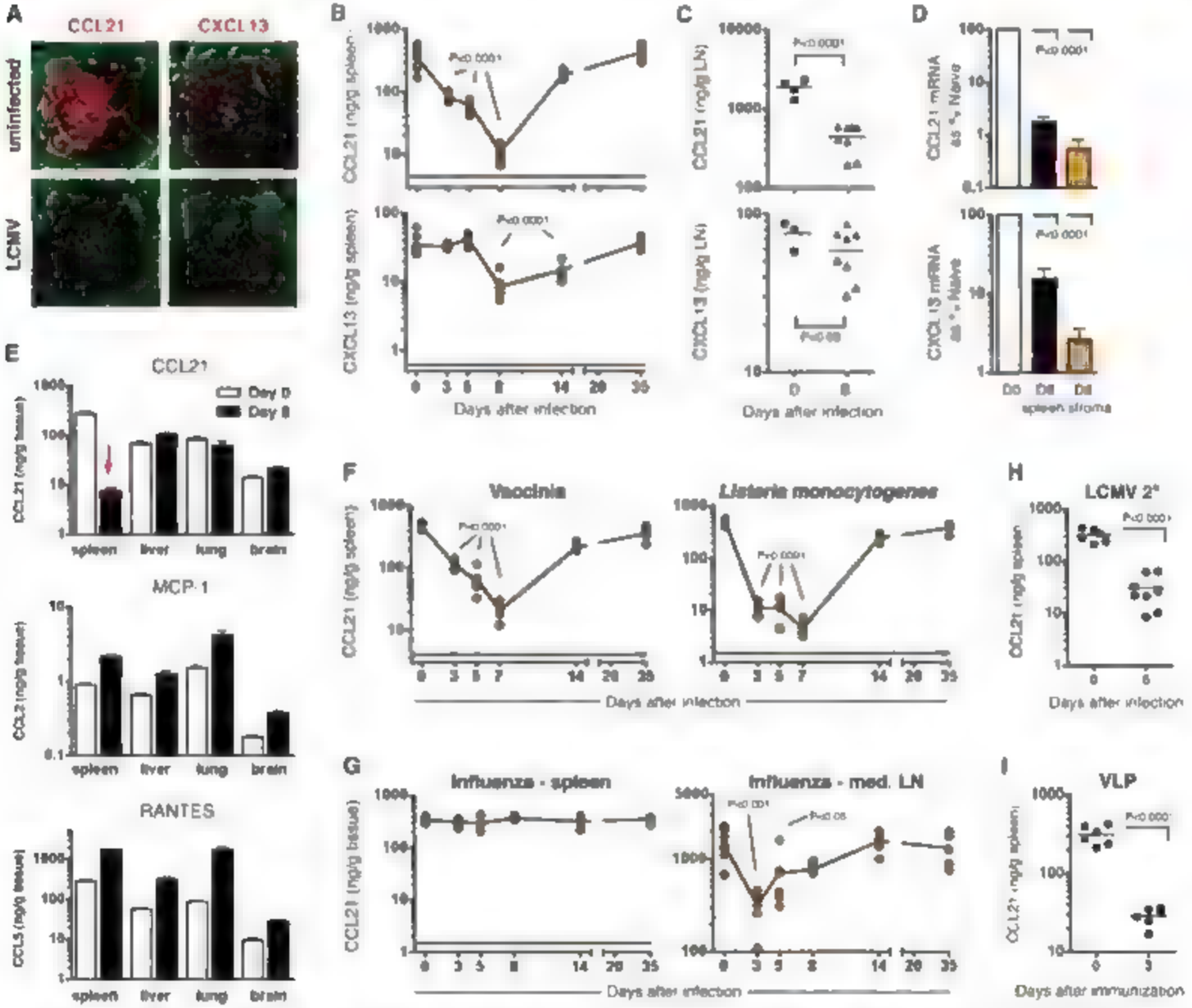

Fig. 1. Transient down-regulation of the lymphoid chemokines occurs during immune responses. (**A**) Spleens from uninfected mice (day 0), or 8 days after LCMV infection, stained for ER-TR7 (green) to detect FRC and anti-CCL21 or anti-CXCL13 (red). White regions indicate co-localization, objective magnification, 20×. (**B** and **C**) Lymphoid chemokine expression in the spleen and inguinal LN after LCMV infection, quantified by ELISA in tissue homogenates. (**D**) Quantitative RT-PCR analysis of chemokine expression in whole spleen or the stromal compartment 0 or 8 days after LCMV infection. Error bars indicate SEM. (**E**) Down-regulation of CCL21 was restricted to lymphoid organs (arrow). CCL21, CCL2 (MCP-1), and CCL5 (RANTES) expression in tissues 0 and 8 days post-LCMV infection. (**F** to **I**) Chemokine modulation during viral and bacterial infections. (F) CCL21 expression in the spleen after systemic VV infection or LM infection, (G) in the draining mediastinal LN and the spleen after intranasal influenza virus infection, (H) in the spleens of LCMV immune mice after secondary infection with LCMV, and (I) in the spleen after immunization with VLPs. *P* values were calculated by *t* test, relative to uninfected mice.

splenic stromal compartment, after LCMV infection (Fig. 1D). Down-regulation of CCL19 protein as well as mRNA was also observed in the lymphoid organs after LCMV infection (fig. S2).

Infection and inflammation can induce up-regulation of various lymphocyte-attracting chemokines in both lymphoid and nonlymphoid tissues (*10*). Interestingly, we found that down-regulation of CCL21 was restricted to lymphoid tissues (Fig. 1E). Yet, up-regulation of the inflammatory chemokines CCL2 and CCL5 occurred in both lymphoid and nonlymphoid tissues (Fig. 1E), indicating that down-regulation was specific to the homeostatic chemokines. To determine whether lymphoid chemokine modulation is a specific feature of LCMV infection or it is a more generalized feature of immune responses to pathogens, we examined chemokine levels after infection of mice with vaccinia virus (VV) or *Listeria monocytogenes* (LM). We observed marked down-regulation of CCL21 and CXCL13 in the spleen after infection with these pathogens (Fig. 1F and fig. S3). We also infected mice intranasally with influenza virus. Although down-regulation of lymphoid chemokine expression was not observed in the spleen after influenza infection, CCL21 and CXCL13 expression was modulated in the draining mediastinal LN (Fig. 1G and fig. S3). These data show that transient chemokine down-regulation occurs during both systemic and localized infections and also make the important point that modulation of lymphoid chemokine expression occurs primarily at the site of the antigen-driven immune response.

A recent study described changes in CCL21 expression after murine cytomegalovirus infection (*11*) and attributed this to virus-induced pathology. However, the modulation of chemokine expression that we found after infection with both viral and bacterial pathogens indicated that this represented a generalized programmed response. We also observed down-regulation of CCL21 during recall responses (Fig. 1H) and after immunization with virus-like particles (VLPs) containing Qβ (Fig. 1I). Similar results were obtained after immunization with ovalbumin (OVA) protein plus lipopolysaccharide

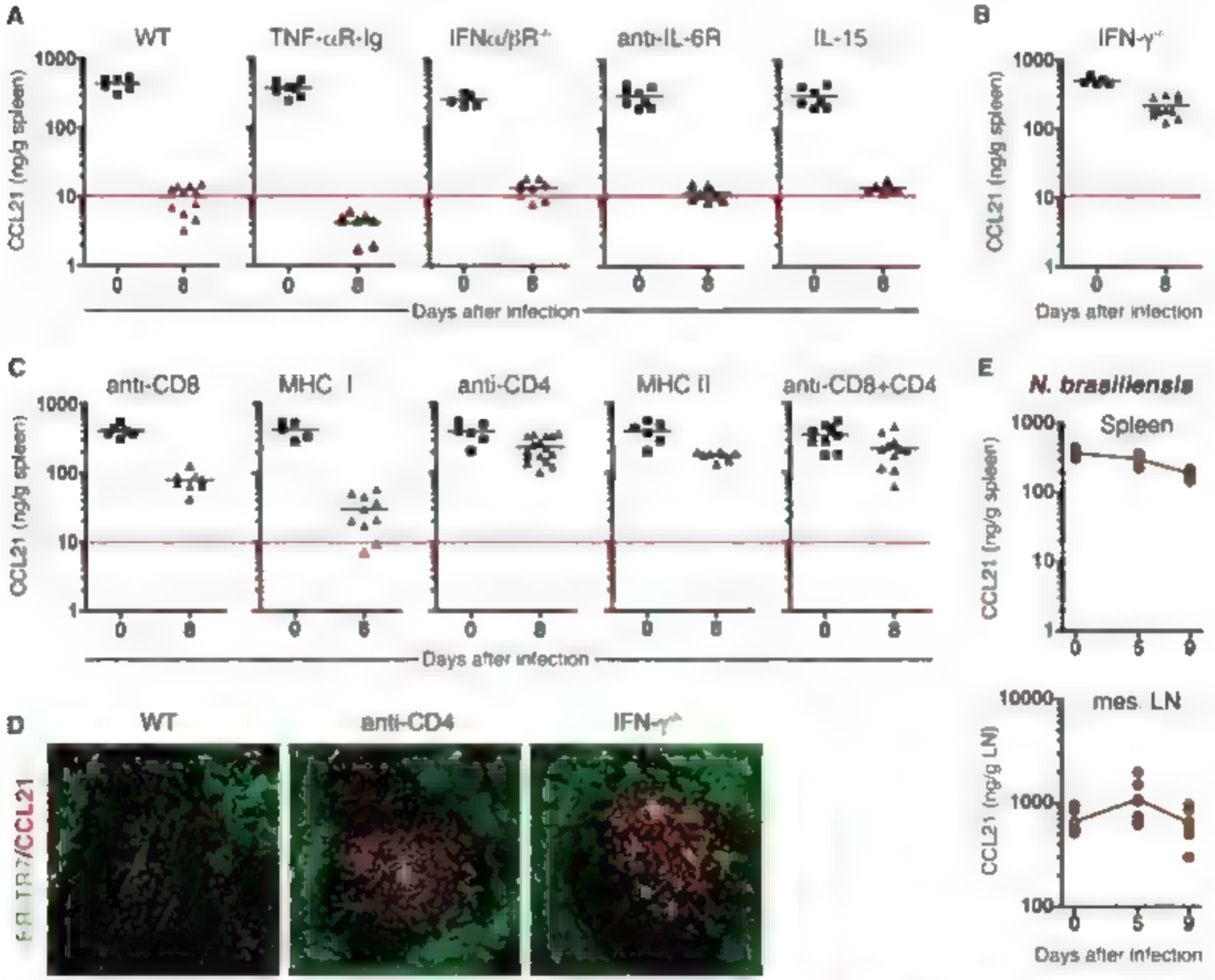

Fig. 2. Role of CD4+ T cells and IFN-γ in lymphoid chemokine down-regulation. (**A**) CCL21 expression after LCMV infection in spleens of wild-type (WT), IFNα/βR$^{-/-}$, or IL-15$^{-/-}$ mice or mice treated with sTNF-αR-Ig or IL-6R antibody. (**B**) CCL21 expression in IFN-γ$^{-/-}$ mice. (**C**) CCL21 expression after LCMV infection in spleens of WT mice depleted of CD8+ T cells (anti-CD8), CD4+ T cells (anti-CD4), or both (anti-CD8+CD4) or in mice deficient in MHC class I or class II molecules. Statistical analysis was performed on day 8 samples, relative to WT values: $P < 0.0001$ for IFN-γ$^{-/-}$, anti-CD8, anti-CD4, anti-CD8+CD4 and MHC II$^{-/-}$; for MHC I$^{-/-}$, $P = 0.0019$. Horizontal red lines represent mean CCLR21 expression in WT mice 8 days after LCMV infection. (**D**) CCL21 expression in spleens from WT, anti-CD4, and IFN-γ$^{-/-}$ mice 8 days after infection. Objective magnification, 20×. (**E**) CCL21 expression in spleen and mesenteric LN after subcutaneous infection with *N. brasiliensis*.

LPS) as an adjuvant, suggesting that pathogen replication was not necessary for chemokine modulation. Together these results suggest that lymphoid chemokine regulation is an integral feature of adaptive immune responses.

Although lymphotoxin β receptor (LTβR) signals are important for lymphoid chemokine expression during organogenesis (*12*), activation or inhibition of the LTβR pathway had minimal effect on CCL21 modulation after infection (Supporting Online Material (SOM) text 1 and fig. S4) (*11*). To understand the mechanism of lymphoid chemokine down-regulation, we determined that many innate cytokines produced after infection such as tumor necrosis factor α (TNF-α), interferon α and interferon β (IFN-α/β), interleukin-6 (IL-6), and IL-15, were not required for this lymphoid chemokine down-regulation (fig. 2A and fig. S4). Our data indicate that IL-12 and IL-1 may play a minor role in lymphoid chemokine regulation (fig. S4). Importantly, IFN-γ was required, because lymphoid chemokine down-regulation was only minimally seen after infection of IFN-γ–deficient mice (fig. 2, B and D).

To ascertain the role of T cells, we infected mice lacking major histocompatibility complex (MHC) class I or II molecules or CD8$^+$ or CD4$^+$ T cells. Minimal down-regulation of chemokine expression occurred in MHC II$^-$ or CD4-depleted mice, indicating that CD4$^+$ T cells were required (fig. 2, C and D). To further examine the role of CD4$^+$ T cells and IFN-γ production (T_H1) in chemokine modulation during immune responses, we infected mice with the nematode *Nippostrongylus brasiliensis* or the protozoa *Leishmania major*. These parasitic infections induce strong T_H2 immune responses, whereas other responses we analyzed were T_H1-driven. We observed minimal modulation of CCL21 or CXCL13 in spleen or LN after *N. brasiliensis* infection and after *L. major* infection (fig. 2I and fig. S5). Thus, we demonstrate two components of type I immune responses (CD4$^+$ T cells and IFN-γ) that are important for lymphoid chemokine modulation during immune responses.

To determine the functional consequences of lymphoid chemokine down-regulation during an ongoing immune response, we examined the migration of naïve carboxyfluorescein diacetate succinimidyl ester (CFSE) labeled CD8$^+$ T cells in the spleen, after adoptive transfer into normal and infected mice (fig. 3A). In uninfected mice the transferred naïve T cells localized predominantly to the T cell zones of the white pulp (WP) (71 ± 19.8%, fig. 3, B and F). In contrast, in LCMV-infected mice the transferred T cells accumulated in the red pulp (RP), and few were found in the WP (4.4 ± 7.2%). This alteration in naïve lymphocyte localization in the spleen after infection correlated with the degree of CCL21 down-regulation (fig. 1). Migration into the T cell zone was intact for at least 3 days after infection, whereas an intermediate phenotype was observed 5 days after infection (fig. 3, B and F). The abrogation of naïve T cell movement into the WP was directly dependent on CCL21 expression, because mice lacking CD4$^+$ T cells or IFN-γ demonstrated normal migration of CFSE$^+$ naïve T cells to the T cell zones (fig. 3, C and F), indicative of CCL21 expression in these mice. Similar results were obtained with transferred naïve CD4$^+$ T cells (fig. S6). Furthermore, mice infected with LCMV in the footpad demonstrated

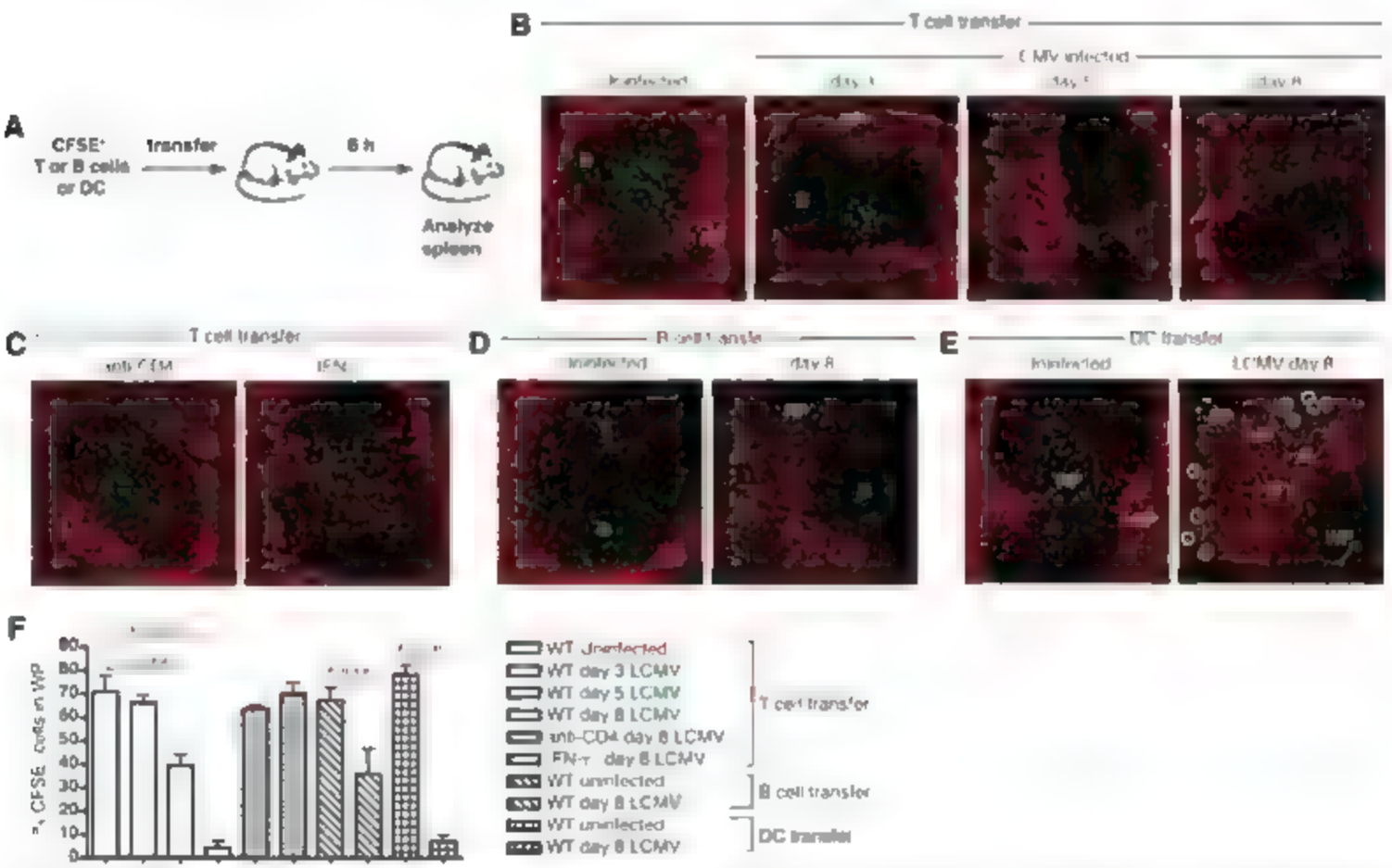

Fig. 3. Altered cell localization after lymphoid chemokine down-regulation. (**A** to **E**) Localization of transferred lymphocytes or DCs in the spleen after infection. (**A**) Naïve T or B lymphocytes or splenic DCs were purified and labeled with CFSE and transferred into mice, and their localization in the spleen was ascertained 6 hours later. CFSE$^+$ CD8$^+$ T cells were transferred into (**B**) WT mice 0 to 8 days after LCMV infection, or into (**C**) CD4-depleted (anti-CD4), or into IFN-γ$^{-/-}$ mice 8 days after infection. (**D**) CFSE$^+$ B cells or (**E**) CFSE$^+$ DCs were transferred into uninfected or day 8 LCMV-infected mice. Spleen sections were co-stained with ER-TR7 (red) to determine the localization of the CFSE$^+$ (green) cells. Objective magnification, 20×; RP, red pulp; WP, white pulp; B, B cell zone; and T, T cell zone. (**F**) Quantitation of CFSE$^+$ cells in the spleen after transfer. The proportion of CFSE$^+$ cells present in WP regions is shown. Data are representative of 5 to 9 mice per group. Error bars indicate SEM.

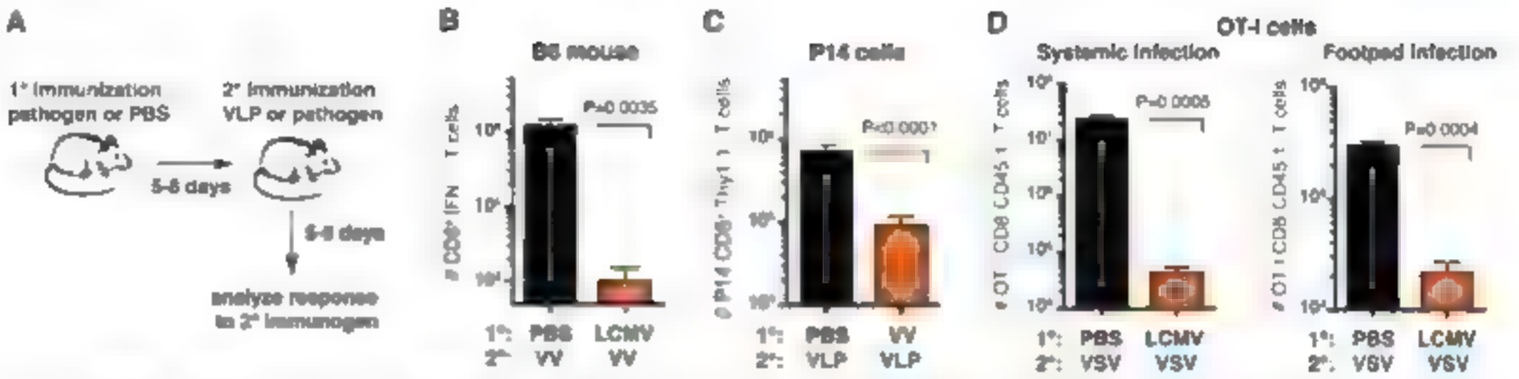

Fig. 4. Impaired priming of naïve CD8$^+$ T cells after lymphoid chemokine modulation. (**A**) Schematic of primary-secondary immunization experiments. Mice were infected with a primary pathogen or given PBS, followed by immunization with VLP or infection with a secondary pathogen after modulation of the lymphoid chemokines (day 5 for VV and day 8 for LCMV). (**B**) Expansion of VV-specific IFN-γ$^+$ CD8$^+$ T cells is shown in spleens 6 days after VV co-infection of LCMV-infected or PBS-treated mice. (**C**) Expansion of P14 Thy1.1$^+$ CD8$^+$ T cells in the spleen 6 days after VLP immunization of VV-infected mice. (**D**) Expansion of OT-I CD45.1$^+$ CD8$^+$ T cells in the spleen (systemic infection) or popliteal LN (footpad infection) 5 days after VSV-OVA infection of LCMV-infected mice. Representative data from two to three experiments are shown. Error bars indicate SEM.

a significant reduction in naïve T cell entry into the draining popliteal LN after chemokine modulation (fig. S7).

We also observed reduced migration of naïve B cells into B cell zones after infection (Fig. 3, D and F). Yet, cells were observed to home to some B cell zones, potentially reflecting the degree of local CXCL13 regulation. Differential regulation of CCL21 and CXCL13 may allow proper orchestration of T and B cell responses. Lastly, because the migration of activated DC into T cell zones is also dependent upon responsiveness to CCL21 (*13*, *14*), we examined the localization of CFSE-labeled mature DC's in the spleen after infection. DC's migrated into the T cells zones of uninfected mice, yet localized to the RP and also to the marginal zone, after infection (Fig. 3, E and F). Together, these data demonstrate that lymphoid chemokine modulation altered lymphocyte and DC localization within lymphoid T and B cell zones, potentially regulating local cellularity and antigen presentation.

These results suggested that priming of naïve T cells may be compromised after chemokine down-regulation. To examine this, we gave acutely infected mice a second distinct immunization or infection after chemokine modulation and measured responses to the second antigen (Fig. 4). Mice infected with either LCMV or LM displayed markedly reduced responses to secondary VV or LCMV infection, respectively (Fig. 4B and fig. S8). Similar results were observed in VV infected mice containing LCMV gp_{33-41}-specific P14 transgenic T cells, which were immunized with VLP containing gp_{33-41} peptide after chemokine modulation (Fig. 4C). Lastly, mice containing OVA-specific OT-I transgenic T cells were infected with LCMV systemically or in the footpad and then co-infected with a recombinant vesicular stomatitis virus expressing OVA (VSV-OVA) when the lymphoid chemokines were most reduced (day 8). Expansion of the OT-I T cells was significantly reduced in comparison with that in control phosphate-buffered saline (PBS) treated mice (Fig. 4D). Thus, altered localization of naïve T cells after down-regulation of the lymphoid chemokines may affect priming against new antigens during an ongoing response. Although other factors, such as the maturation of DCs and inhibition of cross-presentation (*15*), can affect T cell activation during immune responses, lymphoid chemokine modulation may contribute to such transient immunosuppression. Indeed, activation of naïve P14 T cells transferred after LCMV infection was abrogated corresponding with chemokine modulation, despite the presence of antigen-positive DC's in the spleen that were capable of activating T cells in vitro (fig. S9).

The size of an immune response will likely dictate the magnitude of lymphoid chemokine modulation. However, a drawback of this strategy is that it may be difficult to effectively generate an immune response to a second antigen during the period of transient chemokine down-regulation. This may be particularly relevant during acute viral infections and prime-boost vaccine regimes in instances where only a short delay separates immunization doses.

Our results suggest that, by reducing expression of the homeostatic chemokines in responding lymphoid tissues, the adaptive immune response can orchestrate local cellularity and thus competition for space and resources during ongoing immune responses. Reducing local accumulation of T cells and antigen-presenting cells may be beneficial for shutting down the immune response and promoting the generation of memory cells (SOM text 2). Further, it is possible that CCL21 modulation may work in concert with chemokine receptor and S1P1 regulation on effector cells (*16*) to promote exit from the lymphoid tissues. Because CCL21 is also important for interstitial motility of lymphocytes (*17*–*19*), modulation during immune responses may additionally affect the motility of cells within the lymphoid parenchyma. It will be interesting to determine how lymphocyte movement and trafficking through lymphoid tissues is modulated by changes in homeostatic chemokine expression during immune responses.

References and Notes

1. U. H. von Andrian, C. R. Mackay, *N. Engl. J. Med.* **343**, 1020 (2000).
2. J. J. Campbell, E. C. Butcher, *Curr. Opin. Immunol.* **12**, 336 (2000).
3. J. G. Cyster, *Annu. Rev. Immunol.* **23**, 127 (2005).
4. S. A. Luther, H. L. Tang, P. L. Hyman, A. G. Farr, J. G. Cyster, *Proc. Natl. Acad. Sci. U.S.A.* **97**, 12694 (2000).
5. S. Mori *et al.*, *J. Exp. Med.* **193**, 207 (2001).
6. R. S. Friedman, J. Jacobelli, M. F. Krummel, *Nat. Immunol.* **7**, 1101 (2006).
7. Materials and methods are available as supporting material on *Science* Online.
8. H. M. Serra, C. E. Baena-Cagnani, Y. Eberhard, *Allergy* **59**, 1219 (2004).
9. J. E. Moyron-Quiroz *et al.*, *Nat. Med.* **10**, 927 (2004).
10. B. Moser, P. Loetscher, *Nat. Immunol.* **2**, 123 (2001).
11. C. A. Benedict *et al.*, *PLoS Pathog.* **2**, e16 (2006).
12. C. F. Ware, *Annu. Rev. Immunol.* **23**, 787 (2005).
13. H. Saeki, A. M. Moore, M. J. Brown, S. T. Hwang, *J. Immunol.* **162**, 2472 (1999).
14. M. D. Gunn *et al.*, *J. Exp. Med.* **189**, 451 (1999).
15. N. S. Wilson *et al.*, *Nat. Immunol.* **7**, 165 (2006).
16. L. R. Shiow *et al.*, *Nature* **440**, 540 (2006).
17. T. Okada, J. G. Cyster, *J. Immunol.* **178**, 2973 (2007).
18. T. Worbs, T. R. Mempel, J. Bölter, U. H. von Andrian, R. Förster, *J. Exp. Med.* **204**, 489 (2007).
19. M. Bajenoff *et al.*, *Immunity* **25**, 989 (2006).

20. We thank J. Browning for murine LTβR-Ig, a fusion protein of mouse LTβR and human immunoglobulin G (hIgG). This work was supported by grant AI30048 from the NIH to R.A., S.M. was funded by a C. J. Martin postdoctoral fellowship from the National Health and Medical Research Council of Australia. M.M. was supported by research awards from the Arthritis Foundation, the Rosalind Russell Medical Research Center for Arthritis at UCSF, and the Sandler Family Supporting Foundation.

Supporting Online Material

www.sciencemag.org/cgi/content/full/317/5838/670/DC1
Materials and Methods
SOM Text
Figs. S1 to S9
References

8 May 2007; accepted 3 July 2007
10.1126/science.1144830

Negative Regulation of Toll-Like Receptor Signaling by NF-κB p50 Ubiquitination Blockade

Ruaidhrí J. Carmody, Qingguo Ruan, Scott Palmer, Brendan Hilliard, Youhai H. Chen*

Toll-like receptors (TLRs) trigger the production of inflammatory cytokines and shape adaptive and innate immunity to pathogens. We report the identification of B cell leukemia (Bcl)–3 as an essential, negative regulator of TLR signaling. By blocking ubiquitination of p50, a member of the nuclear factor (NF)-κB family, Bcl-3 stabilizes a p50 complex that inhibits gene transcription. As a consequence, Bcl-3–deficient mice and cells were found to be hypersensitive to TLR activation and unable to control responses to lipopolysaccharides. Thus, p50 ubiquitination blockade by Bcl-3 limits the strength of TLR responses and maintains innate immune homeostasis. These findings indicate that the p50 ubiquitination pathway can be selectively targeted to control deleterious inflammatory diseases.

Toll-like receptor (TLR) activation is essential for the development of innate immunity to pathogens (*1*, *2*). However, repeated or prolonged activation of TLRs can render them insensitive or hyporesponsive to subsequent ligand stimulation. This phenomenon is referred to as TLR tolerance (*3*). The molecular mechanisms of TLR tolerance are not well understood, although several negative regulators of TLR signaling have been implicated (*4*–*10*). Bcl-3 is a nuclear member of the inhibitor of NF-κB (IκB) family, which interacts exclusively with the transcriptionally inactive homodimers of p50 and p52, two members of the NF-κB family (*11*–*13*). *Bcl3* deficiency in mice disrupts the microarchitecture of lymphoid organs but does not affect the development of lymphoid or myeloid cells (*14*, *15*). To explore the roles of Bcl-3 in immunity and tolerance, we examined the phenotype and function of *Bcl3*-deficient cells. We found that, although *Bcl3* deficiency did not affect cell surface marker expression or phagocytotic function (fig. S1), *Bcl3*$^{-/-}$ macrophages, dendritic cells, and B cells produced significantly more cytokines than wild-type (WT) cells upon stimulation with several TLR ligands (fig. 1 and figs. S2 and S3).

Department of Pathology and Laboratory Medicine, University of Pennsylvania School of Medicine, Philadelphia, PA 19104, USA.

*To whom correspondence should be addressed. E-mail: yhc@mail.med.upenn.edu

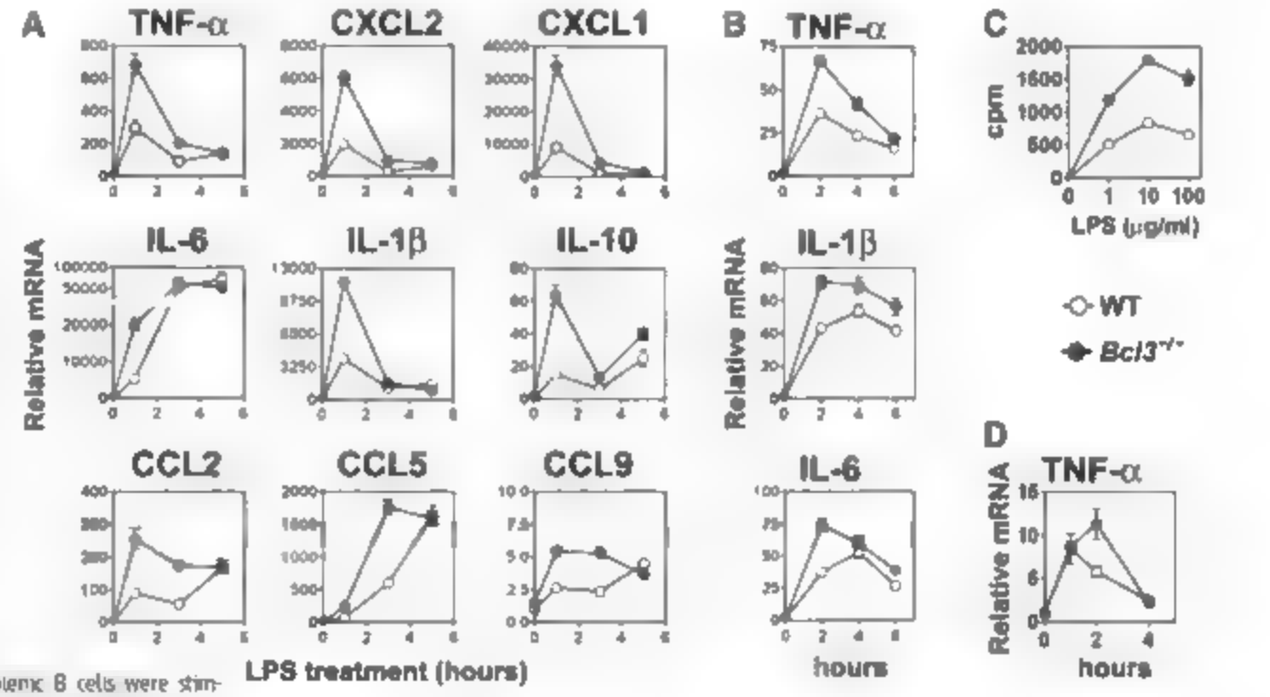

Fig. 1. Bcl-3 inhibits cytokine gene expression and controls NF-κB dimer exchange at gene promoters. (**A**) *Bcl3*$^{-/-}$ macrophages are hyperresponsive to LPS. Bone marrow–derived (BMD) macrophages were stimulated with LPS, and cytokine mRNA was quantified by real-time polymerase chain reaction (PCR) (*25*). Error bars indicate ±SEM. (**B**) *Bcl3*$^{-/-}$ dendritic cells are hyperresponsive to LPS. BMD dendritic cells were stimulated with LPS, and gene expression was measured by real-time PCR. (**C**) Enhanced proliferation of *Bcl3*$^{-/-}$ B cells to LPS. Splenic B cells were stimulated with LPS, and ^{3}H-thymidine incorporation was measured as count per minute (cpm). (**D**) Enhanced gene expression in *Bcl3*$^{-/-}$ B cells. B cells were stimulated with LPS, and *TNFα* gene expression was measured by real-time PCR. (**E**) *Bcl3*$^{-/-}$ macrophages have reduced p50 DNA binding. Nuclear extracts from BMD macrophages were tested by EMSA with the consensus NF-κB–binding sequence and indicated antibodies. Arrow indicates p50 complexes. (**F**) Altered NF-κB dimer loading and exchange at gene promoters in *Bcl3*$^{-/-}$ macrophages. BMD macrophages were treated with LPS, and ChIP was performed with antibodies to the indicated factors.

Additionally, *Bcl3*$^{-/-}$ macrophages were also hypersensitive to interleukin (IL)-1β and tumor necrosis factor (TNF) α stimulation (fig. S3).

The hyperresponsiveness of *Bcl3*$^{-/-}$ cells was not due to increased receptor-proximal signaling (fig. S4A) but could be blocked by a NF-κB inhibitor (fig. S3F). In response to lipopolysaccharides (LPS), *Bcl3*$^{-/-}$ cells displayed a marked reduction in nuclear p50 DNA binding relative to WT controls (Fig. 1E), although nuclear translocations of p50, p65, and c-Rel were normal (fig. S4B). Chromatin immunoprecipitation (ChIP) analysis revealed a similar reduction in p50 binding to promoters of *TNFα* and *CXCL2* (*chemokine C-X-C motif ligand 2*) genes in *Bcl3*$^{-/-}$ cells (Fig. 1F). In unstimulated WT macrophages, *TNFα* and *CXCL2* promoters contained only the p50 subunit of NF-κB, indicating the

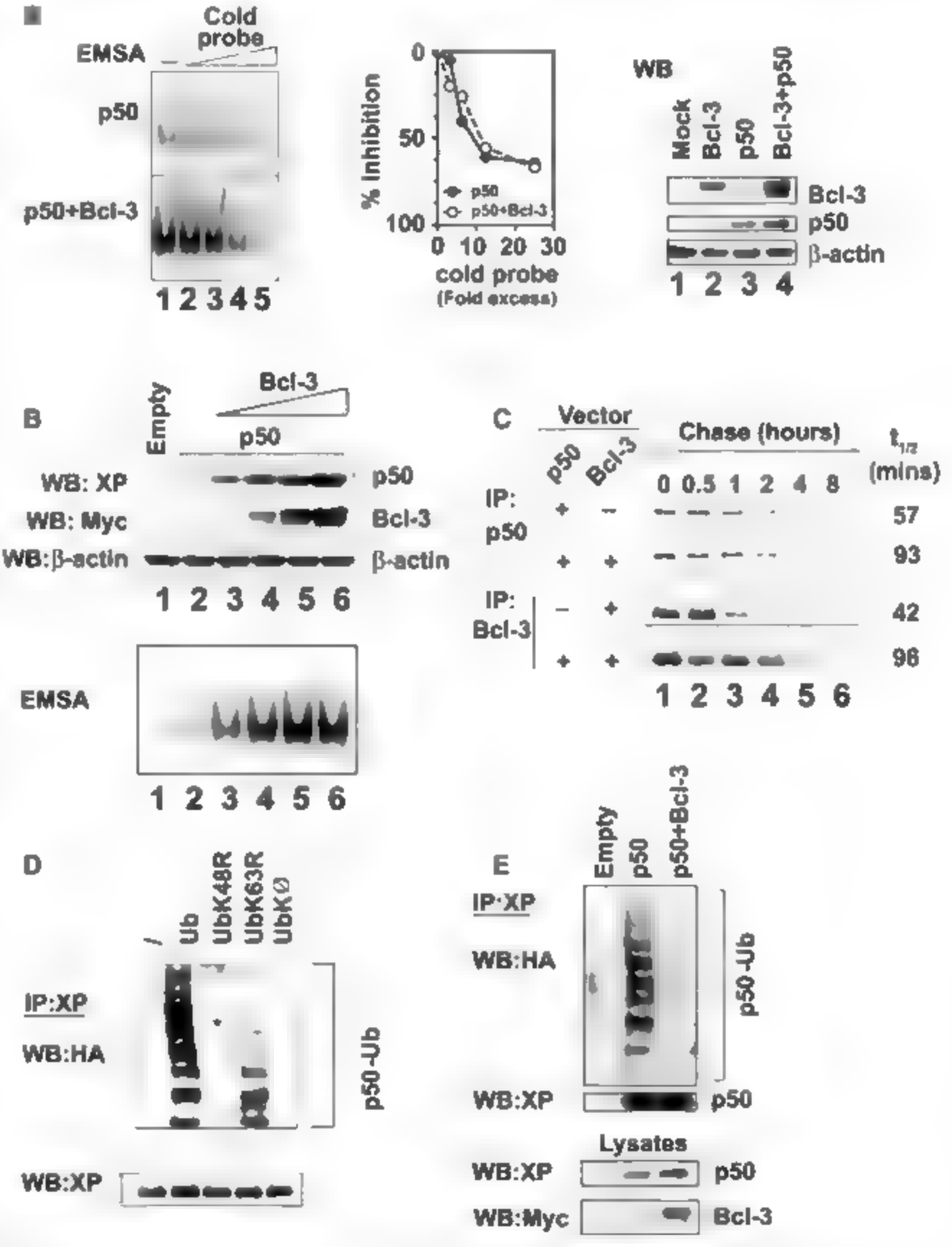

Fig. 2. Bcl-3 inhibits p50 ubiquitination and degradation. (**A**) Bcl-3 increases p50 homodimer binding to DNA without altering its affinity. Human embryonic kidney (HEK) 293T cells were transfected with p50 and Bcl-3 expression plasmids. EMSA was performed with increasing amounts of unlabeled NF-κB consensus oligonucleotides (cold probe) (left), and p50 homodimer DNA binding was measured by densitometry (middle). Relative protein levels were determined by immunoblotting of whole-cell extracts (right). WB, Western blot. (**B**) Increased p50 homodimer DNA binding is associated with increased amounts of p50 protein. HEK 293T cells were transfected with XP-p50 and increasing amounts of myc-Bcl-3 plasmids. p50 and Bcl-3 levels were measured in whole-cell lysates by immunoblotting (top), and p50 homodimer DNA binding was measured by EMSA (bottom). Empty, empty vector alone. (**C**) Bcl-3 increases the half-life of p50. HEK 293T cells were cotransfected with XP-p50 and empty vector or myc-Bcl-3, and the half-life ($t_{1/2}$) of proteins was determined (*25*). IP, immunoprecipitation. (**D**) p50 undergoes Lys^{48} (K48) polyubiquitination. HEK 293T cells were transfected with XP-p50 and expression vectors encoding either WT, Lys^{48}→Arg^{48} (K48R) mutant, Lys^{63}→Arg^{63} (K63R) mutant, or lysine-less (KØ) HA-tagged ubiquitin (Ub). Lysates were immunoprecipitated with antibody against XP and immunoblotted with antibody against HA. (**E**) Bcl-3 inhibits p50 ubiquitination. HEK 293T cells were transfected with XP-p50 and HA-ubiquitin with or without myc-Bcl-3. Ubiquitination was determined as in (D).

presence of p50 homodimer binding. After stimulation with LPS, p50 was transiently replaced by c-Rel and p65 dimers (Fig. 1F). Five hours after stimulation, both *TNFα* and *CXCL2* promoters reverted to the state of p50 occupancy (Fig. 1F). In contrast, unstimulated *Bcl3*$^{-/-}$ macrophages lacked p50 homodimers on the *TNFα* and *CXCL2* promoters, which were instead occupied by p65, c-Rel, and p50 dimers (Fig. 1F). The order of p65 and c-Rel dimer exchange on both *TNFα* and *CXCL2* promoters was severely disrupted in LPS-stimulated *Bcl3*$^{-/-}$ cells (Fig. 1F), indicating an essential role for Bcl-3 and p50 homodimers in regulating NF-κB DNA binding and transcriptional output of target genes.

Although Bcl-3 has previously been reported to enhance p50 homodimer DNA binding (*16*, *17*), the established picomolar dissociation constant of p50 homodimers suggests that any further increase in their affinity is unlikely to be significant (*18*, *19*). In support of this, we observed no measurable differences in the binding affinity of p50 homodimers in the presence or absence of overexpressed Bcl-3 despite a clear increase in p50 DNA binding in cells overexpressing Bcl-3 (Fig. 2A). Overexpressing Bcl-3 increased p50 protein levels in a dose-dependent manner, leading to increased p50 DNA binding, as shown in an electrophoretic mobility shift assay (EMSA) (Fig. 2B). Pulse chase analysis demonstrated that the half-life of p50 protein (57 min) was almost doubled in cells overexpressing Bcl-3 (93 min) (Fig. 2C). These results indicate that Bcl-3 increases p50 DNA binding by extending the half-life of p50 rather than by enhancing its affinity to DNA.

To determine the potential roles of Lys^{48}-mediated ubiquitination pathway in the turnover of p50 homodimers, we examined the polyubiquitination of both overexpressed and endogenous p50. Overexpressed p50 underwent constitutive Lys^{48}-mediated polyubiquitination, which was dramatically inhibited by Bcl-3 (Fig. 2F). Significant ubiquitination of endogenous p50 was detected only after LPS stimulation, which was markedly increased in *Bcl3*$^{-/-}$ macrophages (Fig. 3A). The increased ubiquitination of p50 in *Bcl3*$^{-/-}$ cells led to a fourfold reduction in its half-life (63 min versus 240 min in WT cells) (Fig. 3B). Importantly, *Bcl3* deficiency did not affect the half-life of p65, c-Rel, or the p50 precursor p105. Mutation of Tyr^{57} and Gly^{60} in the DNA binding domain of p50 (*20*) gave rise to a DNA binding defective mutant, p50^{Y57A,G60D}, that was unable to bind to DNA (Fig. 3C) but retained the ability to interact with p65 and Bcl-3 (fig. S5). Ubiquitination of p50^{Y57A,G60D} was dramatically reduced compared with that of WT p50 (Fig. 3D). This was associated with a significant increase in p50^{Y57A,G60D} half-life (Fig. 3E). Taken together, these results establish that p50 homodimer binding to DNA triggers its polyubiquitination and degradation, which are effectively blocked by Bcl-3.

We next examined whether Bcl-3 played a role in TLR tolerance, because p50 homodimers have previously been implicated in this process (*21*). WT and *Bcl3*$^{-/-}$ macrophages were treated with LPS for 24 hours (to induce tolerance), rested, and restimulated with LPS. Pretreatment of WT cells with LPS induced tolerance, characterized by reduced cytokine gene expression upon restimulation (Fig. 4A). By contrast, LPS pretreatment of *Bcl3*$^{-/-}$ macrophages not only failed to repress cytokine gene expression but significantly increased *IL6* and *CCL2* expression upon restimulation (Fig. 4A). *Bcl3* deficiency did not significantly alter the expression of other negative regulators of TLRs or receptor-proximal signals in tolerized cells (fig. S6). However, like IRAK-M (IL-1 receptor associated kinase-M), SOCS-1 (suppressor of cytokine signaling 1), and A20, Bcl-3 was significantly upregulated in tolerized macrophages (fig. S6). As expected, Bcl-3 knockdown by RNA interference diminished LPS tolerance (fig. S7), whereas Bcl-3 overexpression significantly inhibited *TNFα* promoter activity (fig. S8). Re-stimulation of tolerized WT macrophages with LPS led to p50 homodimer binding to the *TNFα* promoter, whereas in *Bcl3*$^{-/-}$ macrophages restimulation led to p65 dimer binding (Fig. 4B). Thus, Bcl-3 mediates LPS tolerance by stabilizing the p50 homodimer on the *TNFα* promoter and by preventing the binding of transcriptionally active p65 dimer.

To determine the roles of Bcl-3 in vivo, we studied TLR tolerance in bone marrow chimeric mice that did or did not express Bcl-3 in their hematopoietic cells. Mice were first tolerized with low doses of LPS and challenged with increasing doses of LPS. LPS pretreatment protected all mice that received WT bone marrow from septic shock. By contrast, the vast majority of mice that received *Bcl3*$^{-/-}$ bone marrow died of the disease a few days after LPS challenge (Fig. 4C).

Taken together, these results establish that Bcl-3 promotes p50 homodimer occupancy of target gene promoters by inhibiting the ubiquitination and subsequent degradation of DNA-bound p50 homodimers. We propose that this state of Bcl-3–p50 homodimer-mediated pro-

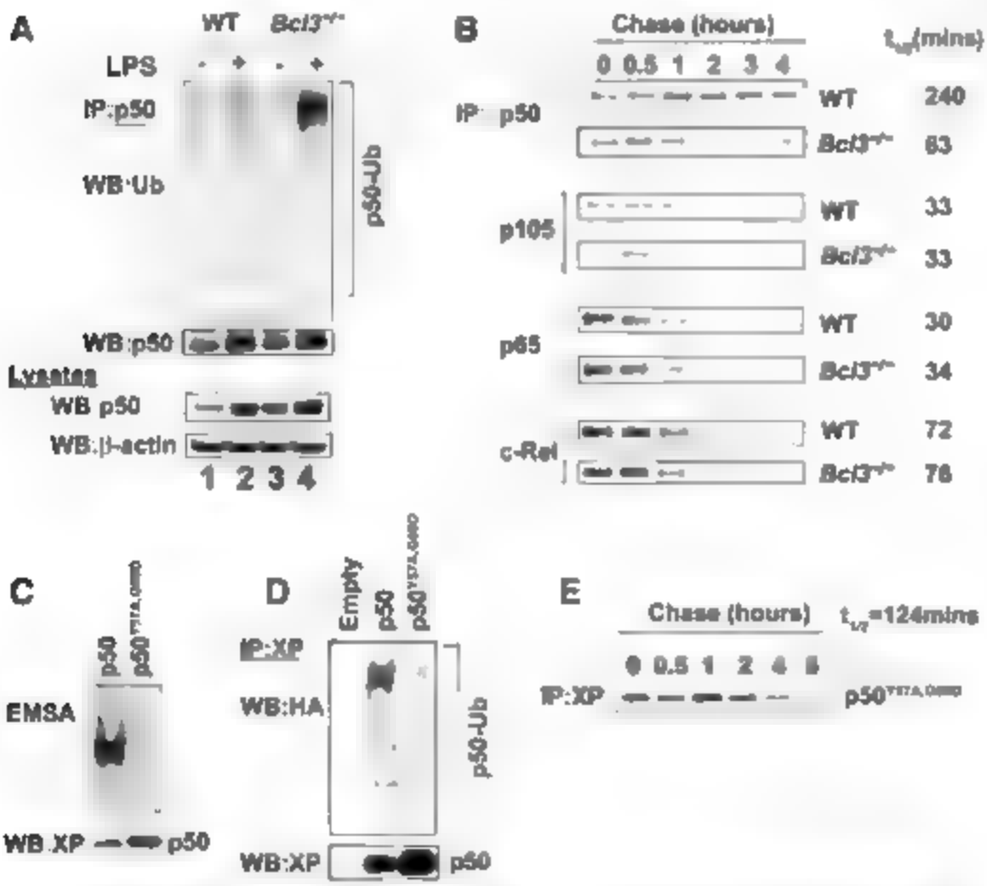

Fig. 3. *Bcl3*$^{-/-}$ macrophages have increased p50 ubiquitination and degradation. (**A**) Increased ubiquitination of p50 in *Bcl3*$^{-/-}$ macrophages. BMD macrophages were treated with (+) or without (–) LPS for 16 hours. Equal amounts of protein were immunoprecipitated with antibody against p50 and immunoblotted with antibody against ubiquitin. (**B**) Reduced p50 half-life in *Bcl3*$^{-/-}$ macrophages. BMD macrophages were treated with LPS, pulse-labeled with ^{35}S-methionine cysteine, and tested as in Fig. 2C. (**C**) Generation of a p50 mutant that does not bind to DNA. HEK 293T cells were transfected with XP-p50 or an XP-p50 mutant containing Lys^{57}–Ala^{57} (Y57A) and Gly^{60}–Asp^{60} (G60D) substitutions in the DNA binding domain. EMSA was performed with the consensus NF-κB binding sequence. (**D**) The p50 mutant is resistant to ubiquitination. Cells were transfected with HA-ubiquitin plus XP-p50, XP-p50^{Y57A,G60D}, or empty vector. Ubiquitination was determined as in Fig. 2D. (**E**) The p50 mutant has a significantly increased half-life. HEK 293T cells were co-transfected with XP-p50 or XP-p50^{Y57A,G60D}, and protein half-life was determined (*25*).

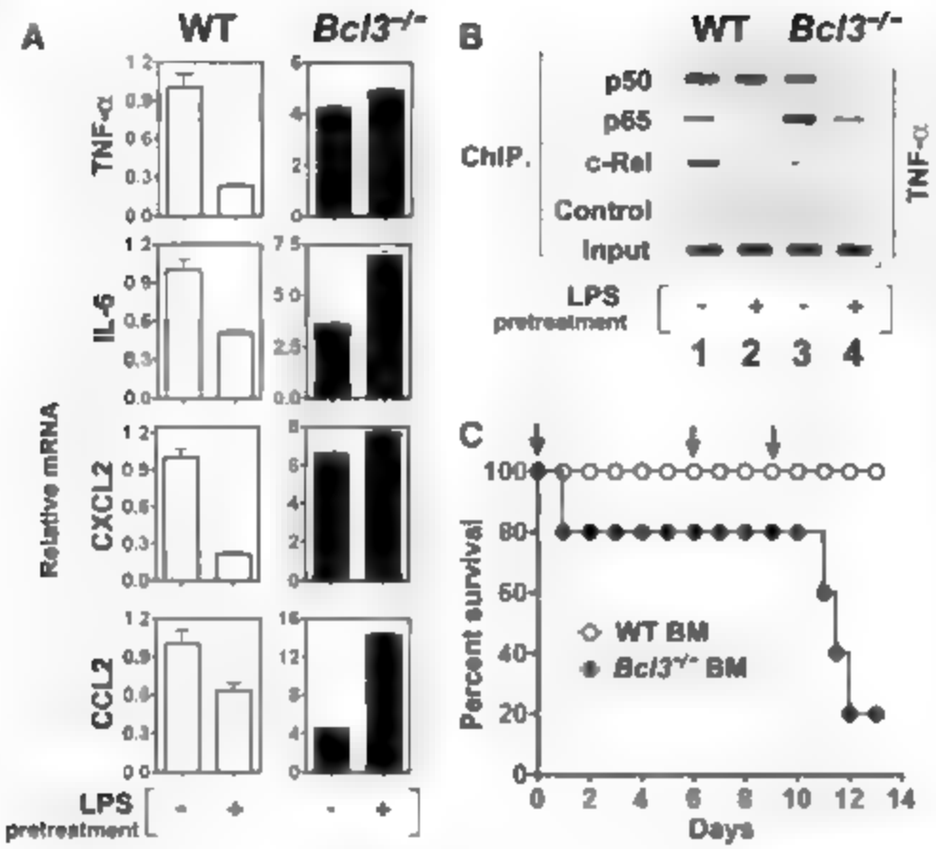

Fig. 4. *Bcl3* deficiency in mice and macrophages abolishes LPS tolerance. (**A**) Lack of LPS tolerance in $Bcl3^{-/-}$ macrophages. BMD macrophages were pretreated with (+) or without (–) LPS for 24 hours. After 1 hour of resting, cells were restimulated with LPS for an additional hour. mRNA levels were determined by real-time PCR. (**B**) Reduced p50 homodimer binding to *TNFα* promoter in $Bcl3^{-/-}$ macrophages under tolerizing conditions. BMD macrophages were treated as in (A). ChIP was performed with antibodies to p50, p65, and c-Rel. (**C**) *Bcl3* deficiency in hematopoietic cells renders mice hypersensitive to septic shock. WT mice were lethally irradiated and reconstituted with either WT or $Bcl3^{-/-}$ bone marrow (BM) cells (n from 3 to 5) (*25*). Eight weeks later, chimeric mice were tolerized with two consecutive injections of low dose LPS (5 mg/kg on day –5 and 10 mg/kg on day –3) and then challenged with three high doses of LPS (15 mg/kg on day 0, 30 mg/kg on day 6, and 90 mg/kg on day 9 as indicated by arrows). Data shown are survival curves of the two groups. The difference between the two groups is statistically significant ($P < 0.01$). Error bars indicate ± SEM.

moter unresponsiveness is the molecular basis of TLR tolerance. Neither Bcl-3 nor p50 alone is sufficient to maintain the tolerant state of gene promoters (Fig. 4) (*22*). In the absence of Bcl-3–p50 complex, the loading of NF-κB subunits on target promoters and the subsequent dimer exchange, critical for appropriate gene expression (*23*, *24*), are disrupted, leading to aberrant expression of inflammatory cytokines. Thus, TLR tolerance and suppression are dependent on the coordinated action of both the activator p50 and its stabilizer, Bcl-3 (fig. S9 and SOM text). These findings provide important insights into the molecular mechanisms of TLR signaling and suggest that deleterious inflammatory responses can be effectively controlled by targeting the NF-κB p50 ubiquitination pathway.

References and Notes

1. S. Akira, K. Takeda, *Nat. Rev. Immunol.* **4**, 499 (2004).
2. A. Iwasaki, R. Medzhitov, *Nat. Immunol.* **5**, 987 (2004).
3. A. E. Medvedev, I. Sabroe, J. D. Hasday, S. N. Vogel, *J. Endotoxin Res.* **12**, 133 (2006).
4. F. Y. Liew, D. Xu, E. K. Brint, L. A. O'Neill, *Nat. Rev. Immunol.* **5**, 446 (2005).
5. R. J. Carmody, Y. H. Chen, *Cell. Mol. Immunol.* **4**, 31 (2007).
6. K. Kobayashi *et al.*, *Cell* **110**, 191 (2002).
7. D. L. Boone *et al.*, *Nat. Immunol.* **5**, 1052 (2004).
8. R. Nakagawa *et al.*, *Immunity* **17**, 677 (2002).
9. I. Kiriyo *et al.*, *Immunity* **17**, 583 (2002).
10. E. K. Brint *et al.*, *Nat. Immunol.* **5**, 373 (2004).
11. L. D. Kerr *et al.*, *Genes Dev.* **6**, 2352 (1992).
12. G. P. Nolan *et al.*, *Mol. Cell. Biol.* **13**, 3557 (1993).
13. J. Inoue, T. Takahara, T. Akizawa, O. Hino, *Oncogene* **8**, 2067 (1993).
14. G. Franzoso *et al.*, *Immunity* **6**, 479 (1997).
15. E. M. Schwarz, P. Krimpenfort, A. Berns, I. M. Verma, *Genes Dev.* **11**, 187 (1997).
16. M. Watanabe, T. Inamura, T. Shonoda, T. Fujita, *EMBO J.* **16**, 3609 (1997).
17. J. H. Caamano, P. Perez, S. A. Lira, R. Bravo, *Mol. Cell. Biol.* **16**, 1342 (1996).
18. M. B. Urban, P. A. Baeuerle, *Genes Dev.* **4**, 1975 (1990).
19. G. Natoli, S. Saccani, D. Bosisio, I. Marazzi, *Nat. Immunol.* **6**, 439 (2005).
20. G. Ghosh, G. van Duyne, S. Ghosh, P. B. Sigler, *Nature* **373**, 303 (1995).
21. H. W. Ziegler-Heitbrock *et al.*, *J. Biol. Chem.* **269**, 17001 (1994).
22. J. Bohuslav *et al.*, *J. Clin. Invest.* **102**, 1645 (1998).
23. S. Saccani, S. Pantano, G. Natoli, *Mol. Cell* **11**, 1563 (2003).
24. D. Bosisio *et al.*, *EMBO J.* **25**, 798 (2006).
25. Materials and methods are available as supporting material on *Science* Online.

26. The authors thank K. Keeshan, M. May, and X. Yang for valuable discussion and critical evaluation of this work and M. Walsh for providing hemagglutinin (HA)-ubiquitin and its mutants. This work was supported by grants from the NIH (AI50059, DK070691, and AI069289).

Supporting Online Material

www.sciencemag.org/cgi/content/full/317/5838/675/DC1

SOM Text
Figs. S1 to S9

23 March 2007; accepted 27 June 2007
10.1126/science.1142953

Immune-like Phagocyte Activity in the Social Amoeba

Guokai Chen,[1]* Olga Zhuchenko,[1]* Adam Kuspa[1,2,3]†

Social amoebae feed on bacteria in the soil but aggregate when starved to form a migrating slug. We describe a previously unknown cell type in the social amoeba, which appears to provide detoxification and immune-like functions and which we term sentinel (S) cells. S cells were observed to engulf bacteria and sequester toxins while circulating within the slug, eventually being sloughed off. A Toll-interleukin 1 receptor (TIR) domain protein, TirA, was also required for some S cell functions and for vegetative amoebae to feed on live bacteria. This apparent innate immune function in social amoebae, and the use of TirA for bacterial feeding, suggest an ancient cellular foraging mechanism that may have been adapted to defense functions well before the diversification of the animals.

Phagocytes that engulf bacteria, first described by Metchnikoff in 1883, form part of the innate immune system of animals in the defense against pathogens (*1*–*4*). Both plants and animals also use innate signaling pathways as a means of sensing microbial pathogens, mainly through Toll-like receptors (TLRs) in animals and resistance (R) proteins in plants (*5*, *6*). Both TLRs and R proteins bind to bacterial effectors through leucine-rich repeats (LRRs) and

signal through adaptor effector proteins such as those containing TIR domains (*4, 6, 8*); thus, in turn, initiates the transcriptional programs that mediate specific defense responses (*4, 9, 10*).

The social amoeba *Dictyostelium discoideum* lives in the soil and feeds on bacteria, so it must defend against environmental toxins and pathogens. However threats to *Dictyostelium*'s survival must also occur during its development, when amoebae aggregate to form a multicellular organism within a semipermeable sheath and eventually produce a fruiting body with spores resistant to environmental dangers and held aloft by a cellular stalk (*11*). Before the formation of fruiting bodies, the cells can migrate as slug-like organisms for several days. During this time, exposure to toxins or bacterial pathogens have the potential of compromising survival by limiting spore production.

We sought to examine potential protective or detoxification pathways that might exist in the social amoeba. To visualize such pathways, we used fluorescent dyes as surrogates for the environmental toxins that *Dictyostelium* slugs might encounter in the soil (*12*). Five fluorescent dyes that we tested were all found to accumulate within a small subset of cells that were scattered throughout the slug (fig. S1) (*13*). Ethidium bromide (EB) displayed the highest differential accumulation within these cells (Fig. 1, A and B). The selective retention of EB suggests that these cells are a distinct population, and the EB labeling allowed us to track the migration of these cells within the slug.

The cells appeared to circulate within the slug as single cells, moving laterally, forward and backward relative to the other cells. The cells also clumped together into immobile groups of 5 to 10 cells that were seen to attach to the inner surface of the slug sheath. These cell clumps were left behind in the discarded sheath as the slug continued to migrate, being deposited at regular intervals (Fig. 1, A and B). Microscopic examination of disaggregated slugs revealed that the identified cells sequester EB within large vesicles (Fig. 1C) and that their numbers within slugs remained stable over time (~1% of slug cells). Because the cells were continuously sloughed off, this suggests that new cells arise continuously within the slug. The cells' ability to sequester EB, along with their movement within, and exit from, the slug suggests that they mediate toxin removal, so we refer to them as sentinel cells, or S cells.

When naïve slugs were disaggregated and exposed to EB, ~1% of the cells sequestered the dye in cytoplasmic vesicles within minutes and came to resemble S cells (Fig. 1D). The number and appearance of these cells did not change over several hours, suggesting that these were S cells present in the stem cell population before EB exposure. We next purified S cells by fluorescence-activated cell sorting (FACS) (fig. S2A) to determine their ability to take up additional EB (*12*) and found that S cells could sequester at least 10 times as much EB as non–S cells after 15 min of exposure (Fig. 1E to G). Similar results were obtained when purified S cells were incubated with another dye, acridine orange (Fig. 1H). This demonstration of dye accumulation by S cells in dilute suspension suggests how S cells might aid in toxin removal from the slug, thus sparing prespore cells from genotoxic stress. EB-exposed S cells also displayed reduced viability, increased sensitivity to killing by ultraviolet light and a higher mutation frequency than other slug cells (fig. S2). S cells appeared to be present in five other species of *Dictyostelia* that we examined as identified by the pattern of cellular EB accumulation within migrating slugs and slime trails (fig. S3), which suggests that they represent a generic characteristic of the social amoeba (*14*).

To determine whether the S cells represent a distinct cell type, we purified them by FACS and estimated the level of specific mRNAs by quantitative, reverse transcriptase polymerase chain reaction (qRT-PCR) (*12*). Genes were examined that distinguished the major cell types, represented in Fig. 2A (*15–17*). The expression of prespore, prestalk A, and prestalk O genes was low in S cells (Fig. 2B), consistent with the results obtained with *ecmB* GFP (green fluorescent protein) and *ecmA* GFP reporter genes (fig. S4). There did appear to be enriched expression of prestalk AB genes in S cells, although S cells were not found to colocalize with prestalk AB cells. Thus, the distribution and gene expression profile of S cells was distinct from all defined cell types (*15–18*), suggesting that they represent a novel cell population.

Given the intriguing properties of S cells, we postulated that they represent a dedicated cellular defense system. A survey of the *Dictyostelium* genome (*19*) identified potential homologs of innate immunity signaling proteins in plants and animals, including a putative WRKY transcription factor (*9*), 6 potential LRR domain receptors, including NwmA, which is most similar to the rice protein Xa21 (*20*); and two proteins, TirA and TirB, with predicted TIR domains similar to those found in *Arabidopsis* RPP5 (*21*). Of these we tested *tirA* and *tirB* by qRT-PCR and found that their mRNAs were enriched by a factor of 8 in S cells (Fig. 2B). Expression of the ABC

[1]Verna and Marrs McLean Department of Biochemistry and Molecular Biology, Baylor College of Medicine, One Baylor Plaza, Houston, TX 77030, USA. [2]Department of Molecular and Human Genetics, Baylor College of Medicine, One Baylor Plaza, Houston, TX 77030, USA. [3]Program in Developmental Biology, Baylor College of Medicine, One Baylor Plaza, Houston, TX 77030, USA.

*These authors contributed equally to this work.
†To whom correspondence should be addressed. E-mail: alvspa@bcm.tmc.edu

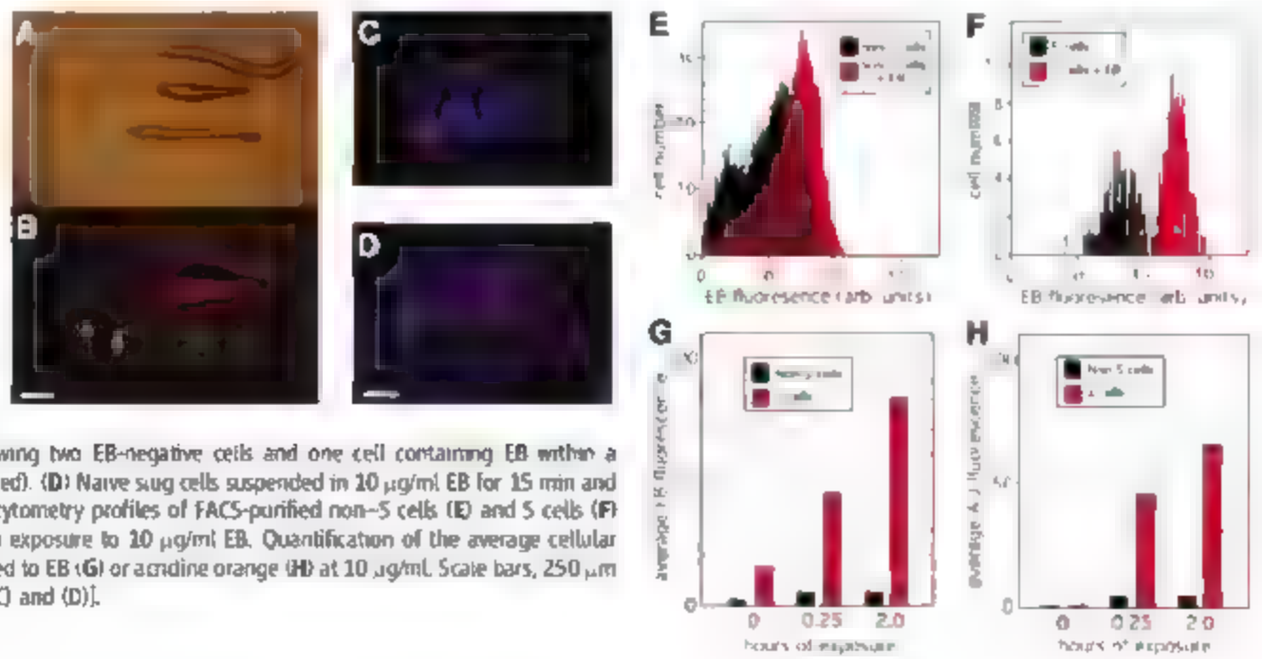

Fig. 1. Accumulation of EB by S cells. Bright-field (**A**) and fluorescence (**B**) images of *Dictyostelium* slugs migrating, left to right, on agar containing 1 μg/ml EB reveals single cells (small arrows) and clumps of cells (large arrows) that are left behind within the sloughed off slug sheaths. (**C**) Fluorescent image of slug cells, with 4′6′ diamidino-2-phenylindole (DAPI)–stained nuclei (blue), showing two EB-negative cells and one cell containing EB within a large cytoplasmic vesicle (red). (**D**) Naïve slug cells suspended in 10 μg/ml EB for 15 min and visualized as in (C). Flow cytometry profiles of FACS-purified non–S cells (**E**) and S cells (**F**) before and after a 15-min exposure to 10 μg/ml EB. Quantification of the average cellular fluorescence of cells exposed to EB (**G**) or acridine orange (**H**) at 10 μg/ml. Scale bars, 250 μm [(A) and (B)], and 2 μm [(C) and (D)].

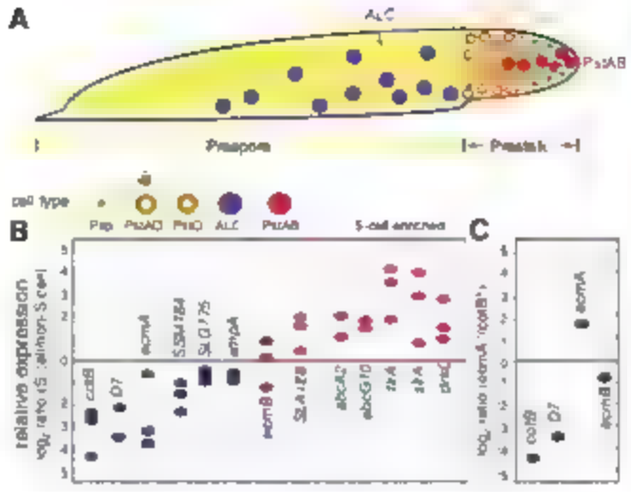

Fig. 2. Gene expression profile of S cells. (**A**) Cartoon of a *Dictyostelium* slug (anterior to the right) with the major cell types indicated by colored circles (yellow, prespore; green, prestalk A; orange, prestalk O; red, prestalk AB; blue, anterior-like cells). (**B**) qRT-PCR was used to compare gene expression in FACS-purified S cells relative to non–S cells (*12*). Blue ovals indicate relatively low expression in S cells; red ovals indicate higher relative expression in S cells (prespore genes, *cotB* and D7; PstAO, *ecmA*; PstO, SSM184 and SLG775, ALC, *ampA*, PstAB, *ecmB* and SLA128). (**C**) Positive control for the qRT-PCR, comparing gene expression in *cotB/gfp*-positive (prespore) and *ecmA/gfp*-positive (prestalk) cells.

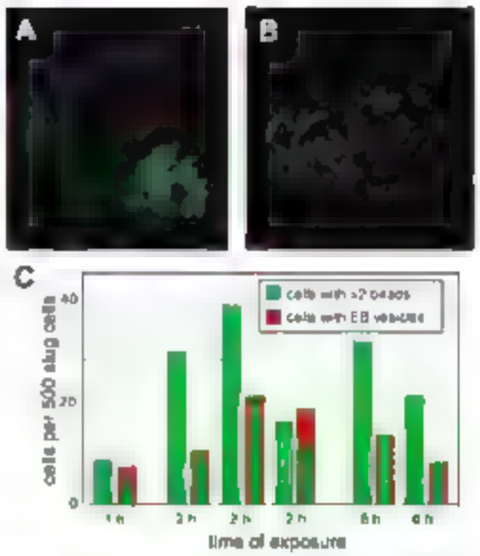

Fig. 3. S cell phagocytosis. Slug cells were incubated with green fluorescent latex beads (**A**) or GFP-labeled *Legionella* bacteria (**B**) for 1 hour, stained with DAPI (blue), and imaged by fluorescence microscopy (*12*). (**C**) The number of slug cells that engulfed beads were scored after the indicated times in separate experiments.

transporter genes *abcA2* and *abcG10* (*22*) was also found to be enriched in S cells (Fig. 2B). For comparison, we purified *ecmA*:GFP-positive cells and detected enrichment of *ecmA* expression by a factor of 3 in these cells (Fig. 2C). Because *ecmA* expression has been shown to be specific to prestalk cells (*23*), this control reflects the limits of purifying minority cell types by FACS and suggests that *tirA* and *dhcA* expression is indeed specific to S cells.

When slugs were disaggregated and mixed with fluorescent latex beads or bacteria, only the S cells were found to have an ability to engulf these efficiently (Fig. 3, A and B) (*12*). Quantification of particle uptake across the entire population of slug cells revealed that all S cells eventually take up a large number of beads (~50) (Fig. 3C). A similar number of cells that could not unequivocally be identified as S cells also engulfed the beads. The EB-negative phagocytes may represent a population of S cells that had not elaborated detectable EB-filled vesicles.

The phagocytic nature of S cells suggested that they might play a role in the defense against pathogens. *Legionella pneumophila* is a bacterial pathogen of soil amoeba that escapes the phagosome maturation pathway normally used by amoebae to digest bacteria and either kills the host or primates its own exocytosis, allowing its dissemination to nearby cells (*24*–*27*). Because a *Legionella* infection within the slug could compromise spore production, it is possible that S cells help prevent or limit such damage. To examine this, we mixed disaggregated slug cells with *Legionella*, allowed them to re-form slugs, following the subsequent fate of the bacteria during continued slug migration (*12*). In these experiments, *Legionella* were swept into re-forming slugs by adhering to amoebae or by being taken up into cells. Within 6 hours, as the slugs migrated away from the site of mixing, the S cells were seen to contain numerous *Legionella*, and the majority of *Legionella* were found inside S cells (table S1). After 18 hours, infected cells or *Legionella* bacteria could not be detected within the slugs, although S cells were still present (table S1). Clumps of *Legionella* bacteria were observed within the collapsed sheaths that are left behind by the slugs, at intervals consistent with their being deposited there by S cells. The bacteria were not visible within cells but appeared to be surrounded by cell debris. We also infected slugs directly by forcing several dozen *Legionella* bacteria through the slug sheath with a needle, without disrupting the integrity of the slug (*12*). After 6 hours, all of the bacteria were found within a small number of cells in the slug, about half of which could be unambiguously identified as S cells (table S1). After 24 hours of migration, no bacteria could be detected within the slugs. Thus, S cells appear to locate and engulf pathogenic bacteria within the context of a migrating slug and show a capacity to clear them from the slug over time.

The ability of S cells to sequester pathogens and remove them from the slug "body" of the social amoeba is akin to neutrophil function in mammals. To explore this possible similarity further, we returned to the role of the *tirA* gene since TIR-domain proteins regulate responses to pathogens in both plants and animals (*6*, *8*, *28*, *29*). Partial deletion mutants were generated in which ~40% of the coding region, including the entire TIR domain, was replaced with a drug-resistance cassette (fig. S5, A to C). The *tirA* mutant slugs produced normal numbers of S cells on EB agar, and the cells themselves appeared grossly normal, with large cytoplasmic EB vesicles (fig. S5D). However, *tirA* mutant S cells were killed by an "avirulent" *Legionella* strain that does not kill wild-type *Dictyostelium* (fig. S5E). These results indicate that, although TirA is not required for S cell differentiation, it is critical for the effective response of S cells to bacteria.

The *tirA*[−] mutants were also observed to form minute colonies on bacterial lawns (Fig. 4, A and B, and fig. S5C). Because the *tirA*[−] mutants grow normally in liquid media, this suggests a specific defect in their ability to feed on bacteria. We tested this by seeding cells on agar plates along with *Klebsiella aerogenes* (*Dictyostelium*'s standard food bacteria) and found that the *tirA*[−] mutant cells grew for ~20 hours but then stopped growing and decreased in number thereafter (Fig. 4C). This growth defect was not due to the mutant's inability to use bacteria as a food source because the mutant cells grew on heat-killed bacteria (Fig. 4C). The growth attenuation of the *tirA*[−] mutant amoebae correlates with a discernable loss of cell viability (Fig. 4D). In addition, *tirA*[−] mutant cells appeared to be more sensitive to killing by *Legionella* (Fig. 4E). Our results suggest that TirA is required by *Dictyostelium* amoebae to respond appropriately to bacteria during vegetative foraging.

S cells in developing social amoebae sequester toxins and bacterial pathogens and carry them away from the presumptive spore population. Given their functional parallels with neutrophils and macrophages, we suggest that S cells provide a simple innate immune system for the social amoebae. We hypothesize that the S cells' compromised fitness is advantageous because it increases the fitness of the prespore cells. This idea, along with the identification of what appear to be S cells in five other species of *Dictyostelia*, adds another layer of complexity to the cellular cooperation observed in the social amoeba (*30*).

Multicellularity likely increased the selective pressure on an organism's ability to avoid exploitation by pathogens (*1*). Although plants and animals share a similar organization of innate immune signaling pathways, the hypothesized conservation of the component proteins has been called into question and has been proposed to have resulted from convergent evolution (*5*, *6*, *31*).

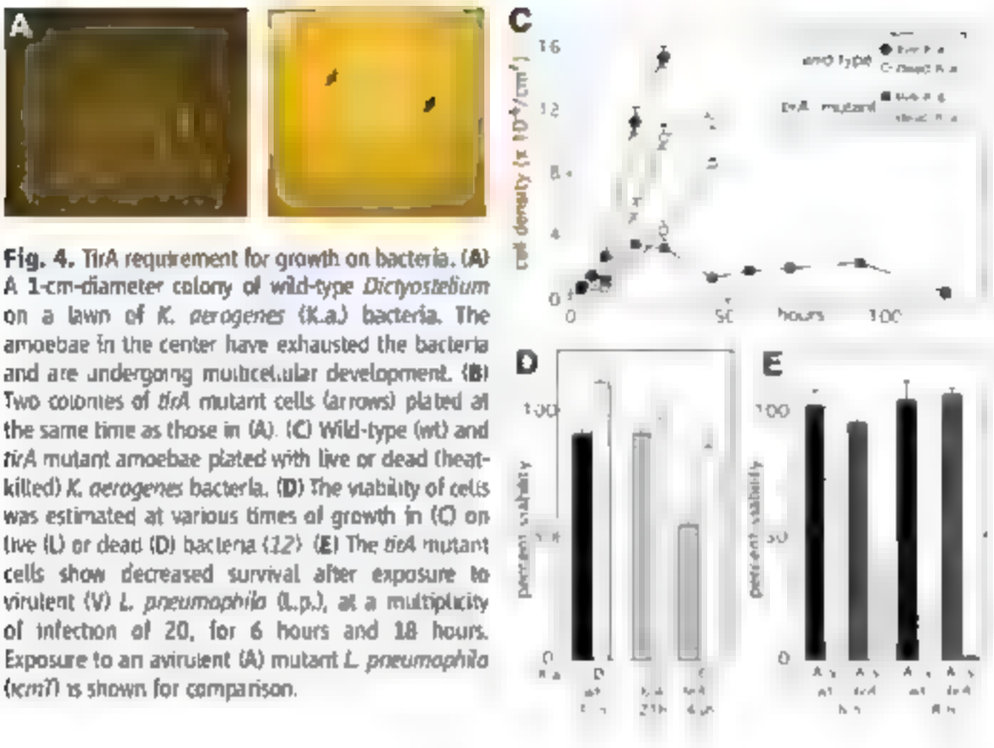

Fig. 4. TirA requirement for growth on bacteria. **(A)** A 1-cm-diameter colony of wild-type *Dictyostelium* on a lawn of *K. aerogenes* (K.a.) bacteria. The amoebae in the center have exhausted the bacteria and are undergoing multicellular development. **(B)** Two colonies of *tirA* mutant cells (arrows) plated at the same time as those in (A). **(C)** Wild-type (wt) and *tirA* mutant amoebae plated with live or dead (heat-killed) *K. aerogenes* bacteria. **(D)** The viability of cells was estimated at various times of growth in (C) on live (L) or dead (D) bacteria (*12*). **(E)** The *tirA* mutant cells show decreased survival after exposure to virulent (V) *L. pneumophila* (L.p.), at a multiplicity of infection of 20, for 6 hours and 18 hours. Exposure to an avirulent (A) mutant *L. pneumophila* (*icmT*) is shown for comparison.

knowing the response of amoebae to bacteria might clarify this issue because the amoebozoa diverged soon after the plant-animal split and are a basal group of the crown group eukaryotes (*13*, *14*). Moreover, amoebae are phagocytic cells that are in constant contact with bacteria and they might have retained key characteristics of plant and animal innate immunity if those functions existed in their common ancestor. The role of TirA in *Dictyostelium*'s response to bacteria provides the first glimpse of an immune-related signaling system in amoeba and suggests that the use of TIR domain based signaling for defense represents an ancient function present in the progenitor of all crown group eukaryotes. If true, it would suggest that this system of pathogen recognition was advantageous to organisms before the evolution of multicellularity.

References and Notes

1. C. A. Janeway Jr., R. Medzhitov, *Annu. Rev. Immunol.* **20**, 197 (2002).
2. A. I. Tauber, *Nat. Rev. Mol. Cell Biol.* **4**, 897 (2003).
3. R. N. Germain, *Nat. Med.* **10**, 1307 (2004).
4. S. Akira, S. Uematsu, O. Takeuchi, *Cell* **124**, 783 (2006).
5. R. Medzhitov, C. A. Janeway Jr., *Curr. Opin. Immunol.* **10**, 12 (1998).
6. F. Blumberger, F. Brunner, B. Kemmerling, L. Pieterse, *Immunol. Rev.* **198**, 249 (2004).
7. Y. Xu *et al.*, *Nature* **408**, 111 (2000).
8. F. M. Burch-Smith *et al.*, *PLoS Biol.* **5**, e68 (2007).
9. F. Eulgem, *Trends Plant Sci.* **10**, 71 (2005).
10. Q. H. Shen *et al.*, *Science* **315**, 1098 (2007).
11. R. H. Kessin, *Dictyostelium: Evolution, Cell Biology, and the Development of Multicellularity* (Cambridge Univ. Press, Cambridge, 2001).
12. Materials and methods are available as supporting material on *Science* online.
13. J. R. Good, A. Kuspa, *Dev. Biol.* **220**, 53 (2000).
14. P. Schaap *et al.*, *Science* **314**, 661 (2006).
15. J. Williams, in *Dictyostelium: A Model System for Cell and Developmental Biology*, Y. Maeda, K. Inouye, I. Takeuchi, Eds. (Universal Academy Press, Tokyo, 1997), pp. 293–304.
16. E. Casademunt, T. B. Varney, J. Dolman, C. Petty, D. D. Blumberg, *Differentiation* **70**, 23 (2002).
17. M. Maeda *et al.*, *Eukaryot. Cell* **2**, 627 (2003).
18. J. Sternfeld, C. N. David, *Differentiation* **20**, 10 (1981).
19. L. Eichinger *et al.*, *Nature* **435**, 43 (2005).
20. S. W. Lee, S. W. Han, L. E. Bartley, P. C. Ronald, *Proc. Natl. Acad. Sci. U.S.A.* **103**, 18395 (2006).
21. J. E. Parker *et al.*, *Plant Cell* **9**, 879 (1997).
22. C. Anjard, W. F. Loomis, *Eukaryot. Cell* **1**, 643 (2002).
23. J. G. Williams, *EMBO Rep.* **7**, 694 (2006).
24. M. A. Horwitz, *J. Exp. Med.* **158**, 2108 (1983).
25. H. A. Shuman, M. Purcell, G. Segal, L. Hales, L. A. Slater, *Curr. Top. Microbiol. Immunol.* **225**, 99 (1998).
26. J. M. Solomon, A. Rupper, J. A. Cardelli, R. R. Isberg, *Infect. Immun.* **68**, 2939 (2000).
27. J. Chen *et al.*, *Science* **303**, 1358 (2004).
28. J. L. Slack *et al.*, *J. Biol. Chem.* **275**, 4670 (2000).
29. V. Braun, R. A. Brown, A. Ozinsky, J. R. Hesselberth, S. Fields, *Eur. J. Immunol.* **36**, 742 (2006).
30. J. E. Strassmann, D. C. Queller, *ASM News* **70**, 526 (2004).
31. F. M. Ausubel, *Nat. Immunol.* **6**, 973 (2005).
32. S. L. Baldauf, W. F. Doolittle, *Proc. Natl. Acad. Sci. U.S.A.* **94**, 12007 (1997).
33. E. Baptiste *et al.*, *Proc. Natl. Acad. Sci. U.S.A.* **99**, 1414 (2002).
34. J. Song *et al.*, *PLoS Comput. Biol.* **1**, e71 (2005).

35. We thank G. Shaulsky, W. Nasser, J. Strassmann, D. Queller, and W. F. Loomis for helpful discussions, C. Zhang for advice on *Legionella* infections, D. Lewis and J. Scott for flow cytometry advice, H. Shuman for *Legionella* strains, and J. Strassmann and D. Queller for additional species of *Dictyostelia*. This work was supported by NIH grants GM52359 and HD39691 to A.K.

Supporting Online Material

www.sciencemag.org/cgi/content/full/317/5838/678/DC1
Materials and Methods
Figs. S1 to S5
Table S1
References

18 April 2007; accepted 2 July 2007
10.1126/science.1143991

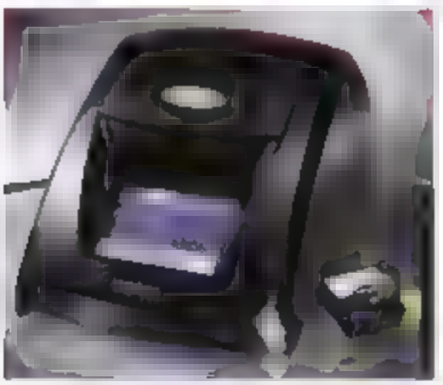

Multimode Reader

The Modulus Microplate Multimode Reader for fluorescence, luminescence, and absorbance applications features an on-board computer, touch screen navigation, and dynamic protocol wizards. Each of the three application modules can be purchased separately or combined. For labs performing luminescence applications, options include single or dual injector systems, curve-fitting software, and a luminescence light standard. The fluorescence module includes four individual optical kits: blue, ultraviolet, green, and red. The absorbance module includes a filter wheel, four filters, and two filter holders. Each of the three detection modules contains individual detectors specific to the application.

Turner Biosystems For information 408-636-2400 www.turnerbiosystems.com

Animal-Free Blocker

Animal Free Blocker is a plant derived blocking agent or diluent for nucleic acid or protein blotting applications that eliminates the possibility of interfering animal proteins. Containing no proteins of animal origin, Animal Free Blocker can be used as an alternative to sera, bovine serum albumin, casein, or non-fat dry milk to avoid potential interaction between the immunoglobulin in these protein solutions and antibodies used for detection, especially anti-goat immunoglobulin or anti-sheep immunoglobulin, the immunoglobulins that may be significant in these commonly used blocking agents/diluents can bind to the detection antibodies and either reduce the signal or produce high background.

Vector Laboratories For information 650-697-3600 www.vectorlabs.com

Biomedical Research Software

BioPathwise DM software for biomedical researchers makes it easier to capture, secure, share, and publish data from any laboratory instrument in any format: images, spreadsheets, documents, and more. The system was developed to address bottlenecks in academic, pharmaceutical, and biotechnology research settings. The BioPathwise DM system fits seamlessly into the research laboratory workflow saving raw data in association with the summary information that makes it meaningful. It is a lightweight application that can be downloaded and set up for small groups by a lab head or principal investigator with basic computer skills. Guidance is offered for larger organizations for server configuration and network installation. The system allows labs to make the information available to anyone it chooses in a secure environment, accessible on the Web from any location. Groups of researchers can easily document, store, and share data along with any reports, records, copies of peer reviewed articles, or other relevant information that helps interpret the raw experimental data.

The BioAnalytics Group For information 609-632-0091 www.bioanalyticsgroup.com

Mathematica Update

Version 6.0 represents the most significant upgrade to Mathematica since its introduction in 1988, according to its maker. The new version introduces more than 1000 new technologies developed over more than 10 years. Mathematica 6 is designed to take technical computing to a new level: more tightly bound, more natural, more automated, and applicable to more areas. Central to this achievement is "instant interactivity"—taking models, simulations, computations, or just about any concepts and turning them into fully interactive applications. Key new features include: dynamic interactivity, allowing sophisticated interactive interfaces to be created from single lines of input; high-impact adaptive visualization for automated creation of high fidelity function and data graphics; language for data integration, including automatic integration of hundreds of standard data formats, load on demand curated data for math, physics, chemistry, finance, geography, linguistics, and more; symbolic interface construction for immediate creation of arbitrary interfaces from simple programs; and automated computational aesthetics, with algorithmic optimization for visual presentation.

Wolfram Research For information 217-398-0700 www.wolfram.com

mRNA Production System

The mScript mRNA Production System provides researchers with a fast and simple method for producing superior eukaryotic messenger RNAs (mRNAs). Incorporating an in vitro transcription system, capping enzymes, and RNA poly(A) tailing reagents, the kit contains everything a researcher needs to produce transfection, electroporation, or microinjection ready mRNA. The system provides the advantages of 100% capped messages, 100% proper cap orientation, and the natural Cap 1 structure—all of which increase in vivo mRNA translation efficiency. Epicentre

Biotechnologies For information 800-284-8474 www.EpiBio.com/mScript.asp

Antigen Immobilization Technology

The Dynabeads M-270 Immunoassay (Carboxyl) is designed to provide precise immobilization of antigens such as proteins, peptides, steroids, and hormones for in vitro diagnostic magnetic bead based immunoassay applications. The antigens are coupled directly or via a cross-linker to carboxylic acid groups on the new 2.8 micrometer Dynabeads. The hydrophilic surface of the beads ensures low nonspecific binding of serum proteins that would otherwise interfere with the assay. The beads disperse well, are easily handled in a wide variety of buffers, and do not inhibit enzymatic activity.

Invitrogen For information 617-897-8258 www.invitrogen.com/ivd

Newly offered instrumentation, apparatus, and laboratory materials of interest to researchers in all disciplines in academic, industrial, and government organizations are featured in this space. Emphasis is given to purpose, chief characteristics, and availability of products and materials. Endorsement by *Science* or AAAS of any products or materials mentioned is not implied. Additional information may be obtained from the manufacturer or supplier.

Science Careers

From the journal Science | AAAS

Classified Advertising

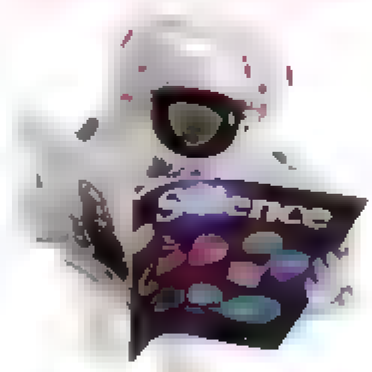

From life on Mars
to life sciences

For full advertising details, go to **www.sciencecareers.org** and click on **For Advertisers**, or call one of our representatives.

United States & Canada

E-mail: advertise@sciencecareers.org
Fax: 202-289-6742

IAN KING Recruitment Sales Manager
Phone: 202-326-6528

NICHOLAS HINTIBIDZE
West Academic
Phone: 202-326-6533

DARYL ANDERSON
Midwest/Canada Academic
Phone: 202-326-6543

ALLISON MILLAR
Industry/Northeast Academic
Phone: 202-326-6572

TINA BURKS
Southeast Academic
Phone: 202-326-6577

Europe & International

E-mail: ads@science-int.co.uk
Fax: +44 (0) 1223 326532

TRACY HOLMES Sales Manager
Phone: +44 (0) 1223 326525

MARIUM HUDDA
Phone: +44 (0) 1223 326517

ALEX PALMER
Phone: +44 (0) 1223 326527

LOUISE MOORE
Phone: +44 (0) 1223 326528

Japan

JASON HANNAFORD
Phone: +81 (0) 52-757-5360
E-mail: jhannaford@sciencemag.jp
Fax: +81 (0) 52-757-5361

To subscribe to Science:
In U.S./Canada call 202-326-6417 or 1-800-731-4939
In the rest of the world call +44 (0) 1223-326-515

Science makes every effort to screen its ads for offensive and/or discriminatory language in accordance with U.S. and non-U.S. law. Since we are an international journal, you may see ads from non-U.S. countries that request applications from specific demographic groups. Since U.S. law does not apply to other countries we try to accommodate recruiting practices of other countries. However, we encourage our readers to alert us to any ads that they feel are discriminatory or offensive.

POSITIONS OPEN

LABORATORY MEDICINE FACULTY

Positions at the University of California, San Diego (UCSD). The Department of Pathology (**website: http://medicine.ucsd.edu/pathology/**) is seeking new faculty in the Division of Laboratory Medicine to support the strategic expansion of UCSD Healthcare and the growth of its regional referral services. Initial recruitments will be in the areas of clinical chemistry/proteomics, toxicology, pharmacogenomics, hematology/hematopathology, microbiology/virology, and molecular diagnostics. Successful candidates will share clinical and administrative responsibilities in the Clinical Laboratories at the campuses in San Diego (Hillcrest), La Jolla (Thornton), and Torrey Pines. Applicants should have strong academic credentials with a track record of basic, translational, or clinical research, and are expected to actively contribute to departmental educational programs including training of residents, fellows, graduate, and medical students. Candidates must possess M.D., Ph.D., or M.D./Ph.D. degrees and be Board-certified/eligible by the American Board of Pathology or a diplomate of an accredited clinical laboratory subspecialty board. California licensure is also required. Preference will be given to individuals with prior subspecialty work experience or fellowship training. Academic series and rank will be commensurate with experience and training. Salary will be consistent with published UCSD pay scales. Applicants should submit their curriculum vitae with a cover letter describing clinical and research interests and the names/addresses of three references to: **Ronald W. McLawhon, M.D., Ph.D., Director, Clinical Laboratories and Professor and Head, Division of Laboratory Medicine, c/o Ms. Catherine Schumacher, Search Coordinator, Department of Pathology 0717, University of California San Diego School of Medicine, 9500 Gilman Drive, La Jolla, CA 92093-0717.** Review of applications will begin August 27, 2007, and will continue until filled. Applications by e-mail are acceptable to **e-mail: cdschumacher@ucsd.edu.** *UCSD is an Affirmative Action/Equal Opportunity Employer with a strong institutional commitment to excellence through diversity.*

FACULTY POSITIONS in ECOLOGY and EVOLUTION
UCLA Department of Ecology and Evolutionary Biology

The Department of Ecology and Evolutionary Biology at UCLA invites applications for two tenure-track positions for an **ECOLOGIST and EVOLUTIONARY BIOLOGIST,** both at the **ASSISTANT PROFESSOR** level. We seek candidates who address central concepts in ecology and evolution using theory and/or experimentation. Applicants working on all systems, particularly those working in the marine realm, are welcome. The Department is also interested in individuals with a history of promoting diversity in education. The expected start date is September 2008. Candidates must have a Ph.D., postdoctoral experience is desired. Salary is commensurate with education and experience. Successful candidates are expected to participate in undergraduate and graduate teaching and to maintain an externally funded research program. UCLA has outstanding resources, including the UC Natural Reserve System, the NSF Institute of Pure and Applied Mathematics (IPAM), the Institute of the Environment's Center for Tropical Research and Coastal Center, a departmental seawater lume facility, re-circulating seawater holding facilities, a coastal research vessel, and many core facilities. Applicants should submit application materials online (**website: http://www.eeb.ucla.edu/eeoevobio**) cover letter, curriculum vitae, statements of research and teaching interests, two to three publications, and names and addresses of three references. Please use job number 0830-0708-01 (Ecologist) or 0830-0708-02 (Evolutionary Biologist) in all correspondence. For additional information, contact: **Search Committee Chair Priyanga Amarasekare (e-mail: amarasek@eeb.ucla.edu).** Review of applications will begin September 15, 2007. *UCLA is an Affirmative Action/Equal Opportunity Employer with a strong institutional commitment to the achievement of diversity among its faculty and staff.*

POSITIONS OPEN

University of Michigan Medical School

FACULTY in MOLECULAR ONCOLOGY
The University of Michigan Medical School

The Department of Pathology is seeking tenure-track faculty to further build our research program in molecular oncology. Areas of particular interest include, but are not limited to, epigenetic regulation of transcription, protein modeling/chemical genomics, and structural biology.

The Department, Medical School, and Health Care System are all in excellent financial condition. Over 350 faculty actively participate in the University of Michigan Comprehensive Cancer Center. The Department operates its own graduate program and has nine endowed chairs and over $25 million annually in research expenditures. Particular areas of research strength include molecular oncology, aging, immunology, proteomics, and informatics. The newly created Divisions of Pathology Informatics and Translational Pathology offer cutting edge technologies in support of research programs. Planning for new building to house the Department's clinical, research, and educational activities is currently underway.

The successful applicant will hold a Ph.D. or M.D./Ph.D. and direct a vigorous research program supported by external funding. Ample resources are available to qualified applicants. Academic rank will be on the tenure track with rank commensurate with experience. Qualified applicants should submit a letter of interest, summary of research interests, curriculum vitae, and names of three references to:

Jay L. Hess, M.D., Ph.D.
Carl V. Weller Professor and Chair
Department of Pathology
University of Michigan Medical School
Medical Science I Building, Room M5240
1301 Catherine Road
Ann Arbor, MI 48109-0602

The University of Michigan Health System is an Affirmative Action Employer and welcomes applications from women and minorities.

ASSISTANT PROFESSOR
Cellular/Developmental Biology
California State University, Fullerton

California State University Fullerton, Department of Biological Science, is seeking applicants for an Assistant Professor (tenure-track) to begin August 2008. All areas of cell biology will be considered with preference given to candidates with expertise in developmental biology. Applicants must have a Ph.D. and postdoctoral research experience. The successful candidates will be expected to develop an active externally funded research program involving undergraduate and Master's level students and be committed to excellence in teaching a diverse population of students. Teaching responsibilities will include an inquiry-based, lower-division cell biology core course, and upper-division/Master's level course in developmental biology, and the candidate will have the opportunity to develop a course in a chosen area of expertise. Interdisciplinary collaborations are strongly encouraged within the Department and College. Send: (1) curriculum vitae (including a history of grant activity), (2) a statement of research plans, (3) two or three related publications, (4) three letters of recommendation, and (5) a statement of teaching philosophy including teaching experience and course preferences to: **Chair, Developmental Biology Search, Department of Biological Science, California State University, Fullerton, P.O. Box 6850, Fullerton, CA 92834-6850 (website: http://biology.fullerton.edu).** Review of applications will begin 1 November 2007, and continue until a suitable candidate is appointed. *Affirmative Action/Equal Opportunity/Title IX/ADA Employer.*

OFFICE OF PORTFOLIO ANALYSIS AND STRATEGIC INITATIVES
DIRECTOR, DIVISION OF RESOURCE DEVELOPMENT AND ANALYSIS

The Office of the Director, National Institutes of Health (NIH) in Bethesda, Maryland, is seeking a Director of the Division of Resource Development and Analysis (DRDA) within the Office of Portfolio Analysis and Strategic Initiatives (OPASI). If you are an exceptional candidate with an M.D. and/or Ph.D., we encourage your application.

The OPASI's primary objective is to develop a transparent process of planning and priority-setting characterized by a defined scope of review with broad input from the scientific community and the public; valid and reliable information resources and tools, including uniform disease coding and accurate, current and comprehensive information on burden of disease; an institutionalized process of regular, scheduled evaluations based on current best practices; the ability to weigh scientific opportunity against public health urgency; a method of assessing outcomes to enhance accountability; and a system for identifying areas of scientific and health improvement opportunities and supporting regular trans-NIH scientific planning and initiatives.

As the DRDA Director, you will be responsible for employing resources (databases, analytic tools, and methodologies) and developing specifications for new resources, when needed, in order to conduct assessments based on NIH-owned and other databases in support of portfolio analyses and priority setting in scientific areas of interest across NIH.

Salary is commensurate with experience and includes a full benefits package. A detailed vacancy announcement with the mandatory qualifications and application procedures can be obtained on **USAJOBS at www.usajobs.gov (OD-07-172841-142) and the NIH Web Site at http://www.jobs.nih.gov**. Questions on the application procedures may be addressed to **Brian Harper on 301-594-5332**. Applications must be received by midnight eastern standard time on **August 10, 2007**.

OFFICE OF PORTFOLIO ANALYSIS AND STRATEGIC INITATIVES
DIRECTOR, DIVISION OF STRATEGIC COORDINATION

The Office of the Director, National Institutes of Health (NIH) in Bethesda, Maryland, is seeking a Director of the Division of Strategic Coordination (DSC) within the Office of Portfolio Analysis and Strategic Initiatives (OPASI). If you are an exceptional candidate with an M.D. and/or Ph.D., we encourage your application.

The OPASI's primary objective is to develop a transparent process of planning and priority-setting characterized by a defined scope of review with broad input from the scientific community and the public; valid and reliable information resources and tools including uniform disease coding and accurate, current and comprehensive information on burden of disease; an institutionalized process of regular, scheduled evaluations based on current best practices; the ability to weigh scientific opportunity against public health urgency; a method of assessing outcomes to enhance accountability; and a system for identifying areas of scientific and health improvement opportunities and supporting regular trans-NIH scientific planning and initiatives.

As the DSC Director, you will be responsible for integrating information and developing recommendations to inform the priority-setting and decision-making processes of the NIH in formulating NIH-wide strategic initiatives. These initiatives will address exceptional scientific opportunities and emerging public health needs (akin to the Roadmap, Obesity, and Neuroscience Blueprint initiatives). You will also be responsible for providing the NIH Director with the information needed to allocate resources effectively for trans-NIH efforts.

Salary is commensurate with experience and includes a full benefits package. A detailed vacancy announcement with the mandatory qualifications and application procedures can be obtained on **USAJOBS at www.usajobs.gov (announcement number OD-07-172844-142) and the NIH Web Site at http://www.jobs.nih.gov**. Questions on the application procedures may be addressed to **Brian Harper on 301-594-5332**. Applications must be received by midnight eastern standard time on **August 10, 2007.**

WWW.NIH.GOV

OFFICE OF PORTFOLIO ANALYSIS AND STRATEGIC INITATIVES
DIRECTOR, DIVISION OF EVALUATION AND SYSTEMIC ASSESSMENTS

The Office of the Director, National Institutes of Health (NIH) in Bethesda, Maryland, is seeking a Director of the Division of Evaluation and Systemic Assessments (DESA) within the Office of Portfolio Analysis and Strategic Initiatives (OPASI). If you are an exceptional candidate with an M.D. and or Ph.D. and the vision and ability to integrate evaluation systems and programs across multiple disciplines and organizations we encourage your application.

The OPASI's primary objective is to develop a transparent process of planning and priority-setting characterized by a defined scope of review with broad input from the scientific community and the public, valid and reliable information resources and tools including outcome data, coding and accurate, current and comprehensive information on burden of disease, an institutionalized process of regularly scheduled evaluations based on current best practices, the ability to weigh scientific opportunity against public health urgency, a method of assessing outcomes to enhance accountability, and a system for identifying areas of scientific and health improvement opportunities and supporting rigorous NIH scientific planning and initiatives.

As the DESA Director, you will be responsible for planning, conducting, supporting, and coordinating specific program evaluations and projects of NIH Institutes and Centers such as the Roadmap, Obesity, and Next Generation Researchers Initiatives, among others. You will serve as the liaison for coordinating governmentally required assessments according to the Government Performance and Results Act (GPRA) and OMB Program Assessment Rating Tool (PART). You will also serve as a member of the OPASI Steering Committee involved in oversight of institute-wide planning and analysis.

Salary is commensurate with experience and includes a full benefits package. A detailed vacancy announcement with the mandatory qualifications and application procedures can be obtained on **USAJOBS at www.usajobs.gov (announcement number OD-07-172847-142) and the NIH Web Site at http://www.jobs.nih.gov**. Questions on the application procedures may be addressed to **Brian Harper on 301-594-5332**. Applications must be received by midnight eastern standard time on **August 10, 2007**.

HUMAN GENETICIST
Tenure-Track/Tenure Position

The newly formed Intramural Laboratory of Translational Genomics (LTG) in the Division of Cancer Epidemiology and Genetics (DCEG), National Cancer Institute (NCI), National Institutes of Health (NIH), Department of Health and Human Services (DHHS), is recruiting two tenure-track tenured investigators. The mission of the LTG is to investigate the genetic basis of strong association signals identified by candidate gene approaches, linkage analyses in high-risk families, or genome-wide association studies (GWAS), particularly loci identified by the ongoing Cancer Genetic Markers of Susceptibility (CGEMS) program involving GWAS of several major cancers. Investigators in the LTG are expected to develop an independent research portfolio in cancer genomics focused on (1) fine mapping and re-sequencing of loci relevant to cancer susceptibility and or outcomes, (2) investigation into the causal gene variants that provide biological plausibility for each locus, and (3) bioinformatic analyses of publicly available datasets derived from germline annotation of genetic variation and somatic alterations in cancers. Each investigator is expected to leverage the NCI resources in molecular epidemiology, high-throughput genotyping and whole genome scans, biostatistics and bioinformatics, as well as in basic and clinical sciences. The incumbent will receive research support for developing a state-of-the-art genomics laboratory, and recruiting two post-doctoral fellows, bioinformaticians and a technician.

Applicants must have an M.D. and or Ph.D. in a relevant field, extensive post-doctoral experience, and a record of publications demonstrating potential for creative independent research in human cancer genetics. Faculty with bioinformatics databases and high dimensional data are highly desirable along with strong communication skills. Interested individuals should send a cover letter, curriculum vitae and a brief summary of research accomplishments and goals, along with copies of three to five publications or preprints, and three letters of reference to:

Ms. Judy Schwadron, Division of Cancer Epidemiology and Genetics, National Cancer Institute, 6120 Executive Blvd. EPS/8073, Bethesda, MD 20892

Recommendations can be included with the package or sent directly by the recommender to Ms. Schwadron. Candidates should submit applications by **October 15, 2007** at this time, the committee will begin to look at suitable candidates. However, the search will continue until qualified scientists are found. Additional information about staff and ongoing research in the NCI Division of Cancer Epidemiology and Genetics is available at **http://www.dceg.cancer.gov**. Please contact **Dr. Stephen Chanock (phone 301-435-7559 at chanocks@mail.nih.gov) or Dr. Peggy Tucker (phone 301-496-8031 at tuckerp@mail.nih.gov)** for questions about the position(s).

WWW.HHS.GOV

Positions NIH

THE NATIONAL INSTITUTES OF HEALTH

Scientific Review Administrator
(Health Scientist Administrator)
Center for Scientific Review
http://cms.csr.nih.gov/

Would you like to work with the most accomplished scientists in your field to provide fair and expert peer review of research and training grant applications submitted to the NIH? The Center for Scientific Review is recruiting dynamic, experienced research scientists in a variety of scientific areas. The successful candidate will be a respected, accomplished scientist with maturity, integrity and outstanding communication skills. Requirements include an M.D. or Ph.D. degree in the biomedical or behavioral sciences (or equivalent training and experience), a record of independent research accomplishments in your field, documented by an outstanding publication record and administrative background.

The Scientific Review Administrator is at the focal point of NIH peer review. SRAs analyze grant applications for key topic areas, recruit experts, conduct study section meetings, and prepare review documents. The position involves travel to scientific meetings, training in health science administration, opportunities to serve the larger NIH community, and career development activities.

Compensation is commensurate with research experience and accomplishments, and a full Civil Service package of benefits is available (including retirement and thrift plans as well as health, life, and long-term care insurance).

For information about current opportunities as a Health Science Administrator at CSR, consult our website: **http://cms.csr.nih.gov/AboutCSR/Employment/**. Feel free to call **(301) 435-1111** as well, if you have any questions.

Biostatistician

The intramural program of NINDS is seeking an experienced Biostatistician to serve in its Biostatistics Unit at the NIH Clinical Center in Bethesda, Maryland beginning in August 2007. This is a full-time position with responsibility for reviewing and providing statistical support toward improving clinical protocols, general statistical consultation service to research staff for data analysis and study design; and substantial collaboration on projects as a coauthor in published work.

A Doctoral Degree is required. Experience in biostatistics or statistics with working experience involving biostatistical applications to clinical trials and/or observational studies is preferred. Appointment will be in the Staff Scientist (non-tenure track) series and salary will be commensurate with experience.

Applicants should send a cover letter, C.V., and names of three references to:

Ms. Caren Collins, NINDS/NIH/DHHS, 10/5N254, 10 Center Drive, MSC 1430, Bethesda, MD 20892, or via E-mail: collinsca@ninds.nih.gov

TENURE TRACK POSITION
LABORATORY OF MOLECULAR BIOLOGY

The Laboratory of Molecular Biology (LMB), Center for Cancer Research, of the National Cancer Institute, National Institutes of Health (http://ccr.cancer.gov/labs/lab.asp?labid=99) uses genetics, molecular biology, cell biology, and molecular modeling to examine and solve a broad range of important biological problems. The Laboratory now invites applications for a tenure track position in the Laboratory of Molecular Biology, CCR, NCI for a scientist working in the field of antibody engineering as it relates to cancer therapy. Candidates must have a Ph.D. or M.D. and a proven record of innovative research and productivity in antibody engineering, display of antibody fragments on phage and mammalian cells and cancer therapeutics. The successful candidate will join an active group of translational and clinical investigators in the LMB working on immunotoxins, humanized antibodies, and tumor biology and carrying out clinical trials with immunotoxins and antibodies. Salary will be commensurate with education and experience. A two-page statement of research interests and goals should be submitted in addition to three letters of recommendation and a curriculum vitae to **Mrs. Ann Schombert, Executive Secretary, Laboratory of Molecular Biology, CCR, NCI, Building 37, Room 5106, Bethesda, MD 20892-4264; phone: 301-451-8714, Fax: 301-402-1344, email: schombea@pop.nci.nih.gov**. NIH Tenure track investigators with educational debts may be eligible for the NIH Loan Repayment Program. The NCI is an Equal Opportunity Employer. The closing date for applications to be accepted is **September 15, 2007**.

Postdoctoral, Research and Clinical Fellowships at the National Institutes of Health

www.training.nih.gov/pdopenings

www.training.nih.gov/clinopenings

Train at the bench, the bedside, or both

Office of Intramural Training and Education
Bethesda, Maryland 20892-0240
800 445 8283

Forschungszentrum Karlsruhe
in der Helmholtz-Gemeinschaft

Universität Karlsruhe (TH)
Research University · founded 1825

The Forschungszentrum Karlsruhe is one of the largest research institutions in Germany and a member of the Helmholtz Association of National Research Centres. Our research programs focus on energy and atmospheric research, micro- and nanotechnology, and structure of matter. At present, the Forschungszentrum Karlsruhe and the Universität Karlsruhe (TH) are combining their activities in the Karlsruhe Institute of Technology, KIT.

Within the framework of KIT, applications are invited for the position of

Head of the Institute of Meteorology and Climate Research
(Atmospheric Trace Constituents and Remote Sensing Division, Successor of Prof. H. Fischer)

associated with the position of a

University Professor (salary group W 3)

at the Universität Karlsruhe (TH) according to the Jülich model.

The Institute of Meteorology and Climate Research studies basic atmospheric processes and their coupling by biogeochemical cycles in the Earth's system. The Atmospheric Trace Constituents and Remote Sensing Division focuses on the investigation of trace constituent budgets and the associated processes, especially in the upper troposphere and stratosphere, and their relevance to global change. In particular, sophisticated remote sensing methods are applied for this purpose. The leading role of the Institute in national and European research projects is due to its outstanding expertise in the development and application of instruments, in particular of infrared spectroscopy, and of modelling tools.

The successful candidate should be a person of outstanding academic ability with wide ranging scientific competence and proven management skills. They should pursue innovative approaches in at least one of the above mentioned research fields. Applicants are expected to participate actively and extensively in national and international research programs.

The holder of the position will be the director of the Atmospheric Trace Constituents and Remote Sensing Division of the Institute of Meteorology and Climate Research of the Forschungszentrum Karlsruhe. A variety of possibilities exists for cooperation with the other three divisions of the institute at the Forschungszentrum and with the Universität Karlsruhe (TH). The Forschungszentrum Karlsruhe is a member of the Helmholtz Association of National Research Centres that pursues long-term research objectives of the state and society in scientific autonomy.

The professorship is assigned to the Faculty of Physics of the Universität Karlsruhe (TH). The holder of the position is expected to participate in training and lecturing in the field of meteorology. In addition, an active role in the development of the Karlsruhe Institute of Technology (KIT) under the planned KIT centre "Climate and Environment" is desired.

Candidates must have a proven record of research and teaching as documented by a habilitation or equivalent qualifications which also may have been acquired in the course of non-university employment.

Applications of qualified women are strongly encouraged, as we wish to increase the proportion of female scientists on the management level.

Handicapped applicants having the same qualification will be given preference.

Applications with the customary documents (curriculum vitae, certificates, list of publications, including selected reprints, as well as documentation of previous research and teaching activities) shall be addressed to **Dr. Peter Fritz, Member of the Executive Board, Forschungszentrum Karlsruhe, P.O. box 3640, 76021 Karlsruhe, Germany** and in parallel to **Prof. Dr. Heinz Kalt, Dean of the faculty of physics, Universität Karlsruhe (TH), Wolfgang-Gaede-Str. 1, 76131 Karlsruhe, Germany** by **September 30, 2007**. In addition, please submit your application in electronic form (e-mail: peter.fritz@vorstand.fzk.de).

Internet: www.fzk.de **www.uni-karlsruhe.de** **www.kit.edu** **institute: www.fzk.de/imk/asf**

U.S. Department of Energy
Office of Science
Deputy for Programs
Announcement #SES-SC-HQ-013 (kd)

The U.S. Department of Energy's (DOE) Office of Science is seeking highly qualified candidates with outstanding scientific achievements to fill the Deputy for Programs position. The Office of Science is the single largest supporter of basic research in the physical sciences in the United States, with a 2007 budget of $3.8 billion. It oversees the Nation's research programs in high-energy and nuclear physics, basic and fusion energy sciences, and biological, environmental and computational sciences. The Office of Science is the Federal Government's largest single funder of materials and chemical sciences, and it supports unique and vital parts of U.S. research in climate change geophysics, genomics, life sciences, and science education. The Office of Science also manages 10 world-class laboratories and oversees the construction and operation of some of the Nation's most advanced R&D user facilities, located at national laboratories and universities. These include particle and nuclear physics accelerators, synchrotron light sources, nanoscale science research centers, neutron scattering facilities, bio-energy research centers, supercomputers and high-speed computer networks. More information on the Office of Science can be found at **http://science.doe.gov**

The Deputy for Programs provides scientific and management oversight of the six program offices by ensuring program activities are strategically conceived and executed; formulating and defending the Office of Science budget request; establishing policies, plans, and procedures related to the management of the program offices; ensuring the research portfolio is integrated across the program offices with other DOE program offices and other Federal agencies; and representing the organization and making commitments for the Department in discussions and meetings with high-level government and private sector officials. The position is within the ranks of the U.S. government's Senior Executive Service (SES); members of the SES serve in key positions just below the top Presidential appointees.

To apply for this position, please see the announcement and application instructions at **https://jobsearch.usajobs.opm.gov/ses.asp** under "Vacancy announcement of #SES-SC-HQ-013 (kd)." Qualified candidates are asked to submit their online applications by **August 29, 2007**.

MASSACHUSETTS GENERAL HOSPITAL
HARVARD STEM CELL INSTITUTE

The Center for Regenerative Medicine (CRM) at Massachusetts General Hospital invites applications for a tenure-track assistant professor position. Outstanding scientists in the field of stem cell biology who have the demonstrated ability to develop a strong independent research program will be considered. Successful candidate(s) will be members of the Harvard Stem Cell Institute and faculty of Harvard University. Candidates must hold a PhD and or MD and have a history of innovative, interactive research. Applicants should send an electronic copy of (1) letter of interest (2) research plan and (3) current curriculum vitae to **Dr. David Scadden c/o Chris Shambaugh cpasker@partners.org.** Three letters of recommendation should also be sent directly to:

Center for Regenerative Medicine
Search Committee
Attention: Chris Shambaugh
Massachusetts General Hospital
185 Cambridge St., CPZN 4265A
Boston, MA 02114

Women and minority candidates are urged to apply. MGH is an Equal Opportunity/Affirmative Action Employer.

MICHIGAN STATE UNIVERSITY

Coupled Human and Natural Systems

Michigan State University seeks three faculty members in the areas of coupled human and natural systems. One of these [illegible] emphasize environmental policy, one land use and one population and [illegible] of environmental policy. We are especially interested in [illegible] appointments will be joint between the Environmental Science and Policy Program and the Departments of Geography (land use position), Political Science (environmental policy position) [illegible] position). The disciplinary department will be the tenure home for each position. The appointments will be [illegible] required at the time of appointment. Candidates should have strong methodological skills and rigorous theoretical focus [illegible] advantage. The positions will be [illegible] internationally renowned research program[illegible] Preference will be given to candidates who could engage in an initiative to introduce computational and other formal modeling techniques into the undergraduate social science curriculum. Letters of application should be accompanied by a curriculum vitae, short [illegible] of professional goals, three letters of reference and examples of published work. Applications will be reviewed starting October 1, 2007 and will be accepted until the positions are filled. Applications can be mailed or sent electronically. Mailed applications should be addressed to: **ESPP CHANS Search Committee, Environmental Science and Policy Program, Michigan State University, 274 Gilmer Hall, East Lansing, MI 48824-1105.** Electronic applications should be sent to ESPP@msu.edu and directed to Search Committee.

MSU IS AN AFFIRMATIVE ACTION, EQUAL OPPORTUNITY EMPLOYER.

Professor and Co-Director
Redox Biology Center and Department of Biochemistry
University of Nebraska-Lincoln (UNL)

The Redox Biology Center (RBC) at UNL, funded as a Center of Biomedical Research Excellence by the National Institutes of Health, invites nominations and applications from established investigators for a **tenured Full Professor** position in the Department of Biochemistry and **Co-Director of the Center**. The RBC is a major focus group for research in redox biology, incorporating various investigators at UNL and the University of Nebraska Medical Center in Omaha. Areas such as thiol-based redox signaling and gene regulation, redox control of neurodegenerative diseases and cancer, biochemistry of redox-active trace elements, structural biology, proteomics/metabolomics, microbial pathogenesis and redox homeostasis are all current targets of investigation. The Center also operates mass-spectrometry and spectroscopy core research facilities. The successful applicant will be expected to lead an internationally recognized, federally funded research program and contribute to the development and leadership of the Center.

The position will be housed in the state-of-the-art George W. Beadle Center, and carries with it a 12-month, state-funded appointment. This senior hire is the first of several new positions that the RBC will fill in various areas of redox biology during the next four years. To learn more about the Center and the Department please visit **http://www.unl.edu/RedoxBiologyCenter** and **http://biochem.unl.edu**

Applicants should go to **www.employment.unl.edu** and search for position **#070421**. Complete the faculty academic-administrative information form. Applicants should submit letter of application, curriculum vitae, a succinct statement of research interests, and three letters of reference sent to: **Dr. Vadim Gladyshev, Redox Biology Center Director, University of Nebraska, N118 Beadle Center, Lincoln, NE 68588-0662, USA** (email: **redox2@unl.edu**). Review of applications will begin on **September 4, 2007** and continue until the position is filled.

The University of Nebraska is committed to a pluralistic campus community through Affirmative Action and Equal Opportunity and is responsive to the needs of dual career couples. We assure accommodation under the Americans with Disabilities Act. contact Sheila Hawes at 402-472-4742 for assistance.

The Max-Planck Society is hosting a Symposium

Neurosensation, Neuroproteomics, and Neurophotonics
– New Vistas of the Brain -

to be held in Bonn/Germany on November 21 22, 2007

This symposium is intended to help define future research directions and to identify candidates for positions at the

Center for Advanced European Studies and Research (CAESAR)

a partner Institute of the Max-Planck Society in Bonn

We invite applications from international scientists with excellent track record both on the senior and junior level. The research areas of interest for CAESAR include neurodegeneration and neuroproteomics, imaging and control of brain function by light ("neurophotonics"), brain interfacing, neurosensory systems, and manipulation of neurons by viral gene transfer.

Scientists who wish to participate in this symposium and who are interested in shaping the future research directions at CAESAR are invited to send their CV and a short statement of their research interests not later than September 24, 2007 to

Max-Planck-Gesellschaft
zur Förderung der Wissenschaften e. V.
Administrative Headquarters
Ms. Dr. Dahrendorf-
Hofgartenstraße 8, D-80539 München/Germany

and in parallel to the following address:

Rheinische Friedrich Wilhelms Universität Bonn
Medizinisches Dekanat
-Prof. Reinhard Buettner
Sigmund-Freud Str. 25, D-53123 Bonn/Germany

STANFORD
SCHOOL OF MEDICINE

Stanford University
School of Medicine
Chair, Department of Comparative Medicine

The Stanford University School of Medicine is initiating a search for the position of Chair for the Department of Comparative Medicine.

The Department is an academic clinical department with active NIH funded research programs and training awards for veterinarians pursuing graduate and research experiences as well as an active teaching program and an ACLAM accredited residency program. The Chair also oversees the Veterinary Service Center, the clinical AAALAC accredited laboratory animal care program and has regulatory oversight of laboratory animals with the Institutional Animal Care and Use Committee and Institutional Official.

Candidates must have received the DVM or VMD degree from an institution accredited by the American Veterinary Medical Association with preference given to candidates with board certification in recognized specialties of veterinary medicine (Laboratory Animal Medicine, Internal Medicine, Veterinary Pathology, Anesthesiology, Surgery) or with appropriate experience and MS or PhD degrees. Candidates should have experience in managing a large animal research program as well as a demonstrable interest in research as evidenced by publications in peer reviewed journals. Among the research opportunities at Stanford are neuroscience, organ transplantation, immunology, genetics, infectious diseases, molecular biology, non-invasive nuclear and magnetic imaging, cancer, anesthesia, primate behavior, and studies using induced mutations in mice.

Stanford University is an equal opportunity employer and is committed to increasing the diversity of its faculty. It welcomes nominations of and applications from women and members of minority groups, as well as others who would bring additional dimensions to the university's research, teaching and clinical missions.

Interested candidates should submit a CV and letter of interest to the search committee by October 31, 2007 to:

William T. Newsome, PhD
Committee to Search for a Chair of the Department of Comparative Medicine
c/o Kendra Baldwin
300 Pasteur Drive Grant S-005
Stanford University School of Medicine
Stanford, CA 94305

Argonne

The Argonne Named Postdoctoral Fellowship Program

The Director's Office initiated these special postdoctoral fellowships at Argonne, to be awarded internationally on an annual basis to outstanding doctoral scientists and engineers who are at early points in promising careers. The fellowships are named after scientific and technical luminaries who have been associated with Argonne and its predecessors, and the University of Chicago, since the 1940's.

Candidates for these fellowships must display superb ability in scientific or engineering research, and must show definite promise of becoming outstanding leaders in the research they pursue. Fellowships are awarded for a two-year term, with a possible renewal for a third year, and carry a stipend of $72,000 per annum with an additional allocation of up to $20,000 per annum for research support and travel.

Requirements for applying for an Argonne Named Postdoctoral Fellowship:

The following documents must be sent via e-mail to Named-Postdoc@anl.gov by October 22, 2007. In the subject line please include the name of the candidate.

- Nomination memo (≤ 2 pages) from ANL sponsor
- Research proposal (≤ 2 pages)
- Three letters of recommendation from other than Argonne staff
- CV
- List of publications, abstracts and significant presentations
- Graduate School and Undergraduate Transcripts

The sponsor could be someone who is already familiar with your research work and accomplishments through previous collaborations or professional societies. If you have not yet identified an ANL sponsor, visit the detailed websites of the various Research Programs and Research Divisions at www.anl.gov.

All correspondence should be addressed to Argonne Named Postdoctoral Fellowship Program. One application is sufficient to be considered for all named fellowships. For additional details, visit the Argonne web site at http://www.dep.anl.gov/postdocs. Argonne is an equal opportunity employer and we value diversity in our workforce.

Argonne is a U.S. Department of Energy laboratory managed by UChicago Argonne, LLC

National Synchrotron Radiation Research Center

National Synchrotron Radiation Research Center
Beamline Scientist/Postdoctoral Positions

The National Synchrotron Radiation Research Center (NSRRC) in Taiwan is planning to construct a new 3 GeV synchrotron, Taiwan Photon Source (TPS), which is scheduled to complete in 2013. The new synchrotron project is seeking qualified beamline scientists and/or postdoctoral research associates. Candidates are preferred with experience in using synchrotron radiation for (a) advanced nano materials research, (b) structural characterization of bio-macromolecules; (c) development of related theories; or (d) inelastic x-ray scattering (IXS) experiments on electronic excitation in various condensed matter systems. Workplace will be at NSRRC or SPring-8, Japan. Applicants should submit an application letter, curriculum vitae, statement of research interest, reprints of three most important papers, and arrange for three letters of recommendation to be sent directly to the **Research Division, National Synchrotron Radiation Research Center, 101 Hsin-Ann Road, Hsinchu Science Park, Hsinchu 30076, Taiwan, R.O.C.** All applications should be made no later than September 15, 2007.

Case Western Reserve University

MetroHealth

DIABETES CENTER DIRECTOR
Case Western Reserve University
Rammelkamp Center for Research and Education
The MetroHealth System Campus

The Diabetes Center is a new initiative to develop a multidisciplinary program involving both laboratory-based and clinical research to study the pathogenesis and treatment of diabetes (and obesity). We seek a national leader in the field of diabetes, obesity or metabolic diseases as the Program Director. This individual will define the specific research focus and recruit a team of 5 to 7 principal investigators and develop collaborations with other basic and clinical investigators at Case. Outstanding facilities, generous start-up funds, and ongoing operational support are available. Preference will be given to M.D. and/or Ph.D. scientists with a demonstrated ability to lead a major research program and a track record of extramural funding. Academic rank and salary commensurate with experience.

Interested individuals should send Curriculum Vitae and names of three references to **John R. Sedor, M.D., Rammelkamp Center for Research and Education, 2500 MetroHealth Drive, R415, Cleveland, OH 44109-1998. E-mail address, pceb@metrohealth.org. Phone: 216-778-4993**

Case Western Reserve University and The MetroHealth System are Equal Opportunity Employers

---

PHYSIOLOGISTS

The **American University of the Caribbean School of Medicine (AUC)**, an accredited institution with over 3,500 graduated physicians, seeks to appoint 2-3 Medical Physiologists.

Candidates should possess a Ph.D. in Physiology or an M.D. with teaching experience at an LCME accredited medical school in any area of medical physiology. The physiology department is committed to providing exceptional instruction in this field. The university seeks individuals who have the ability to integrate medical physiology with other basic and clinical sciences. Candidates with teaching awards will be given preference.

The positions are to be fulfilled at the Basic Sciences campus on the island of St. Maarten in the Netherlands Antilles, approximately 3 hours by air from Miami. AUC possesses an exceptional faculty composed of both basic scientists and clinicians. Students complete their basic sciences training on the island, and then go on to complete clinical clerkships in the U.S., U.K. or Ireland.

Interested parties should send a brief statement of teaching interests, their CV, and contact information for three professional references to Dr. Susan Mesquita, Chair of the Physiology Search Committee, at **sdemesquita@auc-med.edu**.

www.auc-med.edu

School of Medicine

Columbia University Medical Center
Department of Pathology

FACULTY POSITIONS

The Department of Pathology and Cell Biology at Columbia University seeks highly qualified individuals for faculty positions in surgical pathology, anatomic pathology and research. Appointments can be at the Assistant, Associate Professor or Associate Research Scientist level depending on experience and qualifications. Clinical positions require board certification and a license in NYS prior to the start of service. Research positions require record of publication in leading journals and a statement of research directions.

Applicants should submit a curriculum vitae and three letters of reference to:

C. Kitzinger
Department of Pathology
Columbia University
630 West 168th Street
New York, NY 10032

Columbia University takes affirmative action toward equal employment opportunity. Women and minorities are encouraged to apply.

DEAN OF THE SCHOOL OF LIFE SCIENCES
FUDAN UNIVERSITY, SHANGHAI, CHINA

The School of Life Sciences of Fudan University, a premier institution of higher learning in China, is inviting applications from qualified scholars and administrators for the position of Dean regardless of citizenship. The School of Life Sciences was established in 1986 as the first in China and since then has been devoted to superlative teaching and research in Genetics, Developmental Biology, Microbiology, Neurobiology, Ecology and Biochemistry.

The successful candidate will have: demonstrated experience and success leading a major department or large laboratory; research projects of national and/or international significance; a publication record in prominent international journals in the last three years; pioneered research in an area of specialization; assumed important positions in international academic organizations; fluency in English or Chinese.

Salary and Term: The appointment will be made on a three year fixed term basis. The successful candidate should work full time, no less than 9 months per annum. Salary will be commensurate with experiences and qualifications.

Applicants should forward: curriculum vitae; letter of interest addressing vision, objectives, goals and qualifications; papers published in the past three years; addresses, telephone numbers, and e-mail addresses of three to five scholars for reference and consultation; copies of advanced degrees; certification of present employ.

Deadline of Application: **October 30, 2007**

Please direct applications and / or inquiries to:

Ms. Wen Jie/Mr. Zhu Hao
Talent Recruitment Office, Fudan University
Email: yj@fudan.ac.cn
Tel: 86-21-65642953

Ms. Jiang Lei
School of Life Sciences, Fudan University
Email: lifesciences@fudan.edu.cn
Fax: 86-21-65646979
Tel: 86-21-65642812
86-21-65642633

For more information, please visit our website: http://www.tr.fudan.sh.cn/

Yale University
Faculty Position
in
Ecology and Evolutionary Biology

The Department of Ecology and Evolutionary Biology at Yale University invites applications for a faculty position at either the tenured or tenure track in the field of ecology. We are particularly interested in candidates whose research unites theory and empirical work in ways that shed new light on basic questions. A record of outstanding achievement and a promising research program are more important than the specific research area.

Interested candidates should submit their C.V., three relevant reprints or manuscripts, brief research and teaching statements, and the names and addresses of four potential evaluators by **15 September 2007**. The search will remain open until the position is filled. Send materials to: **Department of Ecology and Evolutionary Biology, Yale University, P.O. Box 208106, New Haven, CT 06520-8106 USA, Attn: Francine Horowitz**.

The Department is described at
www.eeb.yale.edu

Yale University is an Equal Opportunity, Affirmative Action Employer. Men and women of diverse racial/ethnic backgrounds and cultures are encouraged to apply.

Emory University

Full Professor and Division Chief
Microbiology & Immunology
Yerkes National Primate Research Center at Emory

The Yerkes National Primate Research Center at Emory University seeks a new Chief for its **Division of Microbiology and Immunology**. The successful candidate will have an established and internationally recognized research program in the areas of vaccine development or microbial pathogenesis and will be expected to play a leadership role at the Primate Center. The Division of Microbiology and Immunology and the associated Emory Vaccine Center have established research programs focusing on HIV, malaria, RSV and biodefense; all have as their foundation a strong commitment to world-class basic science in the immunology and pathogenesis of microbial infections. The Chief of the Division of Microbiology and Immunology will have a tenure track academic appointment in an appropriate Department within Emory University's School of Medicine and will also be a Member of the Emory Vaccine Center. The Emory Vaccine Center is a partner in a new State-wide Initiative launched by the Georgia Research Alliance to develop and deploy next-generation vaccines and therapeutics. The selected candidate will play a major role in this Vaccine Initiative. Applications should be submitted by **September 30, 2007** and should be addressed to:

Dr. Rafi Ahmed
ra@microbio.emory.edu
1510 Clifton Road
Atlanta, GA 30322

Please reference job requisition #1269BR on the Emory employment website
http://emory.hr.emory.edu/careers/index.html

Emory University is an EEO/AA employer

U.S. Department of Energy
Associate Director
Office of Science for
Biological and Environmental Research
Announcement # SES-SC-HQ-014 (kd)

The U.S. Department of Energy's (DOE's) Office of Science is seeking qualified candidates to lead its Biological and Environmental Research (BER) Program. With an annual budget of more than $500 million, the BER Program is the nation's leading program devoted to applications of biology to bio-energy production and use and to environmental remediation. The BER Program supports major research programs in genomics, proteomics, systems biology, and environmental remediation. The Program is also one of the nation's leading contributors to understanding the effects of greenhouse gas emissions, aerosols, and atmospheric particulates on global climate change.

The Director of Biological and Environmental Research is responsible for all strategic program planning in the BER Program, budget formulation and execution, management of the BER office including a federal workforce of more than 70 technical and administrative staff; program integration with other Office of Science activities and with the DOE technology offices; and interagency integration. The position is within the ranks of the U.S. government's Senior Executive Service (SES); members of the SES serve in key positions just below the top Presidential appointees. For more information on the program please go to **http://www.sc.doe.gov/ober/**

For further information about this position and the instructions on how to apply and submit an application, please go to the following website: **http://jobsearch.usajobs.opm.gov/getjob.asp?JobID=58520806&AVSDM_2007%2D06=2006+13*3444%3A02&Logo=0&q=SES-SC-HQ-014+(kd)&FedEmp=N&sort=rv&vw=d&brd=3876&ss=0&FedPub=Y&SUBMIT1.x=47&SUBMIT1.y=12**. To be considered for this position you must apply online. It is important that you follow the instructions as stated on the announcement **SES-SC-HQ-014 (kd)** located at the website above.

Massachusetts Institute of Technology

It takes everyone at MIT to be MIT.

Postdoctoral Associates for SMART Interdisciplinary Research Group in Infectious Disease

In anticipation of the establishment of **Singapore-MIT Alliance in Research and Technology (SMART)**, we are recruiting ten (10) postdoctoral associates in the next six months to join an integrated, cutting-edge research program in infectious disease, involving principal investigators from Massachusetts Institute of Technology (MIT), National University of Singapore (NUS), Nanyang Technological University (NTU), A*Star research institutes, and Temasek Life Sciences Laboratory (TLL). The major goals of the research program are to advance basic understanding of pathogen-host interactions at the cellular and molecular levels and use this basic knowledge to develop diagnostics, prophylactics and therapeutics for specific infectious diseases.

Postdoctoral Associates will work on interdisciplinary projects in one of the following areas: i) cellular and molecular mechanisms of pathogen-host interactions, ii) immune responses to infections (influenza, RSV, malaria, or tuberculosis), iii) novel approaches to manipulate ES cells, stem cells, hematopoiesis, tissue repair and mice, and iv) nano- and micro-mechanics in the biological system.

The ideal candidates should have a Ph.D. in biochemistry/molecular biology, immunology, microbiology/virology, stem cells/hematopoiesis, or biomechanics; a strong publication record; excellent communication skills in English, and an ability to work independently as well as in a team consisting of people with diverse scientific backgrounds.

Postdoctoral associates will be supervised jointly by MIT and Singapore principal investigators. The postdoctoral associates will be based in Singapore with opportunity to conduct research at MIT. They will receive compensations comparable to equivalent positions in the US.

[redacted] and CV and names of three references to
Professor Jianzhu Chen at jchen@mit.edu

MIT is an Affirmative Action/Equal Opportunity Employer

http://web.mit.edu

MICHIGAN STATE UNIVERSITY

Faculty Position in Plant Systems Biology

As part of an initiative in **Systems Biology, the Department of Plant Biology at Michigan State University** seeks to fill a faculty position in genomics-enabled plant systems biology. We are seeking an individual who will address fundamental biological questions in plants and/or in related model systems. Applications from individuals who generate and integrate complex or heterogeneous data from metabolomic, proteomic and genomic studies or build models of metabolic or regulatory networks are especially encouraged. The successful candidate will be expected to develop a vigorous independent research program supported by extramural funding. We are particularly interested in recruiting a colleague who will participate in collaborative interdisciplinary research. The successful candidate may have a joint appointment with another suitable department and will contribute to undergraduate and graduate teaching in their area of expertise.

This faculty position is a tenure track, academic year appointment at the Assistant Professor level. An appointment at the Associate Professor level will be considered for exceptional candidates. Applicants must have a PhD and postdoctoral research experience is highly desirable. Applications should include a curriculum vitae, a summary of research accomplishments and future research objectives, a brief description of teaching philosophy, goals and three letters of reference. Application materials should be sent electronically to **PLBSYS@msu.edu**. Information about the Department of Plant Biology can be found at **http://www.plantbiology.msu.edu**. The review of applications will begin **September 7, 2007** and will continue until suitable candidates are identified. Questions regarding this position may be sent to Yair Shachar-Hill (**yairhill@msu.edu**).

MSU is an Affirmative Action, Equal Opportunity Employer
MSU is committed to achieving excellence through cultural diversity.
The university actively encourages applications and/or nominations of women, persons of color, veterans and persons with disabilities.

University of Heidelberg

The **Institute for Theoretical Physics** of the Ruprecht-Karls-University at Heidelberg, Germany, invites applications for a

Professorship in Theoretical Physics (Complex Systems) (W3)

(Succession of Prof. H. Horner (C4))

The position is available starting with the winter term 2007/2008.

The scientific field of activity of the position holder is expected to be [redacted] Physics with focus on Biophysics. The faculty is especially interested in scientists who develop novel analytical mathematical methods in order to build a theoretical bridge from Physics to Biology.

The new professor is expected to demonstrate a commitment to teaching in Theoretical Physics in its full spectrum and he/she should adequately participate in the basic training in Theoretical Physics (Mechanics, Electrodynamics, Quantum Mechanics, Statistical Physics).

In the case of appointment the applicants have to participate in the self administration of the University.

Applicants are expected to have a Ph.D. in physics and an excellent research record.

Normally, first-time professorial contracts at universities in Baden-Württemberg are temporary for 3 years at first and turn permanent after a review. Exceptions from this rule are possible especially for candidates from abroad or from outside the universities.

[redacted] and, for this reason, especially welcomes applications from women. Handicapped persons with the same qualifications will be given preference.

Qualified candidates are invited to submit their applications until September, 30th 2007 with the usual documents and a research plan to **Prof. M. Bartelmann, Dekan der Fakultät für Physik und Astronomie der Universität Heidelberg, Albert-Ueberle-Str. 3-5, D-69120 Heidelberg.**

ASSISTANT PROFESSOR OF MICROBIOLOGY

UNIVERSITY OF NEW ENGLAND COLLEGE OF OSTEOPATHIC MEDICINE BIDDEFORD, MAINE

University of NEW ENGLAND

A tenure-track, Assistant Professor position is available in the Department of Microbiology. Qualifications include a doctoral degree (Ph.D., D.O., or M.D.), experience in teaching microbiology (with an emphasis in virology), postdoctoral experience, and a commitment to excellent teaching. Candidates will be expected to develop an independent research program that will eventually attract extramural funding. The primary teaching duty will involve instruction in medical virology to first year medical students. The University of New England is surrounded by the natural resources of coastal southern Maine and is situated near the urban offerings of Portland, Portsmouth and Boston.

Applicants should submit copies of their curriculum vitae, statements of teaching experience and philosophy, and research experience and goals, as well as arrange for three letters of recommendation to be sent to: **James M. Vaughn, Ph.D., Chair, Department of Microbiology, UNECOM, 11 Hills Beach Rd., Biddeford, ME 04005, or via email to jvaughn@une.edu.**

Equal Opportunity/Affirmative Action employer and strongly encourages candidates of diverse backgrounds.

PROFESSOR, MOLECULAR ONCOLOGY

ENDOWED CHAIR – MOFFITT CANCER CENTER & RESEARCH INSTITUTE

The University of South Florida (USF) College of Medicine's Department of Interdisciplinary Oncology and the H. Lee Moffitt Cancer Center & Research Institute, an NCI-designated Comprehensive Cancer Center, are seeking a distinguished scientist for a Professorship position in the Molecular Oncology Program. In addition to the academic appointment at USF, this position is also an Endowed Chair at the Moffitt Cancer Center.

The successful candidate must possess a Ph.D. or M.D. degree and an excellent track record of independent research as demonstrated by high quality publications in peer-reviewed journals and sustained extramural funding. The candidate must also have at least five years academic experience at the Associate Professor rank. Preference will be given to individuals who will complement current existing interests in our program including, but not limited to, the broad areas of gene regulation, signal transduction, cancer genetics, proteomics and functional genomics. However, outstanding candidates from all other research areas will be considered. The position is tenure earning and salary is negotiable.

Please reference position no. DR00524. Interested candidates should send curriculum vitae and a brief statement of major academic interests as one single pdf document to the Molecular Oncology Search Committee at Rebecca.Jokarsky@moffitt.org. Application review begins August 1, 2007; position is open until filled.

MOFFITT Cancer Center & Research Institute
The Life Of Cancer Stops Here.

USF University of South Florida College of Medicine

USF Health is committed to increasing its diversity and will give individual consideration to qualified applicants for this position with experience in ethnically diverse settings, who possess select language skills, or who have a record of providing medical care to underserved or economically challenged communities. The University of South Florida is an EEO/EA/AA Employer. For disability accommodations, contact Kathy Jordan at (813) 745-1453 a minimum of five working days in advance. According to FL law, applications and meetings regarding them are open to the public.

www.moffitt.org

RHEUMATOLOGIST/IMMUNOLOGIST

The Division of Rheumatology and the Department of Medicine at Dartmouth-Hitchcock Medical Center (DHMC) in conjunction with the Department of Microbiology and Immunology, Dartmouth Medical School (DMS) are seeking a highly motivated translational faculty member with their established research program in the Immunobiology of autoimmune diseases at the preclinical / translational level. Successful candidates will hold joint appointments in the Department of Microbiology and Immunology and participate in graduate programs of NCI-funded Center of Biomedical Research Excellence (COBRE) in Immunobiology. Opportunity to participate in the Norris Cotton Cancer Center at DMS/DHMC, a comprehensive NCI-core grant supported center that has recently undergone extensive expansion. Prospective candidates must possess a MD and/or PhD or equivalent and be qualified for appointment at the rank of Assistant Professor or higher. The Rheumatology Section has a long history of clinical and research excellence as well as fellowship training at both DHMC and the White River Junction VA Hospital in Vermont. DHMC is a 396-bed tertiary care hospital and the teaching hospital for DMS. DMS, DHMC and the Section of Rheumatology are in a period of vigorous growth with the goal of becoming a major academic focus in all areas of investigation. Dartmouth-Hitchcock Medical Center is a state-of-the-art tertiary facility located in the Upper Valley Region of New Hampshire, an area of Northern New England with cultural, academic and recreational activities readily available. Salary is commensurate with experience. Please forward letter of interest, CV and references to:

Daniel A. Albert, MD
Section Chief, Rheumatology
Dartmouth Hitchcock Medical Center
One Medical Center Drive, Lebanon, NH 03756

DARTMOUTH HITCHCOCK MEDICAL CENTER

www.DHMC.org

Dartmouth-Hitchcock Medical Center is an affirmative action/equal opportunity employer and is especially interested in identifying female and minority candidates.

Department of Health and Human Services
National Institutes of Health
National Human Genome Research Institute

CHIEF OF STAFF, IMMEDIATE OFFICE OF THE DIRECTOR

The National Human Genome Research Institute (NHGRI), a major research component of the National Institutes of Health (NIH) and the Department of Health and Human Services (DHHS), has led the groundbreaking enterprise known as the Human Genome Project, and is now vigorously exploring the application of advances in genome research to human health. The NHGRI is soliciting applications for the career federal position of Chief of Staff in the Immediate Office of the Director, NHGRI. The incumbent will serve as a senior advisor and the Chief of Staff managing and directing the scientific and administrative activities and priority setting for all tasks occurring within the Immediate Office of the Director. The Chief of Staff will have advanced scientific training and maintain an active knowledge of advances in the fields of genetics and genomics and the application of such research to health and disease. Responsibilities will encompass substantive program and policy matters covering the full range of NHGRI's interests and program activities and directing the efficient planning and coordination of operations and staff within the Immediate Office of the Director. The NHGRI vacancy announcement for this position contains complete application procedures and lists all mandatory information which must be submitted with your application. To obtain the vacancy announcement for this position it will be available on **http://www.usajobs.gov** and posted under announcement **#NHGRI-07-203295-CR-DE** or **NHGRI-07-103295-CR-MP**. You may also visit the NIH website at **www.jobs.nih.gov.** Applications must be received no later than **August 24, 2007**.

This is a full time permanent position offering benefits including health and life insurance, retirement, sick and annual leave. U.S. citizenship is required.

DHHS and NIH are Equal Opportunity Employers

Does your next career step need direction?

There's only one place to go for career advice if you value the expertise of *Science* and the long experience of AAAS in supporting career advancement. ScienceCareers.org. The pages of *Science* and our website ScienceCareers.org offer.

- Thousands of job postings
- Funding information
- Career advice articles and tools
- Networking opportunities

www.sciencecareers.org

DIRECTOR
NATIONAL OPTICAL ASTRONOMY OBSERVATORY

The Association of Universities for Research in Astronomy, Inc. (AURA) seeks a new Director of the National Optical Astronomy Observatory (NOAO). We are seeking an individual with an outstanding scientific background, with vision, and with demonstrated leadership and talent for administration in a complex and evolving environment. The director is responsible for all of NOAO including operations and development.

The coming decade will present both outstanding opportunities and significant challenges for NOAO, and for its next director. The recent NSF Senior Review has underscored the crucial role of NOAO in serving the community, and budget increments to upgrade NOAO facilities are already beginning. The new director will have the opportunity and responsibility to work with the community and the NOAO staff to shape the future of the National Observatory in the years ahead.

The Search Committee will begin evaluating applications **on October 1, 2007**. Applications will be accepted until the position is filled. Applications should include scientific and management experience, relevant accomplishments, a resume, bibliography, a list of three references, and the individual's written view of the future role of NOAO in the U. S. and international astronomy communities. Applications will be kept confidential, and should be sent to **Dr. Patrick Osmer, Chair, NOAO Director Search Committee, c/o AURA, Suite 450, 1212 New York Avenue N.W., Washington, DC 20005**.

Questions related to this search should be directed to **Dr. Patrick Osmer, osmer.1@osu.edu**.

Information and updates regarding this search are available on **www.aura-astronomy.org**

Women and minorities are encouraged to apply. AURA is an EOE/AA/E.O. Employer.

University of San Diego

ASSISTANT PROFESSOR Biology

The University of San Diego (USD), Department of Biology, invites applications for a tenure track faculty position beginning in September 2008.

The department seeks applicants with expertise in Ecology or Evolutionary Biology to offer an upper division course with laboratory in their area of specialty and to teach a course in organismal diversity as part of our introductory majors sequence.

Preference will be given to candidates with expertise in terrestrial invertebrate biology. USD is an independent Catholic university whose primary aim is teaching excellence. Active scholarship is integral to this aim, and the candidate is expected to have an ongoing research program that will involve undergraduates.

Applicants should submit a curriculum vitae, a brief statement of teaching philosophy and research interests, and three letters of recommendation by September 15, 2007 to:

Chair, Department of Biology
University of San Diego
5998 Alcala Park
San Diego, CA 92110-2492

Women and minority candidates are encouraged to apply. Additional information about the University can be found at our website: www.sandiego.edu.

www.sandiego.edu *Equal Opportunity Employer*

FOCUS ON CAREERS

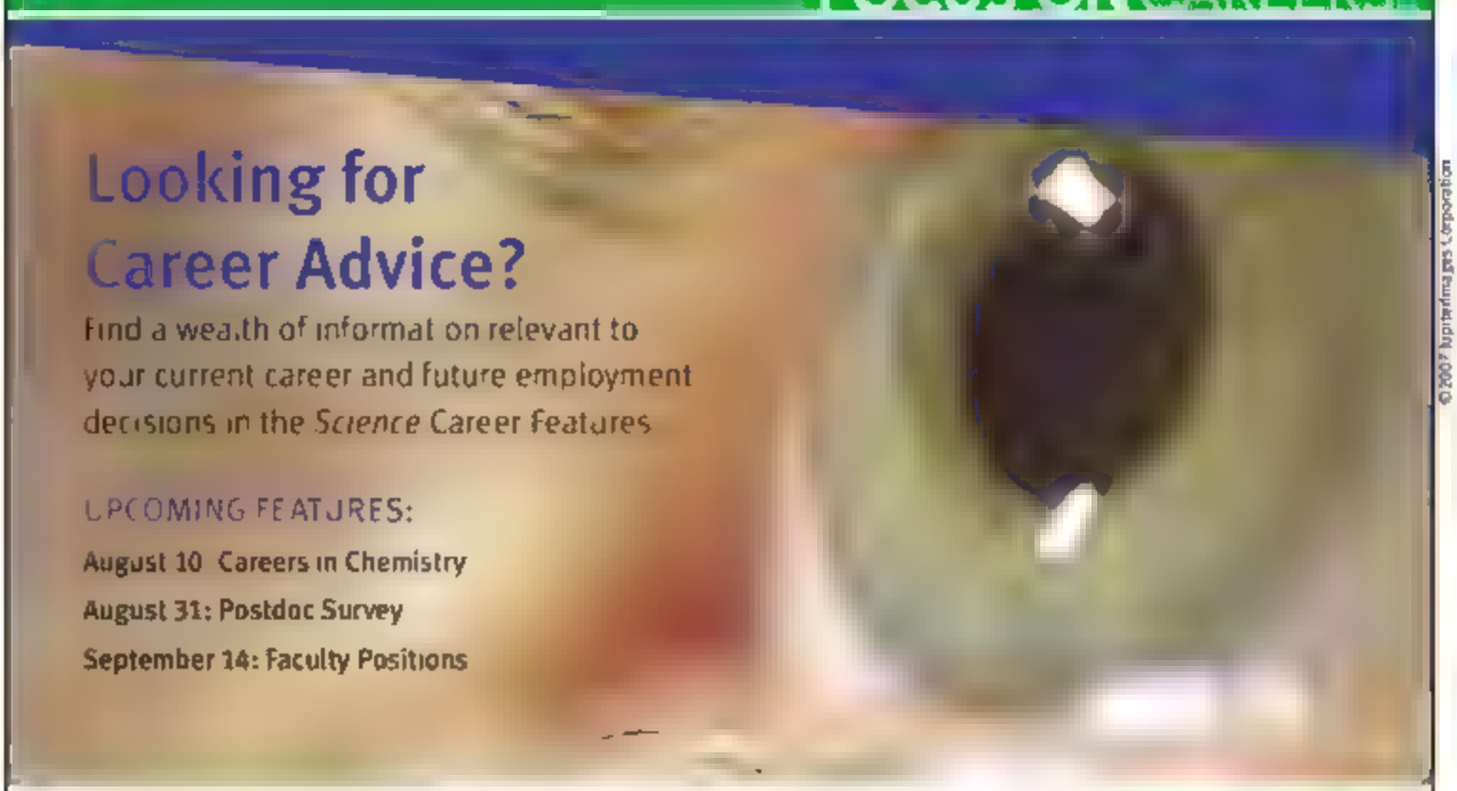

Looking for Career Advice?

Find a wealth of information relevant to your current career and future employment decisions in the *Science* Career Features.

UPCOMING FEATURES:

August 10: Careers in Chemistry

August 31: Postdoc Survey

September 14: Faculty Positions

Also available online at www.sciencecareers.org/businessfeatures

ScienceCareers

From primates to proteomics

For careers in science, turn to *Science*

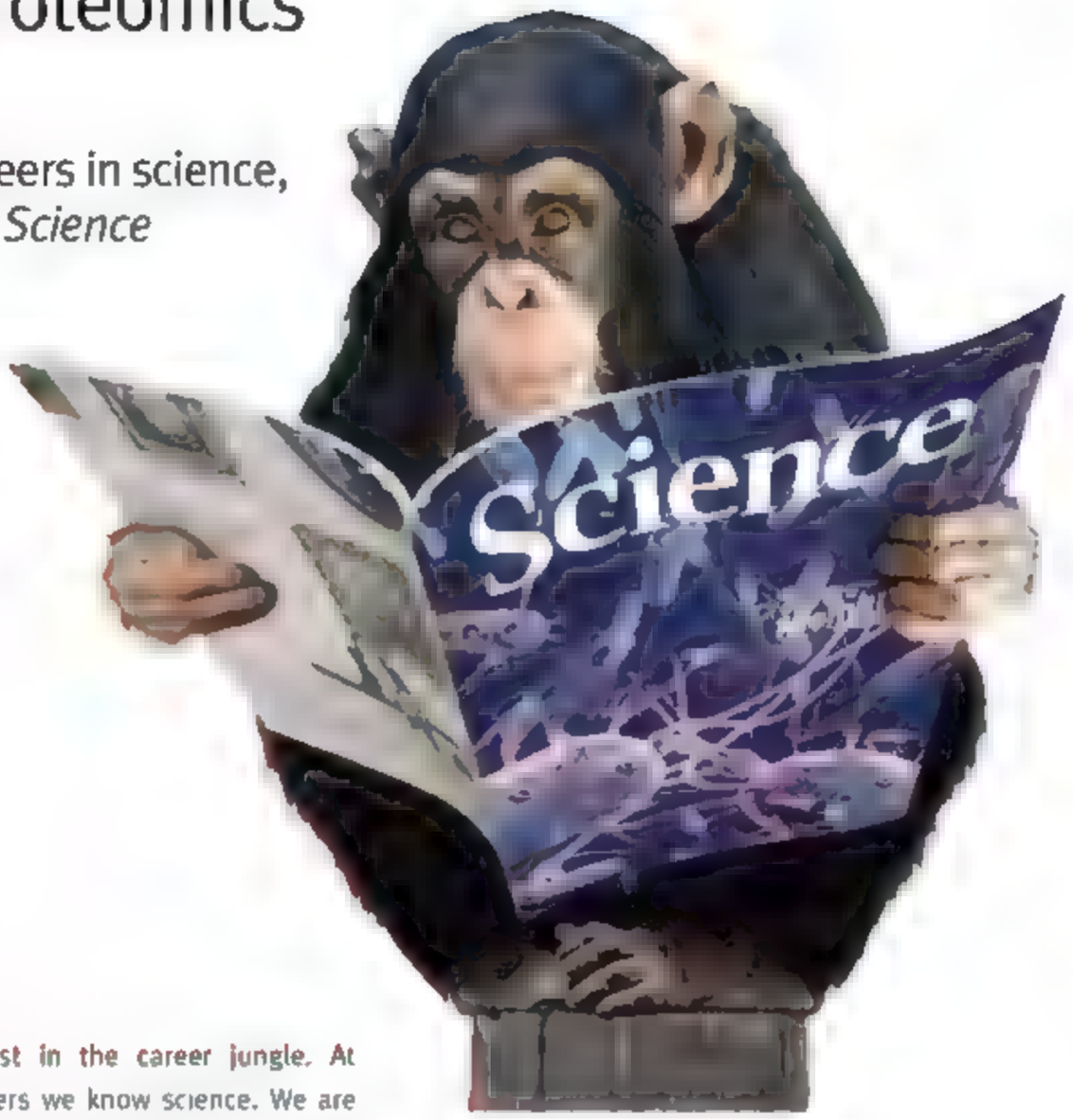

Don't get lost in the career jungle. At *Science* Careers we know science. We are committed to helping you find the right job, and to delivering the useful advice you need. Our knowledge is firmly founded on the expertise of *Science*, the premier scientific journal, and the long experience of AAAS in advancing science around the world. *Science* Careers is the natural selection.

Features include:

- Thousands of job postings
- Career advice
- Grant information
- Resume/CV Database
- Career Forum

www.ScienceCareers.org

Science Careers
From the Journal *Science* AAAS

The **Medical College of Georgia Vascular Biology Center** is recruiting a **physiologist pharmacologist at the Assistant Professor level**, tenure-track. The successful candidates will have an earned Ph.D., M.D. or M.D. Ph.D. degree. They will join an active group of extramurally funded vascular biologists (currently about $8 million annually, see: **http://www.mcg.edu/centers/VBC/index.html**) in recently renovated laboratories utilizing state-of-the-art equipment. They will have the opportunity to participate in the two institutional pre- and post-doctoral training programs in Integrative Cardiovascular Biology. Ample opportunities for collaborative basic and clinical research are available and encouraged. The candidates are expected to develop an active, extramurally funded research program in aspects of hypertension related to the kidney and or endothelial function. Highly competitive salary and start-up package, commensurate with prior experience, will be provided.

Applications should include detailed C.V., statement of career goals and names of three references and be e-mailed to **David M. Pollock, Ph.D. (dpollock@mcg.edu)**

The Medical College of Georgia is an Equal Opportunity and Equal Access Institution. Applications from women and under represented minorities are particularly encouraged.

Education

Elizabethtown COLLEGE

ASSISTANT PROFESSOR OF ECOLOGY

The Biology department at Elizabethtown College has an opening for a tenure-track position at the Assistant Professor level beginning August 2008. Candidates must be committed to undergraduate teaching and research with significant student involvement and must possess a Ph.D.

Teaching responsibilities may include ecology, introductory biology for majors, a non-majors biology course, and an advanced elective course in landscape ecology. Experience teaching at the undergraduate level and successfully obtaining external funding are preferred. Application by candidates whose research incorporates vertebrate species and Geographic Information Systems is particularly encouraged.

Ranked as one of the country's best regional colleges by U.S. News and World Report, Elizabethtown offers its 1900 students 43 major programs in the liberal arts, sciences and professional studies. Marked by a commitment to "Educate for Service," the college prepares students intellectually, socially, aesthetically and ethically for lives of service and leadership as citizens of the world. As signature attributes of its academic excellence, Elizabethtown centers learning in strong relationships, links classroom instruction with experiential learning, emphasizes international and cross-cultural perspectives, and nurtures the capacity for lives of high purpose. For more information, consult www.etown.edu

To apply, send curriculum vitae, statements of teaching and research interests, and up to three reprints, and arrange for at least three letters of reference to be sent to:
Elizabethtown College
Attn: Human Resources
One Alpha Drive, Elizabethtown, PA 17022-2298
hr@etown.edu

For more information visit:
www.etown.edu/humanresources - AA/EOE
Review of applications will begin on Sept. 15, 2007

FDA

DIRECTOR
DIVISION OF APPLIED PHARMACOLOGY RESEARCH

Join us at the frontier of knowledge

The Food and Drug Administration's Center for Drug Evaluation and Research (CDER), Office of Pharmaceutical Science (OPS), Office of Testing and Research (OTR) is recruiting for a Director of its **Division of Applied Pharmacology Research** at the FDA's Research Laboratory in White Oak, Maryland.

Basic Qualifications. **A doctoral level degree** (M.D., Ph.D., D.Sc. etc.), doctoral level knowledge of pharmacology, toxicology, biomedical engineering, clinical pharmacology or closely related fields, and extensive knowledge in one or more of the following: pharmacology, physiology, pharmacodynamics, biopharmaceutics, toxicology and/or pharmacokinetics, with a strong record of peer-reviewed original research.

Applicants should have managerial experience that demonstrates strong executive leadership and the ability to: direct a research laboratory, communicate and effectively interact with high level national and foreign government officials, scientific and academic communities, medical and health related organizations, regulated industry, and others. **It is desirable that applicants have** a practical knowledge of pharmacogenomics, proteomics, and metabonomics relevant to drug therapy and safety and knowledge of the FDA laws and regulations related to human drugs and pharmacology.

Duties: The Director is the Office/Center's principal advisor for planning and conducting laboratory research in pharmacology, toxicology or closely related fields, and he/she maintains an active research program and directs research scientists engaged in pharmacologic research designed to ensure drug safety and efficacy. The incumbent participates fully in policy, planning, and oversight of pharmacology laboratory research activities to insure compliance with FDA Critical Path Initiative and that Center decisions are based on current pharmacology/toxicology science.

Salary: This position may be filled as either Senior Biomedical Research Svc ($110,363-$186,600) Title 42 (Salary negotiable-Title 42 is not capped at $186,600) or Commissioned Corps Officer.

How to Apply: Submit **an electronic curriculum vitae or brief resume** indicating that you are applying for the SBRS position of Director, Division of Applied Research (D-DAPR), Office of Testing and Research (OTR), Office of Pharmaceutical Science (OPS), Center for Drug Evaluation (CDER), Food and Drug Administration (FDA) to: **FOOD AND DRUG ADMINISTRATION, Center for Drug Evaluation and Research, Office of Pharmaceutical Science, 10903 New Hampshire Avenue, Room 3541, Silver Spring, Maryland 20993, Attn: Jim Keady, Project Manager.** For more information on this position contact **Jim Keady** at **james.keady@fda.hhs.gov** on **301-796-1550** (phone), **301-796-9733** (fax) or **Dr. John M. Strong** at **john.strong@fda.hhs.gov** on **301-796-0121** (phone), **301-796-9818** (fax).

FDA IS AN EQUAL OPPORTUNITY EMPLOYER WITH A SMOKE FREE ENVIRONMENT

University of Michigan

Biogerontology
University of Michigan

The **University of Michigan Geriatrics Center** is seeking one or more junior or senior faculty members to carry out independent research focused on the biology of aging and its impact on late life pathophysiology. Research that emphasizes mammalian models or use of proteomic and genomic approaches, would be of particular interest. Successful candidates will be housed in newly constructed Geriatrics Center space, and will receive a primary tenure-track or tenured appointment in a basic science or clinical department as appropriate. Minimum qualifications are a PhD, MD or equivalent degree, several years of highly productive postdoctoral research, and a clear interest in problems relevant to biogerontology. Substantial start-up funding will be available for each selected candidate.

Applicants should submit a CV, a brief (1-2 page) description of research interests, a synopsis of current and previous research support, and contact information for 3 - 5 referees, to **Rich Miller, 3001 BSRB, Box 2200, 109 Zina Pitcher Place, Ann Arbor, MI 48109-2200.**

The University of Michigan is an Equal Opportunity Employer committed to maintaining diversity in its hiring programs.

FACULTY POSITION in PLANT MOLECULAR VIROLOGY
Department of Plant Pathology
The Ohio State University

A nine-month, tenure-track position at the **ASSISTANT PROFESSOR** level is available in the Department of Plant Pathology at the Ohio State University (OSU) in Wooster. The position is 90 percent research and 10 percent teaching.

The successful candidate will be expected to develop a strong, extramurally funded research program in plant virology. Possible research areas include viral gene function, replication, pathogenicity and transmission, or the molecular basis of viral host resistance. The incumbent will have access to state-of-the-art laboratory, phytotron, and greenhouse facilities, as well as a microscopy and genomics center. The incumbent will interact with the USDA-Agricultural Research Service Corn and Soybean Research Group and the OSU Plant Molecular Biology and Biotechnology (PMBB) Program. The incumbent will be expected to advise graduate students, teach a five-week course in plant virology, and participate in advanced team-taught courses in plant-microbe interactions.

A Ph.D. in plant pathology, virology, molecular biology, or closely related discipline is required. Research experience with the characterization of plant viruses, plant virus interactions, viral genes, and/or viral proteins using modern molecular techniques is highly desired. For further information, please contact the **Chair of the Search Committee, Dr. Larry Madden (telephone: 330-263-3839; e-mail: madden.1@osu.edu).** Review of applications will begin October 1, 2007, and continue until a suitable applicant is found. Please submit curriculum vitae, a brief description of proposed research focus and teaching goals, and names and complete addresses of four references to: **Dr. Larry Madden, Department of Plant Pathology, Ohio State University, 1680 Madison Avenue, Wooster, OH 44691.**

To build a diverse workforce, the Ohio State University encourages applications from individuals with disabilities, minorities, veterans, and women. OSU is an Equal Employment Opportunity/Affirmative Action Employer.

CHAIR
Department of Genetics and Biochemistry
Clemson University

The Department of Genetics and Biochemistry at Clemson University, housed within the College of Agriculture, Forestry, and Life Sciences, is seeking an experienced and visionary individual for the position of Chair. The Department offers B.S., M.S., and Ph.D. degrees in the Genetics and the Biochemistry Programs. The Department Chair is responsible for strategic planning, academic administration, and fostering national and international collaborations. Candidates should have a Ph.D. in genetics, biochemistry, or related discipline and demonstrate significant experience in research, teaching, mentorship, and administration of an organizational unit or program. The Department, established in 2001, is particularly interested in an individual who can guide and mentor young faculty through his/her experience, effective leadership and vision. Curriculum vitae that demonstrate significant achievement in research, scholarship, and service including a clear statement of administrative philosophy should be submitted electronically to **Sheryl Banks (e-mail: sherylb@clemson.edu).** Review of nominations and applications will begin on September 15, 2007, and continue until a suitable candidate is found. The applicant should arrange for three letters of recommendation to be sent to the same address by the same date. Please visit **website: http://www.clemson.edu/genbiochem** to learn more about the Department and the University. *Clemson University is an Equal Employment Opportunity/Affirmative Action Employer and does not discriminate against any individual on the basis of age, color, disability, gender, national origin, religion, sexual orientation, or veteran status.*

ASSISTANT or ASSOCIATE PROFESSOR
Kyoto University, Kyoto, Japan
Six Positions Available
Kyoto University Evolution and Biodiversity Global Center of Excellence

The Evolution and Biodiversity Global Center of Excellence (COE) of Kyoto University is seeking candidates for fixed-term positions of Assistant/Associate Professor, depending on qualifications. Successful candidates will be expected to pursue vigorous independent research programs.

Our Program aims to develop novel approaches to understand the development, evolution, behavior, and diversity of organisms, always keeping the genome as our common base. We welcome innovative researchers pursuing not only micro-level studies, such as studies of animal or plant development or diversity (especially using nonmodel organisms), experimental evolutionary biology, the role of epigenetics in evolution, or the variety and evolution of biofunctions from the viewpoint of diversity of biomolecules, but also researchers pursuing macro-level studies such as ecological fieldwork, ethology, or primatology. Kyoto University is unmatched in Japan for its rich tradition and success in fostering such researchers.

Candidates must hold a Ph.D. or equivalent degree and have demonstrated ability to develop novel approaches to study leading-edge problems in biodiversity and evolution.

Successful candidates will be employed through March 31, 2012.

Application deadline: August 16, 2007, 10 a.m. Japan Standard Time. Interview date: August 28, 2007.

Submit applications through **website: http://www.biol.rigaku.kyoto-u.ac.jp/gcoe/.**

Send any enquiries to **Professor Kiyokazu Agata, Global COE Project Leader at e-mail: agata@mdb.biophys.kyoto-u.ac.jp.**

FACULTY POSITIONS
Department of Pharmaceutical Sciences
South Dakota State University

Department of Pharmaceutical Sciences is seeking faculty members for two tenure-track positions. An attractive startup package is available. Qualified applicants with an earned Ph.D. degree in pharmaceutical sciences or a closely related area with teaching and research experience in molecular modeling, molecular biology, cell signaling, pharmacogenomics, pharmacokinetics, or a related area with effective verbal and written communication and interpersonal skills are invited to apply. The successful candidate will be expected to teach professional pharmacy courses (for B.S. and Pharm.D. degree) and graduate courses (for Ph.D. degree) in the area of expertise, as well as develop and maintain an active extramurally funded research program. Preference will be given to candidates in the area of cancer and neurobehavioral research with prior teaching and research experience in the relevant areas and a professional degree in pharmacy. For questions on the position, contact **Dr. Hesham Fahmy at telephone: 605-688-4243, e-mail: hesham.fahmy@sdstate.edu.** Review of applications will begin September 1, 2007, and continue until the positions are filled. To view a full list of qualifications and critical instructions regarding the application process, visit **website: http://YourFuture.sdbor.edu**, search for the position, and follow the electronic application process. For questions on the electronic employment process, contact **South Dakota State University Human Resources at telephone: 605-688-4128.** *SDSU is an Affirmative Action/Equal Employment Opportunity Employer.*

ASSISTANT PROFESSOR
Marine Biology
California State University, Fullerton

The Department of Biological Science, California State University, Fullerton (CSUF) invites applications for a full-time tenure-track Assistant Professor position in marine biology to begin August 2008. Applicants should have a Ph.D. and relevant postdoctoral experience. We are interested in candidates who can contribute to departmental concentrations in marine biology and in biodiversity, ecology, and conservation biology. Possible research areas include, but are not limited to, systematics, population genetics, phylogeography, marine plant-animal interactions, and invasive species. The successful candidate will be expected to maintain an active, externally funded research program involving undergraduate and M.S. students, and be committed to excellence in teaching a diverse population of students. The successful candidate will contribute to an inquiry-based, lower-division core course (either evolution and biodiversity or principles of physiology and ecology), teach an upper-division/graduate-level course in phycology, and develop other upper-division elective courses in his/her area of expertise. CSUF is a member of the Southern California Marine Institute (**website: http://scmi.us/**) and is situated near other major universities that offer possibilities for collaboration. Send (1) curriculum vitae (including history of grant support), (2) a statement of research plans, (3) reprints of two to three recent, peer-reviewed publications, (4) a statement of teaching philosophy and experience, and (5) have three letters of recommendation sent to: **Marine Biology Search Committee, Department of Biological Science, California State University, Fullerton, CA 92834-6850. Website: http://biology.fullerton.edu/.** Review of applicants will begin November 16, 2007, and continue until a suitable candidate is appointed. Salary is competitive and commensurate with experience and qualifications. *Women and minority candidates are particularly encouraged to apply. CSUF is an Affirmative Action/Equal Opportunity/Title IX/ADA Employer.*

FACULTY POSITIONS, EXPERIMENTAL PATHOLOGY. The Department of Pathology at the University of California, San Diego (UCSD), **website: http://medicine.ucsd.edu/pathology/,** seeks outstanding scientists for new faculty positions in the following areas: genetic models of human disease, immunology, and cell biology/signal transduction. Applicants should have an M.D., M.D./Ph.D., or Ph.D. degree, substantial postdoctoral experience, and the ability to develop an extramurally funded research program. Preference will be given to individuals with established NIH support. Successful candidates will be expected to participate in our education mission by teaching in the medical school, pharmacy school, and/or graduate school. Rank will be commensurate with experience. Salary will be consistent with published UCSD pay scales. Review of applications will begin August 23, 2007, and will continue until filled. Please forward application letters together with curriculum vitae and names/addresses of at least three references to: **Search Committee Chair, Dr. David Cheresh, c/o Ms. Catherine Schumacher, Search Coordinator, Department of Pathology 0717, University of California San Diego School of Medicine, 9500 Gilman Drive, La Jolla, CA 92093-0717.** Applications by e-mail are acceptable to **e-mail: cdschumacher@ucsd.edu.** *UCSD is an Affirmative Action/Equal Opportunity Employer with a strong institutional commitment to excellence through diversity.*

ASSOCIATE DIRECTOR
Program Development and New Initiatives (PDNI)

The University of Kansas Transportation Research Institute, **website: https://jobs.ku.edu;** search position number 00206358.

Review of applications begins September 1, 2007.
Equal Opportunity/Affirmative Action Employer.

POSITIONS OPEN

MEDICAL ENTOMOLOGIST, at the level of **ASSISTANT or ASSOCIATE PROFESSIONAL SCIENTIST,** Illinois Natural History Survey (INHS), Champaign, Illinois. Develop and maintain an independent research program and cooperative research endeavor involving the biology, ecology, and management of arthropods and the pathogens they transmit that affect the health and welfare of humans, wild and domestic animals.

Requires Ph.D. in entomology/biology/zoology/epidemiology with a specialization in medical entomology. Responsibilities: develop and maintain a vigorous, extramurally funded research program, maintain a record of frequent publications in peer reviewed, nationally recognized scientific journals, present research at scientific conferences, manage facilities and supervise staff at the Medical Entomology Laboratory, interact with news media, the public, and officials at the international, federal, state, and local levels, serve on INHS-Department of Natural Research committees, and participate in educational and outreach activities. INHS houses a functioning, well-equipped medical entomology laboratory that includes three permanent positions. One research scientist position is available for a new hire. The Laboratory currently receives approximately $400,000 per year in state support for mosquito research and research on other arthropod pests of humans and animals. INHS is part of the Illinois Department of Natural Resources and an Affiliated Agency of the University of Illinois at Urbana-Champaign.

To apply send cover letter, curriculum vitae, statement of research interests, and contact information for three references to our **Human Resources Office, e-mail: hroffice@inhs.uiuc.edu** (electronic applications required). Position reference #1512, **telephone: 217-244-4592, fax: 217/333-4949.** Deadline September 17, 2007. For application requirements and complete position description visit our **website: http://www.inhs.uiuc.edu/opportunities/index.php?action=fulltime&id=133.**

The University of Michigan Department of Medicine, Division of Infectious Diseases seeks M.D. or M.D./Ph.D., candidates for tenure-track positions at the **ASSISTANT, ASSOCIATE, or FULL PROFESSOR** rank to develop and conduct independently funded basic and/or translational research programs in the fields of viral or bacterial pathogenesis. Investigators will join a growing and interactive group of researchers with close ties to both basic science and clinical departments within the University, and joint appointments within graduate departments of the University of Michigan are available. Preference will be given to physician-scientists who are Board-certified/eligible in infectious diseases, although highly qualified Ph.D. candidates will also be considered. Interested individuals should submit curriculum vitae, summary of research and career goals for junior applicants, and contact information along with three references to: **Pawel Kazanjian, M.D., Professor and Chief, Division of Infectious Diseases, Department of Internal Medicine, 1500 E. Medical Center Drive, 3119 Taubman Center, Ann Arbor, MI 48109-5378 or e-mail: francis@umich.edu.** *The University of Michigan is an Equal Opportunity Employer; women and other minorities are encouraged to apply.*

CAREER OPPORTUNITY

This unique program offers the candidate with an earned Doctorate in the life sciences the opportunity to obtain the Doctor of Optometry (O.D.) degree in 27 months (beginning in March of each year). Employment opportunities exist in research, education, industry, and private practice. Contact the **Admissions Office, telephone: 800-824-5526** at the **New England College of Optometry, 424 Beacon Street, Boston, MA 02115.** Additional information at **website: http://www.neco.edu, e-mail: admissions@neco.edu.**

POSITIONS OPEN

INSTITUT PASTEUR

POSTDOCTORAL FELLOWSHIPS
Institut Pasteur, Paris, France

Founded in 1887 by Louis Pasteur and located in the heart of Paris, the Institut Pasteur is a world-renowned private research organization. The Pasteur Foundation of New York is seeking outstanding fellowship applicants. Candidates may apply to any laboratory within 10 Departments: Cell Biology and Infection, Developmental Biology, Genomes and Genetics, Immunology, Infection and Epidemiology, Microbiology, Neuroscience, Parasitology and Mycology, Structural Biology and Chemistry, and Virology. See website for details. Annual package is $70,000 for three years. This is a biannual call for applicants; see website for deadlines. *U.S. citizenship required.*

E-mail: pasteurus@aol.com. Website: http://www.pasteurfoundation.org.

University of Minnesota Cancer Center seeks self-motivated and career-oriented **POSTDOCTORAL ASSOCIATES** to join highly interactive research team working in cell cycle checkpoints, apoptosis regulation, and cancer biology. The Laboratory studies the molecular aspects of prostate cancer with particular focus on: (1) regulation and function of FOXO1 during the cell-division cycle and under genotoxic/oxidative stress, and (2) functional interaction between two tumor suppressor genes CBP and PTEN in prostate tumorigenesis. See **website: http://www.mcdb.umn.edu/faculty/Huang.html** for recent publications. The approaches used range from mammalian cell culture, molecular biology, biochemistry to mouse genetics. A relevant doctoral degree and strong background in molecular and cellular biology is essential. Applicants including curriculum vitae, bibliography, summary of past accomplishments, and the names and contact information of three references should be submitted to: **Haojie Huang, Ph.D.** Please apply to requisition number 149483 online at **website: https://employment.umn.edu.** *The University of Minnesota is an Equal Opportunity Educator and Employer.*

Indiana University, Bloomington and Department of Psychological and Brain Sciences seeks an outstanding faculty to lead and serve as the new **DIRECTOR** for the Imaging Research Facility **(website: http://www.indiana.edu/~imaging/),** a 100 percent research facility located within the Department of Psychological and Brain Sciences. A full position description is available at **website: http://www.indiana.edu/~psych.** Applications will be reviewed as they are received and will continue until the position is filled. A Ph.D. in a relevant field is required. *Indiana University is an Affirmative Action Employer. Applications from women and minority candidates are encouraged.*

ASSISTANT PROFESSOR POSITIONS
Organic Chemistry and Biochemistry

Rider University's Department of Chemistry, Biochemistry, and Physics seeks applicants for two tenure-track positions at the rank of Assistant Professor to begin fall 2008. One position is in the area of organic chemistry (position #207102), and the other in biochemistry (position #209108).

For more information on these positions and for application instructions, please visit our **website: http://www.rider.edu/hr,** Employment Opportunities. *Affirmative Action/Equal Opportunity Employer.*

POSITIONS OPEN

LABORATORY MANAGER (Job Number 38464)
Laser Ablation-Inductively Coupled Plasma Mass Spectrometry, Arizona LaserChron Center

The University of Arizona seeks a highly motivated scientist to serve as Manager of the Arizona LaserChron Center, which is a multi-user facility that focuses on U-Th-Pb geochronology by laser ablation-multicollector-inductively coupled plasma mass spectrometry (LA-MC-ICPMS). Responsibilities would include: (1) directing installation of a new multicollector ICPMS and Excimer laser, (2) developing new analytical techniques and applications using an existing multicollector LA-MC-ICPMS (GVI Isoprobe) and Excimer laser (DUV193), (3) performing minor maintenance and overseeing major repairs of these instruments, (4) supervising visits of research scientists, and (5) conducting independent research. The position is full-time and permanent. Applicants should have an M.S. or Ph.D. in earth science or chemistry, and have demonstrated experience with LA-MC-ICPMS instrumentation. Applications will be reviewed beginning 15 August 2007, and will continue until the position is filled. Applications should be submitted at **website: https://www.uacareertrack.com** for job number 38464. For additional information, please visit the Arizona LaserChron Center **website: http://www.geo.arizona.edu/alc** and contact **George Gehrels (e-mail: ggehrels@e-mail.arizona.edu)** or **Joaquin Ruiz (e-mail: jruiz@e-mail.arizona.edu).** *The University of Arizona is an Equal Opportunity, Affirmative Action Employer.*

ASSISTANT PROFESSOR in CELL BIOLOGY
Carleton College

The Department of Biology invites applications for a tenure-track position starting fall 2008. We seek candidates who have research and teaching interests in cell biology. Teaching responsibilities include a mid-level survey course in cell biology, an upper level course and/or laboratories in area of candidate's expertise, and participation in our introductory course focused on energy transformation in biological systems.

Candidates should be committed to excellence in undergraduate teaching in a liberal arts environment, and dedicated to developing an active research program that engages students. We are particularly interested in applicants who will strengthen the department's commitment to students from underrepresented groups in the biological sciences. Candidates must have a Ph.D. in biology or a related field, and postdoctoral experience is preferred.

Please send letter of application, curriculum vitae, a statement of teaching philosophy and research plans, and three letters of reference to: **Professor Matthew Rand, Department of Biology, Carleton College, Northfield, MN 55057-4025.** Application deadline is September 15, 2007.

Carleton College is an Affirmative Action/Equal Opportunity Employer. We are committed to developing our faculty to better reflect the diversity of our student body and American society. Women and members of minority groups are strongly encouraged to apply.

QUANTITATIVE/THEORETICAL ECOLOGIST

The Department of Ecology and Evolution is seeking to fill a faculty position with an individual working at the interface of theory and data in ecology. Rank is open, with a preference for **ASSISTANT or ASSOCIATE PROFESSOR.** Interested applicants should submit curriculum vitae, selected reprints and preprints, statements of research and teaching interests, and the names and addresses of three references to **website: https://ecologysearch.uchicago.edu;** letters of reference can be submitted at this site as well. Applications will be accepted until the position is filled, but applications should be received before 15 September 2007, to ensure full consideration. *The University of Chicago is an Affirmative Action/Equal Opportunity Employer.*

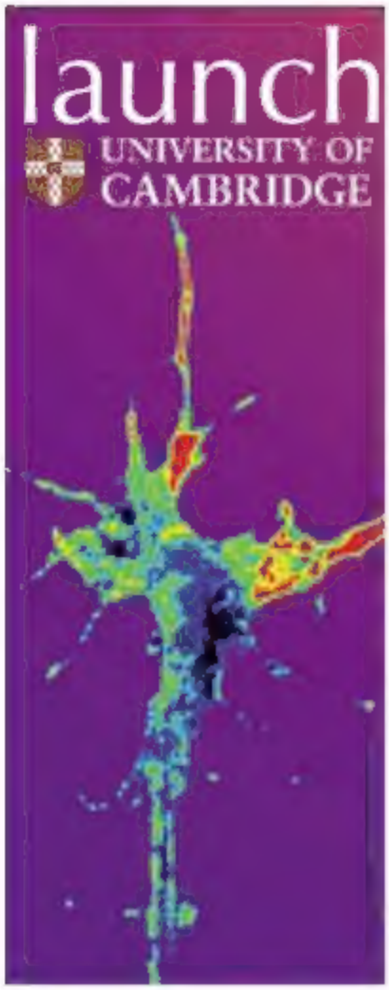

launchsymposium

UNIVERSITY OF CAMBRIDGE

19th-21st September 2007
Cambridge, UK

Keynote speakers

Linda Buck, Antonio Damasio, Tom Jessell

Plenary speakers

Adriano Aguzzi, Earl Miller, Josh Sanes, Mike Shadlen, Daniel Weinberger

CAMBRIDGE NEUROSCIENCE

To register visit www.neuroscience.cam.ac.uk

Sessions in developmental, cellular & molecular, systems & computational, cognitive & behavioural and clinical & veterinary neuroscience

EUROPEAN SCIENCE FOUNDATION
SETTING SCIENCE AGENDAS FOR EUROPE

ESF RESEARCH CONFERENCES
2007 Call for Proposals

The **ESF Research Conferences Scheme** (www.esf.org/conferences) provides the opportunity for leading scientists and younger researchers to meet for discussions on the most recent developments in their fields of research. It acts as a catalyst for creating new contacts throughout Europe and the rest of the world. It develops principally through the establishment of long-term partnerships between the ESF and national and international organisations, including universities.
ESF Research Conferences are open to scientists world-wide, whether from academia or industry. Conferences may be single events, or series, usually with a biennial meeting focusing on specific aspects of the same general topic. Conferences generally last for four or five days and up to 150 participants and invited speakers may attend.

The European Science Foundation now invites proposals for conferences to be held in **2008 and 2009**. The Call is addressed to leading European scientists for conferences to take place in Europe.

CALL FOR PROPOSALS – 2009 CONFERENCES

The following scientific areas will be covered by the Call:
- Biology at the Interface with Other Science Disciplines (ESF-EMBO Symposia)
- Physics/Biophysics and Environmental Sciences (ESF-FWF Conferences in Partnership with LFUI)
- Social Sciences and Humanities (ESF-LiU Conferences)
- Global Change Research (ESF-VR-FORMAS Conferences)

The Proposals will be evaluated through international Peer Review for which Referees will be nominated by the appropriate ESF Scientific Committees. The final assessment and selection of topics, on the basis of three written reviews, will be made jointly by the Partner Organisations through a Review Panel composed of members of the ESF Scientific Committees and scientists nominated by the Partner Organisations.

- Closing Date for on-line Submission:
Monday 1 October 2007 (midnight CET)

CALL FOR PROPOSALS – 2008 CONFERENCES

A second Call is also open for conferences to take place in 2008 in the field of Mathematics. A maximum of three proposals will be selected within the framework of the new partnership established with the Ministry of Science and Higher Education Poland (MSHE) and the Institute of Mathematics of the Polish Academy of Sciences (PAN). The proposals will be assessed by the three Partner Organisations.

- Closing Date for on-line Submission:
Saturday 15 September 2007 (midnight CET)

For further information about the Call, please visit
www.esf.org/conferences/Call2007
or send an email to **conferences-proposals@esf.org**
European Science Foundation | ESF Research Conferences
149 avenue Louise | Box 14 | 1050 Brussels | Belgium
Tel: +32 (0)2533 2020 | Fax: +32 (0)2538 8486
www.esf.org/conferences

POSITIONS OPEN

GENE THERAPEUTICS RESEARCH INSTITUTE CEDARS SINAI MEDICAL CENTER and DEPARTMENT of MOLECULAR and MEDICAL PHARMACOLOGY University of California at Los Angeles

POSTDOCTORAL POSITIONS are available in the Gene Therapeutics Research Institute and the Department of Molecular and Medical Pharmacology, University of California at Los Angeles to study the molecular and cellular mechanisms involved in brain tumor regression; the formation and function of specific immunological synapses in vivo and the in vivo migration of immune cells into the tumor microenvironment. This project also has a strong translational component to develop and implement novel immuno-therapeutics in human clinical trials for brain cancer (See: *The Journal of Experimental Medicine* **203**:2095-107, 2006; *Cancer Res.* **65**:7194-7204, 2005; *Nature Biotechnol.* **19**:582-585, 2001; *Proc. Natl. Acad. Sci. USA* **97**: 7482-7, 2000; *Nature Med.* **5**:1256-63, 1999). A strong background in immunology, cell biology, virology, and image analysis is essential.

Our Institute is located at the Cedars Sinai Medical Center campus and offers state-of-the-art facilities in an exciting environment for postdoctoral research. Interested candidates should have a Ph.D and/or an M.D and have under five years of postdoctoral experience. Salary is dependent on education and research experience, with a range of $36,000 to $45,000. Please submit a cover letter, curriculum vitae including bibliography, and contact information for three references to: **Pedro R. Lowenstein, M.D., Ph.D.** or **Maria G. Castro, Ph.D., Cedars Sinai Medical Center, 8700 Beverly Boulevard, Davis Building, Room: R5090, Los Angeles, CA 90048. E-mail: lowensteinp@cshs.org** or **castrong@cshs.org.**

Two **POSTDOCTORAL POSITIONS** in the Division of Hematology at the Children's Hospital of Philadelphia and the University of Pennsylvania are available immediately. One position will be devoted to studying the biological effects of long-term expression and immune responses to transgene and/or vectors in hemophilia animals and thrombosis models using gene therapy strategies. Applicants for this position should have a strong background in molecular biology and have experience working with transgenic/gene targeted mouse models.

The second position will examine mechanisms contributing to blood coagulation factor specificity and function. Biochemical approaches both in vitro and in vivo are employed to characterize recombinant blood clotting proteins. Applicants for this position should have a strong background in protein biochemistry and have tissue culture and molecular biology experience. Experience with murine models is also desirable. Candidates for both positions should have a Ph.D. or M.D. degree, have good communications skills, be highly motivated, and be willing to work on a multidisciplinary team. Highly competitive salary and benefits are offered. Curriculum vitae and three references should be sent to: **Drs. Valder Arruda and Rodney M. Camire, The Children's Hospital of Philadelphia, ARC, Room 302, Philadelphia, PA 19104. E-mail: arruda@e-mail.chop.edu, rcamire@mail.med.upenn.edu.**

POSTDOCTORAL POSITIONS are open to study biochemical mechanism of ubiquitylation in regulating genomic integrity and tumorigenesis. Candidates with strong background in biochemistry, genomic integrity, and tumor mouse model are encouraged to send curriculum vitae and three references to: **Dr. Yong Wan, Ph.D., University of Pittsburgh Cancer Institute, Hillman Cancer Center, 5117 Centre Avenue, Room 2.6C, Pittsburgh, PA 15213. E-mail: yow4@pitt.edu. Laboratory website: http://www.cbp.pitt.edu/faculty/yong_wan.** *The University of Pittsburgh is an Affirmative Action, Equal Opportunity Institution.*

POSTDOCTORAL POSITION available immediately on a West Virginia-Experimental Program to Stimulate Competitive Research-funded grant in the Cell Differentiation and Development Center at Marshall University. Our Laboratory is interested in the epigenetic/molecular mechanisms which influence cell differentiation and in cancer research. The successful candidate will be highly motivated, have Ph.D., and/or M.D., a strong background in molecular biology and immunology, and exceptional oral and written communication skills. Applicants with demonstrated experience in the latest techniques to analyze chromatin structure and gene regulation will be given preference. Experience with animal models is highly desirable. The candidate will be expected to present research findings at scientific conferences, prepare manuscripts, assist in experimental design, and apply for external postdoctoral funding (NIH, NSF, American Association for Cancer Research, et cetera). Salary is nationally competitive and will be commensurate with experience. Please e-mail curriculum vitae and a brief description of career goals, along with names and contact information of three references to:

Philippe Georgel, Ph.D.
Byrd Biotechnology Center, Room 241-F
One John Marshall Drive
Huntington, WV 25755 U.S.A.
E-mail: georgel@marshall.edu

Marshall University is an Equal Opportunity/Affirmative Action Employer.

POSTDOCTORAL RESEARCH SCIENTIST Department of Neurological Surgery Columbia University

Seeking applicants for Postdoctoral position to work in neurovascular laboratory. Successful applicant will have M.D. or Ph.D. and experience with rodent surgical models, preferably those for strokes. Candidate will interact with multidisciplinary investigators in a collaborative research environment and will be responsible for the stroke model and immunohistochemical procedures. Must speak and write fluent English with strong verbal and written communication skills. Interested applicants should e-mail a letter of interest, curriculum vitae, and list of references to **e-mail: rs604@columbia.edu.** *Columbia University takes Affirmative Action to ensure Equal Employment Opportunity.*

MOLECULAR TUMOR BIOLOGY and DEVELOPMENTAL THERAPEUTICS

A POSTDOCTORAL POSITION is available to study genes and proteins involved in cancer cell signal transduction pathways and to develop targeting strategies in animal models of cancer. Recent Ph.D. with background and training in molecular biology and biochemistry is desirable. Please send curriculum vitae and names of three references to: **Usha Kasid, Ph.D., Professor, Room E208, The Research Building, Georgetown University Medical Center, 3970 Reservoir Road N.W., Washington, DC 20057.** No e-mails please. *An Equal Opportunity/Affirmative Action Employer.*

POSTDOCTORAL POSITION. HIV recombination creates viral diversity that obstructs therapy. We are defining the mechanisms of DNA-RNA strand interactions and viral protein activities that promote recombination within the co-packaged HIV genomes. Strong background in biochemistry and molecular biology required. Send curriculum vitae and three recommendations to: **Dr. Robert Bambara, Biochemistry and Biophysics, P.O. Box 712, University of Rochester, Rochester, NY 14642. (Website: http://www.urmc.rochester.edu/smd/bcbp.)**

POSITIONS OPEN

POSTDOCTORAL FELLOW POSITIONS available to study the role of membrane-anchored metalloproteinases in development and cancer (e.g., *Cell* **125**:577, 2006 and **114**:33, 2003; *Genes Dev.* **20**:2673, 2006). Strong background in cell or molecular biology required. *U.S. citizen and resident aliens only.* Send curriculum vitae and letters of reference to: **Stephen J. Weiss, M.D., Upjohn Professor of Medicine, Chief, Molecular Medicine and Genetics, University of Michigan, 5000 LSI, 210 Washtenaw, Ann Arbor, MI 48109-0640.**

POSTDOCTORAL POSITIONS at Texas A&M University to exploit yeast models of human bone marrow failure and leukemia, and to discover drugs to treat same. High-quality publications in yeast cell biology and/or genetics required. These NIH-funded positions come with excellent benefits and a salary that is commensurate with experience. To apply, please visit **website: http://greatjobs.tamu.edu** and click on job code NOV 02707 or job code NOV 02705. *Texas A&M University is an Equal Opportunity Employer.*

BIOINFORMATICS. We are seeking a **POSTDOCTORAL FELLOW** to work jointly with the **Jacobsen and Pellegrini** Laboratories in the Department of Molecular, Cell, and Developmental Biology at UCLA **(website: http://www.mcdb.ucla.edu)** in the analysis whole genome chromatin profiling data using ultra high throughput sequencing. Candidate will conduct sophisticated data analyses using Matlab, Mathematica, R, C, and C++, and participate in database construction. Please apply to **e-mail: mingh@ucla.edu.**

MARKETPLACE

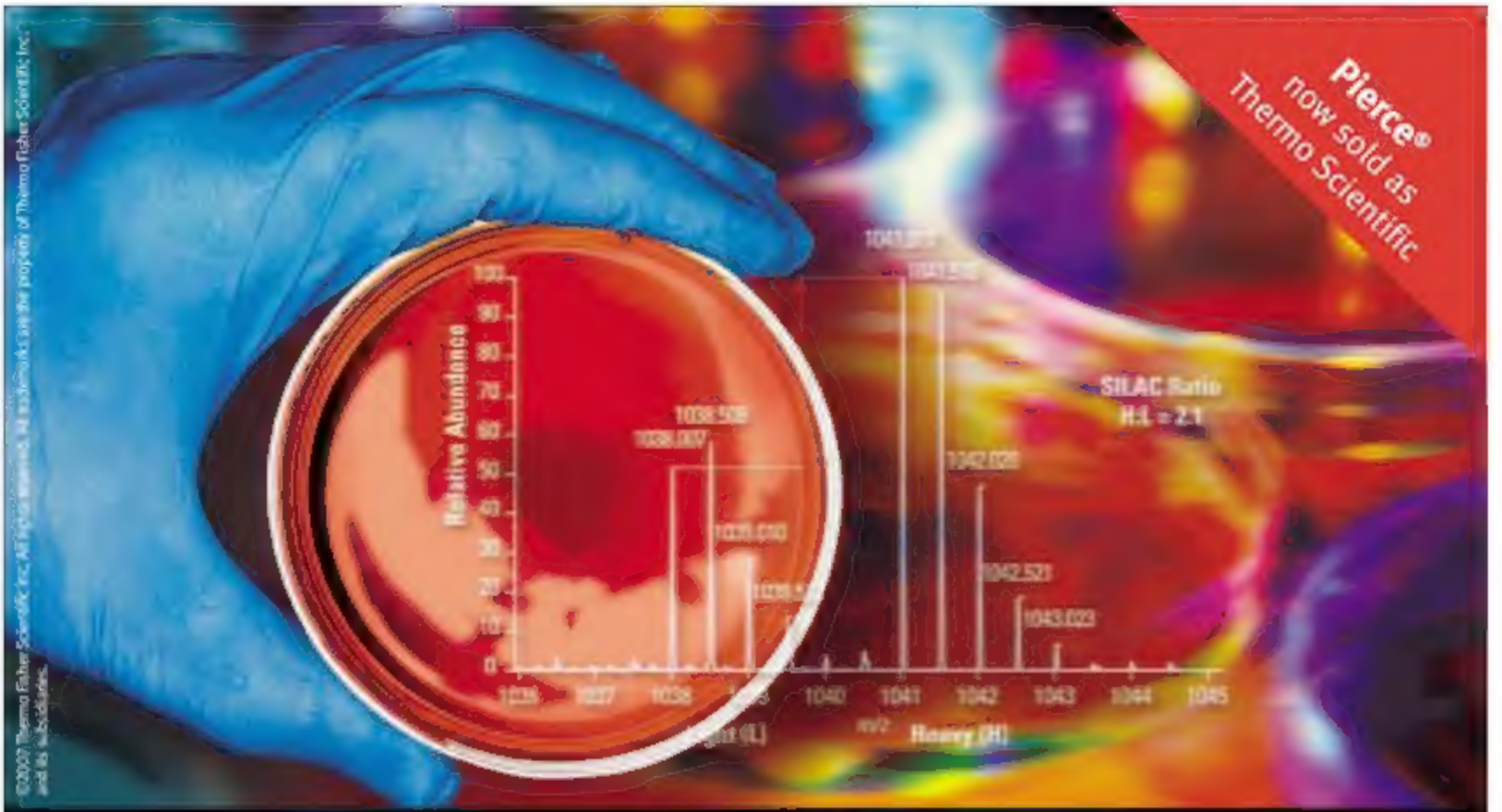

What's up (or down) with your protein? SILAC can tell you.

New Thermo Scientific Pierce SILAC (stable isotope labeling using amino acids in cell culture) Kits identify and quantify relative differential changes in protein samples. These kits and Thermo Scientific MS Instruments provide a complete and validated workflow, making protein quantitation easier, faster and more reproducible.

SILAC Applications:

- Quantitative analysis of protein changes and proteins for which there are no antibodies available
- Proteomic profiling in normal and diseased cells
- Quantitative identification of 100s to 1,000s of proteins in one experiment

Learn more. Visit www.thermo.com/silac or call 800-874-3723 to request your free copy of our SILAC technical brochure.

Thermo Scientific Pierce SILAC Quantitation Kits. Ideal for quantitative analysis of differential protein expression in mammalian cells.

Part of Thermo Fisher Scientific

Thermo SCIENTIFIC

IDT introduces the miRCat™ Cloning Kit for small RNA discovery

miRCat™ small RNA cloning is based on the pre-activated, adenylated linkering method that has been successfully used in many labs since its development in 2001[1]. miRCat™ permits cloning from any RNA source in any species.

Material sufficient for ten cloning experiments is provided in the miRCat™ Small RNA Cloning Kit, and a detailed technical manual provides instructions for cloning and sequencing small RNAs either as individual clones or as concatamers.

www.idtdna.com for more miRCat™ information

References
1. Lau NC, LP Lim, EG Wienstein, and DP Bartel 2001 An abundant class of tiny RNAs with probable regulatory roles in Caenorhabditis elegans. Science 294: 858-862.